5.8.5

COO-2841-1
ESTD 76-07
UC-77

VHTR ENGINEERING DESIGN STUDY

Intermediate Heat Exchanger Program

FINAL REPORT

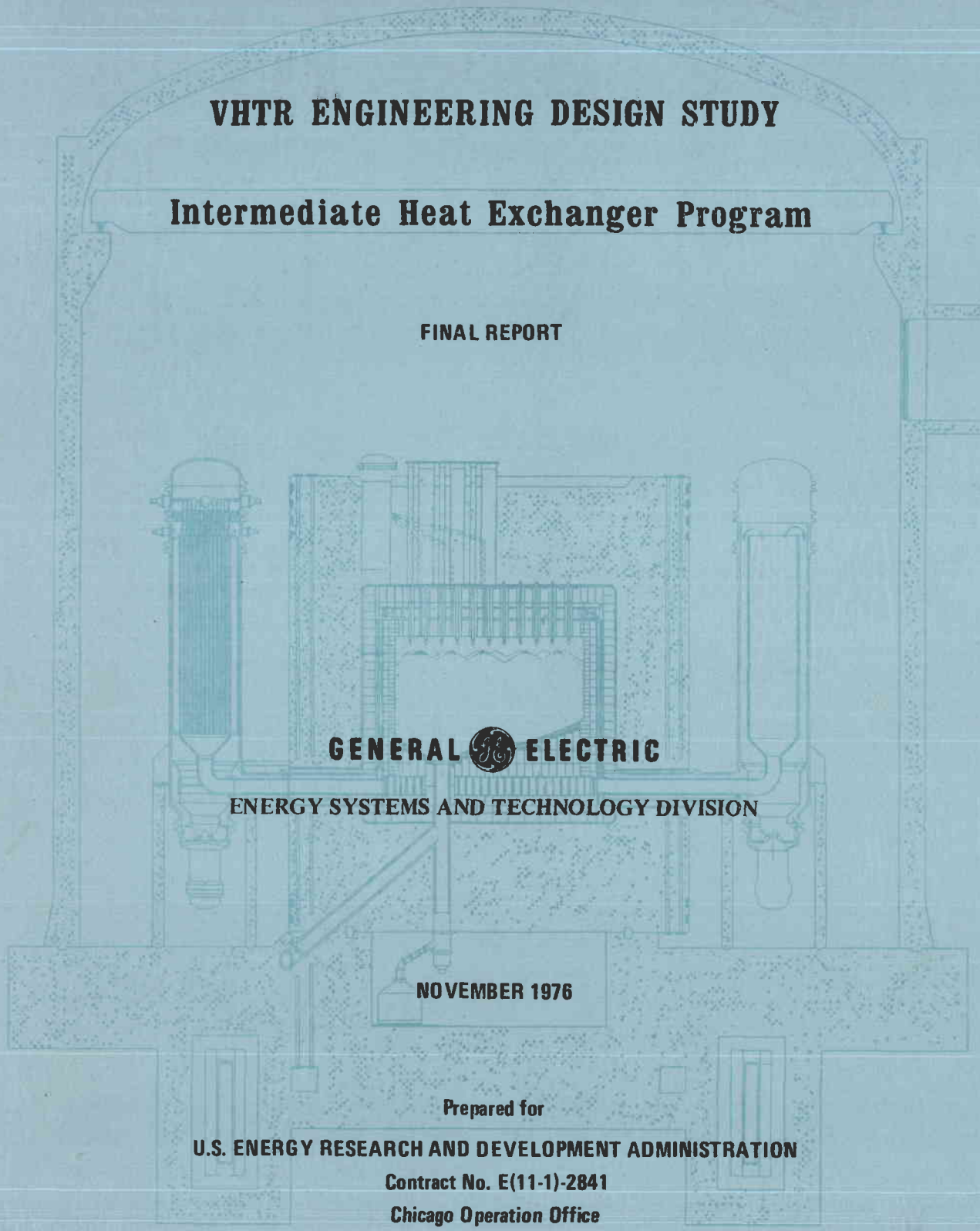

GENERAL ELECTRIC

ENERGY SYSTEMS AND TECHNOLOGY DIVISION

NOVEMBER 1976

Prepared for

U.S. ENERGY RESEARCH AND DEVELOPMENT ADMINISTRATION

Contract No. E(11-1)-2841

Chicago Operation Office

COO-2841-1
ESTD 76-07
UC-77

VHTR ENGINEERING DESIGN STUDY

Intermediate Heat Exchanger Program

Prepared for

U.S. Energy Research and Development Administration
Contract No. E(11-1)-2841
Chicago Operation Office

General Electric Company
Energy Systems & Technology Division

TABLE OF CONTENTS

LIST OF FIGURES

LIST OF TABLES

SECTION 1

SUMMARY

1.1 OBJECTIVE

The work reported in this document is the result of a follow-on program to earlier Very High Temperature Reactor (VHTR) studies[1,2]. The primary use of the VHTR is to provide heat for various industrial processes, such as hydrocarbon reforming and coal gasification. These prior studies identified the method of transferring high temperature heat from the reactor primary cooling circuit to the chemical process as a key area for further investigation. For many processes the use of an intermediate heat transfer barrier between the reactor coolant and the process is desirable; for some processes it is mandatory. Various intermediate heat exchanger (IHX) concepts for the VHTR were investigated with respect to safety, cost, and engineering design considerations. The reference processes chosen were steam-hydrocarbon reforming, with emphasis on the chemical heat pipe, and steam gasification of coal.

1.2 INTRODUCTION

The High Temperature Reactor is uniquely suited for providing the heat energy required for many industrial processes. Among these are steam reforming of light hydrocarbons, coal gasification or liquefaction, thermochemical water splitting, and the long distance transport of thermal energy. Table 1-1 shows the temperature requirements for two of these processes. The capability of the pebble bed reactor fuel to meet these requirements is also shown. This study investigates the critically important area of heat transfer between the reactor coolant, helium, and the various chemical processes.

The many possible schemes for heat transfer can be broadly divided into two groups - (1) those in which the process heat exchanger is heated directly by the reactor coolant, and (2) those in which a second coolant or equivalent barrier is located between the process heat exchanger and

TABLE 1-1

TEMPERATURE REQUIREMENTS FOR NUCLEAR PROCESS HEAT				
	STEAM REFORMING	STEAM GASIFICATION OF COAL		
		DESIGN POINT	GROWTH POTENTIAL	
Primary Helium Temperature, °C	950*	950*	1000*	1100*
Secondary Helium Temperature, °C	-	900	950	1050
Peak Process Temperature, °C	820 - 870	771	783	800
Reference IHX Design	DSR	IHX-L With "U"-Tube Module		
Reference Materials	800H	IN-617 AISI-316	ODS IN-617 AISI-316	

*Pebble Bed Reactor Fuel Capability

- 970°C Helium from Core Outlet Using BISO Fuel Kernel
- 1200°C Helium from Core Outlet Using TRISO Fuel Kernel

the reactor coolant. From a thermodynamic viewpoint, it would be desirable to heat the process heat exchanger directly, however, there are a number of reasons why this may not be appropriate. One reason involves the prevention of leaks which would either allow the release of radioactive material to the process stream or the entrance of process materials into the reactor core. Another reason is the requirement for physical separation of the reactor and process so that the reactor coolant remains in the reactor building and all process materials stay outside.

For coal gasification the latter reason holds. It is not reasonable to either transport many tons of coal per hour into the reactor building, nor to allow the primary reactor coolant to leave the reactor building. Thus, for steam gasification of coal, at least, a separate heat transport loop will be required. This leads to the requirement for the development of a high temperature gas-to-gas intermediate heat exchanger and its associated loop components.

For steam-hydrocarbon reforming, the need for a separate IHX loop (IHXL) is not so clearly defined. The process heat plant under development in the Federal Republic of Germany[10] incorporates a single-wall steam reformer tube, heated by primary reactor coolant, and located within the reactor building. The General Electric Company has proposed a double-wall steam reformer tube, with stagnant helium between the walls, as a superior way of achieving the goals of an IHX loop without its cost and complexity. In this study the comparative merits and disadvantages of each of these methods was compared.

To perform this study, two conceptual design plants were selected, one for the steam reforming of methane, and a second for the steam gasification of coal. The selection of a reference design plant for steam reforming was based on a systematic optimization process.* More than thirty-six different arrangements were investigated. A final selection was made between nine detailed designs. This final selected design is presented in Section 2. It should be noted that many design variables represent a choice made on the basis of prior work[1,2,10]. Table 1-2 shows some of the many design choices made, divided into three

*See Appendix G for these details

TABLE 1-2

STEAM REFORMER PLANT DESIGN CHOICES

INDEPENDENT DESIGN CHOICES	REFERENCE DESIGN SELECTION	COMMENTS
A) Primary Optimization Variables		
1) Duplex versus Single Wall Reformer Tubes	Duplex Tube	Based on Optimization on Economics, Safety, and Engineering Design Consideration. Described in Section 2 and Appendix G.
2) Advanced Catalyst	Conventional Catalyst	
3) Integrated versus Non-Integrated PCRV	Non-Integrated PCRV	
4) Power Split between Reformer and Steam Generator	35.6% Power to Reformers	
5) Use of Intermediate Heat Exchanger Loop	Not Used	
6) Type of Intermediate Heat Exchanger (when used)	"U" Tube	Based on Design Optimization Described in Section 3 and Appendix C
7) Details of IHX	Described in Section 3	
8) IHX Loop Pressure and Temperatures	Described in Section 3	
B) Secondary Optimization Variables		
1) Location of IHX	Within Secondary Containment	Based on Safety and Operational Considerations. Described in Appendix G.
2) Location of Steam Generator(s)	Within Secondary Containment with DSR	
3) Location of Steam Reformers	Within Secondary Containment	
4) Number of Modular Units for IHX, SG, SR	12	Modularity and Standardization
C) Selected (Fixed) Design Choices		
1) Type Service for Reformer Plant	Chemical Heat Pipe	Consistent Plant Basis
2) Power Level of Reactor	3000 MWth	Useful Base-Load Size.
3) Type of Reactors	Pebble Bed	Numerous Advantages Over Prismatic
4) Fuel Cycle and Options	Thorium-U235 → Hi-Conversion	Present Day Optimum with Growth
5) Reactor Exit Gas Temperature	950°C	Proven (AVR) Capability
6) Reactor Internal Design Details	Described in Section 2	Based on KFA/GE Prior Studies
7) Method of Auxiliary Cooling	Separate CACS (4)	Cost Effective
8) Reactor and Process Pressure Levels	∿ 40 bar	Based on Prior Optimization
9) Reactor Power Density	5 MW/m^3	Based on Prior Optimization
10) Type of Primary and Secondary Circulators	Electric Drive	Near Optimum with Low Complexity

classes according to the degree of emphasis placed on them during this study. Section 2 describes the selected optimum steam reforming plant, which utilizes the duplex tube steam reformer (DSR) to transfer the nuclear heat directly to the process stream while maintaining a double barrier between the reactor coolant and the process.

The plant for the steam gasification of coal, described in Section 3, makes use of a compact "U" tube heat exchanger in an intermediate loop to allow the coal gasifier to be located outside the reactor containment building.

At the conclusion of the study, the development needs of both systems were evaluated. Section 4 presents the recommended development needs in the areas of metallic materials for the IHXL and DSR, component test programs (IHXL and DSR), fuel element design and qualification, and preliminary design programs.

1.3 CONCLUSIONS

The following conclusions resulted from this study.

1) For steam gasification of coal, water splitting, and other high temperature processes where corrosive materials are handled (coal, ash, acids, etc.), an intermediate heat exchanger loop (IHXL) is required to keep the process heat exchangers (PHX) outside the secondary containment.

2) At the temperatures needed for these processes, a single oxide barrier is necessary and sufficient to reduce the tritium concentration in process gases to a safe level.

3) For the IHXL it is desirable to have the secondary helium doped with oxygen or steam to maintain an oxide film on the IHX as well as the PHX.

4) A double metal barrier is desirable between the primary coolant and the process stream to prevent fission product or process gas contamination following a crack or failure of one of the barriers. This can be accomplished either through the use of

an IHX loop or through the use of a duplex tube heat exchanger in the primary loop.

5) For steam-hydrocarbon reforming, a duplex tube (DSR) offers the advantages of a separate IHX loop but with significantly less cost and complexity. See Table 1-3.

6) The development of an advanced catalyst for steam-hydrocarbon reforming, which would permit more compact heat exchangers and eliminate periodic catalyst replacement, would allow a significant economic improvement to be realized.

7) When an IHX loop is used, it is desirable to remove the steam generator(s) from the primary loop.

8) Although potential alloys are available for consideration, screening tests have not yet identified alloys which have the demonstrated capability of withstanding the HTR primary environment at 950°C with acceptable corrosion resistance over the required design life.

9) The duplex tube design may allow the use of two different materials, one for the outer tube which would be stable with respect to carburization and/or oxidation in HTR primary coolant, and another for the inner tube which would be stable with respect to the reformer gases.

1.4 RECOMMENDATIONS

It is recommended that the following development activities be pursued for HTR process heat.

1) For the higher temperatures needed for coal gasification, TRISO fuel should be developed to take advantage of the lower metallic fission product release above 1000°C exit gas temperature.

2) For the IHXL, material developments in the areas of:

   - o High temperature oxide dispersed metals for tubes.
   - o Joining technology for dissimilar metals.

TABLE 1-3

DSR VERSUS IHX FOR STEAM HYDROCARBON REFORMING

DSR PROS	DSR CONS
• LESS COMPLEX OVERALL DESIGN, LOWER COST, INCREASED RELIABILITY VS. IHX LOOP.	• MAY REQUIRE INERT SECONDARY CONTAINMENT.
• IF NO METALLURGICAL BOND EXISTS BETWEEN TUBES, A CRACK IN ONE TUBE WILL NOT PROPAGATE THROUGH OTHER TUBE WALL.	• REGARDING "GUILLOTINE" BREAK ASSUMPTION OF BOTH TUBES 1) MUST PROVE THIS INCREDIBLE AND/OR 2) LIMIT CONTAMINATION OF PROCESS STREAM. (NOTE THAT CHEMICAL HEAT PIPE IS A CLOSED LOOP.)
• LOWER REACTOR AND METAL TEMPERATURES REQUIRED FOR A GIVEN PROCESS TEMPERATURE. (LESS HEAT EXCHANGER Δt LOSS)	
• PROVIDES SAME TRITIUM AND HYDROGEN DIFFUSION BARRIER AS IHX LOOP. (BOTH REQUIRE AN OXIDE FILM)	• LICENSEABILITY OF DSR MUST BE ESTABLISHED.
• LEAK DETECTION CAPABILITY AFTER FAILURE IN EITHER WALL.	• LEAK DETECTION METHODS MUST BE DESIGNED AND VERIFIED.

- o Wear coating for sliding joints in HTR primary helium.
- o Nuclear code qualifications in the 900°C and up range for selected alloys.

3) Programs leading to the development and qualifications of advanced catalysts should be pursued.

4) The DSR development should be pursued, especially to demonstrate its acceptability as an IHX from a safety and licenseability standpoint.

5) The reference "U" tube IHX described in this report should be the object of a program to design, build, and test one or more modules under simulated reactor conditions.

6) For coal gasification using the steam gasification process, and for advanced applications, such as water splitting, design work and development efforts should be started on a growth version of the IHX to permit process temperatures above 1000°C, see Figure 1-1.

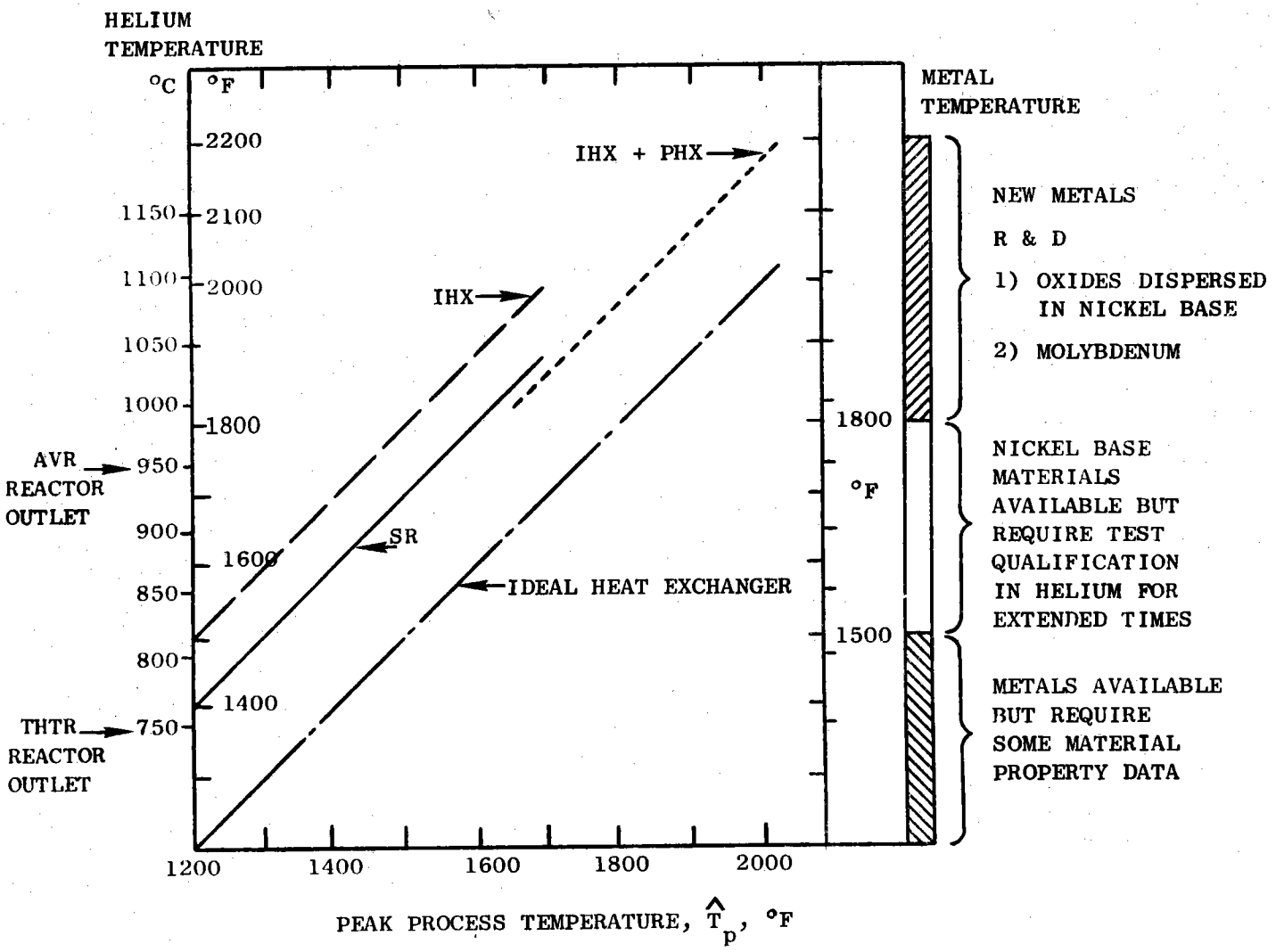

Figure 1-1. Reactor, Heat Exchanger, Process and Metal Temperature Relationships.

SECTION 2

STEAM REFORMER PLANT

This section of the report contains the description of the selected reference steam reformer plant. Also included are the results of the evaluation which led to this choice.

2.1 DUPLEX TUBE STEAM REFORMER REFERENCE PLANT

The reference plant consists of a 3000 MWt pebble bed reactor system coupled to a chemical heat pipe plant by means of twelve duplex tube steam reformer/steam generator modules. Of the 3000 MWt, 35.6% is transferred to the steam reformer process itself with the remainder being used to raise steam for other portions of the reformer process and for electrical power generation. Table 2-1 summarizes the reference plant description.

2.1.1 PROCESS CONDITIONS

The process conditions are set by the chemical heat pipe requirements. Appendix A describes the CHP in some detail. Figure 2-1 shows a schematic diagram of the CHP plant. Figure 2-2 shows the process conditions within the containment building. Table 2-2 summarizes the plant thermal conditions. The net output from this plant is 1080 MW (3690 MBTU/hr) of chemical energy to the ultimate customer, and 591 MW of electrical power available for sale.

2.1.2 REACTOR PLANT

The following drawings, Figures 2-3 through 2-6, show the layout for the reference reactor plant.

Figure 2-3 shows a plan view of the reactor containment building interior and identifies the PCRV, surrounded by the twelve non-integrated reformer-steam generator pods and the four core auxiliary cooling system

TABLE 2-1

GENERAL PLANT DESCRIPTION

CHARACTERISTIC	DESCRIPTION
Plant Output	Product Gas and Electricity
Nuclear Heat Source Power Rating	3000 MW_{th}
Fuel Element Configuration/ Refueling Cycle	Pebble Bed/OTTO (Once-Through-Then-Out)
Reactor Primary Containment Configuration	Prestressed Concrete Reactor Vessel (PCRV)
Reactor Primary Coolant/ Peak Bulk Temperature	Helium/950°C
Number of Primary Coolant Loops	12
Primary Coolant Loop Components	Circulator Steam Generator (SG) Steam-Methane Reformer (SMR)
SG-SMR Assembly Description	Combined Assembly with Circulator, Duplex Tubes in SG and SMR
SG-SMR Assembly Location	Pod Mounted External to PCRV (Non-Integrated)
Number of Core Auxiliary Cooling Loops	4
Containment Building Location/ Construction Material	Above ground/prestressed concrete
Containment Building Internal Atmosphere/Pressure	Nitrogen/Slightly negative

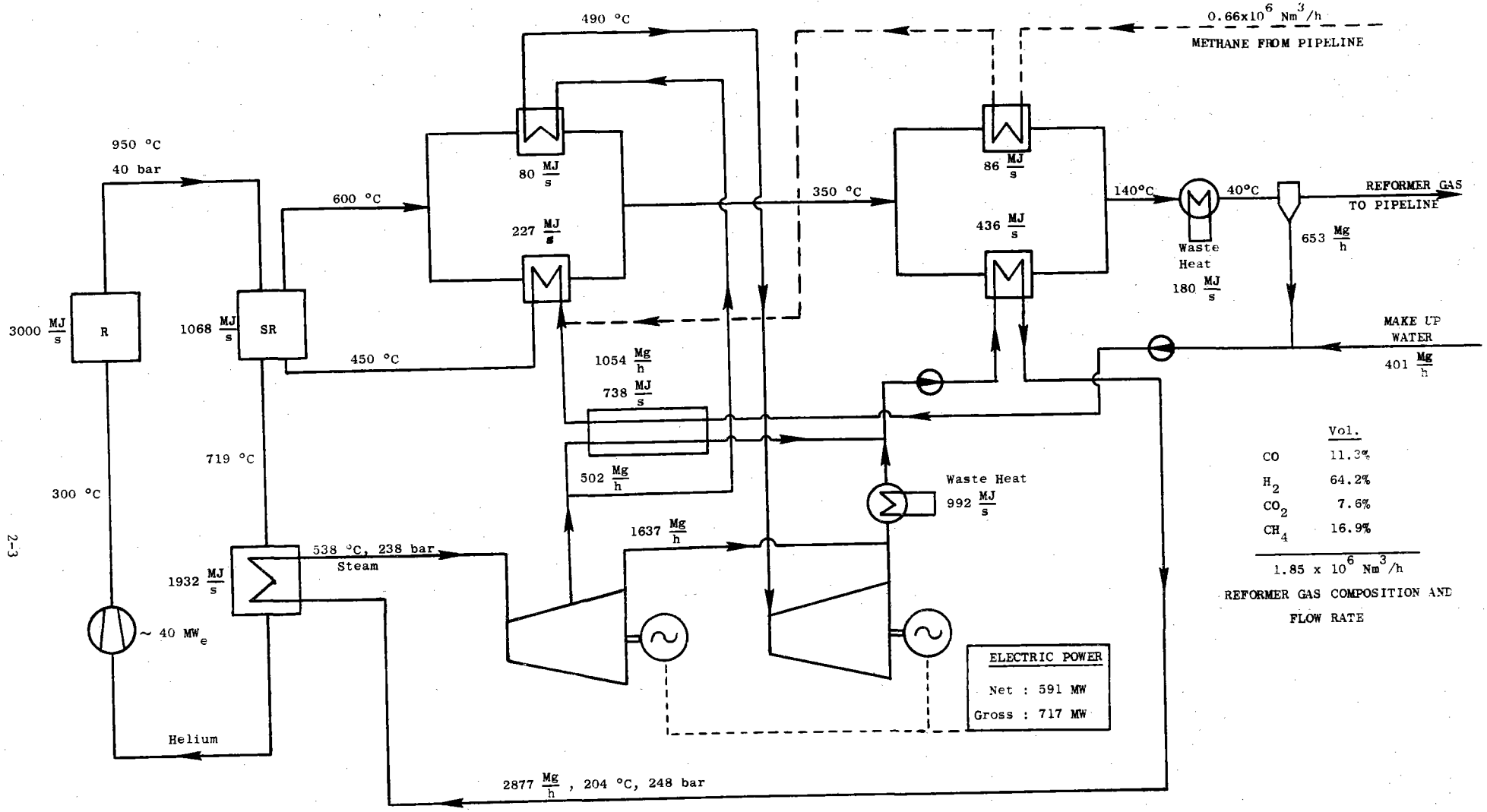

Figure 2-1. Nuclear Plant for Chemical Heat Pipe System

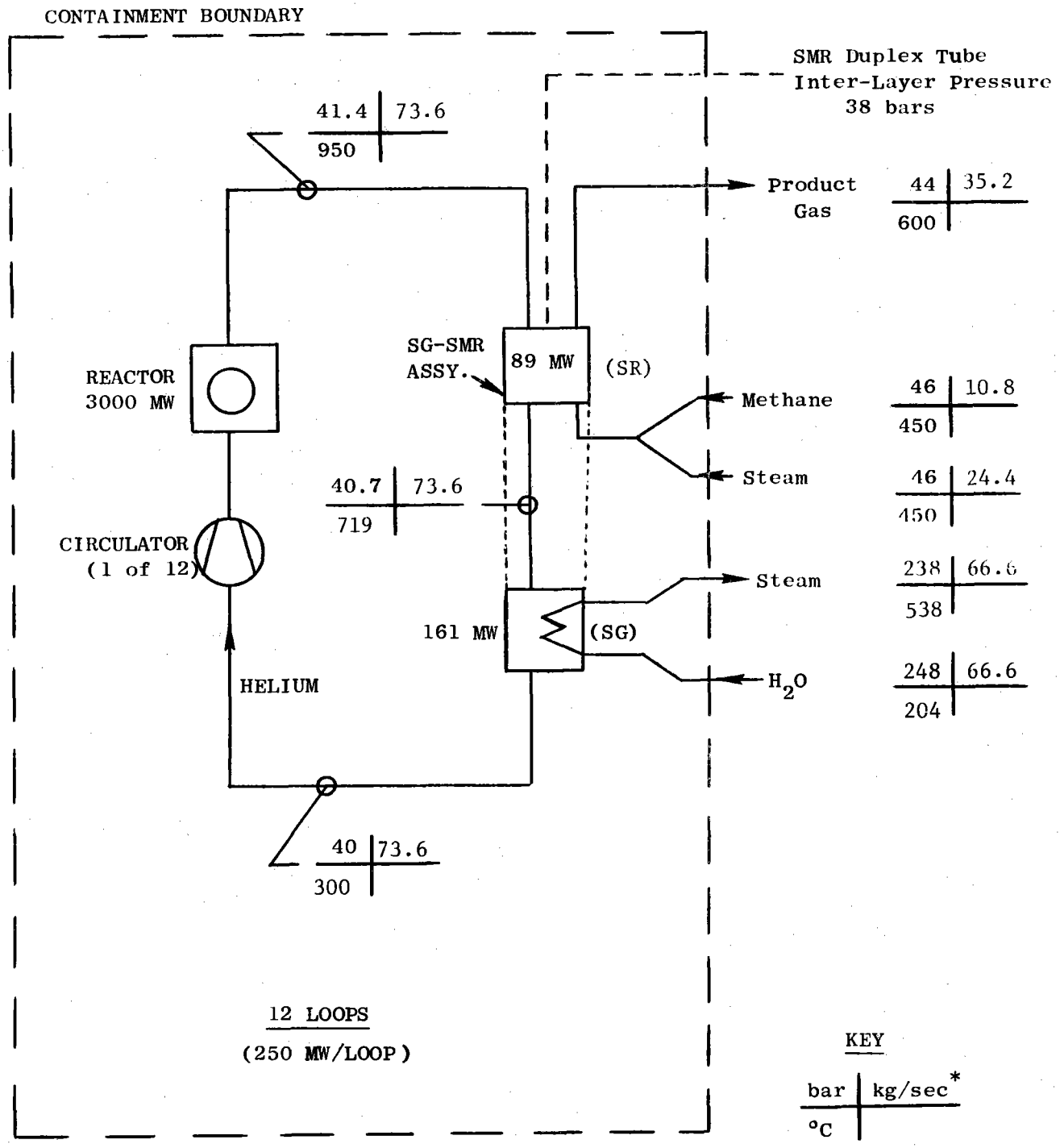

* All flows on a per loop basis.

Figure 2-2. Pressure, Temperature and Flow Rates Within the Containment Building

TABLE 2-2

PLANT THERMAL SUMMARY

	Metric	English
Thermal Reactor Power	3000 MW_t	
Steam Generation Summary		
Exit Temperature	538°C	1000°F
Exit Pressure	238 bar	3451 psi
Total Plant Output	799.2 Kg/sec	6.34×10^6 lb/hr
Feedwater Temperature	204°C	400°F
Feedwater Pressure	∿248 bar	∿3600 psi
Duty	1932 MW_t	-
Steam-Methane Reformer Summary		
Product Gas Exit Temperature	600°C	1112°F
Product Gas Exit Pressure	44 bar	638 psi
Maximum Reactant Temperature	825°C	1517°F
Product Constituents Flow Rate (Total Plant)		
H_2	29.5 Kg/sec	
CO	72.6 Kg/sec	
CO_2	76.8 Kg/sec	
CH_4	62.1 Kg/sec	
H_2O	181.5 Kg/sec	
	422.5 Kg/sec	3.35×10^6 lb/hr
Reactant Flow Rates (Total Plant)		
Steam	292.4 Kg/sec	
Methane	130.1 Kg/sec	
	422.5 Kg/sec	3.35×10^6 lb/hr
Steam & Methane Inlet Temperature	450°C	842°F
Steam & Methane Inlet Pressure	46 bar	667 psi
Helium Inlet/Outlet Temperature	950/719°C	1742/1326°F
Helium Flow Rate (Total Plant)	883.2 Kg/sec	7.01×10^6 lb/hr
Duty	1068 MWt	

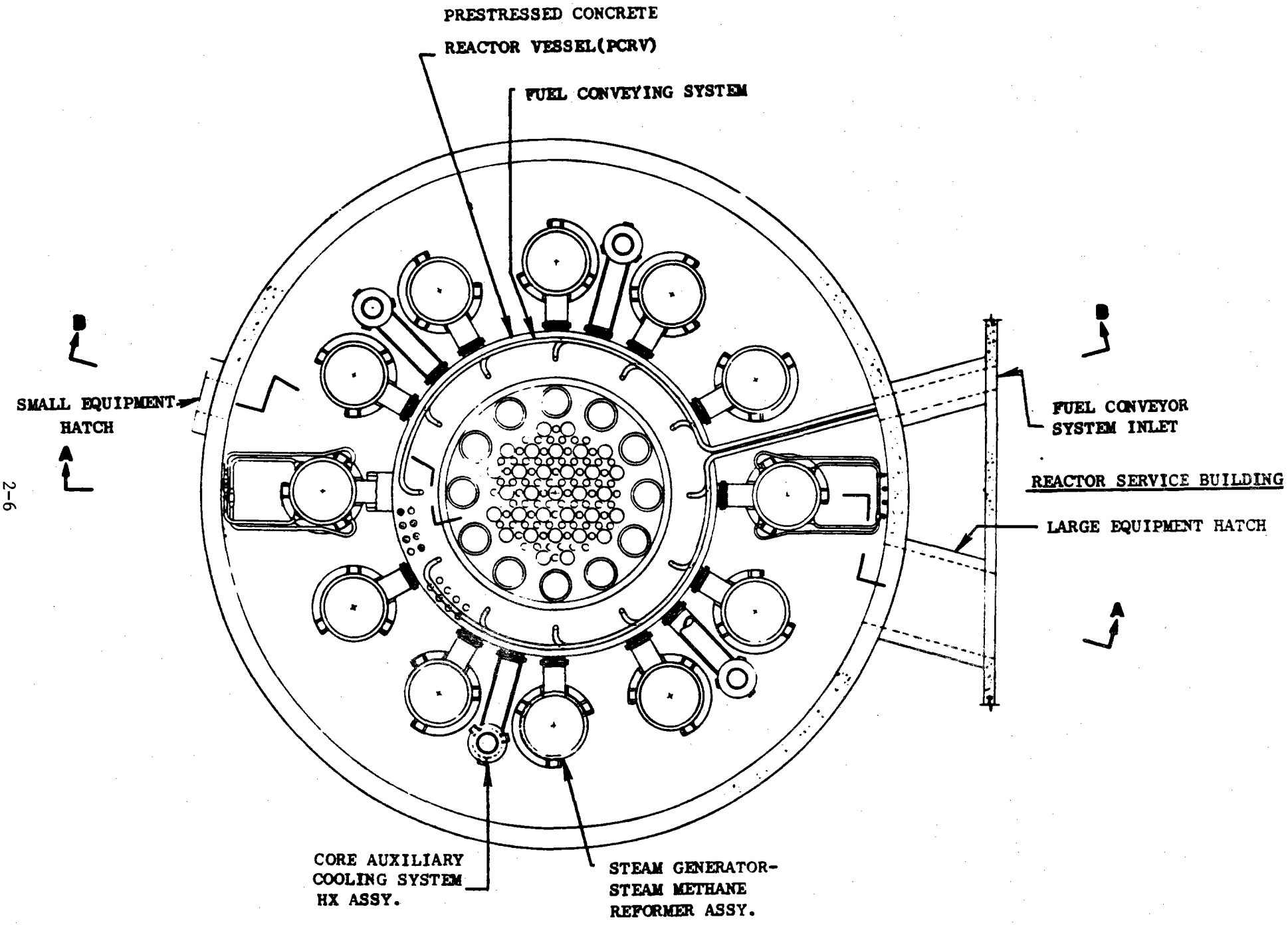

Figure 2-3. Plan View of Reactor Containment Building

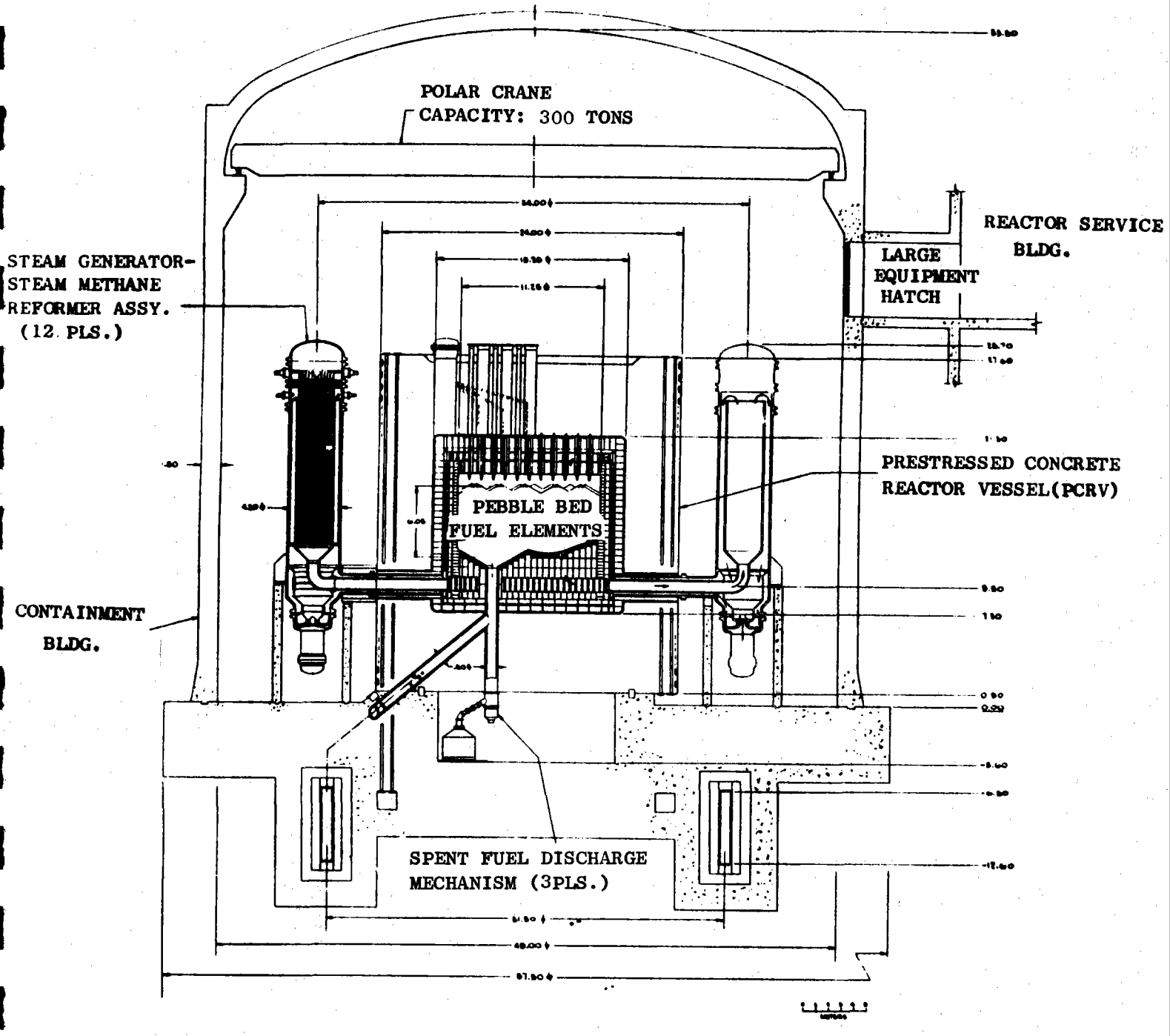

Figure 2-4. Details of Pebble Bed Reactor and the Reformer-Steam Generator Assembly.

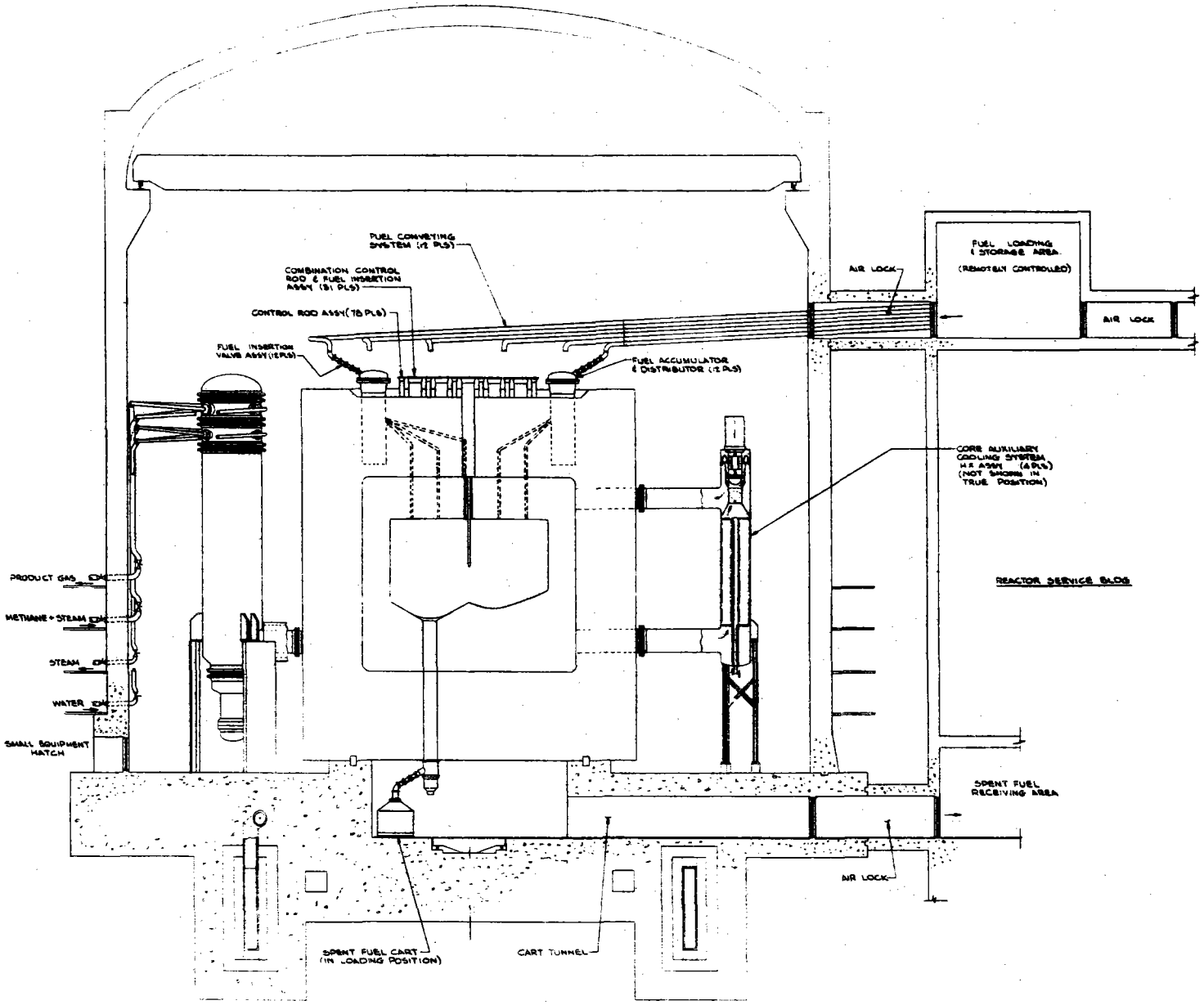

Figure 2-5. Reactor Containment Building Showing Refueling Concept.

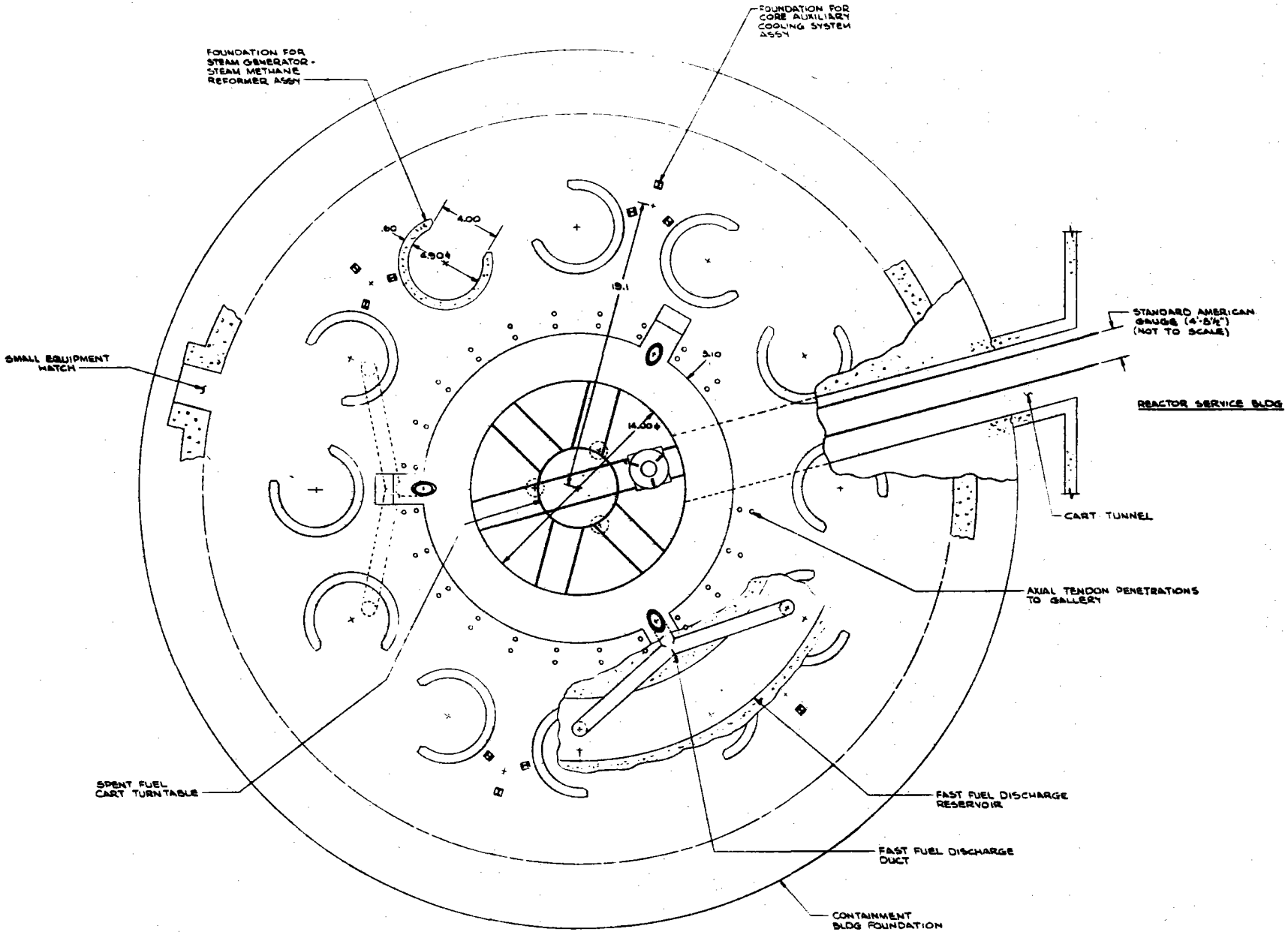

Figure 2-6. Plan View of the Foundation for the PCRV and Containment Building.

loops. Figures 2-3 and 2-5 show the design of the reformer-generator plumbing, wherein the connections to each reformer-steam generator independently penetrate the containment building walls and are manifolded external to the containment building for connection to the CHP system.

Figure 2-4 (Section A-A of Figure 2-3) shows pertinent details of the pebble bed reactor and the reformer-steam generator assembly. The helium flow path of the reactor primary coolant is indicated.

Figure 2-5 (Section B-B of Figure 2-3) shows the OTTO refueling concept wherein pebble fuel elements are batch loaded in the reactor service building and injected into the appropriate portion of the reactor interior via fuel conveyer and distribution mechanisms. The fuel element removal concept and the CACS are indicated.

Figure 2-6 shows a plan view of the foundation for the PCRV and containment building. The fuel cart turntable and track concept is indicated. The fast discharge system ducting arrangement and fuel reservoir are indicated.

Referring to Figure 2-4, the reactor consists of a cylindrical prestressed pressure vessel containing a graphite reflector assembly. The core consists of a fixed bed of spherical graphite balls 6 cm in diameter containing the fuel. Fuel balls are added essentially continuously at the top and removed at the bottom, after a residence time of approximately two years. The coolant flow is downwards through the fuel bed, a key element of the OTTO cycle.

In this scheme, the fissile material content of the fuel balls decreases from the top to the bottom of the core. The heat flux and power distribution tend to have the same distribution so that the highest power density occurs at the top of the core where the coolant enters at its lowest temperature. At the bottom of the core, the power density is low, where the coolant has its highest temperature. Thus, the coolant is rapidly heated in the upper portion of the core by relatively fresh fuel and with a large temperature difference while in the lower portions the temperature difference is relatively low. Thus, the difference between the maximum fuel temperature and the exit gas temperature is

very small. Figure 2-7 shows the temperature axial profiles in a typical OTTO cycle reactor.

The pressure vessel is a nonintegrated design, with the loop components in separate pods attached to the PCRV by means of coaxial ducts. This design appears preferable from the standpoint of cost since more factory fabrication can be used, and the cost of the field-erected PCRV is much less than that of the alternate integrated design. However, the choice between a multicavity integrated design and the nonintegrated design shown is not crucial to the success of the HTR. Either design meets the basic requirements. The final choice was made on the basis of cost, practicability, reliability, and safety considerations.

The PBR is designed for remote fuel handling in anticipation of the use of reprocessed U-233/thorium fuel with its attendant radioactivity. This represents an advance over the presently operating AVR and the presently under-construction THTR. Both of the above plants use fresh fuel balls which can be handled manually (initially).

As shown in Figures 2-3, and 2-5 four core auxiliary cooling units, each capable of providing 50 percent of the required afterheat removal, are provided. In conjunction with the triply redundant liner cooling-water circuits, these systems can handle the shutdowns and emergency heat removal requirements.

Each steam reformer/steam generator assembly module (SRA/SGA) is connected to the PCRV with a coaxial duct which contains both the hot discharge helium and the cool reactor inlet helium. A motor-driven circulator is located in each module. Variable inlet guide vanes on the circulator allow flow variations down to about 20 percent of full flow and, additionally, provide for flow shutoff to enable the reactor to operate on less than the full number of modules.

Additional details of the reactor system are described in Appendix F.

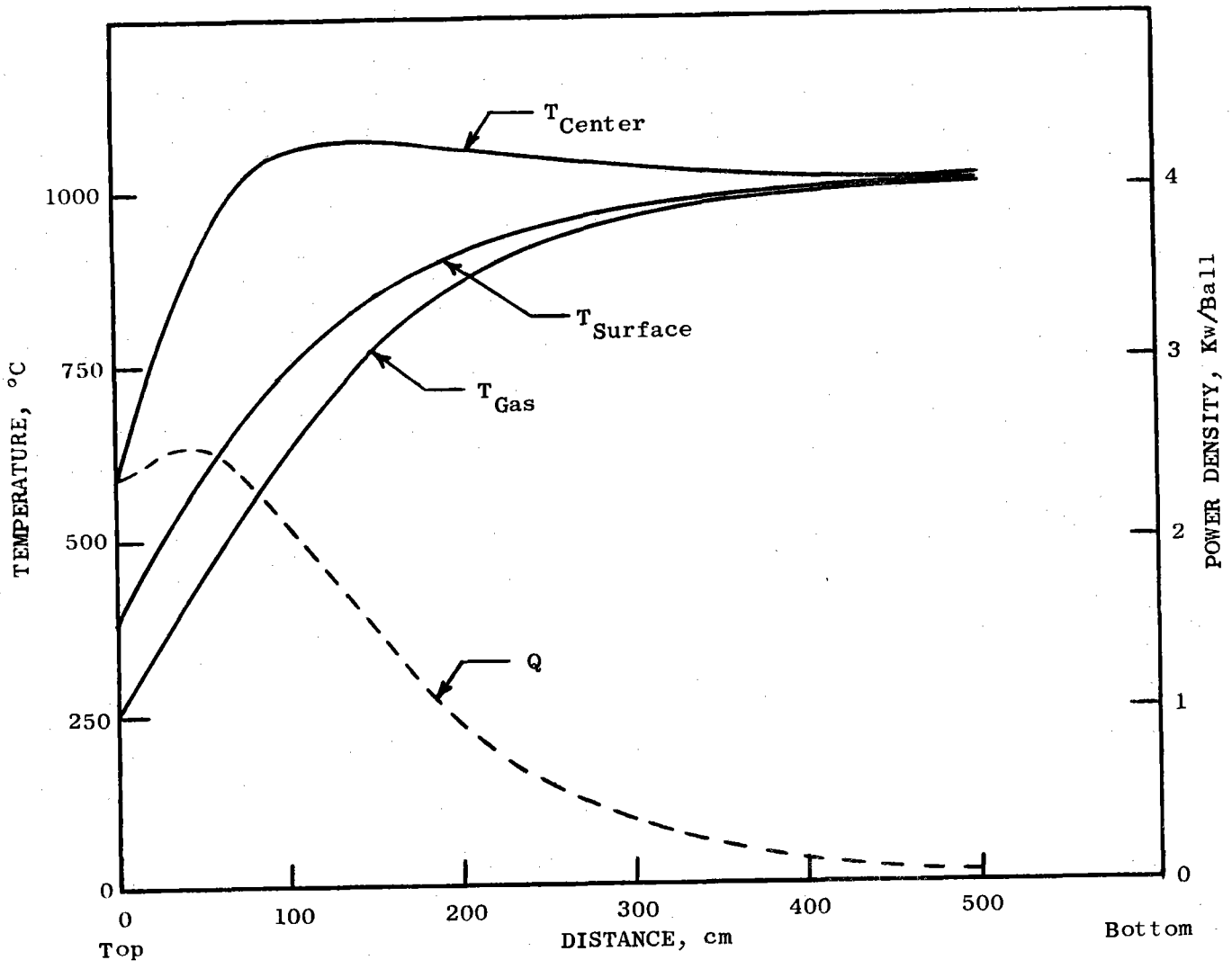

Figure 2-7. Typical Axial Distribution of Power Density and Temperature.

2.1.3 STEAM REFORMER/STEAM GENERATOR

The key component in the steam reforming plant is the steam reformer/steam generator assembly (SRA/SGA). The chosen design makes use of a duplex tube steam reformer (DSR) tube to provide separation between the reactor coolant and the process gas. Twelve of these units are used with a 3000 MWt PBR.

2.1.3.1 Mechanical Design

The steam reformer-steam generator heat exchanger is illustrated in Figure 2-8. Helium from the reactor outlet enters through the inner coaxial duct and flows upward through the space between the reformer tubes which occupy the central portion of the heat exchanger core. At the top of the core the reactor coolant stream is directed into the outer annulus through which it flows downward over the concentric helical tubes of the once through steam generator. The cooled helium is then directed to the inlet of the centrifugal circulator. The circulator is provided with variable diffuser vanes for flow control. From the circulator diffuser the helium stream passes into the outer coaxial duct for return to the reactor.

The design of the duplex tube steam reformer units is discussed in Section 2.1.3.2 and in Appendix E. The reformers are supported from the tube sheet. Two tubes are connected to the top of each steam reformer, one bringing in the steam-methane mixture which flows over the catalyst filling the inner duplex tube, and the other delivering the product gas from the "pigtail" tube which acts as a recuperative heat exchanger between the product gas and the reactant gas in the catalyst space. The reactant gas and product gas tubes from all of the reformers are manifolded at nozzle tube sheets (two for each gas stream) which are accessible from outside the pressure vessel. At these tube sheets leaking tubes can be detected and sealed off. Employment of established steam reformer catalyst technology requires replacement of the catalyst at an interval ranging from two to eight years. Detailed design effort is required to define a tube closure design above the tube sheet which will facilitate catalyst replacement.

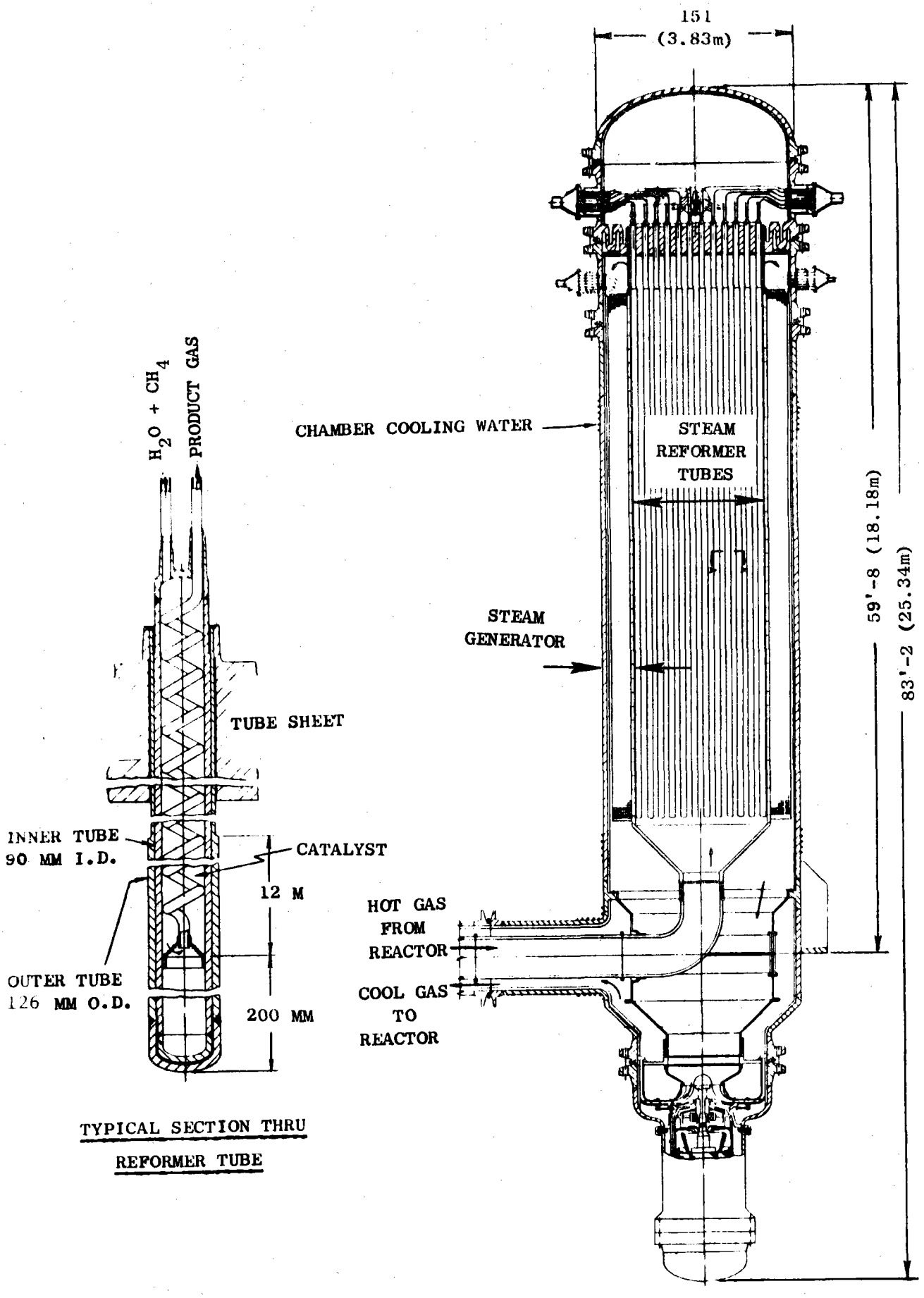

Figure 2-8. Reference Design for the Duplex Tube Steam Reformer/Steam Generator Assembly.

It is necessary to block a portion of the helium flow area between the reformer tubes by use of the alternate means shown in Figure 2-9, in order to realize the design level of helium film convection coefficient (1700 watts/m^2°C). Thermal stress caused by a radial temperature gradient between the tube sheet and the water cooled pressure vessel shell is relieved by the incorporation of a folded thermal sleeve. In order to minimize the temperature gradient across the tube sheet, an insulation blanket, of either fibrous material or metallic foil, is placed against the lower surface of the tube sheet.

The steam generator unit is an assembly of concentric multiple helical tubes which are supported by suspension from supports anchored to the section of pressure vessel shell between the second and third pair of flanges (counting from the top) shown on Figure 2-8. Feedwater and steam tubes are manifolded at four locations in this portion of the shell. The design thus provides for independent assembly of the steam reformer and steam generator sections of the integrated heat exchanger. The integrated heat exchanger is proposed as a space and cost saving alternative to a design involving separate pressure vessels for the reformer and steam generator.

Design data for the reference assembly is presented in Table 2-3. The design is based on 250 MW thermal input from the helium flow of which 35.6%, or 89 MW, are utilized in the steam reformer and the balance, or 161 MW, are utilized in the steam generator.

The steam reformer tube sheet thickness was calculated from the curve shown in Figure 2-10, taken from reference 3. The assumed value of working stress is 24,000 psi. This stress level will be realized only under an abnormal (accident) condition in which 600 psi differential pressure is imposed on the tube sheet. The normal pressure level induced stress is negligible, since the normal differential pressure is very low. Actually the normal differential pressure load is opposed by the weight of the reformer tubes and the tube sheet.

The folded thermal sleeve shown between the tube sheet and the water cooled pressure vessel shell was sized using the curve of Figure 2-11 also taken from reference 3.

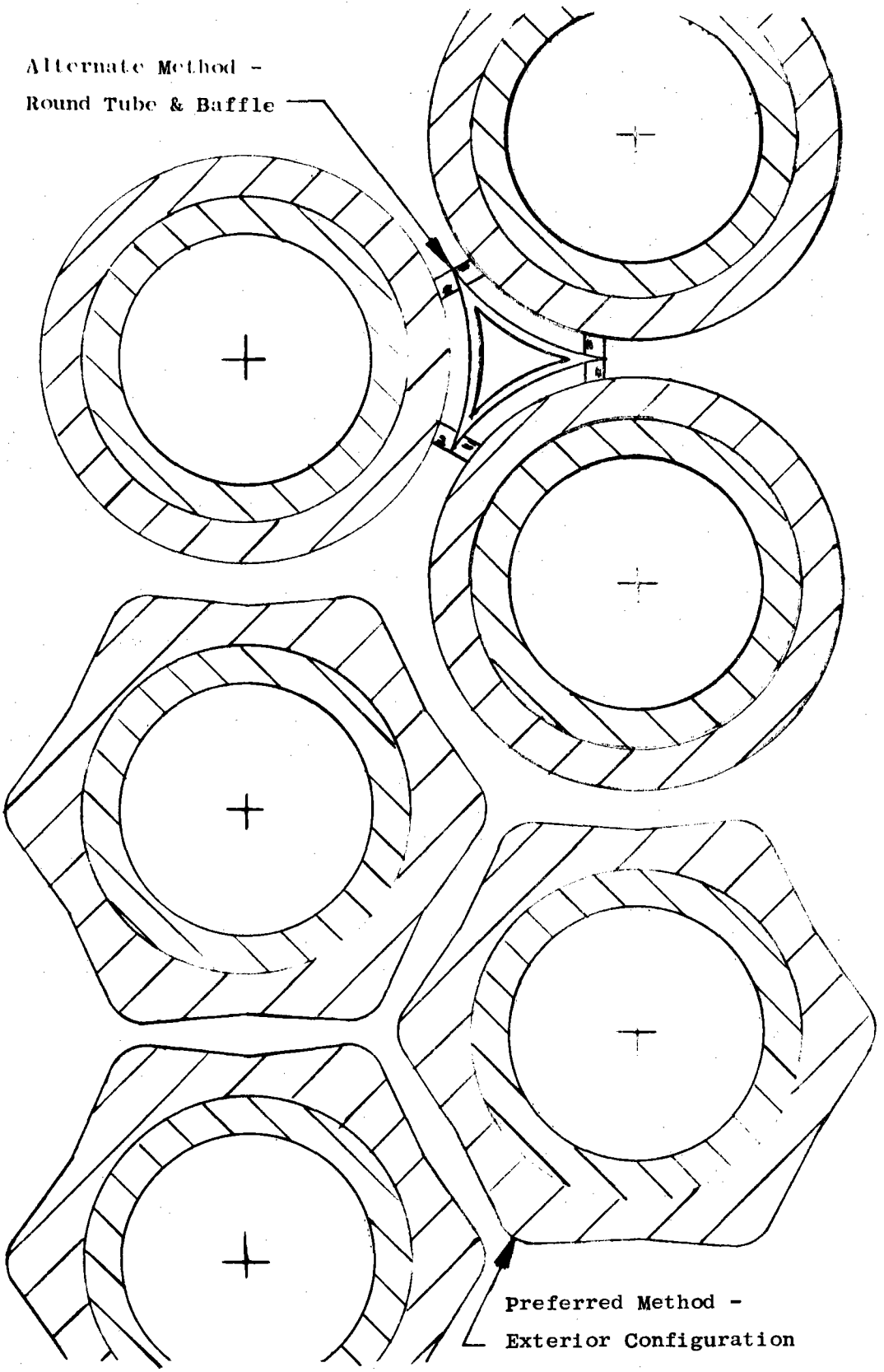

Figure 2-9. Section Through Reformer Tube Bundle Showing Intertube Flow Blockage.

TABLE 2-3

STEAM REFORMER/STEAM GENERATOR ASSEMBLY DESIGN

CHARACTERISTIC	VALUE
STEAM REFORMER	
SR Helium Inlet Temperature	950°C
Reforming Temperature	825°C
SR Helium Outlet Temperature	718.6°C
Reactant Inlet Temperature	450°C
Product Outlet Temperature	600°C
SR Log Mean ΔT	187.7°C
Helium Flow Rate	73.6 Kg/Sec
SR Thermal Conductances (Referred to SR Tube OD)	
Helium Film	1700 $w/m^2°C$
Outer Tube Wall	2672 $w/m^2°C$
Inner Tube Wall	2259 $w/m^2°C$
Product Film	826 $w/m^2°C$
Gap	12000 $w/m^2°C$
SR Overall	370 $w/m^2°C$
SR Power	89 MW
SR Surface Area (Outer Tube O.D.)	1283 sq m
No. of Tubes	270
Outer Tube O.D.	126 mm
Outer Tube I.D.	108 mm
Inner Tube I.D.	90 mm
Tube Spacing Ratio (SR Proper)	1.11
(Tube Sheet)	1.25
SR Tube Bundle O.D.	2.39 m
Tube Sheet Thickness	42.2 cm
SR Pressure Drop	.47 b
Pressure Vessel O.D.	3.83 m
STEAM GENERATOR	
SG Power	161 MW
SG Helium Inlet Temperature	718.6°C
Steam Outlet Temperature	538°C
Steam Pressure	238 b
SG Helium Outlet Temperature	300°C
Feed Water Temperature	204°C
Steam Flow Rate	66.6 Kg/Sec
SG Log Mean ΔT	106°C
SG Thermal Conductances (Referred to SG Tube O.D.)	
Helium Film	1700 $w/m^2°C$
Tube Wall	7500 $w/m^2°C$
Steam/Water Film	12000 $w/m^2°C$
SG Overall	1242 $w/m^2°C$
Tube O.D.	2.54 cm
Tube I.D.	1.90 cm
No. of Tubes in Parallel	56
Tube Distribution	7 Tubes Across 8 Threads in Parallel
Total Tube Surface Area (Tube O.D.)	1221 sq m
SG Pressure Drop	.27 b
SG Tube Bundle I.D./O.D./Length (m)	2.56/3.38/10.6
Overall SR/SG Assembly Weight	373,000 kg
Power per Steam Reformer Tube	.329 mw/Tube

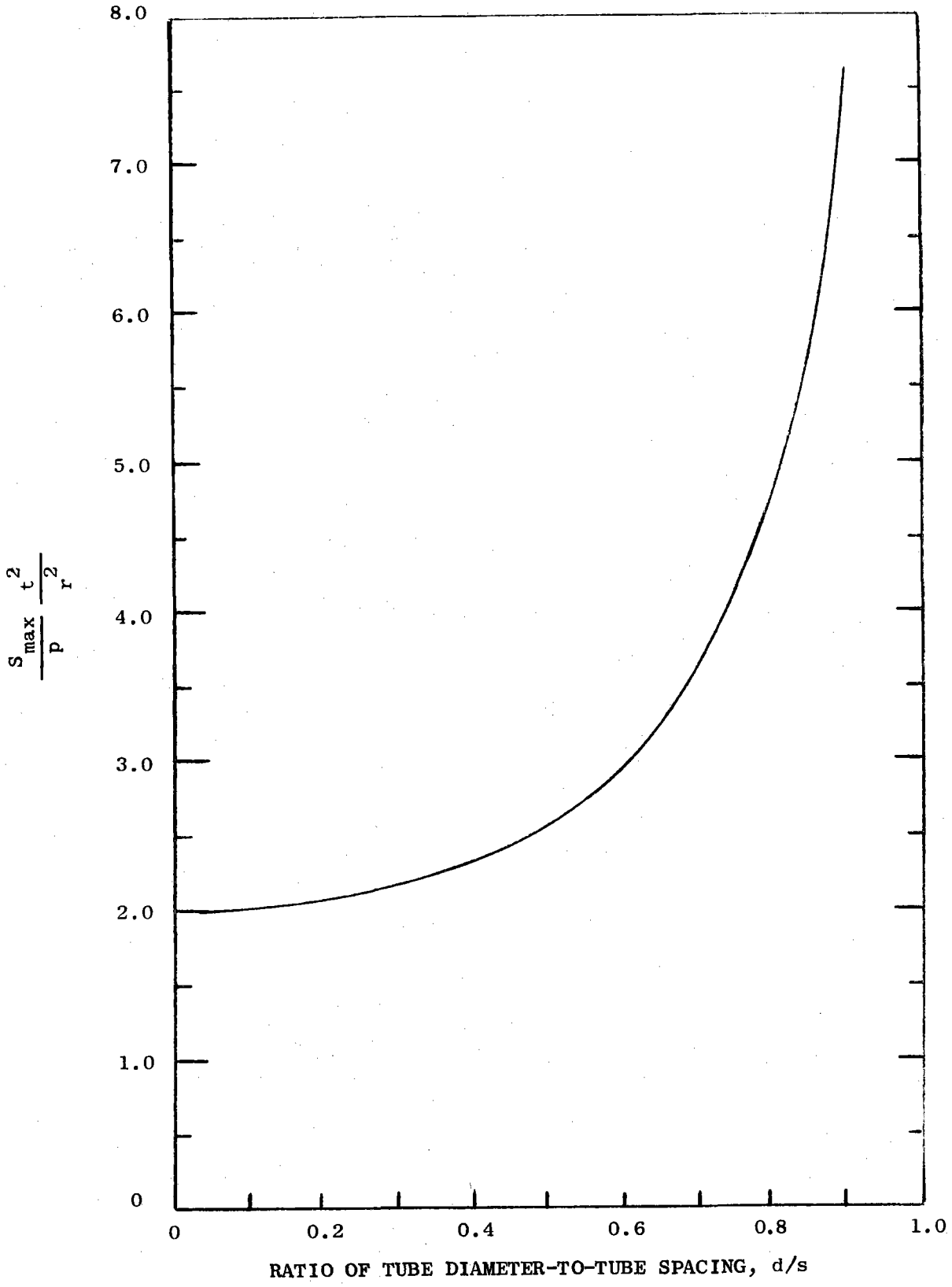

Figure 2-10. Effects of the Ratio of Tube Diameter-to-Tube Spacing on the Maximum Stress in Tube Header Sheets in Which the Tubes are on an Equilateral Triangular Pitch.

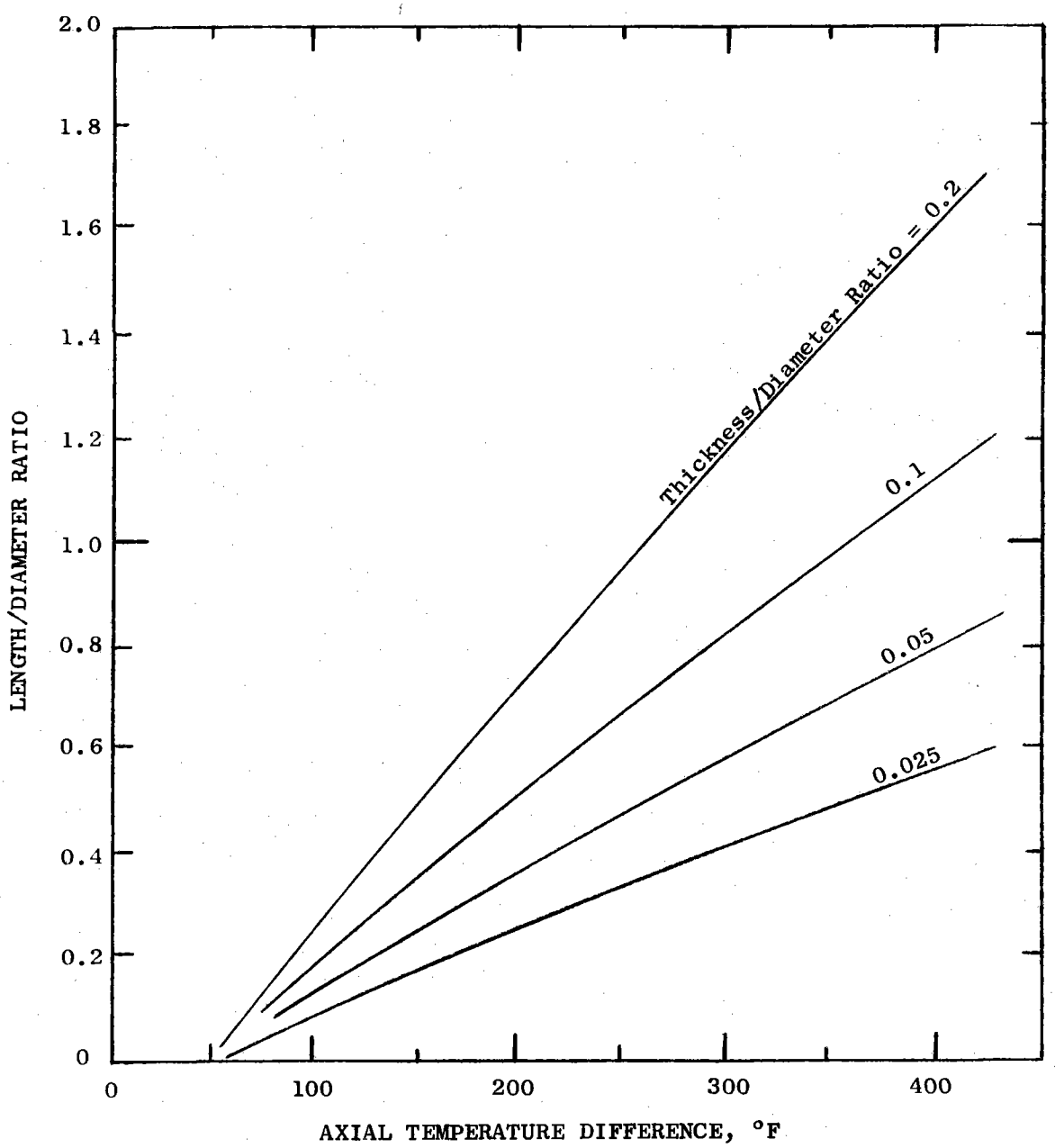

Figure 2-11. Thermal Sleeve Length/Diameter Ratio for Plain Carbon Steel to Give an Allowable Shear Stress of 10,000 psi. (The assumed axial temperature distribution is exponential)

Alloy selection for the reformer tubes was based on considerations of:

- Strength
- Thermal Stability
- Environmental Capability
  - HTR Helium Gas
  - Process Gas
- Ductility
- Fabricability
- Cost
- Availability

A number of commercially available alloys and several developmental alloys which are considered to be suitable candiates for use in duplex reformer tubes are listed below:

- Inconel Alloys 601, 617 and 625
- Incoloy Alloys 800H, 802 and 807
- Hastelloy Alloys C, S and X
- Development Alloys HAST X-280 and Inconel 617 w/o Co.

Alloys containing elements such as cobalt and tantalum may have to be eliminated on the basis of potential problems from radioactive contamination. The Japanese have reported that cobalt whiskers can form on a surface and then be carried away by the helium stream. If these whiskers enter the coolant stream, they will become radioactive on passing through the reactor core and may seriously restrict access to normally low-activity areas of the reactor. Further tests are required to verify the Japanese results. If the cobalt and tantalum containing materials are eliminated, then the remaining candidates are:

- Inconel Alloy 601
- Incoloy Alloys 800H and 802
- Hastelloy Alloy S
- Development Alloys HAST X-280, Inconel 617 w/o Co.

Reference 4 provides the design of a duplex reformer tube to be tested in the EVA test facility at Jülich, FRG. The material selected for that test section was Incoloy alloy 800H. That selection will have to be confirmed by appropriate materials tests before finalizing the design of a reformer assembly. The advantages of Incoloy 800H may be summarized as follows:

- Creep strength comparatively high
- Free from cobalt and tantalum
- Good thermal stability
- Hydrogen permeability comparatively low
- Should oxidize in steam (iron-base alloy)
- Readily available
- Good fabricability
- Lowest cost of candidates
- Same alloy as planned for EVA.

2.1.3.2 Thermal-Hydraulic Design

Heat is transferred from the helium to the process gas through five thermal resistances consisting of the helium film, the outer tube wall, the gap between tubes, the inner tube wall, and the process gas film. Gas-side velocities (which in turn determine the heat transfer coefficients) are determined by allowable pressure drops.

Helium Side - Heat transfer from the helium to the reformer tube occurs by the mechanism of forced convection. For an unbaffled tube bundle in which the helium flows parallel to the tubes, the heat transfer coefficient was calculated from:

$$(1)\quad \frac{h}{C_p G}\left(\frac{C_p \mu}{K}\right)^{2/3} = \frac{0.023}{\left(\frac{D_e V}{\nu}\right)^{0.2}}$$

The helium pressure drop was calculated as the sum of an inlet loss, the friction loss, and an outlet loss:

$$(2) \quad \Delta P = \left[K_i + f \frac{\ell}{D_e} + K_o\right] \frac{\rho V^2}{2}$$

Shown in Figure 2-12 is a plot of the helium side heat transfer coefficient and pressure drop as a function of helium velocity in the tube bundle. The physical properties of helium for this figure were evaluated at a temperature of 825°C (average of helium inlet and helium outlet temperatures) and an average pressure of 41.2 bars. A design point velocity was selected from considerations of helium pumping power as follows.

Fraas[3] discusses the tradeoff between heat exchanger operating costs and capital charges. It has been found that if the pumping power chargeable to the heat exchanger is in the range of 0.5 and 1.0% of the heat transferred, the overall cost will be close to the minimum obtainable. For a helium ΔT of 250°C (950-700), a pressure of 40 bars, and a helium temperature of 250°C at the circulator, the above criterion establishes the helium pressure drop across the reformer as 0.24 to 0.48 bar for 0.5% and 1.0% of the heat transferred, respectively. The corresponding helium velocities are 30.7 m/s and 43.5 m/s. A design point helium velocity of 30 m/ was selected, which is consistent with HTR reactor studies now underway. The corresponding heat transfer coefficient and pressure drop are 1224 $w/m^{2\circ}C$ (216 Btu/hr $ft^{2\circ}F$) and 0.23 bar (3.3 psi), respectively.

Process Side - On the process side the heat is transferred from the tube wall to the process gas which is flowing through a packed bed of catalyst pellets. The chemical performance of the reformer was calculated using a reformer computer code developed at the Los Alamos Scientific Laboratory[5]. In that code, the process-side heat transfer coefficient is calculated using the following correlation:

$$(3) \quad h = \frac{K_g}{D_p} \left[2.58 \left(\frac{D_p V}{\nu}\right)^{1/3} N_{Pr}^{1/3} + 0.094 \left(\frac{D_p V}{\nu}\right)^{0.8} N_{Pr}^{0.4}\right]$$

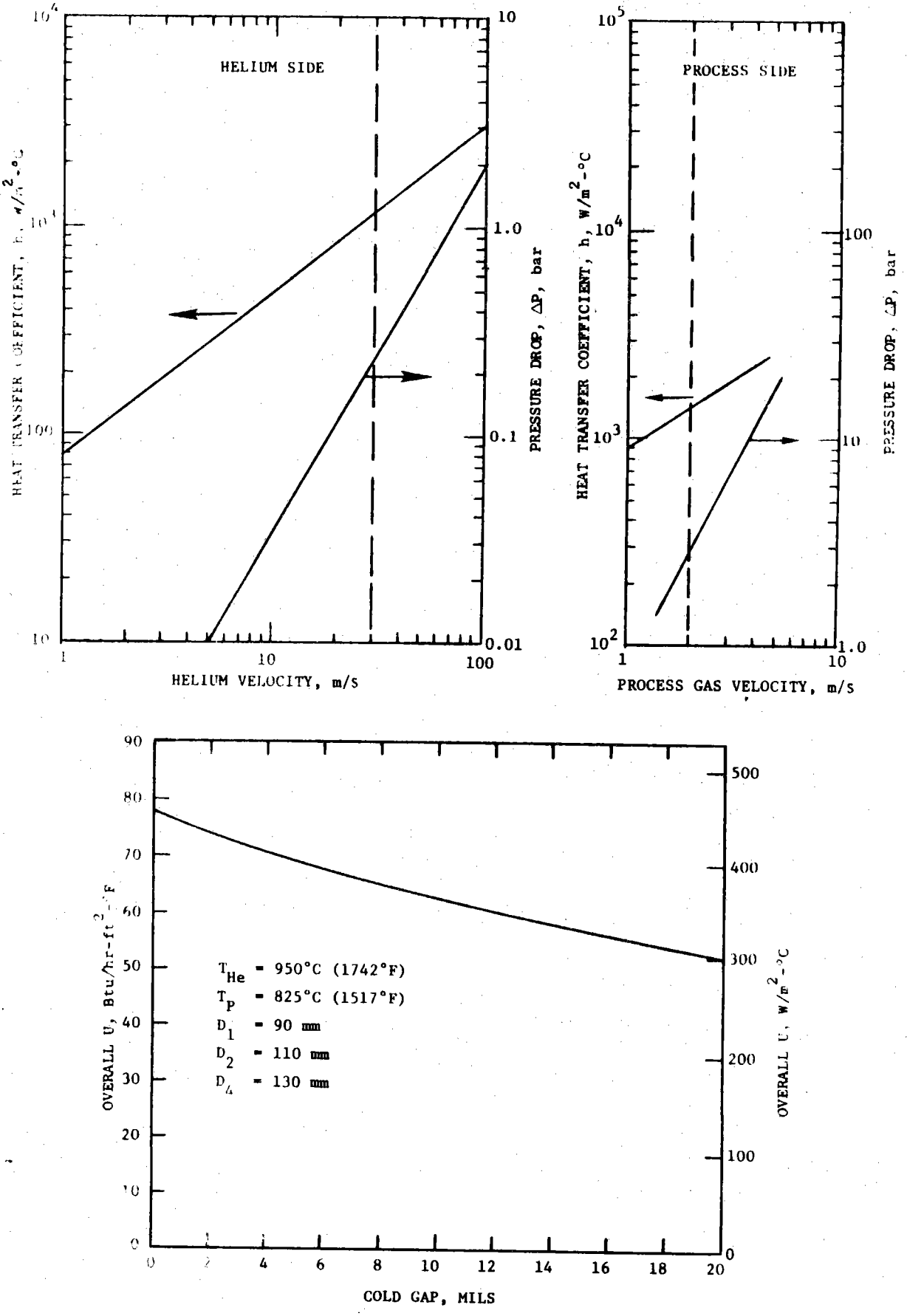

Figure 2-12. Heat Transfer and Pressure Drop Considerations in the Duplex Tube Reformer

The process-side pressure drop through packed beds is calculated from the Ergun equation:

$$(4)\quad \frac{dP}{dZ} = -\left[\frac{150(1-\varepsilon)}{(N_R)_P} + 1.75\right] \frac{1}{D_P} \left(\frac{1-\varepsilon}{\varepsilon^3}\right) \frac{G_o^2}{\rho}$$

For particle Reynolds numbers, $(N_R)_P$ greater than about 1000 (which is typical in steam methane reformers), the first term may be neglected and the Ergun equation reduces to the Burke-Plummer equation:

$$(5)\quad \frac{dP}{dZ} = -\left(\frac{1.75}{D_P}\right) \left(\frac{1-\varepsilon}{\varepsilon^3}\right) \frac{G_o^2}{\rho}$$

Figure 2-12 shows the process side heat transfer coefficient and pressure drop as a function of superficial velocity of the gas. Superficial velocities between 2 and 3 m/s are typical for conventional reformers. A value of 2 m/s was chosen for the design point of the duplex tube reformer.

The Overall Heat Transfer Coefficient - The overall thermal resistance between the primary helium and the process gas is the sum of the resistances due to the helium gas film, the duplex tube, and the process gas film. The calculations presented here are for the case of a duplex tube having a gap between the OD of the inner tube and the ID of the outer tube. The helium-filled gap was assumed to be uniform around the circumference with no metal-to-metal contact. It was also assumed that the mechanism of heat transfer across the gas-filled gap is conduction; radiation and convection effects were neglected. The overall heat transfer coefficient is given by:

$$(6)\quad \frac{1}{U_1} = \frac{1}{h_1} + \frac{D_1\, \ell n(D_2/D_1)}{2\, K_{12}} + \frac{D_1\, \ell n(D_3/D_2)}{2\, K_{gap}} + \frac{D_1\, \ell n(D_4/D_3)}{2\, K_{34}} + \frac{1}{\left(\frac{D_4}{D_1}\right) h_4}$$

Using typical values of the helium and process-side heat transfer coefficients (h_1 and h_4), calculations were performed to determine the effect of gap dimension on the overall heat transfer coefficient which determines the reformer size. Figure 2-12 shows the results of these calculations for an overall helium-to-process ΔT typical of the hot end of the tube. This shows that the effect of gap dimension on overall U is not severe because the controlling thermal resistances are the helium and process side gas films. This is in contrast to a sodium-heated boiler such as the LMFBR evaporator. In that case, the water-side and the sodium-side coefficients are large and the wall resistance is controlling so that small variations in wall resistance severely affect the overall coefficient. Figure 2-13 shows the effect of the gap on the overall U normalized to the zero-gap case, U_o. For a given heat transfer rate and overall ΔT, the heat transfer areas and overall U's are related by:

$$(7) \quad \frac{A}{A_o} = \frac{U_o}{U}$$

Consequently, Figure 2-13 can be interpreted as the penalty in heat exchanger size due to the gap. The upper curve is for the overall ΔT near the cold end and the lower curve is for the hot end. For a gap of 3 mils, the required area is less than 10% more than that required for the zero gap case. A fabrication goal is to achieve a gap dimension of from 0 to 3 mils.

Figure 2-14 illustrates the radial temperature distribution through the duplex wall and the relative importance of the five resistances in series. A total of 67% of the overall ΔT is taken in the two gas films which are controlling. As can be seen, the ΔT across the gap is only 5% of the total.

2.1.3.3 Performance

The reformer performance calculations were made with the aid of a computer code developed especially for helium-heated reformers by personnel at the Los Alamos Scientific Laboratory[5]. The LASL program assumes a counterflow shell-and-tube configuration with hot helium on the shell side. The following options are available:

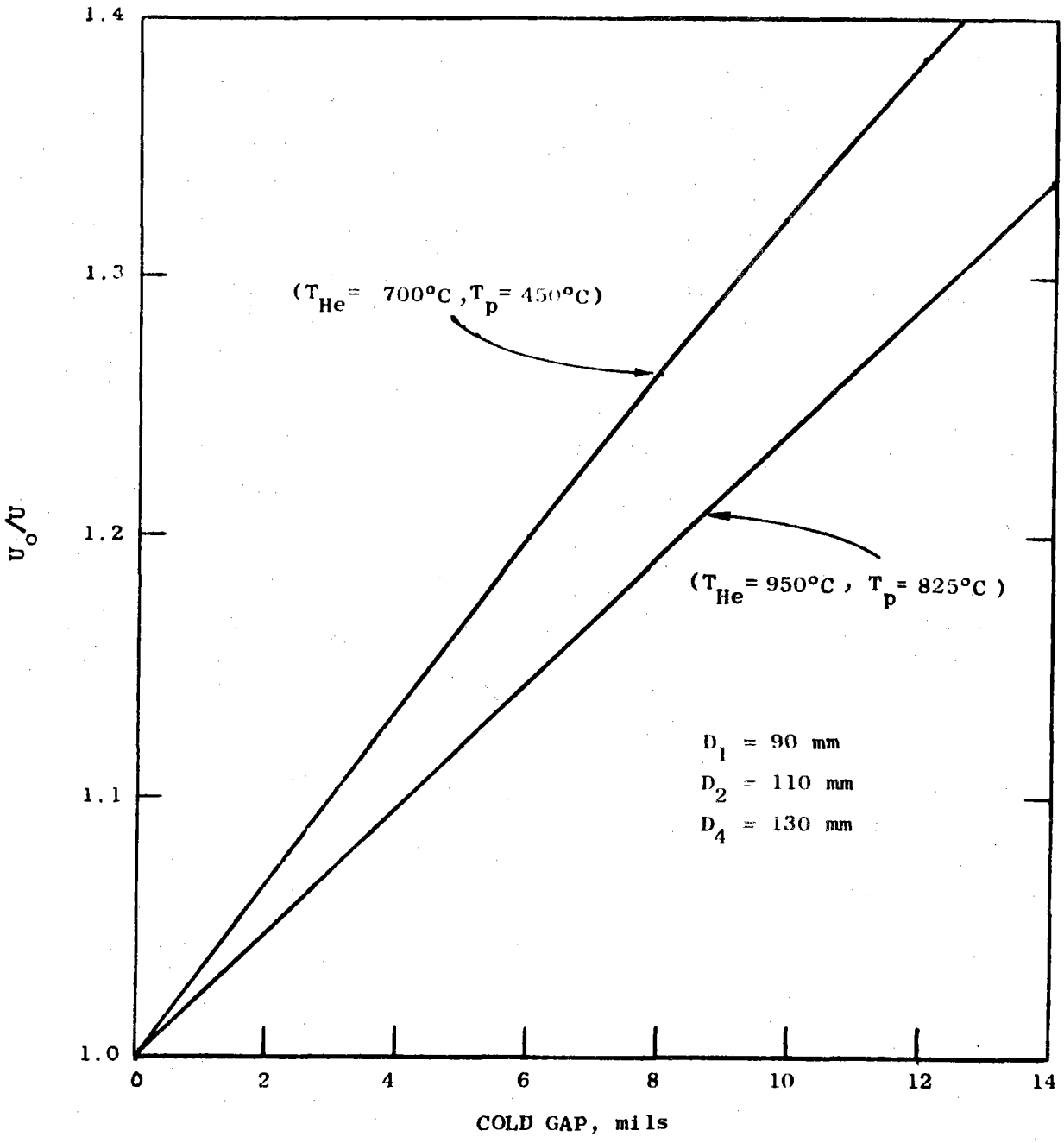

Figure 2-13. Effect of Gap on Tube Area

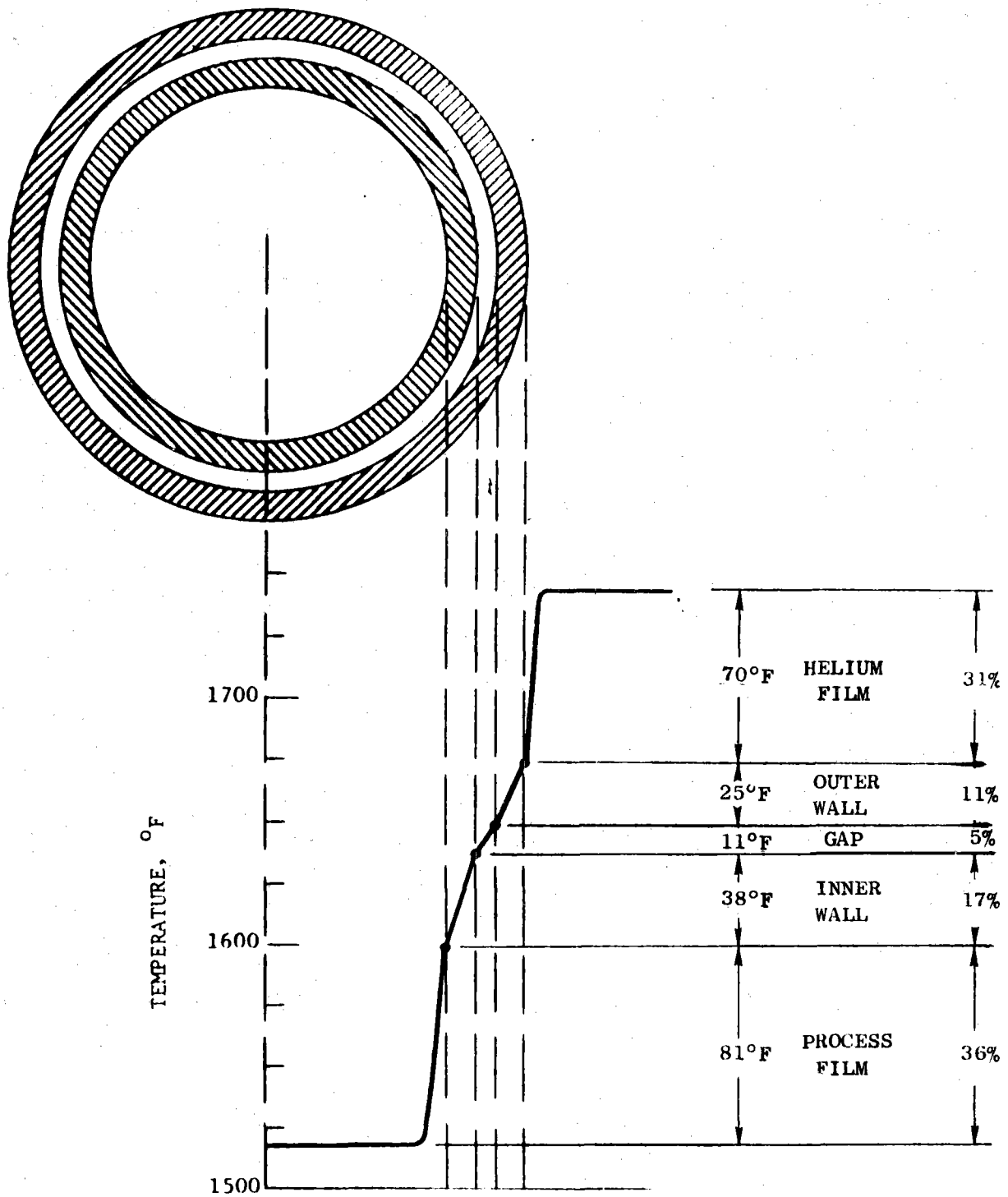

Figure 2-14. Typical Temperature Profile in a Duplex Tube (2 mil gap).

1. Parallel flow or baffled cross flow on the helium side.

2. Reformer gas flowing inside tubes filled with catalyst, discharging at the opposite end from entry.

3. Reformer gas flowing as in (2), but discharging at the entry and through an internal pigtail with heat recuperation.

4. Solid metal tube walls, or duplex tubes (concentric tubes with stagnant helium in the small gap).

For a given geometry and inlet conditions, the LASL code calculates the one-dimensional temperature, pressure and composition distributions along the tube length. The mathematical model simulating the methane reformer reactions was based on the model developed by Hyman[6].

Figure 2-15 shows the calculated performance of a typical duplex reformer tube. The upper chart shows the process gas constituent distributions and the lower chart shows the helium and process gas temperature distributions. An active tube length of 12 m results in a peak process temperature of 828°C and a corresponding methane conversion of 60.3%.

2.2 STEAM REFORMER PLANT EVALUATION

In order to arrive at the optimum plant described above, a detailed optimization and evaluation was conducted. Appendix G contains a complete description of the process followed. In addition, capital costs and cost of energy were estimated for nine different plant designs. Appendix H contains the details of the costing process.

2.2.1 PLANT COMPARISONS

More than thirty-six arrangements were originally considered. These were reduced to the nine cases shown in Table 2-4.

Four types of comparison were performed. The first set (the A-1a plants) explored the range of steam reformer power from 13% to 58.4%. All three designs used the 90 mm duplex tube steam reformer module described in Appendix E. Table 2-5 shows the quantitative results.

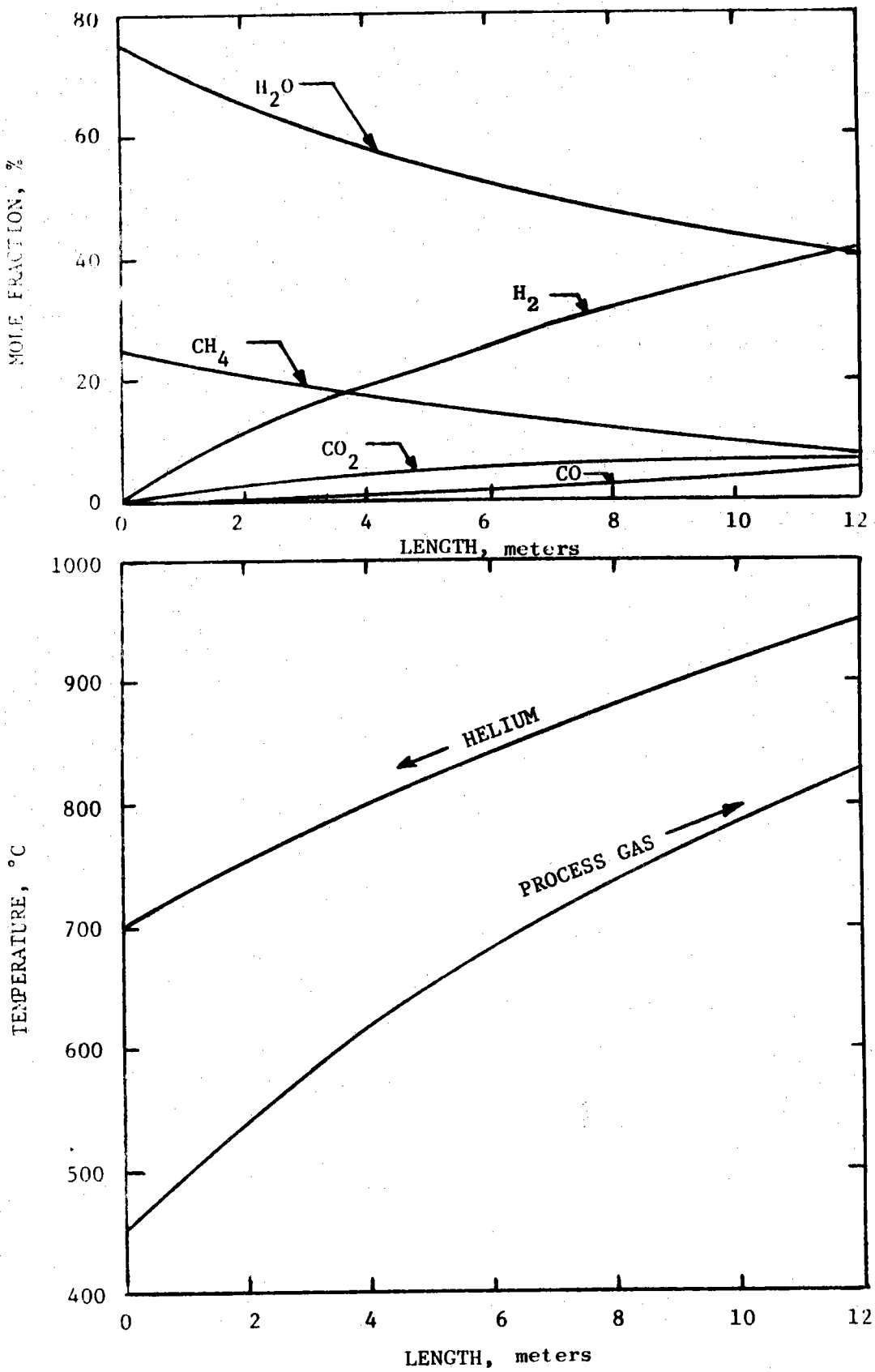

Figure 2-15. Calculated Performance Of Duplex Tube Reformer

TABLE 2-4

PLANT DESIGN CONCEPTS

A-1	DUPLEX TUBE STEAM REFORMER PLANTS
A-1a	90 mm ID TUBES
A-1a1	13% POWER TO REFORMER
Reference System A-1a2	35.6% POWER TO REFORMER
A-1a3	58.4% POWER TO REFORMER
A-1b	50 mm ID TUBES (ADVANCED CATALYST)
A-1b1	58.4% POWER TO REFORMER
A-1b2	35.6% POWER TO REFORMER
A-1c	90 mm ID TUBES WITH INTEGRATED PCRV
A-2	SINGLE WALL STEAM REFORMER PLANTS
	35.6% POWER TO REFORMER
A-2a	90 mm ID TUBES WITH 9 mm WALL
A-2b	90 mm ID TUBES WITH 12 mm WALL
A-3	INTERMEDIATE HEAT EXCHANGER LOOP PLANT
-	35.6% POWER TO REFORMER
-	90 mm ID TUBES, SINGLE, 9 mm WALL

TABLE 2-5

A-1a PLANT DESIGN VARIATIONS
(90 mm Duplex Tube Steam Reformers)

Parameter		A-1a1	Reference A-1a2	A-1a3
Power to Reformer,	%	13	35.6	58.4
Power to CHP User,	MWt	394	1080	1772
Electric Power,	MWe	932	591	241
Height of Reactor Building,	m	51.2	52.7	54.9
Diameter of Reactor Building,	m	46.3	48.2	50.0
SRA/SGA Module				
Diameter of Shell,	m	3.00	3.83	4.82
Height of Shell,	m	18.85	20.54	22.53
Total Weight,	Mg	166.5	371.9	736.6
Number of 90 mm DSR Tubes,	-	77	270	606
Steam Generator Surface Area,	m^2	1275	1221	1333
Total Plant Investment,	$\$x10^{-6}$	695.6	723.0	813.4
Thermal Energy Cost,	¢/MBTU	326	284	305
Electrical Energy Cost,	¢/KWH	1.63	1.72	1.92

The use of an advanced catalyst was considered with the next set of cases (A-1b). The concept of an advanced catalyst is that of removing two limitations of the present steam reformer catalyst and tube design. First, the present catalyst life is between two and eight years, much less than the 30-40 year design life of the entire plant. The replacement of catalyst requires both costly shutdowns as well as requiring that the reformer tube be accessible enough and of such a size that periodic catalyst removal is feasible. In addition, the present 90 mm I.D. tubes, which permit catalyst removal, are heat transfer limited rather than reaction rate limited. An "advanced" catalyst is one whcih, by unspecified means, allows a reduction in tube diameter to a point where the reaction rate limits heat transfer and also allows either in-place catalyst regeneration or 30 year plus catalyst life, thus permitting the use of a sealed reformer tube. Table 2-6 shows the comparison between the 90 mm reference duplex tubes and hypothetical 50 mm advanced catalyst plants. Note the significant gain in all important parameters.

Figure 2-16 shows the combined effect of steam reformer power split and the use of an advanced catalyst. Of these designs, the one involving conversion of 35.6% of the power in the steam reformer is clearly superior if the 90 mm duplex tubes must be used. Thus, existing catalyst technology forms the reference design in which 35.6% of the power is used in the steam reformer; but there is a real cost incentive to develop the advanced catalyst technology.

The effect of using an integrated PCRV was investigated by designing a PCRV to hold the twelve SRA/SGA modules (the 35.6%, 90 mm DSR units) in pods within the PCRV. Although there is a good fit mechanically, the energy costs increased 9%, due primarily to the larger cost of the integrated PCRV itself.

For the purpose of showing what the economic penalties are in using either a duplex tube or IHXL plant design two plant designs were examined in which single wall reformer tubes were used. The single wall reformer tube plants are based on German (KFA) design, but sized for the same conditions as the 35.6% reference DSR plant (A-1a2). Two tube wall thick-

TABLE 2-6

A-1b PLANT DESIGN VARIATIONS
(Advanced Catalyst Variations)

PARAMETER	A-1a2	A-1b2	A-1a3	A-1b1
Duplex Tube I.D., mm	90 (Ref)	50* (Adv)	90 (Ref)	50 (Adv)
Power to Reformer, %	35.6		58.4	
Power to CHP User, MWt	1080		1772	
Electric Power, MWe	591		241	
Height of Reactor Building, m	52.7	51.8	54.9	53.0
Diameter of Reactor Building, m	48.2	46.9	50.0	48.5
SR/SG Assembly				
Diameter of Shell, m	3.83	3.27	4.82	3.99
Height of Shell, m	20.54	19.42	22.53	20.85
Number of Tubes -	270	423	606	951
Total Weight, Mg	372	234	737	430
Steam Generator Area, m^2	1221	1221	1337	1333
Total Plant Investment, $\$x10^{-6}$	723.0	667.4	813.4	690.6
Thermal Energy Cost, ¢/MBTU	284	263	305	262
Electrical Energy Cost, ¢/KWH	1.72	1.59	1.92	1.65

*Note lower investment and energy costs for incorporation of advanced catalyst designs.

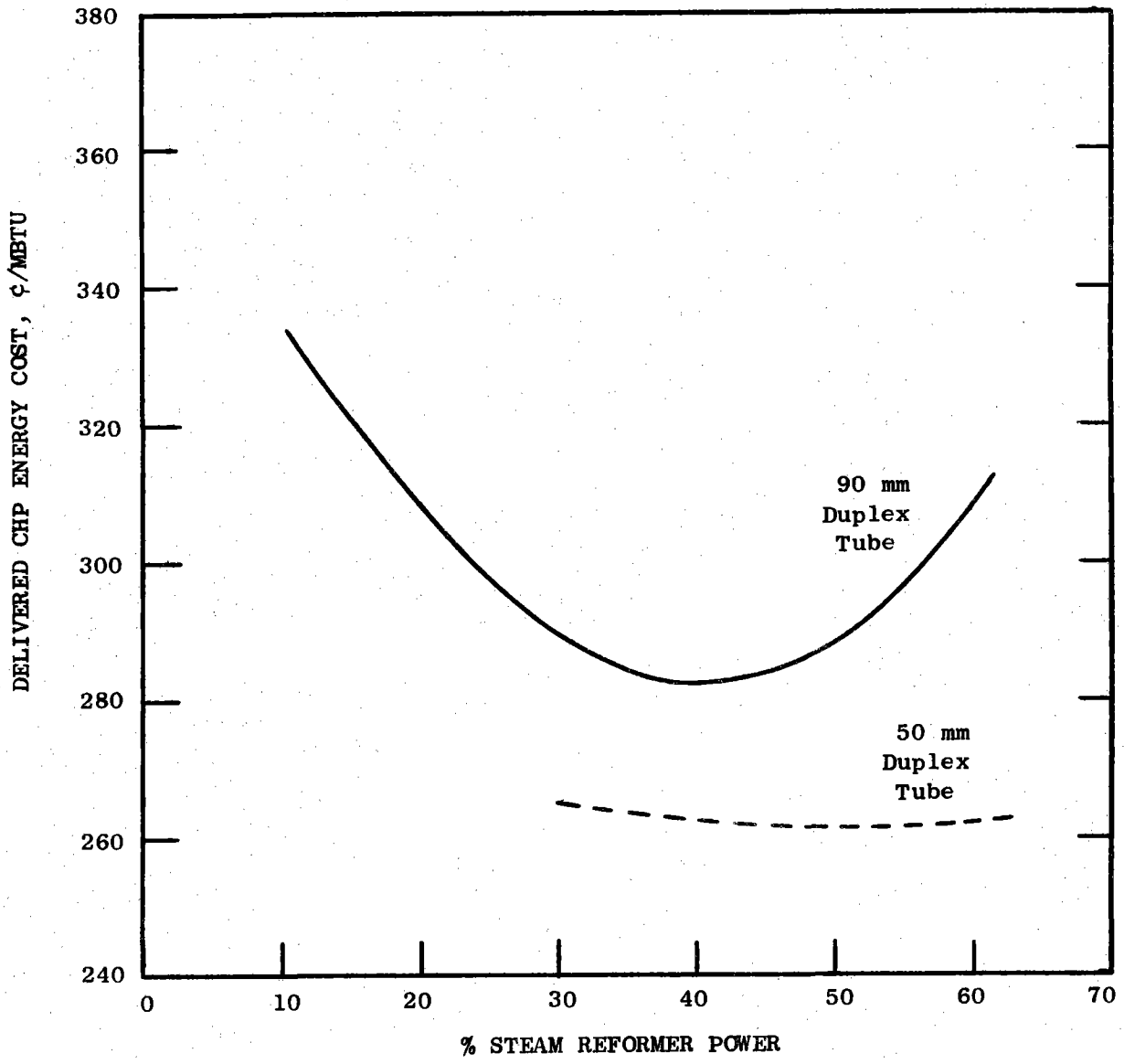

Figure 2-16. Cost of Thermal Energy vs. Steam Reformer Power and Duplex Tube I.D.

nesses were evaluated, an optimistic 9 mm wall, which is about half that of a duplex tube, and a more realistic 12 mm wall tube. For comparison, a KFA-designed single wall reformer tube had an I.D. of 100 mm and a wall thickness of 15 mm. Even with the optimistic 9 mm wall, only 6% is saved in energy cost, and, as discussed later in this section, these plants do not meet the safety and reliability standards we believe are required.

An alternative to the use of a duplex tube for placing a double barrier between the reactor core and the customer is to provide a dynamic closed cycle heat transfer loop between the reactor loop and the SRA/SGA loop. An intermediate heat exchanger in that loop acts as an interface between the reactor loop and this dynamic loop. The heat exchanger was designed and coupled to a single wall steam reformer/steam generator module located outside the containment building. Appendix C describes the selection and evaluation of a realistic, near-optimum IHX design. Figure 2-17 shows an elevation of the reactor plant showing, for comparison purposes, both a steam reformer/steam generator module on the left and an intermediate heat exchanger coupled to an external steam reformer/steam generator module on the right. Table 2-7 shows the pertinent parameters of a plant with an IHXL compared with a duplex tube steam reformer plant. The IHXL plant shows a 17% higher energy cost. Much of this difference is due to the larger size of the steam reformer components. Because of the lower helium temperature at the reformer entrance, occasioned by the additional temperature loss in the added heat exchanger, 33% more tubes were required to provide the same amount of reforming. The cost of energy to pump the helium in the second loop is also significant.

2.2.2 EVALUATIONS

Table 2-8 shows the evaluation criteria used to select the "best" steam-methane reforming plants. The approach used for the selection process was to divide the various criteria into "needs" and "wants". To be selected, a plant had to meet all "needs" criteria, and then was rated on the "wants" criteria. In addition, for those plants which meet the mandatory criteria, the two key items which affect the selection are the cost of energy, and the required development programs. Table 2-9 compares all nine plants.

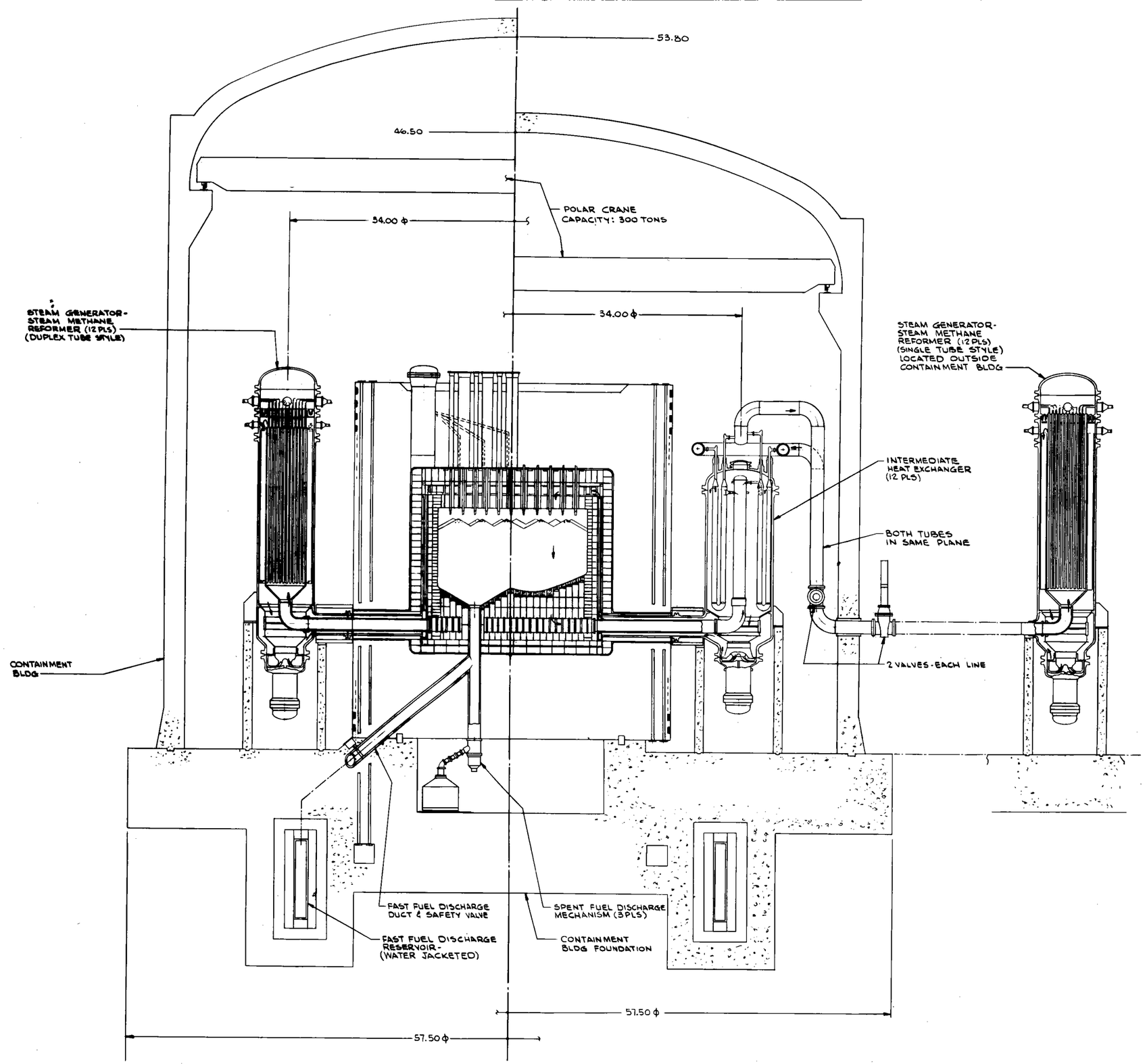

Figure 2-17. 3000 Mw_t Plant Layout Showing Steam - Hydrocarbon Reforming Alternates.

TABLE 2.7

IHX vs DSR PLANT DESIGN VARIATIONS

PARAMETERS		A-1a2	A-3
Type Plant		Duplex Steam Reformer	IHXL
Power to Reformer	, %	35.6	
Power to CHP User	MWt	1080	
Net Electric Power	MWe	591	547
Height of Reactor Building, m		52.7	51.2
Diameter of Reactor Building, m		48.2	50.0
Helium Inlet Temperature to Reformer	°C	950	900
Primary Heat Transfer Module			
Type		DSR/SGA	IHX
Diameter of Shell	m	3.83	4.78
Height of Shell	m	20.54	13.68
Total Weight	Mg	372	232
Total Plant Investment	$\$x10^{-6}$	723	800.8
Thermal Energy Cost	¢/MBTU	284	333
Electrical Energy Cost	¢/KWH	1.72	1.88

TABLE 2-8

VHTR-IHX PROGRAM

EVALUATION CRITERIA

STEAM-METHANE REFORMING PLANTS

MEASUREMENT (CRITERION)	
SAFETY -	CHEMICAL EXPLOSION FISSION PRODUCT CONTAMINATION SEISMIC
CAPITAL COST Δ -	INCLUDES PIPES, DUCTS, VALVES, CLEANUP LOOPS, ETC.
ENERGY COST -	COST OF THERMAL ENERGY LESS ELECTRIC CREDIT
MAINTENANCE -	
REPAIRABILITY -	
WEIGHT -	
RELIABILITY -	
PLANT AVAILABILITY -	
HYDROGEN DIFFUSION -	H_2 TO REACTOR HELIUM T_2 TO PROCESS GAS
REQUIRED DEVELOPMENT PROGRAM-	

TABLE 2-9

OVERALL PLANT EVALUATION

	PLANT DESCRIPTION								
	A-1a1	A-1a2	A-1a3	A-1b1	A-1c	A-2a	A-3	A-2b	A-1b2
Plant Description									
Type of Primary Heat Transfer	DSR	DSR	DSR	DSR	DSR	SR	IHX	SR	DSR
Power to Steam Reformer, %	13	35.6	58.4	58.4	35.6	35.6	35.6	35.6	35.6
Steam Reformer Tube I.D., mm	90	90	90	50	90	90	90	90	50
Containment Method	Non-Int.	Non-Int.	Non-Int.	Non-Int.	Integrated	Non-Int.	Non-Int.	Non-Int	Non-Int.
Notes		Reference				9mm wall		12mm wall	
Mandatory Criteria ("Needs")									
Safety									
Chemical Explosion	✓	✓	✓	✓	✓	✓	✓	✓	✓
Fission Product Contamination	✓	✓	✓	✓	✓	X	✓	X	✓
Maintenance	✓	✓	✓	✓	✓	✓	✓	✓	✓
Repairability	✓	✓	✓	✓	✓	✓	✓	✓	✓
Reliability	✓	✓	✓	✓	✓	✓	✓	✓	✓
Hydrogen Diffusion (Tritium)	✓	✓	✓	✓	✓	X	✓	X	✓
Desirable Criteria ("Wants")									
Plant Availability	Fair	Fair	Fair	Excellent	Fair	-	Good	-	Excellent
Component Weight	Excellent	Good	Poor	Good	Excellent	-	Excellent	-	Excellent
Required Development Program	Good	Good	Good	Fair	Good	-	Moderate	-	Fair
Economic Criteria									
Capital Cost, $\$x10^{-6}$	696	723	813	691	806	-	801	-	667
Delivered Thermal Energy Cost, ¢/MBTU	326	284	305	262	310	-	333	-	263
Delivered Electrical Energy Cost, ¢/KWH	1.63	1.72	1.92	1.65	1.87	-	1.88	-	1.59
Economic Rank (Based on Energy Cost)	4	2	3	1	3	-	4	-	1

The two single wall reformer plants are disqualified on the basis of not providing sufficient barriers between the customer and the reactor fission products,(including tritium). All other plants meet the mandatory criteria. See Appendix D for discussion of safety related matters.

Among the desired criteria, there is a trade-off between the excellent projected plant availability of the advanced catalyst plants with their long term catalyst life and the programs required to develop the advanced catalyst concept.

The key economic criteria is delivered energy cost. The following statements are pertinent. First, in a comparison between the IHX plant (A-3) and those plants which deliver the same amount of energy, the A-3 plant is clearly more expensive. Second, the advanced catalyst plants (A-1b1 and A-1b2) are clearly superior to the reference plants at the same delivered power ratings. Third, the integrated PCRV plant (A-1c) is more costly than its non-integrated counterpart (A-1a2). Lastly, within the power range covered by the 90 mm DSR plants, the 35.6% power-to-reformer plant (A-1a2) is slightly superior to the 58.4% plant (A-1a3).

The selected plant is thus the A-1a2 reference plant based upon current technology, with the second choice being the advanced catalyst plants, A-1b1 and A-1b2, which can be undertaken when the advanced catalyst is developed.

Nomenclature

h - convection heat transfer coefficient

Cp - specific heat of gas

G - mass flow velocity

Pr - Prandtl No. $\frac{Cp\mu}{k}$

Re - Reynolds No. $\frac{DG}{\mu}$

f - friction factor

ΔP - pressure drop

L/D- flow passage length/diameter ratio

ρ - gas density

V - gas velocity

g - gravitational constant

SECTION 3

COAL GASIFICATION PLANT

This section contains the description of a HTR plant to gasify coal using the steam gasification of coal process. The plant includes an intermediate heat exchanger loop to separate the primary reactor coolant from the coal gasifier.

3.1 PROCESS CONDITIONS

The selected process for the gasification of coal is the steam gasification process shown schematically in Figure 3-1. Appendix B contains a description of the many approaches which have been studied or used in the past.

Coal gasification using nuclear energy provides a way of combining the two most available energy sources to provide a source of a premium fuel, natural gas, which is reaching the end of its availability. Much work is currently underway concerning the coal gasification processes in which coal combustion supplies the necessary thermal energy to the process. The use of nuclear power to provide the thermal energy for the gasification process is potentially advantageous for two reasons. First, the amount of coal processed is decreased and the coal becomes only a chemical feed stock. Second, as a consequence of the lower coal thruput, less pollutants have to be removed in order to meet environmental requirements.

The basic reaction for steam gasification using an IHX is the water gas reaction:

$$C + H_2O \rightarrow CO + H_2$$

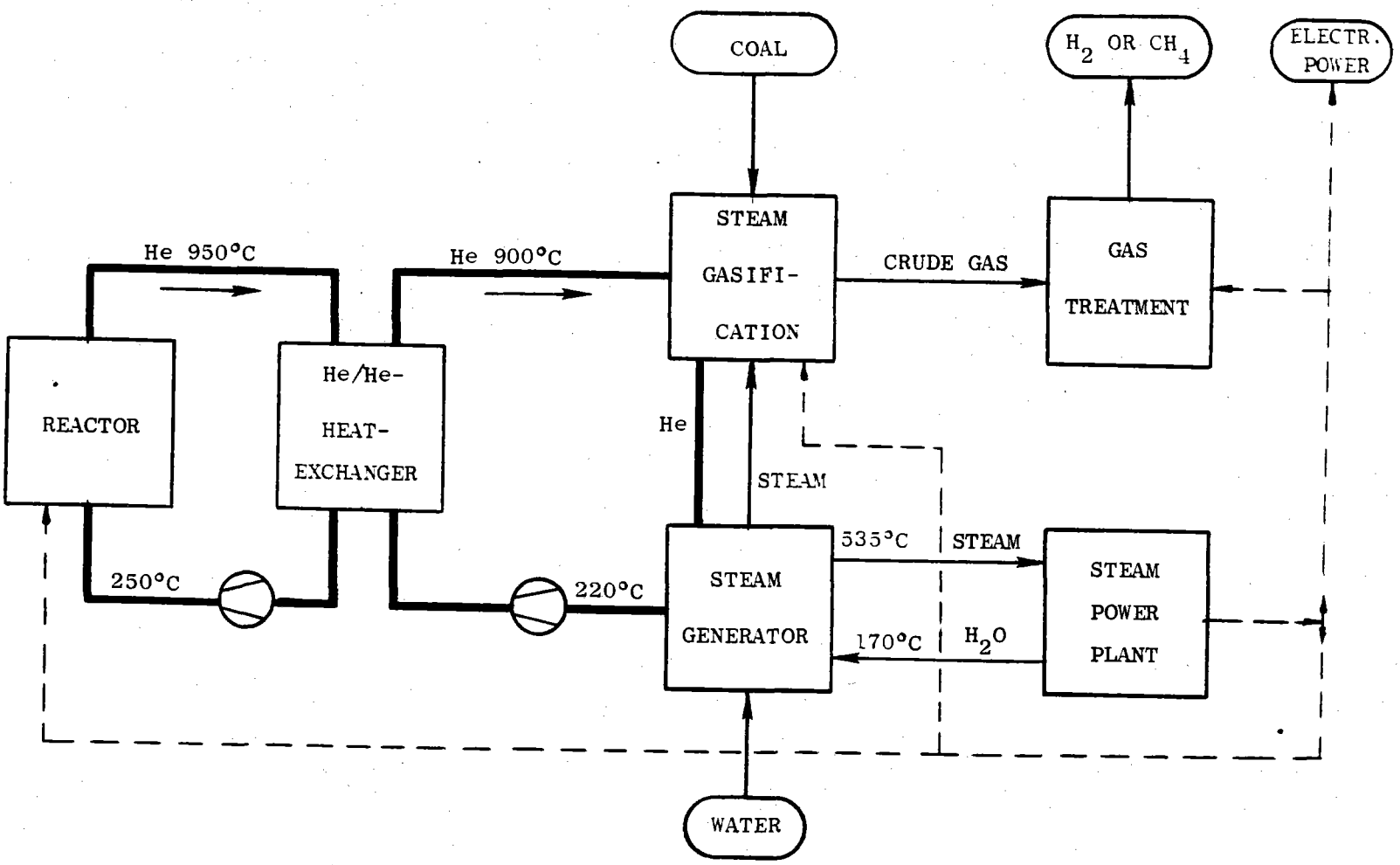

Figure 3-1. Steam Gasification Using an Intermediate He Circuit.

This gas has an energy content $(\frac{BTU}{SCF})$ which is only one-third that of methane. Additional reactions are possible to either proceed to the maximum amount of hydrogen or the maximum amount of methane, depending on pressure, temperature, and reaction processes. A typical gas would be the result of the following reaction chain:

$$4C + 4H_2O \rightarrow 4CO + 4H_2 \rightarrow CH_4 + 3CO + 2H_2O$$

where the final mixture, after removal of the water, has a heating value of slightly less than half that of pure methane.

In both of the above cases, high temperatures, and high heat transfer rates are required for high conversion efficiencies. Figure 3-2 shows the effect of process temperature on the conversion of various types of coal. Note that 900°C does an excellent job for lignite, but is not nearly as good for bituminous coal. As shown in Figure 3-1, the helium temperature to the steam gasifier unit is only 900°C. Thus there is a real incentive to raise the reactor exit temperature level to at least 1000°C in order to get good conversion from the plentiful bituminous coal available in the United States. An intermediate heat transfer loop permits the entire coal handling process to be located outside the reactor building, and allows replacement and/or repair of the helium-to-coal heat transfer equipment without going inside the reactor building.

Table 3-1 lists the key system parameters for three reactor exit temperatures, the lower (950°C) being the reference design point and the higher (1000°C and 1100°C) being goals for future development.

3.2 PLANT LAYOUT

Figure 3-3 shows the overall plant layout. The reactor plant is essentially identical to that described in Section 2.1.2. In place of the steam reformer/steam generator modules are twelve heat exchangers of 250 MWt each. These are coupled to four steam gasifier units, whose location is shown outside the reactor building. Not shown in Figure 3-3 are the necessary secondary circulators, steam generators, and turbo-generators to use the steam not required by the gasifier.

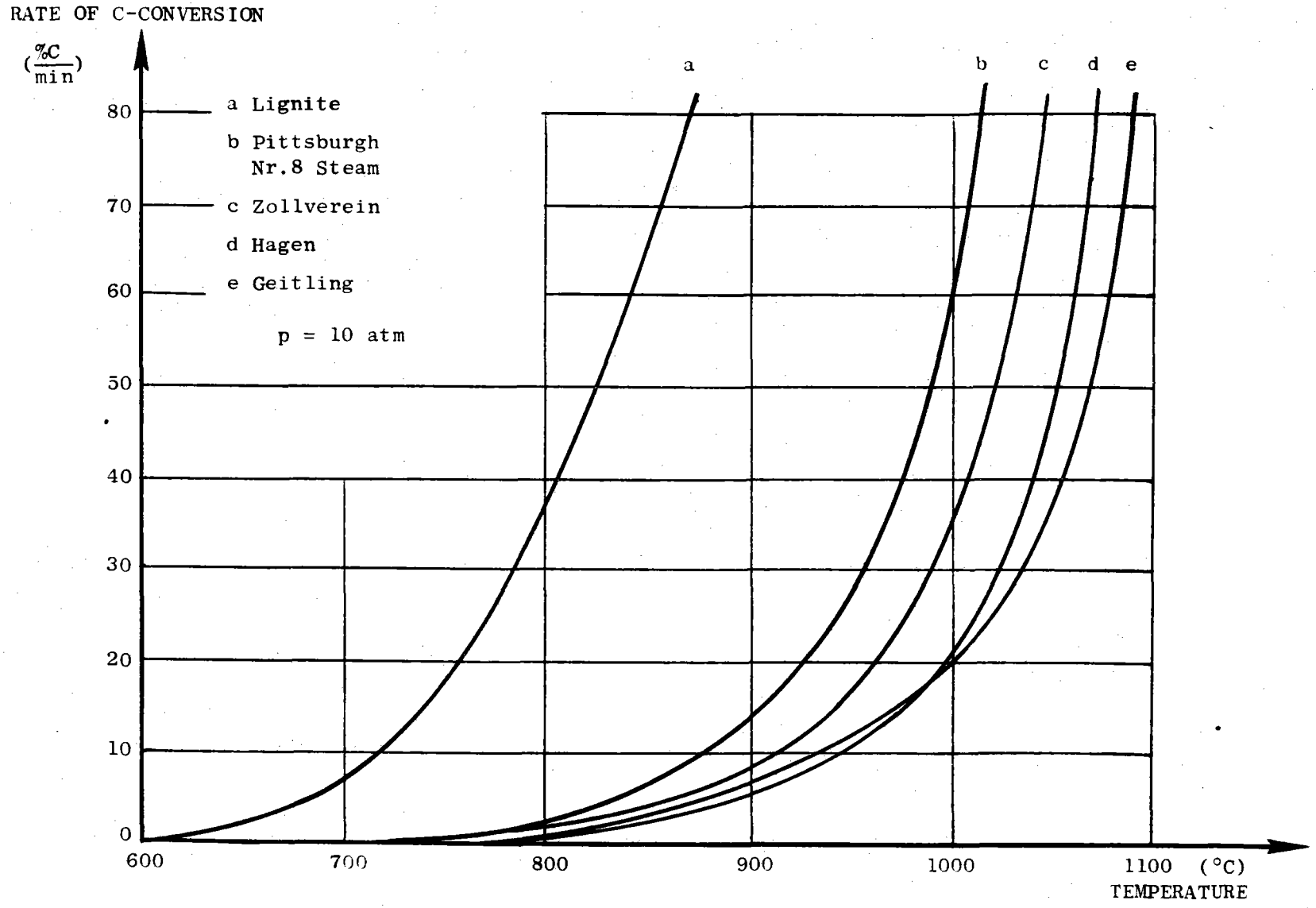

Figure 3-2. Rate of Gasification as a Function of Isothermal Process Temperature.(7)

TABLE 3-1

COAL GASIFICATION PLANT PARAMETERS*

	REFERENCE	ADVANCED	
Reactor Exit Temperature, °C	950	1000	1100
Gasifier Helium Inlet Temperature, °C	900	950	1050
Gasifier Helium Exit Temperature, °C	821	833	850
Peak Process Temperature, °C	771	783	800
Coal Thruput (3000 MW plant) Mg/h	188	220	280
Approximate Plant Efficiency, %	62	67	73

*Data from Reference 8

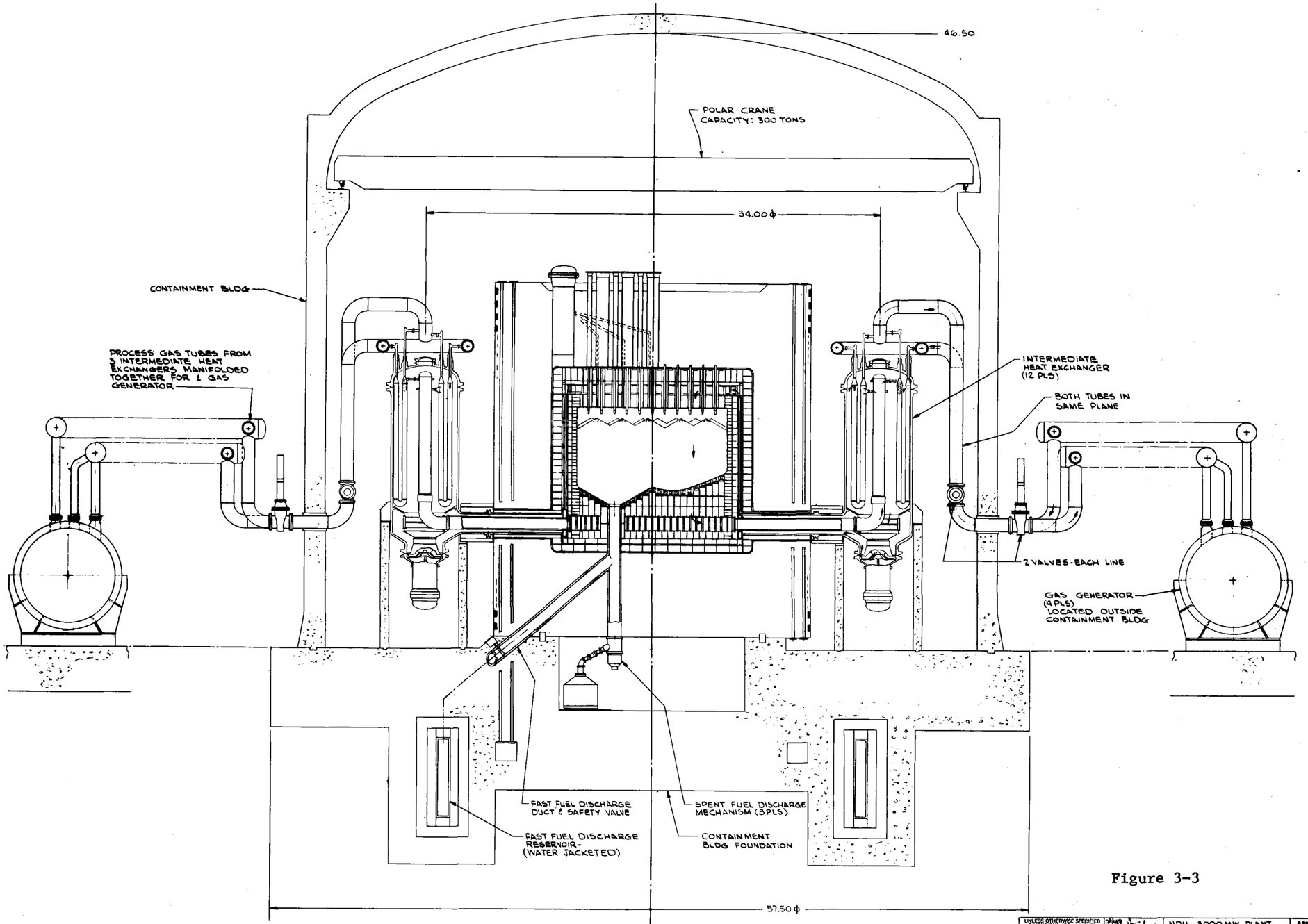
46.50
POLAR CRANE
CAPACITY: 300 TONS
34.00 ϕ
CONTAINMENT BLDG
PROCESS GAS TUBES FROM 3 INTERMEDIATE HEAT EXCHANGERS MANIFOLDED TOGETHER FOR 1 GAS GENERATOR
INTERMEDIATE HEAT EXCHANGER (12 PLS)
BOTH TUBES IN SAME PLANE
2 VALVES-EACH LINE
GAS GENERATOR (4 PLS) LOCATED OUTSIDE CONTAINMENT BLDG
FAST FUEL DISCHARGE DUCT & SAFETY VALVE
FAST FUEL DISCHARGE RESERVOIR - (WATER JACKETED)
SPENT FUEL DISCHARGE MECHANISM (3 PLS)
CONTAINMENT BLDG FOUNDATION
57.50 ϕ
0 1 2 3 4 5
METERS

Figure 3-3

The steam gasifier is shown in Figure 3-4 and is taken from current German (FRG) work[7,8]. Table 3-2 shows the major features of this unit.

From the data shown in Table 3-1 and Figure 3-2, the advantages of going to higher temperature can be clearly seen. Not only does the thruput increase, but the conversion efficiency also improves rapidly with increasing temperature.

The hot gas ducts are also based on current German technology. It is anticipated that ducts like those used in the HHV facility at Jülich, and shown in Figure 3-5, would be used. These ducts use a thin metallic liner to separate the hot gas flow from an insulation blanket. The pressure containing membrane is a water cooled shell built to ASME codes which can be solidly mounted to the containment building. The technology of such hot gas ducts are discussed more fully in Appendix I.

Hot gas valves are also water cooled, and are designed to seal against gas flow in either direction.

3.3 INTERMEDIATE HEAT EXCHANGER

This section describes the IHX designed for use either with steam reforming plants or with the steam gasification of coal. Complete details of the IHX, and factors influencing its design are given in Appendix C.

The reader should note that the reference design described in Section 3.3.1 below is not identical to the design selected from the configuration assessment summary described in Section 3.3.2. Once the U-tube design had been selected as the best configuration, an additional design iteration was performed, including internal design reviews, to improve and define the initial concept.

3.3.1 DESIGN SUMMARY

Figure 3-6 shows the overall design of the selected IHX assembly featuring thirty-six U-tube modules assembled in a (non-integrated) cylindrical pressure vessel. The assembly is rated at 250 MW and is approximately 17 feet in diameter by 60 feet overall length. The primary fluid is on the shell side with its motor driven circulator directly attached to the lower portion of the pressure vessel.

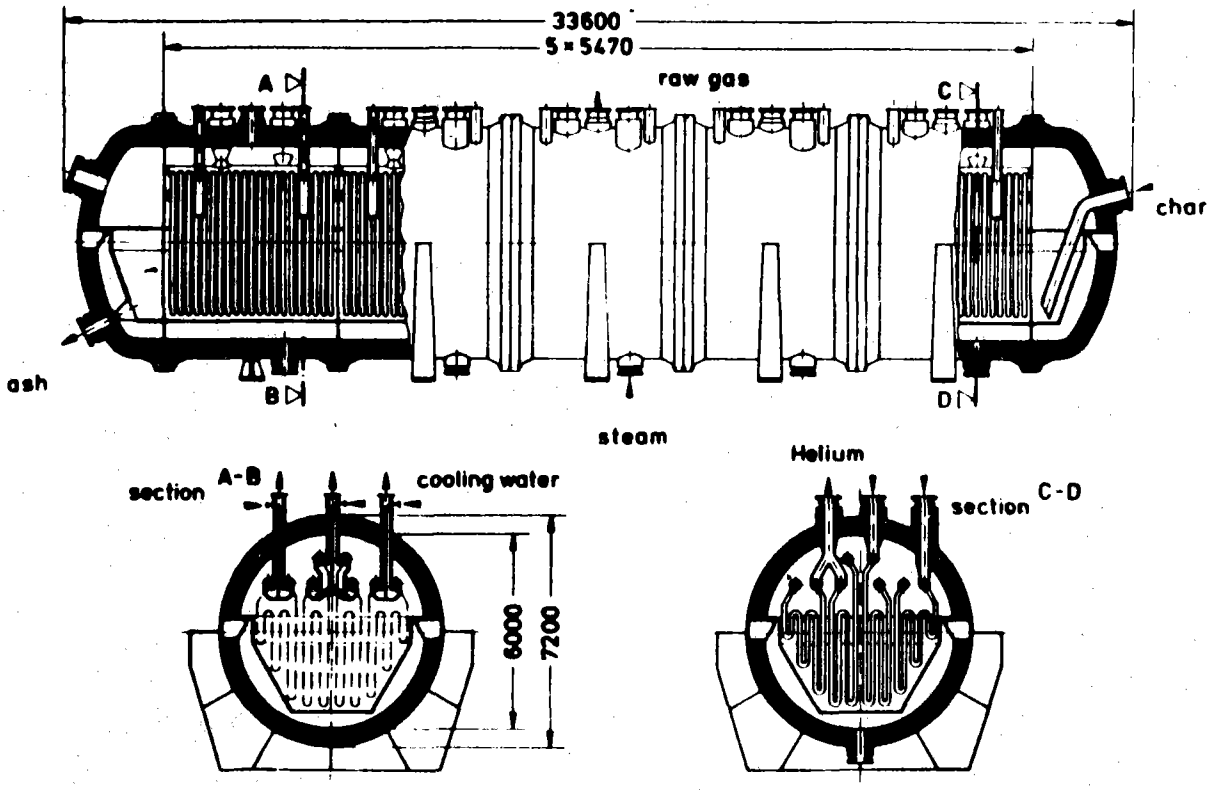

Figure 3-4. Gas Generator - Heating Area 4000m^2 (B-15)

TABLE 3-2

COAL GASIFIER PARAMETERS

Length	33.6 m
Diameter	7.2 m
Inlet Helium Temperature	900°C
Exit Helium Temperature	821°C
Process Temperature	771°C
Coal Thruput	47 Mg/hr
Heat Transfer Area	4000 m^2
Effective Bed Value	318 m^3
Reactor Power to Helium*	∿365 MW
Reactor Power to Process Steam*	∿840 MW
Gross Electric Power*	∿718 MW

*Approximate values subject to confirmation.

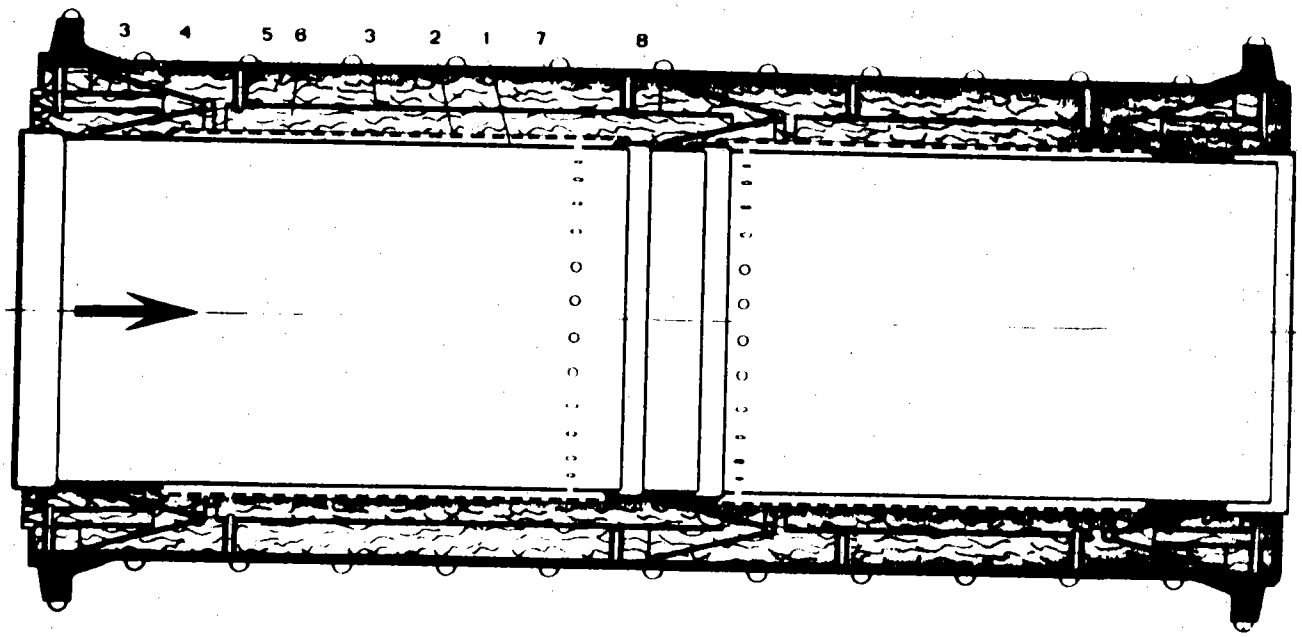

1 - Inner Liner
2 - Perforated Sheet Metal
3 - Intermediate Sheet Metal
4 - Support Member
5 - Spacer Bolt
6 - Insulation
7 - Pressure Containment
8 - Water Cooling

Figure 3-5. Cross-section of a Hot Gas Duct.

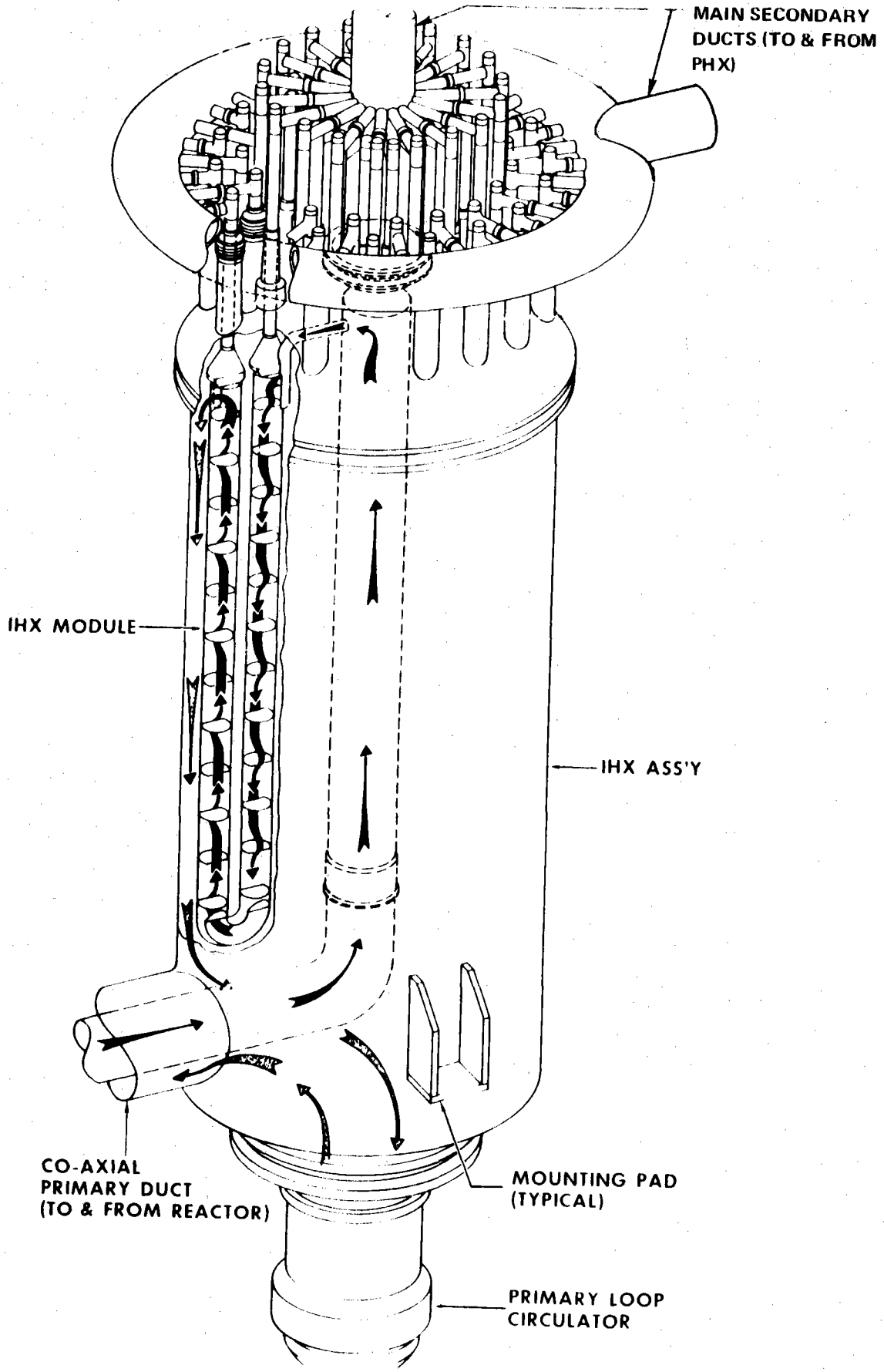

Figure 3-6. U-Tube Style Intermediate Heat Exchanger Assembly (Reference Design).

Figure 3-7 shows an exploded parts view of a typical module. Each module is approximately 30 feet in length, contains 251 1/2" O.D. U-tubes and is arranged so that the primary helium makes twenty-four passes across the heat exchanger tubes. Each module leg is circular in cross section and is approximately 16 inches in diameter.

Table 3-3 summarizes the significant data relating to the IHX design. Figures 3-8 and 3-9 indicate, respectively, engineering drawings of the complete reference IHX and of one of the thirty-six individual modules.

Table 3-4 shows the advantages of the reference IHX design. The U-tube thermal/hydraulic design is second only to that of the straight tube, counterflow design; the U-tube design approaching the thermal advantages of the straight tube design due to the relatively large number of cross flow passes in the former.

A major cost advantage of the U-tube style is achieved by avoiding large massive tube sheets where thickness varies directly with the overall diameter. In addition, the configuration readily lends itself toward utilization of small diameter tubes which directly reduces the core volume for the required heat transfer surface.

The safety related aspects of the U-tube style are significant in that modules may be readily inspected and isolated, if required, without disassembly of the IHX. Boroscopic inspection of the tube sheets and tube interior surface is possible without breaking the hermetic seal of the primary coolant fluid. The design lends itself toward the potential to find, plug and seal leaky tubes. All these activities could be accomplished by internally probing the U-tube ends from outside the IHX assembly, with access achieved through sealed access ports welded in the external plumbing.

Mechanical design features of the U-tube cross flow style include good support of the tube bundle with low shell-side pressure loss, outstanding capability to channel and control the primary coolant flow in the IHX assembly, and inherent ability to handle differential thermal expansion, both as a module and as individual tubes.

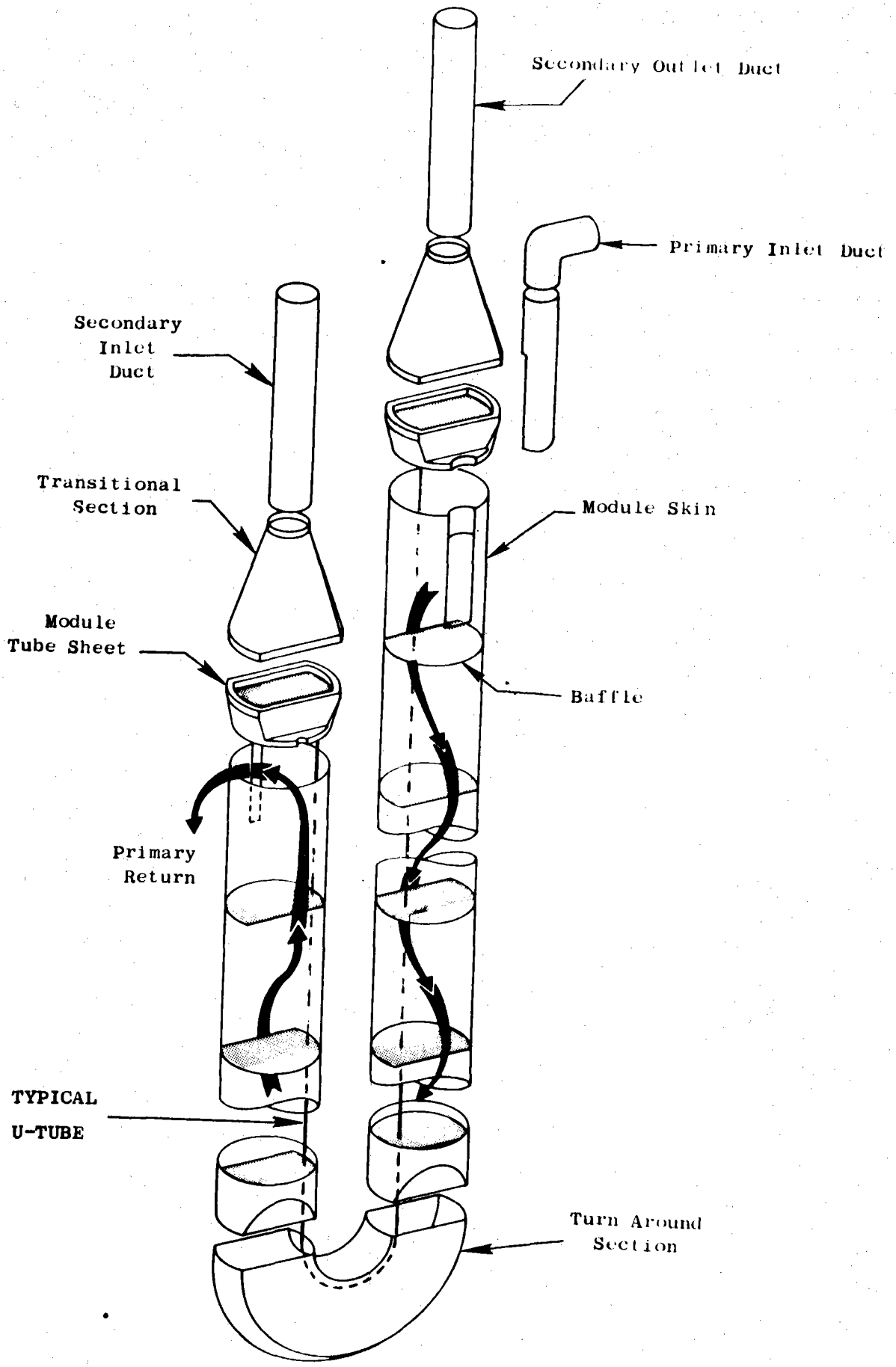

Figure 3-7. Exploded Parts View of U-tube IHX Module (Reference Design)

TABLE 3-3

SUMMARY DATA FOR REFERENCE DESIGN IHX

PLANT DATA

Chemical Process	Steam Gasification of Coal
Thermal Power	3000 MW
No. of Process Loops	12
Reactor Primary Coolant	Helium
Core Outlet/Inlet Temperature	950/350°C
Gasifier Inlet Temperature	900°C
IHX Inlet Temperature	300°C

IHXA DATA

IHX Power Rating	250 MW
No. of Modules	36
Primary Inlet/Exit Temperature	950/350°C
Secondary Exit/Inlet Temperature	900/300°C
Pressure Vessel O.D.	16' - 10-7/8"
Overall Height	62' - 6-1/2"
Approximate Weight	500K lbs
Primary/Secondary Flow	$.63 \times 10^6$ lb/hr
Primary ΔP (Shell Side)	15.9 psi
Secondary ΔP (Tube Side)	15.5 psi
No. of U-tubes	9036
Tube O.D. x Wall	0.500 x .050 inch

MODULE DATA

Module Power Rating	6.94 MW
Primary/Secondary Flow	4.861 lbs/sec
Primary ΔP (Shell Side)	15.9 psid
Secondary ΔP (Tube Side)	15.5 psid
Inlet Pressure Primary/Secondary	600/638 psi
IHX Cavity Pressure	585 psi
No. of U-tubes	251
No. of Cross Flow Passes	24
Tube O.D. x Wall	0.500 x .050 inch
Module Header O.D./Thick	15.62/3.5 inch
Module Skin O.D./Thick	15.62/.0625 inch
Tube Spacing-to-O.D. Trav/Long.	2.0/0.9
Overall Length	32' - 4-1/2"
Approximate Weight	4000 lbs

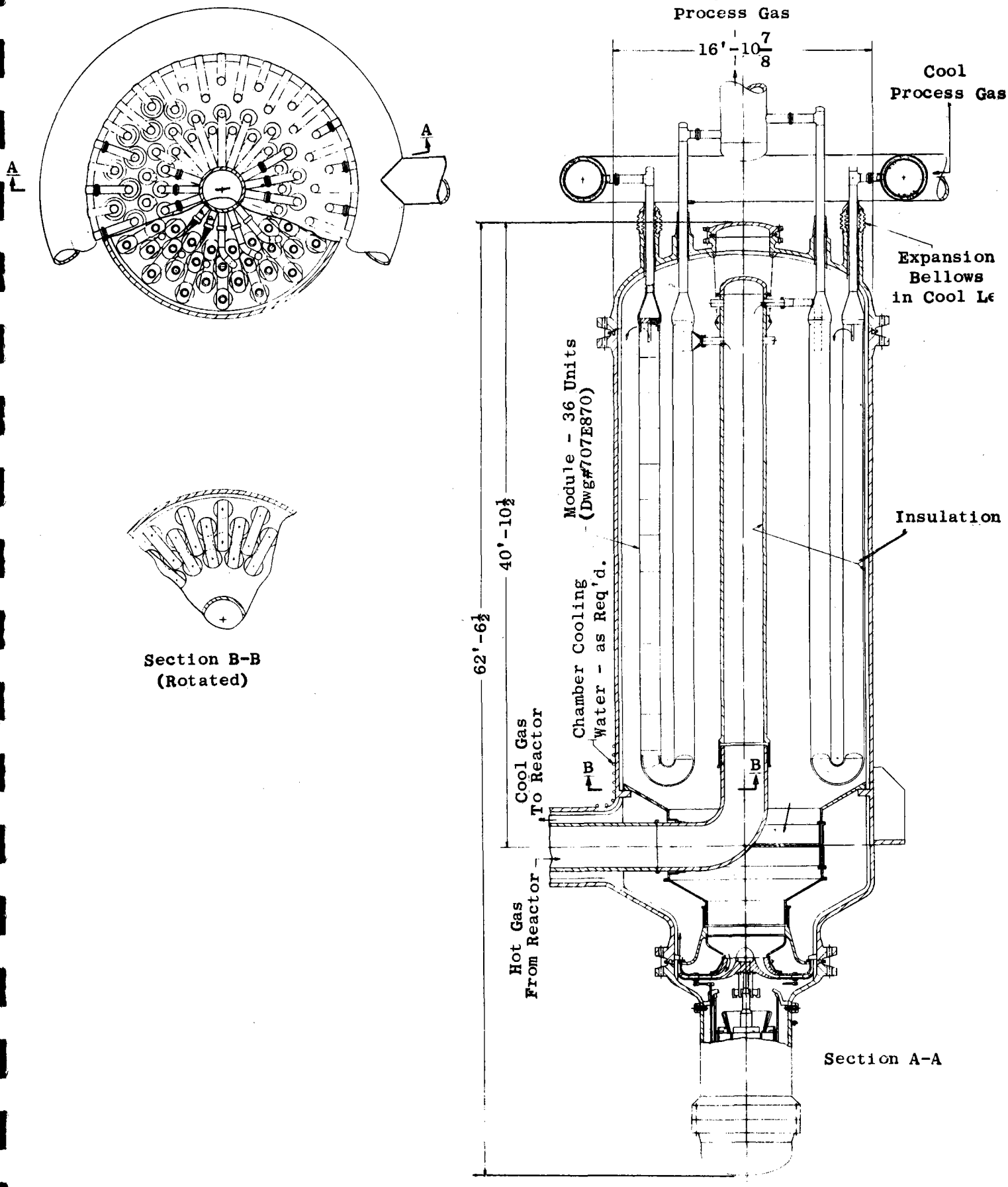

Figure 3-8. Engineering Drawing of Reference Design IHX Featuring 36 U-tube Style Modules. (Drawing No. 707E871)

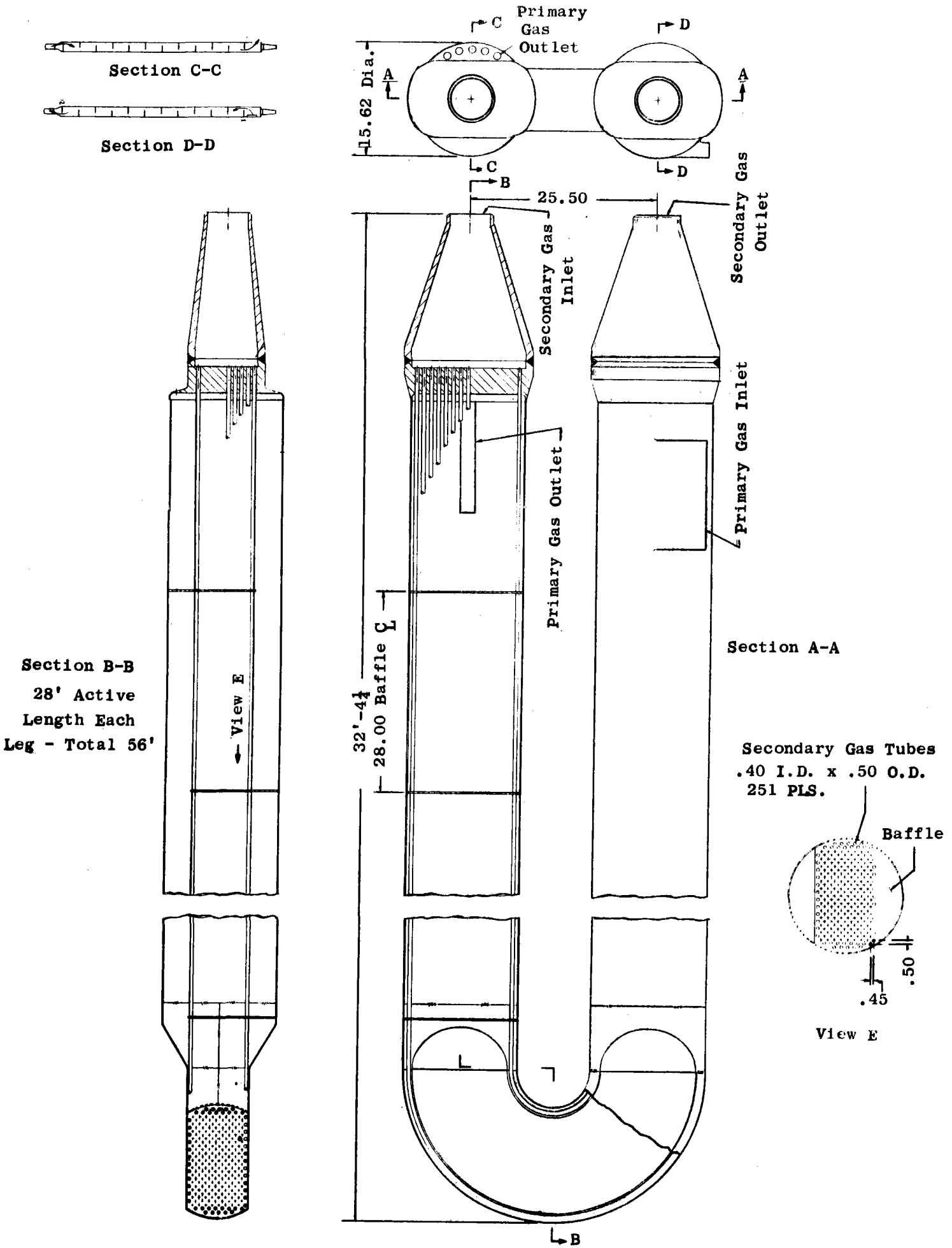

Figure 3-9. Module Assembly Drawing for Reference Design IHX (U-tube Concept). (Reference Drawing No. 707E)

TABLE 3-4

ADVANTAGES OF U-TUBE STYLE IHX

- FEATURES OF U-TUBE IHX
  - UTILIZES ESSENTIALLY SIMPLE STRAIGHT TUBES
  - GOOD THERMAL UTILIZATION OF VOLUME
  - GOOD PRIMARY DUCTING AND TUBE SUPPORT
  - IN SITU INSPECTION, BOROSCOPIC INSPECTION
  - INDIVIDUAL TUBE PLUGGING POTENTIAL
  - SINGLE MODULE ISOLATION FROM OUTSIDE
  - MINIMUM COST - NO MASSIVE TUBE SHEETS
  - INHERENT THERMAL EXPANSION CAPABILITY

- ABSTRACT
  - GOOD MECHANICAL DESIGN
  - GOOD THERMAL/HYDRAULIC DESIGN
  - MINIMUM COST
  - EXCELLENT SAFETY RELATED ASPECTS

3.3.2 CONFIGURATION ASSESSMENT SUMMARY

Initial screening of current IHX design efforts and consideration of the overall operating conditions indicated the suitability of the following four basic design styles for this application.

- straight tube counterflow, (two versions considered)
- U-tube multi-pass cross flow
- helical tube multi-pass cross flow, (two versions considered)
- bayonet tube folded flow

Six design layouts involving these styles were generated to serve as a reference for comparative evaluation. Using the digital computer as a design tool, each configuration was thermally and hydraulically optimized on the basis of cost within appropriate mechanical or other limitations. An overall assessment of each configuration was made with weighted consideration given to safety related aspects, mechanical design, thermal/hydraulic design, size and cost. Appendix C describes this assessment in detail.

The overall assessment clearly identifies the U-tube style as the most optimum of the candidates studied. This style was rated superior to all other candidates in the area of cost, mechanical design and safety related considerations.

Figure 3-10 shows the relative outline sketches of the IHX candidate configurations which resulted from the original optimization study, and clearly shows the size and cost superiority of the U-tube design.

Table 3-5 shows a numerical assessment of the IHX candidate configurations in the areas of safety, mechanical and thermal/hydraulic design and relative cost. This table indicates the overall superiority of the U-tube design configuration. The straight tube counterflow styles are judged to be the second most desirable; the helical style and folded flow configurations are judged to be least desirable.

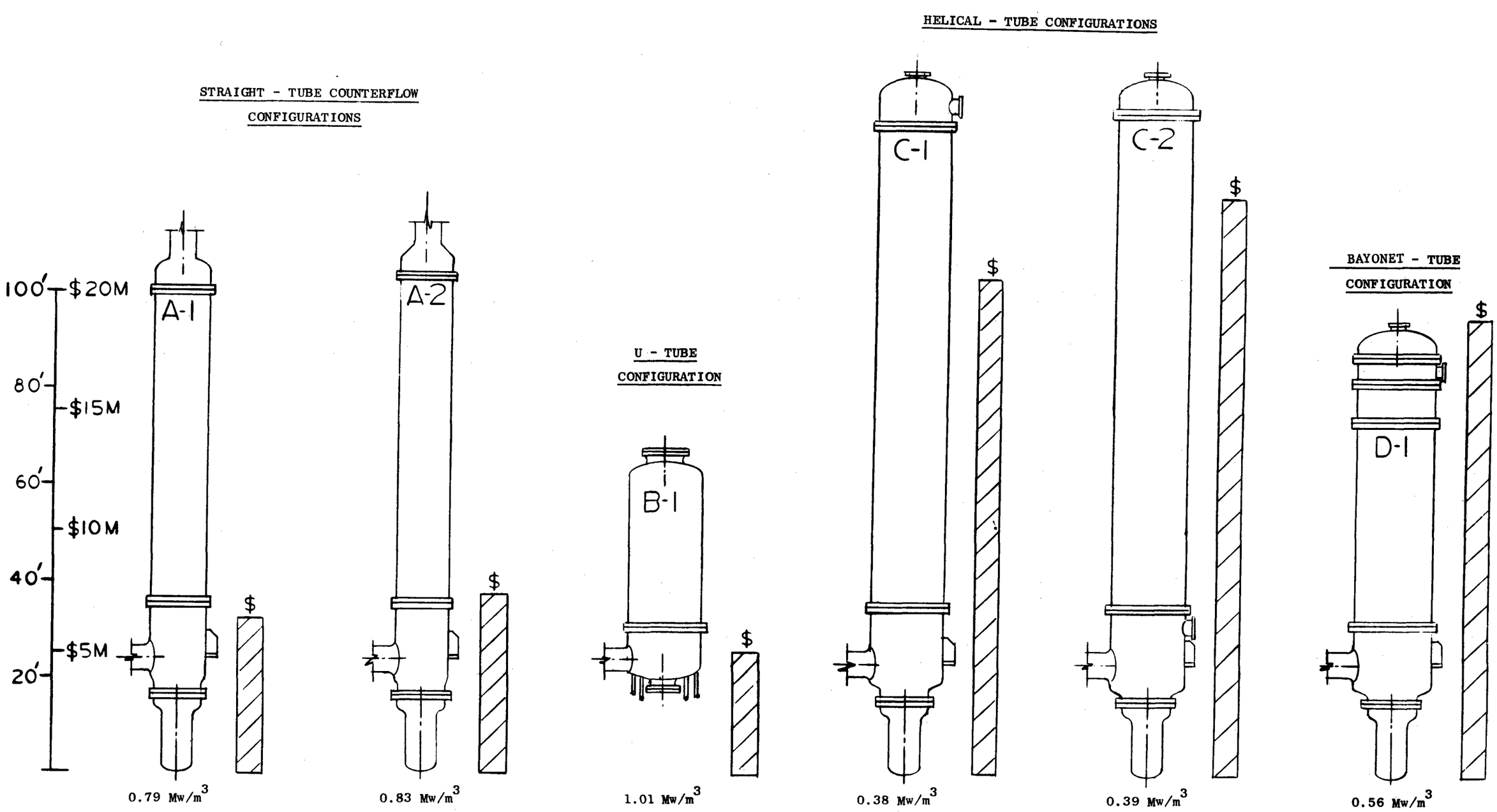

Figure 3-10. Size and Cost Comparison of IHX Candidate Configuration

TABLE 3-5

OVERALL ASSESSMENT OF CANDIDATE IHX CONFIGURATIONS

Evaluation Aspect	IHX CONFIGURATION DESCRIPTION					
	Straight-Tube		U-Tube	Helical-Tube		Bayonet Tube
	*A-1	A-2	B-1	C-1	C-2	D-1
Safety Related	87	87	98	89	92	83
Mechanical Design	59	52	93	57	57	61
Thermal/ Hydraulic Design	100	89	67	61	61	56
Cost	78	80	100	25	22	27
Overall Assessment	83	77	95	67	67	65

Note: All ratings on the basis of 100. The tabulated data shown in this Table summarizes the evaluation results presented in Table C-11 and Appendix C.4.4.2.

*See Appendix C for schematic description of candidate IHX configuration and definition of identification code.

Table 3-6 summarizes the size, weight, cost and other significant features of the candidate configurations. The tube diameters indicated were somewhat arbitrarily established with 1/2-inch O.D. considered to be the minimum acceptable based upon handling considerations. The pressure drop allocated to each side of the heat exchanger was selected to result in the lowest cost for the sum of (1) the capital cost of the heat exchanger, (2) the capital cost of the circulator and (3) the plant life time circulator operating cost.

TABLE 3-6

SUMMARY OF SIGNIFICANT DATA FOR VARIOUS COMPUTER OPTIMIZED IHX CONFIGURATIONS

IHX CONFIGURATION DESCRIPTION*	Straight-Tube		U-Tube	Helical-Tube		Bayonet Tube
	A-1 (780C)	A-2 (780C)	B-1 (780)	C-1 (777-9)	C-2 (777-9)	D-1 (777)
TUBES ($M)	$1.91	$1.65	$2.11	$10.11	$10.19	$8.03
O.D. (INCH	0.5	0.5	0.5	1.50	1.50	2.244
NO. OF TUBES	8558	7135	9070	1804	1863	3087
WT (LBS X 10^6)	.127	.110	.140	.474	.629	.535
PRESSURE VESSEL ($M)	$2.28	$2.34	$2.03	$5.36	$5.18	$4.06
OVERALL HEIGHT (FT)	86.6	88.7	44.9	129	128	77.1
OVERALL DIAMETER (FT)	12.5	12.0	1.57	15.0	14.8	15.8
WEIGHT	.284	.293	.254	.670	.647	.507
TUBE SHEETS ($M)	$1.19	$1.20	$0.13	$2.97	$5.96	$3.73
WEIGHT	.099	.100	.011	.248	.496	.310
TOTAL IHX WEIGHT	.636	.632	.502	1.82	1.99	.1697
ΔP DATA						
ΔP PRIMARY (PSI)	9.0	13.0	2.4	9	10	10
ΔP SECONDARY (PSI)	16.0	23.0	15.5	3.8	3.5	47.5
COST DATA ($M)						
TOTAL IHX (NET)	$6.5	$6.4	$5.1	$20.5	$22.9	$18.9
CIRCULATORS	5.1	6.3	4.3	4.0	4.0	8.2
TOTAL IHX	$11.6	$12.7	$9.5	$24.5	$26.9	$27.1

*SEE APPENDIX C FOR SCHEMATIC DESCRIPTION OF CANDIDATE IHX CONFIGURATIONS AND DEFINITION OF IDENTIFICATION CODE. THE DATA TABULATED HEREIN IS SUMMARIZED FROM THE COMPUTER OUTPUT SHEETS FIGURES C-40 THROUGH C-45 WHICH REFLECT THE OPTIMIZED DESIGN FOR EACH CANDIDATE CONFIGURATION.

SECTION 4

DEVELOPMENT

This section presents the key developments required for a successful VHTR-IHX program. A fuel development summary is also included. Further VHTR development details can be found in reference 1. The table below indicates process and helium requirements.

Requirements	Steam Reforming	Steam Gasification of Coal
Peak process temperature	820-870°C	771°C-800°C
Secondary helium temperature	-	900°C-1050°C
Primary helium temperature	950°C	950°C-1100°C

4.1 IHX METALLIC PARTS DEVELOPMENT PROGRAMS

This section discusses the development required for the metallic parts of the heat transport system, especially the intermediate heat exchanger.

4.1.1 DESIGN PHILOSOPHY

The key design philosophy upon which all HTR development work should be based is to keep as much of the overall plant as conventional as possible. This leads to three specific points.

First, all pressure vessels, piping, and valves which see system pressure are designed for water cooling to meet existing ASME codes. This implies the development of liners and insulations which will work with the low temperature pressure barrier to provide a reliable, economic, coded system.

Second, the selections of simple, modular component designs for the high temperature parts will permit much simpler component testing and development which should result in decreased overall development costs.

Third, the next steps are the detailed design of the IHX module followed by the testing described below.

4.1.2 MATERIAL TEST PROGRAMS (See also Appendix I)

4.1.2.1 Separately Funded Programs

Development of the IHX will be supported by several separately funded programs appropriate to many components of the high temperature gas cooled reactor; in addition, it will be supported by materials programs directly related to the specific needs of the IHX design. The former includes the broad materials evaluation and development program[9] covering the long term environmental effects of helium on selected alloys. A similar basic program would involve fundamental studies of the diffusion of tritium and hydrogen through selected coolant containment alloys.

4.1.2.2 IHX Directly Related Programs

In addition to the above basic programs, the following effort will be necessary to meet the specific engineering design requirements of such components as the IHX.

Design Data - The development of ASME code qualified design data will be required for the final selected heat exchanger alloy or alloys in those environmental areas and for those temperature regimes where the alloys are not currently code qualified.

Fabrication Development - Effort will be required to confirm the manufacturability of the various components, to certify the weld joining processes, to determine weld joint mechanical properties of specific joint configurations such as tube to header joints and joints between dissimilar alloys, and to certify other special processes such as the application of wear coatings on different components.

Cold Wall Insulation Development - Additional effort will be required to further develop insulation systems and prove their reliability. A detailed and current assessment should be made of the actual operating performance characteristics, maintenance experience and life of various types of insulating materials in actual reactors. Evaluation of more promising insulation systems, design features and insulating materials should

be made at the higher proposed temperatures (950°C and higher). The work should be guided by design effort intended to optimize the insulation system at these higher temperatures.

Wear Coating Development - A basic testing program for the selection and evaluation of wear coating materials will be required. Plasma arc spraying and other forms of coating application, will be used to apply wear coatings on one or both mating alloy surfaces in simple materials rub test experiments. Various combinations of materials will be evaluated under appropriate rubbing contact conditions in helium; materials such as metal bonded tungsten, titanium and chromium carbides.

4.1.3 BENCH TEST PROGRAMS

Several component design confirmation testing programs will be required using modular components or simulations of final design configurations.

Cold-flow mockups of a "U" tube bundle section will be required for initial evaluation of flow distribution and pressure drop in the primary and secondary fluid flow areas.

Simulations of various design configurations for rub test evaluation of wear surface coatings will be required. These will be performed under representative design configuration and under the environment and sliding conditions of temperature, contact pressure, displacement, frequency and number of cycles expected in final design components. Such testing will utilize the most promising technology developed in the materials wear tests; it will confirm the satisfactory nature of the selected design and the materials and processes for expected resistance to wear, seizing and excessive gas leakage at each of the critical sliding contact areas in the IHX design.

The preparation of closely simulated tube-to-header joints, the fabrication of process demonstration components, and the preparation of dissimilar alloy welds in full size components will be necessary both for the final certification of the fabrication processes and also for non-destructive and destructive tests necessary to certify the design capability.

4.1.4 COMPONENT TEST PROGRAMS

Single module heat exchanger "U" tube bundles provide a relatively economic basis for evaluating the design limits, performance characteristics and endurance capability of the IHX. The construction of a total of 3 modules is suggested. One module would be operated in air or combustion gases over the design temperature range at a test facility in the USA. This module test would provide data concerning such characteristics as hot gas flow performance, pressure drop in both circuits, preliminary heat transfer data, tube bundle thermal distortions under transient conditions, tube vibration characteristics, and high cycle fatigue problem analysis at design and off-design conditions. In addition to various tests involving exploration of design capabilities, this component could serve as a test vehicle to evaluate the adequacy of the design in the event of a simulated abrupt rupture failure in the secondary loop. The design calculations establishing the acceptability of retaining full pressure in the primary loop for a time interval such as a ten hour fault period could be verified, the capability of the system to withstand a significant number of fatigue cycles could be verified and the mode of failure of the module under the large pressure differential occasioned by a fault period much longer than the design requirement could be determined.

The preparation of two additional "U" tube bundles is suggested, one for test at the Los Alamos Scientific Laboratories and one for test at KFA in the Federal Republic of Germany. Both tube bundles would be tested under helium atmospheres at temperatures and heat flux rates required by the design. Design performance could be verified and off-design characteristics should be determined. Tests could be run to determine the effect of tube plugging; effects of variations in leakage at various seal areas could be noted; and the long term performance reliability and structural endurance characteristics of the component could be verified. In addition special techniques could be developed for determining the presence of primary to secondary circuit leakage and for borescopic examination of the tubes on each side of the hairpin tube bundle by entry through the secondary flow passages above the tube headers.

4.1.5 GROWTH VERSIONS OF THE IHX

It would appear that growth versions of the IHX can use essentially the same design as presented herein with only a direct replacement of materials with higher temperature capability in a partial length of the heat exchanger tubes at the inlet end of the hairpin modules. Changing from a chromium-nickel base alloy such as Inconel 617 to an oxide dispersion strengthened (ODS) alloy such as MA 754 has the potential advantage of several fold increase in rupture strength at 950°C.

The formability of the high strength ODS alloys is relatively poor and, when welded, the ODS structure which provides their basic strengthening mechanism is lost. Thus, the use of ODS alloys in aircraft turbine engines, as nozzle vanes employing limited air cooling at extremely high temperatures, has been in extruded bar form rather than in formed and welded sheet metal structures. Parts are joined by brazing instead of welding; brazing alloys and processing techniques are well established both in the brazing process itself, and in the satisfactory behavior of brazed joints operating at very high temperatures.

For use in the growth version of the IHX, the ODS alloys would probably be employed as extruded tubes. An immediately achievable development goal would be the production of extruded tubes in ten foot lengths. Brazed joints with relatively large lap shear areas would be used to minimize stresses in the brazed joint. The design would provide essentially a mechanical joint with the braze acting as a leak tight sealant and providing shear resistance against joint disassembly. Joining with dissimilar alloys, such as Inconel 617, using brazed joints, should not cause any great difficulties.

While the ODS alloys are limited in available sizes and in their fabricability and while their cost is currently somewhat excessive ($25-40/lb), there appears to be no reason why such alloys could not be used in growth versions of the IHX in those limited areas where uncooled hot gas tubing header plates or heat exchanger tube surfaces were required.

4.1.6 IHX LOOP DEVELOPMENT PROGRAM SUMMARY

Table 4-1 shows the summary of the development required for the IHX loop and components.

TABLE 4-1

IHX-LOOP COMPONENT AND MATERIALS DEVELOPMENT PROGRAM

COMPONENT	REQUIREMENT	COMPONENT TEST	BENCH TEST	MATERIALS TEST	COMMENTS
IHXL	• 1000 LCF Cycles • 10 Hour Fault • 300,000 Hour Life	• LCF o FAULT • PERFORMANCE • ENDURANCE			
• IHXA - "U" Tube Modules	Reference Design 7 MWt, 950°C Primary Helium	Helium (KFA & USA Facilities) Air (USA Facility)	Flow Distribution & Proof Tests (Wear Coatings)		Growth version limited in temperature by (1) tube materials, and (2) insulation & liners
Tubes	INCO 617 Design Point, 0.5" dia, Pri-Sec barrier, 50 mil wall includes 22 mil corrosion allowance	• Operation with up to 10% of tubes plugged. • Borescope inspection • Tube leak tests • Tube plugging tests	• Sliding wear resistance • Corrosion resistance • T & H_2 permeation resistance • Bi-metallic tube joint	• INCO 617/618 • ODS Tube Dev. including joint - Coatings - Cost	Materials Program Summary: 15 materials + coating, (1) corrosio and (2) wear & rupture tests and mission mix. (3) doped helium tests.
Baffles	Wear Coat, 0.5" dia. and 16" dia. sliding *		• Sliding	• Metal alloy • Graphite (especially growth version)	
Skin	Welding 16" dia. sliding *		• Sliding	Compatibility/ Welding • Sliding	
Inlet	Sliding Joint 5" dia. tube		• Sliding	Compatibility	
Insulation in Secondary Outlet Leg	5" dia. blanket		Compatibility/ Reactions Liner Fatigue/ Reliability		
Tubesheet	Welding *			ODS - size limitation	

* Materials requirements less stringent than for tubes

TABLE 4-1 (Continued)

IHX-LOOP COMPONENT AND MATERIALS DEVELOPMENT PROGRAM

COMPONENT	REQUIREMENT	COMPONENT TEST	BENCH TEST	MATERIALS TEST	COMMENTS
- Hot Primary Supply Duct Insulation Duct	Sliding Joint - 32" diameter				
- External Bellows Assy. Sec. Inlet Leg	<600°F (Pri-Inside containment)		Fatigue/ Reliability		
• Secondary Outlet Duct - Insulation - Liner	1 m O.D. 8" t 30" dia.				
• Containment Valves	Water cooled base and Seats				
• Circulator	Oil/Buffer Gas System				
• Secondary Helium	T, H_2 diffusion - O_2 film	"U" tube module test	Doped helium	Doped helium (O_2 for Ni & Fe Steam for Fe)	

4.2 STEAM REFORMER DUPLEX TUBE DEVELOPMENT PROGRAMS

The development of a duplex tube steam reformer has been started[4]. Specific development work required includes:

1. Fabrication development of the full size tubes,
2. Materials qualification for both the process side and helium side (similar to IHX),
3. Design and qualification of closures, tube sheet attachments, and gas ducting within the module,
4. Testing of full size reformer tubes under realistic conditions,
5. Advanced catalyst development.

4.3 FUEL DEVELOPMENT PROGRAMS

4.3.1 INTRODUCTION

The THTR fuel ball with the BISO kernel clad is the reference fuel for the HTR reference reactor. This fuel is already qualified for the 760°C helium exit temperature in the THTR. The 950°C helium temperature has been demonstrated in the AVR research reactor for over two years. THTR fuel balls have been in production at HOBEG at a rate of 200,000 per year. Additional developments desired for the BISO coating mixed oxide fuel are:

- Irradiation tests under OTTO cycle conditions,
- Fabrication development to reduce the uranium contamination on the outside of the kernel,
- Special high temperature tests, i.e., 1800-2000°C to determine fission product release under postulated worst accident cases.

For steam gasification of coal to improve the process yield, the primary helium from the core should be raised from 950°C toward 1100°C. Here a TRISO coated particle would be required to reduce the release of metallic fission products.

The table below lists the various particle failure modes which limit the average reactor outlet helium temperature to the following values:

Particle Type \ Failure Mode	Fission Gas Pressure	Irradiation Cracking	Kernel Migration	Metallic Fission Product Release
BISO	>>1500°C	>1350°C	>1170°C	970°C
TRISO	>>1500°C	>1350°C	>1170°C	>1170°C

Up to 1150°C helium temperature the principal cause of fission product release from TRISO coated fuel is due to mechanical failure of the SiC coating. The probability of such failure is minimized by good process control during fuel manufacture. Amoeba motion has not been observed in irradiated fuel balls.

4.3.2 FISSION PRODUCT RELEASE

Fuel particle coatings do not need to fail mechanically for fission products to be released. Although some fission products are released from defective coatings or coatings broken during fuel element fabrication, there are two other means for fission products release as well. Some of the released fission products come from the heavy metal contamination of the matrix outside the particles which occurs inadvertently during manufacture. And even intact coatings release some fission products. These move through the coating by the diffusion process, and some have sufficient mobility to traverse the entire coating thickness. Fission products that do traverse the entire thickness of the coating must diffuse through the graphite matrix and shell, and evaporate from the pebble surface in order to reach the helium coolant. The release of fission products such as Cs, I, and Ag restricts the repair and maintenance of components of the primary heat transport circuits. Estimates of the plate-out of fission products in the colder parts of the AVR circuits suggest for Cs 137 an upper release limit of about 100 Ci/year, (i.e., a R/B* ratio of $\sim 2 \times 10^{-5}$).

*R/B = rate of release/rate of birth

Fission products are divided into three main categories with respect to their effect on HTR safety:

1. Inert gases (Kr and Xe)
2. Electronegative elements (principally I), and,
3. Electropositive elements (principally the metals Cs, Ag, and Sr).

The primary barrier to the inert gases is the inner high-density pyrocarbon coating. Kr and Xe have very low diffusion coefficients in pyrocarbon (on the order of 10^{-15} cm^2/sec at 1250°C), and are therefore released only from broken fuel particles and from heavy metal contamination of the matrix outside the fuel particles.

At HTR core temperatures, iodine behaves like a rare gas of equivalent half-life. Much of the iodine that does reach the helium coolant is deposited on metal or graphite surfaces in the low temperature parts of the circuit.

Electropositive elements (e.g., Cs, Ag, Sr) have significant mobility in pyrolytic carbon coatings as shown by the data in Table 4-2, where fractional release of Sr-90 from BISO- and TRISO-coated fuel particles is given for three temperature ranges. The table also shows that TRISO coatings retain Sr-90 much better than BISO coatings at the higher temperatures. This is substantiated by comparing the diffusion coefficients of Sr and Cs in pyrocarbon and silicon carbide in Table 4.3. The coefficients are several decades lower in SiC than in pyrocarbon. The ability of the SiC layer of TRISO coatings to better retain metallic fission products allows TRISO coated particles to be operated at higher temperatures than BISO coated particles for a given fission product release rate.

Calculations for Cs 137 release in an OTTO-cycle pebble bed reactor were performed at KFA for a process heat reactor for different gas outlet temperatures (770°, 870°, 970°, 1070°, 1170°C) and for different fuel designs. For these calculations the reactor core was divided into six vertical loading regions of equal volumes. The Cs 137 release was calculated in each region as a function of the power and temperature history of a fuel element residing in this region. Since there is a temperature gradient within a pebble moving through the core, the pebble was divided into three temperature zones. In each zone the Cs release was calculated for a representative coated particle.

TABLE 4-2

FRACTIONAL RELEASE OF Sr-90 THROUGH BISO OR TRISO PARTICLE COATINGS

Particle Type			Fuel Temperature Range, °C		
Name	Retaining Layer	Design	900-1000	1040-1150	1160-1230
BISO	P_yC		4.6×10^{-6}	1.7×10^{-4}	1.4×10^{-2}
TRISO	$P_yC/SiC/P_yC$		4.3×10^{-6}	3.0×10^{-6}	3.3×10^{-6}

Fuel burnup 3.5% FIMA, 280 days irradiation

TABLE 4-3

COMPARISON OF DIFFUSION COEFFICIENTS
MEASURED AT 1400°C, CM^2/SEC

	Pyrocarbon ($2.0\ g/cm^3$)	Silicon Carbide	
		$T_{dep.}$ 1400°C	$T_{dep.}$ 1500°C
SR	3.5×10^{-8}	$2. \times 10^{-8}$	5×10^{-13}
Cs	1.5×10^{-12}	1×10^{-10}	6×10^{-17}

The diffusion coefficients and the release model were tested against irradiation experiments performed in reactors in Studsvik and Jülich. Encapsulated pebbles were irradiated and the measured Cs concentration profiles were shown to agree with those calculated from the above diffusion coefficients. The calculated release rate also agreed with the release rate from the AVR as measured in the VAMPYR experiments. The calculated Cs-137 release rates from the above fuel types are shown in Figure 4-1, as a function of matrix contamination and exit gas temperature for a 3000 MW_{th} reactor operating in an OTTO-cycle mode.

For a 100 Ci/year Cs release, curve 3 of Figure 4-1 shows that the THTR fuel pebble with its BISO propylene coated mixed oxide fuel may be used up to mean gas outlet temperature of 970°C with an initial U contamination of the matrix of no more than 2.5×10^{-5}*. Since the present contamination is about 2.5×10^{-4}, however, Figure 4-1 shows that the existing THTR fuel would release about 700 Ci/year of ^{137}Cs. A uranium contamination of 2.5×10^{-5} has been reached in small fabrication batches but development is necessary to reach this level in large scale fuel production. Little improvement beyond the latter value of contamination can be expected since the uranium level in the natural graphite used in the fuel element matrix is about 10^{-6}, i.e., curve 6 of Figure 4-1 is the lowest release possible.

The following conclusions may be drawn from the above:

1. Up to a He-outlet temperature of 950°C the uranium contamination of the fuel matrix (all of the pebble except the coated particles) determines the Cs release.

2. The well-developed THTR fuel pebble with coated particle coatings deposited from propylene (BISO) is acceptable up to a He outlet temperature of 970°C if the uranium level in the fuel matrix is $\leq 2.5 \times 10^{-5}$.

3. TRISO coated particles in the THTR fuel element form will give acceptable fission product release up to at

*$\frac{\text{This is wt. of U in the graphite}}{\text{Total wt. of U in the fuel}}$

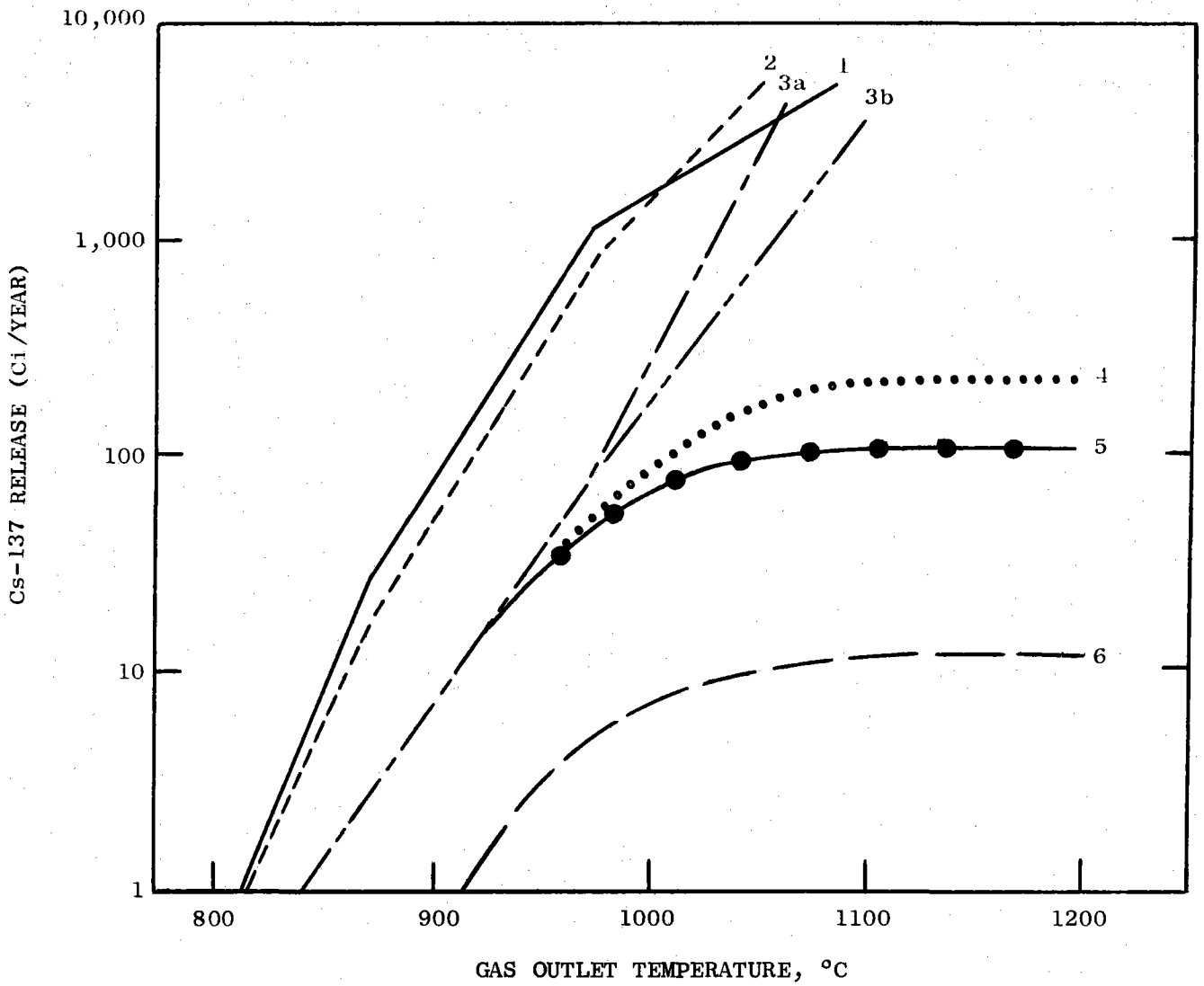

CYCLE: OTTO
POWER: 3000 MWt
BURN P: 100,000 MWd/T
GAS INLET TEMPERATURE: 250 °C
FUEL RESIDENCE TIME: 890 DAYS
POWER DENSITY: 9MW/m^3

CURVE NO.	SYMBOL	FUEL	MATRIX COMBINATION	FRACTION OF FAILED PARTICLES	FUEL ELEMENT
1		FEED-TRISO BREED-BISO	2.5×10^{-4}	10^{-3}	CONVENTIONAL
2		MIXED-BISO	2.5×10^{-4}	NONE	CONVENTIONAL
3a		MIXED-BISO	2.5×10^{-5}	NONE	CONVENTIONAL
3b		MIXED-BISO	2.5×10^{-5}	NONE	ZONED
4		FEED-TRISO BREED-TRISO	2.5×10^{-5}	10^{-4}	CONVENTIONAL
5		MIXED-TRISO	2.5×10^{-5}	NONE	CONVENTIONAL
6		MIXED-TRISO	2.5×10^{-6}	NONE	CONVENTIONAL

Figure 4-1. Release of Cs-137 as a Function of Gas Outlet Temperature.

least 1170°C if the matrix contamination is $\leq 2.5 \times 10^{-5}$ and the irradiation induced pyrolytic coating failure fraction is $< 10^{-4}$.

4.3.3 FUEL ELEMENT SPECIFICATIONS

I. Fuel Element - Coated fuel particles in A3 matrix

Conventional Element

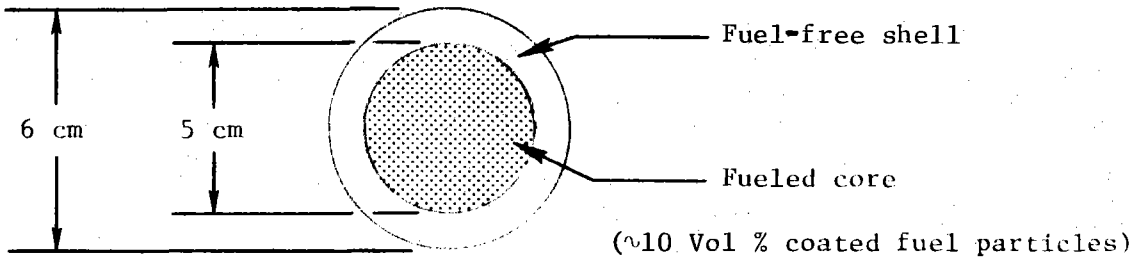

II. Matrix

75 % natural flake graphite
15 % petroleum coke
10 % phenol resin

III. Coated particles

A. BISO

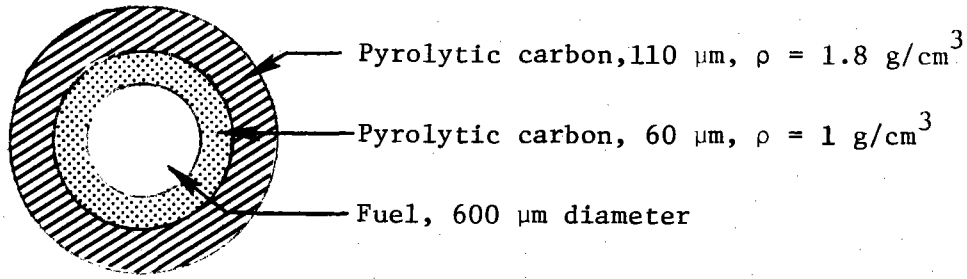

B. TRISO

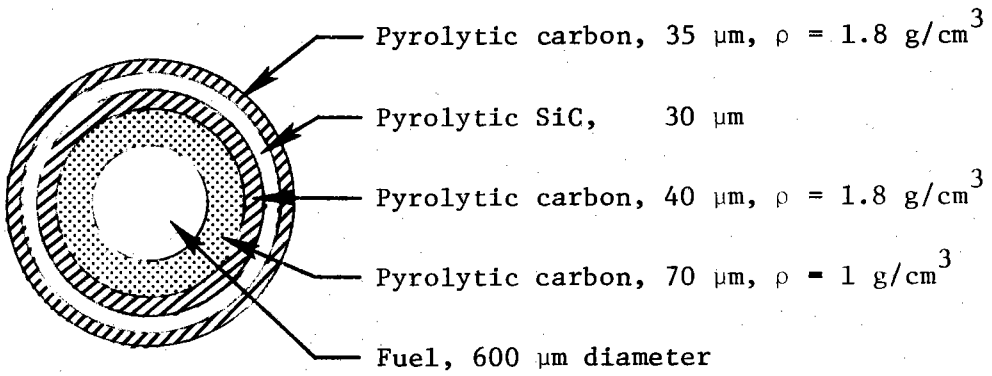

IV. Specifications

A comparison of THTR, AVR and PR3000 Fuel Elements

Quantity	Units	THTR	AVR	PR3000 (Case 4021)
$T_{aver.\ gas\ outlet}$	°C	750	950	950
Power density	MW/m^3	6	2.5	5
Power	MW_T	750	50	3000
Diameter of balls	cm	6	6	6
No. balls/m^3		5400	5400	5400
Ball type		Convent.	Convent.	Conventional
Shell thickness	cm	0.5	0.5	0.5
Particle Type		Mixed	Mixed	Mixed
Particle cladding		BISO	BISO	BISO
Diameter of Particles	μm	400		600
Thickness of Coatings	μm	60 μm acetylene	-	80 μm acetylene
		110 μm HTI-methane		80 μm LTI propylene
Heavy metal/ball	g/ball	11	6	10

Quantity	Units	THTR	AVR	PR3000 (Case 4021)
Vol. fraction of coated particles in matrix	Vol. %	8	5	8
Matrix		A3	A3	A3
Fuel		(U,Th)02	(U,Th)02	(U,Th)02
Enrichment of Fuel	% $\frac{U-235}{U}$	93	93	93
Ratio $\frac{Th}{U}$ (first core)		Zone 1 10 2	5	Zone 1 11 2
$\frac{N_C}{N_{HM}}$			350	
Density of fuel	g/cm^3	10	10	10
X-133 release	R/B	$5x10^{-4}$	$1x10^{-5}$	10^{-5}
Burn up (max)	MWd/T_{HM}	130,000	161,000 (1974)	118,000
Burn up (mean)	MWd/T_{HM}	115,000	95,000	109,000
Fast dose (max) E >0.1 MeV ($.10^{21}$)	n/cm^2	6.3	3.1 (1974	6.0
Fast dose (mean) E >0.1 MeV ($.10^{21}$)	n/cm^2	6.0	2.0	5.7
Maximum power/ball	KW_t/ball	3.2	1.7	2.4
Mean power/ball	KW_T/ball	1.1	0.52	0.93
$T_{max.fuel}$ (material tested up to:)	°C	1250	1250	1250
$T_{max.surface}$ (material tested up to:)	°C	1050	1050	1050

Quantity	Units	THTR	AVR	PR3000 (Case 4021)
$T_{max.\ fuel\ (nominal)}$	°C	1050	1041Tg=850 1154Tg=950	1010
$T_{max.\ surface}$ (nominal)	°C	910	973Tg=850 1081Tg=950	994
Hot spot adder for $T_{max.\ fuel}$	°C			48
Hot spot adder for $T_{max.\ surface}$	°C			30
$T_{random\ peak\ fuel}$	°C			1058
$T_{random\ peak\ fuel\ surface}$	°C			1024
Residence time (max)* (full power days)	days	1450		2320
Residence time (aver)* (full power days)	days	1260	1950	1633

4.3.4 FUEL DEVELOPMENTS FOR NEAR BREEDERS

To achieve a high breeder rate requires an optimization of the neutron economy in the reactor. On the basis of a favorable η value of U-233 even a breeder rate of one is achievable for the thorium cycle, Figure 4.2. A preliminary study shows the influence of different parameters on the breeding relationship. Factors favoring high breeding rates are:

1. A high proportion of U-233 in the mixture of fission material isotope.
2. High thorium input into the core.
3. Low fission product poisoning

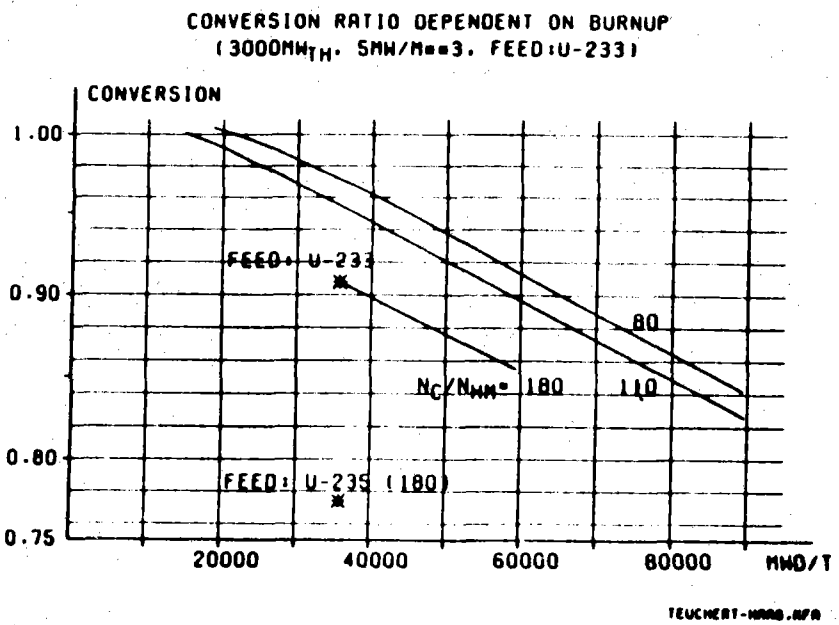

Figure 4-2. Conversion Rate U Functions of Heavy Metal Input and Burnup

4. Low U-236 content.
5. Small average power density (minimal Pa- and Xe-Absorption).
6. Large core volume (minimum neutron leakage).
7. Base load operation (minimum control poison input).
8. Most homogeneous possible distribution of coated particles in the pebbles.
9. Small coated particle kernels diameter.

A heavy metal load of 20.1 gm/pebble corresponds to a moderation ratio of 180. Fuel elements of this kind are at the present time being tested (AVR). A load of 32.4 gm/pebble corresponds to the relationship of N_C/N_{HM} = 110. This can be realized through a filling density of 21% for the coated particles in the matrix and a thickness, reduced to 3 mm, of the outer pebble shell which is free of fuel. In a view of the present pebble press procedure these data represent an upper limit of the possible specifications. A moderation ratio of 80 appears achievable with a warm press manufacturing technique.

To minimize neutron losses to fission products the high converter fuel balls pass through the core in approximately six months rather than the three years of the normal converter fuel. The fuel burnup is approximately 20,000 MWD/T rather than 100,000. Because of the lower fission product inventory in the reactor a reduced fission product release is expected.

SECTION 5

REFERENCES

1. Tschamper, P., et al., "The VHTR for Process Heat", General Electric Co., GEAP-14018, Sept. 1974.

2. Woike, O. G., et al., "Small Nuclear Process Heat Plants (SNPH)" General Electric Co., GEEST 75-001 (ORNL-Sub-4352-1), Nov. 1975.

3. Fraas, A. P., and Ozisik, M. N., Heat Exchanger Design, Wiley, 1965.

4. Bond, J. A., et al., "Design of a Helium-Heated Duplex-Tube Steam Methane Reformer", General Electric Company, ESTD Report ESTD 76-06, to be published.

5. Cooper, K. C., "Steam-Methane Reforming and Intermediate Heat Exchanger Model (PHXSTP) for Nuclear Process Heat", Office Memorandum, Los Alamos Scientific Laboratory.

6. Hyman, M. H., "Simulate Methane Reforming Reactions", Hydrocarbon Processing, July 1968, Volume 217, n. 7.

7. Juntgen, H., Van Heek, K. H., and Klein, J., "Comparative Investigations into the Kinetics of Gasification with Steam or Hydrogen and Conclusions for Gasifier Design", Gordon Research Conference on Coal Science, July 2-6, 1973.

8. Juentgen, H., Van Heek, K. H., Duerrfeld, R., and Feistel, P. O., "Steam Gasification of Coal Using Heat from HTR's", Traus Am Nuc. Soc. The European Nuclear Conference, April 21-25, 1975, p. 715-717.

9. Anon, Advanced Gas Cooled Nuclear Reactor Materials Evaluation and Development Program, General Electric Co. Proposal CFEX P-75-12 (ERDA RFQ, Dated October 9, 1975), December 8, 1975.

APPENDIX A

CHEMICAL HEAT PIPE SYSTEM

TABLE OF CONTENTS

LIST OF FIGURES

LIST OF TABLES

APPENDIX A

CHEMICAL HEAT PIPE SYSTEM

Steam-Methane reforming is one of the most promising applications of nuclear process heat. Figure A-1 shows how the use of the HTR to reform water and methane into hydrogen and carbon monoxide can be the basis for many applications. For the purposes of this particular study, one of these applications, the chemical heat pipe, was selected as representative of the entire class of uses. This choice allows the design of different heat transport systems to be related to a common end use, thus allowing a fair comparison between competing heat transport concepts.

A.1 INTRODUCTION

The chemical heat pipe (Figure A-2) is a system for the conversion of heat energy to chemical energy and the reconversion of the chemical energy to heat at a remote place and/or time. Energy transmission and storage are accomplished by pumping and storing a heat-converted chemical substance. Inherent in the scheme is a reversible endothermic/exothermic chemical reaction. The chemical heat pipe chemical reaction(s) should have the following characteristics:

(1) reversibility of the chemical reaction system, i.e. no loss of reactant through irreversible subsidiary reactions;

(2) sufficiently large reaction enthalpy and as high a conversion as possible so that high energy densities result for the products to be transported;

(3) favourable temperature region for the forward and the back reaction (i.e. for the endothermic reaction, up to 850°C and for the exothermic reaction, possibly higher than 500°C);

(4) the required catalysts should be available in sufficient amount and at low costs;

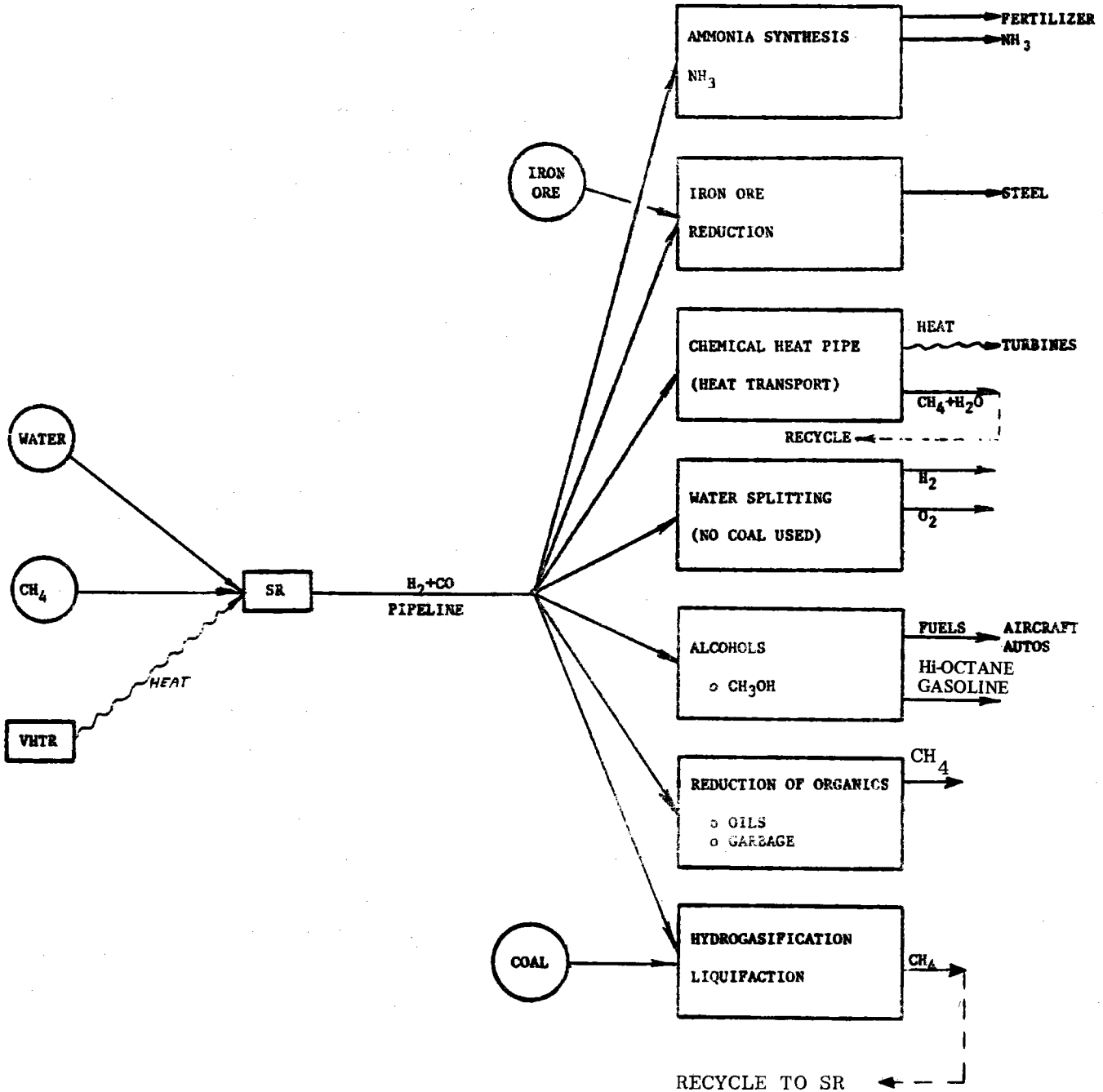

Figure A-1. Potential Uses of the HTR for Process Heat.

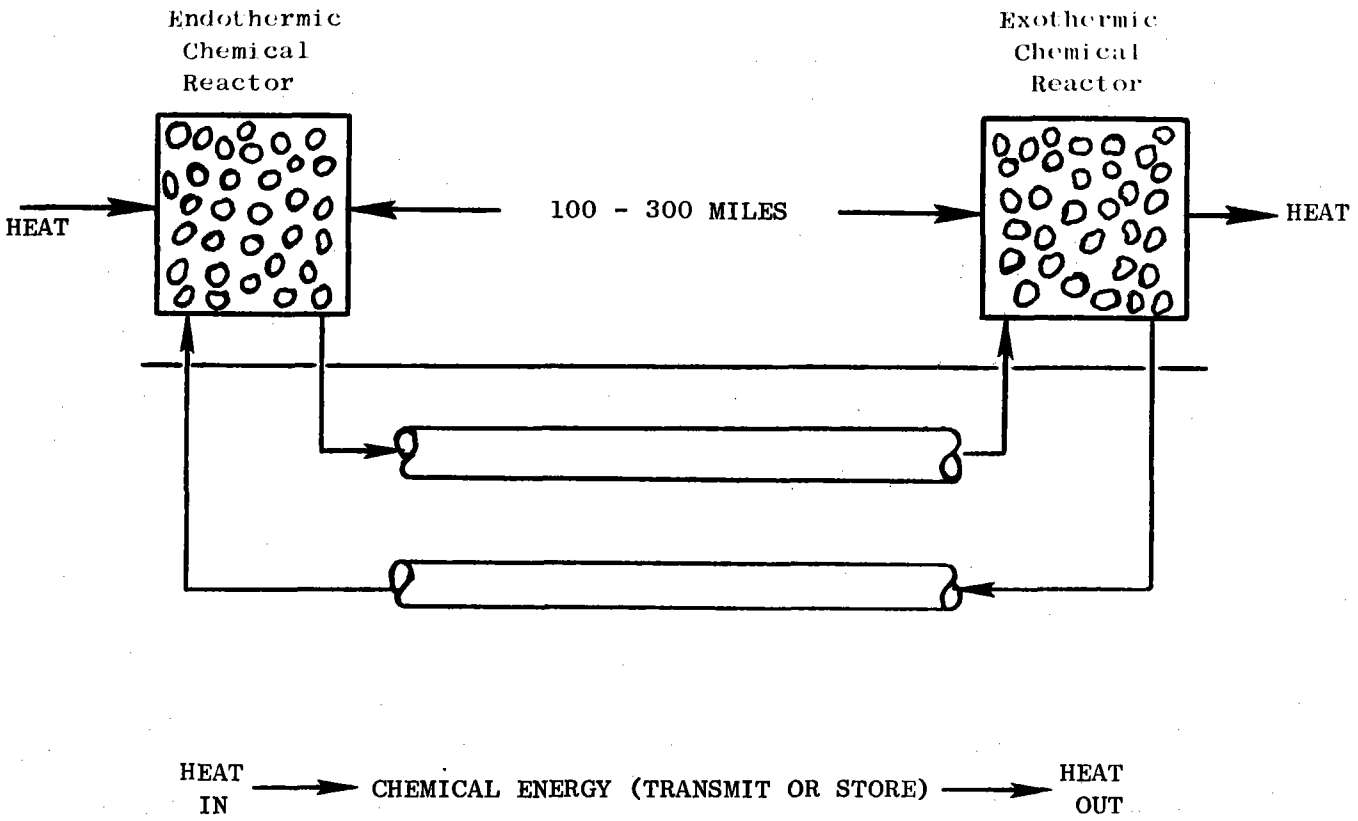

Figure A-2. Chemical Heat Pipe Concept.

(5) use of strongly corrosive or toxic substances should be avoided; and

(6) availability of the utilized substances in large amounts and at low costs.

For the HTR heat source application in which heat is delivered as high-temperature steam, the reactions below were selected.

$$CO + 3H_2 \rightleftarrows CH_4 + H_2O \quad \Delta H = 49 \text{ KCAL/Mol}$$

$$CO_2 + 4H_2 \rightleftarrows CH_4 + 2H_2O \quad \Delta H = 39 \text{ KCAL/Mol}$$

Considerations supporting this selection include compatibility of the endothermic and exothermic reactions with the heat source temperature/pressure levels, and with the desired heat delivery temperature level, the high state of technology development, a long record of successful experience, the relative freedom from problems of side reactions, coke formation and corrosion, and the low cost of methane.

A chemical heat pipe system using a HTR heat source and based on the steam-methane reactions is illustrated schematically in Figure A-3. In succeeding portions of this appendix, this system including the reformer - heat recovery heat exchanger - steam/power generation plant, the pipeline/storage subsystem, and the methanator plants distributed at heat user locations will be discussed in some detail.

Such a system has been under preliminary design study by KFA in the FRG for some time, and KFA is presently engaged in development of the helium-heated steam reformer component. Methanator technology for temperature levels as high as 1400°F is under development in this country (Reference A-1). Pipeline technology is presently well developed, for CO-CH_4 gas mixtures. The General Electric Corporate Research and Development Laboratory is currently engaged in a chemical heat pipe technology assessment/conceptual design/economic evaluation study contract for ERDA.

Both KFA and General Electric have identified the nuclear-powered chemical heat pipe system as a potentially attractive source of industrial process steam and in-plant-generated electricity for the time period of 1990 and beyond. Specific advantages of this concept include the following:

(1) the cost of heat supplied as process steam is (even at current fuel prices) competitive with coal and other fossil fuel heat sources in large capacity installations and is significantly lower in cost for small-size units (below 100 MWth) and for low-capacity factor users (less than 4,000 hrs/year);

(2) the system is environmentally clean from a stack emissions standpoint and also provides a greatly reduced waste heat rejection rate at the nuclear site as compared with nuclear electric plants of equal thermal capacity;

(3) the concept provides for the utilization of nuclear heat by customers dispersed over a large, heavily populated area while permitting remote, secure location of the nuclear reactor.

A.2 CHEMICAL HEAT PIPE NUCLEAR PLANT

A system for the application of nuclear heat to the steam-methane reforming reactions and for efficiently interfacing these reactions with the cold gas delivery and return pipelines is shown schematically in Figure A-3. One configuration of a methanator plant in which the reverse (exothermic) reactions occur in order to deliver the transmitted energy as heat for the generation of process steam is indicated in Figure A-4.

Reactor heat is delivered to helium coolant circulating in the primary loop. The helium flow is cooled from 950°C to 600°C in the steam reformer and is then further cooled to an acceptable return temperature of 350°C in a steam generator. Thus, 58% of the reactor heat is delivered to the steam reformer, and 42% is used for the generation of steam. Limitation of steam reformer heating to the temperature range above 600°C (450°C process gas entering temperature) is required by the reforming reaction kinetics and equilibrium characteristics. The principal means for increasing the percentage of reactor power fed to the steam reformer is to raise the reactor outlet temperature. The helium coolant temperature range between 600°C and 350°C is ideal for the generation of high-pressure high-temperature steam. This steam is expanded through a turbine which generates power needed for the chemical heat pipe system compressors, and also provides extraction steam at a pressure somewhat above the pressure of the reformer process. An excess of power is also produced for utility distribu-

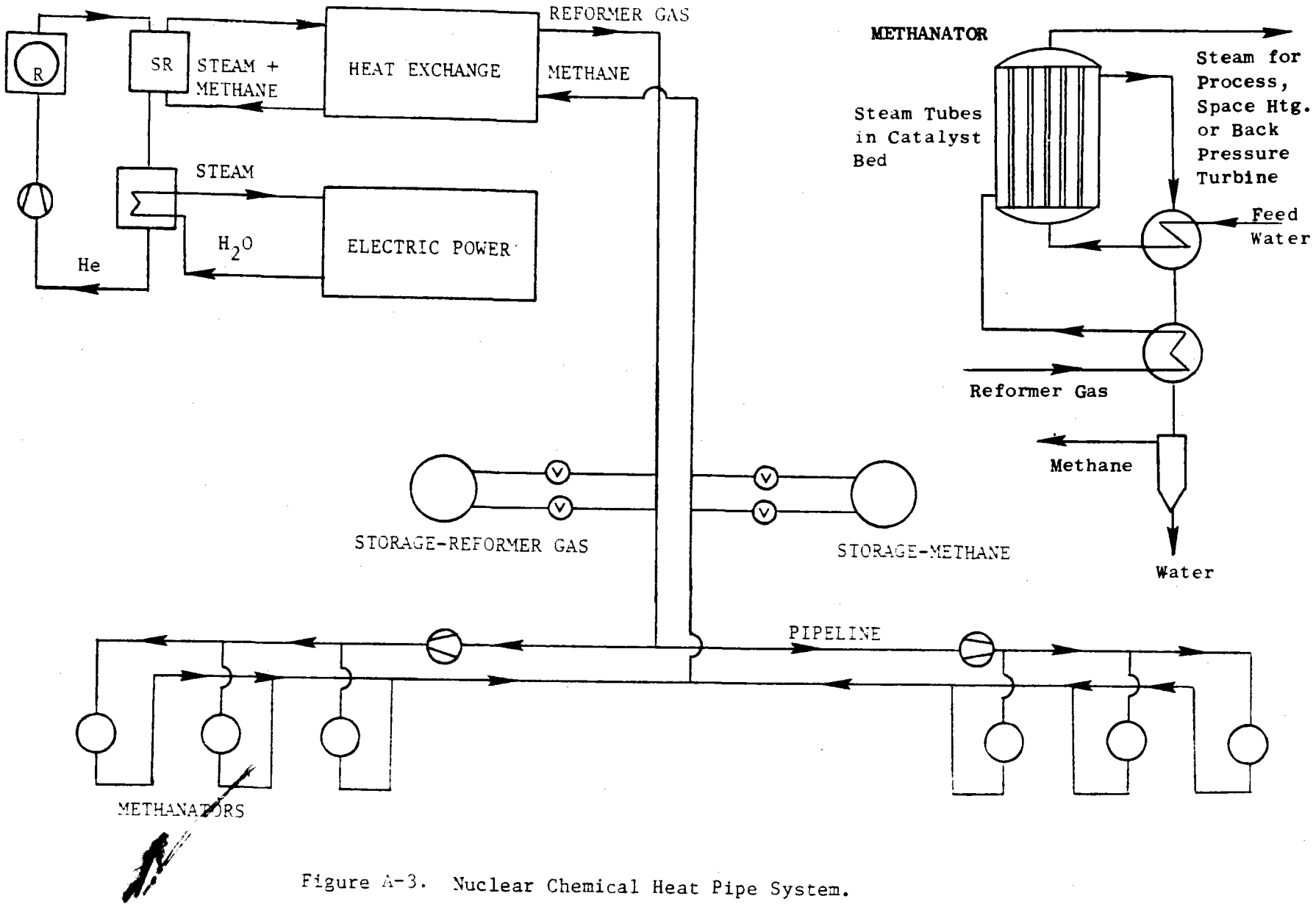

Figure A-3. Nuclear Chemical Heat Pipe System.

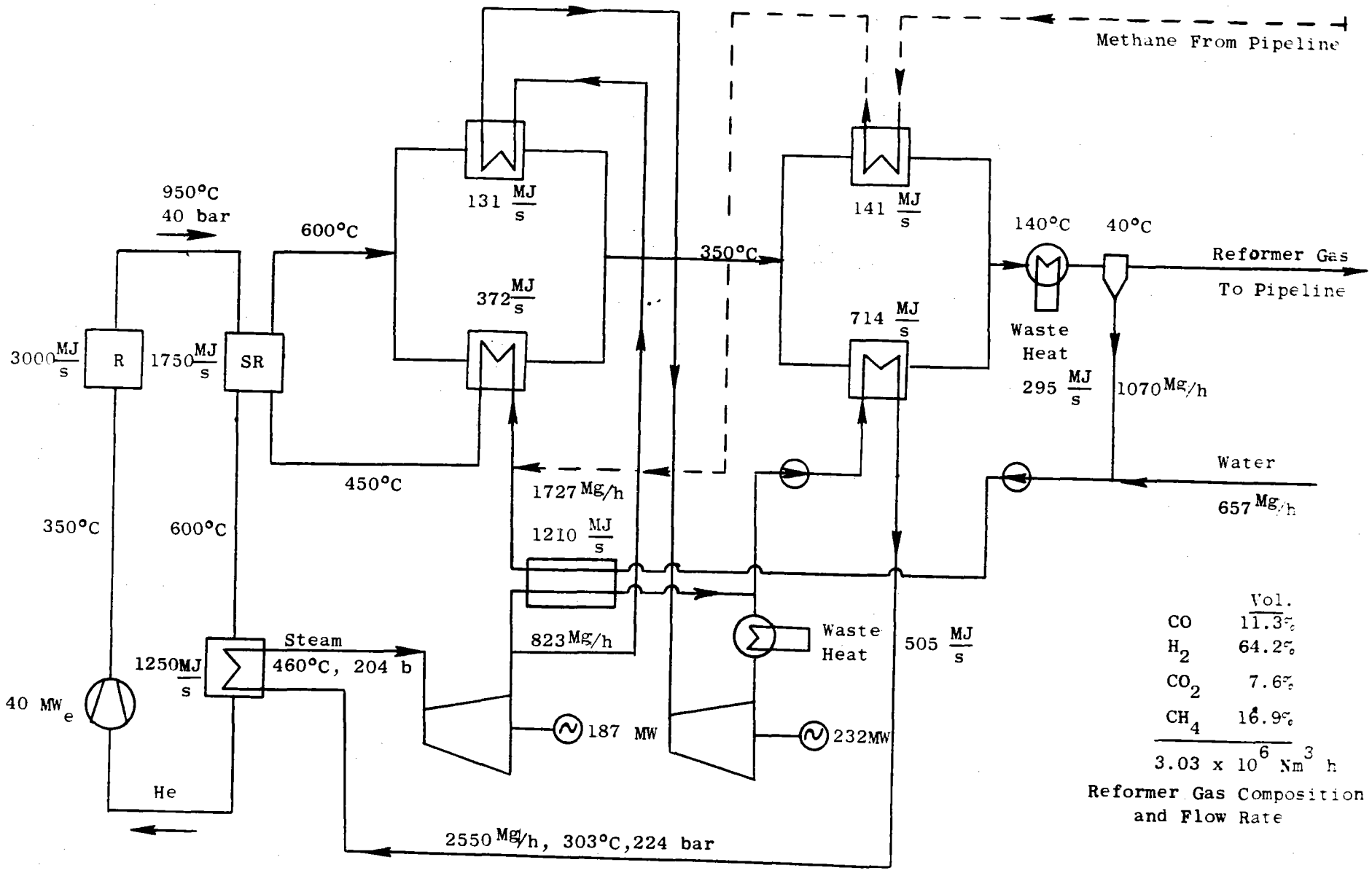

Figure A-4. Nuclear Plant for Chemical Heat Pipe System

tion. As shown in Figure A-4, the turbine extraction steam is not used directly for supply of the reformer but is condensed and subcooled in a heat exchanger (reboiler) in which reformer steam is generated. This provides a desirable isolation of the reactor-coolant-heated steam and the chemical heat pipe system gases. Duplex tube construction employed in the reformer tubes for isolation of the reactor coolant and the reformer gases is not required in the steam generator.

As a result of the extraction of turbine steam for the generation of reformer steam, a substantial transfer of energy occurs between the power generation system and the steam reformer (CHP) system. This results in a reduction in power generation. Net power output is further reduced by the portion of the primary loop circulator power chargeable to the reformer, by the portion of the feed pump power chargeable to the supply of steam for extraction, and by the consumption of power by the chemical heat pipe compressors. These effects are partially compensated by the supply of reheat energy and feed water heating energy to the power system from the reformer output gas cooling heat exchangers. Additional removal of sensible and latent (water condensation) heat from the reformer output gas is accomplished through preheating of the methane (returning to the reformer from the pipeline) and the steam-methane mixture. Although the total heat removal from the reformer gases is approximately equal to the heat addition to the methane plus the heat required for reformer steam generation and superheating, it is not possible to accomplish these two functions by direct transfer of heat, largely because the heat of condensation of the water in the reformer gas is available at a lower temperature than that required for steam generation. Thus, the necessity for the interchange of energy between the chemical heat pipe and the power generation flow steams. The efficiency of the chemical heat pipe system defined below, is largely a function of the effectiveness with which available energy is conserved in this interchange of heat. Changes in efficiency are reflected not in the power supplied directly to the steam reformer or in the rate of pipeline energy flow, but in the amount of excess electric power generated by the plant.

Two parameters of major importance are the steam/methane mole ratio in the reformer inlet steam and the maximum reforming temperature.

The reference system of Figure A-4 has a ratio of 2 and a maximum reforming temperature of 825°C. Increasing this ratio increases the percentage conversion of methane in the reformer, thus reducing the pipeline volume flow for a given rate of energy transport and also reducing the storage volume required. However, an increase in the water/methane mole ratio also increases the amount of steam which must be generated and condensed from the reformer discharge flow, an effect which results in larger heat exchanger capacity and plant compressor/pump power. KFA (Reference A-2) concludes that a ratio of 2 is close to optimum. The pipeline energy density is also critically affected by the maximum reforming temperature, since the equilibrium conversion of CH_4 increases with temperature.

A.3 PERFORMANCE EVALUATION OF REFERENCE DESIGN CHEMICAL HEAT PIPE SYSTEM

In Table A-1, the key performance numbers are tabulated for the reference design chemical heat pipe system (Figures A-3 and A-4) and the efficiency of this system is defined and calculated as a plant efficiency (.752), which includes the pipeline compressor power. As stated above, the losses involved in the plant efficiency stem from two principal sources: (1) parasitic electric power chargeable to the chemical heat pipe system, and (2) loss of available energy in the reformer plant heat exchangers. For the reference system, about 43% of the total loss is ascribable to parasitic power and 57% to net loss of available energy of the steam turbine resulting from steam extraction and other energy exchanges described above.

The .40 efficiency figure used in Table A-1 for the evaluation of reactor heat chargeable to net electric power generation is a reasonable nuclear electric plant efficiency for the steam conditions indicated in Figure A-4. Except for energy used by the chemical heat pipe system, only the indicated amount of reactor power would be required to supply the net electric power.

A.4 STEAM REFORMERS AND METHANATOR ASSEMBLIES

The configuration of the steam reformer - steam generator assembly is described in some detail in Appendix E. This heat exchanger unit is designed for location outside the primary PCRV containment but inside the

TABLE A-1

PERFORMANCE EVALUATION OF REFERENCE CHEMICAL HEAT PIPE SYSTEM

Power Input to Steam Reformer	1750 MW
Power Input to Steam Generator	1250 MW
Parasitic Power of Complete Nuclear Plant Primary Loop Circulator	40 MW
Compressor Power Required for Reformer Plant Heat Exchangers	30 MW
Miscellaneous Generation Plant Parasitic Power	31 MW
Compressor Power Required for 200-Mile Pipeline and Methanator Plants	60 MW
Thermal Power Delivered to Users	1772 MW
Net Electric Power Generated Before Subtraction of Pipeline Compressor Power	318 MW
Net Electric Power After Subtraction of Pipeline Compressor Power	258 MW
Thermal Power Chargeable to Net Electrical Generation at .40 Efficiency	
(a) Based on 318 Net MW	795 MW
(b) Based on 258 Net MW	645 MW
Total Reactor Power Chargeable to Chemical Heat Pipe System	
(a)	$1250 - 795 + 1750 = 2205$
(b)	$1250 - 645 + 1750 = 2355$
Chemical Heat Pipe System Efficiency	
(a) Not Including Pipeline Compressor Power	$\frac{1772}{2205} = .803$
(b) Including Pipeline Compressor Power	$\frac{1772}{2355} = .752$

secondary containment. The reformer units are designed as duplex tubes 12 meters in length having an inside diameter of 90 mm for the catalyst space. A helical "pigtail" tube removes the product gases and transfers sensible heat, corresponding to a 225°C temperature difference between the maximum process temperature and the product gas exit temperature, back into the process.

The duplex tube provides double containment isolation between the reactor coolant and the reformer gas. The internal design of the reformer tubes is based on proven technology demonstrated by KFA in the EVA facility (Reference A-3). At the design values of pressure, temperature, reactant gas composition, and flow rate, the reforming reactions proceed essentially to equilibrium, and the process is heat transfer limited.

A methanator configuration which is typical of the high-temperature (1400°F) technology that has been demonstrated by the Ralph M. Parsons Company is illustrated in Figure A-5. This design incorporates several adiabatic catalyst beds with heat delivery heat exchangers located between beds. Steam injection is required for some reactant gas compositions in order to eliminate coke formation. Design criteria for determination of the minimum amount of steam have been well developed (Reference A-1). It is necessary to provide heat recovery heat exchangers with the methanator for preheat of the reformer gas, cooling of the product gas, and condensation of the steam in the product gas. Recovery of the heat of condensation of the product steam represents an important portion of the delivered heat. If steam recirculation is required, this steam can be generated in a mixed flow evaporator designed as part of the heat recovery heat exchanger unit. With such a device, condensation of product steam can be directly employed for evaporation of recirculated steam. With independently generated injection steam, this is not possible since the partial pressure of the product gas steam is less than the required pressure of the injection steam.

An alternate advanced design concept proposed by KFA (Reference A-2) shown earlier in Figure A-3. This incorporates direct cooling of the catalyst bed. Some recirculation of product gas (by means of a compressor) may be required for coke elimination.

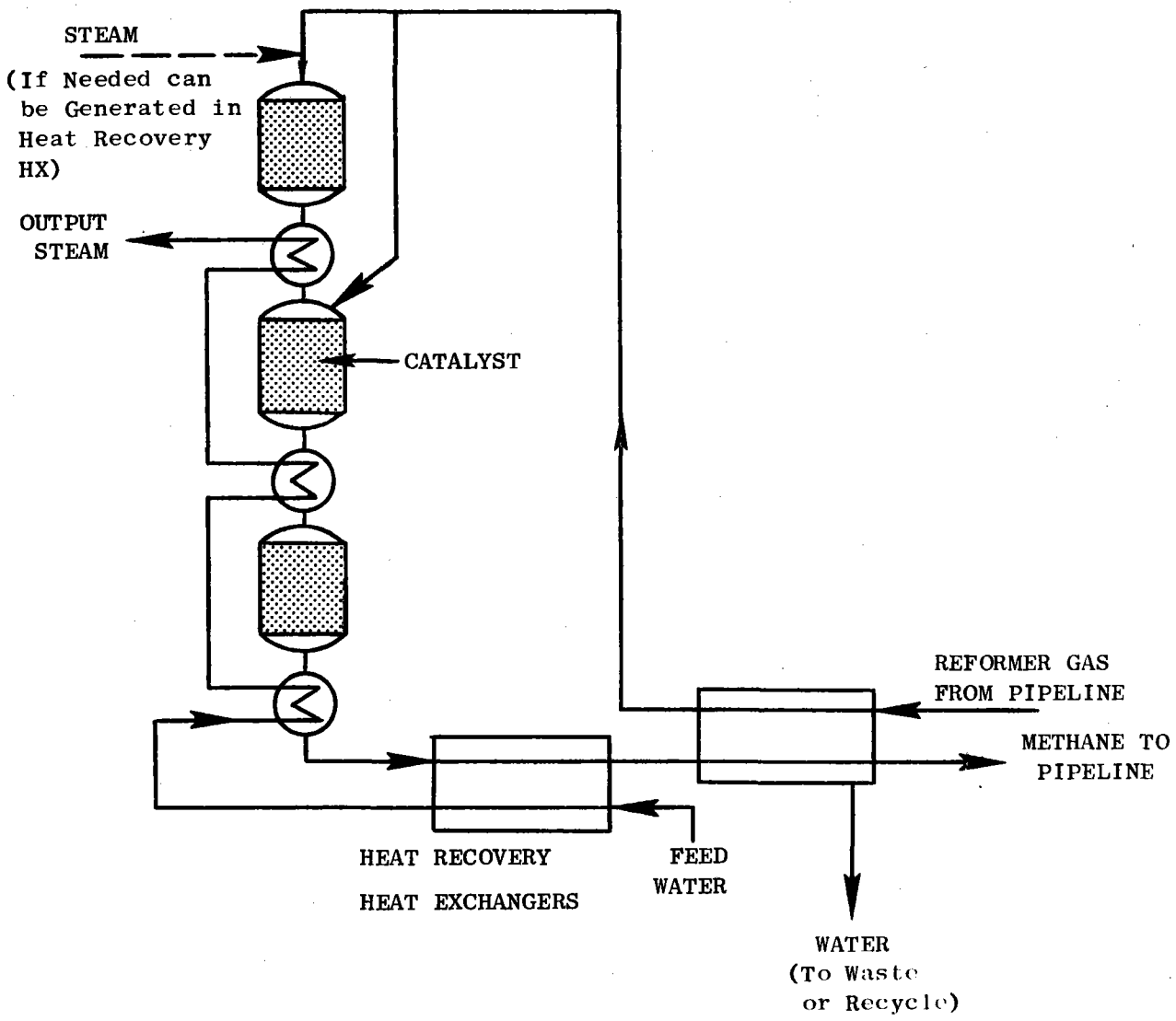

Figure A-5. Typical Methanator Configuration.

REFERENCES

A-1. "The RM Process," G. A. White, el at., The Ralph M. Parsons Company, Pasadena, California.

A-2. "Transport of Nuclear Heat by Means of Chemical Engineering," K. Kugeler, et al., Nuclear Engineering and Design 34 (1975), North Holland Publishing Company.

A-3. "Steam Reformers Heated by Helium from High-Temperature Reactors," K. Kugeler, et al., Nuclear Engineering and Design 34 (1975), North Holland Publishing Company.

A-4. "Nuclear District Heating and Nuclear Long Distance Energy," Th. Bohn, G. Dietrich, et al., June 1974.

APPENDIX B

NUCLEAR PROCESS HEAT TO GASIFY COAL

TABLE OF CONTENTS

LIST OF FIGURES

LIST OF TABLES

APPENDIX B

NUCLEAR PROCESS HEAT TO GASIFY COAL

The application of nuclear heat to gasify coal provides a way of combining the two most available energy sources to provide a source of premium fuel, natural gas, which is in declining supply. The use of nuclear energy reduces the amount of coal needed as the coal becomes only a chemical feed stock. In this study, two ways of coupling an HTR to coal gasification plants are described.

B.1 INTRODUCTION

The present depletion of natural gas reserves has led to the need for development of coal gasification plants. Many atmospheric pressure fixed-fuel-bed gas producer units were in operation about 50 years ago, but these were phased out because of the then plentiful supply of natural gas. There are many processes being developed for coal gasification, and these have been previously reviewed[B-1,B-2,B-3]. The main parts of all processes, however, generally follow three main steps: coal preparation, gasification, and raw gas upgrading. Each of these main steps may have several parts: coal preparation can include handling, storage, size reduction, and pretreatment (i.e., removing volatiles) of the coal feed; gasification may be in multiple stages and possibly include an auxiliary for H_2 preparation; and various parts of raw gas upgrading may involve such items as the shift for H_2 formation, acid gas removal, and methanation. This has been schematically depicted by Siegel and Kalina [B-2] as shown in Figure B-1. The reduction of steam with coal can be performed in a fixed bed, fluidized bed, or entrained phase; and the necessary heat supplied by burning coal or by heat transfer using either directly with solids, liquids, or gases or indirectly through a heat transfer system (i.e., through a wall barrier). Thus, it is possible to have 15 types of basic gasification process systems.

Various processes for coal gasification are shown in Table B-1 listing several critical features for each process [B-1,B-2,B-3,B-7]. Typical gas compositions resulting from some of the processes are shown in Table B-2 [B-3].

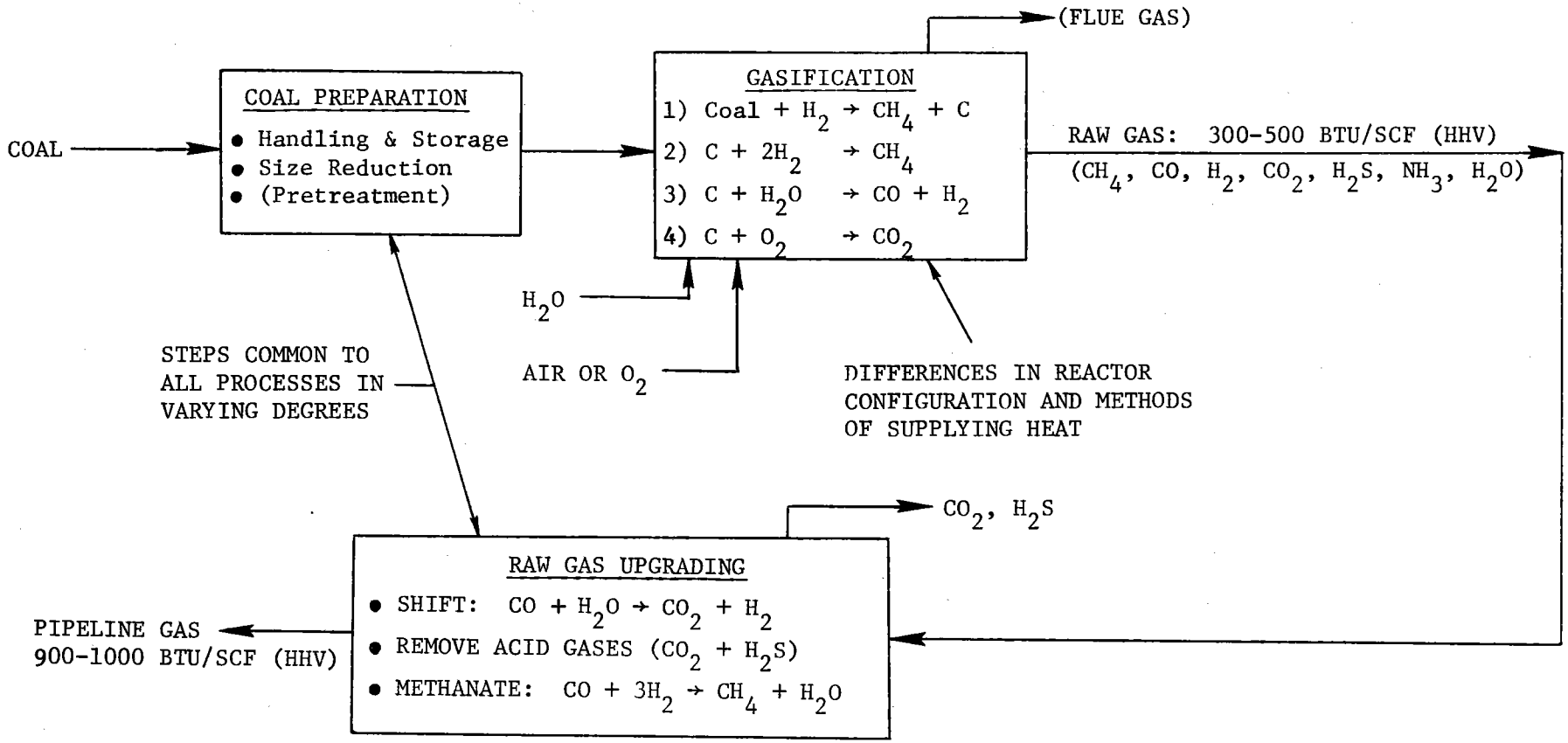

Figure B-1. General Process Scheme for Producing SNG From Coal[B-2].

TABLE B-1

TYPICAL PROCESSES FOR SYNTHESIS OF GAS FROM COAL

	Lurgi	HYGAS	BIGAS	Koppers-Totzek	Synthane	GA-SW	Kellog	BCR	German	
									Hydro gasification	Steam gasification
Coal Pretreatment	lump	slurried	slurried	pulverized	pulverized	liquidation of coal	pulverized add Na_2CO_3	pulverized		
Coal Degassing	none	combined	none	none	800°F		none	1200°F separate	none	combined
Gasification Bed	fixed	fluidized	entrained, fixed	entrained, fixed	entrained, fluidized		molten salt	fluidized	fluidized	fluidized
Bed Pressure, psi	300-500	1000-1500	1000-1500	15	600-1000		1200		~ 1200	~ 600
Max. Temp., °F	2400	1700	2700	2800	1850	1800	1700	2000	1830	1660
Gases Added	O_2, air + H_2O	H_2 rich	O_2, H_2O	O_2, H_2O	O_2, H_2O		O_2, H_2O	air, H_2O	H_2	H_2O
Char Bed Location	combined	separate	combined	one bed	separate	separate		separate (2100°F)	separate(1)	separate(2)
Ash	semi-slag	semi-slag	slag	slag			slag	semi-slag	dry	dry
Products	syn. gas + tars	syn. gas	syn. gas	syn. gas	syn. gas	syn. gas + liquids	syn. gas	syn. gas	CH_4	CH_4
Developer	Lurgi	IGT	BCR	Koppers	BOM	GA-SW	Kellog	Bituminous Coal Research	R Bkw AG	BF GmbH
Status	comm.	pilot plant	pilot plant	pilot plant	pilot plant	research stage	research stage	research stage		

(1) The R Bkw AG plant presently is based on using dry lignite directly or bituminous coal char from the BF GmbH process. Char from R Bkw AG is fed to a conventional steam plant.

(2) Char is fed either to R Bkw AG plant or to a conventional steam plant.

TABLE B-2

TYPICAL GAS PRODUCTS FROM THE GASIFICATION OF COAL[B-3]

	Lurgi (W/O_2)	Lurgi W/Air	Winkler W/O_2	Winkler W/Air	Bi-Gas	Synthane	HYGAS W/O_2	HYGAS W/Air	Hydrane	Koppers-Totzek	CO_2 Acceptor	Kellog Molten Salt	U-Gas
CO	9.2	13.3	25.7	19.0	22.9	10.5	18.0	13.5	3.9	50.4	14.1	26.0	17.0
CO_2	14.7	13.3	15.8	6.2	7.3	18.2	18.5	12.7		5.6	5.5	10.3	8.8
H_2	20.1	19.6	32.2	11.7	12.7	17.5	22.8	16.6	22.9	33.1	49.6	34.8	11.6
H_2O	50.2	10.1	23.1	11.5	48.0	37.1	24.4	18.3		9.6	17.1	22.6	12.0
CH_4	4.7	5.5	2.4	0.5	8.1	15.4	14.1	8.4	73.2		17.3	5.8	4.1
C_2H_6	0.5					0.5	0.5	0.6			0.4		
N_2, H_2S, etc.	0.6	38.2	3.5	51.3	1.0	0.8	1.7	29.9		1.3	1.0	0.5	46.0
Total	100.0	100.0	100.0	100.0	100.0	100.0	100.0	100.0	100.0	100.0	100.0	100.0	100.0
Heating Value (Dry Basis) BTU/SCF	302	180	275	118	378	405	374	236	826	298	440	329	150

The advent of relatively low cost process heat (with respect to fossil fuel) from the HTR* suggests that this approach has economic advantages for the production of gaseous, and possibly liquid, fuels from coal. One approach to this has been proposed by the GA/SW** team[B-5] using coal liquefaction as a feed. However, this proposed process has been reviewed for economy [B-6] with the suggestion that another approach would be more economical. Pilot plants for the steam gasification and hydrogasification of lignite and hard coal using pressurized fluidized beds are being constructed[B-7,B-8,B-9] in the Federal Republic of Germany for use with the HTR reactor process heat. Further the FRG is planning a 150 MW_t demonstration nuclear coal gasification plant.

The use of nuclear process heat for coal gasification has the potential to produce an environmentally acceptable gaseous fuel (synthesis gas) with minimum processing and maximum thermal efficiency. This gas can be produced as substitute natural gas (SNG) and/or as an intermediate BTU gas for general heat applications. The proposed general process flow patterns are shown in Figure B-2 for hydro-gasification to produce SNG and in Figure B-3 for steam gasification to produce the intermediate BTU gas. The processes, of course, can be arranged in other configurations depending on the demand for synthesis gas.

The general background of coal gasification is discussed below along with comment on some of the economic factors comparing this source of heat with that obtained by burning part of the coal. These comments are followed by suggestions on the work needed to more carefully evaluate these processes.

B.2 BACKGROUND DATA

The general background of coal gasification involves the basic reactions involved, the heat content of the resulting gases, and the factors influencing the gasification processes. These are described briefly below in terms of reactions and physical aspects.

---

*High Temperature Reactor

**General Atomic/Stone & Webster

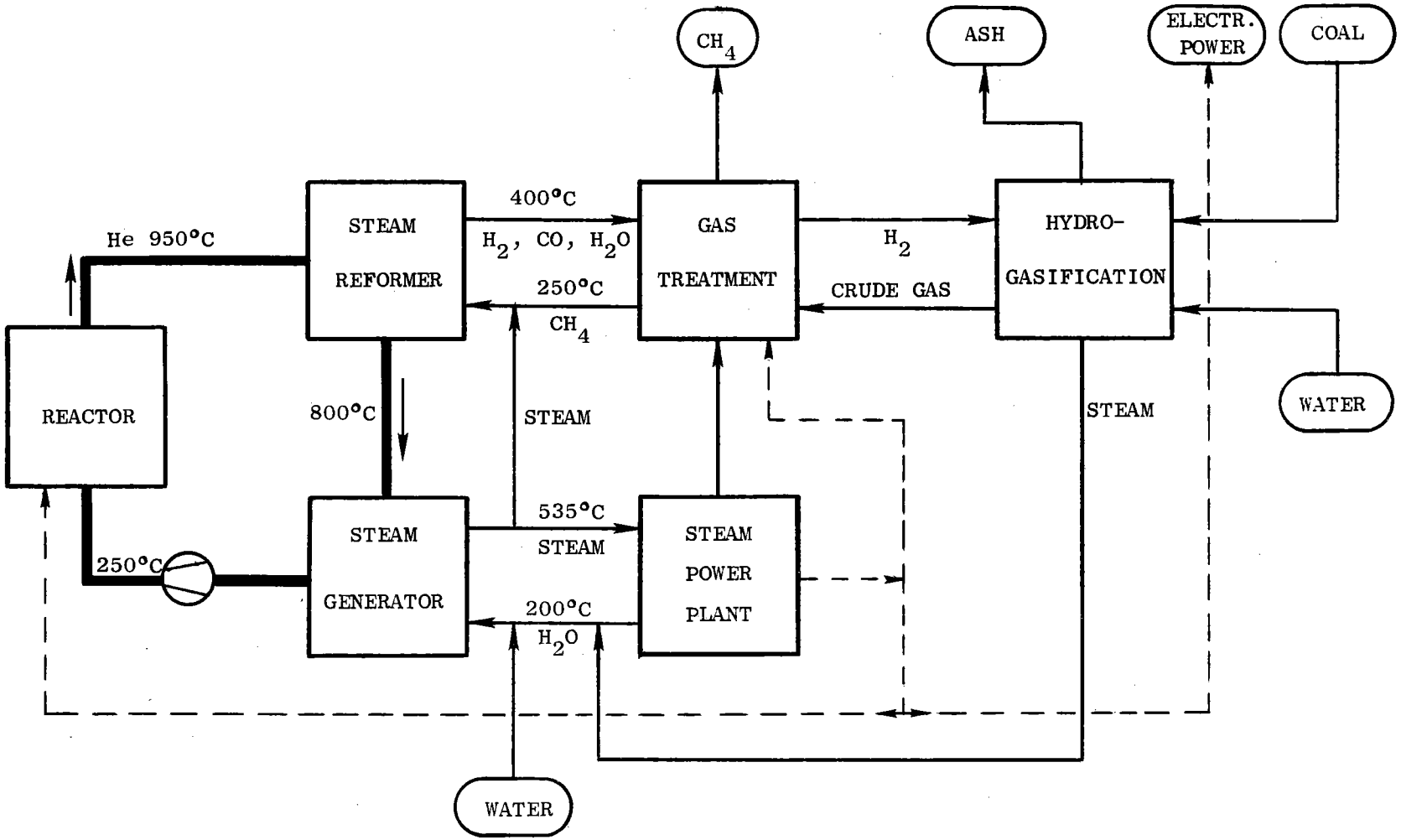

Figure B-2. Hydrogasification

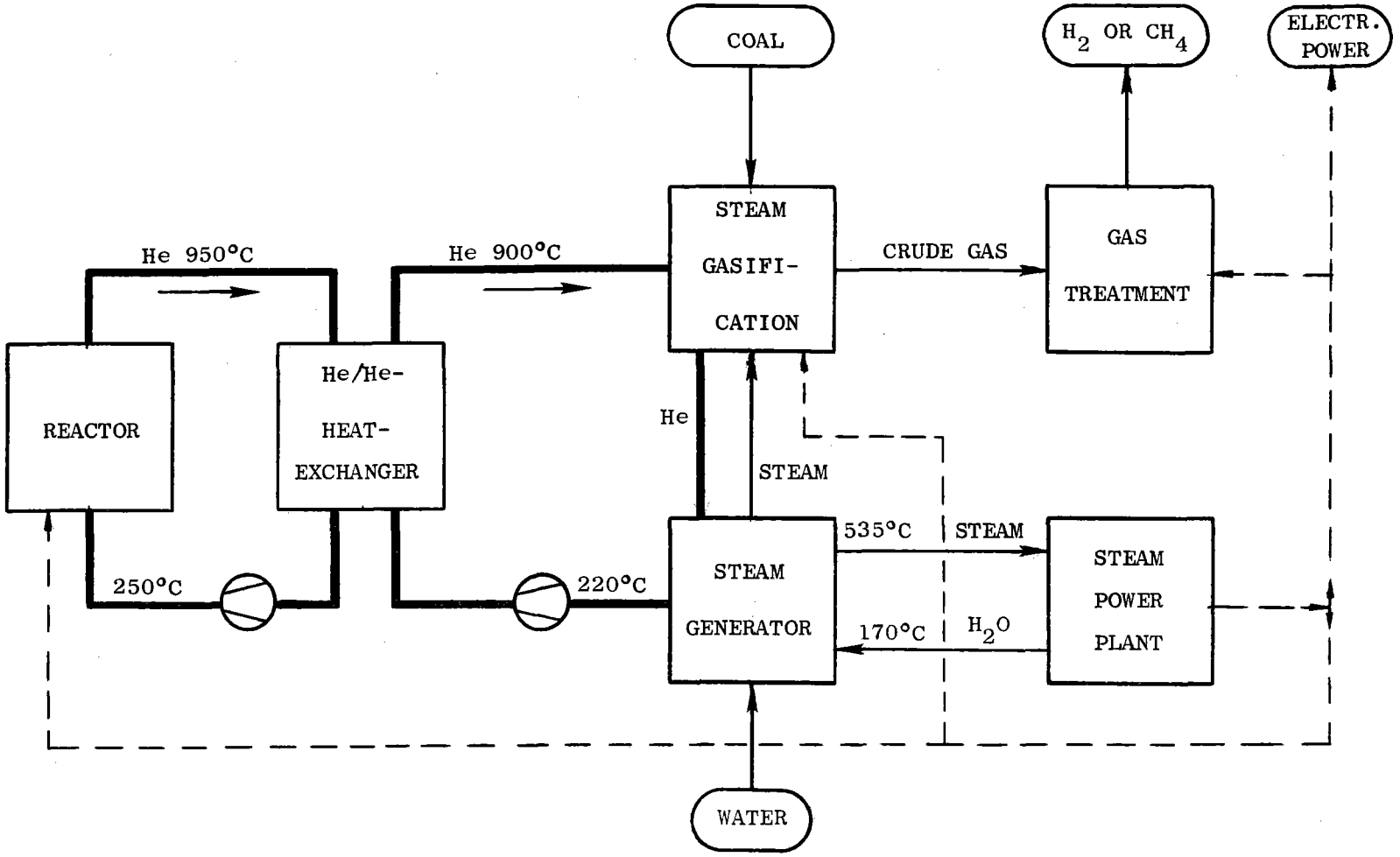

Figure B-3. Steam Gasification Using an Intermediate He Circuit.

B.2.1 Reactions and Gas Heat Values

The basic equations which are important in the gasification of coal are:

$C + H_2O = CO + H_2$; $\Delta H = +28.3$ kcal/mol (1)

$CO + H_2O = CO_2 + H_2$; $\Delta H = -9.9$ kcal/mol (2)

$C + 2H_2O = CO_2 + 2H_2$; $\Delta H = +18.5$ kcal/mol (3)

$C + CO_2 = 2CO$; $\Delta H = +38.2$ kcal/mol (4)

$C + 2H_2 = CH_4$; $\Delta H = -20.6$ kcal/mol (5)

$CO + 3H_2 = CH_4 + H_2O$; $\Delta H = -49.0$ kcal/mol (6)

$CO_2 + 4H_2 = CH_4 + 2H_2O$; $\Delta H = -39.1$ kcal/mol (7)

$CH_4 + H_2O = CO + 3H_2$ $\Delta H = +49.0$ kcal/mol (8)

$CH_4 + 2H_2O = CO_2 + 4H_2$; $\Delta H = +39.1$ kcal/mol (9)

In general, the primary reaction of steam gasification of coal is reaction (1) forming predominately hydrogen and carbon monoxide. The carbon monoxide may react with more steam to form carbon dioxide [equation (2)], the so-called shift reaction. Equation (3) then summarizes equations (1) and (2) to show the maximum yield of hydrogen. The carbon dioxide then can further react with carbon to form more carbon monoxide [equation (4)]. The hydrogen then reacts with carbon to form methane and carbon monoxide and carbon dioxide to form methane plus water [equations (5-7)]. The methane then can react with water to form carbon monoxide plus hydrogen [equation (8), the steam reformer equation] or, if conditions are suitable, carbon dioxide and hydrogen [equation (9)]. Thus, gas from the steam gasification of coal is a mixture of H_2, CO, CO_2, and CH_4 which becomes predominately H_2 and CO as the temperature is increased while increasing pressure raises the amount of CH_4.

The heating values for gases produced from coal are as follows:

$C + 1/2\ O_2 = CO$; $\Delta H_{298} = -26.4$ k Cal/Mol C (10)

$C + O_2 = CO_2$; $\Delta H_{298} = -94.05$ k Cal/Mol C (11)

$CO + 1/2\ O_2 = CO_2$; $\Delta H_{298} = (2)-(1) = -67.55$ k Cal/Mol C (12)

$H_2 = 1/2\ O_2 = H_2O$; $\Delta H_{298} = -68.32$ k Cal/Mol H_2 (13)

$CH_4 + 2O_2 = CO_2 + 2H_2O$; -210.8 kg Cal/Mol CH_4 (14)

$CO + 3H_2 + 2O_2 = CO_2 + 3H_2O$; $(-67.55)+(-68.3243) = -272.51$ k Cal/4 Mols Gas (15)

$CH_4 + H_2O = CO + 3H_2$; $+ 49$ k Cal/Mol CH_4 (16)

Reactions #10 plus #13 gives 135.87 x 3.968/0.835 x 2 = 323 Btu/cu ft gas which represents 646 Btu/cu ft CO. Reaction #14 gives 210.8 x 3.968/ 0.835 = 1002 Btu/cu ft gas.

Steam gasification requires coal plus steam to produce water gas $CO + H_2$ (reaction #1). This can, of course, be up-graded by methanation, by blending in methane prepared by hydrogasification or by some similar secondary process. In the first case the limiting factor is reaction #8 which shows that the final gas would be one made of CH_4 plus 3 moles of CO, (i.e., $4CO + 4H_2 \rightarrow CH_4 + 3CO + 2H_2O$), which would result, after removal of the H_2O, in a heating value of 493 Btu/cu ft of gas if only the methanation step is used.

The comparison of the heat values for methane (CH_4), water gas ($CO + H_2$), a mixture of these two, and typical synthetic gases produced by coal gasification are shown in Figure B-4.

Hydrogasification of coal produces CH_4 at the expense of adding hydrogen (reaction #5) which is mostly obtained by the steam reformer route (reaction #4) plus the shift reaction (reaction #2). There is some hydrogen in the coal but this is minor compared to the total amount needed to produce CH_4. While hydrogasification produces a gas of high heat value (i.e., CH_4 has 1002 Btu/cu ft), the process requires twice the amount of coal so that the net result is about the same available heat content of this gas per pound of coal feed as with steam gasification

The reaction rate of steam with coal depends on the coal structure and the temperature. This is illustrated in the data shown in Figure B-5[(B-11)] which shows the remarkably lower temperatures for gasification of the lignite as compared to the bituminous coal.

The reaction of hydrogen with coal [equation (5)] is also dependent on the reaction temperature. This is illustrated in Figure B-6 which shows the methane formation of lignite and bituminous coals as a function of hydrogen pressure and temperature for coal heated at the rate of 10°C/minute. The decrease in the curves suggest that after a peak rate diffusion becomes rate controlling (see also Ref. B-12 and B-13).

Since coals normally contain some oxygen, hydrogen, nitrogen, and sulfur, the effects of these are noticed in the gasification. Thus, even

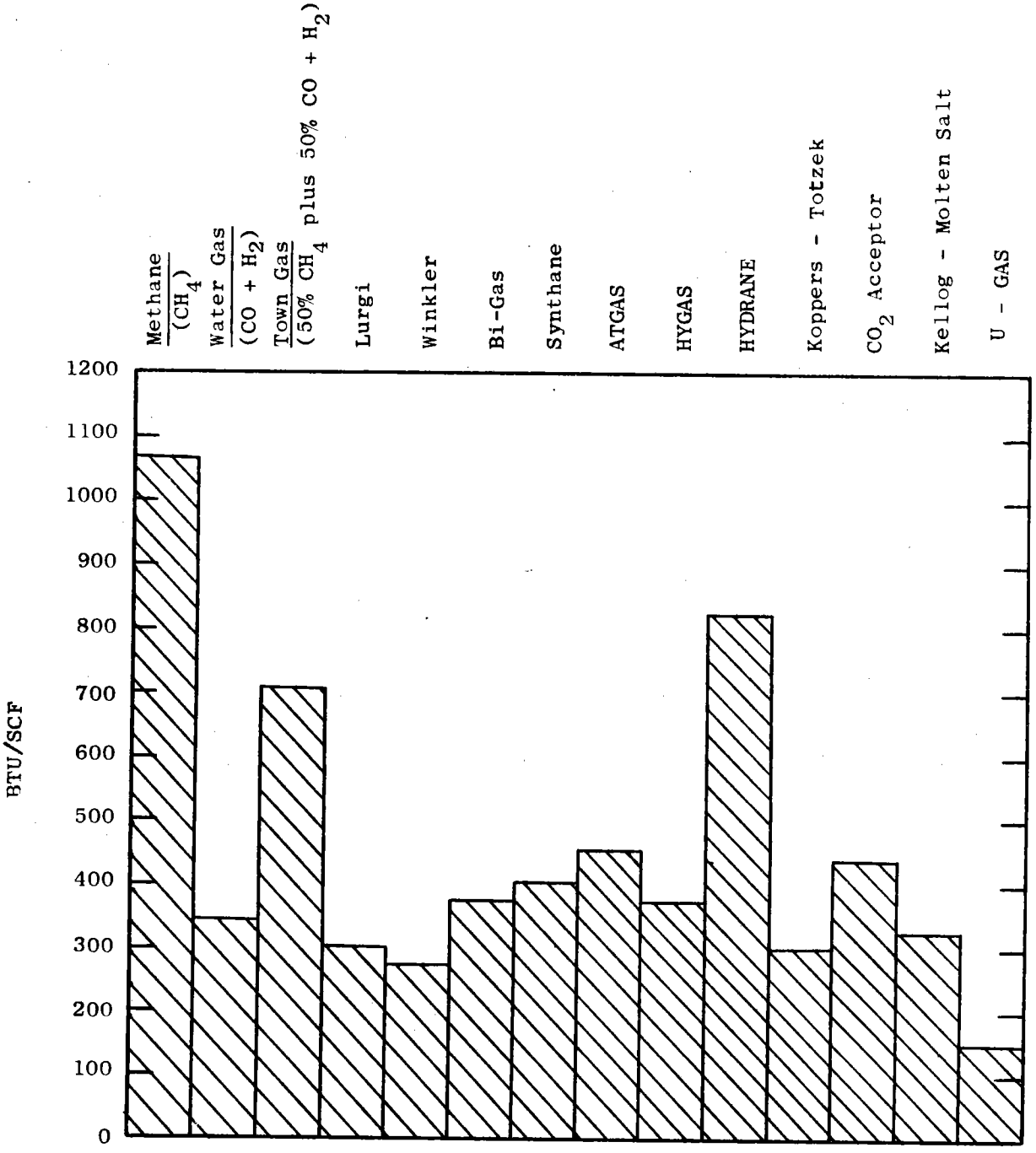

Figure B-4 Comparison of Heating Values of Products From Various Coal Gasification Processes.(B-4)

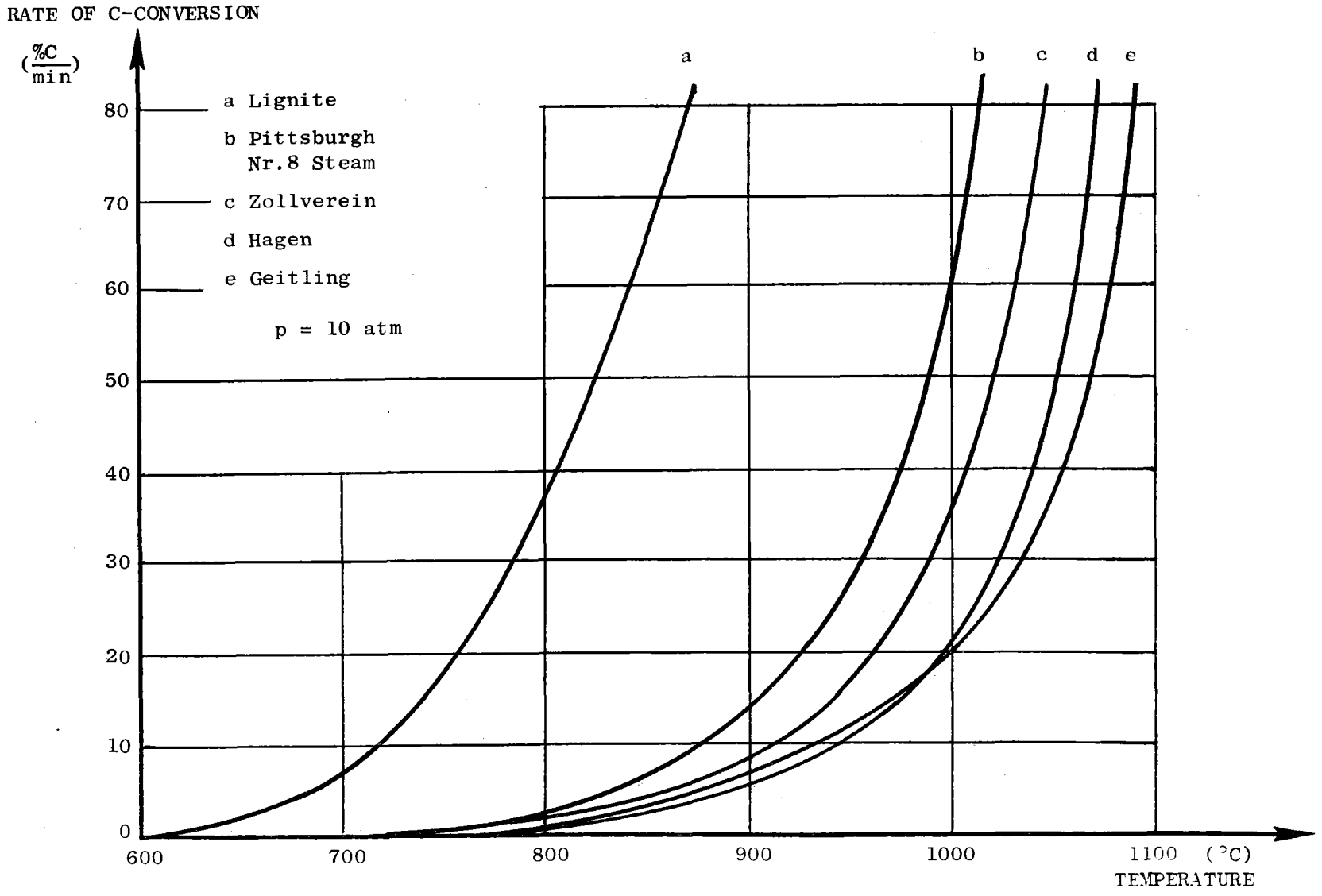

Figure B-5. Rate of Gasification as a Function of Isothermal Process Temperature.(B-11)

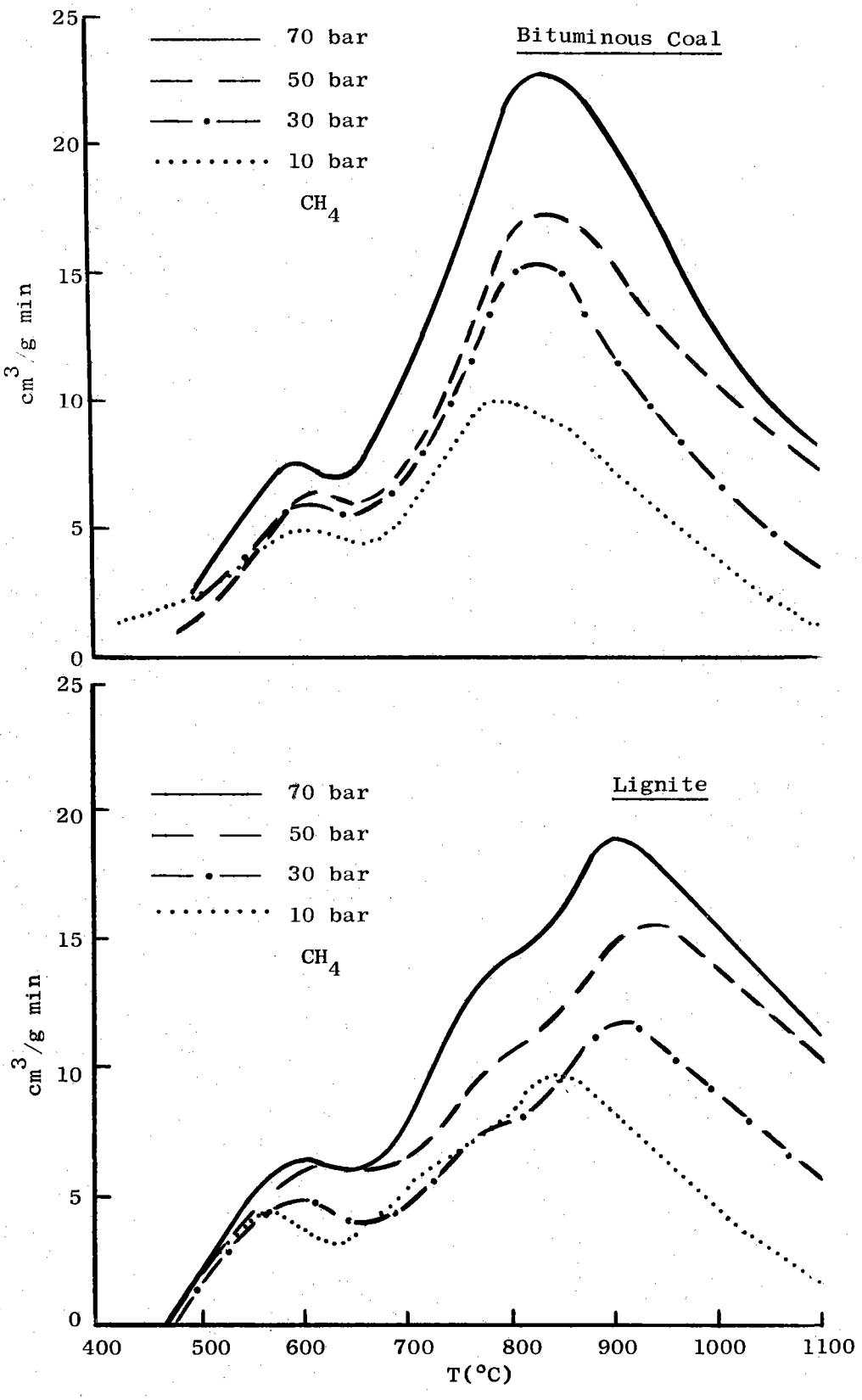

Figure B-6. Methane Formation During Hydrogasification; Heating Rate = 10 °C/min

with hydrogasification some CO_2 and CO will be present along with H_2S and NH_3. The effects of the oxygen are illustrated in Figure B-7[B-9] which show data on hydrogasification of bituminous coal and lignite as a function of temperature with 10 bar H_2. These data show that carbonization is occurring below the temperatures required for steam gasification (i.e., 300° to 700°C). Consequently, if the coal is heated slowly, the gaseous carbonization products (tars, etc.) will be present in the produced gas and, thus, require removal. On the other hand, if the coal is heated rapidly, the carbonization products are reacted to the same products CO_2, CO, H, and CH_4 as formed by the steam-carbon reactions.

The nitrogen content of coal is generally small. Consequently, if the coal is heated rapidly any ammonia formed will be rapidly split, leaving the produced gas with only nitrogen present which probably can be tolerated as a minor diluent. The sulfur, however, will form as hydrogen sulfide which has to be removed from the gas.

B.2.2 Physical Aspects

The coal bed can exist as a fixed bed (often with stirring), as a fluidized bed, or as an entrained phase. In the case of steam gasification, heat is supplied either by burning part of the coal with oxygen or by some heat transfer mechanism. The heat transfer by a gas medium such as a He heat exchanger is, of course, the most probable means to be used with HTR process heat.

The introduction of coal into a gasifier can take any of many forms - "powdered" coal, "solid" coal, "liquefied" coal, and "slurried" coal. The basic problems, of course, are related to bringing a high-surface-area solid into a pressurized system by the most economical technique because the high-pressure system shows higher rates of reaction and thus much more promise for high production rates with minimum capital investment.

The possibilities of ash acting as a catalyst has been noted above. These phenomena are generally related to the presence of transition elements and their availability to act as catalysts.[B-14] The ash also can be utilized for preheating the coal feed to recover this sensible heat. However, in any case, ash removal should be at the lowest practicable carbon content.

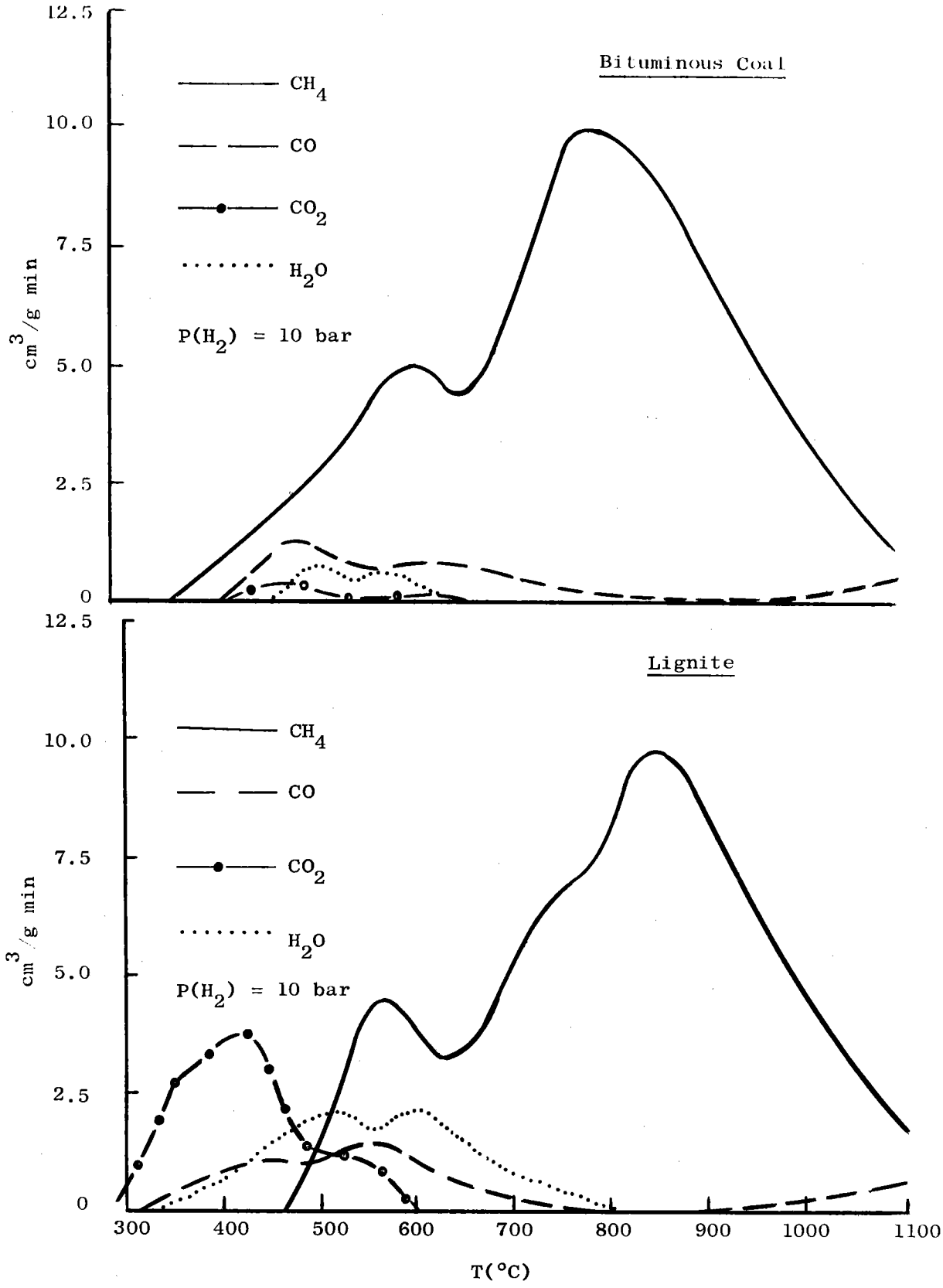

Figure B-7. Gas Formation During Hydrogasification; Heating Rate = 10 °C/min

The processes which occur are obviously complicated because of short residence time at temperature as well as by the competing mechanisms and other factors.[B-12,B-13] Process complication is also affected by possible caking of the feed due to the coal hydrocarbon content, volatilization of these hydrocarbons as oils and tars, excessive carbon in the discharged ash, and, as suggested above, the removal of fly ash and volatile impurities (S, N, etc.) from the synthesized gas.

B.3 SOME ECONOMIC CONSIDERATIONS FOR COAL GASIFICATION USING NUCLEAR HEAT

The use of nuclear heat for coal gasification has the obvious advantages of reducing the amount of coal used by eliminating the need for burning part of the coal to produce heat. The economic advantages of this approach will, of course, depend on the local economic factors which include the following:

1. The local cost of nuclear heat versus burning coal.
2. Cost of special equipment for transferring the nuclear heat to the coal gasification process.
3. The cost of auxiliary equipment for processes such as heat recovery, gas purification, etc.
4. Coal caking characteristics.
5. Process temperature limitations of nuclear heat.
6. Process parameters defined by local coal gasification kinetics, especially those which may be influenced by nuclear heat temperature limitations.
7. Process selection based on local conditions which are reflected in the market demand for coal gasification and/or liquifaction products including the question of using only steam gasification, only hydrogasification or a combination of both.
8. Extenuating circumstances related to combining coal gasification with other uses for char such as the use of char in conventional fuel burning electric power generation, etc.

Several of these factors are briefly discussed below.

B.3.1. Local Cost of Nuclear Heat Versus Burning Coal

The initial concept of coal gasification by nuclear heat as compared to producing the needed heat by burning coal assumes that in both cases generally similar equipment would be used. Significant exceptions include the need for a heat exchanger in steam gasification by using nuclear heat (described below) and the auxiliary equipment needed for heat recovery, etc. (which is briefly discussed in Section B.3.3).

B.3.2 Cost of Heat Transfer Equipment for Steam Gasification

Among the several possibilities of transferring the heat of the primary gas circuit into the gasifier, the best way seems to be to use an intermediate circuit of He as shown in Figure B-8[B-15]. This He passes through a heat-exchanger similar to an immersion-heater in a fluidized bed of coal and steam, and provides the heat necessary for the gasification of coal. The primary helium loop, intermediate loop and fluidized bed operate at the same pressure of about 40 bar. Steam required is generated and superheated with helium at a lower temperature level.

The intermediate circuit separates the nuclear part of the plant from the gasification unit. Thus it gives a higher degree of safety for the total plant, and inhibits permeation of hydrogen from the gasifier into the core of the reactor and of tritium from the nuclear part into the gas generator. Moreover, inspection and replacement of parts of the gasifier is easier. The amount of coal gasified in a thermal gas generator can be determined from the heat balance as given by the following equation:

$$\text{heat consumed} = \text{heat transferred}$$

$$q.k(T).\gamma.V = h.F.\theta(T,T_1,T_2,) \quad (B\text{-}8)$$

q = heat of reaction — Gcal/Mg

k = gasification rate — 1/h

T = gasification temperature — K

γ = density of the fluidized bed — Mg/m^3

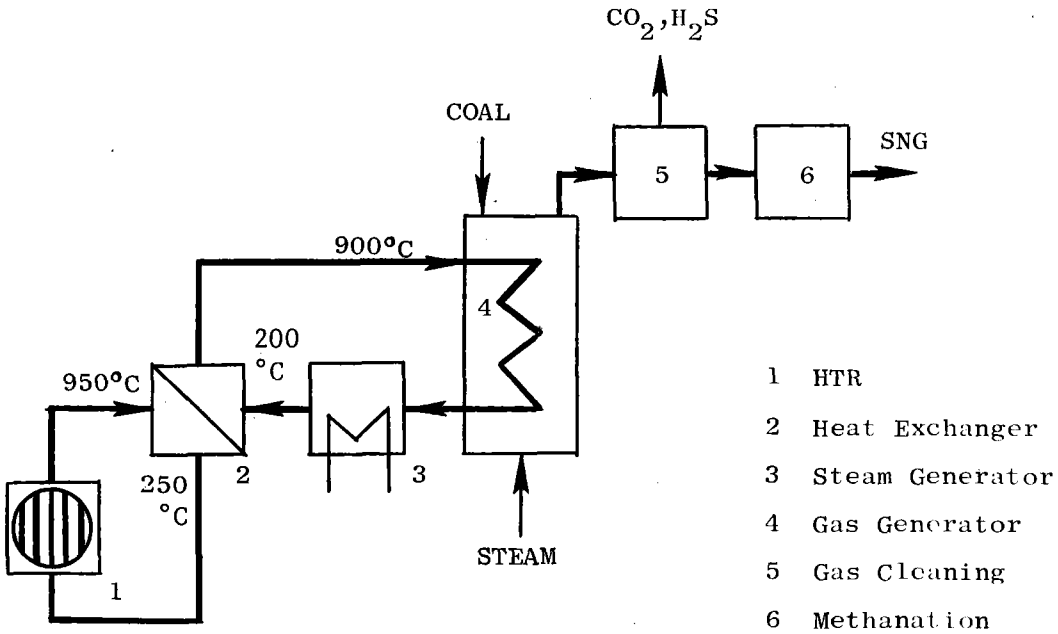

Figure B-8. Steam Gasification of Coal[B-8].

V = volume of the fluidized bed	m^3
h = overall heat transfer coeff.	$kcal/m^2 h°C$
F - heat transferring area	m^2
θ = log temperature difference	K
T_1 = helium inlet temperature	K
T_2 = helium outlet temperature	K

The heat transferred depends mainly on the overall heat transfer coefficient, whereas the heat consumed by gasification is mainly set by the gasification rate. Both sides of the equation depend on temperature. The gasification temperature at steady state is such that the heat consumed by the gasification reaction is equal to the heat transferred from the intermediate circuit into the fluidized bed.

An initial evaluation of the heat balance has been made. It was found that a heat transfer area of about 4000 m^2 and a fluidized bed volume of about 300 m^3 are necessary to assure a total throughput of approximately 50 Mg/h. This gasifier is shown in Figure B-9 (B-15). It consists of a horizontal cylindrical pressure vessel. In its interior is a trough whose walls serve as the inlet distributor for the steam entering the fluidized bed from below. The heat exchanger tubes, through which helium from the intermediate circuit flows, project from above into the fluidized bed which is bounded by the trough. According to present ideas, the coal (possibly after preliminary low temperature devolatilization) is introduced at one end of the gas generator. It moves in the longitudinal direction through the fluidized bed and is increasingly gasified. The ash accumulates at the other end and can be removed through an opening at the left hand end on the fluidized bed.

Thus, the use of a 3000 MW pebble bed reactor with eight to twelve intermediate heat exchangers can feed hot He to four such units at 750 MW each and thereby process approximately 200 Mg of coal per hour.

The most obvious item of special equipment thus is that of the heat exchanger for the steam gasification of coal which is expected to operate

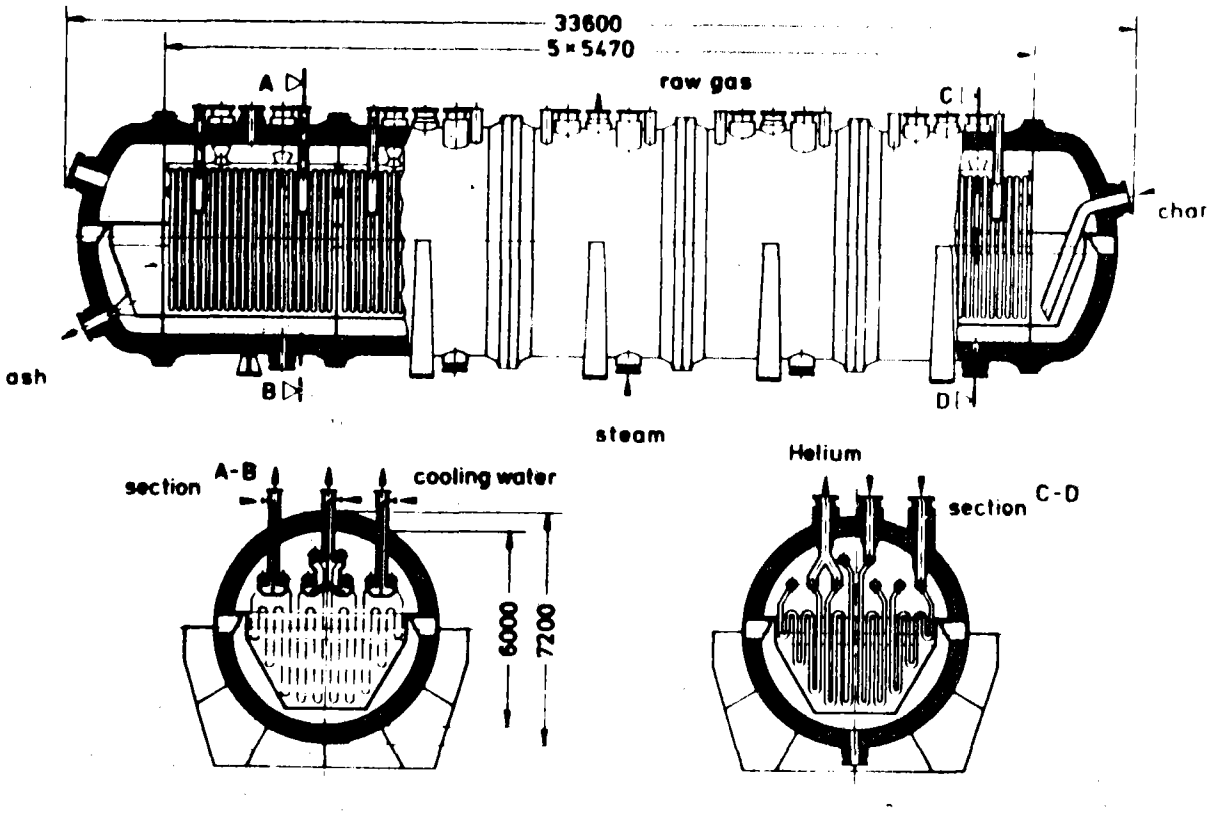

Figure B-9. Gas Generator - Heating Area 4000 m^2 (B-15).

economically using nuclear heat. This plus other process savings anticipated from using nuclear heat (i.e., less ash, less sulfur to remove, etc. as compared to burning coal) may offset this apparent higher cost of steam gasification due to the heat exchanger.

B.3.3 Cost of Auxiliary Equipment

The cost of other (i.e., other than the heat exchanger described above in Section B.3.2) auxiliary equipment associated with the gasification of coal will probably be slightly higher for using coal as a heat source as compared to using nuclear heat because of the need to handle more coal with the associated processing problems. This would, for example, include the need to remove more sulfur per product unit, increase the heat exchanger economy because of the greater quantity of waste products, etc.

B.3.4 Coal Coking Characteristics

The bituminous coals generally show strong coking behavior when heated due to the separation of the complex hydrocarbon polymers by thermal effects. Such behavior obviously will seriously affect the performance of a fluidized bed. One method of solving this problem is to thermally treat the coal as a "conditioning" step to volatilize these hydrocarbons. This solution has limited applications because of the limited market for these hydrocarbons (tars) and the added cost of the extra processing. A more preferred solution is to heat the coal particles very rapidly in the gasification unit to pyrolyze the hydrocarbons into the more desirable gases CO and CH_4. This process may be difficult to achieve economically in the steam gasification process using nuclear heat (i.e., through a heat exchanger). This problem obviously needs more study involving experimental work.

B.3.5 Process Temperature Limitations of Nuclear Heat

The present nuclear heat temperature limitation is about 1000°C which represents the upper limit of economical malleable metallic construction materials. These materials are the solution strengthened Ni base alloys which may be further strengthened by various precipitated phases. These can also be rendered more oxidation resistant by "surface" treatment with Al. Higher temperatures can be tolerated with the ceramic materials such as graphite and SiC but these require considerable development for use as construction materials for nuclear process heat handling.

These temperature limitations may not necessarily be a deterring factor, however, since, as noted above, the coal gasification process can be accomplished by these temperatures. The most probable limitation may be that of the steam gassifier heat exchanger which cannot provide temperatures above 850-900°C for the dehydrocarborization of the coal being fed to the unit. (See above under Section B.3.4).

B.3.6 Coal Gasification Kinetics

While much has been published on coal gasification kinetics, the questions of process economy on this subject relate to how rates of steam gasification using nuclear heat are limited due to the temperature limitations of the heat exchanger. For example, it is recognized that the $C + H_2O$ reaction of a high

ash coal can be diffusion rate limited, but the details of this are obviously dependent on local coal characteristics. This problem can, of course, be related to the use of char in certain localities. In other words, it may be most economical to remove only a portion of the carbon in the steam gasification process.

B.3.7 Effects of Local Markets

An example of this matter can be seen by comparing the gasification product market for the lignite of the Western states with the market for the gasification of Eastern bituminous coal. In the East there is a large demand for petrochemical needs and similar industrial requirements plus that of home heating which represents a demand for both "energy pipe" products such as $CO + H_2$ and the high energy gas CH_4. On the other hand, in Western areas, where industrial markets are at far distances, the demand will most probably be for mostly the high energy gas CH_4.

B.3.8 Extenuating Circumstances Relating to Char as a Product

The most effective use of nuclear heat for coal gasification is, of course, to gasify the carbon at the highest possible rate. Since the coal will almost always contain substantial ash, the rate of carbon gasification will decrease at 850-900°C. This unit, as mentioned above, requires about 43,000 square feet of heat transfer area to process 50 Mg of coal per hour. Using 1" OD pipe, this requires about 165,000 linear ft. of pipe. Data on corrosion studies[B-16] of this process show that Incoloy 800 is probably the most suitable alloy available today for this use. This much of that alloy in 1" OD pipe with about 0.070" wall would cost today about $700,000. Fabrication costs for the heat exchanger would probably double this cost. Thus, it would appear that the savings in the use of nuclear heat as compares to burning coal would need to be substantial to off-set this estimated heat exchanger cost when compared to the cost of a similar coal fired unit (which would include the cost of oxygen, about 10% of the coal to be burned plus the relatively small added cost of constructing the necessary parts for making the vessel suitable for burning coal). On the other hand, local market conditions may necessitate complex processing procedures more attractive

as a function of time because the particle surface becomes depleted in carbon and further gasification may be mostly rate controlled by a diffusion mechanism. High gasification rates can, therefore, be maintained only by discharging char with a high carbon content. Utilization of this high carbon char may be economically attractive by burning as a fuel in a conventional fossil fuel power generation station or some similar utilization method.

B.4 CONCLUSIONS

In summary, the use of nuclear heat for coal gasification is obviously attractive for those places where this type of heat is more economical than burning coal. The local market conditions will, of course, have a strong influence on the details of the coal gasification system selected and this may in turn affect the heat source economy especially in the case of steam gasification which involves a heat exchanger.When using nuclear heat, other extenuating circumstances may also affect the economy. These will include such matters as auxiliary process equipment (heat exchangers, etc.) and local market conditions.

Much work needs to be done on developing a process for utilizing nuclear heat for coal gasification. The work presently in progress in West Germany is a strong forerunner for this concept and every effort should be made to keep abreast of this work.

Items which can also be readily undertaken to lead to a more detailed understanding of the use of nuclear heat to gasify coal include market evaluations, systems studies, gasification technology related to the use of nuclear heat, material development for improved process equipment life, and the possibilities of combining more than simply coal gasification to affect the greatest economy in coal utilization. These are discussed briefly below.

B.4.1 Systems Analyses

There is need to make a detailed comparison of the economy of the use of nuclear heat for coal gasification as compared to the burning of part of the coal for heat. In particular, these analyses should include auxiliary process equipment such as that necessary for energy conservation as well as those processes associated with the preparation of the finished gas (and hydrocarbon) products. These analyses should result in more clearly defining the details of the economy

of coal gasification including the parts associated with producing specialized products.

B.4.2 Market Analyses

The local market will probably vary depending on the hydrocarbon needs by the local industries as well as the home fuel requirements. Consequently, it seems unlikely that coal gasification will always be directed to producing a single product for all markets. Such is the case of gasification of the Eastern bituminous coal which will most probably serve the petrochemical market as well as home heating. Other market outlets may be present and could thus be used when the economy is suitable. Another, and apparently different, example is gasification of the Western lignite where the main market is probably pipe-line gas.

B.4.3 Prevention of Caking

The caking of bituminous coals can be prevented by heating the particles rapidly such that the hydrocarbons are decomposed thermally before they can cement particles together. While considerable work has been done on this problem it needs to be reviewed to determine the operating procedures necessary for this process to be most effective in beds using nuclear process heat. This review should, of course, include a continuing search of the literature for information relating to this problem. There is need also for developing more experimental data on coal particle conglomeration as a function of ash content and as a function of size for temperature ranges and at heating rates expected in coal gasification by nuclear process heat.

B.4.4 Gasification Kinetics

While there are many reports dealing with gasification rates, there needs to be developed specific data relating to the rates as related to the particle size and ash content. These data should be developed under conditions commensurate with those of the gasification conditions expected with using nuclear heat. These data will be needed to calculate the economy of coal gasification as related to optimum carbon removal during gasification.

B.4.5 Materials Development

There is need to develop data on corrosion of materials used in processing

coal during gasification. This need is probably most pronounced in the case of the heat exchanger used to heat the coal for steam gasification. There may be other material applications in these processes used for coal gasification which show similar corrosion problems.

B.4.6 Process Combinations

There is need to evaluate the local market demand with the various possible processes to most effectively utilize the coal. In other words develop the most economical process combinations commensurate with local market demands and the local process economy. For example, in the extreme case it may be most desirable economically to treat the coal thermally for removal of the tars (i.e., hydrocarbons), remove part of the carbon by steam gasification, part of the carbon by hydrogasification and the balance by conventional burning.

REFERENCES

B-1. Evaluation of Coal Conversion Processes to Provide Clean Fuels, EPRI 206-0-0, Final Report, Parts II and III, Feb. 1974.

B-2. Technology and Cost of Coal Gasification, H.M. Siegel, and T. Kalina, ASME Pub. 72-WA/Fu-2.

B-3. Symposium "Clean Fuels From Coal", Sept. 10-14, 1973, Inst. of Gas Tech., Chicago, Ill., 1973.

B-4. Federal Register, EPA, Standards for Performance for New Stationary Sources, Vol. 36, No. 159, Part II, Tuesday, Aug. 17, 1971.

B-5. Final Report - Application Study of a Nuclear Coal Solution Gasification Process for Oklahoma Coal, Vols. 1 & 2, May 1972, General Atomic/ Stone & Webster (GA-A12068).

B-6. Engineering Evaluation of Process Heat Applications for Very High Temperature Nuclear Reactors, prepared for Holifield National Laboratory under ERDA contract No. AT(11-1) 2477, June 30, 1975. United Engineers & Constructors, Inc.

B-7. Nuclear Heat Generation System of a Process Heat Plant for Hydrogasification of Lignite - H. Baumgartner, Hochtemperatureaktorbau GmbH, Mannheim, Federal Republic of Germany, IAEA-SM-200/65, Julich, Federal Republic of Germany, Oct. 13-17, 1975.

B-8. Van Heek, K.H., "Hydrogen production by steam gasification of coal with special regard to the unitization of nuclear heat", ISPRA lecture, September 29 - October 3, 1975.

B-9. Huettner, R., Strauss, W., and Teggers, H., "Technology of hydrogen production from coal gasification", ISPRA lecture, September 29 - October 3, 1975.

B-10. "Origin, Petrography and Classification of Coal", by Parks, B.C., from Chemistry of Coal Utilization, Supplementary Volume, by Lowry, H.H., John Wiley & Sons, New York, 1963.

B-11. Juntgen, H., Van Heek, K.H., and Klein, J., "Comparative investigations into the kinetics of gasification with steam or hydrogen and conclusions for gasifier design", Gordon Research Conference on Coal Science, July 2-6, 1973.

B-12. Curran, G.P., Fink, C.E., and Gorin, E., "Kinetics of Lignite Char Gasification", I&EC, Process Design and Development, Vol. 8, No. 4, Oct. 1969, pp. 559-567.

B-13. Zielke, C. W., and Gorin, E., " Kinetics of Carbon Gasification", Ind. & Engr. Chem., Vol. 49, No. 3, March 1957, pp. 396-403

B-14. Samsonov, G.V., and Kharlamov, A.I., "Catalytic Properties of Powders of Refractory Compounds", Poroshoraya Mettallurgia, No. 9 (153), 1975, pp. 4-14.

B -15. H. Juentgen, K.H. Van Heek, R. Duerrfeld and P.O. Feistel, "Steam Gasification of Coal Using Heat From HTR's", Traus Am. Nuc. Soc. The European Nuclear Conference, April 21-25, 1975, p. 715-717.

B -16. Van Heek, K.H. - Private communication.

TABLE OF CONTENTS

TABLE OF CONTENTS continued

LIST OF FIGURES

LIST OF TABLES

APPENDIX C

IHX DESIGN OPTIMIZATION

C.1 INTRODUCTION

This appendix presents the design details of a U-tube style IHX which has been selected as the optimum configuration based upon an overall assessment of cost, safety and other engineering considerations. A modular assembly has been conceived. This appendix also describes the other IHX styles and designs which were considered in the selection of the optimum design. The evaluation procedure and a discussion of the various pros and cons of each configuration is presented.

Section C.2 summarizes the selected design and selection method. Section C.3 presents a detailed description of the modular IHX assembly. Section C.4 presents the details of the optimization assessment and selection method.

C.2 SUMMARY

C.2.1 DESIGN SUMMARY OF REFERENCE IHX

Figure C-1 shows the overall design of the selected IHX assembly featuring thirty-six U-tube modules assembled in a (non-integrated) cylindrical pressure vessel. The assembly is rated at 250 MW and is approximately 17 feet in diameter by 60 feet overall height. The primary fluid is on the shell side with its motor driven circulator directly attached to the lower portion of the pressure vessel.

Figure C-2 shows an exploded parts view of a typical module. Each module is approximately 30 feet in length, contains 251 1/2" O.D. U-tubes and is arranged so that the primary helium makes twenty-four shell side cross flow passes. Each module leg is circular in cross section and is approximately 16 inches in diameter.

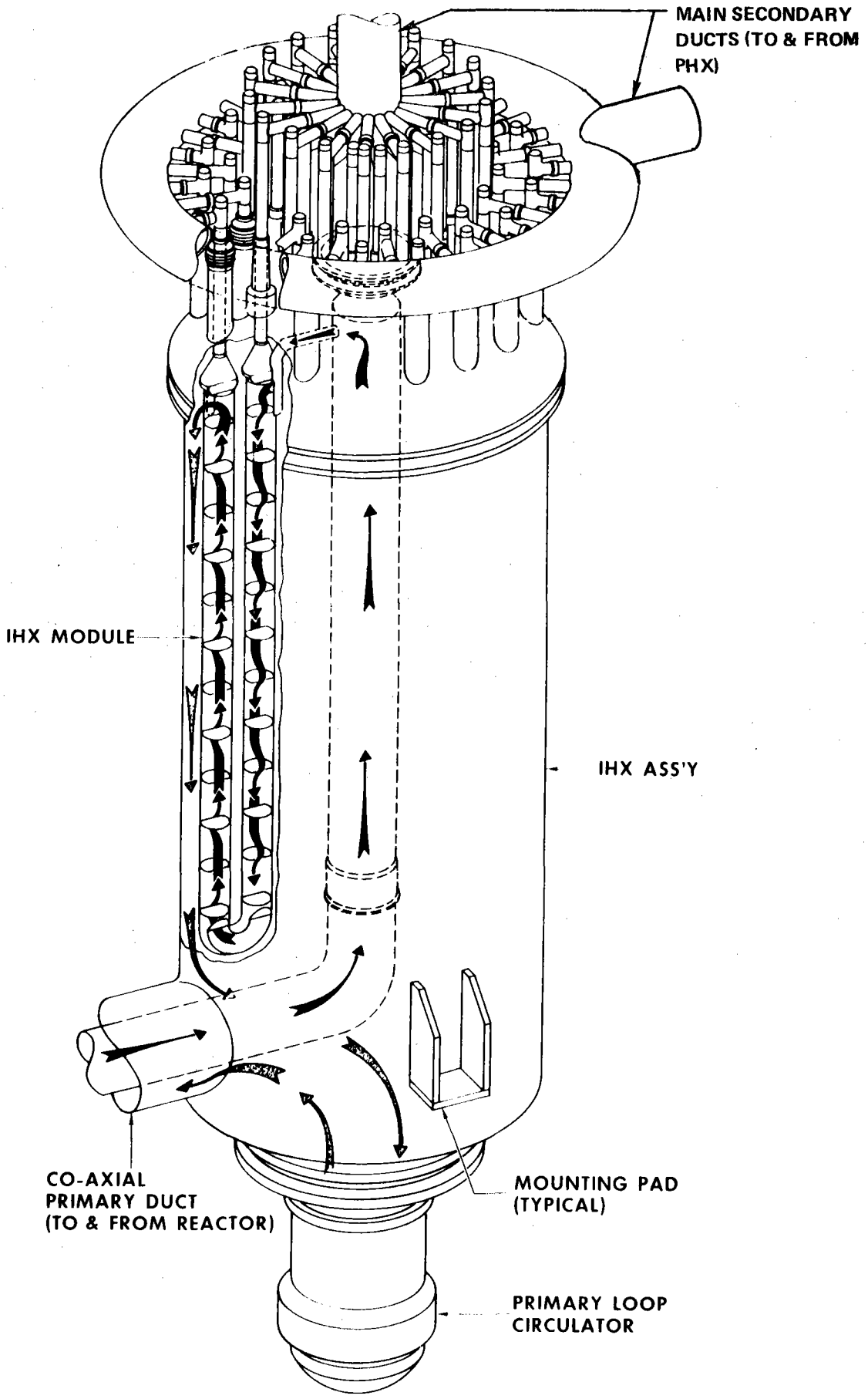

Figure C-1. U-Tube Style Intermediate Heat Exchanger Assembly (Reference Design).

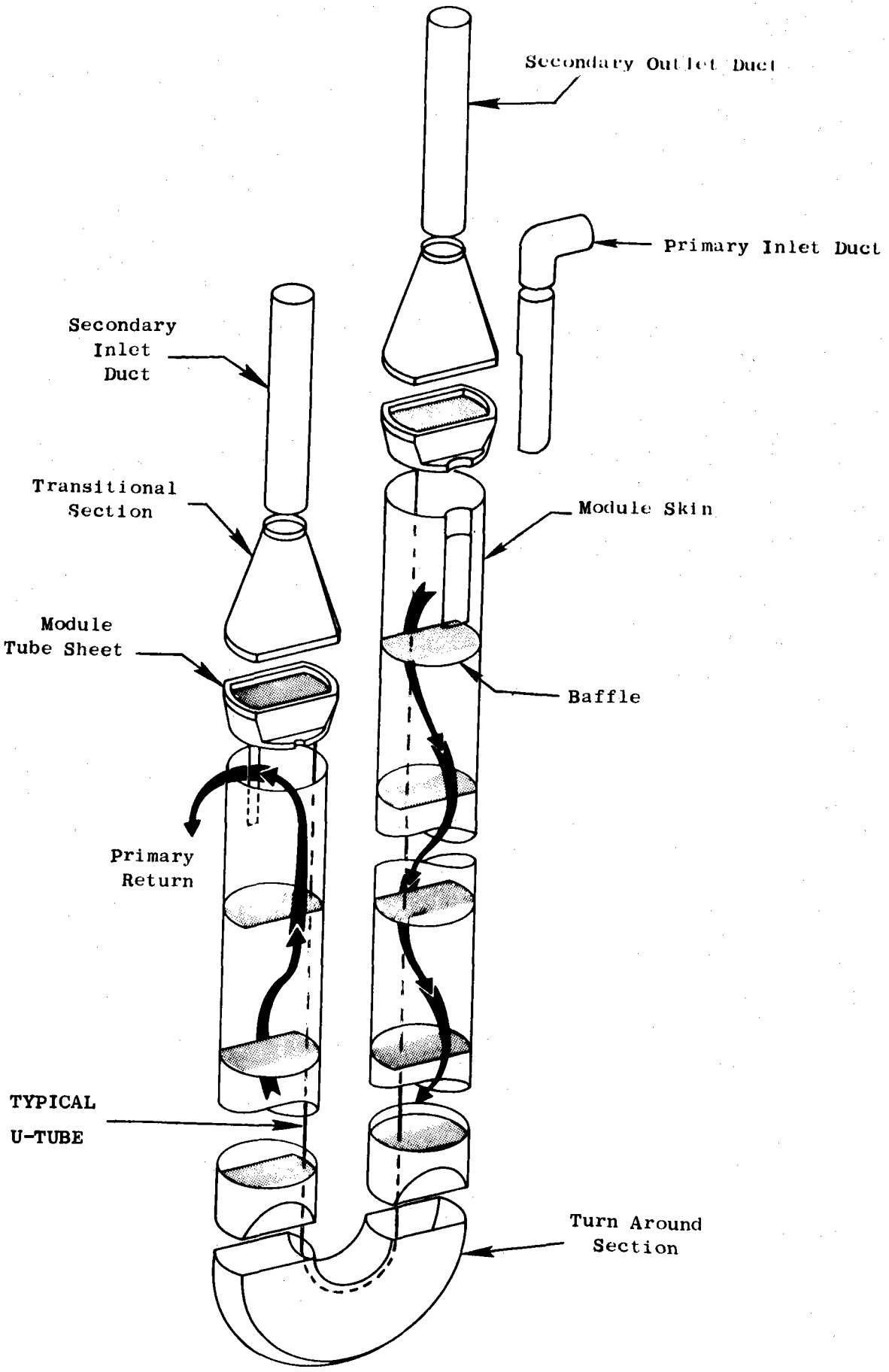

Figure C-2. Exploded Parts View of U-tube IHX Module (Reference Design)

Table C-1 provides an overall summary of significant thermal, hydraulic and other physical data related to the overall plant, the IHX assembly and the IHX module.

The justification for or against the use of an IHX loop will not be discussed in this section but if such a loop is required for safety or other reasons, a typical plant schematic would be similar to that shown in Figure C-3 which illustrates a steam methane reformer process heat plant. The relative pressure levels and temperatures at key locations are indicated. The significant point relative to these parameters is that: (1) rupture of the IHX primary-secondary barrier wall permits inward leakage only and (2) a 50°C thermal potential is typically employed to drive the heat from the primary loop to the secondary loop.

Figure C-4 illustrates the ducting arrangement of both the primary and secondary portions of the loop including the isolation valving where the ducting penetrates the walls of the secondary containment vessel. For the process heat plant illustrated each of the twelve steam reformers is individually coupled to the reactor heat source via its own IHX loop. The steam reformer design details are presented in Appendix E. Other major plant components such as the reactor, PCRV, and secondary containment building have been previously reported (in other parts of this report, Section 2.3, Appendix F) and are not further discussed in this section.

The U-tube heat exchanger is composed of modules which channel the two fluid streams in the manner illustrated in Figure C-5. A major cost advantage of the U-tube style is achieved by avoiding large massive tube sheets where thickness varies directly with the diameter. In addition the configuration readily lends itself toward utilization of small diameter tubes which directly reduce the core volume for a required heat transfer surface.

TABLE C-1

SUMMARY DATA FOR REFERENCE DESIGN IHX

PLANT DATA

Chemical Process	Steam Methane Reforming
Thermal Power	3000 MW
No. of Process Loops	12
Reactor Primary Coolant	Helium
Core Outlet/Inlet Temperature	950/350°C
Reformer Inlet Temperature	900°C
Reformer Peak Process Temperature	825°C
Reformer Power Ratio	35.6%
S.G. Inlet/Exit Temperature	600/300°C

IHXA DATA

IHX Power Rating	250 MW
No. of Modules	36
Primary Inlet/Exit Temperature	950/350°C
Secondary Exit/Inlet Temperature	900/300°C
Pressure Vessel O.D.	16' - 10-7/8"
Overall Height	62' - 6-1/2"
Approximate Weight	500K lbs
Primary/Secondary Flow	.63 x 10^6 lb/hr
Primary ΔP (Shell Side)	15.9 psi
Secondary ΔP (Tube Side)	15.5 psi
No. of U-tubes	9036
Tube O.D. x Wall	0.500 x .050 inch

MODULE DATA

Module Power Rating	6.94 MW
Primary/Secondary Flow	4.861 lbs/sec
Primary ΔP (Shell Side)	15.9 psid
Secondary ΔP (Tube Side)	15.5 psid
Inlet Pressure Primary/Secondary	600/638 psi
IHX Cavity Pressure	585 psi
No. of U-tubes	251
No. of Cross Flow Passes	24
Tube O.D. x Wall	0.500 x .050 inch
Module Header O.D./Thick	15.62/3.5 inch
Module Skin O.D./Thick	15.62/.0625 inch
Tube Spacing-to-O.D. Tran/Long.	2.0/0.9
Overall Length	32' - 4-1/2"
Approximate Weight	4000 lbs

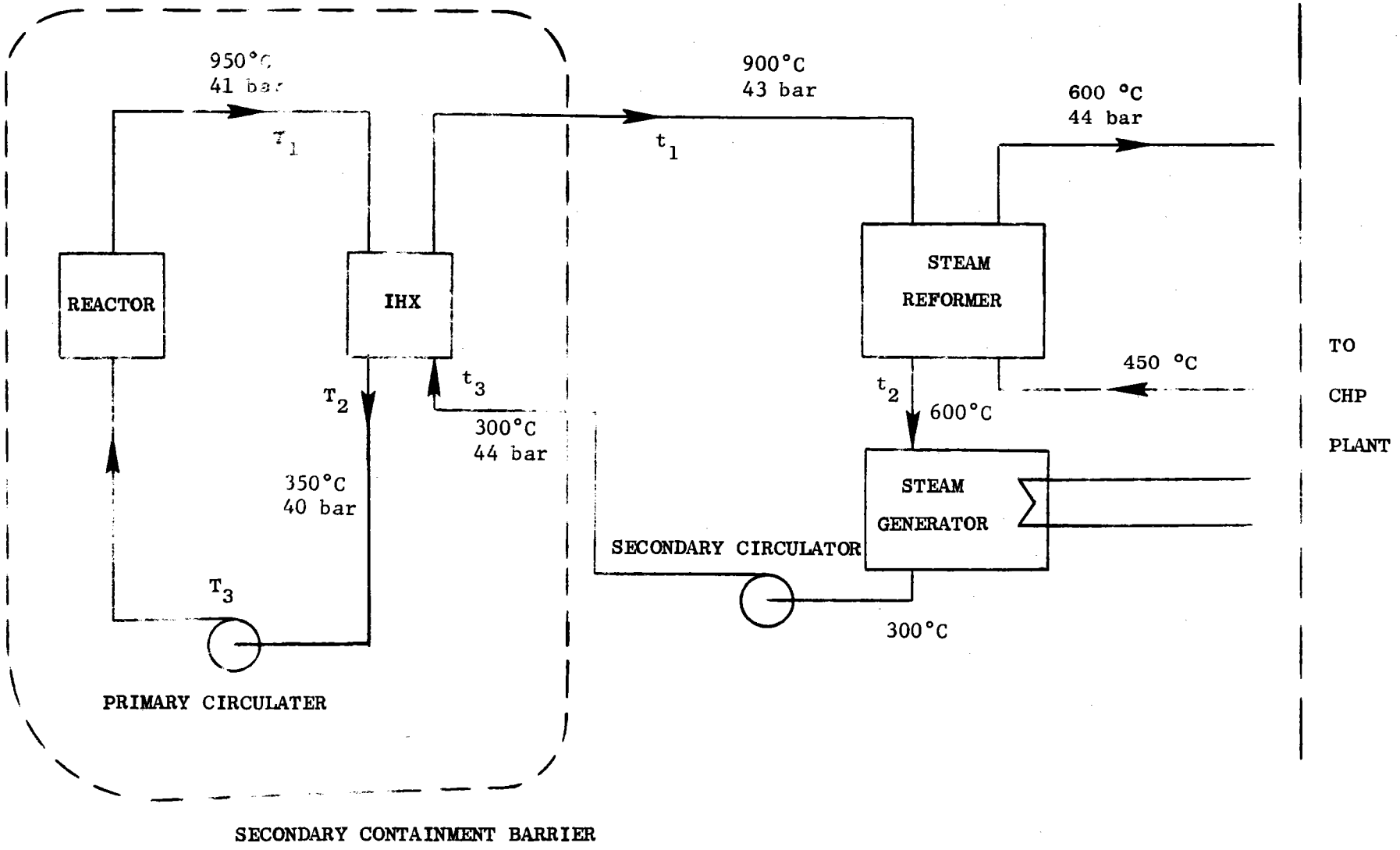

Figure C-3. Steam Reformer Plant Schematic With Intermediate Heat Transfer Loop.

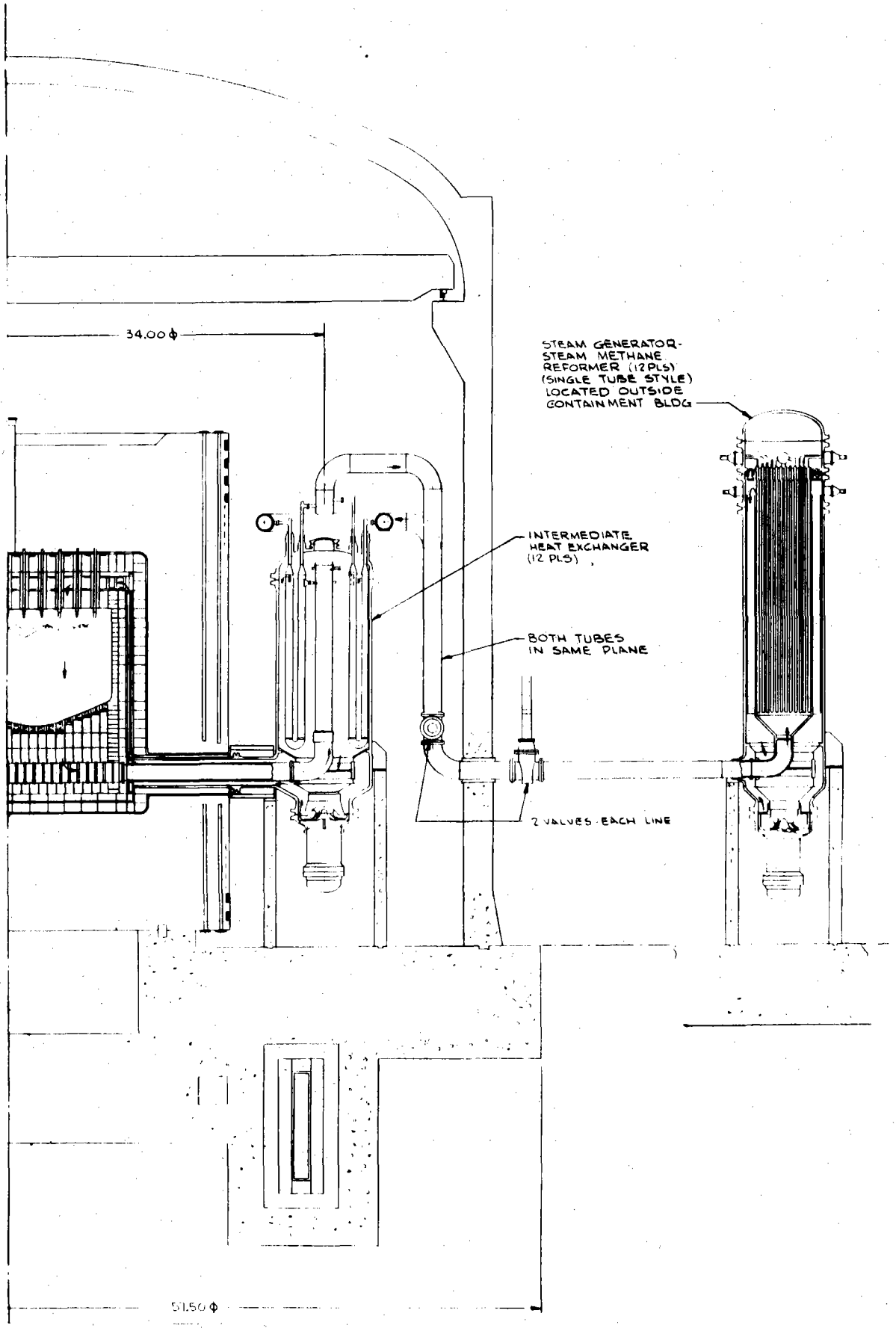

Figure C-4. Ducting Arrangement for Intermediate Heat Transfer Loop.

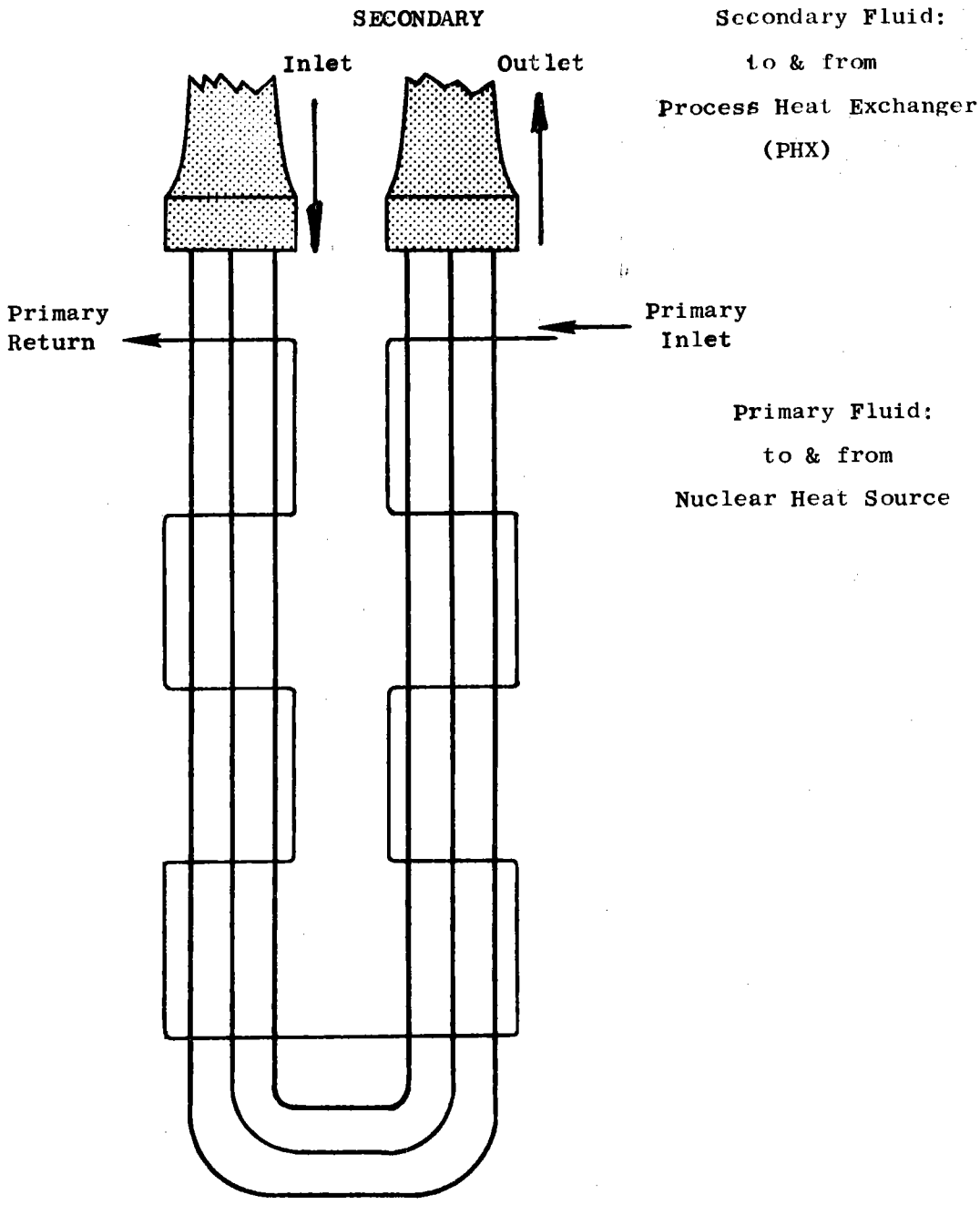

Figure C-5. Schematic Flow Diagram for the U-tube Style Intermediate Heat Exchanger.

The safety related aspects of the U-tube style are significant in that modules may be readily inspected and isolated if required without disassembly of the IHX. Borescopic inspection of the tube sheets and tube interior surface is possible without breaking the hermetic seal of the primary coolant fluid. The design lends itself toward the potential to find, plug and seal leaky tubes. All these activities could be accomplished by internally probing the U-tube ends from outside the IHX assembly with access achieved through sealed access ports welded in the external plumbing.

Mechanical design features of the U-tube cross flow style include good support of the tube bundle with low shell-side pressure loss, outstanding capability to channel and control the primary coolant flow in the IHX assembly, and inherent ability to handle differential thermal expansion, both as a module and as individual tubes.

Table C-2 summarizes the overall features of the U-tube configuration which led to its selection as the optimum design.

C.2.2 CONFIGURATION ASSESSMENT SUMMARY

Initial screening of current IHX design efforts and consideration of the overall operating conditions indicate the suitability of the following four basic design styles for this application.

- o straight tube counterflow, (two versions considered)
- o U-tube multi-pass cross-flow
- o helical tube multi-pass cross-flow, (two versions considered)
- o bayonet tube folded flow

Six design layouts involving these styles were generated to serve as a reference for optimization and evaluation. Using the digital computer as a design tool each configuration was thermally and hydraulically optimized on the basis of cost within appropriate mechanical or other limitations.

TABLE C-2

ASSESSMENT SUMMARY OF U-TUBE STYLE IHX

- o U-TUBE CONFIGURATION CLEARLY IDENTIFIED AS MOST OPTIMUM OF CANDIDATES STUDIED

- o FEATURES OF U-TUBE
  - UTILIZES ESSENTIALLY SIMPLE STRAIGHT TUBES
  - GOOD THERMAL UTILIZATION OF VOLUME
  - GOOD PRIMARY DUCTING AND TUBE SUPPORT
  - IN SITU BORESCOPIC INSPECTION
  - INDIVIDUAL TUBE PLUGGING POTENTIAL
  - SINGLE MODULE ISOLATION FROM OUTSIDE
  - MINIMUM COST - NO MASSIVE TUBE SHEETS
  - INHERENT THERMAL EXPANSION CAPABILITY

- o ABSTRACT
  - GOOD MECHANICAL DESIGN
  - GOOD THERMAL/HYDRAULIC DESIGN
  - MINIMUM COST
  - EXCELLENT SAFETY RELATED ASPECTS

Table C-3 summarizes the size, weight, cost and other significant features of the computer optimized candidate configurations. For this optimization a minimum tube diameter of 1/2-inch O.D. was arbitrarily established based upon handling considerations and was utilized in the candidate designs where appropriate. In addition, the pressure drop allocated to each side of the heat exchanger was selected to result in the lowest cost for the sum of (1) the capital cost of the heat exchanger, (2) the capital cost of the circulator and (3) the plant life time circulator operating cost.

An overall assessment of each computer optimzed configuration was made with weighted consideration given to safety related aspects, mechanical design, thermal/hydraulic design, size and cost. Table C-4 shows a numerical assessment of the IHX candidate configurations in these areas and indicates the overall superiority of the U-tube design configuration. This style rates superior to all other candidates in the area of cost, mechanical design and safety related considerations. The thermal/hydraulic design is second only to that of the straight tube counterflow. In the overall assessment the straight tube counterflow styles are judged to be the second most desirable with the helical style and folded flow configurations least desirable. Section C.4 of this appendix discusses in further detail this evaluation assessment of the various candidate designs.

Figure C-6 shows the relative outline sketches of the optimized IHX candidate configurations and clearly shows the size and cost superiority of the U-tube design.

For reader clarity it should be pointed out that the reference design summarized in the previous section C.2.1 and presented in detail in section C.3 is not identical to the computer optimized "B-1" U-tube configuration which was used to substantiate the configuration selection. Chronologically once the conclusion was reached that the U-tube style indicated an optimum configuration, it was then subjected to an additional design iteration to further define and improve the initial concept. This refined version, the so-called reference design, is described in the two above referenced sections.

TABLE C-3

SUMMARY OF SIGNIFICANT DATA FOR VARIOUS COMPUTER OPTIMIZED IHX CONFIGURATIONS

	IHX CONFIGURATION DESCRIPTION*					
	Straight-Tube		U-Tube	Helical-Tube		Bayonet Tube
	A-1 (780C)	A-2 (780C)	B-1 (780)	C-1 (777-9)	C-2 (777-9)	D-1 (777)
TUBES ($M)	$1.91	$1.65	$2.11	$10.11	$10.19	$8.03
O.D. (INCH)	0.5	0.5	0.5	1.50	1.50	2.244
NO. OF TUBES	8558	7135	9070	1804	1863	3087
WT (LBS X 10^6)	.127	.110	.140	.474	.629	.535
PRESSURE VESSEL ($M)	$2.28	$2.34	$2.03	$5.36	$5.18	$4.06
OVERALL HEIGHT (FT)	86.6	88.7	44.9	129	128	77.1
OVERALL DIAMETER (FT)	12.5	12.0	1.57	15.0	14.8	15.8
WEIGHT	.284	.293	.254	.670	.647	.507
TUBE SHEETS ($M)	$1.19	$1.20	$0.13	$2.97	$5.96	$3.73
WEIGHT	.099	.100	.011	.248	.496	.310
TOTAL IHX WEIGHT	.636	.632	.502	1.82	1.99	.1697
ΔP DATA						
ΔP PRIMARY (PSI)	9.0	13.0	2.4	9	10	10
ΔP SECONDARY (PSI)	16.0	23.0	15.5	3.8	3.5	47.5
COST DATA ($M)						
TOTAL IHX (NET)	$6.5	$6.4	$5.1	$20.5	$22.9	$18.9
CIRCULATORS	5.1	6.3	4.3	4.0	4.0	8.2
TOTAL IHX	$11.6	$12.7	$9.5	$24.5	$26.9	$27.1

*SEE PAGE C-53 FOR SCHEMATIC DESCRIPTION OF CANDIDATE IHX CONFIGURATIONS AND DEFINITION OF IDENTIFICATION CODE. THE DATA TABULATED HEREIN IS SUMMARIZED FROM THE COMPUTER OUTPUT SHEETS FIGURES C-40 THROUGH C-45 WHICH REFLECT THE OPTIMIZED DESIGN FOR EACH CANDIDATE CONFIGURATION.

TABLE C-4

OVERALL ASSESSMENT OF CANDIDATE IHX CONFIGURATIONS

Evaluation Aspect	IHX CONFIGURATION DESCRIPTION*					
	Straight-Tube		U-Tube	Helical-Tube		Bayonet Tube
	A-1	A-2	B-1	C-1	C-2	D-1
Safety Related	87	87	98	89	92	83
Mechanical Design	59	52	93	57	57	61
Thermal/ Hydraulic Design	100	89	67	61	61	56
Cost	78	80	100	25	22	27
Overall Assessment	83	77	95	67	67	65

Note: All ratings on the basis of 100. The tabulated data shown in this Table summarizes the evaluation results presented in Table C-11 and Appendix C.4.4.2.

*See Page C-53 for schematic description of candidate IHX configuration and definition of identification code.

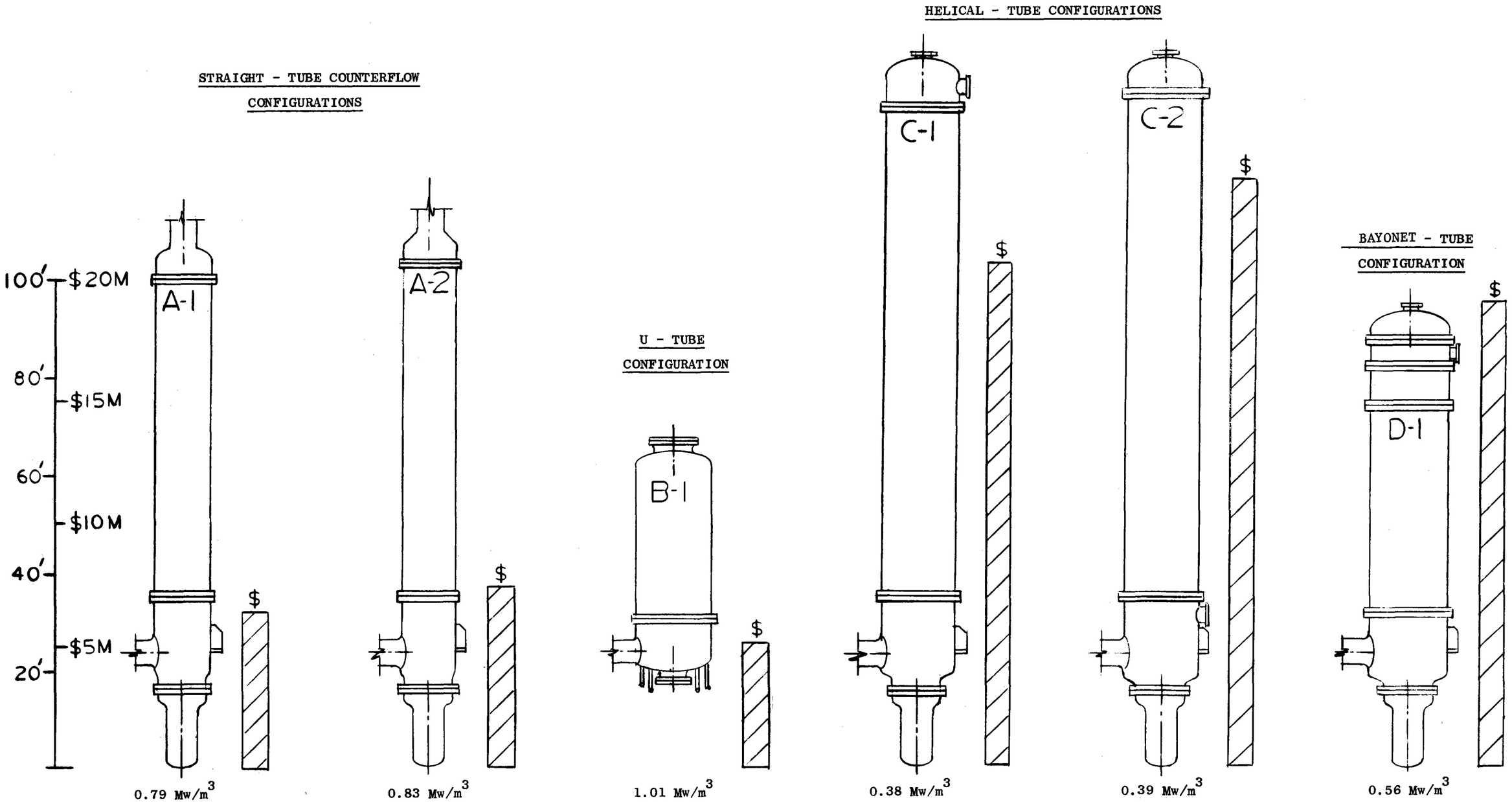

Figure C-6. Size and Cost Comparison of IHX Candidate Configurations.

C.3 DETAIL DESCRIPTION OF REFERENCE DESIGN IHX

C.3.1 IHX ASSEMBLY DESCRIPTION

C.3.1.1 Overall Assembly

Figure C-1 shows an isometric sketch of the selected IHX assembly featuring thirty-six U-tube modules assembled in a free standing cylindrical pressure vessel. The assembly is rated at 250 MW and is approximately 17 feet in diameter by 60 feet overall height. Figure C-7 shows an engineering drawing of this assembly and indicates the manner in which the modules are packaged around the centerline of the cylindrical pressure vessel.

C.3.1.2 Primary Coolant Duct

A coaxial duct brings the heated primary helium into the heat exchanger and returns the cooled fluid to the reactor after it has given up its heat to the secondary fluid and has passed through the circulator. The cooler return flow is in the outer coaxial duct thus easing the ducting temperature-strength problem. The inner supply duct with an I.D. in the order of 31.5" is internally insulated so that the metal wall temperature approaches the cool helium return temperature (300°C).

After entering the IHX the hot supply duct rises vertically to the top of the pressure vessel where smaller radial ducts supply each module. At the lower elbow the duct is supported by a sliding seal arrangement which accommodates axial expansion. At the upper end the module supply ducts which are approximately 4-1/2" I.D. each contain a piston ring type seal to accommodate radial differential expansion.

C.3.1.3 Primary Coolant Flow Path

The primary helium is caused to flow in successive cross flow passes down the inner U-tube leg and up the outer. The primary flow exhausts from each module directly into the pressure vessel interior. The relatively cool gas then finds its way to the circulator inlet located at the bottom of the IHX assembly. During this downward pass the

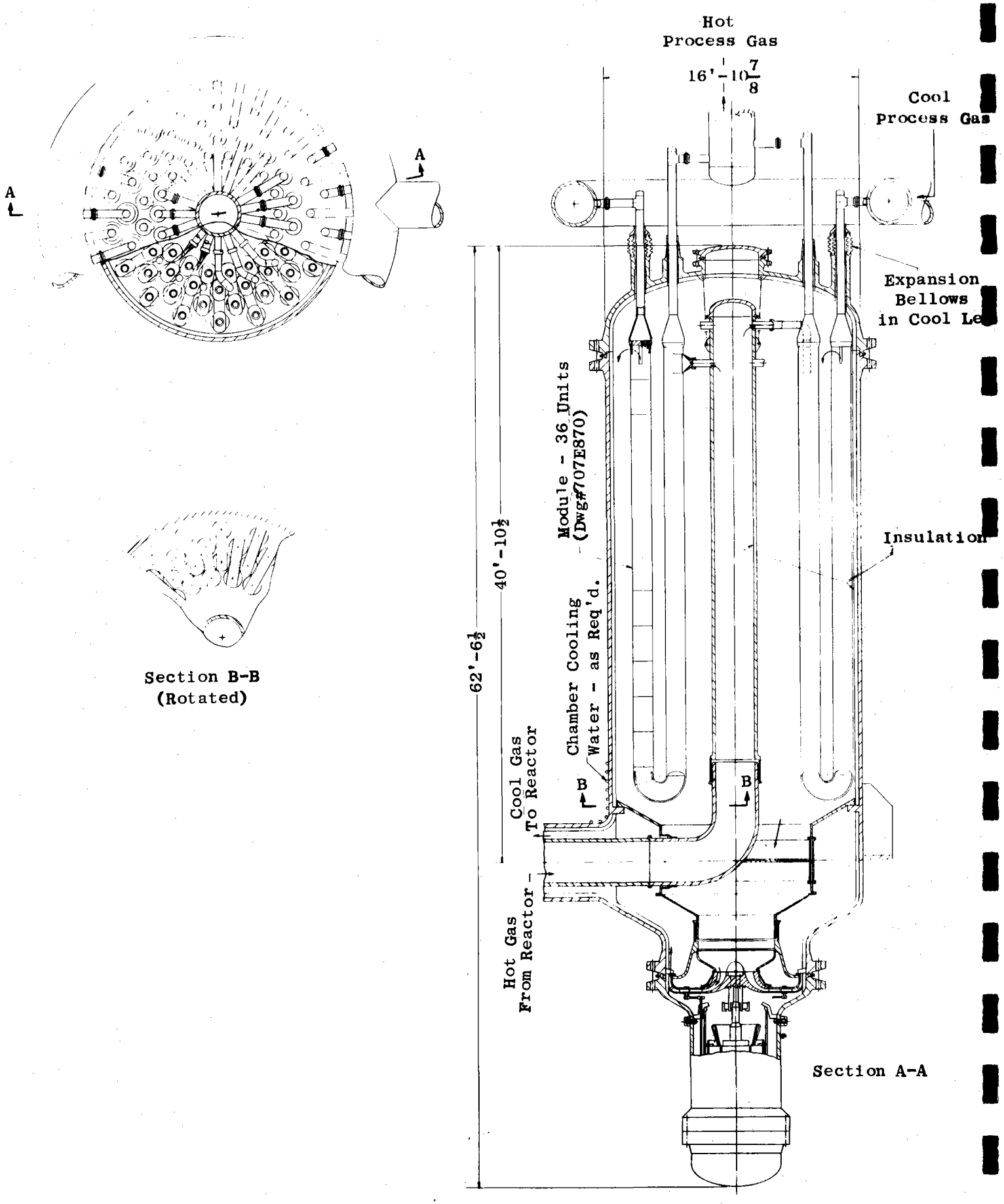

Figure C-7. Engineering Drawing of Reference Design IHX Featuring 36 U-tube Style Modules. (Drawing No. 707E871)

cool flow bathes the central supply duct which as stated earlier is internally insulated. The pressure vessel interior walls are also insulated. With water cooling coils attached to the outer surface of the pressure vessel, the metal wall temperature is maintained at approximately room temperature rather than at the 300°C return helium temperature. The modules themselves are insulated on the outside to prevent excessive loss of heat of the hot primary fluid to the cool primary bath.

C.3.1.4 Secondary Helium Ducts and Manifolds

The cool secondary helium from the process heat exchanger is ducted to a toroidal manifold which is located above and around the upper end of the IHX assembly. Each module has its own supply duct welded directly to the toroidal manifold. (See Figure C-7) The hot outlet ducts from each module after leaving the pressure vessel are attached to a central duct located above the IHX. The two main secondary ducts between the IHX and the PHX individually penetrate the secondary containment building whereas the primary side is ducted coaxially to the reactor. As indicated in Figure C-4 each main secondary duct contains two isolation valves, one on each side of the containment vessel wall. These valves are required for safety reasons. As indicated in Figure C-4 the main secondary ducting contains generous bends to prevent thermal stress problems due to end attachments.

C.3.1.5 Number of Modules

The number of modules shown in the reference design was arbitrarily picked at thirty-six so that the power rating of one module would approach the approximate rating of a potentially available test facility. The following tabulation shows the module power rating versus the number of modules for an assumed 250 MW assembly.

No. of Modules	24	36	48
Power per Module (MW)	10.4	6.9	5.2

A smaller number of modules would eliminate some of the congestion in the region of the upper secondary ducting. There appears to be no geometric packaging advantage or disadvantage associated with smaller modules.

C.3.1.6 Core and Secondary Ducting Support

In the reference IHX assembly (Figure C-7) the hot and cold secondary ducts penetrate the PV shell in straight sections which allow the safety related inspection features discussed in the following section. This approach also allows the following features to be incorporated in the mechanical support of the IHX core.

1. The hot secondary duct is welded to the pressure vessel using a thermal sleeve to accommodate radial expansion mismatch. This attachment point establishes the vertical reference location for each module.

2. The U-tube modules are supported from outside the IHX pressure vessel by counter weights or constant force hangers attached to the upper secondary manifolds. The major part of the IHX core weight is not supported by the pressure vessel. The thermal sleeve mentioned above is not a structural member.

3. The module secondary ducts to each of the upper manifolds serve as hockey-stick deflection members to equalize any stresses which may result from unequal module-to-module expansion.

4. The hot module secondary ducts and the main secondary duct itself will be internally insulated to allow metal temperatures to operate at controlled levels.

C.3.1.7 Safety Related Inspection Features

As indicated in Figure C-3 the average pressure level in the secondary loop is slightly higher than that of the primary loop. Any failure of the barrier between the primary and secondary fluid thus allows inward flow of the secondary helium into the primary loop rather than the reverse situation whereby radioactive particles could enter the secondary loop.

The detection of a leak at any point in the secondary loop inside the containment building can be readily made by closing the loop isolation valves at the wall penetration and monitoring the static pressure. A falling pressure would indicate a leak. The primary helium flow would need to be stopped during the check to avoid rising metal temperatures with resultant thermodynamically induced pressure variations. The determination of the specific module(s) containing the leak is theoretically possible by monitoring the pressure level in the secondary inlet ducts since a leaking module would result in a flow with local pressure reduction in the effected secondary inlet duct. Assuming a leaky IHX assembly has been detected, plant operation could continue during a critical period using only the remaining sound loops. The faulty IHX would be isolated from the process heat exchangers by the redundant valves in each main secondary duct.

During periods of plant shutdown, detection of the specific leaky module could be determined with assurity by isolating each module one by one and conducting a vacuum or pressure leak test. The module isolation can be accomplished in a relatively easy manner by inserting blank-off plates in the module secondary ducts at the module flanges.

The tee located at the upper end of each module secondary duct (reference Figure C-7) provide an inspection access port with a direct view of the module tube sheets. Inspection of the tube-tube sheet seal weld can be readily accomplished at plant shut downs. In addition a boroscope could be inserted into each tube interior and traversed all the way down to the tube turn-around section. With both ends of the U-tube accessible it is possible to locate specific leaky tubes by reaching down the secondary ducts with extension devices which would enable vacuum leak tests to be conducted on individual U-tubes. The extension devices could essentially be the equivalent of a rubber stopper on the end of small tube (maybe 1/4" O.D.). By wedging the stopper in each end of a U-tube a vacuum leak test can be conducted in situ.

It is conceivably possible that a means of plug welding a leaking U-tube could be developed and accomplished through the secondary ducts. In any event, isolation of the module containing the leaking tube is readily accomplished by seal welding a blank-off plate at the secondary duct flanges. This expedient would allow plant operation to be resumed until an IHX overhaul could be scheduled. A thermal heat loss of less than 3% would result per module on a thirty-six module basis.

C.3.1.8 Pressure Vessel Cavity Pressure

The modules which make up the IHX assembly are in the shape of a hair pin with each leg having a circular cross section. The cylindrical legs make excellent pressure vessels to contain the primary helium fluid. The plate-out of any nuclear reactant products carried by the primary coolant would largely be confined by the module skin. The pressure loss of the primary coolant as it flows through the module is in the order of 3.5 to 15 psi depending on the specific packaging selected. Since the module primary flow exhausts directly into the IHX pressure vessel cavity, the maximum module internal pressure will be this same value and will tend to bulge the module cylindrical legs. The pressure differential will decrease linearly with length in the flow direction through the module. With this arrangement the module skin need not exceed .062" since the pressure loading is very low and the best possible shape has been utilized.

C.3.2 IHX MODULE DESCRIPTION

C.3.2.1 Reference Design Description

Figure C-2 shows an isometric sketch of the reference design IHX module. Figure C-8 shows an engineering drawing of the module assembly. As indicated the legs of the U-tube module are circular in cross section with the exception of the turn around area which is flattened to allow close nesting of the modules in the IHX assembly. Each module contains 251 U-tubes with each straight leg approximately 28 feet long. The tubes are supported by 24 primary baffle plates which channel the primary flow in the desired multi-pass cross flow arrangement. The tube sheets at

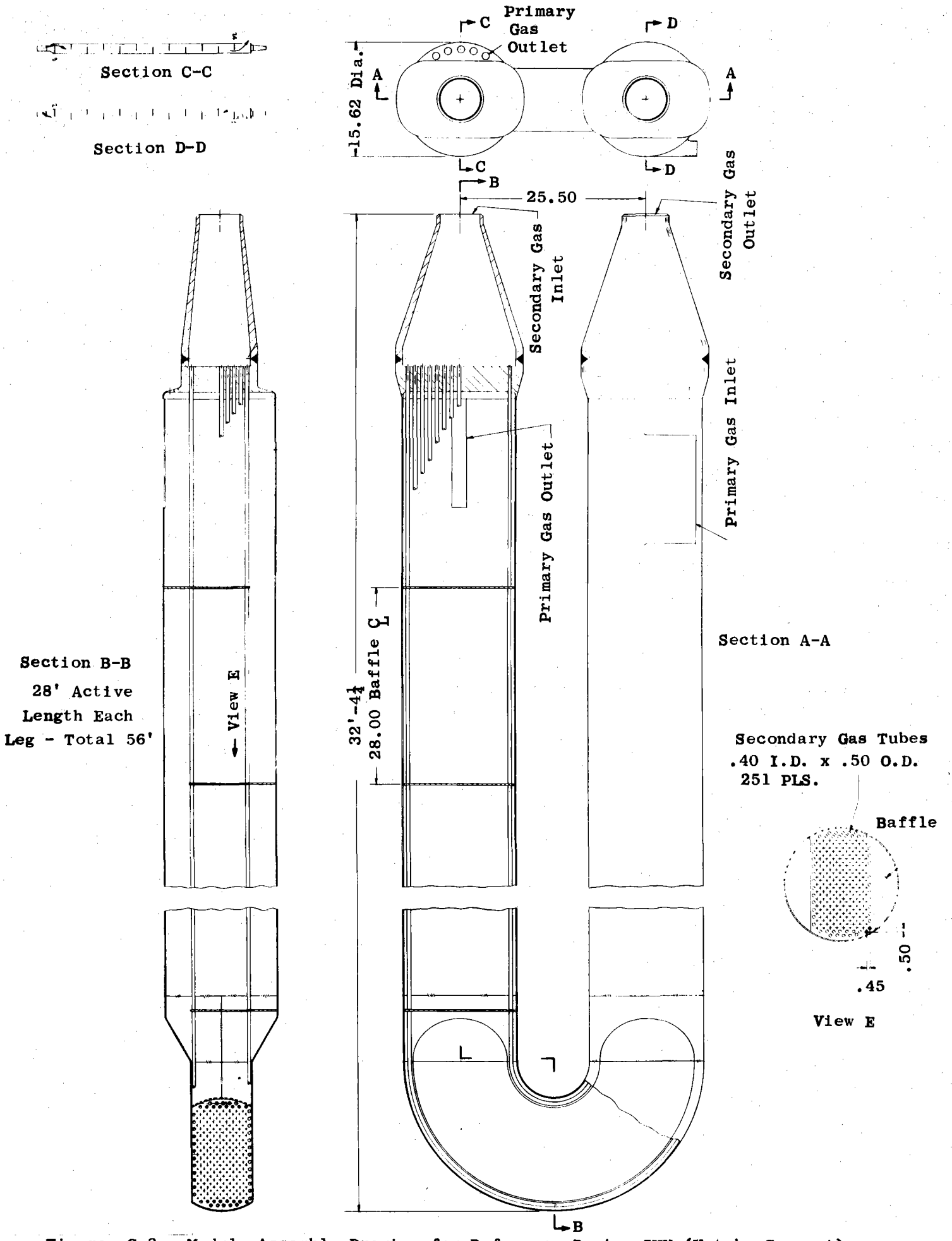

Figure C-8. Module Assembly Drawing for Reference Design IHX (U-tube Concept). (Reference Drawing No. 707E870)

each end of the U-tube legs are completely independent of each other to allow ease of assembly and expansion freedom during operation. The transition section at each header connects the circular secondary ducts to the rectangular-like area taken by the tubes. The module skin constrains primary flow within the module and supports any necessary module external insulation.

C.3.2.2 Module Fabrication Sequence

To illustrate the design simplicity of the U-tube module the following tentative assembly sequence is presented.

1. The baffle plates and the tube sheets would be positioned in their approximate orientation by a fixture.

2. The pre-formed and inspected U-tubes would be individually threaded through the baffle plates and into the tube sheets. The module assembly would be built up from the inner U-tubes to the outermost.

3. The tube-tube sheet joints would be made. Tentatively this would consist of mechanical expansion of the tube by explosive forming or other process. Seal welds between the tubes and tube sheet would also be made. Figure C-9 shows a tentative tube-tube sheet joint.

4. The module skin would then be installed. Longitudinal closure seam welds would join two identical half sections to form the turn-around. The circular legs could be similarly installed or other methods employed. At the hot leg the skin would be welded to the tube sheet. At the cold header a close fitting slip joint would be used to accommodate any mismatch in thermal expansion between the skin legs and the tube-tube sheet bundle. This joint need not be leak tight since a zero pressure differential exists there locally.

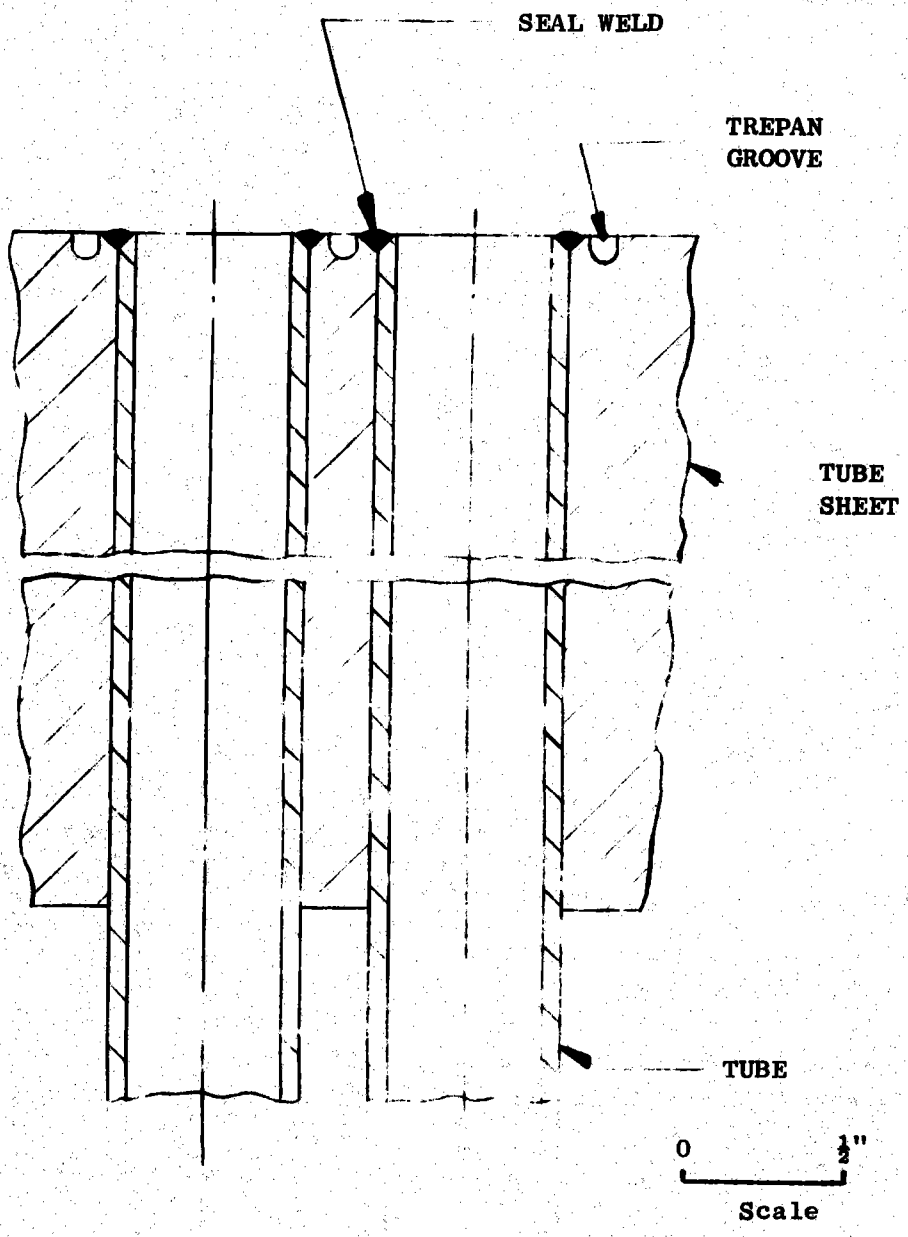

Figure C-9. Tube-to-tube Sheet Joint.

5. After adequate NDT inspection the transition section would be welded to the tube sheets. The transition section could be a forging or a split welded subassembly. Adequate welding accessability is provided.

C.3.2.3 Thermal-Hydraulic Design

IHX module sizing and parametric design studies were accomplished with the aid of a gas-to-gas heat exchanger design code. Thermal-hydraulic performance requirements, tube size and geometrical configuration data are inputs to the program. The code calculates the number of tubes and the dimensions of the heat exchanger.

The computer code uses the effectiveness-NTU approach described by Kays and London in reference C-4. The inputs to the code determine the effectiveness, ε, which is given by:

$$\varepsilon = \frac{(\Delta T)_{max}}{T_H(in) - T_C(in)} \qquad (1)$$

where

$(\Delta T)_{max}$ = temperature rise of cold stream at temperature drop of hot stream, whichever is larger.

Given the heat exchanger effectiveness, the circulation ratio, and the heat exchanger type (counterflow, crossflow, etc.), the number of heat transfer units, NTU, can be calculated:

$$NTU = \phi\ (t,\ CR) \qquad (2)$$

where

$$NTU = \frac{UA}{(W\ Cp)_{min}} \qquad (3)$$

$$CR \equiv \frac{(WCp)_{min}}{(WCp)_{max}} = \text{Circulation Ratio} \qquad (4)$$

The function ϕ in equation (2) is determined once the heat exchanger type is specified. The U-tube design is a crossflow unit with shell-side passes. For a crossflow unit, the appropriate relations are as follows. The required thermal effectiveness per pass, ε_p, is given in terms of the overall effectiveness (Equation 1), and the circulation ratio, CR (Equation 4):

$$\varepsilon_p = \frac{E^*-1}{E^*-CR} \tag{5}$$

where

$$E^* = \left(\frac{1-\varepsilon CR}{1-\varepsilon}\right)^{1/n_p} \tag{6}$$

where n_p is the selected number of shell-side passes.

For crossflow when the minimum value of the WC_p product occurs on the shell side (the mixed side), the required number of heat transfer units per pass, NTU_p, is calculated from the relationship:

$$NTU_p = -\frac{1}{CR} \log_e \left\{1 + CR \log_e (1-\varepsilon_p)\right\} \tag{7}$$

The term "mixed" in the context of crossflow refers to the fact that the shell-side flow is free to be thermodynamically mixed in the direction perpendicular to the flow direction in each pass; in distinction, the "unmixed" fluid in the tubes is not thermodynamically mixed since the flow is segregated by the tubes.

When the minimum value of the WC_p product occurs on the tube side (the unmixed side), the NTU_p is calculated with:

$$NTU_p = -\log_e \left\{1 + \frac{1}{CR} \log_e (1-\varepsilon_p CR)\right\} \tag{8}$$

In either case, the total number of NTU's required is determined as:

$$NTU = n_p \, NTU_p \tag{9}$$

For flow inside a tube, the appropriate heat transfer correlation for turbulent flow is:

$$\frac{h_i d_i}{k_g} = 0.023 \left(\frac{G_i d_i}{\mu} \right)^{0.8} \left(\frac{\mu C_p}{k_g} \right)^{0.4} \tag{10}$$

where G is the mass flux inside the tube, and d_i is the inside diameter; μ, C_p, and k are the viscosity, specific heat, and thermal conductivity of the flowing helium, evaluated at the average bulk temperature.

The shell-side heat transfer coefficient for crossflow is given by the relations presented in Reference C-5a:

$$\frac{h_o d_o}{k_g}_o = C \left(\frac{G_{max} \, d_o}{\mu} \right)^n \times 1.13 \left(\frac{\mu C_p}{k} \right)_o^{1/3} \tag{11}$$

G_{max} is the mass flow based on the minimum flow area. This equation is valid for banks having ten or more transverse rows of tubes and for values of the Reynolds number in the range: $2{,}000 < (G_{max} do/\mu) < 40{,}000$. Strictly, the gas properties are to be evaluated at a temperature halfway between the bulk temperature and the wall temperature. However, the code evaluates the gas properties at the average bulk temperature; but this evaluation has only a small effect on the overall designs obtained in the parametric analysis.

The values of n and C to be used in Equation 11 were determined by Grimison based on data for air obtained by Pierson and by Huge. Table C-5 (taken from reference C-5a) summarizes the values of n and C to be used in equation 11 for both staggered and in-line tube arrangements as a function of the longitudinal bank spacing (S_L) and the transverse tube spacing (S_T), as made nondimensional by the outside diameter of the tube. The geometry of the tube spacing is shown in Figure C-10.

The pressure drop for crossflow across tube banks is calculated with the following equations (which are from reference C-5b):

$$\Delta P = 4\, f_{TB} N^* \frac{G_{max}^2}{2\rho_{go} g_c} \tag{12}$$

where N^* is the number of major restrictions encountered by the flow through the tube bank of N_T transverse banks. For all in-line arrangements and for staggered arrangements where S_T is less than S_L:

$$N^* = N_T \tag{13}$$

For staggered arrangements where S_T is greater than S_L,

then
$$N^* = N_T - 1 \tag{14}$$

For staggered arrangements, the friction factor for the tube banks, f_{TB}, is:

$$f_{TB} = \left(Re_o\right)^{-0.16} \left\{ 0.25 + \frac{0.1175}{\left(\frac{S_T}{d_o} - 1\right)^{1.08}} \right\} \tag{15}$$

where the Reynolds number Re_o is calculated as:

$$Re_o = \frac{G_{max}\, d_o}{\mu_o} \tag{16}$$

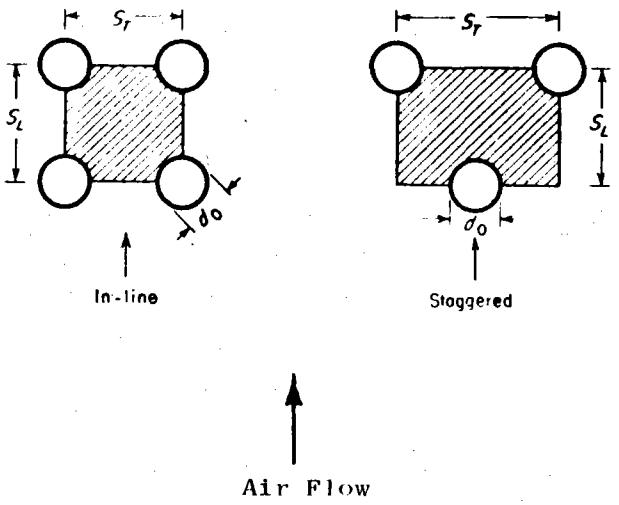

Figure C-10. Definitions of pitch for crossflow over tube banks.

Arrangement	S_T/d_0 / S_L/d_0	1.25		1.50		2.0		3.0	
		c	n	c	n	c	n	c	n
Staggered	0.6							0.213	0.636
	0.9					0.446	0.571	0.401	0.581
	1.0			0.497	0.558				
	1.125					0.478	0.565	0.518	0.560
	1.250	0.518	0.556	0.505	0.554	0.519	0.556	0.522	0.562
	1.50	0.451	0.568	0.460	0.562	0.452	0.568	0.488	0.568
	2.0	0.404	0.572	0.416	0.568	0.482	0.556	0.449	0.570
	3.0	0.310	0.592	0.356	0.580	0.440	0.562	0.421	0.574
In-line	1.25	0.348	0.592	0.275	0.608	0.100	0.704	0.0633	0.752
	1.50	0.367	0.586	0.250	0.620	0.101	0.702	0.0678	0.744
	2.0	0.418	0.570	0.299	0.602	0.229	0.632	0.198	0.648
	3.0	0.290	0.601	0.357	0.584	0.374	0.581	0.286	0.608

Table C-5. Values of c and n to be used in Equation 11 for banks of tubes having more than 10 transverse rows

For in-line arrangements, the appropriate friction factor is:

$$f_{TB} = (Re_o)^{-0.15} \left\{ 0.044 + \frac{0.08(S_L/d_o)}{\left(\frac{S_T}{d_o} - 1\right)^{0.43+(1.13d_o/S_L)}} \right\} \qquad (17)$$

These correlations are valid for: $5{,}000 < Re_o < 40{,}000$.

The thermal hydraulic design parameters calculated by the design code are summarized in Table C-6.

The analyses described above assumes uniform flow distribution on both the tube-side and the shell-side. In the reference U-tube design, there should be no problem with flow distribution on the tube side. The shell-side,however, involves flow in headers between each cross flow pass as illustrated in Figure C-11a. This is a parallel-flow header arrangement (not to be confused with heat exchanger type) in which the inlet header flow is parallel to the flow in the outlet header. Pressure variations in the headers are a result of frictional losses and momentum effects. In the inlet header, frictional effects contribute a negative pressure gradient while momentum effects (due to loss of fluid to the core) contribute a positive pressure gradient. Whether the pressure actually increases or decreases in the direction of flow depends upon the relative magnitudes of the two effects. In the outlet header, the friction and momentum effects act in the same sense and the pressure decreases in the direction of flow. The overall result, as illustrated in Figure C-11b, could be an increasing core ΔP which would lead to flow maldistribution.

Reference C-6 presents an analysis of flow headers for heat exchangers. The purpose of that analysis is to determine the header configuration required for uniform flow distribution and to analyze the pressure losses chargeable to the headers. As a guide, the following limits of applicability of the design equations are given in this reference.

TABLE C-6

THERMAL-HYDRAULIC DESIGN SUMMARY U-TUBE MODULE

CONFIGURATION

Heat Exchanger Type: Multi-Pass, Cross-Counterflow, U-Tube	
Tube O.D.	12.7 mm
Tube Wall Thickness	1.27 mm
Transverse Tube Pitch	25.4 mm
Longitudinal Tube Pitch	11.43 mm
Number of Shell-Side Passes	24
Number of Tubes	251
Tube-Side Flow Length	17.68 m
No-Flow Length	410.38 mm

THERMAL-HYDRAULIC PARAMETERS

	Shell-Side	Tube-Side
Fluid	Primary Helium	Secondary Helium
Inlet Temperature, °C	950	300
Outlet Temperature, °C	350	900
Effectiveness	0.923	
Flow Rate, Kg/S	2.21	2.21
Mass Flux, Kg/S M^2	22.8	108.3
Heat Transfer Coefficient, $W/M^2°C$	1736	2116
Core Pressure Drop, bar	0.165	1.07
Header Pressure Drop, bar	0.931	-

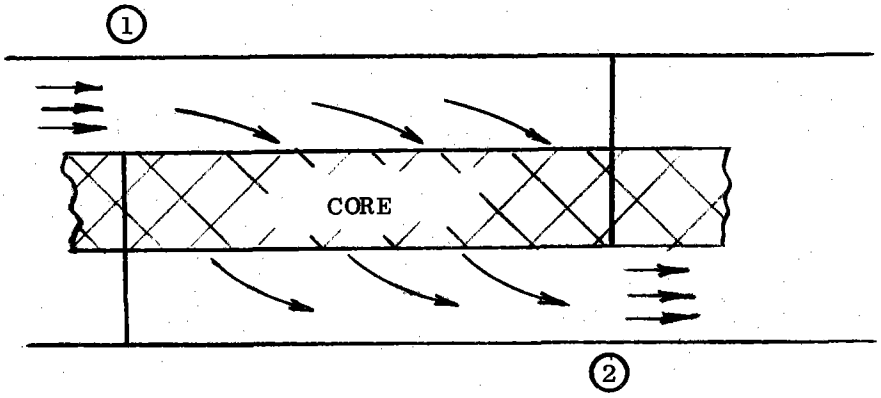

(a) Parallel Header Arrangement

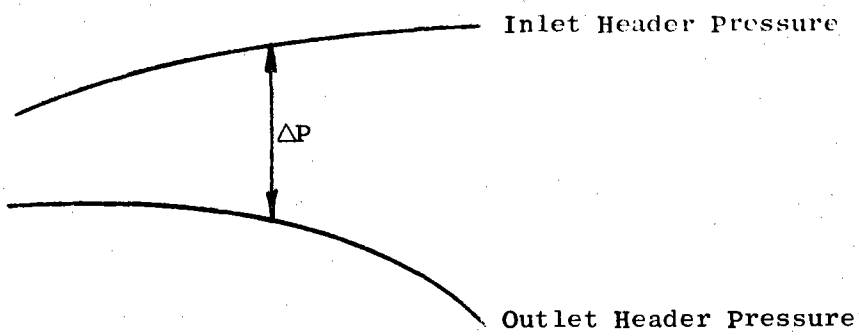

(b) Header Pressures vs. Length

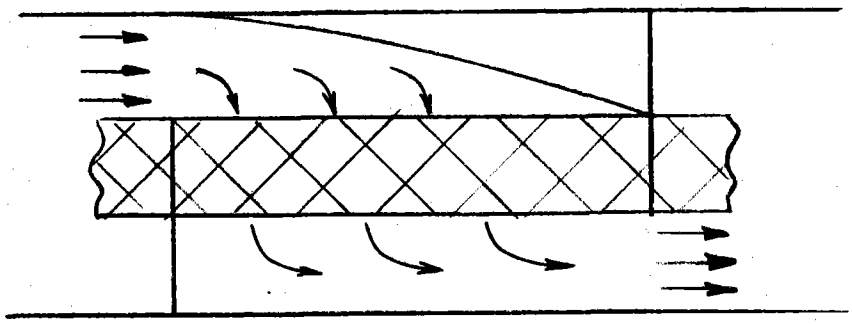

(c) Typically Shaped Inlet Header

Figure C-11. Header Arrangements for Cross Flow Configuration.

$$\frac{(\Delta P)_{core}}{h_1} > 1/2$$

$$\frac{A_1}{A_c} < 1/3$$

where

$(\Delta P)_{core}$ = pressure drop across the heat exchanger core (per pass)

h_1 = fluid velocity head at section 1

A_1 = flow cross-sectional area at section 1

A_c = core area normal to flow

In the reference design, $A_1/A_c = .096$ which is well within the limit of applicability. The ratio $(\Delta P)c/h_1 = 0.43$ which is a bit low. An 8% increase in A_1 would bring that ratio within limits. Using the analysis of Reference C-6, the shell-side pressure drop chargeable to the headers is 13.5 psi.

As mentioned previously, one result of the Reference C-6 analysis was to determine the header configuration required for uniform flow distribution. For the parallel flow headers, a requirement is that the inlet header be tapered such that the flow area varies linearly with length. This may require shaped inlet headers as illustrated in Figure C-11c. Before a full scale module is built, further analyses and bench tests of the shell-side flow distribution is recommended.

C.3.2.4 Module Thermal Profile and Stress Analysis

The temperature versus flow length relationship for both fluid streams is approximately linear as indicated in the following sketch.

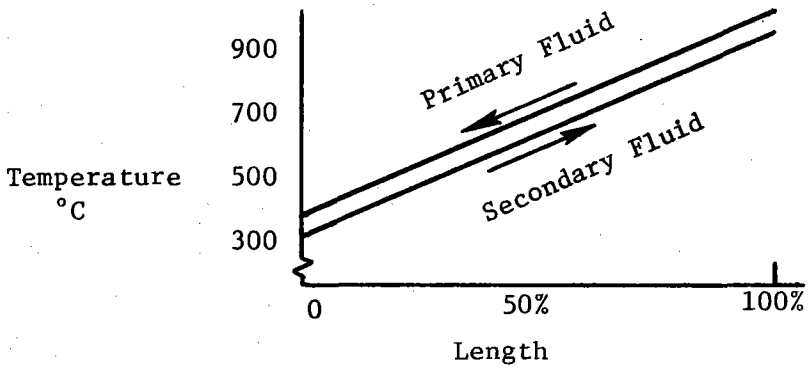

The tube metal temperature is assumed to be midway between the two fluid stream temperatures. The module skin temperature is assumed to be the same as the primary helium. These temperature profiles indicate that the two legs of the U-tube will expand differing amounts since the average temperature of the hot leg is approximately 775°C versus 475°C for the cold leg. Typical expansion coefficients indicate that free hot leg expansion will exceed that of the cold leg by approximately 2-inches. This differential expansion will result in a secondary (thermal) stress which must be controlled within fatigue-creep limitations established from the plant design life, cyclic operation and the material properties. In this instance all three of these items are not precisely known and the allowable thermal stress becomes a matter of judgement.

A computer library program* was employed to investigate the U-tube thermal stress-deflection situation. The following items summarize this investigation phase:

1. With both U-tube ends rigidly welded to the pressure vessel the legs lengthen approximately 4.8-inches from room temperature to operating conditions. (800H Inconel alloy assumed.)

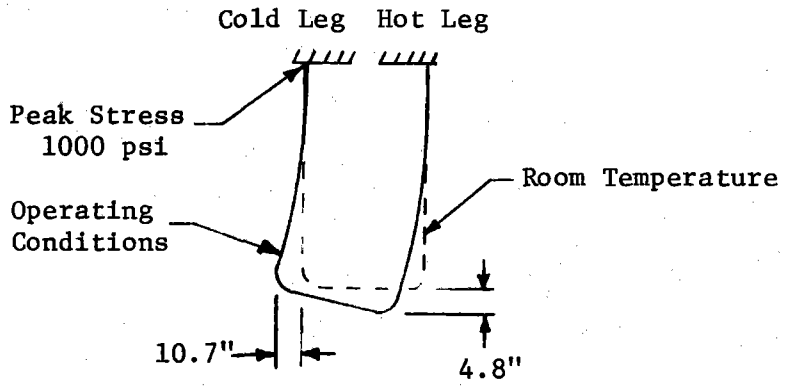

2. In a single outer U-tube (same assumptions as #1) the turnaround section would distort sideways (radially in the IHX assembly) approximately 10.7 inches due to the unequal leg lengthening.

* ASIST: General Electric Mark III Time Sharing Service

3. The maximum thermal stress resulting in this instance (assumption #1) is approximately 1000 psi and results at the cold leg attachment point.

4. When an isolated inner U-tube is examined under the same assumptions as #1, the axial growth, lateral (radial) deflection and maximum stress become 4.7 inches, 29.6 inches and 3000 psi stress respectively. This data indicates a significant difference between inner and outer U-tubes and shows that the tube core must be analyzed as a system with interacting constraints (baffles).

5. In an effort to minimize the stress-deflection situation, U-tubes made of dissimilar metals were examined. The hot leg was assumed to be fabricated from INCO 617 which has a relatively low coefficient of linear expansion and the cold leg fabricated from 316 stainless steel with a high coefficient. An isolated, rigidly welded inner U-tube showed an axial growth of 4.0 inches, a lateral (radial) deflection of 15.5 inches and a 1900 psi stress.

6. When bi-metallic inner and outer U-tubes (as in 5 above) are examined as a system the axial growth is found to be 4.0 inches, the lateral deflection 13.1 inches and the maximum thermal stress approximately 8700 psi at the inner U-tube turnaround.

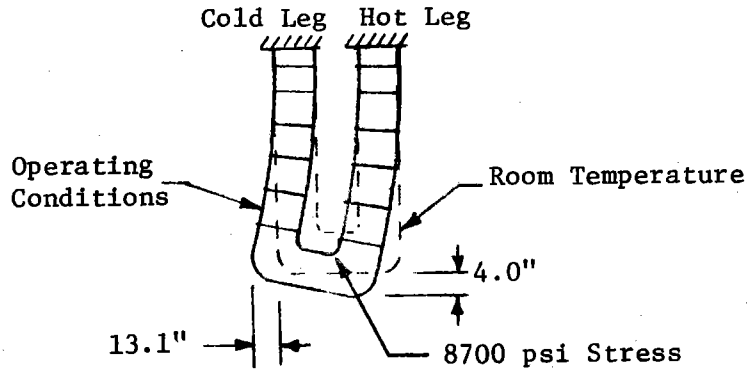

Additional stress analysis in conjunction with a detail design is required to completely resolve the U-tube thermal stress problem. Several questions which need to be answered are:

1. Can a lateral deflection of approximately 13 inches be tolerated in the IHX assembly? Perhaps it can. Figure C-7 indicates a fair amount of space between the U-tube turn around and the central primary supply duct. By "cold springing" at assembly this space could potentially be utilized and the thermal stress in the order of 8700 psi would result with the tubes deflected to a nearly vertical position.

2. Is an 8700 psi thermal stress acceptable considering the design life of the plant? Preliminary indications are that it is. The thermal stress profile varies with the tube location but tentatively reaches its maximum value in the turn around portion of the inner most U-tubes where the metal temperatures are in the order of 625°C (1157°F). The procedure for determining the structural acceptability of the IHX involves determining that all points in the heat exchanger have the capability to survive the design life without rupture as indicated by an accumulated damage analysis. The accumulated damage is calculated using the Miner Rule to combine both cyclic and steady stress effects. The total creep and fatigue damage is defined as:

$$\sum_{j=1}^{p}\left(\frac{n}{N_d}\right)_j + \sum_{k=1}^{q}\left(\frac{t}{T_d}\right)_k \leq D$$

D = total creep-fatigue damage

n = number of applied cycles of loading condition j

N_d = number of design allowable cycles of loading condition j

t = time duration of load condition k

T_d = allowable time at a given stress intensity for load k

To survive without rupture the accumulated creep-fatigue damage must be less than unity for all points for all loading conditions. A complete specification of the design life, cyclic operation, temperature, and material properties are required to accomplish this analysis. Preliminary calculations (assuming 800H Inconel) indicate a satisfactory damage analysis for the U-tube turn around section primarily as a result of the relatively low temperature and the relatively low number of thermal cycles (10^3).

3. What is the peak stress and is it tolerable when the lateral deflection of the turn around sections is constrained? These answers can be obtained from a detailed stress analysis which can be expeditiously accomplished using available computer stress analysis programs. If resultant stresses are too severe a bellows can be utilized to accomplish the attachment of one end of the U-tube module to the pressure vessel shell. Although it is felt that a bellows will not be required the reference design heat exchanger does incorporate this feature since it represents one solution to the U-tube thermal stress problem. The following section (C.3.2.5) presents a design discussion of this bellows.

The module skin is subjected to essentially the same temperature profile as the tubes and will require axial expansion freedom in one leg to allow stress free deflection. A close clearance slip joint between the module skin and the cold header readily provides this freedom and is readily accomplished since a positive gas seal is not required.

C.3.2.5 Bellows Design

The IHX reference design indicates that a bellows is used with each module to provide a flexible seal between the cold secondary inlet leg and the pressure vessel. The bellows allows the cold U-tube leg to expand less than the hot leg without producing thermal stresses and deflection in the primary-to-secondary heat transfer tubes. The bellows design indicated in Figure C-7 consists of a dual bellows configuration with the following features:

1. The bellows is in the cold leg and is not a structural member.

2. The bellows is readily inspectable being located at the outer, upper edge of the IHX pressure vessel.

3. A redundant bellows design is used with the space between the two bellows pressurized to greater than the IHX internal cavity. Any leakage due to failure of the inner bellows results in inward flow to the primary rather than vice versa and is detectable due to buffer gas flow.

4. A failure of either the inner or the outer bellows would be indicated by the resultant flow of the normally static buffer gas.

5. A failure of the outer bellows would be immediately detectable by inspection and would result in buffer gas flow into the secondary containment building.

6. A complete failure of both bellows sections would not result in the distribution of the primary coolant gas to the process heat exchanger. The flow would be retained within the secondary containment building with the same consequences as any primary containment rupture except that in this case the flow rate would be controlled to a low value due to the small area, labyrinth type clearance rings built into the penetration feedthru.

C.3.2.6 Baffle Design Considerations

Since the module skin is approximately 25°C above the tube temperature, a 30 foot length of skin will grow approximately 1/8" longer than the tubes. Clearance of this magnitude must be factored into the turnaround section but of more significance is how this effect relates to the baffle plates. It is assumed the baffle plates will be located by the friction of the 251 tubes which penetrate the close clearance holes (.005 - .010 diameter clearance). Thus the baffle plates will move with the tubes with as much as 1/8"inch of relative motion between the baffle plate edges and the skin interior. The development of a hard coating or ceramic coating of some nature is required to insure that sliding does occur at these locations. See discussion in Appendix I. Use of a skin material with a slightly lower coefficient of expansion than that of the tube material could eliminate this motion. A convolution-deflection type section in the skin (or baffle plate) could also provide an acceptable solution to this problem.

C.3.3 DESIGN VARIATIONS OF THE REFERENCE DESIGN

This section presents alternate design variations of the U-tube style IHX which were conceived during the study and which may have future value.

C.3.3.1 IHX Cavity Pressure Variations

The U-tube concept with the primary helium on the shell side results in the IHX pressure vessel cavity always being subjected to essentially the same pressure as the reactor core. However three distinct variations of the IHX can be determined by slight design variations of the specific cavity pressure with resultant advantages and disadvantages. Specifically, the IHX cavity pressure can be vented to either the HX core inlet, the core HX outlet or the circulator outlet.

With the cavity pressure at the core inlet level there is no need for the central hot supply duct shown in the reference design. The hot coaxial duct could simply terminate at the IHX shell. The hot helium would find its way to the module inlets which would simply be openings in the module skin. The module's exhaust would be contained in sealed

ducts to the circulator inlet and the primary flow would essentially be sucked through the modules. This arrangement simplifies the hot inlet ducting by eliminating it and replacing it with cold outlet ducts. There would always be a collapsing pressure gradient across the module skin which would be zero at the hot end and be equal to the core pressure drop at the cold end. The uncontrolled hot inlet streaking discouraged the selection of this variation as the reference design.

The reference design vents the cavity pressure to the HX core outlet A hot sealed supply duct into each module is required but no ducting is required for the core outlet. The cool outlet flow tends to bathe the metal surfaces as it finds it way to the circulator inlet. This arrangement puts an internal bulging pressure gradient across the module skin which would be zero at the cold module exhaust and would be equal to the core pressure drop at the hot module inlet.

In the third variation the hot duct into the module is required as well as a sealed core outlet duct to the circulator inlet. By venting the pressure vessel cavity to the circulator outlet pressure (or any intermediate value by appropriate circulator bleed-off) a collapsing pressure is developed across all sections of the module skin with the maximum gradient occurring at the cold end. With this arrangement any cracks in the skin which open by-pass leakage paths would always result in cold-streaking, i.e., cold circulator discharge flow into a lower pressure hot region. By venting the IHX cavity through a controlled line, a direct means of sensing internal by-pass leakage of the primary circuit is obtained. Since there is normally no flow in the vent line from the circulator discharge to the main IHX cavity any measured flow would indicate an internal leak. Figure C-12 illustrates this design arrangement.

C.3.3.2 Circulator Location

Figure C-13 shows a U-tube design variation in which the circulator is internally top mounted. Core inlet and outlet manifolds are located at the bottom of the IHX. The sealed module inlet and outlet allows the cavity pressurization to be established so as to result in the cold-streaking previously discussed. The main secondary ducting to and from the process heat exchanger would be located at ground level rather than

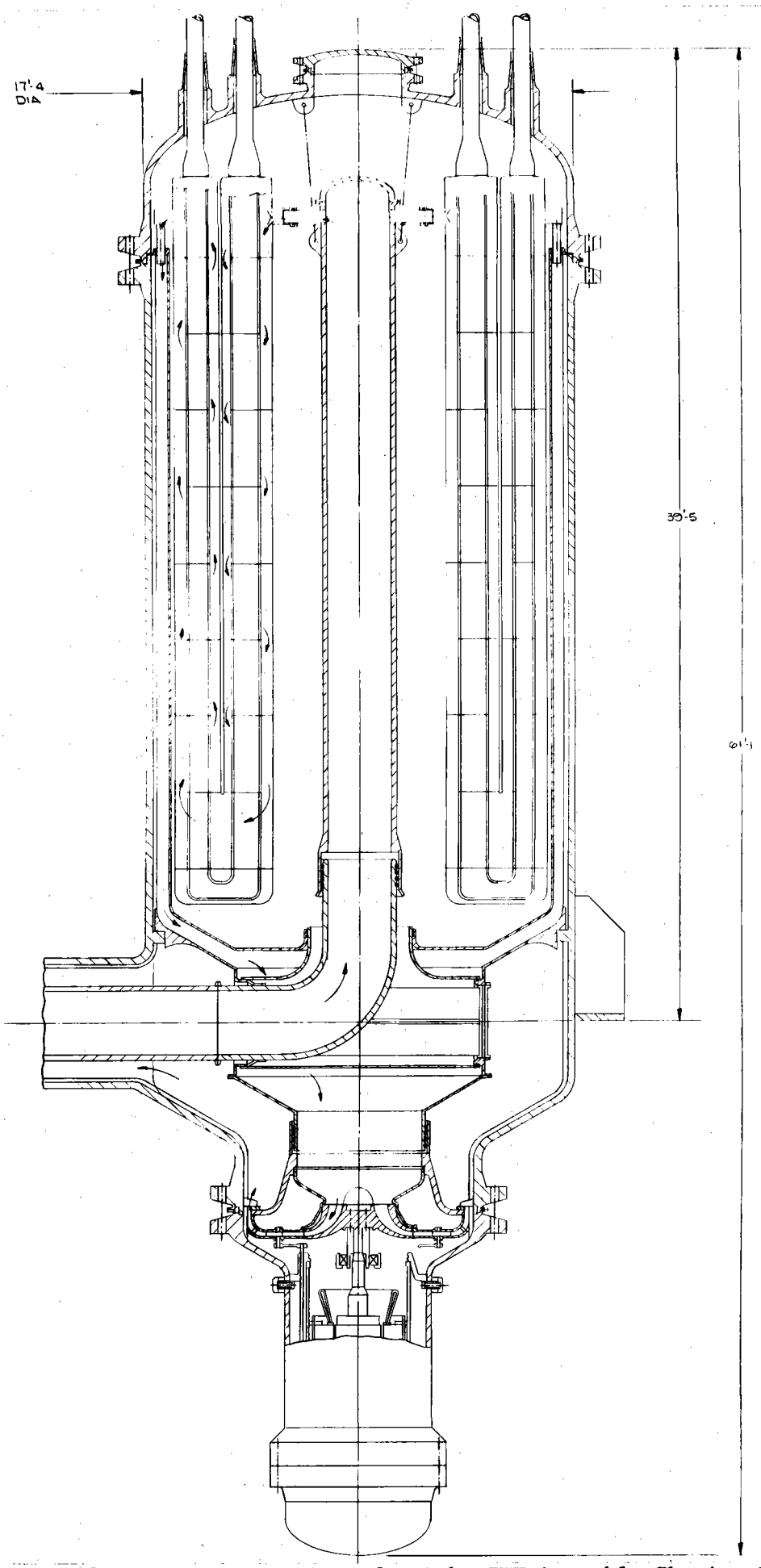

Figure C-12. Design Variation of U-tube IHX Assembly Showing Primary Inlet and Outlet Ducts at Each Module.

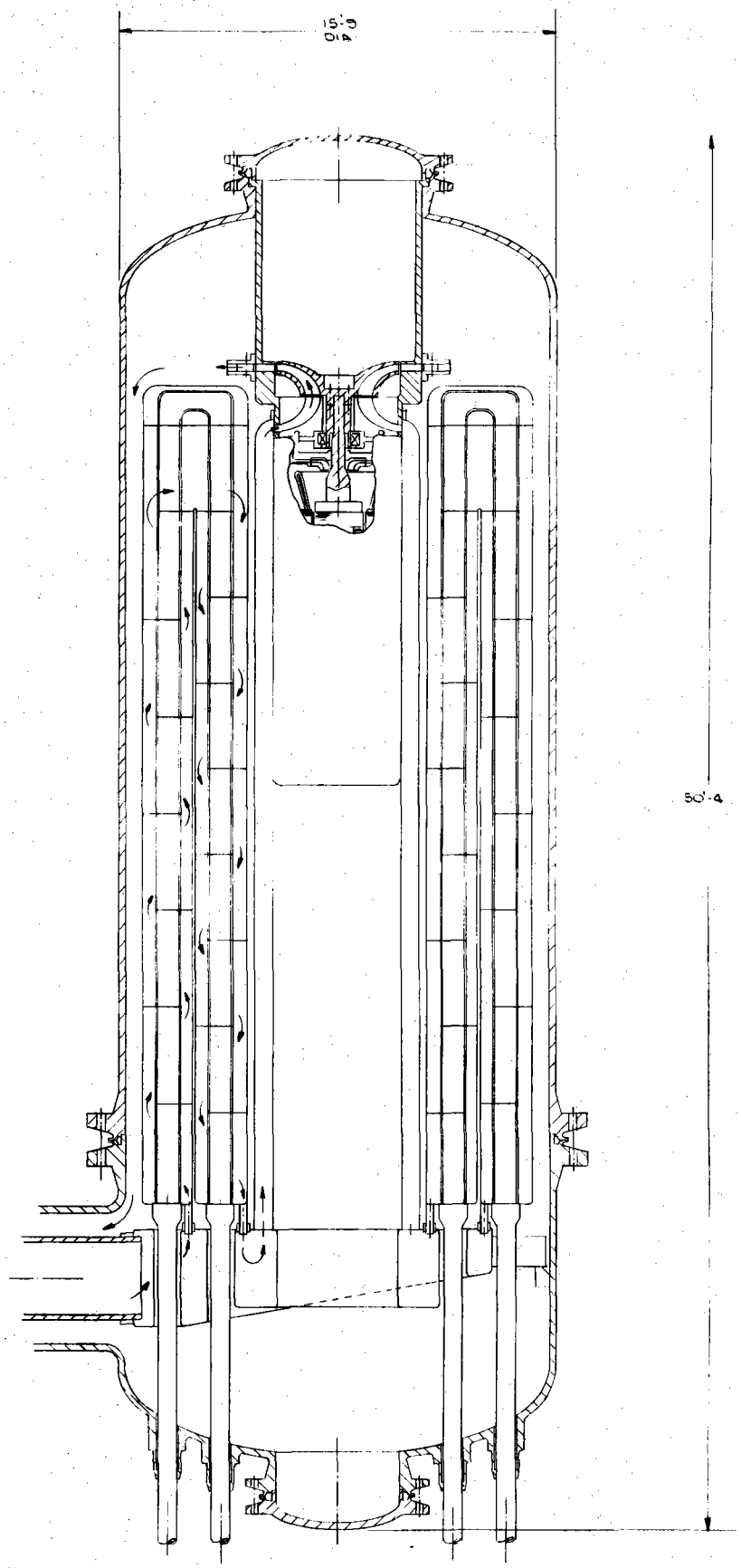

Figure C-13. Internal Circulator Design Variation of U-tube IHX Assembly.

elevated as in the reference design. Modules are inverted from the previous designs and would require some sort of support in the turn-around area.

C.3.3.3 Buried Circulator Design

Figure C-14 illustrates a design which attempts to eliminate the hot gas supply ducting without inverting the U-tube. The primary coolant flow goes directly from the coaxial duct into a toroidal manifold which feeds each module. Any of the cavity pressurization schemes discussed in C.3.3.1 could be utilized.

Since the coaxial inlet duct elevation is located by the PCRV this configuration results in the lower end of the IHX pressure vessel being below ground level and possibly requiring some penetration in the foundation. Figure C-15 shows such a tentative arrangement for the power levels specified herein.

C.3.3.4 Non-Circular Module Cross Section

The nesting of the U-tube modules is somewhat impaired by using circular cross sectional U-tube legs since there is always a lost space between tangent circles. Key stone-shaped modules as shown in Figure C-16 make better utilization of the PV internal space with the disadvantage that the flat surfaces do not make as good a pressure vessel as the cylindrical design. However, by compact nesting against each other so that the flat surface touched each other they could reinforce each other and collectively could accommodate the relatively small pressure differential across the module skin. Channels or hat-section reinforcement of the flat surfaces would be required for individual module testing.

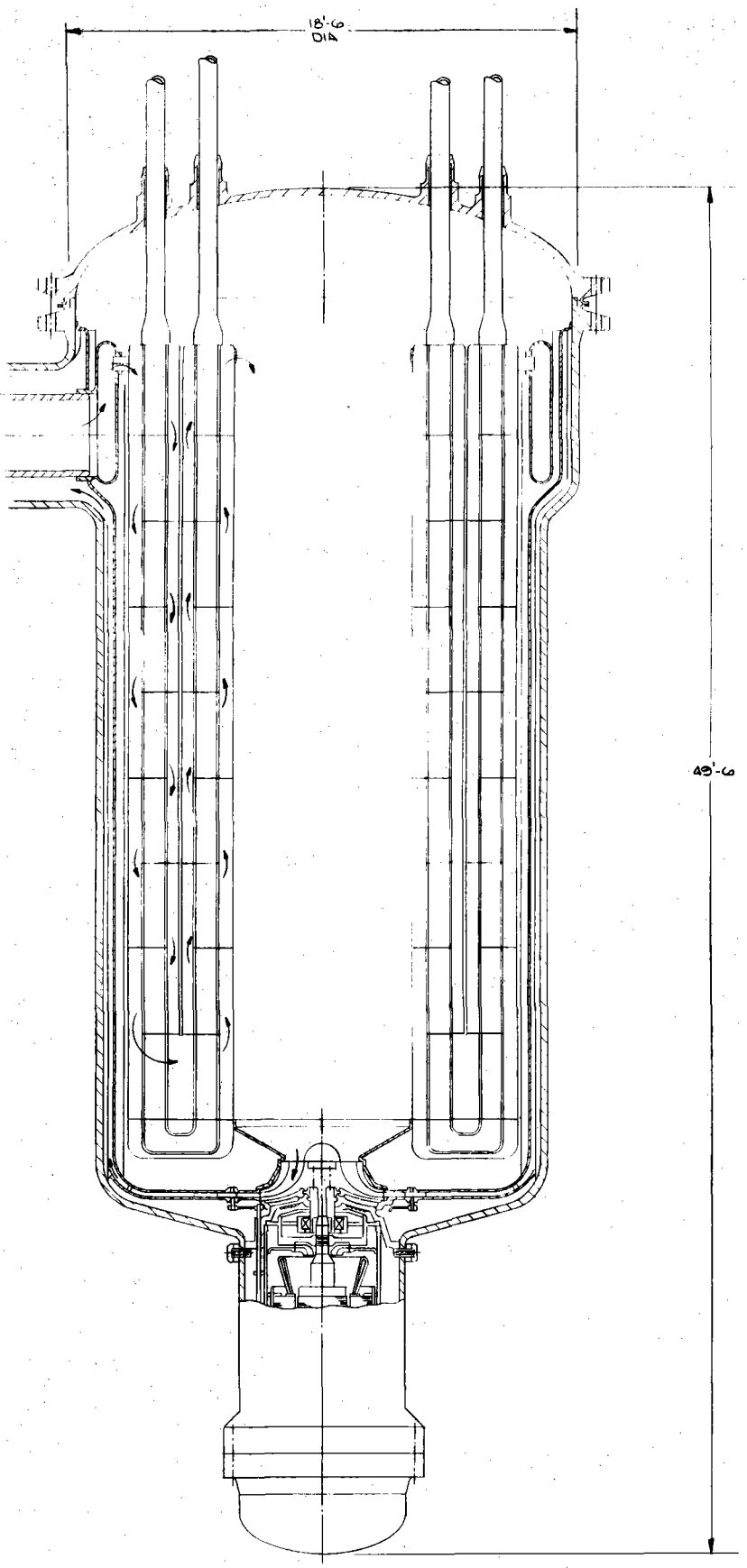

Figure C-14. Buried Circulator Design Variation of U-tube IHX Assembly.

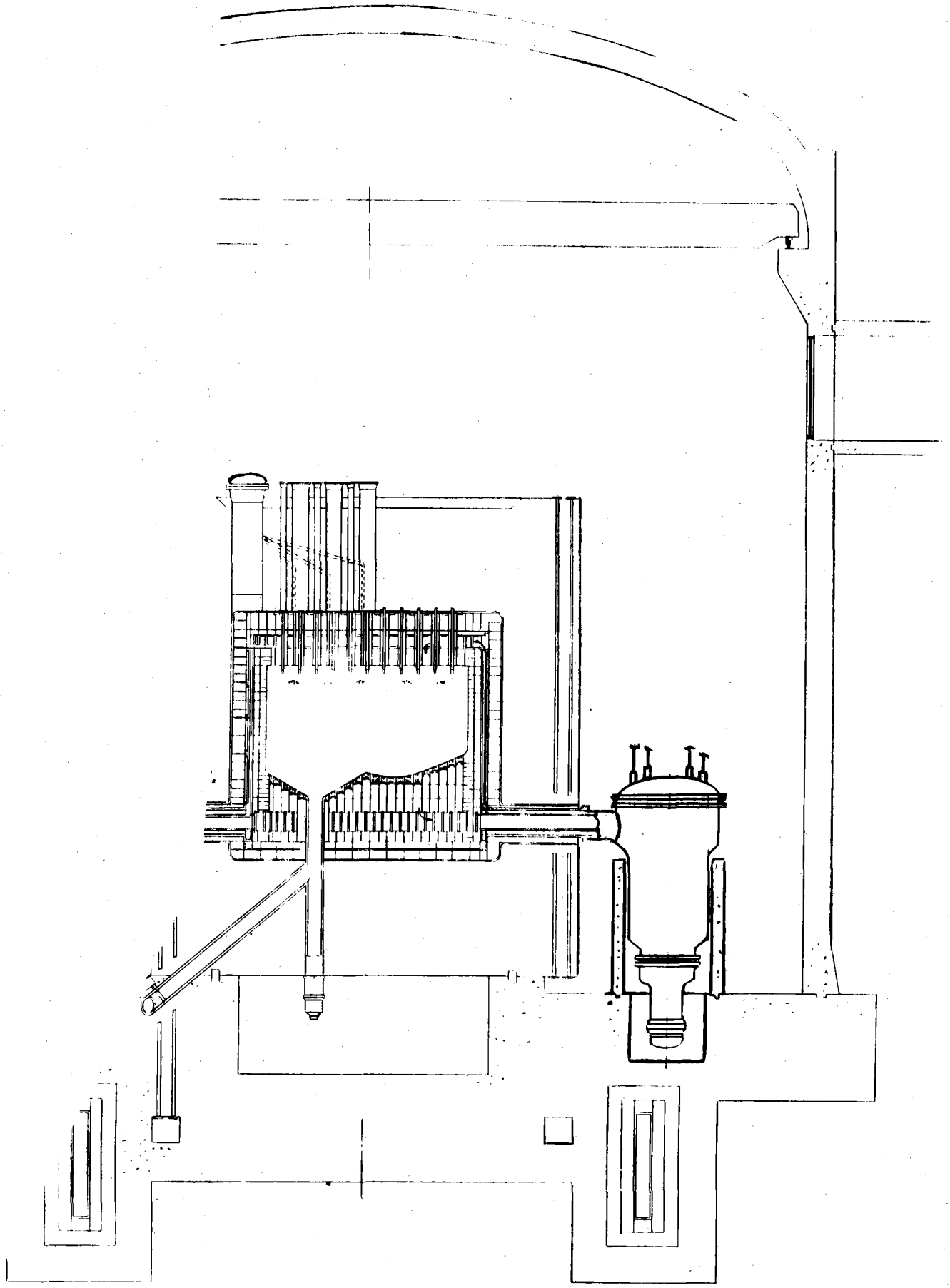

Figure C-15. Steam Reformer Plant with "Buried Circulator" IHX.

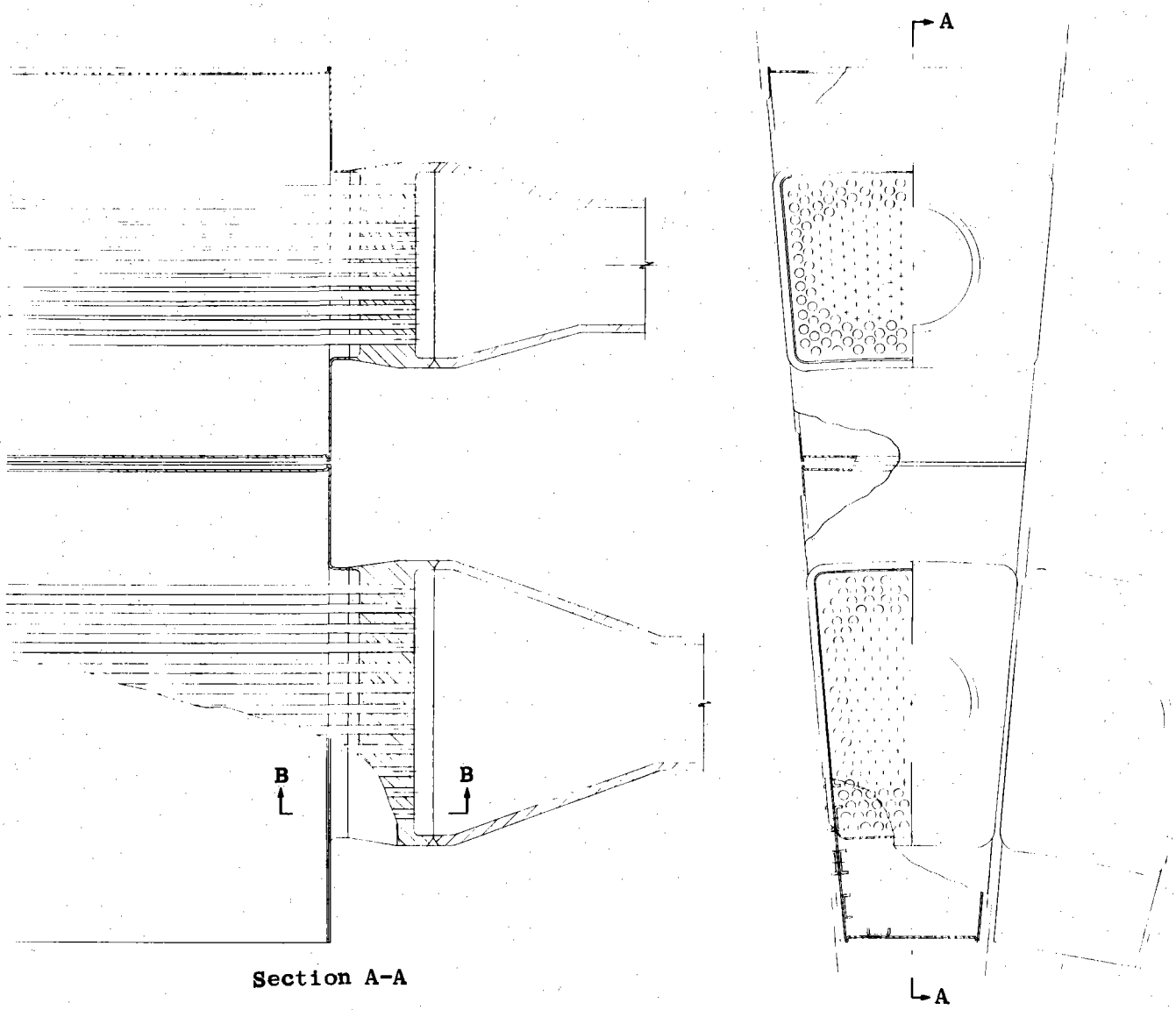

Figure C-16. Module Design Variation Showing Keystone-shaped Cross-section.

C.4 ASSESSMENT OF HEAT EXCHANGER CONFIGURATIONS

C.4.1 IHX SPECIFICATIONS

The selection of an optimum design heat exchanger depends upon an overall assessment of numerous considerations, some of more importance than others. A precise weighing and evaluation of the various aspects is difficult but nevertheless is attempted and described in this section. As an initial assumption the specific thermal requirements shown in Figure C-17 are assumed a priori and are fundamental to the conclusions reached. These thermal requirements dictate a large heat exchanger (250 MW) with a high effectiveness (.923) and a moderately low LMDT (50°C).

The basis of design optimization is contractually identified in the work statement as the following:

- o Safety
- o Cost
- o Other Engineering Considerations

Additional contractual requirements related to the IHX phase are to provide definition of any material development required by the design.

Contractual reference to previous studies[C-1,C-2,C-3] implies the system specifications listed in Table C-7. A noteable requirement/assumption concerns the faulted design condition which establishes the stress basis for design. In this area it is assumed that a guillotine fracture of the secondary loop could occur as the fault condition. Figure C-18 taken from the ASME B&PV Code shows the analyses flow diagram required for the faulted and other conditions. When this assumed fault occurs a large pressure differential is developed across the primary-to-secondary barriers, i.e., the tubes and tube sheets. The primary flow would be stopped as soon as possible within the reactor shutdown limitations. A ten hours application of this faulted condition has been assumed for the total plant life. (i.e., in ASME language, S_t is the ten hour time - temperature allowable stress.)

THERMAL DESIGN POINT

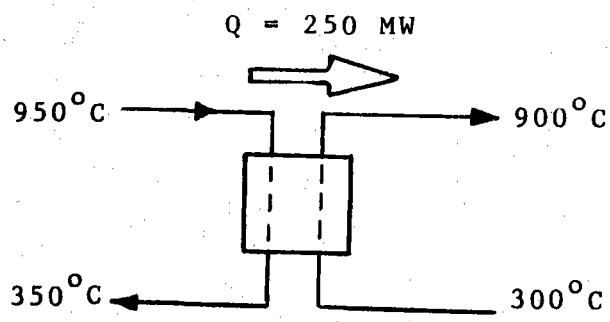

CONTRACTUAL REQUIREMENTS

OPTIMIZE IHX DESIGN RELATIVE TO:

- SAFETY
- COST
- OTHER ENGINEERING CONSIDERATIONS

PROVIDE RELATED MAT'L. (& FUEL) DEV. REQ'TS.

Figure C-17 Thermal Design Point and Contractual Requirements for IHX Assembly.

TABLE C-7

REFERENCED SYSTEM DESIGN REQUIREMENTS

PLANT DESIGN LIFE	30 YRS.
BASIC PLANT SIZE	3000 MW(t)
PRIMARY REACTOR COOLANT	HELIUM
NO. OF LOOPS	12
CYCLIC OPERATION	1000 THERMAL CYCLES
PRIMARY COOLANT DUCTS	31.5 INCH (I.D.)
COOLANT SUPPLY TEMP.	950°C
COOLANT RETURN TEMP.	350°C
NON-INTEGRATED IHX	
PRI. & SEC PRESSURE	$\approx$ 40 BARS
ASSUMED LIMITING FAULT CONDITION	SECONDARY RUPTURE
MODULAR IHX EXTREMELY DESIRABLE	

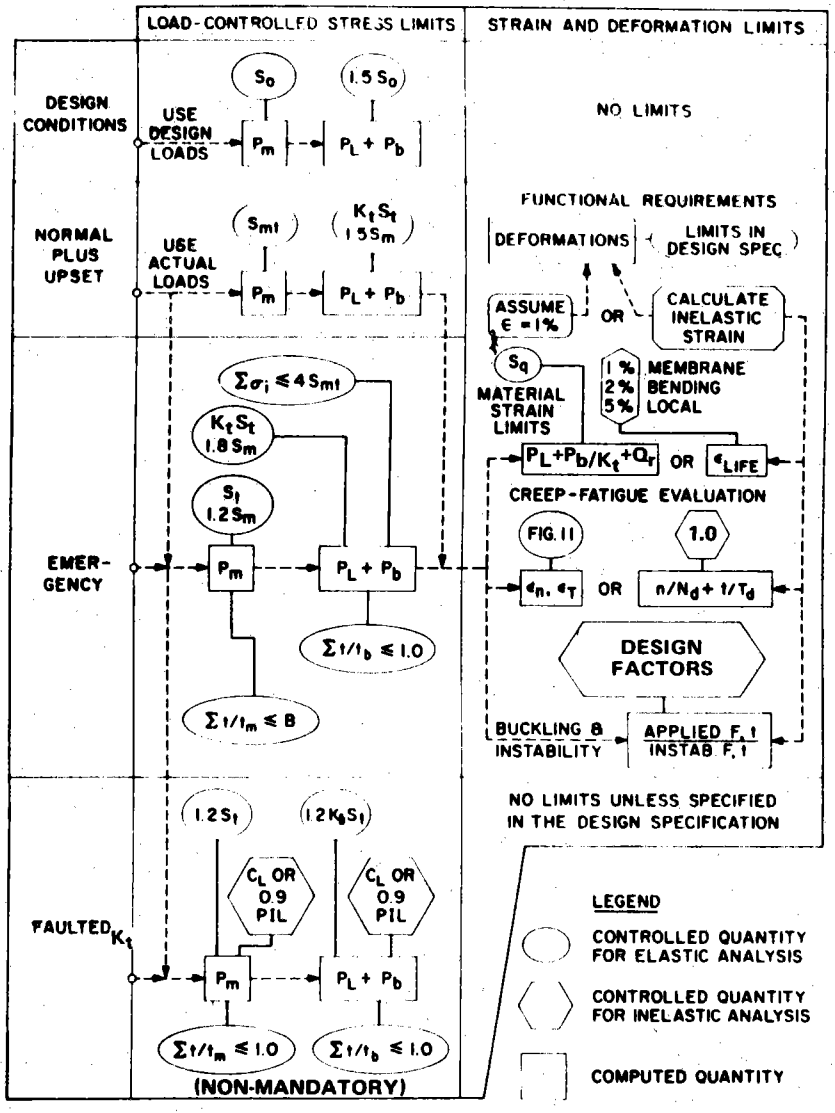

Figure C-18 Flow Diagram for Elevated Temperature Analyses

A guillotine fracture of the primary loop while undoubtedly of more severe consequence to the reactor plant, is less demanding on the IHX. A sudden drop in pressure on the primary side can almost immediately be matched on the secondary side by shutting off and/or regulating the secondary helium pressure and flow. The worst possible magnitude of the ΔP is approximately the same for either guillotine failure but the time duration application is considerably longer with a secondary failure since there is considerably less flexibility for variation of the primary (reactor side) pressure. In addition a primary failure stops the heat input to the IHX metal whereas this is not necessarily true with a secondary failure.

C.4.2 CONFIGURATION CANDIDATES

A review of related studies and proposals coupled with consideration of the specific requirements indicate the IHX heat transfer surfaces should be tubular and should be patterned in one of the following basic styles:

Style A - straight tubes with counterflow fluid streams

Style B - U-tube with multi pass cross flow

Style C - helical tubes with multi pass cross flow

Style D - bayonet tubes with folded counterflow

Figure C-19 illustrates these fundamental styles and briefly lists some of the advantages and disadvantages which are generally associated with each.

Two variations of the straight tube counterflow style and of the helical tube style made a total of six conceptual designs which were thoroughly examined in an effort to identify an optimum design. General assumptions which were made relative to all styles are:

1. Primary helium is shell side. This would allow a steam generator to be integrated with the IHX in the primary loop if this were desired.

STYLE A STRAIGHT-TUBE COUNTERFLOW

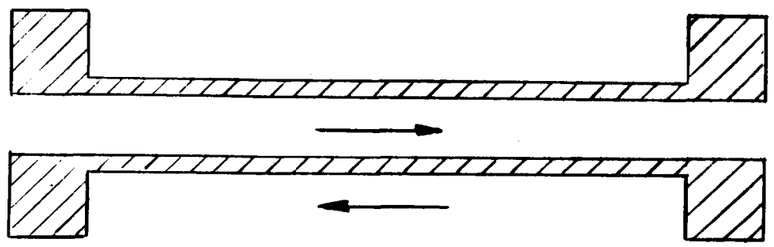

Advantages
- o Thermally Ideal
- o Small, Simple Tubes

Disadvantages
- o Axial Expansion
- o Tube Support

STYLE B U-TUBE MULTIPASS CROSSFLOW

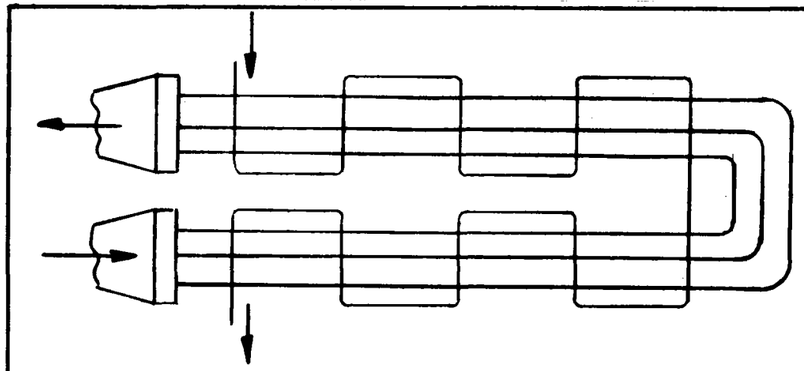

Advantages
- o Approaches Ideal Thermal
- o Small, Simple Tubes
- o Tube Support
- o Axial Expansion

Disadvantages
- o Δp Turning Losses
- o Packaging

STYLE C HELICAL-TUBE MULTIPASS CROSSFLOW

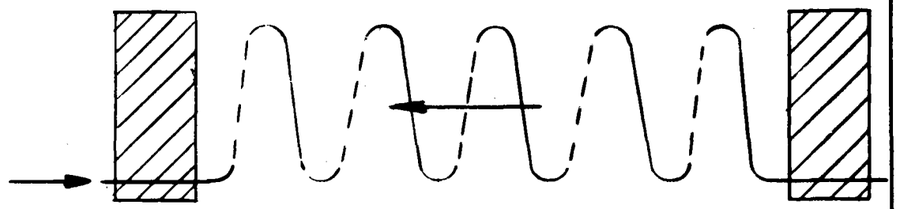

Advantages
- o Thermal Expansion
- o Approaches Ideal Thermal

Disadvantages
- o Non-modular
- o Difficult Assy.
- o Central Void
- o Long, Big O.D. Tubes

STYLE D BAYONETTE-TUBE FOLDED FLOW

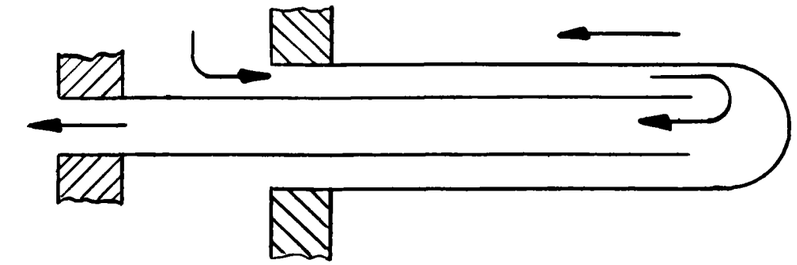

Advantages
- o Axial Expansion
- o 2 - Temp. Zones Possible
- o Annular Flow Area Independent of Tube Spacing

Disadvantages
- o Heavy
- o Tube Support
- o Thermal Feedback
- o Leak Isolation

Figure C-19. Fundamental HX Styles and General Assessment of Their Features.

2. Bare tubes will be used with no fins. Smaller diameter tubes will be used to achieve a higher surface to volume ratio. This approach makes better use of the metal since no fin efficiency factor is required. In addition there is no significant mismatch of the inside/outside heat transfer coefficient which is the general condition which leads to the desirability of using fins.

The method of evaluation is discussed in the ensuing section. The following paragraphs briefly describe each design candidate.

Note: The reader is again cautioned not to confuse any of the U-tube design layouts shown in this C.4 assessment section with the U-tube Reference Design heat exchanger presented in section C.2 and C.3. The "B-1" coding distinction is applied to the U-tube IHX design, discussed in this section, which was used for comparison with other style IHX's. The "B-1" design led to the selection of the U-tube style as optimum. Following this selection, design refinements and improvements were accomplished which resulted in the U-tube Reference Design which is discussed in other sections of this report.

C.4.2.1 Design A-1 - Straight Tube Counterflow - Central Return

The tubes are packaged in modules with module tube sheets at each end. One end of each module attaches to a large main tube sheet. A large central return duct collects the module flow, pierces the main tube sheet and the upper surface of the pressure vessel. The primary flow is contained in individual channels surrounding each module. A primary circulator could be attached to the lower portion of the pressure vessel. Axial thermal expansion would require a "hockey stick" deflection approach at the lower end of each module or a bellows would be required as a primary to secondary barrier. This latter could be located in each module or in the central return duct.

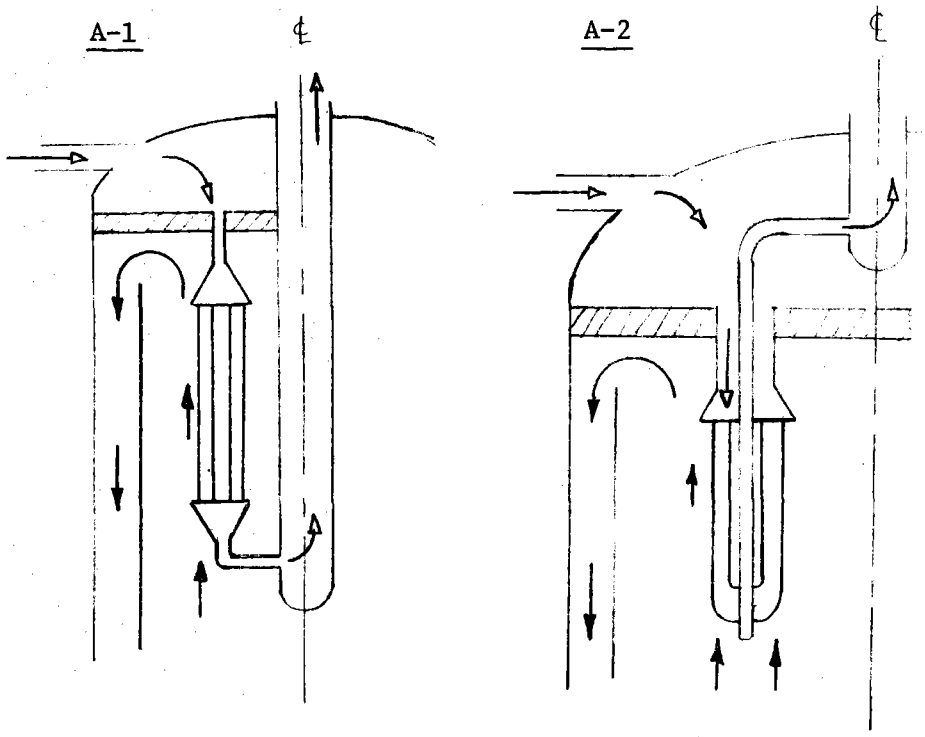

Figure C-20. Straight-Tube Counterflow IHX Schematic Diagrams

C.4.2.2 Design A-2 - Straight Tube Counterflow - Modular Return

The tubes are packaged in modules with a module tube sheet at the upper end only. The module exit flow is collected in a relatively small return duct centrally located in each module. Each return leg collects into a large central duct above the main tube sheet. Axial thermal expansion requires a "hockey stick" approach at the central return manifold or a bellows either in each module return or in the central manifold. Failure of the bellows would allow secondary flow to by-pass the heat transfer surfaces but would not void the primary-secondary separation. Primary flow is contained in individual channels surrounding each module. A primary circulator could be attached to the lower portion of the pressure vessel.

C.4.2.3 Design B-1 - U-Tube Cross Flow

The U-tubes are packaged in modules with separate module tube sheets at each tube end. Each module is enclosed in a shell which, in conjunction with the tube support baffle plate, channels the primary flow in a multipass crossflow arrangement. The module header ducts directly pierce the pressure vessel shell. Axial differential expansion is directly accommodated by the U shape or requires a bellows in one leg of each module at the pressure vessel penetration. A bellows failure would allow the primary coolant helium to leak into the secondary containment building.

B-1

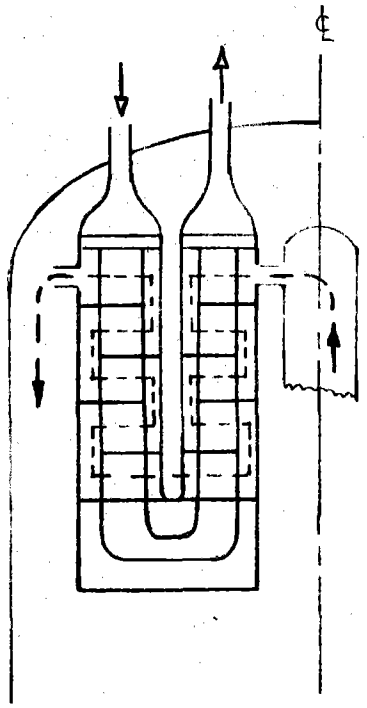

Figure C-21. U-Tube IHX Schematic Diagram

C.4.2.4 Design C-1 - Helical Tube - Central Return Duct

The tubes are wound in helices and are attached to an upper main tube sheet. The lower end of each helix connects to a large central return duct which collects the tube side flow, pierces the upper main tube sheet and the upper surface of the pressure vessel. Helices are stacked in concentric shells as well as in a multiple thread arrangement in each shell. A non-modular design results which is rather difficult to assemble due to the interlocking of the multiple helices. If the number of shell side flow passes (helical turns) is maintained constant, the tube side flow length varies from shell to shell directly as the shell diameter. Tube side flow mal-distribution could be prevented by orificing or by varying the tube I.D. in each shell.

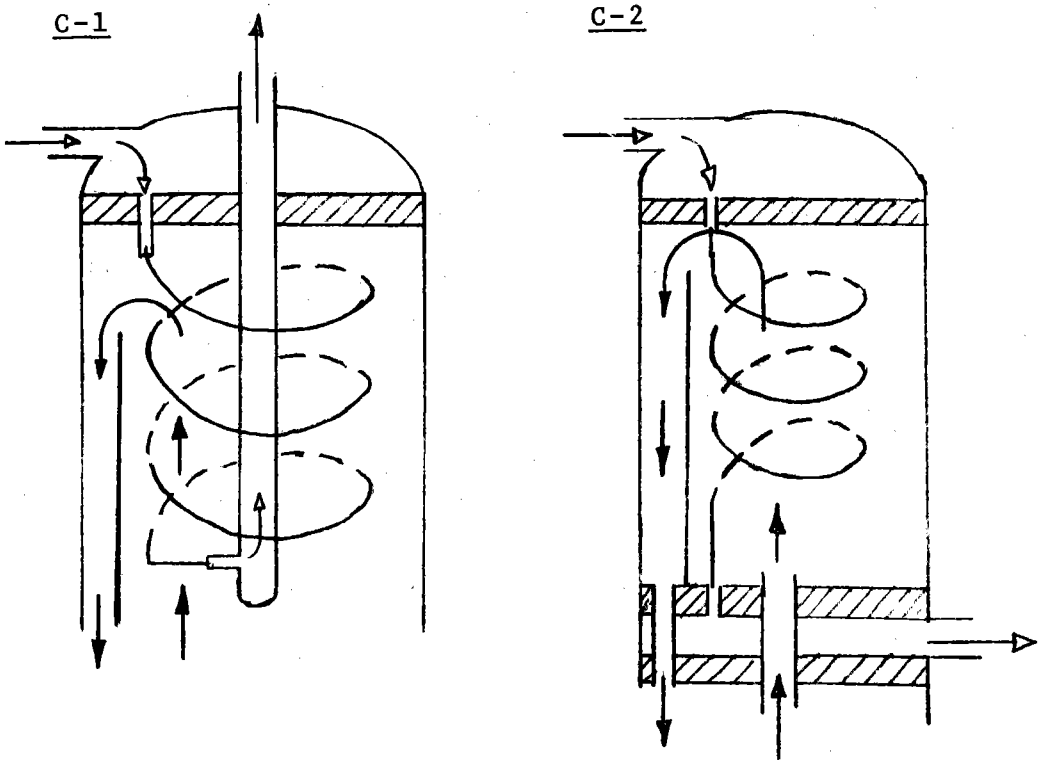

Figure C-22. Helical-Tube IHX Schematic Diagram Showing the Two Variations Evaluated.

C.4.2.5 Design C-2 - Helical Tubes - Upper and Lower Main Tube Sheet

The tubes are wound in helices which attach to an upper and lower main tube sheet. The helices are arranged in concentric shells with a multiple lead in each shell. Since the inner shell requires a certain minimum coiling diameter, a central restriction of some form is needed to prevent primary helium flow from by-passing the helical coils. The lower tube sheet requires entrance and exit penetrations for the primary flow. Thermal expansion of the tube coils is inherently accomplished provided the tube support system has adequate flexibility.

C.4.2.6 Design D-1 - Bayonet Tubes with Folded Counterflow (2-Zone)

This style IHX, designed by the KFA, is described in a technical paper presented at a HTGR conference held in Petten, the Netherlands, May 1975. The IHX is divided in two parts which are packaged concentrically. The lower temperature section is non-modular and contains approximately 2000 tube-plug tube pairs located near the periphery of the cylindrical pressure vessel. The inner plug tube ducts the cool secondary gas to the bottom of the heat transfer tube where it then receives heat during the return flow in the annular space between the plug tube and the heat transfer tube. A main tube sheet and a smaller auxiliary tube sheet attach to the tube and plug tube respectively. The collected annular flow then enters the centrally located high temperature section of the IHX. The initial flow is in the annular region where additional heating occurs. The exit flow occurs in the plug tubes which are attached in seven tube clusters to a module tube sheet. Each module exit duct contains a bellow between the auxiliary tube sheet and the pressure vesel skin to accommodate axial thermal expansion. A bellow failure allows secondary flow to by-pass the heat exchanger but the integrity of both fluid streams and their isolation is maintained.

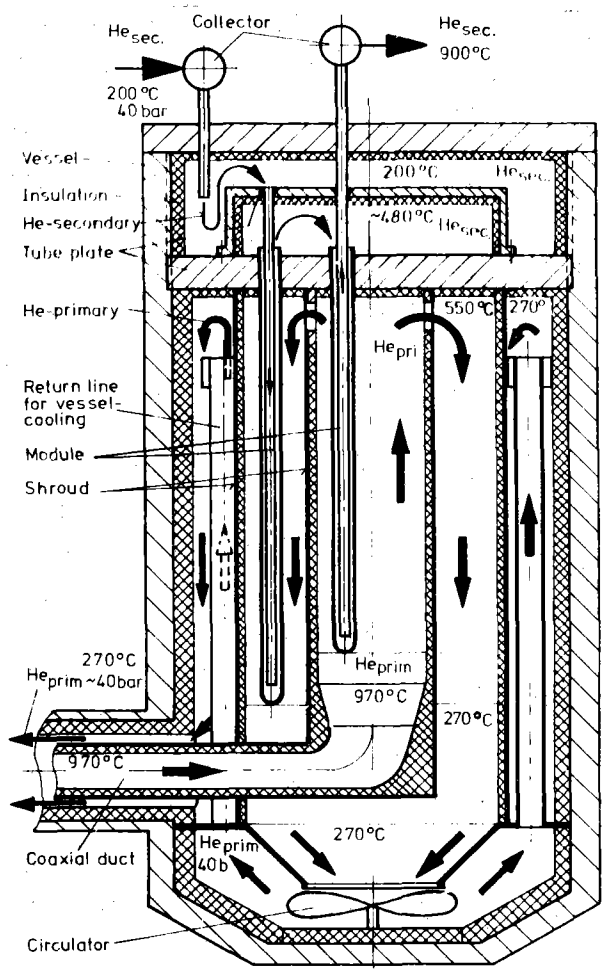

Figure C-23. Bayonet-Tube IHX Schematic Diagram

C.4.3 EVALUATION METHOD

C.4.3.1 Summary of Method

Table C-8 summarizes the evaluation procedure as a five step operation consisting of the following.

1. An evaluation system was established which considered all aspects of a design with appropriate weighting. The system involved the use of a score card and resulted in one overall grade for each candidate.

2. Engineering layout drawings were prepared for each candidate design. The purpose of the layout was to address the mechanical and thermal design problems associated with each style and was needed to provide the background necessary for evaluation in these areas.

3. Computer programs were written for each IHX style based upon the layouts to enable thermal and hydraulic variations to be rapidly investigated for sensitivity effects upon the overall assembly.

4. Optimization of each IHX style was accomplished using the computer as a design tool. Cost optimization of the fluid pressure drops was a major activity accomplished for each design.

5. Evaluation of each optimized design using the scoring system developed in 1. was accomplished.

C.4.3.2 Evaluation System

Figure C-24 illustrates a blank evaluation sheet with the evaluation criteria categorized under the general headings of Safety, Engineering Considerations (consisting of Mechanical Design and Thermal/Hydraulic Design Evaluation) and Cost. The method of weighting the various criteria is illustrated wherein Safety was arbitrarily assigned 48 "rating points", Mechanical and Thermal/Hydraulic Design 32 points and Cost 20 points.

TABLE C-8

SUMMARY OF IHX DESIGN EVALUATION PROCEDURE

1. EVALUATION SYSTEM ESTABLISHED WHICH CONSIDERS ALL DESIGN ASPECTS WITH APPROPRIATE WEIGHTING.

2. DESIGN LAYOUTS PREPARED FOR EACH CANDIDATE
   - MECHANICAL & THERMAL DESIGN PROBLEMS ADDRESSED

3. COMPUTER PROGRAMS WRITTEN FROM THE LAYOUTS WHICH:
   - ACCOMPLISH THE THERMAL/HYDRAULIC DESIGN. OUTPUTS ARE:
     - NO. OF TUBES, TUBE LENGTHS, CORE DIMENSIONS
   - ACCOMPLISH THE MECHANICAL DESIGN. OUTPUTS ARE:
     - P.V. DIMENSIONS, TUBE SHEET THICKNESS, OVERALL DIMENSION AND WEIGHT
   - COST ESTIMATES THE IHX (WT. X RATE IN 4 CATEGORIES)
     - P.V., TUBES, TUBE SHEETS & INTERNALS
   - DETERMINES REQUIRED CIRCULATOR POWER, CAPITAL COST & PUMPING COSTS

4. OPTIMIZE (FINE-TUNE) EACH CONFIGURATION WITH COMPUTER FOR MINIMUM COST DESIGN.

5. EACH DESIGN EVALUATED AGAINST THE SYSTEM ESTABLISHED IN STEP 1.

EVALUATION SHEET

	Max. Avail. Points	A-1	A-2	B-1	C-1	C-2	D-1
(1) Safety Related							
• Reliability of Pri. Containment	8						
• Reliability of Fluid Isolation Barrier	8						
• NDT at Fab-Assy & In-Service	8						
• Buffer Gas System	8						
• Failure Case Consequences	8						
• Intangible (Gut Feeling)	8						
Sub-Total	48						
(2) Engineering Consideration							
Mechanical							
• Accommodation of Thermal Expansion	3						
• Tube Support & Vibration Control	3						
• Tube Sheets, Return Ducts, Framing Core Support, Flange Design	3						
• Blower Replacement &/or Module Replacement (ease of)	3						
• Leaky Tube Isolation	3						
• Dimensions (Practical & Seismic)	2						
• Assembly Ease	2						
• Intangible	4						
Thermal Hydraulic							
• Confidence in thermal design	3						
• Confidence in hydraulic design	3						
• Intangible	3						
Sub-Total	32						
(3) Cost							
	20						
Sub-Total	20						
Total	100						

Figure C-24. Evaluation Sheet Showing Criteria Weighting Used for the Configuration Assessment.

This weighting system stresses the safety aspects and tends to minimize the cost as a basis for optimization. Other weighting can be employed.

Figure C-25 provides guidelines for evaluating each candidate configuration against a specific criterion. An attempt was made to establish criteria and guidelines which would provide a sound evaluation basis without being repetitive.

C.4.3.3 Design Layouts

The six design layouts are shown in Figures C-26 through C-31. Each layout is representative of one of the IHX styles being investigated. However the layouts are not directly comparable in that different thermal/hydraulic design points are employed for each design. The reason for this dissimilarity is that each style was patterned from an existing study, if one existed. This allowed the computer design programs to be checked against other study results where they existed. Thus the folded flow layout copies the KFA thermal/hydraulic design point and the straight tube counterflow - central return style copies the G.E. VHTR design point presented in reference 1. Table C-9 tabulates the various thermal/hydraulic design points related to each layout.

It should also be pointed out that the U-tube configuration shown in Figure C-28 is not the U-tube reference design described previously in this appendix and other portions of this report. The reference design shown in Figures C-1 and C-7 features design variations which chronologically were conceived following the selection of the U-tube style as the optimum approach.

Tentative Grading Guidelines

100% of Max. Avail. Points - Superior Design
75% of Max. Avail. Points - Good
50% of Max. Avail. Points - Fair
25% of Max. Avail. Points - Marginal

- Desirable - clean smooth shell, no stress conc. factors, good streamlines, no apparent thermal stress problems.
- Avoid using pri to sec separation barriers which are difficult to analyze for stress (i.e. massive flat plates, bellows, etc.)
- Can welded joints be inspected at assy per all NDT req. (X-ray, zyglo, mass spec). Is in-service insp. easily accomplished?
- Consider the shaft seal at circulators & other locations. Is reliability of buffer gas sys. compromised by IHX design?
- With sec. sudden rupture, can pri flow be stopped quickly, does large ΔP pri.>sec. jeopardize pri containment? Can metal temperature readily be reduced?
- Intangible assessment of overall safety related characteristics.

- Can all parts handle thermal expansion in a nearly stress free manner, (particularly the core)?
- Is the tube support & prevention of fluid induced vibration competently handled without incurring ΔP problems?
- Overall design adequacy and accomplishment of good mechanical design in subject areas.

- How readily does the design lend itself to replacement of failed or worn out parts? Is plant down time for replacement minimized?
- Capability to find and detect a pri-sec leak & to isolate same to enable plant operation until convenient overhaul time.
- Consider crane capability, excessive tallness,seismic desirability, transition thru access hatch if required.
- How much factory assy can be accomplished vs field assy. Relative assy ease regardless of location.
- Intangible assessment of overall mechanical characteristic of design.

- Does design utilize well established correlations, realistic heat xfer coefficients,etc. no extensive extrapolation etc.
- Overall confidence in hydraulic design, is by-pass leakage or flow mal-distribution a potential problem?
- Intangible assessment of thermal/hydraulic design characteristics.

- Lowest cost IHX receives maximum available.
- Others receive points inversely proportional to the relative cost.

Figure C-25. Evaluation Guidelines.

Figure C-26. Layout Drawing for IHX Concept A-1.

REVISIONS

ZONE	SYM	DESCRIPTION	DATE	APPROVAL

106'-1 (32.3M)

82'-5 (25.12M)

52.00'

HOT PROCESS GAS

COOL PROCESS GAS

BLANK OFF SHEET

FLOW LINER TOP SHEET

I BEAM FRAMING

OUTER FLOW LINER CHANNEL

INSULATION

BOTTOM SHEET

180 DIA (4.57M)

A

A

RETURN DUCT LINER

CHAMBER COOLING WATER - AS REQ'D

TYPICAL ELEVATION

15'-4 (4.67M)

HOT GAS FROM REACTOR

COOL GAS TO REACTOR

COUNTERWEIGHT

IHX TUBE SHEET

MODULE TUBE SHEET (11.50 DIA)

INSULATION

FLOW LINER TOP SHEET

TUBE -.50 O.D.

5.00 DIA

6.40 DIA

4.00 DIA

HOT PROCESS GAS HEADER

COOL PROCESS GAS HEADER

INNER FLOW LINER CHANNEL

OUTER FLOW LINER CHANNEL

MODULE DETAIL
SCALE 1/4

BLANK OFF SHEET ON FRAMING

MODULE SUPPORT FRAMING - 5.00 I BEAM

MODULE LOCATION 109 MODULES PER UNIT

RETURN DUCT LINER

13.00

FLOW LINER TOP SHEET (13.00)

OUTER FLOW LINER CHANNEL (8.75)

MODULE TUBE SHEET (11.50 DIA)

FULL SECTION AT A-A

LATERAL SUPPORT RODS (ALTERNATE DIRECTION AT VARIOUS STATIONS)

FLOW LINER TOP SHEET (13.00)

108 TUBES .50 O.D. x .43 I.D (108 TUBES/MODULE x 108 MODULES = 11772 TUBES)

11.50 DIA MODULE TUBE SHEET

5.18 INNER FLOW LINER CHANNEL

8.75 OUTER FLOW LINER CHANNEL

HOT PROCESS GAS HEADER 3.00 O.D. x .31 WALL

INSULATION (4.00 I.D.)

SECTION THRU MODULE AT A-A

I BEAM FRAMING

FLOW LINER TOP SHEET

BOTTOM SHEET

OUTER FLOW LINER CHANNEL

MODULE TUBE SHEET (11.50 DIA)

MODULE ARRANGEMENT

POWER DENSITY = 1.28 W/cc

DESIGN PARAMETERS OF THIS UNIT

950°C (1742°F) — ΔP SHELL = 3.6 PSI* — 350°C (662°F)

Q = 250 MW

300°C (1652°F) — ΔP TUBE = 25 PSI* — 300°C (572°F)

* ENTRANCE/EXIT LOSS NOT INCLUDED

UNLESS OTHERWISE SPECIFIED DIMENSIONS ARE IN INCHES TOLERANCES ON FRACTIONS DECIMALS ANGLES ± ± ±					
ALL SURFACES ✓					
MATERIAL					
GOVT. OR COML.					
DRAWN	J. Stanley	DATE	9-11-70		
APPD.		ISSUED			
	APPROVED	DATE			
ENGR					
MFG					
MATL					

INTERMEDIATE HEAT EXCHANGER

CONCEPT A-2

GENERAL ELECTRIC ASD

DIV OR DEPT. CINCINNATI, O

LOCATION

SIZE 707E860

SCALE WT (LBS)

CONT ON SHEET

DWG NO. 707E860 REV

PRINTS TO

Figure C-27. Layout Drawing for IHX Concept A-2.

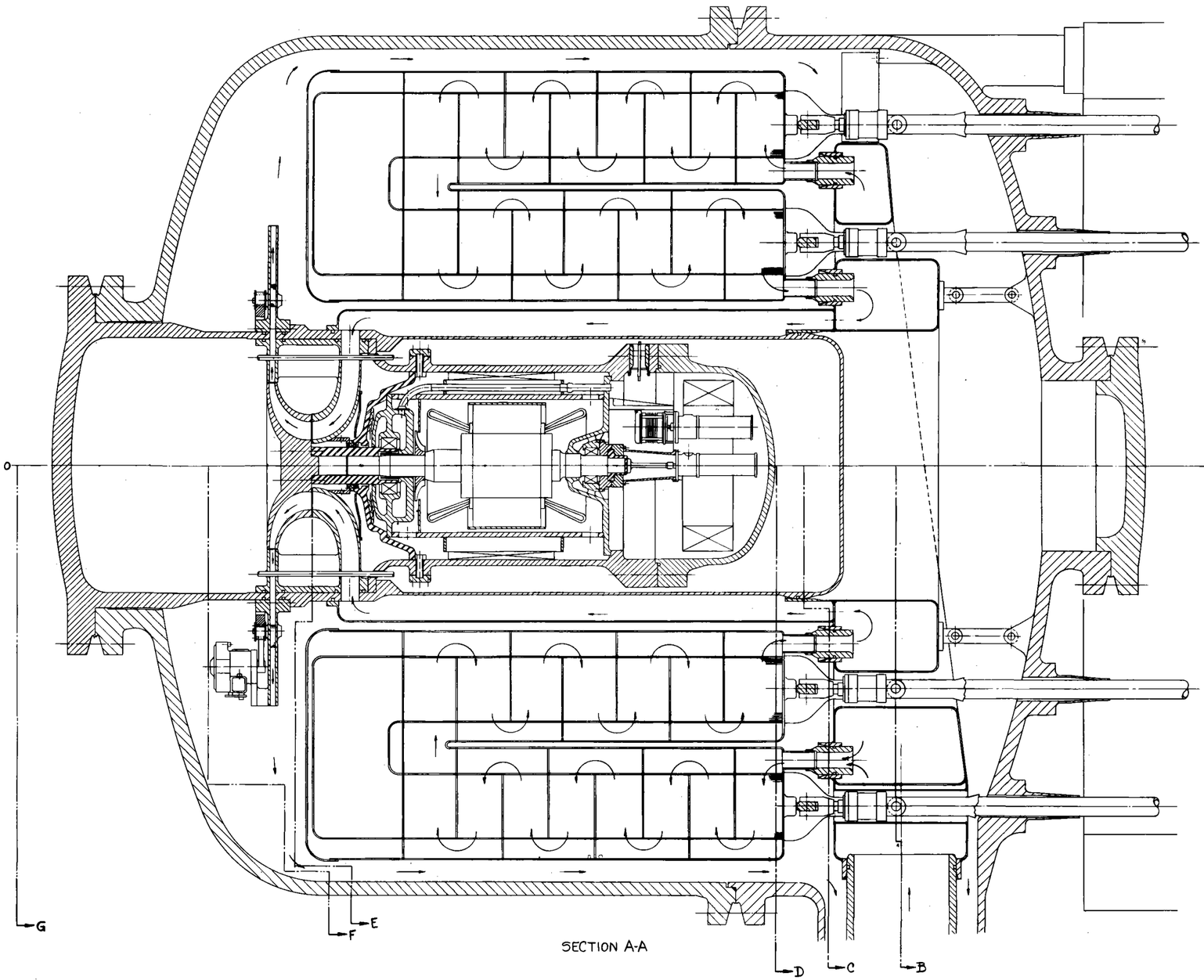

Figure C-28(a). Layout Drawing for IHX Concept B-1 (Sheet 1)

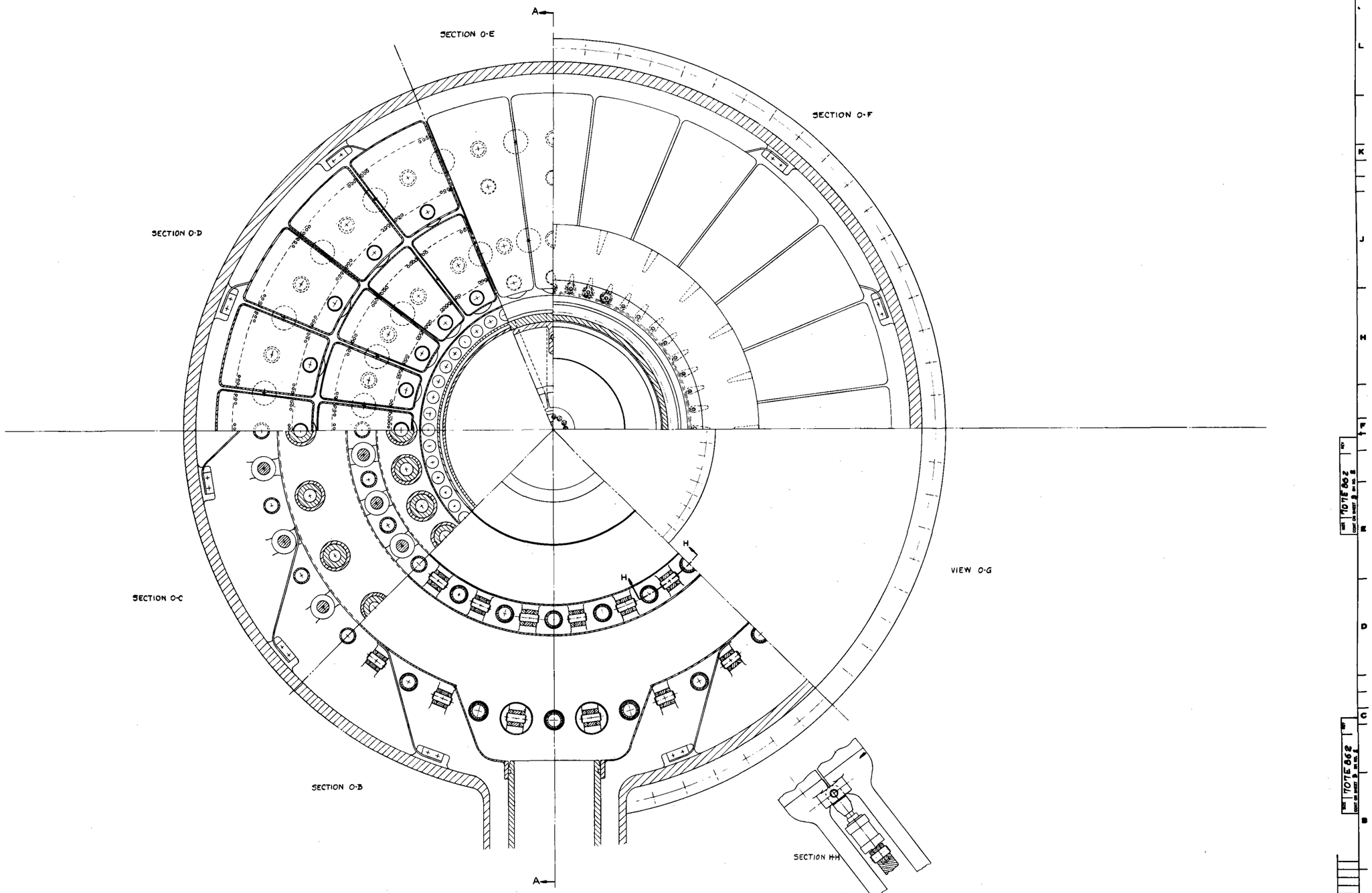

Figure C-28(b). Layout Drawing for IHX Concept B-1 (Sheet 2)

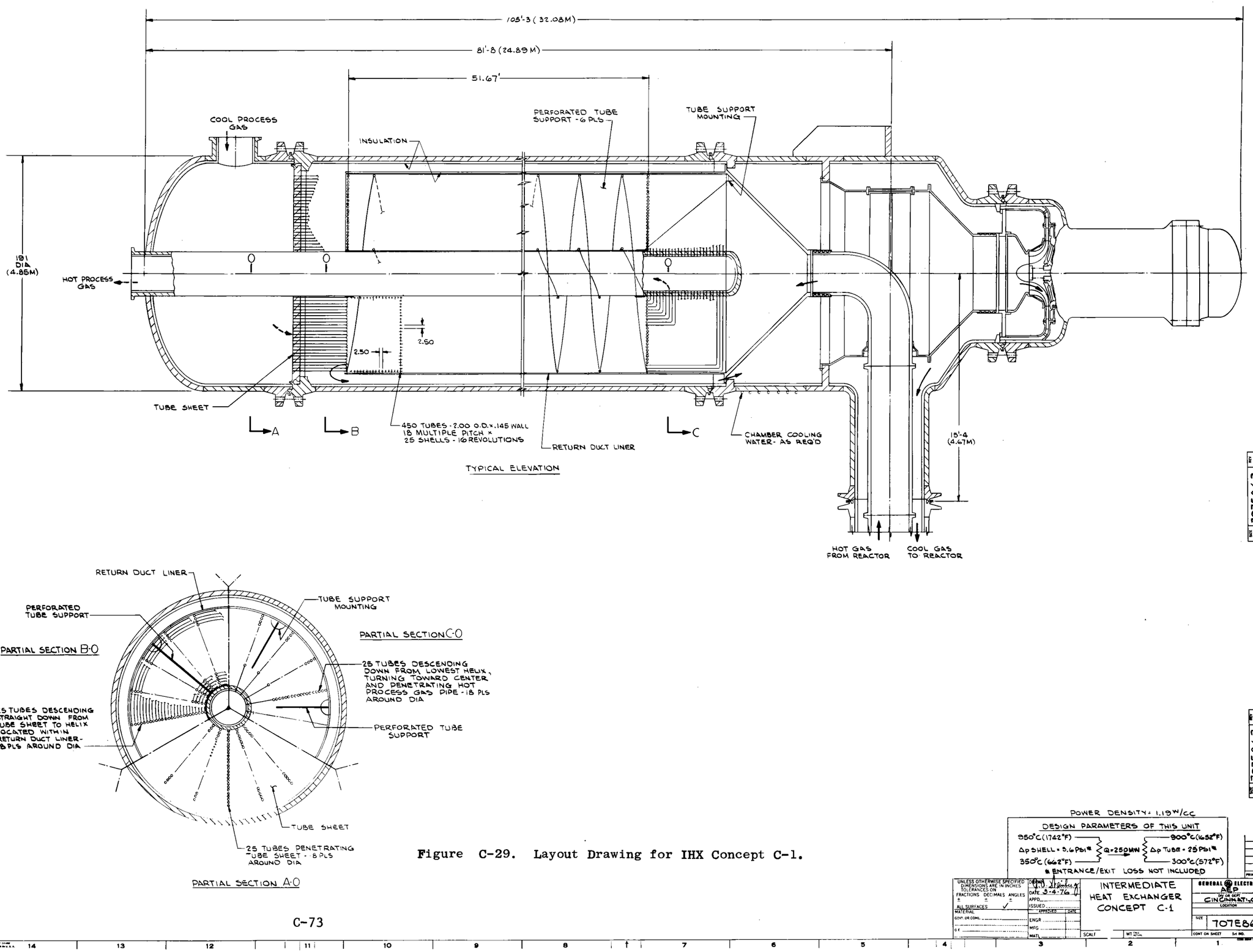

TYPICAL ELEVATION

Figure C-29. Layout Drawing for IHX Concept C-1.

POWER DENSITY = 1.19 W/CC

DESIGN PARAMETERS OF THIS UNIT

950°C (1742°F) — 900°C (1652°F)

ΔP SHELL = 5.6 PSI* — Q = 250 MW — ΔP TUBE = 25 PSI*

350°C (662°F) — 300°C (572°F)

* ENTRANCE/EXIT LOSS NOT INCLUDED

UNLESS OTHERWISE SPECIFIED DIMENSIONS ARE IN INCHES. TOLERANCES ON FRACTIONS DECIMALS ANGLES ± ± ± ALL SURFACES ✓ MATERIAL GOVT. OR COML.	DRAWN J.W. Hanna DATE 5-4-76 APPD. ISSUED	APPROVED DATE ENGR MFG MATL	INTERMEDIATE HEAT EXCHANGER CONCEPT C-1
SCALE	WT (LBS) NETT	SIZE	GENERAL ELECTRIC AEP DIV OR DEPT CINCINNATI, O LOCATION
		CONT OR SHEET	707E863 SH NO.

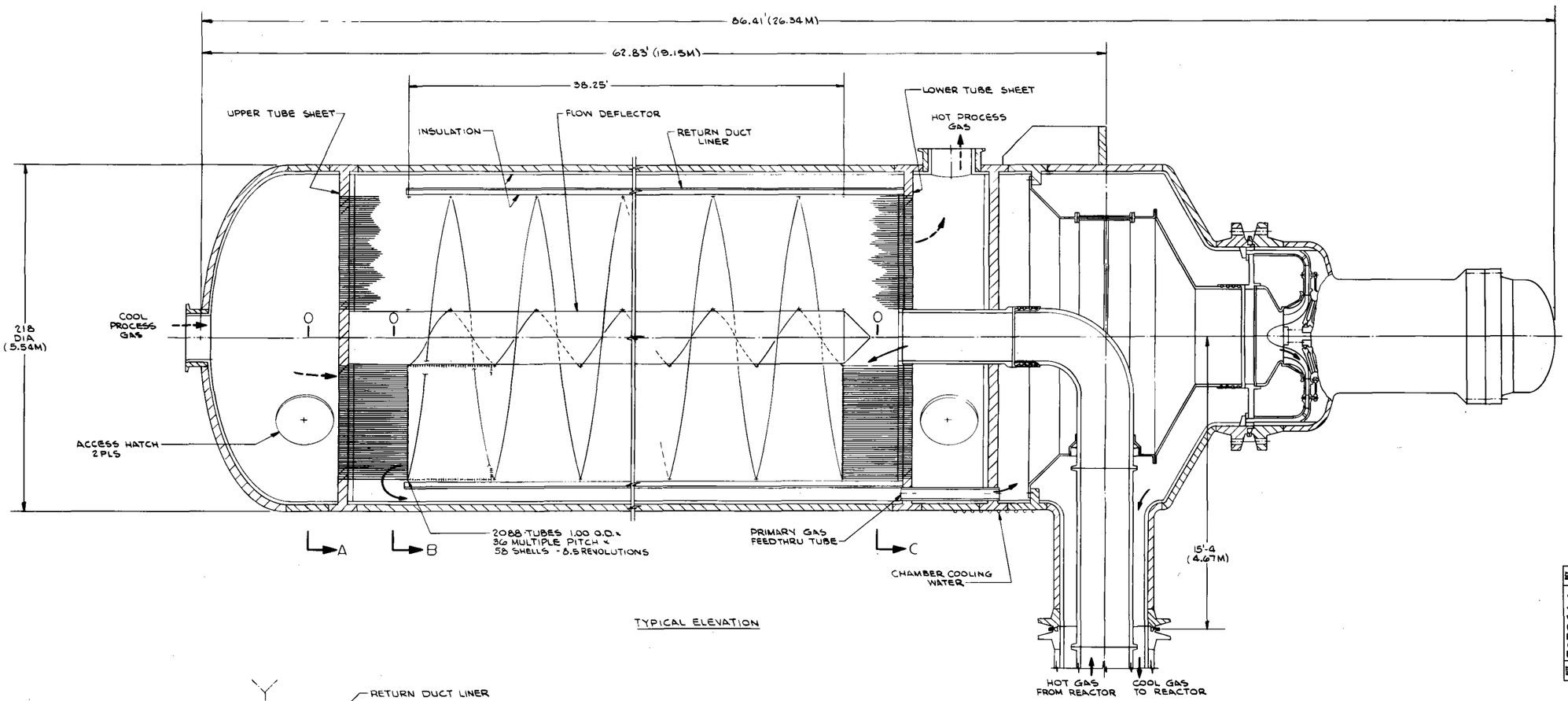

TYPICAL ELEVATION

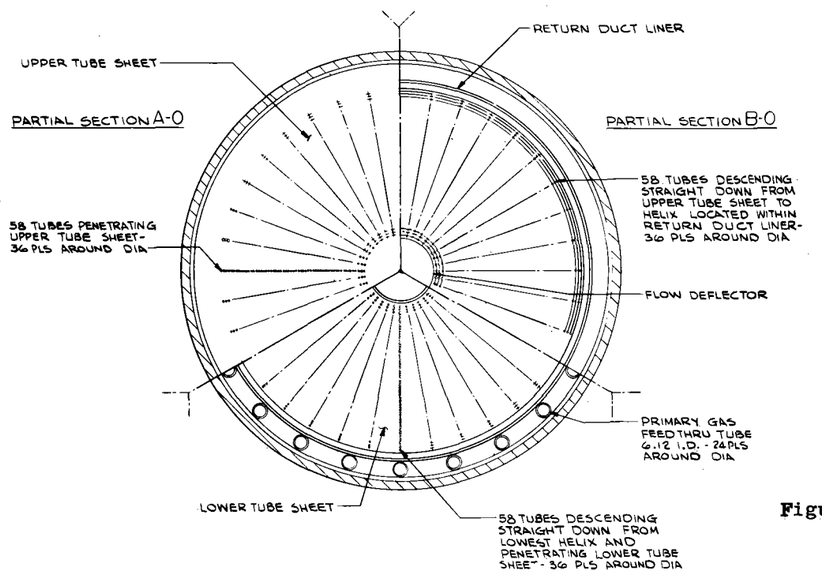

PARTIAL SECTION A-0

PARTIAL SECTION B-0

PARTIAL SECTION C-0

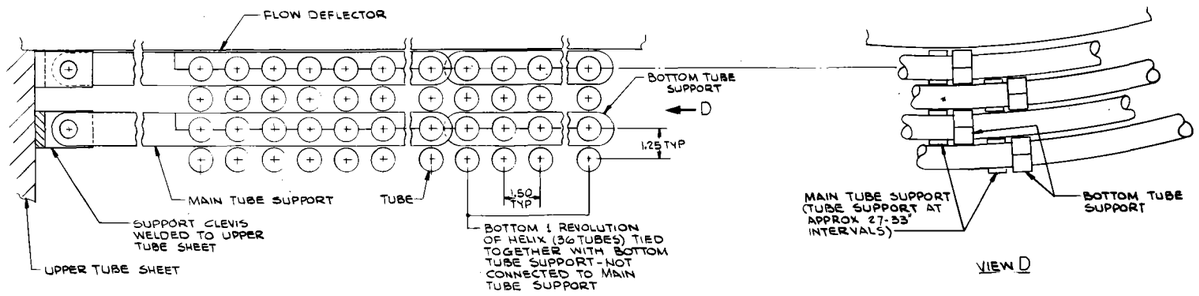

TUBE SUPPORT DETAIL

VIEW D

Figure C-30. Layout Drawing for IHX Concept C-2.

POWER DENSITY = 1.38 W/CC

DESIGN PARAMETERS OF THIS UNIT

950°C (1742°F) — Q = 250 MW — 900°C (1652°F)

Δp SHELL = 5.6 PSI — Δp TUBE = 25 PSI @ 350°C (662°F) — 300°C (572°F)

* ENTRANCE / EXIT LOSS NOT INCLUDED

UNLESS OTHERWISE SPECIFIED DIMENSIONS ARE IN INCHES TOLERANCES ON FRACTIONS DECIMALS ANGLES ± ± ±	DRAWN		INTERMEDIATE HEAT EXCHANGER CONCEPT C-2
	DATE 5-11-76		
ALL SURFACES ✓	APPD.		
MATERIAL	ISSUED		
GOVT. OR COML.	APPROVED	DATE	
G-E	ENGR.		
	MFG.		
	MATL.		
	SCALE	WT. EACH	

GENERAL ELECTRIC — AEP — CINCINNATI, O — LOCATION

SIZE 107E864 — CONT ON SHEET — DWG. NO.

REVISIONS

ZONE	SYM	DESCRIPTION	DATE	APPROVAL

92'-2 (28.1M)

68'-5 (20.8M)

42.65'

37.73'

COOL PROCESS GAS

CHAMBER COOLING TUBE

INSULATION

LOW TEMP SHROUD

HIGH TEMP SHROUD

226 DIA (5.74M)

HOT PROCESS GAS

A B C D

MAIN TUBE SHEET

INTERMEDIATE TUBE SHEET

COLLECTOR TUBE SHEET

MODULE MOUNTING

HIGH TEMP MODULES

LOW TEMP MODULES

CHAMBER COOLING WATER - AS REQ'D

TYPICAL ELEVATION

15-4 (4.67M)

HOT GAS FROM REACTOR

COOL GAS TO REACTOR

STANDOFF

MODULE

MODULE MOUNTING

VIEW E

48 CHAMBER COOLING TUBES 6.00 DIA

QUARTER SECTION AT D-0

HIGH TEMP SHROUD

HIGH TEMP MODULE

LOW TEMP MODULE

LOW TEMP SHROUD

1998 LOW TEMP MODULES

MAIN TUBE SHEET

QUARTER SECTION AT C-0

1936 HIGH TEMP MODULES ARRANGED IN 285 GROUPS OF 7

QUARTER SECTION AT A-0

COLLECTOR TUBE SHEET

285 COLLECTOR TUBES

INNER TUBE OF LOW TEMP MODULE

INTERMEDIATE TUBE SHEET

COLLECTOR TUBE PASSING THRU INTERMEDIATE TUBE SHEET

QUARTER SECTION AT B-0

COLLECTOR TUBE SHEET

COLLECTOR TUBE 3.24 O.D. x 2.85 I.D.

INTERMEDIATE TUBE SHEET

INSULATION

INNER TUBE 1.67 O.D. x 1.35 I.D.

MAIN TUBE SHEET

.98 DIA

2.44 DIA

EXPANSION BELLOWS

SPLIT RING SUPPORT COLLARS

2.56

E

HIGH TEMP MODULE

HIGH TEMP SHROUD

LOW TEMP MODULE

MODULE MOUNTING

OUTER TUBE 2.24 O.D. x 1.85 I.D.

MODULE DETAIL

Figure C-31. Layout Drawing for IHX Concept D-1.

POWER DENSITY = 1.18 W/cc

DESIGN PARAMETERS OF THIS UNIT

970°C (1778°F) → 900°C (1652°F)

ΔP_{SHELL} = 2.9 PSI

Q = 150 MW

ΔP_{TUBE} = 18 PSI

550°C (1022°F) → 480°C (896°F)

ΔP_{SHELL} = 1.5 PSI

Q = 100 MW

ΔP_{TUBE} = 11.7 PSI

270°C (518°F) → 200°C (392°F)

UNLESS OTHERWISE SPECIFIED DIMENSIONS ARE IN INCHES
TOLERANCES ON FRACTIONS ± DECIMALS ± ANGLES ±
ALL SURFACES ✓
MATERIAL
GOVT. OR COML.
G E

	APPROVED	DATE
DRWN	W.D. Yarnay	
DATE	2/26/74	
APPD.		
ISSUED		
ENGR		
MFG		
MATL		

SCALE

INTERMEDIATE HEAT EXCHANGER CONCEPT D-1

GENERAL ELECTRIC
AEP
CINCINNATI, O.

SIZE 707E861

WT (lbs)

CONT ON SHEET

SH NO.

707E861 SH NO. 1 CONT ON SHEET

707E861 SH NO. 2 CONT ON SHEET

PRINTS TO

TABLE C-9

THERMAL-HYDRAULIC DESIGN POINTS FOR CANDIDATE CONFIGURATIONS

	DESIGN STYLE	Q	T_1	T_2	t_1	t_3	ΔP PRI	ΔP SEC
A-1	GE VHTR IHX	273	950	633	918	427	7.56	6.2
A-2	VARIATION OF A-1	250	950	350	900	300	3.6	25
B-1	U-TUBE	190	950	633	894	403	3.6	7.0
C-1	HELICAL	250	950	350	900	300	3.6	25
C-2	HELICAL (JAPANESE)	250	950	350	900	300	3.6	25
D-1	KFA BAYONET	250	970	270	900	200	4.4	30

C.4.3.4 Computer Program

In order to equitably compare the design concepts it was necessary to relate them to the same thermal/hydraulic design point. This was accomplished using the digital computer to redesign each candidate to the single thermal design point shown in Figure C-17. (250 MW primary temperatures 950-350°C, secondary temperatures 900-300°C.)

Figure C-32 shows a sample computer print out for the U-tube style IHX. Input data to the program in addition to the thermal/hydraulic characteristics include mechanical design parameters such as the tube O.D., wall thickness and geometric spacing. Additional mechanical input parameters include items such as the number of flanges, the fault condition pressure and time duration, the pressure vessel allowable loop stress and the allowable time-temperature stress characteristics of the tube sheet material.

The computer program determines the required heat transfer geometry by solving simultaneously the appropriate equations. In addition, all significant mechanical dimensions such as the pressure vessel wall, tube sheet thickness and the overall assembly dimensions are determined. The cost of the IHX is estimated by multiplying the weight by an assumed rate in four categories. These categories and the rates assumed are as follows:

Category	Rate
Pressure Vessel	$8/lb
Tube Sheets	$12/lb
Internals	$9/lb
Tubes	$15/lb

The rates are assumed to include raw material procurement, manufacture, inspection and assembly (see Section H). The variations of the rates is based on judgement of the differing complexity associated with each category. The program also determines the capital cost of the circulator and the cost of its operation pro-rated over the life of the plant. These latter costs were a function of the ΔP specified as part of the thermal/hydraulic input data. A cost optimization is possible in this area

```
MHLB1       08:08EDT    05/28/76

ENTER NAME OF DATA FILE?MHINB1


          PARAMETRIC DESIGN CODE FOR HELIUM-HELIUM IHX FOR VHTR

             STYLE B-1          U-TUBE              CASE NUMBER 777

          STAGGERED BARE TUBES - SHELL-SIDE MULTI-PASS CROSS FLOW
                RADIAL TURNING SPACE/FLUID STREAM = 6 INCHES

INPUT:

QMW          250.00 MW          NO. OF MAIN FLANGES     1.00
THOT1        950.00 DEG.C       FLANGE BULK FACTOR      1.000
THOT2        350.00 DEG.C       NO. OF PASSES           17.
TCOLD2       900.00 DEG.C       HOOP STRESS             20000. PSI
TCOLD1       300.00 DEG.C       DEFORMATION FACTOR      1.000
DP PRI.(NET)   2.40 PSI         NO. OF MODULES          24.0
DP SEC.       15.50 PSI         FAULT TIME DURATION     10.00 HRS.
DP FAULTED   580.00 PSI         DENSITY                 0.280 LB/IN3
TUBE OD        0.500 IN.        P/D TRANSVERSE          2.000
WALL THICK.    0.050 IN.        P/D LONGITUDINAL        0.900
                                METAL PROPERTIES        TABLE A


      NRE(SHELL) =     6.7410091E+03
OUTPUT:

                                                          INCHES    FEET
H(SHELL) (B/HR-FT2-DF)      305.80   LENGTH(SHELL FLOW)     10.53    0.88
H(TUBE)  (B/HR-FT2-DF)      372.74   LENGTH(TUBE)          687.07   57.26
G(SHELL) (LBM/HR-FT2)     16825.56   LENGTH(NO-FLOW)       387.76   32.31
G(TUBE)  (LBM/HR-FT2)     79891.96   AS-BUILT AXIAL LENGTH 343.53   28.63
MISC. WEIGHT FACTOR           0.237  AS-BUILT BUNDLE OD    156.48   13.04
NO. OF TUBES               9070.9    AS-BUILT BUNDLE ID     90.37    7.53
NO. OF TUBES/MODULE         378.0

SHELL-SIDE EXPANSION & CONTRACTION LOSSES TOTAL =  0.4004 PSI

OVERALL LENGTH (FT.)        44.89    OVERALL DIAMETER (FT.)   15.70

COST SUMMARY:

                                DIA.     THICK.    WEIGHT    COST/LB.  COST
                                IN.      IN.       LBS.      $         $(K)

PRESSURE VESSEL
   SHELL (ID)                183.096    2.655    236410.
   MAIN FLANGE                                    16822.
   INSPECTION FLANGE                                432.
      SUBTOTAL                                   253663.      8.00    2029.

TUBE SHEETS (EQUIV. DIA.
      SUBTOTAL                15.505     6.171    15659.     12.00     188.

INTERNALS
   SEC.RETURN DUCT ASSY.       7.776     0.599    30462.
   SEC.INLET DUCT ASSY.        7.776     0.599    30462.
   PRIMARY MANIFOLDS                   (0.125)    2815.
   MODULE MISC.(SKIN,ETC.)             (0.0625)  33334.
   CORE SUPPORT SYSTEM                            4964.
      SUBTOTAL                                   102037.      9.00     918.

TUBES (ID)
      SUBTOTAL                 0.400              140500.     15.00    2107.


      TOTAL IHX (NET)                             511859.              5243.


CIRCULATOR CAPITAL COST
   PRI. LOOP                                                           439.
   SEC. LOOP                                                           628.

PUMPING COSTS EQUATED TO COMPONENT PRESENT WORTH
   PRI. LOOP (QPRI=  2.49 MW) (COST OF ELECT.=  524. $(K)/YR)         1164.
   SEC. LOOP (QSEC=  4.52 MW) (COST OF ELECT.=  949. $(K)/YR)         2110.


TOTAL IHX                                                             9584.
```

Figure C-32. Sample Computer Printout (24 Module U-tube Design)

because the IHX becomes smaller and cheaper as more pressure drop is allocated to it but the circulators require more power and cost more to operate. Figure C-33 illustrates this optimization for the A-1 configuration and also indicates the tube spacing constraint. (Tube spacing less than S/D=1.3 was considered mechanically impractical for this tube size.)

Additional features or aspects of the computer programs are indicated in the following figures. Figure C-34 pictorially summarizes the information flow diagram for each computer diagram program.

Figure C-35 shows the procedure used to estimate flange dimensions and weight. Flanges designed to the proportions indicated were found to have satisfactory stress levels when analyzed by the methods described in the ASME B&PV Code, Section III (Subsection NA).

Figure C-36 shows the procedure used to estimate tube sheet dimensions and weight. This design curve extracted from reference C-7 is in accordance with the above mentioned ASME B&PV code. The procedure establishes the tube sheet thickness as directly proportional to the diameter thus indicating the desirability of avoiding large diameter tube sheets. The thickness also varies directly as the square root of the fault pressure difference and inversely as the square root of the allowable stress. The ligament dimension inversely effects the thickness as a higher order function.

Table C-10 shows the allowable stress intensity used to calculate the tube sheet thickness as a function of the metal temperature and fault duration. The stress levels shown are the S_t values specified in Code Case 1592 of the ASME B&PV Code. This code case addresses the problem of high temperature design of nuclear power plant components. Up to 1200°F the data shown was extracted directly from the code case. Above this temperature, the allowable stress intensity has been extrapolated from published INCO data using the prescribed ASME methods.

Figure C-37 shows the relationship assumed between the tube O.D. and wall. Two significant aspects of the tube material are assumed, one concerning strength of material and the other concerning corrosion allowance. This figure indicates that the Lame´ thick walled tube

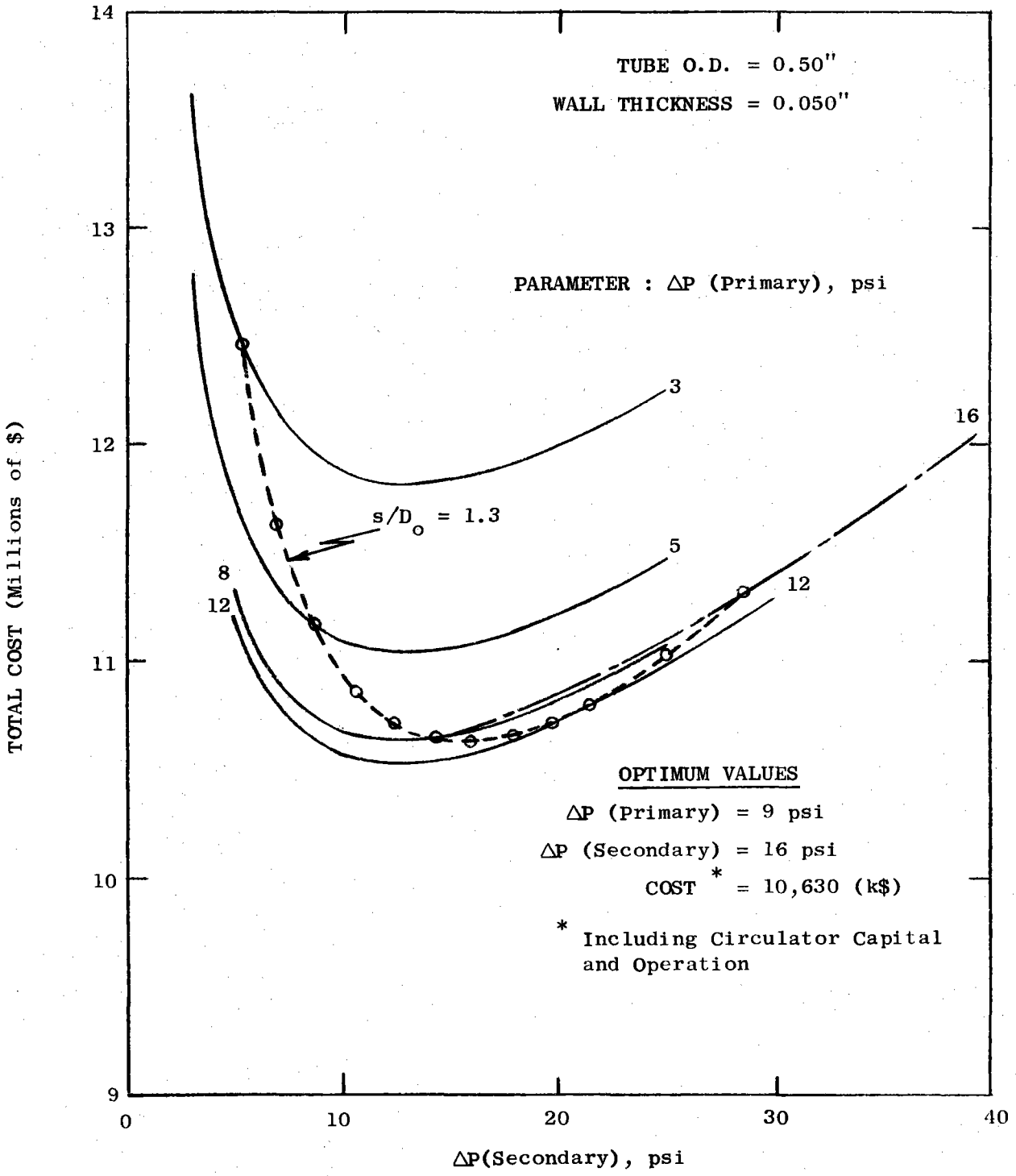

Figure C-33. Curve Illustrating Selection of ΔP Ratings for Minimum Cost within Minimum Tube Spacing Constraints.

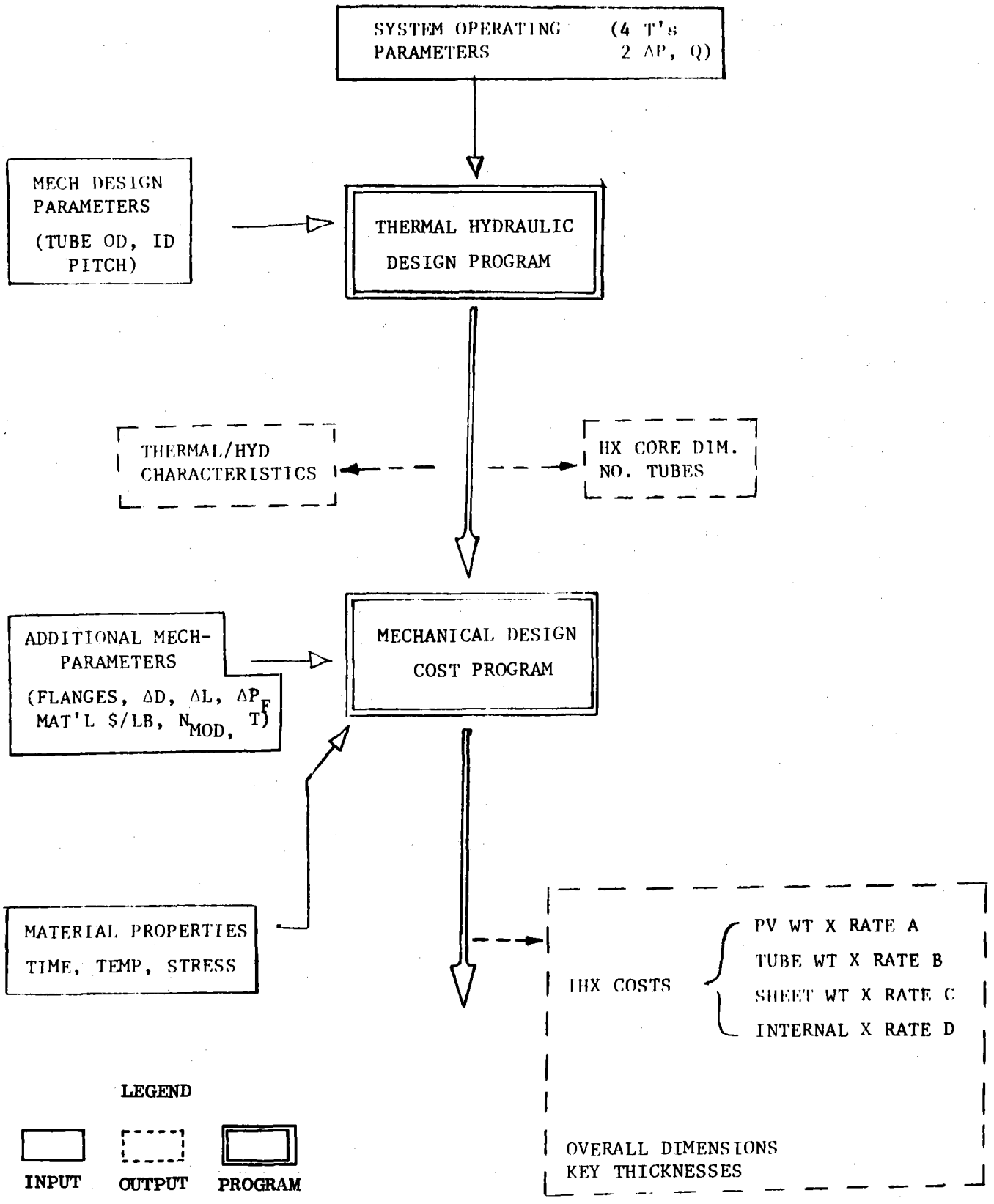

Figure C-34. IHX Computer Design Program Flow Schematic.

PROCEDURE FOR FLANGES

1. SIZE THE WALL THICKNESS ON THE BASIS OF THE HOOP STRESS $t = \frac{PD}{2\sigma}$

2. MAINTAIN FLANGE PROPORTIONS AS FOLLOWS:

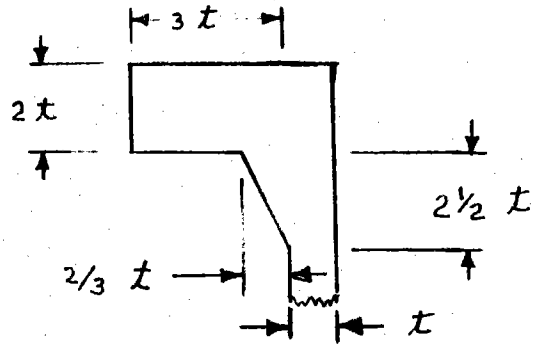

3. THIS WILL MAKE EACH FLANGE PAIR WT. =

$$WT_{FLANGE} = D^3 \rho (11) \left(\frac{P}{\sigma}\right)^2 \left[1 + 2\frac{P}{\sigma}\right]$$

AT $P = 600$ PSI

$\sigma = 12{,}750$ PSI

$\rho = .284$ #/IN^3

$WT = D^3 [.0069]$

Figure C-35. Flange Design Procedure.

1. Basic Method - ASME B&PV Code Section III

2. Basic Equation (Circular Tube Sheets)

$$(\text{Thickness})^2 = \frac{\text{Pressure} \times (\text{Radius})^2}{\text{Allowable Stress}} \times \text{Tube Spacing Function}$$

3. At the limiting design basis, i.e., Faulted Condition (Reference Figure C-18)

Pressure = ΔP Faulted

Allowable Stress = $1.2\ K_t\ S_t$

K_t = plastic deformation factor (1.0)

S_t = 10 hrs temp.-stress intensity (see discussion Section C.4.3)

Tube Spacing Function - Figure E-4

Figure C-36. Sizing Procedure for Tube Sheets

TABLE C-10

METAL TEMPERATURE PROPERTIES

(This data is identified as Table A in the computer program)

INCO 800H EXTENDED (CODE CASE 1592)

	S_t (KSI)	
TEMP. ^{o}F	T = 10 HRS.	T = 30 HRS.
$\leq$ 100	21.4	21.4
800	20.2	20.2
900	19.8	19.8
1000	19.4	19.4
1100	19.1	19.0
1200	17.6	17.3
1300	14.5	12.4
1400	9.2	8.0
1500	6.5	5.6
1600	4.2	3.6
1700	3.1	2.7
($950^{o}C$)	(2.8)	
1800	2.5	1.9

ASME ALLOWABLE $P_m = 1.2\ S_t$ (FAULTED CONDITIONS)

TUBE O.D. VS. WALL

LIMITING STRESS CONDITION @ FAULTED CONDITION

LAME' EQUATIONS → PRINCIPAL STRESS

STRESS INTENSITY = LARGEST ABSOLUTE DIFFERENCE BETWEEN PRINCIPAL STRESSES

$$\sigma_{INT} = 2\ P_2 \left[\frac{1}{1 - (r_1/r_2)^2} \right]$$

WALL THICKNESS = .022 + $\frac{\text{TUBE O.D.}}{17.85588}$

(P_2 = 39 BARS GAGE)

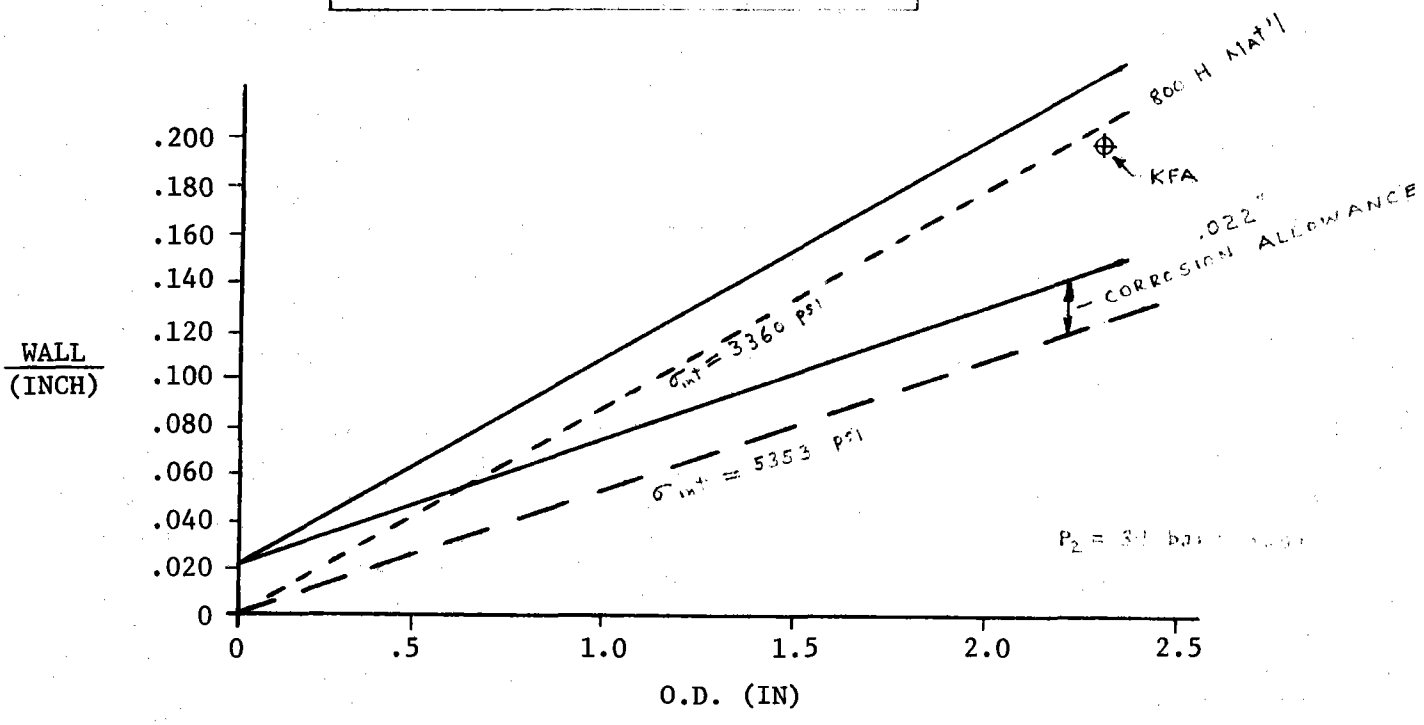

Figure C-37. Tube Wall Thickness vs. Diameter.

equations were used to determine the relationship between the faulted pressure difference, the tube I.D. and O.D. and the resulting stress. The assumption was made that a material would be developed that would have a creep strength approximately 50% stronger than the INCO 800H data tabulated in Table C-10 at the ten hour duration condition. Data published by the INCO indicates that Inconel 617 has this approximate temperature-strength capability but it has not as yet been sanctioned by the ASME for use at the high temperatures indicated. A corrosion allowance of .011 per tube surface has been assumed based upon extrapolation of relatively short term data. (Reference C-8 and Appendix I).

Figure C-38 shows the pressure drop assumed in the primary and secondary loop in addition to the IHX pressure drops. The data shown was taken from previous studies[C-1, C-2, C-3].

Figure C-39 shows the equations used to determine the circulator capital cost and operational cost. Significant assumptions involved are: (1) that a 0.6 power law is used to extrapolate circulator costs from WASH 1230 base and (2) cost of electricity to operate the plant is assumed constant at 3¢/KW-Hr.

C.4.3.5 Tubing Diameter Selection

In an effort to evaluate each design in a fair manner, consistent with any unique packaging requirements, the following steps are applicable:

(1) All IHX designs meet the thermal design requirements shown in Figure C-17.

(2) The IHX pressure drop for both the primary and secondary is individually optimized for minimum cost of the IHX and circulator,

(3) Identical raw material fabrication rates are used for estimating costs from material weights,

LOOP ASSUMPTIONS

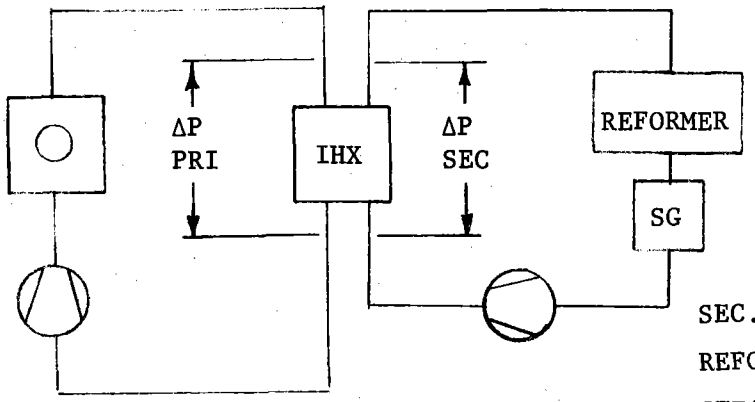

SEC. DUCTING = 5.5
REFORMER SHELL = 2.5
STEAM GEN. = 6.5
14.5 PSI

PRI. DUCTING = 5.5
CORE = 5.5
11.0 PSI

Figure C-38. Primary and Secondary Loop Pressure Drop Assumptions Excluding IHX Losses.

- CAPITAL COST

CIRCULATOR COST = $75/HP BASIS: WASH 1230(WITH ESCALATION) 13,600 HP SIZE

0.6 POWER LAW

$$\text{COST CIRCULATOR X (\$)} = \left[\frac{\text{POWER CIRCULATOR X (MW)}}{10.14\ (\text{MW})}\right]^{0.6} * \$1{,}020{,}000$$

- OPERATIONAL COST

$$\text{COST} = \frac{0.4}{0.18}\ (0.03)\ (8760)\ (.8) * \text{POWER}$$

$\frac{0.4}{0.18}$: 0.4 = COMP $ / INVEST $; 0.18 = FCR

(0.03): $/Kw-hr

Figure C-39. Circulator Costing Equations (Capital Cost and Operational).

(4) Identical stress design procedures are used. In general the ASME B&PV Code procedures prescribed in Section III were utilized, and

(5) Identical thermal/hydraulic design procedures are utilized.

However, one significant parameter which was rather arbitrarily established is the tubing O.D. Smaller tubing drastically reduces the IHX size, weight and cost. Thus the 0.5" diameter tubing assumed for the straight tube and U-tube designs give these candidates a substantial advantage over the helical and bayonet tube designs. However these small diameters are not possible for the bayonet design where an annular space between a tube within a tube is required for flow area and insulation. In the helical design small diameters lead to a very large number of helices as indicated in the following table. For the helical styles, 1-1/2" diameter was selected as a compromise between IHX size, weight, and cost versus number of tubes and assembly complexity.

Tube O.D. (in.)	No. Helices (-)	Core Ht (ft)	Core Wt (lbs)
1.0	1700	30	$.3\ (10)^6$
1.5	790	44	$.43\ (10)^6$
2.0	450	63	$.55\ (10)^6$

The 2.24 inch diameter used for the bayonet tube is taken directly from the metric size specified in the KFA design. The 1/2" O.D. used for the straight tube and U-tube styles was arbitrarily selected as being the smallest acceptable size from a handling view point. Perhaps this should be reassessed at a later point in the overall study since 3/8" diameter and even 1/4" diameter tubing might conceivably be acceptable when additional materials and design information are known

C.4.4 EVALUATION RESULTS

C.4.4.1 Cost, Size and Weight Comparison

The optimized computer print-out sheets for the six IHX candidates are attached as Figures C-40 through C-45. These sheets show many of the details relative to inputs and outputs for each style and enable

PARAMETRIC DESIGN CODE FOR HELIUM-HELIUM IHX FOR VHTR

STYLE A-1 STRAIGHT TUBE CASE NUMBER 780

COUNTER FLOW - EQUILATERAL TRIANGULAR PITCH - CENTRAL SECONDARY RETURN DUCT

INPUT:

QMW	250.00 MW	NUMBER OF FLANGES	2.00
THOT1	950.00 DEG.C	FLANGE BULK FACTOR	1.250
THOT2	350.00 DEG.C	CORE PACKING FACTOR	3.88
TCOLD2	900.00 DEG.C	HOOP STRESS	20000. PSI
TCOLD1	300.00 DEG.C	DEFORMATION FACTOR	1.000
DP PRIMARY	9.00 PSI	MISC.WT./TUBE WT.	0.500
DP SECONDARY	16.00 PSI	NO. OF TUBES/MODULE	127.0
DP FAULTED	580.00 PSI	TRANSIENT 1	60.00 DEG.C
TUBE OD	0.500 IN.	TRANSIENT 2	60.00 DEG.C
WALL THICK.	0.050 IN.	FAULT TIME DURATION	10.00 HRS.
CORE ID	31.50 IN.	DENSITY	0.280 LB/IN3
		METAL PROPERTIES	TABLE A

OUTPUT:

PRI.RET.DUCT ID	128.25 IN.	IHX EFFECTIVENESS	0.9231
S/OD	1.2994	NUMBER OF TUBES	8558.4
GOUT(LBM/HR-FT2)	62889.	EACH TUBE LENGTH	55.049 FT.
HO(B/HR-FT2-DF)	303.1	TUBE VEL. HEAD	0.4058 PSI
HI(B/HR-FT2-DF)	390.3	NUMBER OF MODULES	67.39

OVERALL LENGTH 85.56 FT. OVERALL DIAMETER 12.45 FT.

COST SUMMARY:

	DIA. IN.	THICK. IN.	WEIGHT LBS.	COST/LB. $	COST $(K)
PRESSURE VESSEL					
SHELL (ID)	139.371	2.021	265991.		
FLANGES			18548.		
SUBTOTAL			284539.	8.00	2276.
TUBE SHEETS					
UPPER MAIN	139.371	22.520	91284.		
MODULE UPPER	9.745	1.581	2225.		
MODULE LOWER	9.745	4.214	5932.		
SUBTOTAL			99440.	12.00	1193.
INTERNALS					
SEC.INLET DUCT (ID)	3.284	0.050	934.		
SEC.RETURN DUCT (ID)	31.500	2.672	59568.		
MISC. SUPPORTS			63727.		
SUBTOTAL			124230.	9.00	1118.
TUBES (ID)					
SUBTOTAL	0.400		127455.	15.00	1912.
TOTAL IHX(NET)			635665.		6499.
CIRCULATOR CAPITAL COST					
PRI.LOOP					556.
SEC.LOOP					639.
PUMPING COSTS EQUATED TO COMPONENT PRESENT WORTH					
PRI.LOOP (QPRI= 3.68 MW) (COST OF ELECT.= 774. $(K)/YR)					1721.
SEC.LOOP (QSEC= 4.66 MW) (COST OF ELECT.= 979. $(K)/YR)					2176.
TOTAL IHX					11591.

Figure C-40. Design Code Output for Style A-1 (Straight Tube) IHX.

PARAMETRIC DESIGN CODE FOR HELIUM-HELIUM IHX FOR VHTR

STYLE A-2 STRAIGHT TUBE CASE NUMBER 780

CTR. FLOW - EQUILATERAL TRIANGULAR PITCH - SEC. RETURN DUCT IN EACH MODULE

INPUT:

QMW	250.00	MW	NUMBER OF FLANGES	2.00	
THOT1	950.00	DEG.C	FLANGE BULK FACTOR	1.250	
THOT2	350.00	DEG.C	CORE PACKING FACTOR	4.50	
TCOLD2	900.00	DEG.C	HOOP STRESS	20000.	PSI
TCOLD1	300.00	DEG.C	DEFORMATION FACTOR	1.000	
DP PRIMARY	13.00	PSI	MISC.WT./TUBE WT.	0.500	
DP SECONDARY	23.00	PSI	NO. OF TUBES/MODULE	108.0	
DP FAULTED	580.00	PSI	TRANSIENT 1	60.00	DEG.C
TUBE OD	0.500	IN.	TRANSIENT 2	60.00	DEG.C
WALL THICK.	0.050	IN.	FAULT TIME DURATION	10.00	HRS.
CORE ID	0.	IN.	DENSITY	0.280	LB/IN3
			METAL PROPERTIES	TABLE A	

OUTPUT:

PRI.RET.DUCT ID	122.20	IN.	IHX EFFECTIVENESS	0.9231	
S/OD	1.2989		NUMBER OF TUBES	7135.3	
GOUT(LBM/HR-FT2)	75553.		EACH TUBE LENGTH	57.042	FT.
HO(B/HR-FT2-DF)	351.2		TUBE VEL. HEAD	0.5839	PSI
HI(B/HR-FT2-DF)	451.5		NUMBER OF MODULES	66.07	

OVERALL LENGTH 88.65 FT. OVERALL DIAMETER 11.99 FT.

COST SUMMARY:

	DIA. IN.	THICK. IN.	WEIGHT LBS.	COST/LB. $	COST $(K)
PRESSURE VESSEL					
SHELL (ID)	139.828	2.028	274013.		
FLANGES			18731.		
SUBTOTAL			292744.	8.00	2342.
TUBE SHEETS					
UPPER MAIN	139.828	22.602	97183.		
MODULE UPPER	10.515	1.706	2741.		
SUBTOTAL			99923.	12.00	1199.
INTERNALS					
SEC.INLET DUCT (ID)	6.397	0.543	5648.		
SEC.RETURN DUCT (ID)	4.157	0.353	68871.		
MISC. SUPPORTS			55054.		
SUBTOTAL			129573.	9.00	1166.
TUBES (ID)					
SUBTOTAL	0.400		110108.	15.00	1652.
TOTAL IHX(NET)			632347.		6359.
CIRCULATOR CAPITAL COST					
PRI.LOOP					622.
SEC.LOOP					752.
PUMPING COSTS EQUATED TO COMPONENT PRESENT WORTH					
PRI.LOOP (QPRI= 4.45 MW) (COST OF ELECT.= 936. $(K)/YR)					2079.
SEC.LOOP (QSEC= 6.10 MW) (COST OF ELECT.= 1282. $(K)/YR)					2849.
TOTAL IHX					12661.

Figure C-41. Design Code Output for Style A-2 (Alternate) IHX.

STYLE B-1 U-TUBE CASE NUMBER 780

STAGGERED BARE TUBES - SHELL-SIDE MULTI-PASS CROSS FLOW
RADIAL TURNING SPACE/FLUID STREAM = 6 INCHES

INPUT:

QMW	250.00 Mw	NO. OF MAIN FLANGES	1.00
THOT1	950.00 DEG.C	FLANGE BULK FACTOR	1.000
THOT2	350.00 DEG.C	NO. OF PASSES	17.
TCOLD2	900.00 DEG.C	HOOP STRESS	20000. PSI
TCOLD1	300.00 DEG.C	DEFORMATION FACTOR	1.000
DP PRI.(NET)	2.40 PSI	NO. OF MODULES	36.0
DP SEC.	15.50 PSI	FAULT TIME DURATION	10.00 HRS.
DP FAULTED	580.00 PSI	DENSITY	0.280 LB/IN3
TUBE OD	0.500 IN.	P/D TRANSVERSE	2.000
WALL THICK.	0.050 IN.	P/D LONGITUDINAL	0.900
		METAL PROPERTIES	TABLE A

NRE(SHELL) = 6.7410091E+03

OUTPUT:

			INCHES	FEET
H(SHELL) (B/HR-FT2-DF)	305.80	LENGTH(SHELL FLOW)	10.53	0.88
H(TUBE) (B/HR-FT2-DF)	372.74	LENGTH(TUBE)	687.07	57.26
G(SHELL) (LBM/HR-FT2)	16825.56	LENGTH(NO-FLOW)	387.76	32.31
G(TUBE) (LBM/HR-FT2)	79891.96	AS-BUILT AXIAL LENGTH	343.53	28.63
MISC. WEIGHT FACTOR	0.285	AS-BUILT BUNDLE OD	156.48	13.04
NO. OF TUBES	9070.9	AS-BUILT BUNDLE ID	90.37	7.53
NO. OF TUBES/MODULE	252.0			

SHELL-SIDE EXPANSION & CONTRACTION LOSSES TOTAL = 0.4004 PSI

OVERALL LENGTH (FT.) 44.89 OVERALL DIAMETER (FT.) 15.70

COST SUMMARY:

	DIA. IN.	THICK. IN.	WEIGHT LBS.	COST/LB. $	COST $(K)
PRESSURE VESSEL					
SHELL (ID)	183.096	2.655	236410.		
MAIN FLANGE			16822.		
INSPECTION FLANGE			432.		
SUBTOTAL			253663.	8.00	2029.
TUBE SHEETS (EQUIV. DIA.					
SUBTOTAL	12.091	4.812	11139.	12.00	134.
INTERNALS					
SEC.RETURN DUCT ASSY.	6.349	0.489	25229.		
SEC.INLET DUCT ASSY.	6.349	0.489	25229.		
PRIMARY MANIFOLDS		(0.125)	2815.		
MODULE MISC.(SKIN,ETC.)		(0.0625)	40005.		
CORE SUPPORT SYSTEM			4053.		
SUBTOTAL			97330.	9.00	876.
TUBES (ID)					
SUBTOTAL	0.400		140500.	15.00	2107.
TOTAL IHX (NET)			502632.		5146.
CIRCULATOR CAPITAL COST					
PRI. LOOP					439.
SEC. LOOP					628.
PUMPING COSTS EQUATED TO COMPONENT PRESENT WORTH					
PRI. LOOP (QPRI= 2.49 MW) (COST OF ELECT.= 524. $(K)/YR)					1164.
SEC. LOOP (QSEC= 4.52 MW) (COST OF ELECT.= 949. $(K)/YR)					2110.
TOTAL IHX					9487.

Figure C-42. Design Code Output for Style B-1 (U-tube) IHX.

PARAMETRIC DESIGN CODE FOR HELIUM-HELIUM IHX FOR VHTR

STYLE C-1 HELICAL GEOMETRY CASE NUMBER 777

CROSS-FLOW OVER IN-LINE TUBES - CENTRAL SEC. RETURN DUCT

INPUT:

QMW	250.00 MW	NUMBER OF FLANGES	2.00	
THOT1	950.00 DEG.C	FLANGE BULK FACTOR	1.750	
THOT2	350.00 DEG.C	TRANSIENT TEMP.	60.00	DEG.C
TCOLD2	900.00 DEG.C	HOOP STRESS	20000.	PSI
TCOLD1	300.00 DEG.C	DEFORMATION FACTOR	1.000	
DP PRIMARY	9.00 PSI	FAULT TIME DURATION	10.00	HRS.
DP SECONDARY	3.80 PSI	DENSITY	0.280	LB/IN3
DP FAULTED	580.00 PSI	P/D TRANSVERSE	1.250	
TUBE OD	1.500 IN.	P/D LONGITUDINAL	1.500	
WALL THICK.	0.106 IN.	HXID DESIRED	30.000	IN.
		METAL PROPERTIES	TABLE A	

OUTPUT FOR 9 TUBE-SIDE PASSES:

			INCHES	FEET
H(SHELL) (B/HR-FT2-DF)	224.25	LENGTH(SHELL FLOW)	1043.58	86.96
H(TUBE) (B/HR-FT2-DF)	165.37	LENGTH(TUBE)	289.49	24.12
G(SHELL) (LBM/HR-FT2)	23969.15	LENGTH(NO-FLOW)	65.62	5.47
G(TUBE) (LBM/HR-FT2)	38751.69	AS-BUILT AXIAL LENGTH	1043.58	86.96
NO.OF HELICAL TUBES	1803.6	AS-BUILT OD	157.77	13.15
NO.OF HELIX SHELLS	35.00	AS-BUILT ID	26.52	2.21
MULTIPLE HELICES	51.53			

OVERALL LENGTH (FT.) 128.56 OVERALL DIAMETER (FT.) 14.99

COST SUMMARY FOR 9 TUBE-SIDE PASSES:

	DIA. IN.	THICK. IN.	WEIGHT LBS.	COST/LB. $	COST $(K)
PRESSURE VESSEL					
SHELL (ID)	174.827	2.535	618473.		
FLANGES			51254.		
SUBTOTAL			669728.	8.00	5358.
TUBE SHEETS					
SUBTOTAL	174.827	36.842	247637.	12.00	2972.
INTERNALS					
SEC.RETURN DUCT (OD)	26.524	2.450	73204.		
SEC.INLET DUCT (OD)	1.500	0.106	9950.		
CORE SUPPORT			107801.		
MISCELLANEOUS			38484.		
SUBTOTAL			229438.	9.00	2065.
TUBES (ID)					
SUBTOTAL	1.288		673756.	15.00	10106.
TOTAL IHX(NET)			1820559.		20501.
CIRCULATOR CAPITAL COST					
PRI.LOOP					545.
SEC.LOOP					470.
PUMPING COSTS EQUATED TO COMPONENT PRESENT WORTH					
PRI.LOOP (QPRI= 3.57 MW) (COST OF ELECT.= 750. $(K)/YR)					1666.
SEC.LOOP (QSEC= 2.79 MW) (COST OF ELECT.= 587. $(K)/YR)					1304.
TOTAL IHX					24486.

Figure C-43. Design Code Output for Style C-1 (Helical Geometry) IHX.

PARAMETRIC DESIGN CODE FOR HELIUM-HELIUM IHX FOR VHTR

STYLE C-2 HELICAL GEOMETRY CASE NUMBER 777

CROSS-FLOW OVER IN-LINE TUBES - SEC. EXIT AT LOWER TUBE SHEET

INPUT:

QMW	250.00 MW	NUMBER OF FLANGES	2.00	
THOT1	950.00 DEG.C	FLANGE BULK FACTOR	1.750	
THOT2	350.00 DEG.C	TRANSIENT TEMP.	60.00	DEG.C
TCOLD2	900.00 DEG.C	HOOP STRESS	20000.	PSI
TCOLD1	300.00 DEG.C	DEFORMATION FACTOR	1.000	
DP PRIMARY	10.00 PSI	FAULT TIME DURATION	10.00	HRS.
DP SECONDARY	3.50 PSI	DENSITY	0.280	LB/IN3
DP FAULTED	580.00 PSI	P/D TRANSVERSE	1.250	
TUBE OD	1.500 IN.	P/D LONGITUDINAL	1.500	
WALL THICK.	0.106 IN.	HXID DESIRED	30.000	IN.
		METAL PROPERTIES	TABLE A	

OUTPUT FOR 9 TUBE-SIDE PASSES:

			INCHES	FEET
H(SHELL) (B/HR-FT2-DF)	228.76	LENGTH(SHELL FLOW)	1088.77	90.73
H(TUBE) (B/HR-FT2-DF)	161.15	LENGTH(TUBE)	282.62	23.55
G(SHELL) (LBM/HR-FT2)	24798.93	LENGTH(NO-FLOW)	64.97	5.41
G(TUBE) (LBM/HR-FT2)	37517.80	AS-BUILT AXIAL LENGTH	1088.77	90.73
NO.OF HELICAL TUBES	1863.0	AS-BUILT OD	154.93	12.91
NO.OF HELIX SHELLS	34.65	AS-BUILT ID	25.00	2.08
MULTIPLE HELICES	53.77			

OVERALL LENGTH (FT.) 128.37 OVERALL DIAMETER (FT.) 14.76

COST SUMMARY FOR 9 TUBE-SIDE PASSES:

	DIA. IN.	THICK. IN.	WEIGHT LBS.	COST/LB. $	COST $(K)
PRESSURE VESSEL					
SHELL (ID)	172.142	2.496	598517.		
FLANGES			48929.		
SUBTOTAL			647446.	8.00	5180.
TUBE SHEETS					
UPPER MAIN TUBE SHEET	172.142	36.277	236401.		
LOWER TUBE SHEET ASSY	172.142	(36.277)	260041.		
SUBTOTAL			496441.	12.00	5957.
INTERNALS					
SEC.RETURN DUCT (OD)	1.500	0.106	10092.		
SEC.INLET DUCT (OD)	1.500	0.106	10092.		
CORE SUPPORT			108707.		
MISCELLANEOUS			44612.		
SUBTOTAL			173503.	9.00	1562.
TUBES (ID)					
SUBTOTAL	1.288		679417.	15.00	10191.
TOTAL IHX(NET)			1996807.		22890.
CIRCULATOR CAPITAL COST					
PRI.LOOP					561.
SEC.LOOP					464.
PUMPING COSTS EQUATED TO COMPONENT PRESENT WORTH					
PRI.LOOP (QPRI= 3.75 MW) (COST OF ELECT.= 787. $(K)/YR)					1750.
SEC.LOOP (QSEC= 2.73 MW) (COST OF ELECT.= 574. $(K)/YR)					1276.
TOTAL IHX					26940.

Figure C-44. Design Code Output for Style C-2 (Hel. Geometry Alt.) IHX.

PARAMETRIC DESIGN CODE FOR HELIUM-HELIUM IHX FOR VHTR

STYLE D-1 FOLDED FLOW - 2 ZONES CASE NUMBER 777

COUNTER FLOW - EQUILATERAL TRIANGULAR PITCH - INDIVIDUAL TUBE SEC. RETURN

INPUT:

QMW	250.00 MW	NUMBER OF FLANGES	4.00	
THOT1	950.00 DEG.C	FLANGE BULK FACTOR	1.250	
THOT2	350.00 DEG.C	TRANSIENT TEMP.	60.00	DEG.C
TCOLD2	900.00 DEG.C	HOOP STRESS	20000.	PSI
TCOLD1	300.00 DEG.C	DEFORMATION FACTOR	1.000	
DP PRIMARY	10.00 PSI	FAULT TIME DURATION	10.00	HRS.
DP SECONDARY	47.50 PSI	DENSITY	0.280	LB/IN3
DP FAULTED	580.00 PSI	PRI.FLOW BLOCKAGE FACTOR	0.560	
TUBE OD	2.244 IN.	DP ANN/DP SEC.	0.70	
WALL THICK.	0.148 IN.	K PLUG TUBE INSULATION	0.100	B/HR-FT-DF
S/OD	1.2000	PLUG TUBE OD/ID RATIO	1.14	
		METAL PROPERTIES	TABLE A	

*** DPIN, DPOUT = 3.3400383E+01 1.0000000E+01

OUTPUT:

*H(SHELL) (B/HR-FT2-DF)	286.72	IHX EFFECTIVENESS	0.9231
*H(TUBE) (B/HR-FT2-DF)	384.99	TUBE VELOCITY HEAD	0.40617 PSI
*G(SHELL) (LBM/HR-FT2)	61464.51	INSULATION THICKNESS	0.2738 IN.
*G(TUBE) (LBM/HR-FT2)	75087.82	ID OF INSULATION	0.9015 IN.
AS-BUILT NO. OF TUBES	3087.4	TEMP.LOSS OF SEC.GAS	9.75 DEG.C
AS-BUILT TUBE LENGTH (FT)	42.920	HI TEMP.ZONE OD (DCORE)	9.257 FT.
		LO TEMP.ZONE OD (HXOD)	13.450 FT.

* UNCORRECTED

% INCREASE IN HX VOL.(2 EQUAL ZONES) 19.497

OVERALL LENGTH (FT.) 77.12 OVERALL DIAMETER (FT.) 15.81

COST SUMMARY:

	DIA. IN.	THICK. IN.	WEIGHT LBS.	COST/LB. $	COST $(K)
PRESSURE VESSEL					
SHELL (ID)	184.329	2.67	421011.		
FLANGES			85819.		
SUBTOTAL			506830.	8.00	4055.
TUBE SHEETS					
COLLECTOR	184.329	2.67	19971.		
INTERMEDIATE	184.329	2.67	19971.		
UPPER MAIN	184.329	36.08	269575.		
MODULE	0.673		1294.		
SUBTOTAL			310811.	12.00	3730.
INTERNALS					
PLUG TUBE (OD)	1.652		225500.		
PLUG TUBE EXTENSIONS			43952.		
PRIMARY RETURN BAFFLE			65113.		
PRIMARY CORE MATRIX			9645.		
SUBTOTAL			344211.	9.00	3098.
TUBES					
TUBES (ID)	1.948		476219.		
TUBE EXTENSIONS			59037.		
SUBTOTAL			535256.	15.00	8029.
TOTAL IHX (NET)			1697107.		18911.

CIRCULATOR CAPITAL COST	
PRI. LOOP	577.
SEC. LOOP	1018.
PUMPING COSTS EQUATED TO COMPONENT PRESENT WORTH	
PRI. LOOP (QPRI= 3.92 MW) (COST OF ELECT.= 825. $(K)/YR)	1832.
SEC. LOOP (QSEC= 10.11 MW) (COST OF ELECT.= 2126. $(K)/YR)	4725.
TOTAL IHX	27064.

Figure C-45. Design Code Output for Style D-1 (Folded Flow-2 zones) IHX.

an exact comparison of the estimated cost, size, and weight. Table C-3 summarizes the significant data for the candidate designs taken from these sheets. Figure C-6 shows the outline drawing of the various styles. This table and figure show the U-tube concept to cost $5.1 million with other concepts ranging from $6.5 to 23.9 million. The weight advantages favor the U-tube with .502 million pounds per assembly versus other concepts from .632 to 1.99 million pounds. The IHX size comparison is conveniently made by examining the power density where the U-tube style is approximately 1.01 MW/m^3 with the other styles varying from 0.38 to 0.83. The following listing tabulates the specific power density for each IHX envelope including the circulator.

IHX Style	Power Density (MW/m^3)
A-1 Straight Tube Counter Flow (Central Return)	0.79
A-2 Straight Tube Counter Flow (Modular Return)	0.83
B-1 U-tube Cross Flow	1.01
C-1 Helical (Central Return)	0.38
C-2 Helical (Two Tube Sheets)	0.39
D-1 Bayonet (Folded Flow)	0.56

C.4.4.2 Overall Comparison

Table C-11 shows the results of the author's overall evaluation of the IHX styles. The U-tube is indicated as a clear winner over the two straight tube counterflow candidates. The helical designs and the bayonet design are judged to be least optimum with a rating of approximately 65% versus 95% and 80% for the U-tube and straight tube designs respectively. All the styles are judged to meet the specified minimum requirements in all areas for safety, engineering and cost with the possible exception of the strong desire for a modular design, which the helical units cannot meet.

While any two evaluators probably will not agree exactly on the specific ratings shown in Table C-11, it is anticipated that the final rankings would be substantiated. The following paragraphs present a discussion of the various aspects which led to the ratings indicated. The comments are grouped under paragraph headings identical to those indicated on the evaluation table.

TABLE C-11

ITEMIZED EVALUATION OF CANDIDATE CONFIGURATIONS AND OVERALL RANKING

	Max. Avail. Points	A-1	A-2	B-1	C-1	C-2	D-1
(1) Safety Related							
• Reliability of Pri. Containment	8	8	8	8	8	7	7
• Reliability of Fluid Isolation Barrier	8	7	6	8	7	7	7
• NDT at Fab-Assy & In-Service	8	5	6	8	5	7	6
• Buffer Gas System	8	8	8	7	8	8	8
• Failure Case Consequences	8	8	8	8	8	8	8
• Intangible (Gut Feeling)	8	6	6	8	7	7	4
Sub-Total	48	42	42	47	43	44	40
(2) Engineering Consideration							
Mechanical							
• Accommodation of Thermal Expansion	3	1	1	2	3	3	2
• Tube Support & Vibration Control	3	2	2	3	2.5	2.5	2
• Tube Sheets, Return Ducts, Framing Core Support, Flange Design	3	2	1	3	2	2	2
• Blower Replacement &/or Module Replacement (ease of)	3	2	2	3	1	1	1.5
• Leaky Tube Isolation	3	1	1	3	1	1	1
• Dimensions (Practical & Seismic)	2	1.5	1.5	2	1	1	1.5
• Assembly Ease	2	1.0	1.0	2	.5	.5	1
• Intangible	4	3	2.5	3.5	2	2	3
		13.5	12	21.5	13	13	14
Thermal Hydraulic							
• Confidence in thermal design	3	3	3	2	2	2	1.5
• Confidence in hydraulic design	3	3	3	2	1.5	1.5	2
• Intangible	3	3	2	2	2	2	1.5
Sub-Total	32	9	8	6	5.5	5.5	5
(3) Cost	20	18.7	15.2	20	5	4.5	5.4
Sub-Total	20						
Total	100	83.2	77.2	94.5	66.5	67	64.4

(1) Safety Related

- o Reliability of Primary Containment

  Massive tube sheets are judged to be an undesirable source of potential stress concentration factors and related problems.

- o Reliability of Fluid Isolation Barrier

  Primary-secondary fluid isolation barriers should not be subjected to thermal deflection and possible fatigue. The short hockey stick legs in the A-2 modules are poor in this respect relative to tube-to-tube expansion. Additionally it is felt that small diameter tube sheets (15") should be more reliable than large (13 ft.) diameter tube sheets due to improved inspection and handling capability.

- o NDT at Fabrication-Assembly and In-Service

  The U-tube design allows tubes and tube sheets to be easily inspected at assembly and during in-service shutdowns. Hockey stick joint inspection in large central return duct areas has poor accessibility. The dual lower tube sheet in the C-2 design is an effort to improve tube - tube sheet inspection.

- o Buffer Gas System

  The circulator dynamic seals require buffer gas to insure inward leakage only. The U-tube design with the centrally contained circulator (reference Figure C-28) potentially compromises the buffer gas supply lines. This situation is not true with the bottom mounted circulator shown in Figure C-7.

- Failure Case Consequences

All the candidates were judged approximately equal in ability to handle the failure case. The hot gas shutoff feature in the accident case is considered to be a function of the circulator design which is common to all styles.

- Intangible Safety Related

In the intangible area, the use of insulation in the annular tube area of the D-1 design raises some concern that pieces may loosen and be circulated around the loop with potential flow blockages. Also, the tubing spacing matrix on the primary side seems likely to lead to fatigue or cyclic failure of the heat transfer tubes.

(2) Mechanical Design Related

- Accommodation of Thermal Expansion

The helical design handles thermal expansion very nicely provided the tubing support spacers do not defeat the inherent flexibility of the tubing coils. The bayonet design requires a bellows for each module to accommodate thermal expansion between the intermediate header, the pressure vessel,and the module outlet ducts. The hockey stick deflection method of handling expansion generally requires more length than is available and accounts for the poor ratings of the A units. The U-tube is intermediately rated since the entire U-legs can deflect to accommodate axial expansion, or dissimilar material legs or bellows may be used.

- Tube Support and Vibration Control

Tube support in cross flow arrangements is nicely handled without pressure loss by utilizing baffle plates. These generally can be placed as close as required to prevent fluid induced vibration. The large size and/or assembly problem of the helix influenced the intermediate rating indicated.

- Internals Design, etc

  The clean flow ducting for the secondary of the U-tube style influenced the superior rating in this category and likewise the complex secondary ducting for the A-2 design had the opposite effect.

- Blower and Module Replacement

  The U-tube design readily allows temporary isolation of defective modules until plant shutdown and repair can be conveniently scheduled. The non-modular helical design rated lowest in this category. The large internal tube sheets work against module isolation. Blower replacement is approximately equal in all styles.

- Leak Isolation

  Leaky tube isolation is most easily accomplished when both tube ends are readily accessible. This consideration led to the appraisal indicated.

- Dimensions

  Figure C-6 showing the relative outline dimensions, gives an indication of the reasons for the appraisal shown. The helical designs are approximately 128 feet in height and probably cannot be factory assembled. Seismic considerations tended to favor the short U-tube unit with the numerous flexible secondary ducts.

- Assembly Ease

  Assembly ease distinctly and adversely affects the assessment of the helical styles. Stacking, welding, and inspection of the U-tube modules seems easier than for the straight tube units. The rather complex bayonet-scabbard assembly

with the auxiliary tube sheet seems less desirable than that of the U-tube.

- o Intangible (Mechanical Design)

  An intangible assessment of the mechanical design features does not show any drastic trends other than to substantiate the assembly difficulties associated with the large multiple helices.

Thermal-Hydraulic

- o Thermal Design

  The bayonet tube design was rated lowest here because of the temperature loss of the secondary gas to itself on the folded return flow. The straight tube counterflow received the highest thermal ratings since it is consistent with classical solutions to thermal design optimization.

- o Hydraulic Design

  The hydraulic design aspects of the straight tube counterflow styles is also judged superior to the other styles. The tube flow length mismatch in the inner versus the outer helices penalize the "C" designs. The U-tube and folded flow seem intermediate with some disadvantage due to turning losses.

- o Intangible (Thermal/Hydraulic)

  An intangible assessment in the thermal-hydraulic area slightly favor the straight tube counterflow units. The thermal feedback losses of the folded flow design influenced the lower rating indicated for the D-1 design.

(3) Cost

The cost assessment is taken directly from the optimized computer print out sheets shown as Figures C-40 through C-45. The ratings indicated are inversely proportional to the estimated costs consistent with the concept that cheaper is better.

REFERENCES

C-1 Tschamper, P. M., "The VHTR for Process Heat", General Electric, GEAP-14018, September 1974.

C-2 "High-Temperature Nuclear Heat Source Study", General Atomic, GA-A13158, December 30, 1974.

C-3 "The Very High Temperature Reactor for Process Heat", Westinghouse Astronuclear Laboratory, WANL-2445-1, December 1974.

C-4 Kays, W. M. and London, A. L., "Compact Heat Exchangers", McGraw-Hill, 1964

C-5 Knudsen, J.C. and D. L. Katz, Fluid Dynamics and Heat Transfer, 1958.

a. pp. 514-515.

b. p. 339.

C-6 London, A. L., Klopfer, G. and Wolf, S., "Oblique Flow Headers for Heat Exchangers", Journal of Engineering for Power, pp 271-286, July 1968.

C-7 Fraas, A. P., and Ozisik, M. N. "Heat Exchanger Design", John Wiley, 1965.

C-8 Duderstadt, E. C., "Corrosion Allowance Determination for Duplex Tube Steam Reformer for EVA Test" General Electric internal letter to J. A. Bond, January 30, 1976.

APPENDIX D

SAFETY CONSIDERATIONS

TABLE OF CONTENTS

LIST OF FIGURES

LIST OF TABLES

APPENDIX D

SAFETY CONSIDERATIONS

D.1 INTRODUCTION

Detailed safety and licenseability evaluations of the pebble bed reactor system have been previously reported[D-1,D-2]. In both cases, it was concluded that the reactor itself is a basically stable, tractable system in which operational and emergency events cause slow, easily controlled effects. This appendix will not repeat all of this prior work, although additional safety-related work is definitely required. The next section will summarize the safety characteristics of the PBR. The following sections will discuss the specific problem areas caused by the use of duplex tube steam reformers and/or an intermediate heat exchanger loop. A section on tritium diffusion effects concludes this appendix.

D.2 SAFETY CHARACTERISTICS

The principal safety features of the pebble bed reactor system are listed in Table D-1. The pebble-bed reactor is inherently stable for power transients due to the large negative temperature coefficient of the core. The reactivity effect of coolant density change is negligible. There is no significant coolant effect on the coefficient of reactivity in the pebble-bed system. The core is self correcting in the event of fuel loading errors since local power peaks tend to be suppressed due to the negative temperature coefficient and cumulative burnup effects. Xenon transients which may occur are damped by the negative temperature coefficient. Furthermore, the axial dimension of the core is not large enough for xenon instabilities to occur.

TABLE D-1

PBR PLANT SAFETY CHARACTERISTICS

REACTOR	CONTRIBUTING FACTORS
1. Nuclear Stability	Negative Doppler Effect Large Negative Temperature Coefficient No Coolant Density Effects on Reactivity Continuous Axial Fuel Shuffling Minimum Excess Reactivity Required
2. On-Line Refueling	Continous Fuel Feed and Discharge Reduced Fuel Storage Requirements Remote Handling of Spent Fuel Optimal Control of Reactivity On-Line Fuel Changes Permissible
3. High Temperature/Low Power Density Ceramic Fuel	High Temperature/Strength Core Low Power Density and Thermal Gradients Power Skewed Toward Cooler Core Inlet Flat Power Shape Near Core Outlet Large Fuel Temperature Margins
4. Large Core Thermal Inertia	Large Core Mass High Volumetric Heat Capacity High Fuel Element Conductance Low Coolant Void Fraction
REACTOR COOLANT SYSTEMS	
5. Inert Reactor Coolant	Small Helium Coolant Inventory Total Loss of Coolant Not Possible No Phase Change Effects Chemically Inert Perfect Gas No Coolant - Fuel Reactions
6. Unalterable Core Cooling Geometry	Random Fuel Element Geometry No Mechanism for Flow Blockage Three-Dimensional Flow Distribution
7. Modular PCRV and Heat Exchange Units	Core Enclosed by high Integrity PCRV Water Cooled PCRV Liners Built-In Reactor Shielding Multi Loop Heat Transport System All Process Fluids Outside PCRV Accessibility to Heat Transport Equipment
8. Coaxial Coolant Ducting	Cooling Helium as Thermal Barrier Water Cooled Pressure Boundary Ducting Accessible for Inspection

Continuous refueling of the pebble-bed limits the excess reactivity in the core to only that amount required for power maneuvering. This excess reactivity is contained by control rods which penetrate the top reflector and void regions.

Unlike the conventional off-line refueling systems, the pebble-bed system offers an automated fuel handling concept which eliminates many special operations required during refueling shutdowns.

The large graphite to fuel mass ratio in the core provides a thermal sink for excess energy produced. Even with total loss of core cooling, the fuel temperature does not exceed the operating range for an hour or more. In addition, with helium as coolant, sudden changes in fuel temperature due to coolant thermal transients are not possible. Subsequent to a loss of main helium circulation accident, the reduced core power due to a reactor trip results in a reduction of core fuel temperatures. The one hour time lag effect gives the plant operator ample time to take corrective action to restore reactor cooling and reduces the response time for the operation of emergency cooling systems. Furthermore, it has been shown for a hypothetical complete loss of helium circulation for the pebble-bed system, that with the reactor shutdown and the aid of the PCRV liner cooling systems, that core temperatures will increase for about 40 hours and eventually reach a maximum of less than 2310°C (4200°F) due to conduction and thermal radiation heat transfer from the core. At this time, fission products will, of course, be released from the peak temperature fuel balls, a small portion of the core. The graphite is well below its vaporization point,and no catastrophic failure will occur even in this worst-case event.

The random configuration of core fuel elements above the core support and inside the radial reflector boundary preclude the possibility of a fuel element rearrangement which could degrade core coolant flow through the pebble bed. Thus, the core geometry always remains amenable to cooling. In the event that local core flow blockage were to occur, the coolant flow distribution and freedom for cross-flow would compensate for reduced flow in a core region.

Special engineered safety features include the use of four independent core auxiliary cooling systems (CACS), each capable of removing 50% of the core afterheat. A fast discharge system (FDS) provides a static way of providing for a walk-away safe shutdown of the entire plant. The FDS provides a rapid removal of all fuel from the core to a shielded location where a nuclearly noncritical configuration exists and where static afterheat removal can be provided. This system is designed as an ultimate backup safety system, supplementing the redundant core auxiliary cooling system (CACS) and the redundant liner cooling systems.

In the highly unlikely event of complete failure of all safety systems, and after the passage of many hours, it is possible that fuel temperatures may exceed some predetermined safe limit. At this point, either automatically or by operator actions, the FDS will be activated. Valves located below the reactor cavity will open, allowing the fuel balls to flow into a subterranean, water-cooled annulus. This annulus is inherently safe from a criticality standpoint. The water outside the annulus can retain all afterheat without boiling so that no cooling system is required. At a future date, the fuel can be removed, either for reprocessing or reuse.

D.3 HEAT TRANSPORT SAFETY CONSIDERATIONS

D.3.1 DESIGN BASIS ACCIDENTS AND FAULT CONDITIONS

Past work[D-1,D-2] has focused attention on the reactor design basis accidents (DBA). Three DBA's were analyzed.

DBA No. 1 Reactor Coolant Depressurization

DBA No. 2 Loss of Primary Circulation

DBA No. 3 Secondary Containment Pressurization (Steam-Water Ingress to Core)

These are still the primary faults which affect the reactor system. Listed below are these DBA's with special stress on the effect on the heat transport system.

D.3.1.1 Reactor Primary Coolant Circuit Depressurization

This occurrence is one of the Design Basis Accidents (DBA) reported in the SNPH Final Report, references D-1 and D-2. It is assumed that a hypothetical rupture of 1000 cm^2 (155 in^2) occurs in the primary helium boundary. The first effect is a loss of primary coolant pressure. Within 16 seconds the pressure drops to approximately 2 bar ($\sim$29 psia). The reactor would be shutdown, the process isolation values closed, and the CACS used for emergency cooling.

The buffer gas pressure in the DSR or IHXL could be regulated as desired to control stress, but the first consideration will be the safety of the reactor and the prevention of radioactive release to the environment.

D.3.1.2 Loss of Helium Circulation

Loss of total helium circulation (all circulators) is a DBA. For this case, the primary coolant pressure would be maintained for several hours until either circulation is restored or it becomes apparent that it will not be. In the latter case, the primary circuit will be depressurized over a 17 hour period using the helium gas management system. This period should give the operators plenty of time to adjust the process feed pressures and the buffer gas system to prevent excess stress in the heat transport system.

If only one circulator fails, pressure will be maintained in the primary loop. The failed module will be isolated (no flow) at the reactor pressure level. The other units will have their flows adjusted at somewhere between 100% and 15% full flow. Process flow will probably be reduced and/or stopped in the operating modules, and definitely stopped in the failed module.

D.3.1.3 Secondary Containment Pressurization

This DBA occurs primarily as a result of steam/water ingress into the core following a steam generator tube failure.

Steam water ingress to the core produces a number of safety related conditions, including:

- Primary coolant pressure transients
- Steam graphite reactions
- Steam fuel reactions
- Possible release of adsorbed fission products from the reactor core
- Possible reduction of core graphite structural strength
- Generation of combustible gases from the steam-graphite reactions.

Sources of steam/water leakage into the primary coolant include a defective steam generator or the reactor core auxiliary cooling heat exchangers. All other water systems operate significantly below the primary coolant pressure. The steam generator leak is the most severe accident of this type.

The sequence of events following a design basis steam leak with normal action of the reactor protection system would be as follows:

1. Steam leak occurs at time zero

2. Moisture monitors in the defective loop detect high coolant humidity in excess of the high setpoint level within ten seconds.

3. The reactor is tripped, steam generator isolation and circulator trip for the defective loop is initiated. Primary circuit flow drops to about 80% and reactor power drops to 5% by 40 seconds.

4. Steam generator blowdown in the leaking loop is initiated shortly after high coolant humidity is detected.

5. The steam leak is terminated due to simultaneous initiation of the steam generator blowdown and steam circuit isolation.

6. The steam mixes with the helium coolant and reacts with graphite as it is circulated through the core.

7. The core is cooled on all but one main helium circuit to temperatures where steam graphite reaction rates are insignificant (below 1300°F).

With no reactor trip and no protective action (isolation of the defective loop) the PCRV relief valves will open and vent primary coolant and reaction products to the containment. Normal protective action will result in a gradual decrease in the PCRV pressure due to isolation of the defective loop and continuous cooling of the reactor in the shutdown condition. Isolation of the wrong loop with reactor trip leads to opening of the relief valve after a gradual pressure increase. The total amount of steam entering the primary system with normal control action and a leak rate of 100 pounds/second is approximately 1500 pounds.

Reactions of steam with graphite occur at significant rates when temperatures exceed 1300°F. The reaction is:

$$H_2O + C \rightarrow CO + H_2 - Q$$

Other secondary reactions are insignificant for the time periods of interest. The reaction rate for the oxidation of graphite can be accelerated by the catalytic action of metallic fission products, particularly barium. For the maximum predicted steam leakage accident (1500 pounds of water), the total amount of graphite reacted is 1000 pounds, assuming complete reaction of the steam and graphite. This is less than 1% of the total core graphite. The mechanical strength of the fuel and structural graphite is not expected to be significantly affected by this oxidation.

D.3.1.4 Failure of Process Equipment

A failure of a process line or a secondary helium line in the case of a plant with an IHX would not cause a DBA, but would result in a fault condition for the heat transfer equipment. Since the main purpose of this study is to examine the engineering details of the heat transport system, this fault becomes a key one for the design of the heat transport equipment. The following sequence is postulated.

1. A failure of the process system outside the reactor building or a break in a process pipe within the secondary containment causes a decrease in the pressure on the process (or secondary helium) side of the main heat transfer device.

2. The reactor is shutdown using normal procedures. (At least one of each pair of isolation valves operates successfully)

3. The pressure in the primary loop is reduced, as is the gas temperature, over a ten hour period.

Thus the requirement on the main heat transfer device is that it be able to withstand ten hours at maximum temperature with a primary pressure of approximately 40 b and zero pressure on the secondary side. This requirement was used for the design of both the duplex tube steam reformer and all IHX designs.

D.3.2 DUPLEX STEAM REFORMER

In addition to withstanding the above fault conditions, two other safety areas require discussion. Assessment of the duplex tube as a licenseable alternate to the use of an independent IHX requires the favorable resolution of two items. These are:

1. Leak detection, monitoring, and tritium cleanup from the DSR intertube gap, and

2. Credibility of a guillotine failure of a reformer tube.

D.3.2.1 DSR Leak Detection, Monitoring and Intertube Cleanup

The design of the duplex tube steam reformer includes the use of a gap between the two tubes. This gap is filled with static helium at a pressure approximately 2 b (30 psi) lower than either the process gas or the primary core coolant. Thus a leak in either stream can be detected by monitoring the intertube gas for fission products and/or hydrogen, methane, carbon monoxide, or water vapor. Grooves have been placed in the intertube gap to insure flow to the top of the tube in the event of a leak. As presently shown in Figure D-1, all intertube gaps are connected to the domed head of the assembly.

There are two potential ways to monitor this space. One is to attach a pigtail tube to each gap, and monitor each tube in a sequential manner. The second is to place a number of sampling tubes in a pattern in

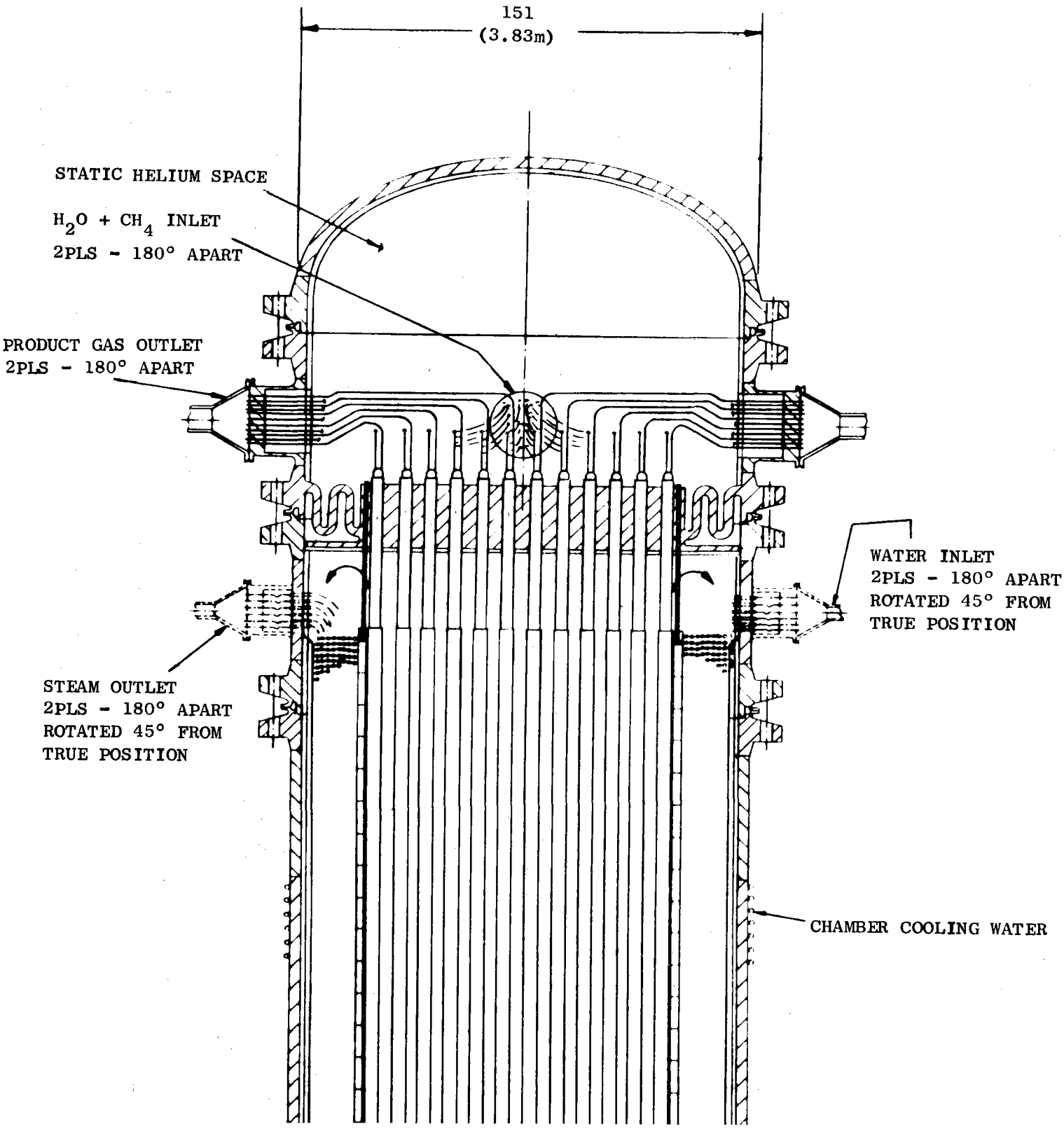

Figure D-1. Steam Reformer Assembly : Duplex Tube

the head, and use these to localize a leaky tube. This latter method would require development testing. In all cases, if a leak is large enough to be significant, it would be detected, so that appropriate action could be taken.

A gas cleanup system would be used for the intertube helium. Although no flow is provided within the gaps themselves, the domed space would be slowly swept by clean helium to allow the removal of impurities, especially tritium. By maintaining a low partial pressure of tritium, diffusion to the product can be held at an appropriate level. (See Appendix Section D.4.)

D.3.2.2 Guillotine Reformer Tube Failure

In order to compete with the intermediate heat exchanger on a safety basis, the duplex tube steam reformer must be no more susceptible than the IHX with respect to single mode failures which might allow fission products to escape the secondary containment. The only conceivable failure which could cause this is a massive, nearly simultaneous failure of both tubes of the duplex tube. Only two initiating mechanisms have been identified which could cause this.

The first is a crack propagating from one tube to the other. Experience with other types of duplex tubes and structures suggest that this is highly unlikely. Statistically, the cracking of each tube should be independent. The results of the work now underway at GE on the duplex steam reformer tube should resolve this issue, but additional tests and analysis are certainly desirable.

The second potential failure is a guillotine failure of a duplex tube. The credibility of this depends on an initiating incident. There are no ways in which a tube can be struck while inside the module. A missile penetrating the module is the only conceivable way to break a tube. This would also cause a loss of core coolant pressure and be one of the DBA's. Again, this would be one of the areas where additional analysis and testing would be desirable.

D.3.3 INTERMEDIATE HEAT EXCHANGER

The IHX concepts described in Appendix C are all designed for the fault conditions mentioned above, i.e., a failure of the secondary pressure level. A cleanup gas purification system insures the removal of tritium from the secondary loop. The removal of the steam generator from the primary loop drastically reduces the chance for the ingress of steam to the reactor core.

D.4 TRITIUM PERMEATION

Tritium, (the heavy isotope of hydrogen, ^{3}H) is formed in all nuclear reactor systems through the fission process (ternary fission) and through neutron interactions in various materials. In the PBR, there are three main sources of tritium:

1. ternary fission in the fuel element (balls)
2. neutron reaction with the isotope Lithium 6 present in impurities, $^{6}Li(n,\alpha)T$
3. neutron reaction with the isotope Helium 3, $^{3}He(n,p)T$

Tritium produced through the ternary fission process and neutron interactions with Lithium 6 is retained primarily by the core materials. For example, the fuel particles are coated to retain fission products and in addition, the fissile core material is surrounded by a thick layer of graphite to form the completed fuel sphere. The main source of tritium in the primary helium is due to the neutron reaction with the Helium 3 isotope.

Most of the tritium which is released will be removed via helium purification systems, but a small fraction will diffuse through heat exchanger surfaces and enter the process gas stream. Control of these permeation rates is essential in the design of a nuclear process heat system.

D.4.1 PERMEATION DATA

Reference D-3 is a treatise on the general problem of diffusion in and through solids. A considerable body of data exists on permeation of hydrogen isotopes through various materials[D-4 - D-9]. Hydrogen permeation through metals is characterized, with small deviations, by a $\sqrt{P}$ law, which means that the driving potential for permeation at a given temperature is the square root of the hydrogen partial pressure. Strehlow and Savage [D-5] present hydrogen permeation data which follows the $\sqrt{P}$ dependence over six orders of magnitude of pressure. An explanation of this behavior is that the diffusion of hydrogen in metals occurs as atoms. Figure D-2 shows some typical data for permeation of hydrogen isotopes through bright metals.

The presence of an oxide film on the metal surface can drastically affect the permeation behavior. As discussed by Strehlow and Savage, permeation through an oxidized metal is expected to be much slower than through pure metal; also, the driving potential in this case becomes P instead of $\sqrt{P}$. Figure D-3 illustrates these points. Plotted on log-log coordinates, the permeation relationships are straight lines. On the process side of a reformer tube, the hydrogen partial pressure will be in the order of 10 bar. At this pressure level, the effect of an oxide film could be to reduce the permeation rate about one order of magnitude below the corresponding value for a bright metal. In the primary helium stream, the partial pressure of tritium in the primary helium is expected to be in the order of 0.5×10^{-8} bar[D-9]. If the trends illustrated in Figure D-3 are extrapolated back to that pressure, the permeation rate for an oxidized metal would be five orders of magnitude lower than that for the bright metal. These results suggest that oxide films may be effective in controlling the permeation of hydrogen isotopes (especially at low pressure). The effect of oxide films on hydrogen permeation has not been thoroughly investigated. Additional information on the nature and stability of oxide films is needed before a system design which depends on the oxide film can be completed.

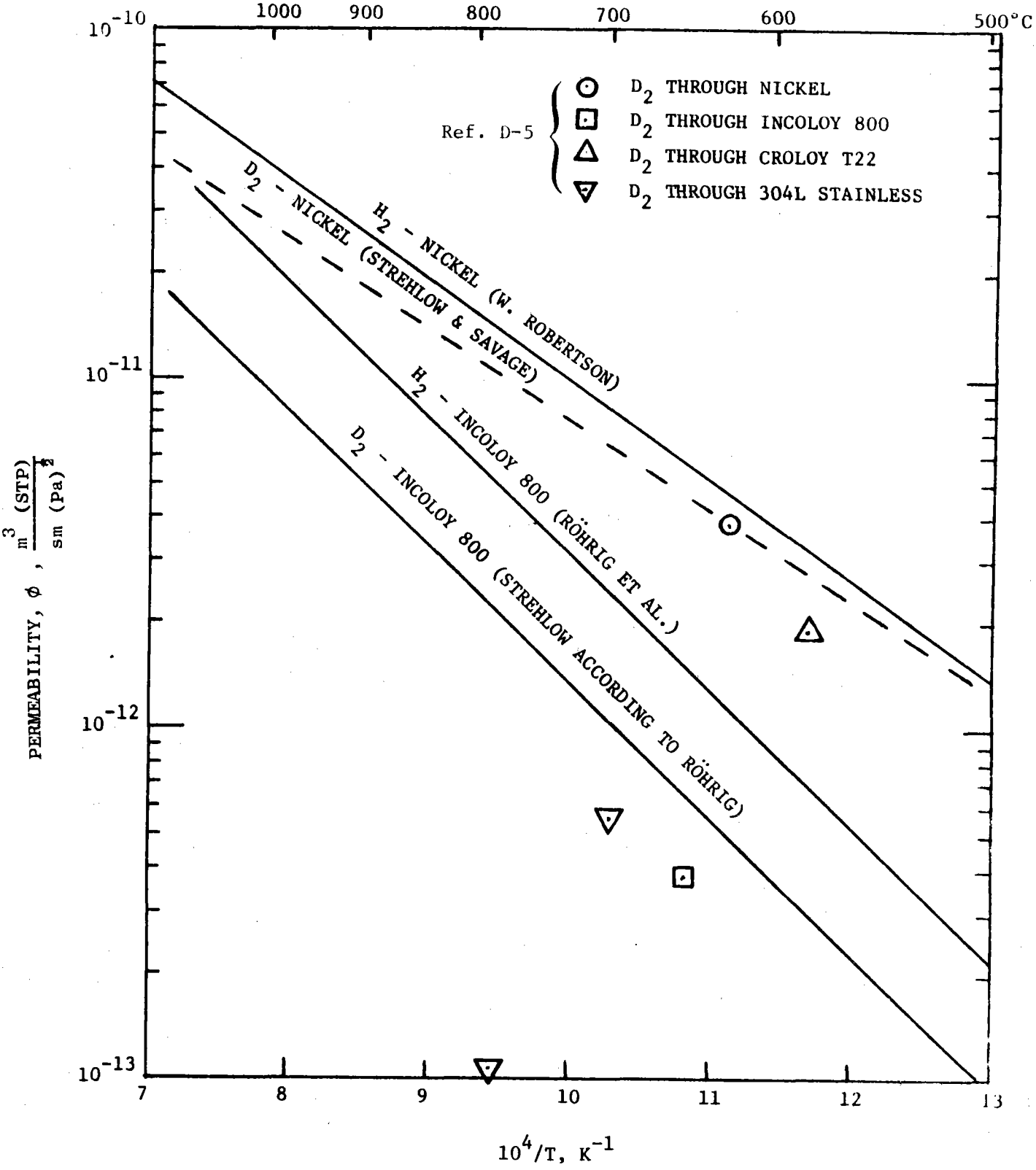

Figure D-2. Hydrogen Permeation Data

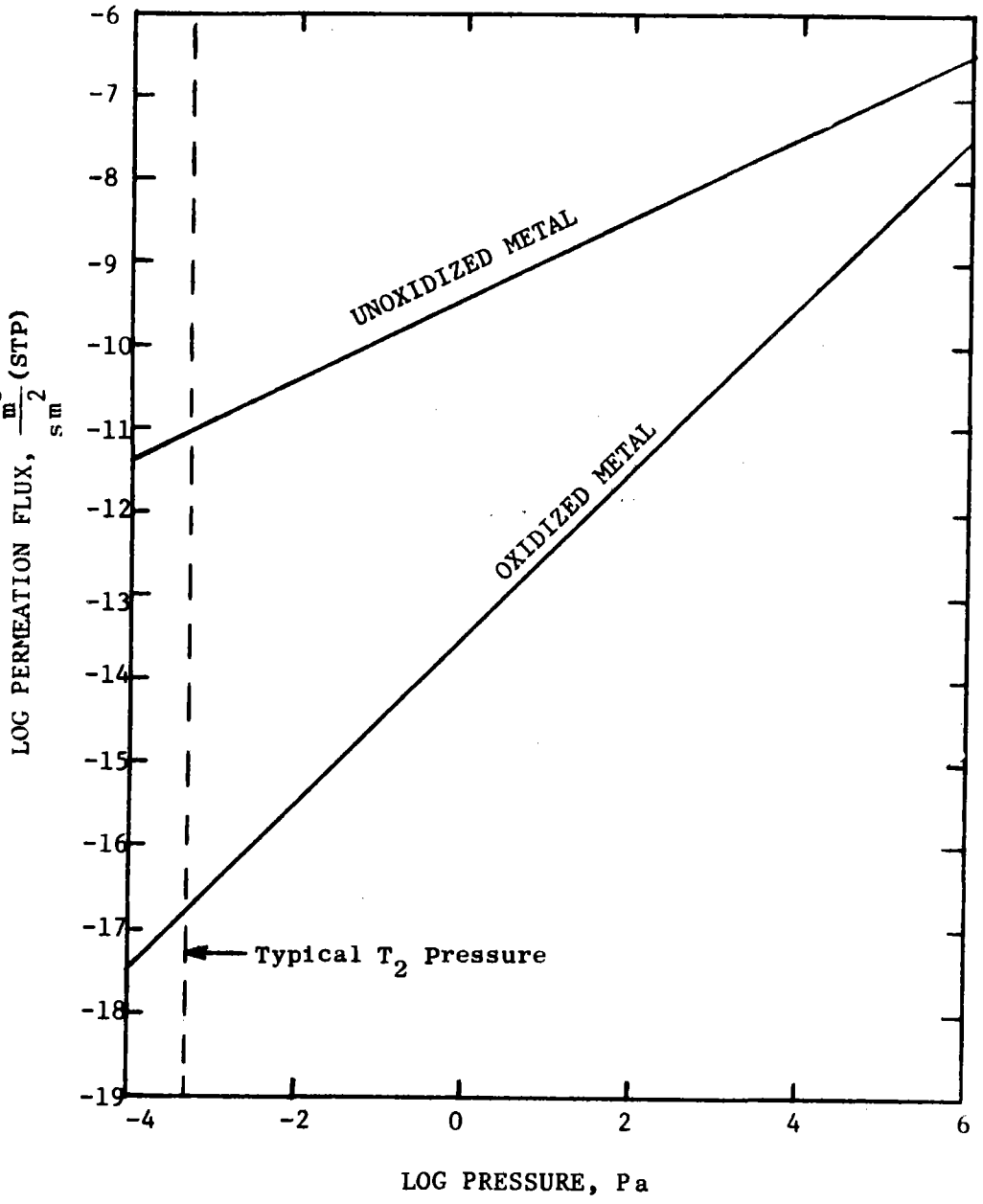

Figure D-3. Pressure Dependence of Permeation For Oxidized and Unoxidized Metals

D.4.2 DIRECT HEATED SYSTEM (NO IHX LOOP)

Figure D-4 illustrates a gas-cooled reactor system in which a reformer and a steam generator are heated directly by the primary helium stream. The steam from the steam generator may either be used in a closed Rankine engine or a portion may be extracted for use in the methane reformer. Figure D-5 illustrates the tritium mass balance.

Under equilibrium conditions, the transport of tritium generated and released into the primary helium stream will be governed by the following mass balance:

$$\begin{matrix}\text{Generation} \\ \text{Rate}\end{matrix} = \begin{matrix}\text{Purification} \\ \text{Rate}\end{matrix} + \begin{matrix}\text{Reformer} \\ \text{Permeation}\end{matrix} + \begin{matrix}\text{Steam Generator} \\ \text{Permeation}\end{matrix}$$

The generation rate is a constant and each of the terms in the right member of the mass balance is a function of the tritium partial pressure in the primary helium. (This assumes no change in tritium partial pressure as the helium passes through the reformer.) The solution of the mass balance equation, then, yields the tritium partial pressure which can then be used to calculate the permeation rates in the reformer and in the steam generator.

Table D-2 summarizes the calculated tritium permeation rates for a reference 3000 MW_t process heat plant. The calculations were performed for bright metal tubes and for oxidized tubes. For the bright metal tubes (no oxide film) the permeation rates were high which results in a low equilibrium tritium partial pressure in the helium. The corresponding purification system removal rate is so low that the purification system is ineffective. The results for a single oxide film show the opposite result. In this case, over 95.5% of the tritium is removed by the purification system. Additional oxide films in series reduce the permeation rates even further. These films could be present on the surfaces of a duplex tube which has four surfaces on which oxide films could be present.

The above results are based on an assumed gas purification system flow rate equal to 60,000 m^3/day (STP). Additional calculations were performed to determine the effect of gas purification flow rate on the permeation rates. The results of those calculations are shown in

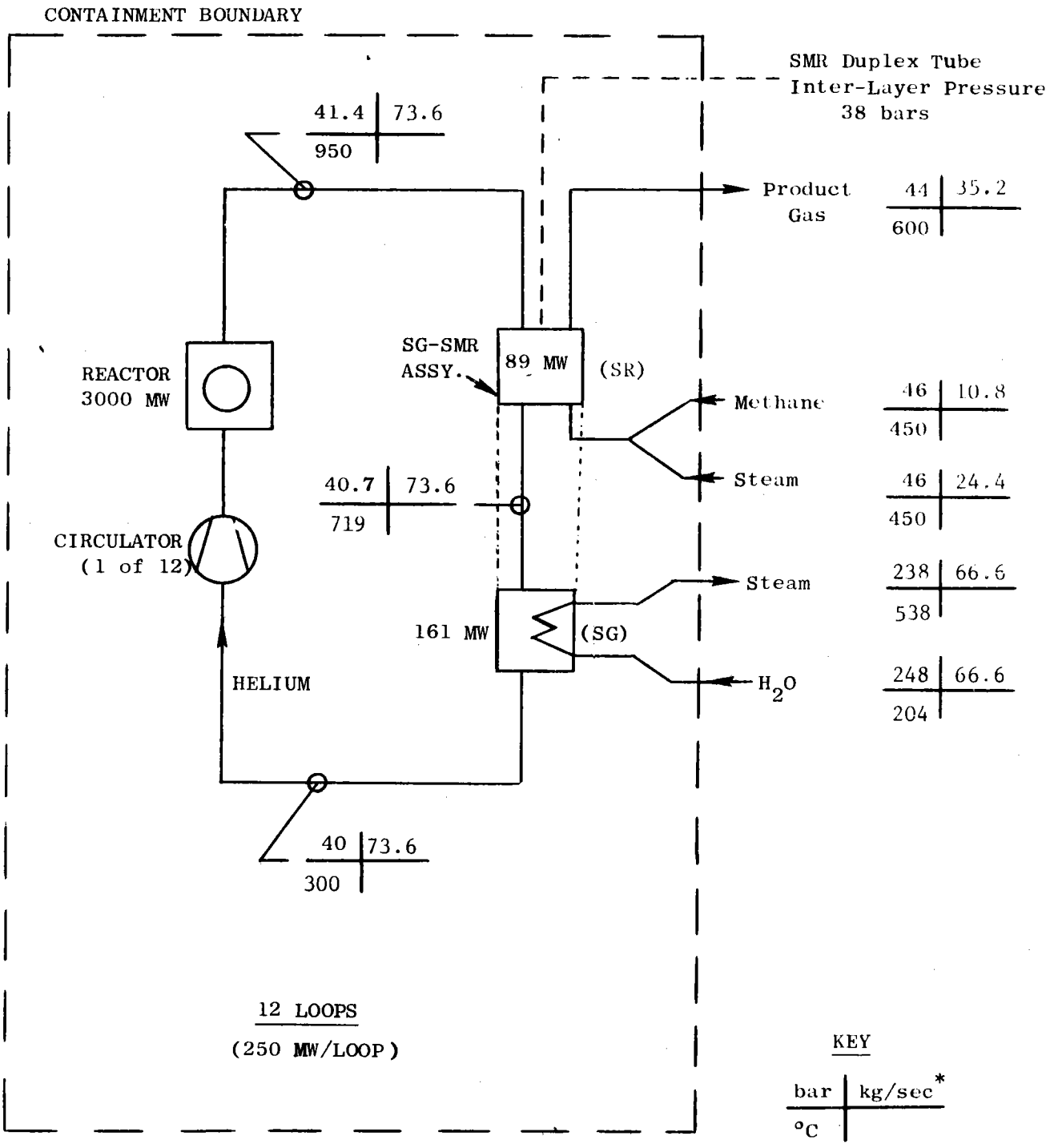

* All flows on a per loop basis.

Figure D-4. Pressure, Temperature and Flow Rates Within the Containment Building

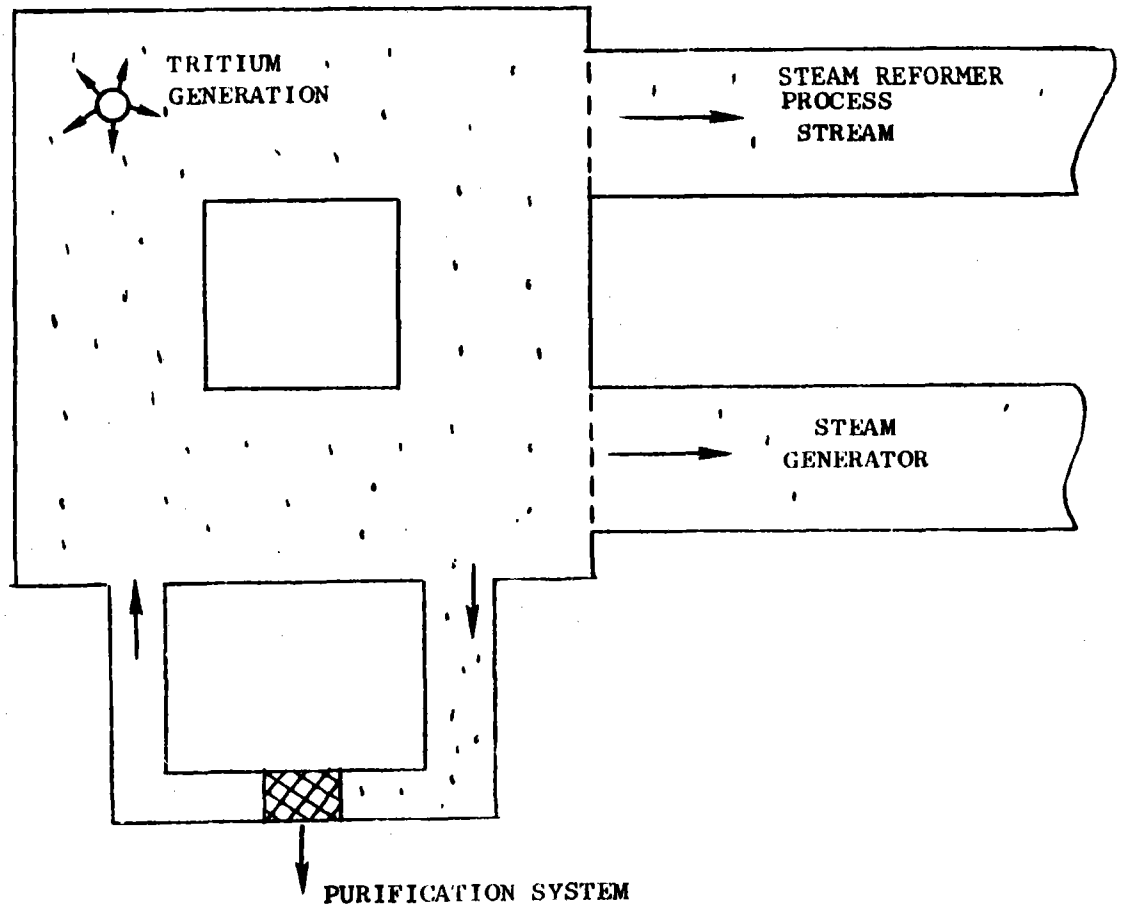

GENERATION RATE = PURIFICATION RATE + REFORMER RATE + STEAM GENERATOR RATE

Figure D-5. Illustration of the Tritium Mass Balance

TABLE D-2

CALCULATED TRITIUM PERMEATION RATES

NUMBER OF OXIDE FILMS	REMOVED BY PURIFICATION SYSTEM Ci/YR	PERMEATION THROUGH REFORMER Ci/YR	PERMEATION THROUGH STEAM GENERATOR Ci/YR	PRIMARY LOOP TRITIUM PARTIAL PRESSURE Pa
0	15	9234	1701	1.3×10^{-9}
1	10,896	43	11	8.5×10^{-4}
2	10,922	22	6	8.5×10^{-4}
3	10,932	14	4	8.5×10^{-4}
4	10,936	11	3	8.5×10^{-4}

ASSUMPTIONS

GENERATION RATE = PURIFICATION RATE + REFORMER RATE + STEAM GENERATOR RATE

GENERATION	=	30 Ci/d = 10,950 Ci/YR
PURIFICATION SYSTEM FLOW	=	60,000 m^3/d (STP)
REFORMER SURFACE AREA	=	19,700 m^2
REFORMER METAL TEMPERATURE	=	740°C
STEAM GENERATOR AREA	=	21,000 m^2
STEAM GENERATOR TEMPERATURE	=	440°C

Figure D-6. As would be expected, the permeation rates decrease with increasing flow rate but at a decreasing rate.

The tritium permeation rates shown in Table D-2 were used to determine concentrations of tritium in the product gas stream. The results are summarized in Table D-3, and show that tritium concentrations in the product gas stream will be in the order of 8×10^{-7} μ Ci/cm^3 for a single oxide layer.

Based on the work performed by Barton[D-10]* et al, the extent to which a residential atmosphere would become contaminated with tritium would depend on a variety of factors. Barton was able to identify the limiting case as an unvented gas heating unit and unvented gas appliances. Even for this situation, the tritium contamination in the residential atmosphere would be reduced by a factor of 170 below the level in the pipeline gas. Thus, the worst case, conservative tritium levels would be in the order of 4.4×10^{-9} μ Ci/cm^3 for the no oxide layer design and 2.0×10^{-11} μ Ci/cm^3 for the oxide layer design.

These levels, which are calculated to be present in the residential atmosphere under the worst conditions, compare favorably with the Maximum Permissible Concentration values in air, $(MPC)_a$, established by the International Commission on Radiological Protection (ICRP). In the USA, these recommended MPC values were accepted by the Federal Radiation Council (FRC) and implemented into practice by the former AEC.

Recent publications by the NRC[D-11], show the $(MPC)_a$ values for tritium to be 2×10^{-7} μ Ci/cm^3 for exposure to the general public. Some typical MPC air and water values are shown:

---

*The product gas was used as a replacement for natural gas for residential heating, cooking and appliances.

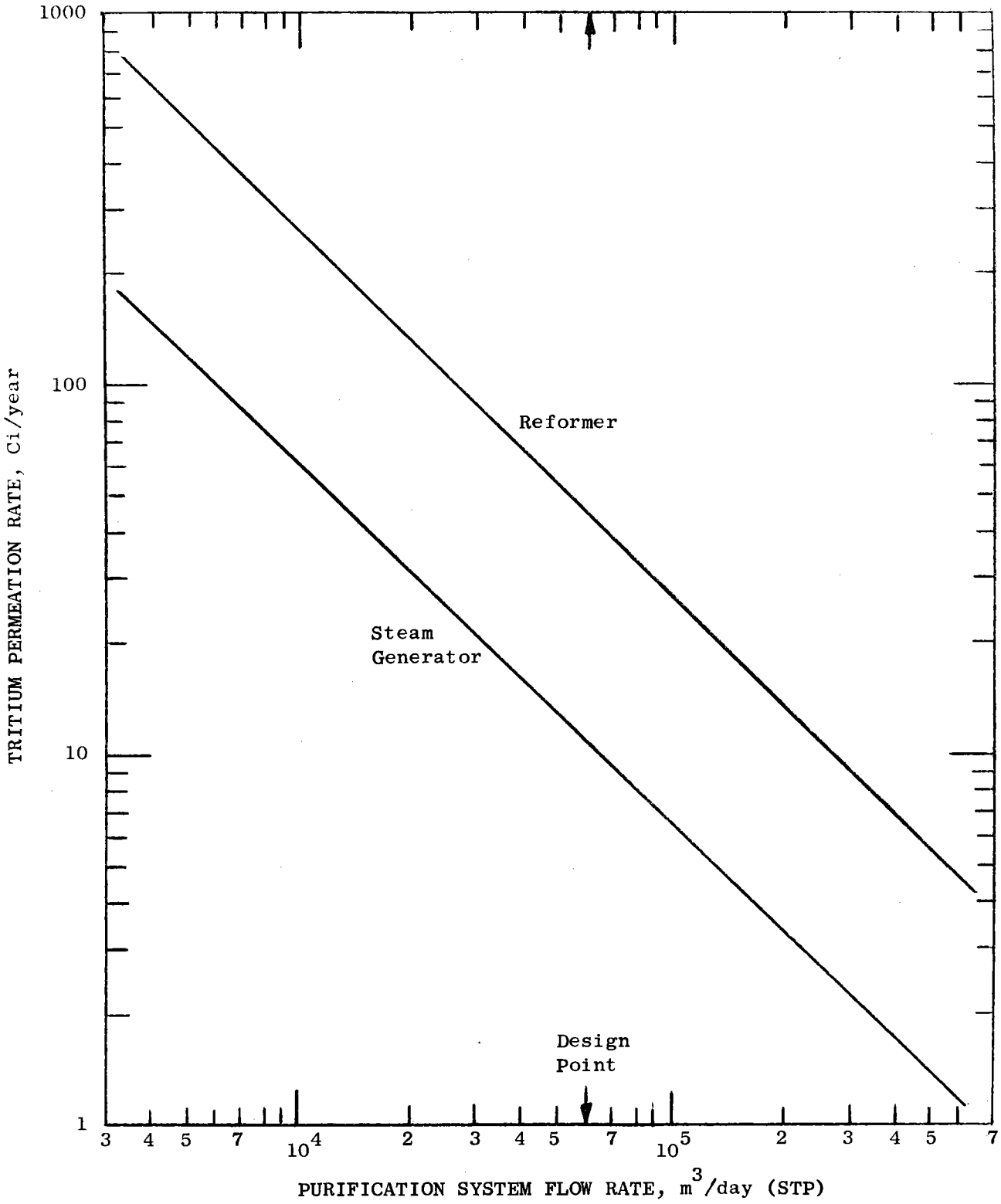

Figure D-6. Effect of Purification Flow Rate on Tritium Permeation.

TABLE D-3

TRITIUM CONCENTRATIONS AND LIMITS

NUMBER OF OXIDE FILMS	PIPELINE PRODUCT GAS CONCENTRATION $\mu Ci/cm^3$	WITH 170 X DILUTION* $\mu Ci/cm^3$
0	7.5×10^{-7}	4.4×10^{-9}
1	3.5×10^{-9}	2.0×10^{-11}
2	1.8×10^{-9}	1.0×10^{-11}
3	1.2×10^{-9}	7.0×10^{-12}
4	8.8×10^{-10}	5.2×10^{-12}

*BASED ON WORK OF BARTON, THE TRITIUM CONTAMINATION IN THE RESIDENTIAL ATMOSPHERE (WITH UNVENTED GAS HEATING UNIT AND UNVENTED GAS APPLIANCE) WOULD BE REDUCED BY A FACTOR OF 170 BELOW THE LEVEL OF PIPELINE GAS.

MAXIMUM PERMISSIBLE CONCENTRATION IN AIR $(MPC)_a$

1975 NRC VALUES FOR TRITIUM

1. $(MPC)_a$ FOR OCCUPATIONAL EXPOSURE = 5×10^{-6} $\mu Ci/cm^3$

2. $(MPC)_a$ FOR GENERAL PUBLIC = 2×10^{-7} $\mu Ci/cm^3$

MAXIMUM PERMISSIBLE CONCENTRATIONS IN MICROCURIES PER cm^3 OF AIR AND WATER OF SELECTED RADIONUCLIDES FOR OCCUPATIONAL EXPOSURE (40-HR WEEK) AND EXPOSURE TO THE GENERAL PUBLIC

	OCCUPATIONAL EXPOSURE		GENERAL PUBLIC	
RADIONUCLIDE	$(MPC)_a$	$(MPC)_w$	$(MPC)_a$	$(MPC)_w$
^{3}H	5×10^{-6}	0.1	2×10^{-7}	3×10^{-3}
^{14}C	4×10^{-6}	0.02	1×10^{-7}	8×10^{-4}
^{24}Na	1×10^{-6}	6×10^{-3}	4×10^{-8}	2×10^{-4}
^{41}Ar	2×10^{-6}	*	4×10^{-8}	*
^{60}Co	3×10^{-7}	1×10^{-3}	1×10^{-8}	5×10^{-5}
^{87}Kr	1×10^{-6}	*	2×10^{-8}	*
^{90}Sr	1×10^{-9}	1×10^{-5}	3×10^{-11}	3×10^{-7}
^{131}I	9×10^{-9}	6×10^{-5}	1×10^{-10}	3×10^{-7}
^{137}Cs	6×10^{-8}	4×10^{-4}	2×10^{-9}	2×10^{-5}
^{226}Ra	3×10^{-11}	4×10^{-7}	3×10^{-12}	3×10^{-8}
^{235}U	5×10^{-10}	8×10^{-4}	$2\times10^{=11}$	3×10^{-5}
^{239}Pu	2×10^{-12}	1×10^{-4}	6×10^{-14}	5×10^{-6}

*Noble gases are not soluble in water; $(MPC)_a$ based on dose a person would receive if surrounded by an infinite hemispherical cloud of radioactive gas. The radiation from the cloud delivers a higher dose than that from gas held in the lungs or other internal organs.

Thus, the contamination of tritium in the product gas is considerably less than the allowed value even under the worst conditions. Even if future standards were reduced by a factor of 10 or 100, the calculated concentrations could be tolerated.

D.4.3 SYSTEM WITH IHX LOOP

Figure D-7 illustrates a system in which the reformer and steam generator are isolated from the primary helium stream by an intermediate heat exchanger. The possibility of helium purification systems in both the primary and secondary loops is illustrated. In this case, there are two tritium mass balances:

$$\begin{matrix}\text{GENERATION} \\ \text{RATE}\end{matrix} = \begin{matrix}\text{PRIMARY} \\ \text{PURIFICATION}\end{matrix} + \begin{matrix}\text{IHX} \\ \text{PERMEATION}\end{matrix}$$

$$\begin{matrix}\text{IHX} \\ \text{PERMEATION}\end{matrix} = \begin{matrix}\text{SECONDARY} \\ \text{PURIFICATION}\end{matrix} + \begin{matrix}\text{REFORMER} \\ \text{PERMEATION}\end{matrix} + \begin{matrix}\text{STEAM GENERATOR} \\ \text{PERMEATION}\end{matrix}$$

This is a system of two equations in two unknowns (the tritium partial pressure in the primary and in the secondary loops). As shown previously, the presence of oxide film on heat exchanger surfaces can drastically effect the permeation rates. The calculations made for this system have assumed oxide films on the reformer and steam generator surfaces. Calculations have been made for an IHX without an oxide film and for the case in which the IHX is oxidized. The results are summarized in Table D-4. The results for the direct heated system are those given previously. Results with an IHX loop are given for unoxidized and for oxidized IHX surfaces. Results are given for no secondary purification system in order to compare directly with the direct heated cases. The effect of a secondary purification system is shown in the last column. These results suggest that a single oxide barrier (or its equivalent) between the primary helium and the process gas is a necessary and sufficient condition to reduce tritium in the process gas to safe values.

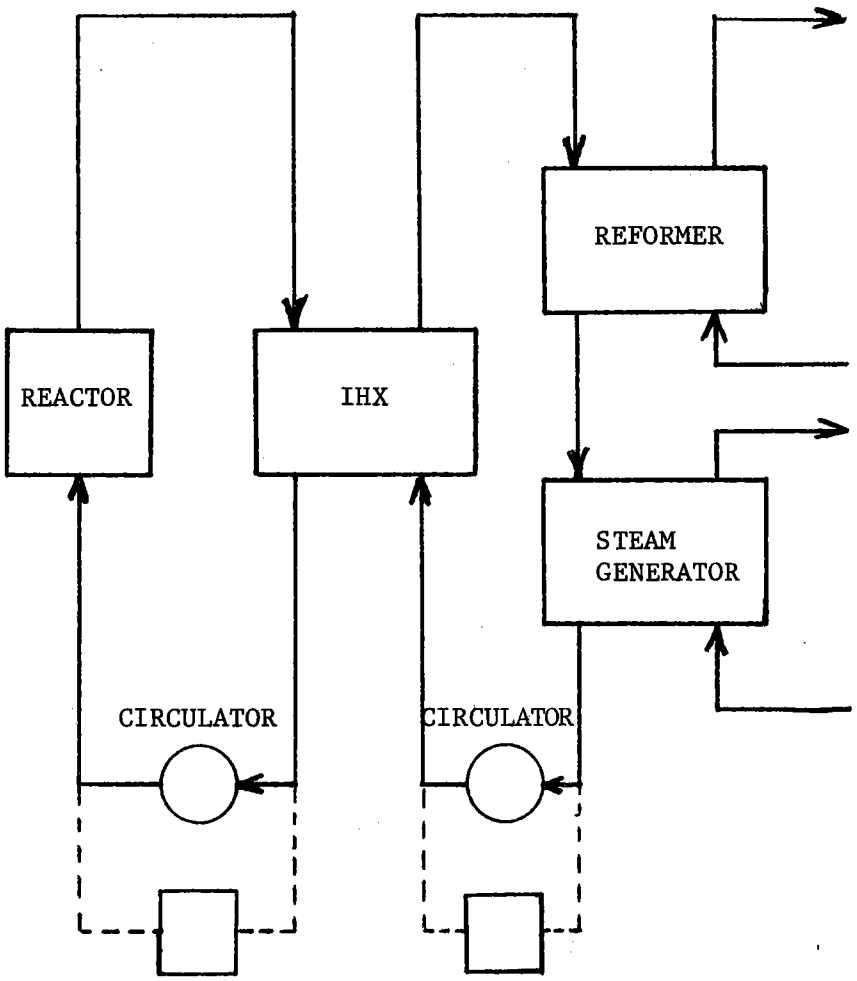

Figure D-7. Illustration of System with IHX Loop.

TABLE D-4

TRITIUM PERMEATION

TRITIUM RELEASE INTO PRIMARY HELIUM, Ci/YR	10,950	10,950	10,950	10,950	10,950
PRIMARY PURIFICATION FLOW RATE, m^3/DAY	60,000	60,000	60,000	60,000	60,000
SECONDARY PURIFICATION FLOW RATE, m^3/DAY	-	-	0	0	60,000
PRIMARY PURIFICATION, Ci/YR	15	10,896	10,909	10,924	10,795
PERMEATION THROUGH IHX, Ci/YR	-	-	41	33	155
SECONDARY PURIFICATION, Ci/YR	-	-	0	0	154.4
PERMEATION THROUGH REFORMER, Ci/YR	9,234	43	34	27	0.5
PERMEATION THROUGH STEAM GENERATOR, Ci/YR	1,701	11	7	6	0.1
PRODUCT GAS CONCENTRATION, μ Ci/Cm^3	7.5×10^{-7}	3.5×10^{-9}	2.8×10^{-9}	2.2×10^{-9}	4.1×10^{-11}
WITH 170 x DILUTION, μ Ci/Cm^3	4.4×10^{-9}	2.0×10^{-11}	1.6×10^{-11}	1.3×10^{-11}	2.4×10^{-13}
IHX TUBES	-	-	NOT OXIDIZED	OXIDIZED	OXIDIZED
REFORMER & STEAM GENERATOR TUBES	NOT OXIDIZED	OXIDIZED	OXIDIZED	OXIDIZED	OXIDIZED

MAXIMUM PERMISSIBLE CONCENTRATION IN AIR $(MPC)_a$ 1975 NRC VALUES FOR TRITIUM

1. $(MPC)_a$ FOR OCCUPTAIONAL EXPOSURE = 5×10^{-6} μ Ci/cm^3

2. $(MPC)_a$ FOR GENERAL PUBLIC = 2×10^{-7} μ Ci/cm^3

REFERENCES

D-1 Woike, O.G., "Small Nuclear Process Heat Plants (SNPH) Using Pebble Bed Reactor", General Electric Company, GEEST 75-001, November 1975.

D-2 Tschamper, P.M., "The VHTR for Process Heat", General Electric, GEAP-14018, September 1974.

D-3 Barrier, R. M., Diffusion In and Through Solids, Cambridge University Press, 1951.

D-4 Robertson, W. M., "Hydrogen Permeation, Diffusion and Solution in Nickel", Zeitschrift Für Metalkunde, Vol. 64, No. 6, June 1973

D-5 Strehlow, R. A., and H. C. Savage, "The Permeation of Hydrogen Isotopes Through Structural Metals at Low Pressures and Through Metals with Oxide Film Barriers", Nuclear Technology, V Vol. 22, April, 1974.

D-6 Röhrig, H. D., J. Blumensaat, and J. Schaefer, "Experimental Facilities for the Investigation of Hydrogen and Tritium Permeation Problems Involved with Steam Methane Reforming by Nuclear Process Heat", British Nuclear Energy Society - International Conference, 26-28, Nov., 1974.

D-7 Bell, J. T., R. A. Strehlow, J. D. Redman, and F. J. Smith, "Tritium Permeation Through Steam Generator Materials", International Conference on Radiation Effects and Tritium Technology for Fusion Reactors, Gatlinburg, Tenn., October 1-3, 1975.

D-8 Bell, J. T., R. A. Strehlow, J. D. Redman, H. C. Savage, and F. J. Smith, "Tritium Permeation through Materials for Steam Generator Systems", Proc. 23rd Conf. Remote Systems Technology, 1975.

D-9 Röhrig, H. D., R. Hecker, J. Blumensaat, and J. Schaeffer, "Studies on the Permeation of Hydrogen and Tritium in Nuclear Process Heat Installations", Nuclear Engineering and Design, Vol. 34, No. 1, October, 1975.

D-10 Barton, C. J., et al., Nuclear Technology, Vol. II, p 335 (1971)

D-11 Title 10, Chapter 1, Code of Federal Regulations, Part 20 (10 CFR 20) Appendix B, April, 1975.

APPENDIX E

STEAM REFORMER DESIGN

TABLE OF CONTENTS

LIST OF FIGURES

LIST OF TABLES

APPENDIX E

STEAM REFORMER DESIGN

This appendix discusses the design of the steam reformer/steam generator module (SRA/SGA) which is used for the steam reforming plants described in Section 2.

E.1 STEAM REFORMER-STEAM GENERATOR ASSEMBLY

The steam reformer-steam generator heat exchanger is illustrated in Figure E-1. Helium from the reactor outlet enters through the inner coaxial duct and flows upward through the space between the reformer tubes which occupy the central portion of the heat exchanger core. At the top of the core the reactor coolant stream is directed into the outer annulus through which it flows downward over the concentric helical tubes of the once through steam generator. The cooled helium is then directed to the inlet of the centrifugal circulator. The circulator is provided with variable diffuser vanes for flow control. From the circulator diffuser the helium stream passes into the outer coaxial duct for return to the reactor.

The design of the duplex tube steam reformer units is discussed in Section E.2. The reformers are supported from the tube sheet. Two tubes are connected to the top of each steam reformer, one bringing in the steam-methane mixture which flows over the catalyst filling the inner duplex tube, and the other delivering the product gas from the "pigtail" tube which acts as a recuperative heat exchanger between the product gas and the reactant gas in the catalyst space. The reactant gas and product gas tubes from all of the reformers are manifolded at nozzle tube sheets (two for each gas stream) which are accessible from outside the pressure vessel. At these tube sheets, leaking tubes can be detected and sealed off. Employment of established steam reformer catalyst technology requires replacement of the catalyst at an interval ranging from two to eight years. Detailed design effort is required to define a tube closure design above the tube sheet which will facilitate catalyst replacement. As a long range goal it is projected that development of an advanced reformer catalyst will eliminate the necessity

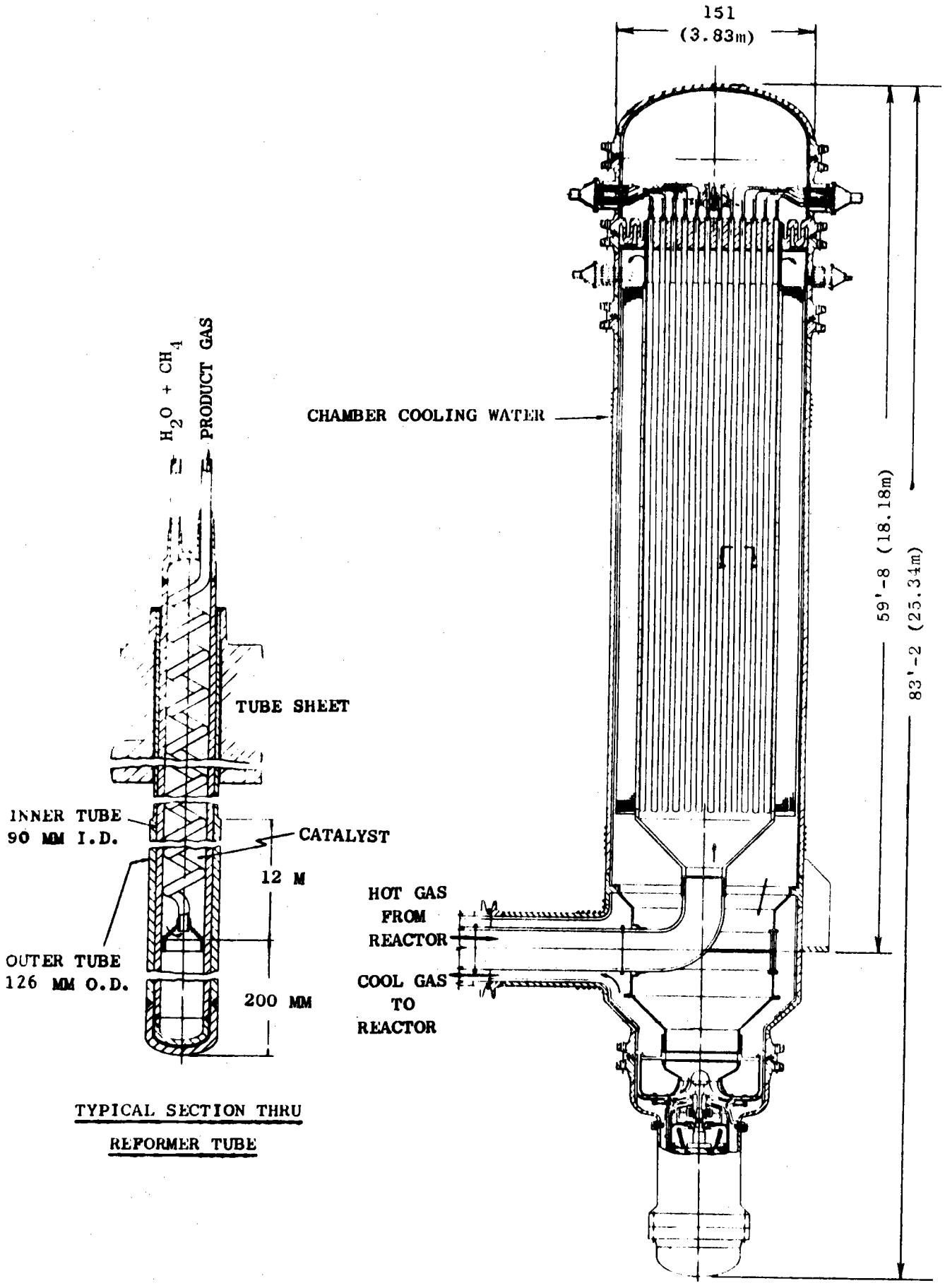

Figure E-1. Reference Design for the Duplex Tube Steam Reformer/Steam Generator Assembly.

for periodic catalyst replacement. With such a catalyst, activity renewal can be accomplished through steam or hydrogen injection. By reduction of the outer duplex tube wall thickness in the upper end of the reformer a larger spacing to diameter ratio is achieved in the tube sheet than in the heat transfer section of the core. In all design cases except for that involving a very small reformer (13% of the total heat transfer to the reformer) it is necessary to block a portion of the helium flow area between the reformer tubes by use of the alternate means shown in Figure E-2, in order to realize the design level of helium film convection coefficient (1700 watts/m^2°C). Thermal stress caused by a radial temperature gradient between the tube sheet and the water cooled pressure vessel shell is relieved by the incorporation of a folded thermal sleeve. In order to minimize the temperature gradient across the tube sheet, an insulation blanket, of either fibrous material or metallic foil, is placed against the lower surface of the tube sheet.

The steam generator unit is an assembly of concentric multiple helical tubes which are supported by suspension from supports anchored to the section of pressure vessel shell between the second and third pair of flanges (counting from the top) shown on Figure E-1. Feed water and steam tubes are manifolded at four locations in this portion of the shell. The design thus provides for independent assembly of the steam reformer and steam generator sections of the integrated heat exchanger. The integrated heat exchanger is proposed as a practical space and cost saving alternative to a design involving separate pressure vessels for the reformer and steam generator.

E.1.1 STEAM REFORMER-STEAM GENERATOR DESIGN DATA

Design data for six design cases is presented in Table E-1. These designs are based on 250 MW thermal input from the helium flow and cover a range of power input to the steam reformer from 13% to 58.4%, the former being appropriate for a base load/peaking power plant with chemical energy storage and the latter being suitable for a chemical heat pipe system with maximum power delivery by the chemical heat pipe (see Appendix A). A comparison of design 2 and 3 shows the difference in heat exchanger size/weight between a duplex tube steam reformer design and

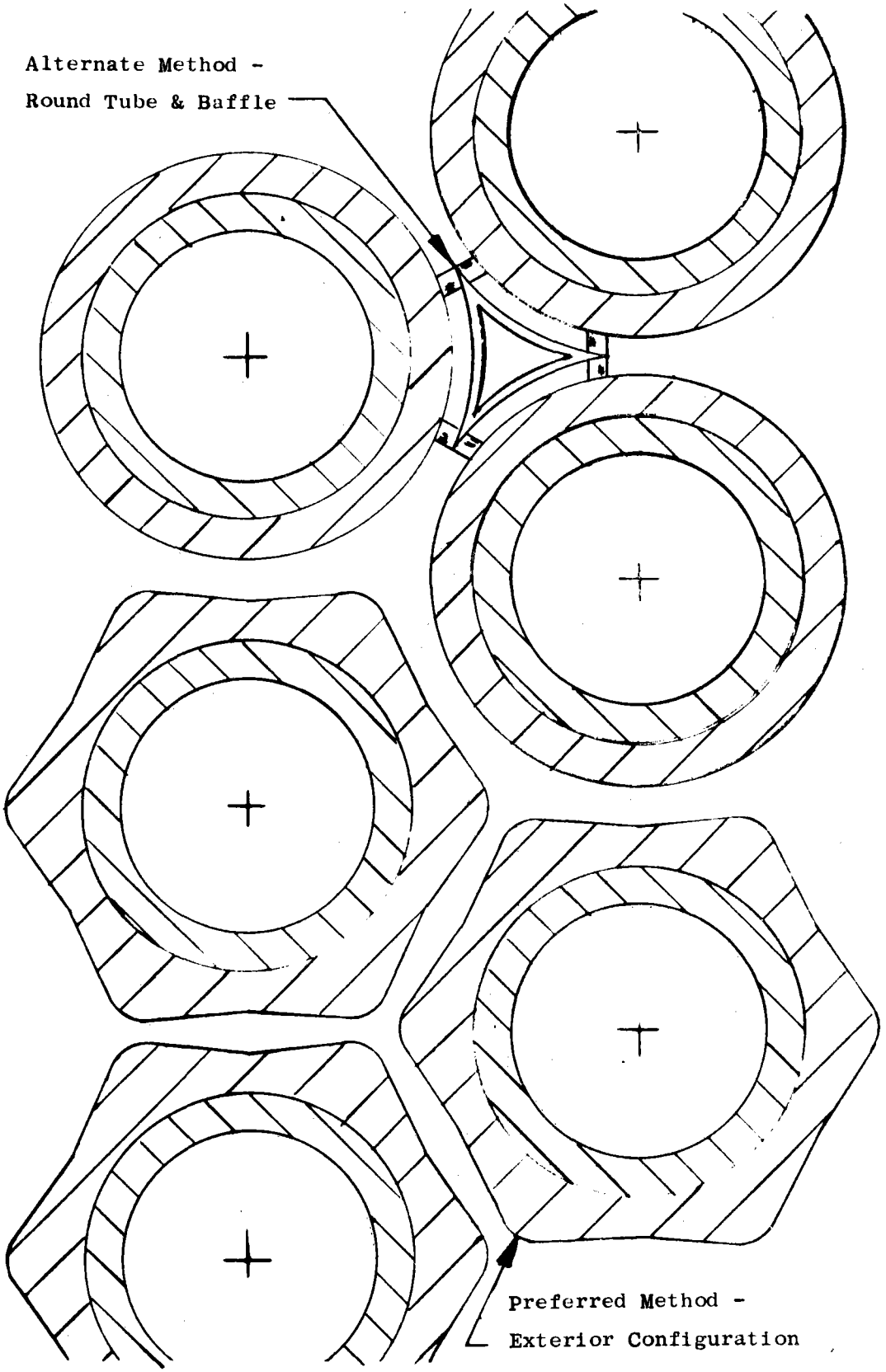

Figure E-2 Section Through Reformer Tube Bundle Showing Intertube Flow Blockage.

Table E-1

Steam Reformer/Steam Generator Assembly Designs

		Reference Design				
Design #	1	2	3	4	5	6
Thermal Power to Steam Reformer	13 %	35.6%	35.6%	58.4%	58.4%	35.6%
S.R. Tube I.D.	90 mm	90 mm	90 mm	90 mm	50 mm	90 mm
IHX Type	DSR	DSR	SR	DSR	DSR	SR IHX
SR Helium Inlet Temperature	950°C	950°C	950°C	950°C	950°C	900°C
Reforming Temperature	825°C	825°C	825°C	825°C	825°C	825°C
SR Helium Outlet Temperature	865.5°C	718.6°C	718.6°C	600°C	600°C	686.4°C
Reactant Inlet Temperature	450°C	450°C	450°C	450°C	450°C	450°C
Product Outlet Temperature	600°C	600°C	600°C	600°C	600°C	600°C
SR Log Mean ΔT	242°C	187.7°C	187.7°C	137°C	137°C	140.6°C
Helium Flow Rate	73.6 Kg/Sec	73.6 Kg/Sec	73.6 Kg/Sec	79.8 Kg/Sec	79.8 Kg/Sec	79.8 Kg/Sec
SR Thermal Conductances (Referred to SR Tube OD)						
Helium Film	1700 $W/m^2°C$	1700	1700	1700	1700	1700
Outer Tube Wall	2672	2672	2635	2672	4348	2635
Inner Tube Wall	2259	2259		2259	3625	
Product Film	826	826	964	826	803	964
Gap	12000	12000		12000	12000	
SR Overall	370 $W/m^2°C$	370	498	370	413	498
SR Power	32.5 MW	89 MW	89 MW	146 MW	146 MW	89 MW
SR Surface Area (Outer Tube O.D.)	366 sq m	1283 sq m	952 sq m	2880 sq m	2580 sq m	1271 sq m
No. of Tubes	77	270	234	606	951	312
Outer Tube O.D.	126 mm	126 mm	108 mm	126 mm	72 mm	108 mm
Outer Tube I.D.	108 mm	108 mm	90 mm	108 mm	61 mm	90 mm
Inner Tube I.D.	90 mm	90 mm		90 mm	50 mm	
Tube Spacing Ratio						
(SR Proper)	1.17	1.11	1.2	1.11	1.11	1.2
(Tube Sheet)	1.25	1.25	1.30	1.25	1.46	1.3
SR Tube Bundle O.D.	1.35 m	2.39 m	2.05 m	3.58 m	2.56 m	2.37 m
Tube Sheet Thickness	23.9 cm	42.2 cm	36.1 cm	63.4 cm	45.3 cm	41.9 cm
SR Pressure Drop	.47 b	.47 b	.47 b	.47 b	.47 b	.47 b
Pressure Vessel O.D.	3 m	3.83 m	3.48 m	4.82 m	4.0 m	3.81 m

Table E-1 continued

Design #	1	Reference Design 2	3	4	5	6
Thermal Power to Steam Reformer	13 %	35.6%	35.6%	58.4%	58.4%	35.6%
S.R. Tube I.D.	90 mm	90 mm	90 mm	90 mm	50 mm	90 mm
IHX Type	DSR	DSR	SR	DSR	DSR	SR IHX
SG Power	217.5 MW	161 MW	161 MW	104 MW	104 MW	161 MW
SG Helium Inlet Temperature	865.5°C	718.6°C	718.6°C	600°C	600°C	686.4°C
Steam Outlet Temperature	538°C	538°C	538°C	538°C	538°C	538°C
Steam Pressure	238 b	238 b	238 b	238 b	238 b	238 b
SG Helium Outlet Temperature	300°C	300°C	300°C	350°C	350°C	300°C
Feed Water Temperature	260°C	204°C	204°C	260°C	260°C	204°C
Steam Flow Rate	100.2 Kg/Sec	66.6 Kg/Sec	66.6 Kg/Sec	48 Kg/Sec	48 Kg/Sec	66.6 Kg/Sec
SG Log Mean ΔT	137°C	106°C	106°C	62.8°C	62.8°C	95°C
SG Thermal Conductances (Referred to SG Tube O.D.)						
Helium Film	1700 $W/m^2°C$	1700	1700	1700	1700	1900
Tube Wall	7500	7500	7500	7500	7500	7500
Steam/Water Film	12000	12000	12000	12000	12000	12000
SG Overall	1242	1242	1242	1242	1242	1345
Tube O.D.	2.54 cm	2.54 cm	2.54	2.54	2.54	2.54
Tube I.D.	1.90 cm	1.90 cm	1.90	1.90	1.90	1.90
No. of Tubes in Parallel	80	56	56	36	40	56
Tube Distribution	10 Tubes Across 8 Threads In Parallel	7 Tubes Across 8 Threads In Parallel	8 Tubes Across 7 Threads In Parallel	6 Tubes Across 6 Threads In Parallel	8 Tubes Across 5 Threads in Parallel	8 Tubes Across 7 Threads In Parallel
Total Tube Surface Area (Tube O.D.)	1275 sq m	1221 sq m	1221 sq m	1333 sq m	1333 sq m	1260 sq m
SG Pressure Drop	.27 b	.27 b	.27 b	.27 b	.27 b	.34 b
SG Tube Bundle I.D./O.D./Length	1.52m/2.53/ 11.1	2.56/3.38/ 10.6	2.21/3.02/ 10.6	3.75/4.36/ 10.9	2.73/3.54/ 10.7	2.53/3.35/ 10.8
Overall SR/SG Assembly Weight (Kg)	167,000	373,000	235,000	738,000	431,000	
MW Tube	.422	.329	.38	.241	.154	.285

a single tube steam reformer design. The effect of variation of duplex tube steam reformer tube diameter is indicated by a comparison of designs 4 and 5. The sixth case in the matrix is that of a steam reformer/steam generator heated by a helium stream from the secondary side of an IHX, rather than by primary reactor coolant. Figure E-3 shows the envelope of each of the six designs.

E.1.2 HEAT TRANSFER/PRESSURE DROP CORRELATIONS

For the calculation of forced convection heat transfer to the steam reformer tubes, equation (1) was used.

$$\frac{h}{Cp\ G}\ (Pr)^{2/3} = \frac{.023}{(Re)^{.2}} \qquad (1)$$

The corresponding friction factor used for pressure drop calculations is given by equation (2).

$$f = 8 \times \frac{.023}{(Re)^{.2}} \qquad (2)$$

where $$\Delta P = 4fL/D\ \frac{\rho V^2}{2g} \quad .$$

For the evaluation of Re and L/D in these equations, an equivalent diameter equal to four times the hydraulic radius (flow cross section/ wetted perimeter) was calculated for the inter tube helium flow passage, with sufficient blockage to achieve a helium convection coefficent of 1700 watts/m^2°C. The catalyst space heat transfer coefficient was taken from an experimental value presented in reference E-1.

Figure E-4 shows the helium side heat transfer/pressure drop correlations used for the steam generator design calculations. Because of the fact that the steam generator tube heat transfer is controlled by the helium side heat transfer coefficient, a conservatively chosen value of 12000 W/m^2°C was used for all sections of the steam generator on the water/steam side. Variations in this number of up to 25% have a negligible effect on the overall thermal conductance.

Scale 0 20'

(dimensions in meters)

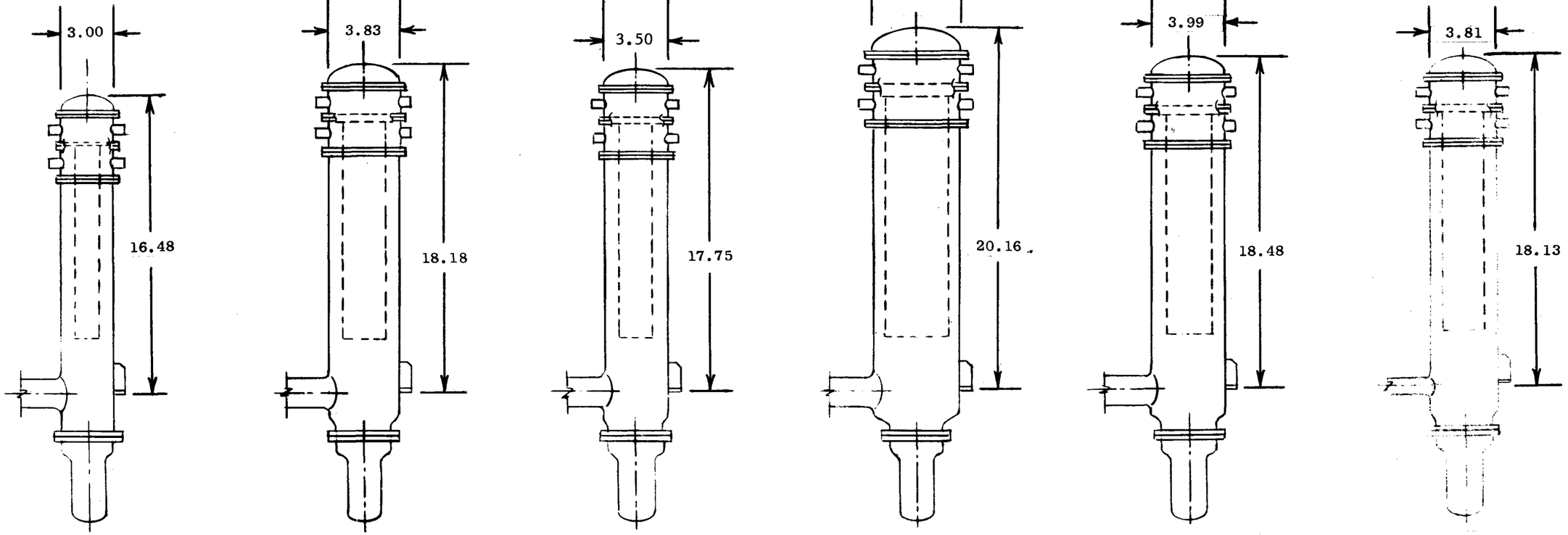

Type	A	B	C	D	E	F
% Power to Reformer	13	35.6	35.6	58.4	58.4	35.6
Tube I.D., mm	90	90	90	90	50	50
Type Wall	DSR	DSR	SR	DSR	DSR	SR
Notes :		Ref. Design	9 mm Wall			9 mm Wall/IHX

Figure E-3. SRA/SGA Size Comparisons

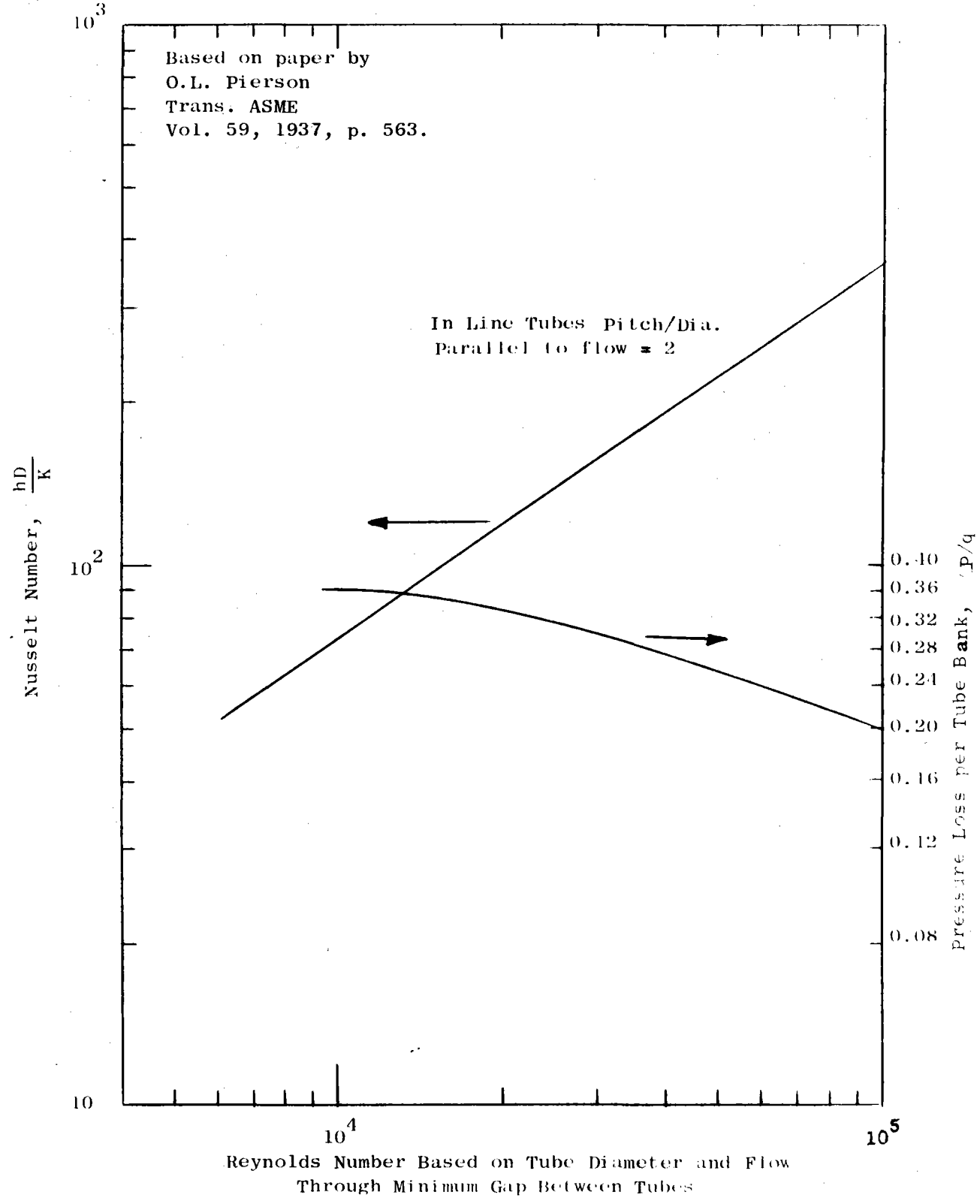

Figure E-4. Correlations for Steam Generator Helium-Side Heat Transfer and Pressure Drop.

E.1.3 TUBE SHEET STRESS

The steam reformer tube sheet thickness was calculated from the curve shown in Figure E-5,taken from reference E-2. The assumed value of working stress is 24,000 psi. This stress level will be realized only under an abnormal (accident) condition in which 600 psi differential pressure is imposed on the tube sheet. The normal pressure level induced stress is negligible, since the normal differential pressure is very low. Actually the normal differential pressure load is opposed by the weight of the reformer tubes and the tube sheet. The folded thermal sleeve shown between the tube sheet and the water cooled pressure vessel shell was sized using the curve of Figure E-6 taken from reference E-2.

E.1.4 EFFECT OF SR/SG POWER SPLIT

As the percentage of reactor power fed to the steam reformer increases the log mean temperature difference for both the steam reformer and steam generator heat exchangers decreases. The effect of this on thermal flux is shown in Figure E-7 and the effect on overall SR/SG weight is shown in Figure E-8. Both figures apply to designs incorporating 90 mm I.D. DSR steam reformer tubes and 25.4 mm single wall steam generator tubes. Figure E-9 shows the effect of power split on power density in the heat exchangers.

E.1.5 EFFECT OF DSR TUBE DIAMETER

The steam reformer performance is basically limited by heat transfer rather than reaction kinetics. As a result of this fact it is possible to make the steam reformer assembly more compact and to achieve significant size and weight reductions by reducing the steam reformer tube diameter to increase the heat transfer surface per unit of core volume. In addition when the tube diameter is reduced the tube wall thickness can also be reduced which increases the thermal conductance. In order to circumvent the problem of prohibitively small inter tube spacing of the tube sheet welds, the reformer tube diameter at the section above the catalyst space can be reduced in the manner

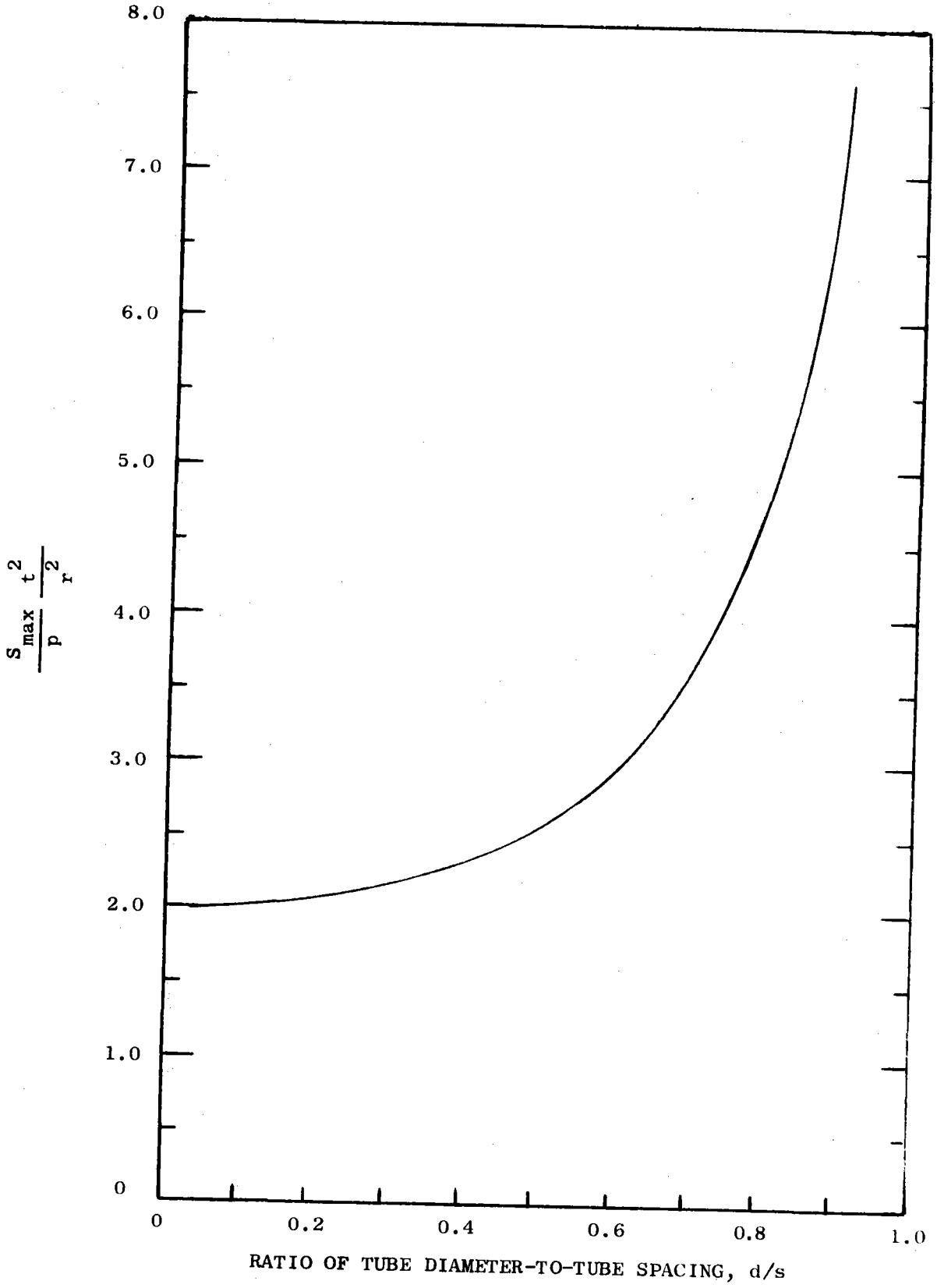

Figure E-5 Effects of the Ratio of Tube Diameter-to-Tube Spacing on the Maximum Stress in Tube Header Sheets in Which the Tubes are on an Equilateral Triangular Pitch.

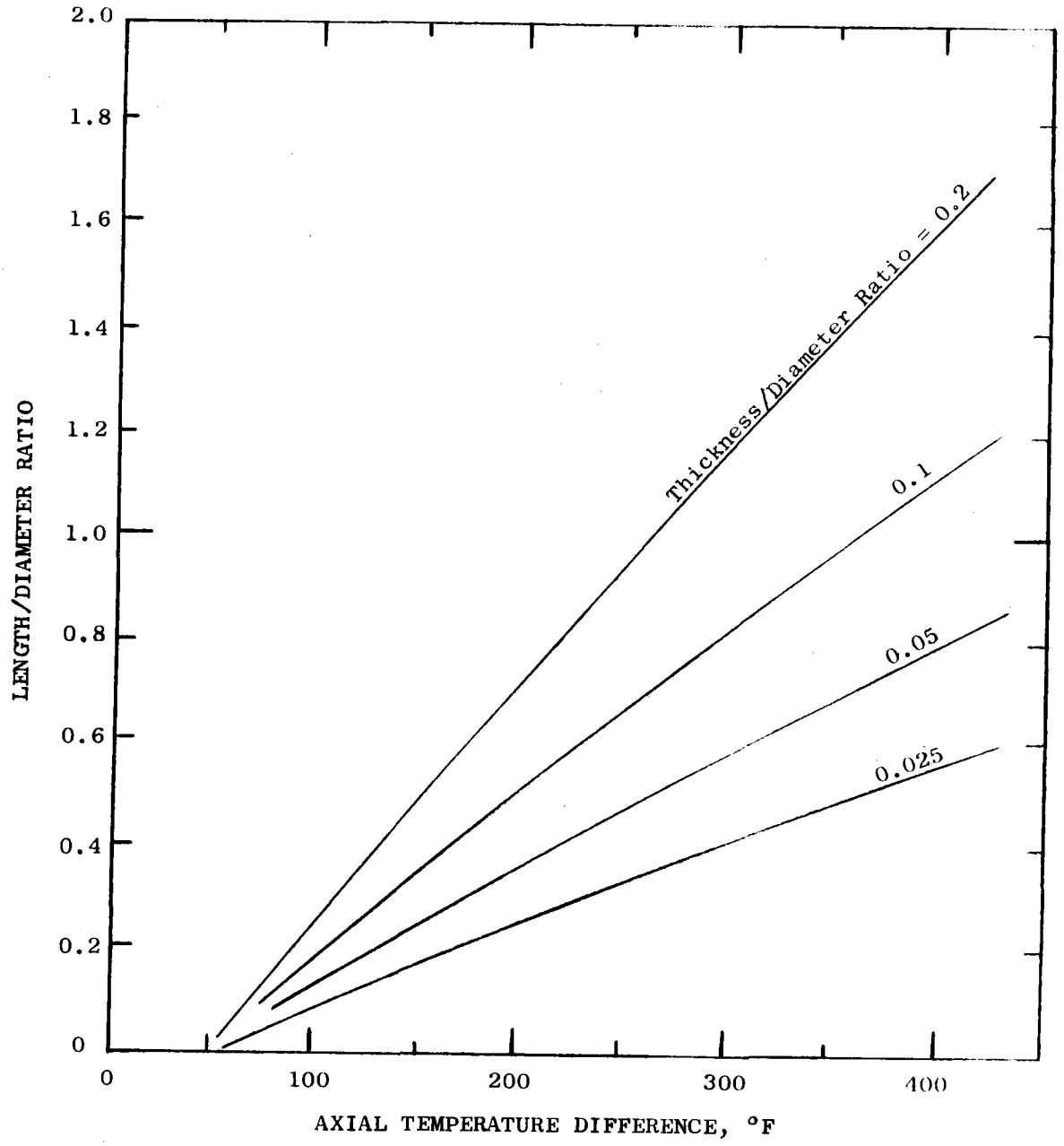

Figure E-6 Thermal Sleeve Length/Diameter Ratio for Plain Carbon Steel to Give an Allowable Shear Stress of 10,000 psi. (The assumed axial temperature distribution is exponential)

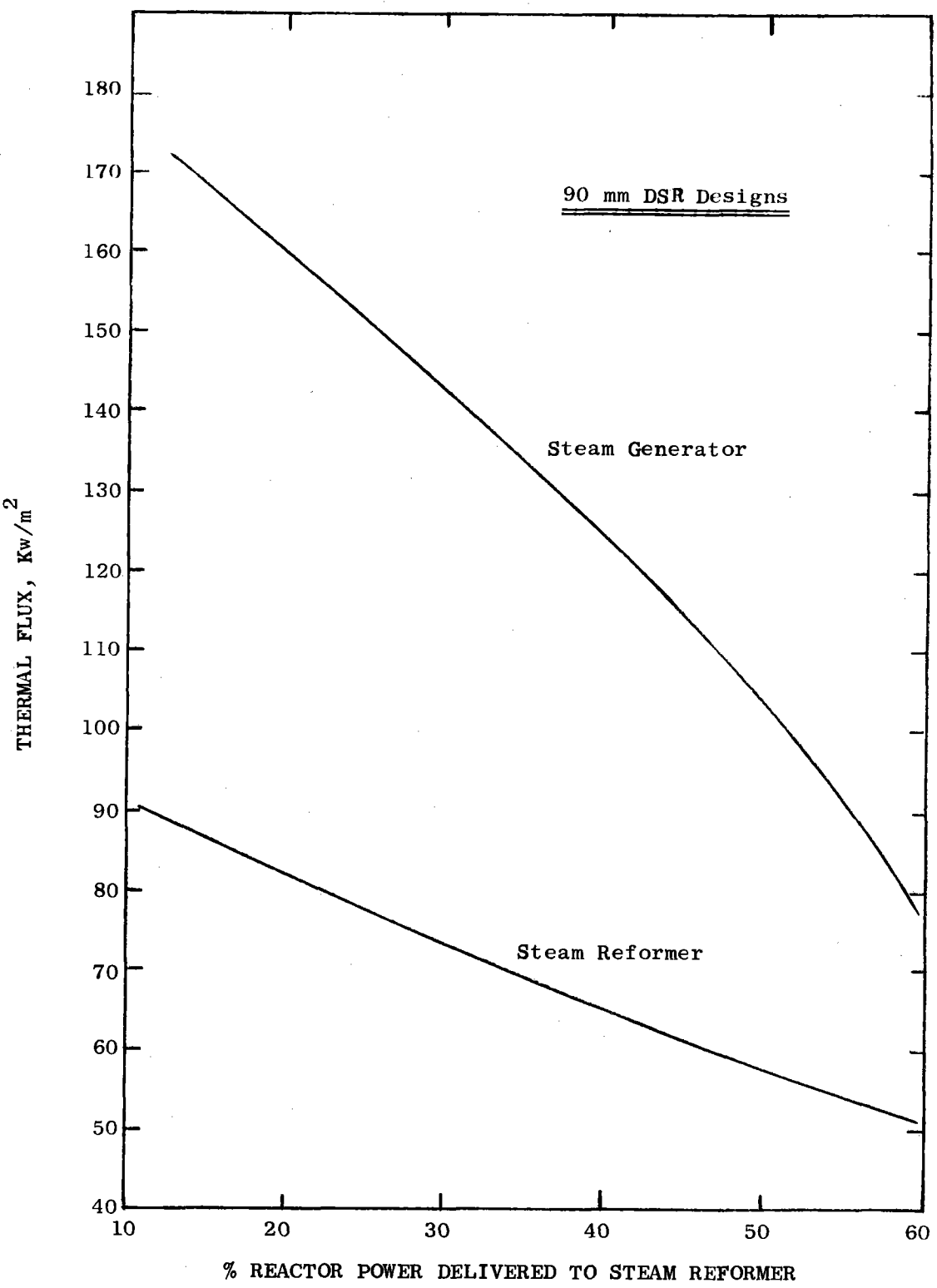

Figure E-7 Heat Exchanger Thermal Flux vs. SR/SG Power Split.

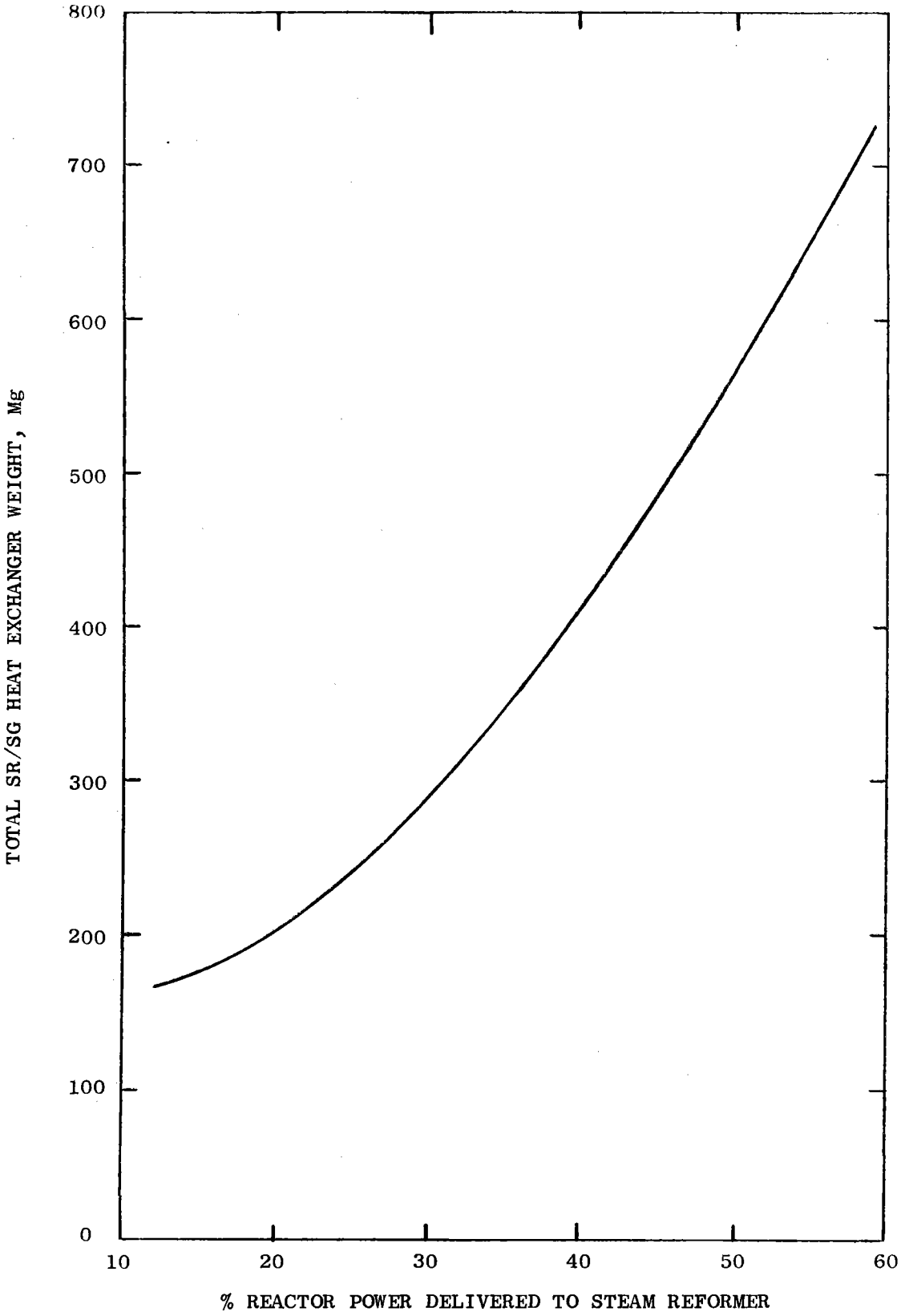

Figure E-8 Total Heat Exchanger Weight vs. SR/SG Power Split.

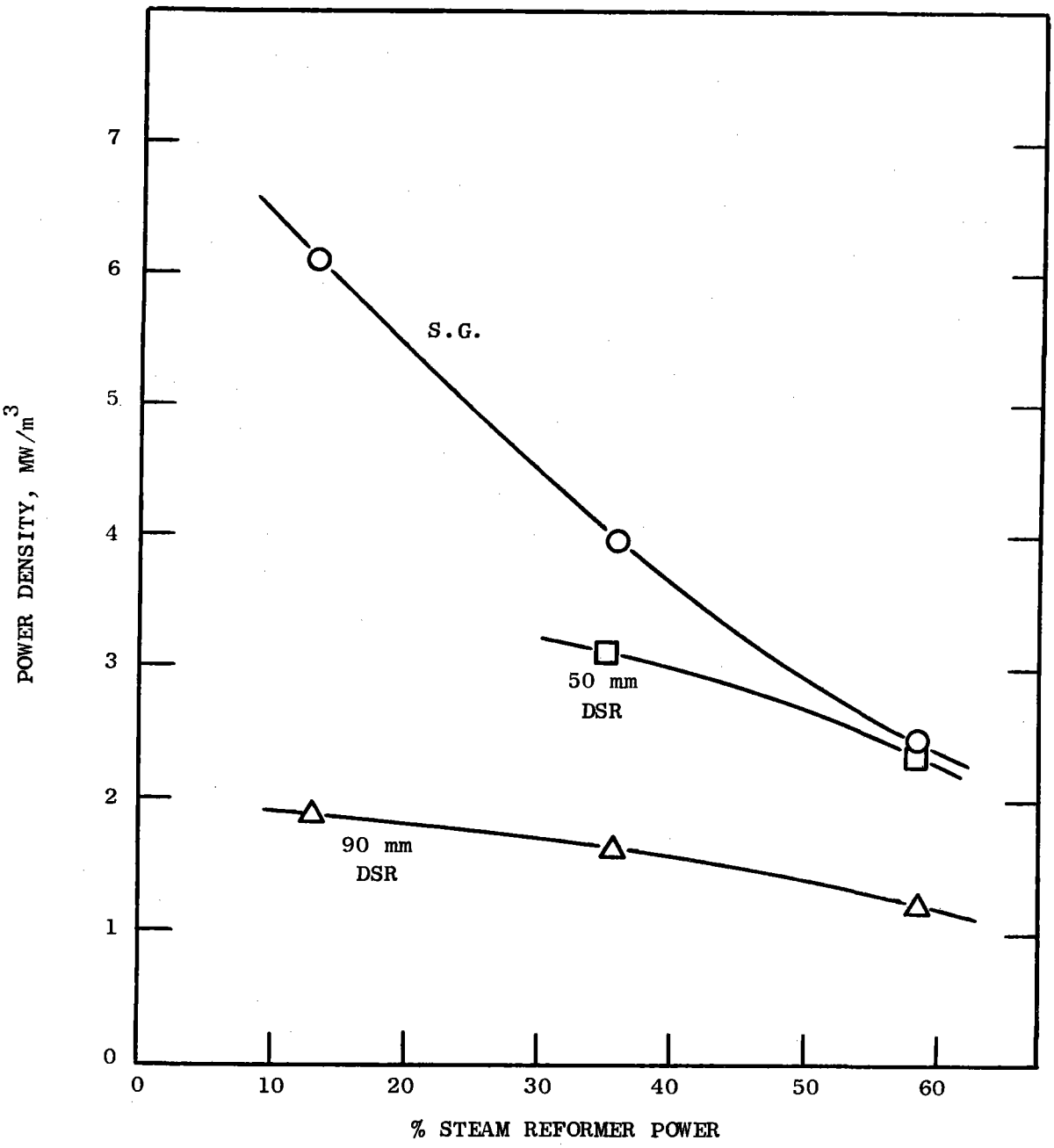

Figure E-9 Specific Power Densities for Steam Generators and Steam Reformers.

shown in Figure E-10. Such a design is based upon successful development of an advanced catalyst which does not require periodic replacement. The effect of DSR tube diameter on SR tube bundle diameter, overall heat exchanger pressure vessel diameter, and on the total SR/SG heat exchanger weight is shown in Figure E-11.

Reduction in DSR diameter increases the reformer tube internal gas volume flow per unit area and thus increases the tube space velocity and the internal pressure drop. The designs for which diameters less than 90 mm have been considered involve the 58.4% power split, for which the basic design space velocity is moderate and essentially 100% of the equilibrium methane conversion is achieved. Estimates based on reference E-3 indicate that for 70 mm and 50 mm designs, the conversion percentages are respectively reduced to 90% and 85% of equilibrium. As a result of increased mass flux the internal pressure drop, most of which occurs in the "pigtail" tube, increases from 6.5 atmospheres in the 90 mm design to approximately 10 atmospheres in the 50 mm design.

E.1.6 COMPARISON OF DSR DESIGNS WITH SINGLE WALL REFORMER TUBE DESIGNS

A comparison of designs 2 and 3, Table E-1, indicates that the single wall reformer design has 26% less surface requirement, is 9% smaller in pressure vessel diameter and is 37% lower in overall weight. If the single wall reformer tube is 12 mm thick, as opposed to 9 mm for the above comparison, the single wall design has 21% less surface, is 6% smaller in pressure vessel diameter and is 29% lower in overall weight.

E.1.7 DEVELOPMENT REQUIREMENTS

Design features of the steam reformer/steam generator assembly which require development include the following:

1. Duplex tube steam reformer fabrication procedures for long duplex tubes of selected high temperature materials. (Test verification of the helium heated reformer performance and endurance characteristics is required.)

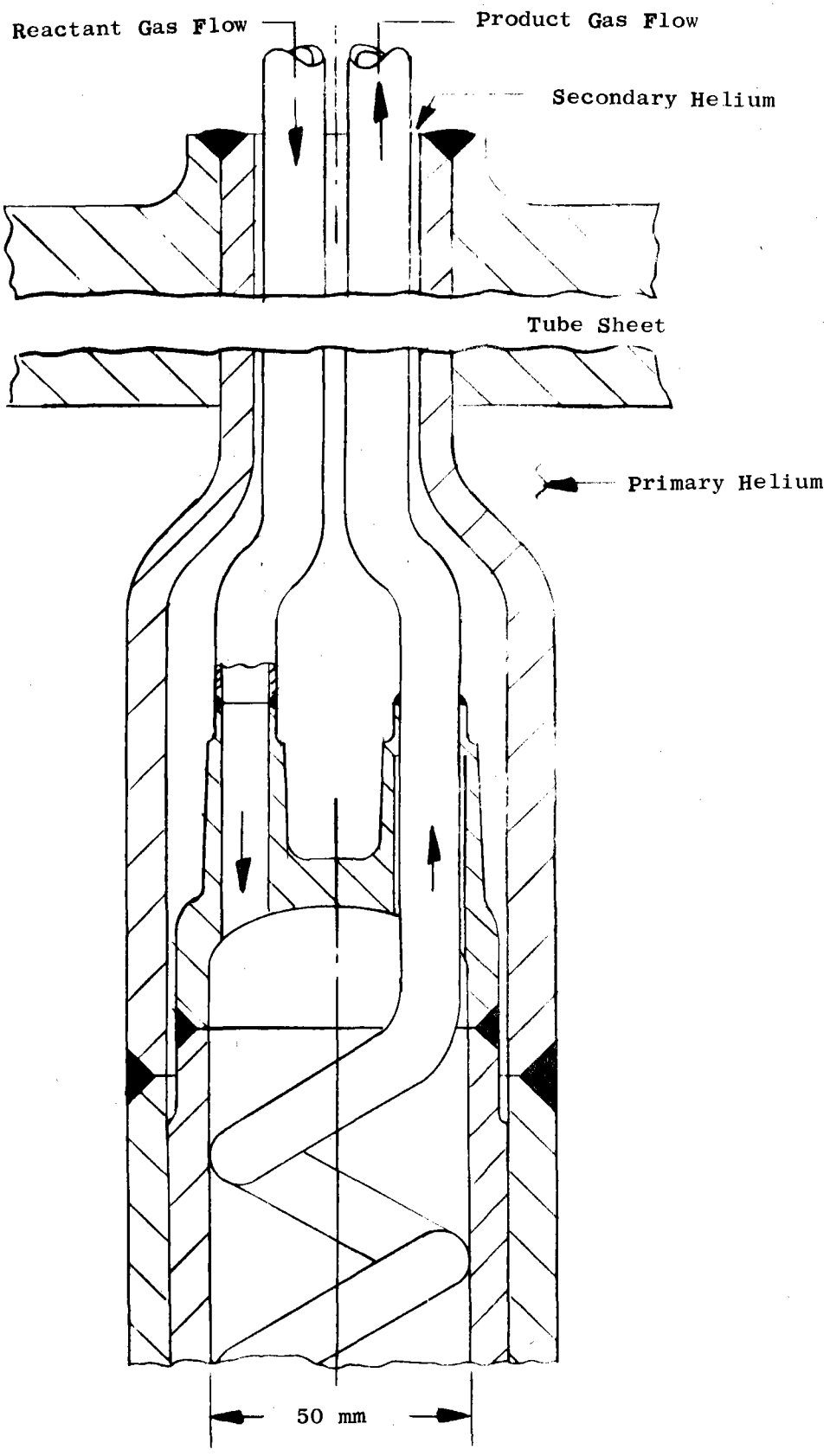

Figure E-10. Design Concept for a Small Diameter Duplex Tube Steam Reformer.

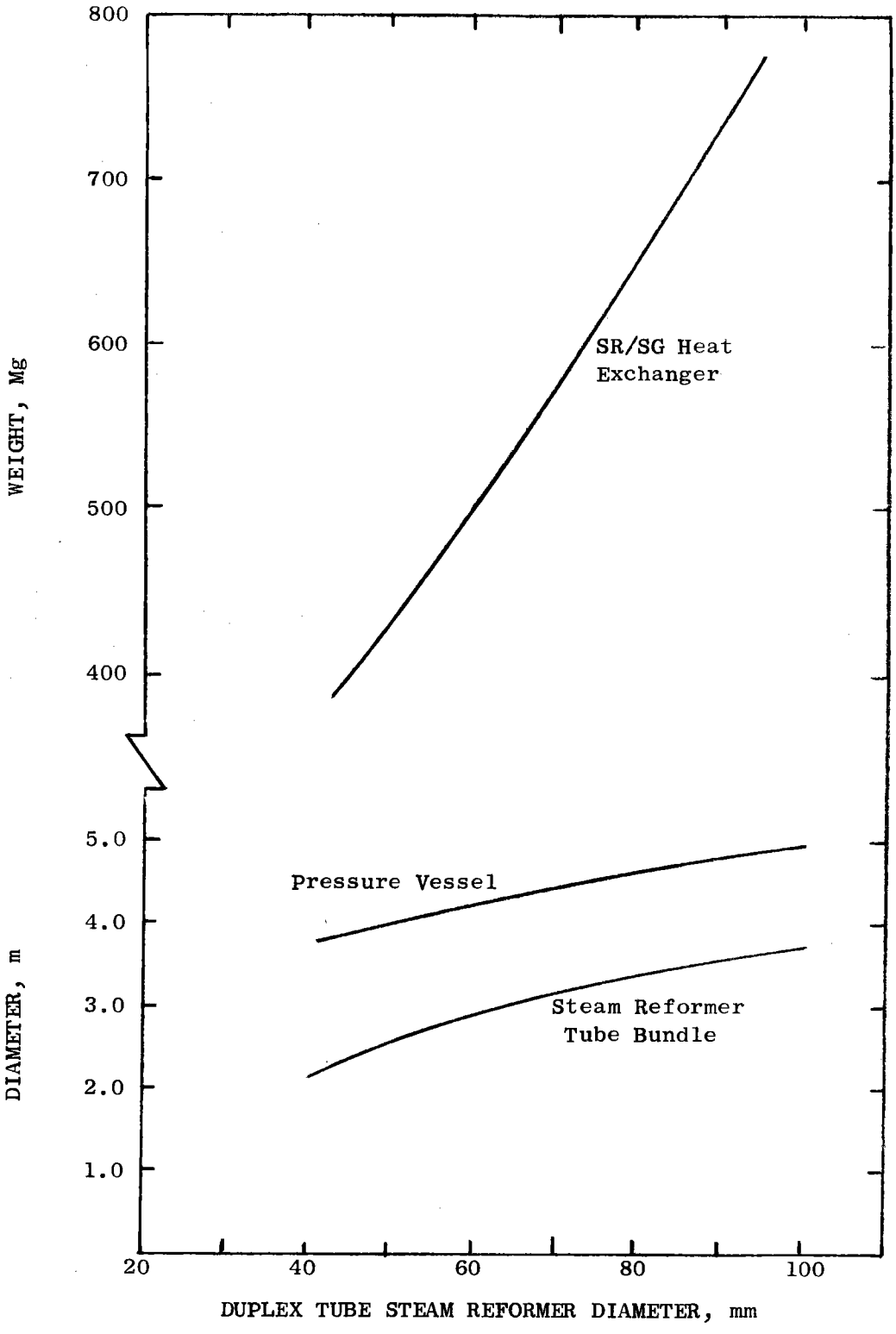

Figure E-11 Heat Exchanger Dimensions and Weight vs. Duplex Tube Diameter.

2. High temperature sliding joints require development with respect to design and materials selection and test verification.

3. High temperature insulation. Insulation for the high temperature ducting and for the pressure vessel requires development with respect to design and materials selection and verification. (This is discussed in Appendix I with reference to the IHX)

4. Advanced Catalyst. Ultimate minimization of the SR/SG assembly weight, cost and downtime for maintenance can be achieved through development of an advanced catalyst. Development goals for the advanced catalyst include (1) capability for activity renewal through internal injection of steam, hydrogen or other fluid, without the need for catalyst removal; (2) capability for operation under heat transfer limited conditions with small diameter (i.e. 50 mm) duplex tubes. This implies the need for a catalyst capable of achieving a methane conversion of the order of 90% of equilibrium conversion at high levels of space velocity.

E.2 DUPLEX TUBE DESIGN CONSIDERATIONS

The design of the steam-methane reformer/steam generator assembly (discussed in Section E.1), uses duplex tubes in the reformer. Although the duplex tube reformer represents a departure from conventional fossil-fired reformers, there exists a body of relevant technology which can be applied in the design of these units. The chemical process design is based on conventional reformers which have been operated for over 40 years. Conventional reformers, however, are heated in the radiant section of fossil-fired furnaces which is quite different than heating with helium in forced convection. This technology has been developed over the past several years by the KFA in Germany. A number of full-scale single-wall reformer tubes have been successfully tested in the EVA helium test facility[E-4]. Duplex tubes have been used for years in sodium heated steam generators. As discussed by Krankota[E-5], a number of steam generator units for sodium-cooled reactors have been

built which employed a double-wall tube as a barrier between the sodium and water. These included units developed by GE-KAPL for the Navy submarine reactor steam generators, steam generators for the Sodium Reactor Experiment, steam generators for the Hallam Nuclear Power Facility, the EBR-II steam generators, and the Small Steam Generator Model built by Westinghouse. The required technologies are available separately and need only be combined for a successful duplex tube reformer design.

E.2.1 THERMAL-HYDRAULIC CONSIDERATIONS

Heat is transferred from the helium to the process gas through five thermal resistances consisting of the helium film, the outer tube wall, the gap between tubes, the inner tube wall, and the process gas film. Gas-side velocities (which in turn determine the heat transfer coefficients) are determined by allowable pressure drops.

E.2.1.1 Helium Side

Heat transfer from the helium to the reformer tube occurs by the mechanism of forced convection. For an unbaffled tube bundle in which the helium flows parallel to the tubes, the heat transfer coefficient was calculated from:

$$(1)\quad \frac{h}{C_p G}\left(\frac{C_p \mu}{K}\right)^{2/3} = \frac{0.023}{\left(\frac{D_e V}{\nu}\right)^{0.2}}$$

The helium pressure drop was calculated as the sum of an inlet loss, the friction loss, and an outlet loss:

$$(2)\quad \Delta P = \left[K_i + f\frac{\ell}{D_e} + K_o\right]\frac{\rho V^2}{2}$$

Shown in Figure E-12 is a plot of the helium side heat transfer coefficent and pressure drop as a function of helium velocity in the tube bundle. The physical properties of helium for this figure were evaluated at a temperature of 825°C (average of helium inlet and helium outlet temperatures) and an average pressure of 41.2 bars. A design point velocity was selected from considerations of helium pumping power as follows.

Fraas[E-2] discusses the tradeoff between heat exchanger operating costs and capital charges. It has been found that if the pumping power chargeable to the heat exchanger is in the range of 0.5 and 1.0% of the heat transferred, the overall cost will be close to the minimum obtainable. For a helium ΔT of 250°C (950-700), a pressure of 40 bars, and a helium temperature of 250°C at the circulator, the above criterion establishes the helium pressure drop across the reformer as 0.24 to 0.48 bar for 0.5% and 1.0% of the heat transferred, respectively. The corresponding helium velocities are 30.7 m/s and 43.5 m/s. A design point helium velocity of 30 m/s was selected, which is consistent with HTR reactor studies now underway. The corresponding heat transfer coefficient and pressure drop are 1224 $w/m^{2\circ}C$ (216 Btu/hr $ft^{2\circ}F$) and 0.23 bar (3.3 psi), respectively.

E.2.1.2 Process Side

On the process side the heat is transferred from the tube wall to the process gas which is flowing through a packed bed of catalyst pellets. The chemical performance of the reformer was calculated using a reformer computer code developed at the Los Alamos Scientific Laboratory[E-6]. In that code, the process-side heat transfer coefficient is calculated using the following correlation:

$$(3)\quad h = \frac{K_g}{D_p}\left[2.58\left(\frac{D_p V}{\nu}\right)^{1/3} N_{Pr}^{1/3} + 0.094\left(\frac{D_p V}{\nu}\right)^{0.8} N_{Pr}^{0.4}\right]$$

The process-side pressure drop through packed beds is calculated from the Ergun equation:

$$(4)\quad \frac{dP}{dZ} = -\left[\frac{150(1-\varepsilon)}{(N_R)_p} + 1.75\right]\frac{1}{D_p}\left(\frac{1-\varepsilon}{\varepsilon^3}\right)\frac{G_o^2}{\rho}$$

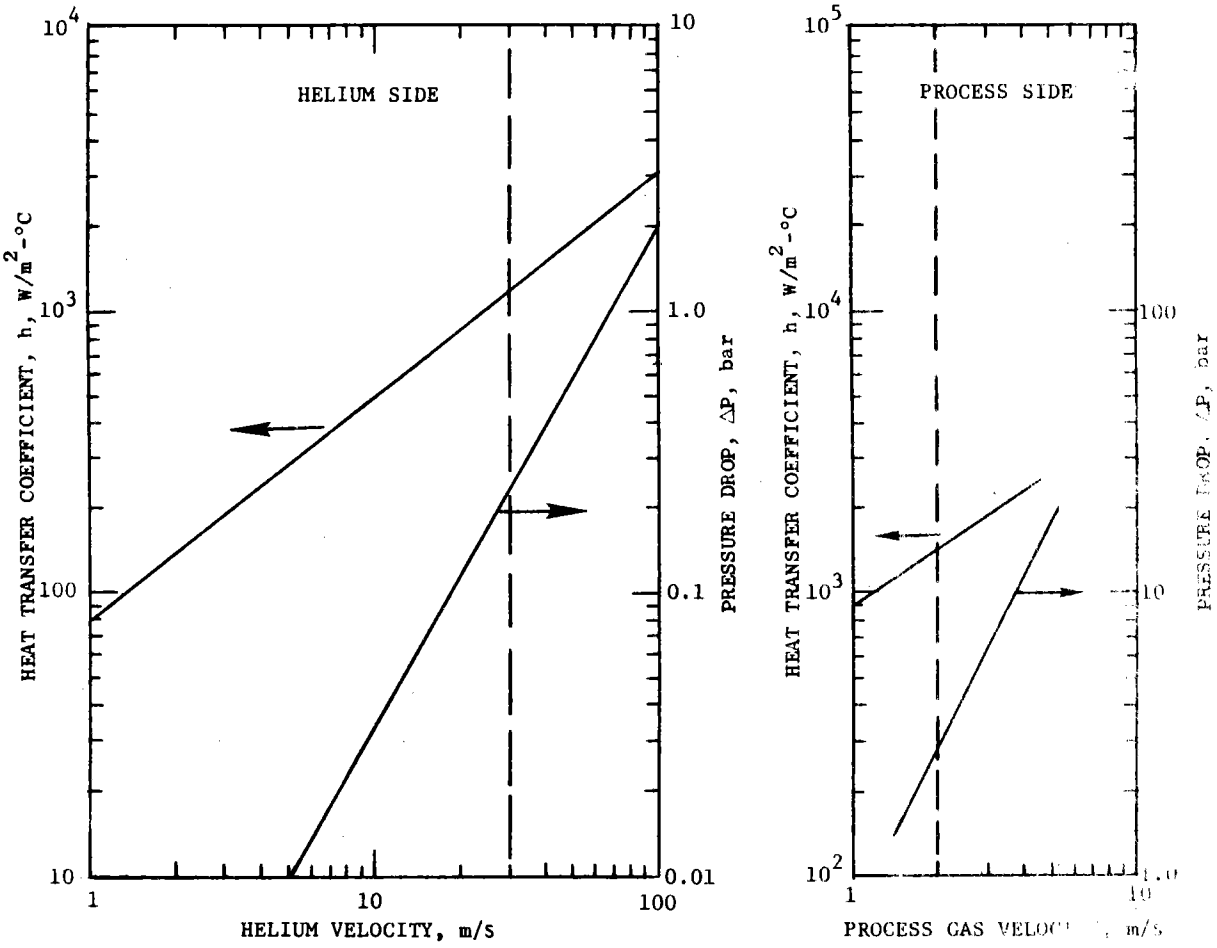

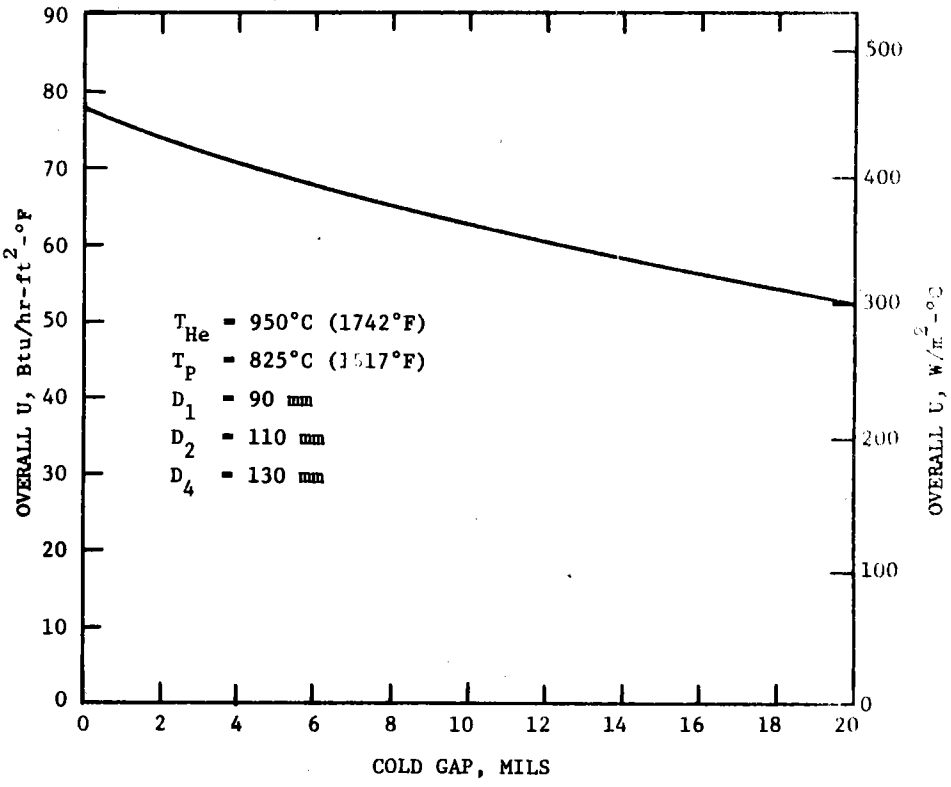

Figure E-12 Heat Transfer and Pressure Drop Considerations in the Duplex Tube Reformer

For particle Reynolds numbers, $(N_R)_p$ greater than about 1000 (which is typical in steam methane reformers), the first term may be neglected and the Ergun equation reduces to the Borke-Plummer equation:

$$(5) \quad \frac{dP}{dZ} = - \left(\frac{1.75}{D_P}\right)\left(\frac{1 - \epsilon}{\epsilon^3}\right)\frac{G_o^2}{\rho}$$

Figure E-12 shows the process side heat transfer coefficient and pressure drop as a function of superficial velocity of the gas. Superficial velocities between 2 and 3 m/s are typical for conventional reformers. A value of 2 m/s was chosen for the design point of the duplex tube reformer.

E.2.1.3 The Overall Heat Transfer Coefficient

The overall thermal resistance between the primary helium and the process gas is the sum of the resistances due to the helium gas film, the duplex tube, and the process gas film. The calculations presented here are for the case of a duplex tube having a gap between the OD of the inner tube and the ID of the outer tube. The helium-filled gap was assumed to be uniform around the circumference with no metal-to-metal contact. It was also assumed that the mechanism of heat transfer across the gas-filled gap is conduction; radiation and convection effects were neglected. The overall heat transfer coefficient is given by:

$$(6) \quad \frac{1}{U_1} = \frac{1}{h_1} + \frac{D_1 \ln(D_2/D_1)}{2 K_{12}} + \frac{D_1 \ln(D_3/D_2)}{2 K_{gap}} + \frac{D_1 \ln(D_4/D_3)}{2 K_{34}} + \frac{1}{\left(\frac{D_4}{D_1}\right) h_4}$$

Using typical values of the helium and process-side heat transfer coefficients (h_1 and h_4), calculations were performed to determine the effect of gap dimension on the overall heat transfer coefficient which determines the reformer size. Figure E-12 shows the results of these calculations for an overall helium-to-process ΔT typical of the hot end of the tube. This shows that the effect of gap dimension on overall U is not severe because the controlling thermal resistances are the helium and process side gas films. This is in contrast to a sodium-heated boiler such as the LMFBR evaporator. In that case, the water-side and the sodium-side coefficients are large and the wall resistance

is controlling so that small variations in wall resistance severely affect the overall coefficient. Figure E-13 shows the effect of the gap on the overall U normalized to the zero-gap case, U_o. For a given heat transfer rate and overall ΔT, the heat transfer areas and overall U's are related by:

$$(7) \quad \frac{A}{A_o} = \frac{U_o}{U}$$

Consequently, Figure E-13 can be interpreted as the penalty in heat exchanger size due to the gap. The upper curve is for the overall ΔT near the cold end and the lower curve is for the hot end. For a gap of 3 mils, the required area is less than 10% more than that required for the zero gap case. A fabrication goal is to achieve a gap dimension of from 0 to 3 mils.

Figure E-14 illustrates the radial temperature distribution through the duplex wall and the relative importance of the five resistances in series. A total of 67% of the overall ΔT is taken in the two gas films which are controlling. As can be seen, the ΔT across the gap is only 5% of the total.

E.2.2 CHEMICAL PERFORMANCE

The reformer performance calculations were made with the aid of a computer code developed especially for helium-heated reformers by personnel at the Los Alamos Scientific Laboratory[E-6]. The LASL program assumes a counter-flow shell-and-tube configuration with hot helium on the shell side. The following options are available.

1. Parallel flow or baffled cross flow on the helium side.

2. Reformer gas flowing inside tubes filled with catalyst, discharging at the opposite end from entry.

3. Reformer gas flowing as in (2), but discharging at the entry end through an internal pigtail with heat recuperation.

4. Solid metal tube walls, or duplex tubes (concentric tubes with stagnant helium in the small gap).

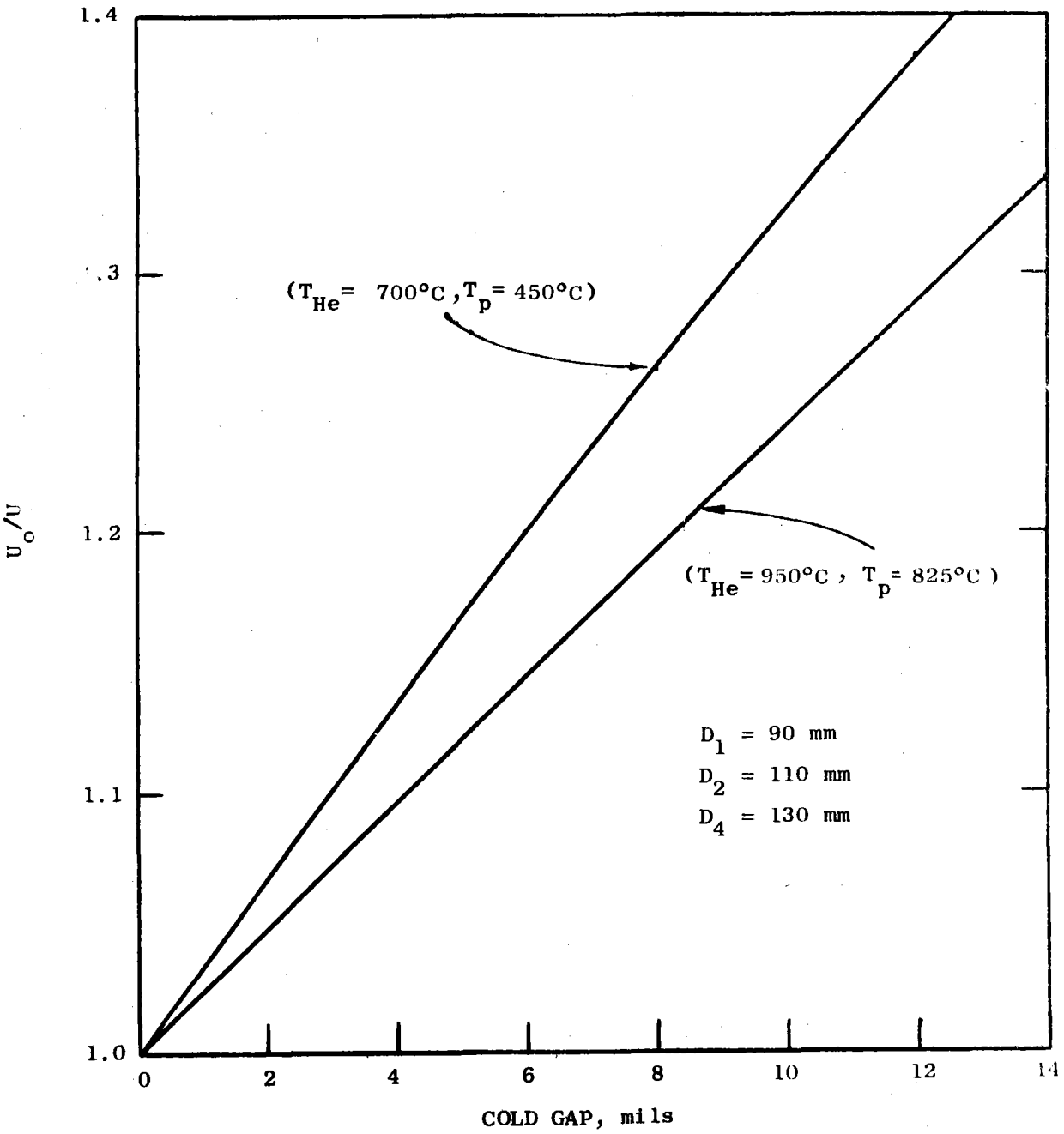

Figure E-13 Effect of Gap on Tube Area

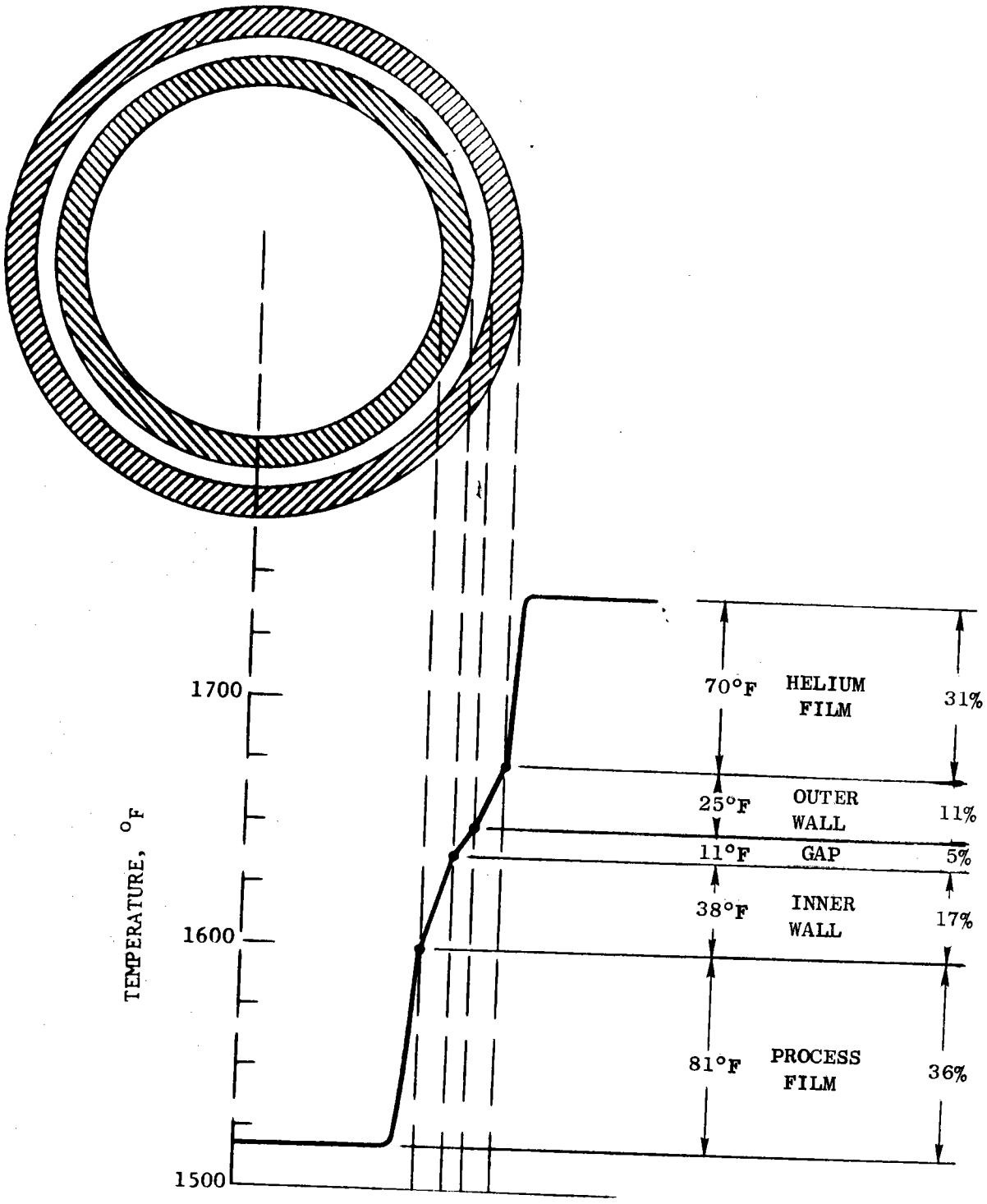

Figure E-14. Typical Temperature Profile in a Duplex Tube (2 mil gap).

For a given geometry and inlet conditions, the LASL code calculates the one-dimensional temperature, pressure and composition distributions along the tube length. The mathematical model simulating the methane reformer reactions was based on the model developed by Hyman[E-7].

Figure E-15 shows the calculated performance of a typical duplex reformer tube. The upper chart shows the process gas constituent distributions and the lower chart shows the helium and process gas temperature distributions. An active tube length of 12 m results in a peak process temperature of 828°C and a corresponding methane conversion of 60.3%.

E.2.3 ALLOY SELECTION

The factors which must be considered in the selection of the reformer tube material include:

- o Strength
- o Thermal Stability
- o Environmental Compatibility
  - GCR Helium Gas
  - Process Gas (CH_4, H_2O, CO, H_2)
- o Ductility
- o Fabricability
- o Cost
- o Availability

A number of commercially available alloys and several developmental alloys which are considered to be suitable candidates for use in duplex reformer tubes are listed below:

- o Inconel Alloys 601, 617, 625
- o Incoloy Alloys 800H, 802, 807
- o Hastelloy Alloys C, S, X
- o Development Alloys HAST X-280, Inconel 617 w/o Co.

Alloys containing elements such as cobalt and tantalum may have to be eliminated on the basis of potential problems from radioactive contamination. Cobalt (and tantalum), when bombarded with neutrons, become

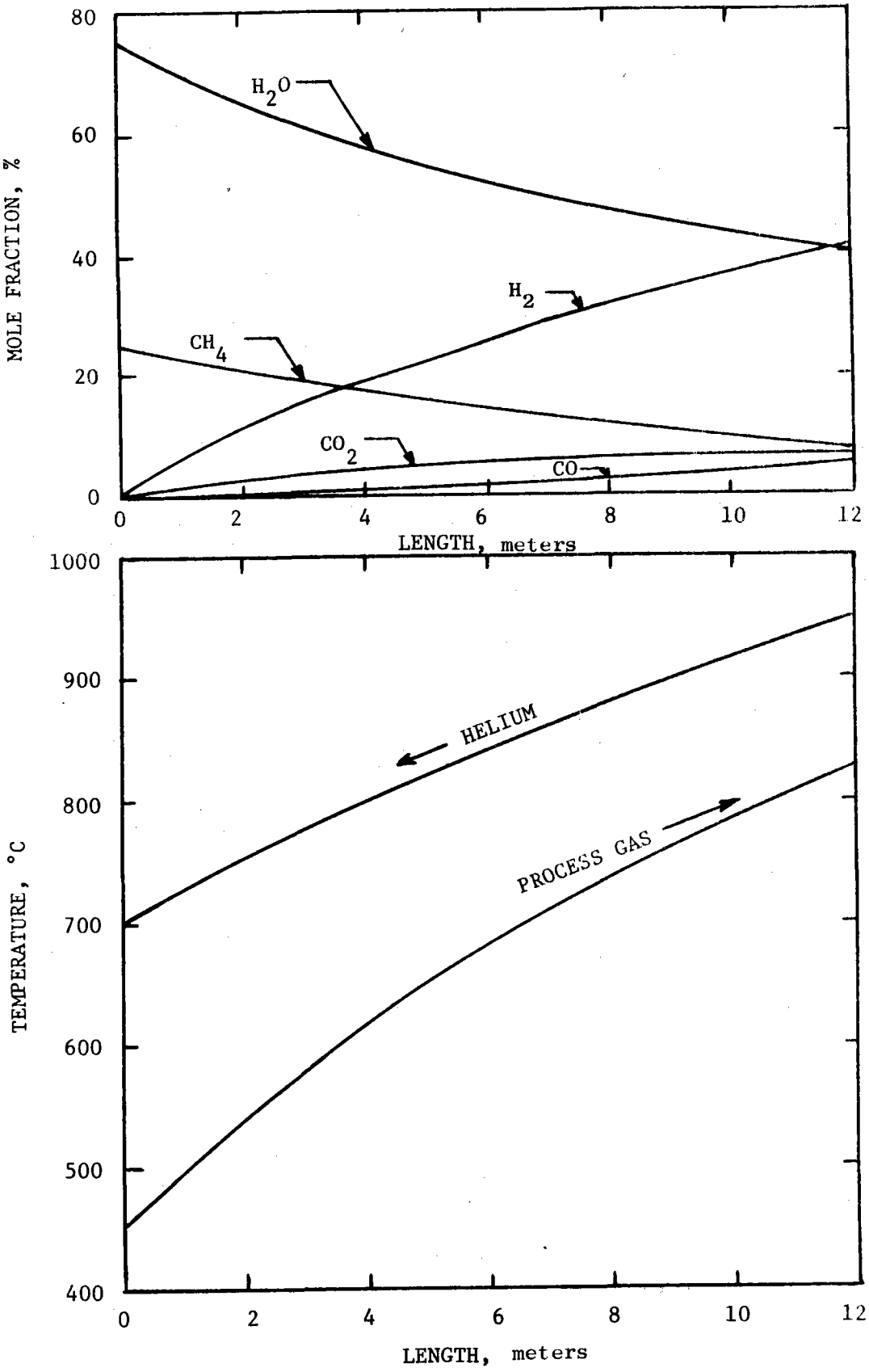

Figure E-15 Calculated Performance Of Duplex Tube Reformer

activated and highly radioactive. The Japanese have reported that cobalt whiskers can form on a surface and then be carried away by the helium stream. If these whiskers enter the coolant stream, they will become radioactive on passing through the reactor core and may seriously restrict access to normally low-activity areas of the reactor. Further tests are required to verify the Japanese results. If the cobalt and tantalum containing materials are eliminated, then the remaining candidates are:

- o Inconel Alloy 601
- o Incoloy Alloys 800H, 802
- o Hastelloy Alloy S
- o Development Alloys HAST X-280, Inconel 617 w/o Co.

Reference E-8 gives the design of a duplex reformer tube to be tested in the EVA test facility at Jülich, FRG. The material selected for that test section was Incoloy alloy 800H. That selection will have to be confirmed by appropriate materials tests before finalizing the design of a reformer assembly. The advantages of Incoloy 800H may be summarized as follows:

- o Creep strength comparatively high
- o Free from cobalt and tantalum
- o Good thermal stability
- o Hydrogen permeability compartively low
- o Should oxidize in steam (iron-base alloy)
- o Readily available
- o Good fabricability
- o Lowest cost of candidates
- o Same alloy as planned for EVA 2.

An advantage of the duplex tube which has not yet been fully explored is the possibility of using different tube materials for the inner and outer tubes. The inner tube material can be selected to be compatible with the process gases and the lower temperatures. The outer tube can be selected for compatibility with the helium reactor coolant and the higher temperatures to which the outer tube is exposed.

Nomenclature

h - convection heat transfer coefficient

Cp - specific heat of gas

G - mass flow velocity

Pr - Prandtl No. $\frac{Cp\mu}{k}$

Re - Reynolds No. $\frac{DG}{\mu}$

f - friction factor

ΔP - pressure drop

L/D- flow passage length/diameter ratio

ρ - gas density

V - gas velocity

g - gravitational constant

References

E-1. The Pebble Bed High Temperature Reactor as a Source of Nuclear Process Heat, Volume 1, Conceptual Design, R. Schulten, et. al, October 1974

E-2. Heat Exchanger Design, A. P. Fraas, M. N. Ozisik, Wiley, 1965.

E-3. An Analytical Model for a Steam-Methane Reformer, C. S. Herrick, GE, CRD Report No. 70C-119

E-4. Fedders, H., R. Harth and B. Höhlein, "Experiments for Combining Nuclear Heat with the Methane Steam-Reforming Process", Nuclear Engineering and Design, Volume 34, No. 1, October, 1975, North-Holland Publishing Company.

E-5. Krankota, J. L., "Double-Wall Steam Generator Tube and Weld Development Study", General Electric Company, NEDM-14072, September, 1975.

E-6. Cooper, K. C., "Steam-Methane Reforming and Intermediate Heat Exchanger Model (PHXSTP) for Nuclear Process Heat", Office Memorandum, Los Alamos Scientific Laboratory.

E-7. Hyman, M. H., "Simulate Methane Reforming Reactions", Hydrocarbon Processing, July 1968, Volume 217, n. 7.

E-8. Bond, J. A., et. al., "Design of a Helium-Heated Duplex-Tube Steam Methane Reformer", General Electric Company, ESTD Report ESTD 76-06, to be published.

APPENDIX F

REACTOR PLANT

TABLE OF CONTENTS

LIST OF FIGURES

LIST OF TABLES

APPENDIX F

REACTOR PLANT

F.1 SUMMARY

This appendix presents the description of the common reactor plant used for this entire study. Table F-1 shows the components included, either explicitly, or implicitly for costing purposes (see Appendix H also).

The reactor selected for this study is the pebble bed reactor (PBR), an advanced graphite-moderated, gas-cooled, reactor design. It is a logical growth version of the German PBR design, on which nearly fifteen years of experience has been accumulated[F-1].

The outlet gas temperature of 950°C (1742°F), proven by the experience of pebble bed fuel in the AVR[F-2], is sufficient for steam-methane reforming. An increase to 1000°C (1832°F), using programmed developmental fuel, would allow this reactor system to provide nuclear heat for the steam gasification of coal.

The reactor plant is designed so that, initially, present-day fuel utilizing the U-235-thorium cycle with a conversion ratio of ~0.6 can be used. As U-233 becomes available, the reactor can be switched over to a U-233-thorium cycle (C.R. $\tilde{=}$ 0.97), and eventually to a true thermal breeder cycle.

Subsequent sections of this appendix describe the PBR reference design.

Table F-1

COMPONENTS INCLUDED IN COMMON REACTOR PLANT

AEC ACCOUNT	DESCRIPTION	CLASS*
20	Land and Land Rights	A
21	Structures and Site Facilities	
211	Site Improvements and Facilities	A
212	Reactor Containment Building	B
213	Turbine Building	B
214	Intake and Discharge Structure	A
215	Reactor Service Building	A
216	Radwaste Building (in 215)	A
217	Fuel Storage Building (in 215)	A
218A	Control Room Building	A
218B	Diesel Generator Building	A
218C	Administrative Building (not included)	-
218D	Turbine Service Building	B
218E	Helium Storage Building	A
218F	Diesel Fuel Storage Building	A
22	Reactor Plant Equipment	
221	Reactor Equipment	A**
222	Main Heat Transfer and Transport Systems	C
223	Safeguards Cooling Systems	A
224	Radwaste Treatment and Disposal	A
225	Nuclear Fuel Handling and Storage	A
226	Other Reactor Plant Equipment	A
227	Instrumentation and Control	A
23	Turbine Plant Equipment	C
24	Electric Plant Equipment	B
25	Miscellaneous Plant Equipment	A

* A = Fixed for entire study, B = Minor variation with type of plant, C = Major study variable

** Except PCRV which is Class C

F.2 SYSTEM REQUIREMENTS AND DESIGN FEATURES

For steam-methane reforming, and for other process heat applications, the primary system requirement is that the reactor be capable of at least 900°C (1652°F) helium discharge temperature. Other requirements are:

1) Proven technology in the area of fuels and reactor configurations.

2) Licenseability and safety characteristics which will be acceptable.

3) Growth capability so as to be competitive in the 1990-2010 time period.

4) Fuel growth capability to above 1000°C (1832°F).

The reactor meeting these requirements is designated the NPH-3000 and is delineated by the following features.

- Graphite fuel in the form of 60 mm diameter balls. A proven design tested for over two years at 950°C outlet temperature in the AVR.

- Continuous fuel flow: The OTTO (Once-Through-Then-Out) fuel cycle whence the fuel balls are introduced at the top of the reactor and flow slowly downwards until discharged at the bottom.

- Carbon stone and graphite reactor structure: The fuel balls are contained in a graphite lined cupola which acts as a nuclear reflector. This liner is enclosed in an insulating layer of carbon stone.

- Single Cavity Prestressed Concrete Pressure Vessel: The reactor is contained in the central cavity of a PCRV. A water-cooled liner maintains the concrete at a safe temperature. (An alternate multi-cavity PCRV was also considered.)

- Coaxial Ducts: A single set of penetrations connects the reactor with the assemblies containing the steam reformer, steam generators, and/or the intermediate heat exchangers. (The multi-cavity PCRV does not require coaxial ducts.)

- Downward Coolant Flow: The helium coolant passes through the reactor in a downwards direction, thus flowing in the same direction as the fuel balls. As a consequence, the temperature profile in the axial direction is highly conducive to low temperatures and temperature gradients in the areas of highest burnup.

- Fast Discharge System: A novel feature of this design is the incorporation of a system for the removal of all fuel from the core to a shielded location where a nuclearly non-critical configuration exists and where static afterheat removal can be provided. This system is designed as an ultimate backup safety system, supplementing the redundant core auxiliary cooling system (CACS), and the redundant liner cooling systems.

  In the highly unlikely event of complete failure of all safety systems, and after the passage of many hours, it is possible that fuel temperatures may exceed some predetermined safe limit. At this point, either automatically, or by operator actions, the fast discharge system will be activated. Valves located below the reactor cavity will open, allowing the fuel balls to flow into a subterranean, water cooled annulus. This annulus is inherently safe from a criticality standpoint. Calculations at KFA have shown that the water outside the annulus can retain all afterheat without boiling so that no dynamic system is needed. At a future date the fuel can be removed, either for reprocessing or reuse.

  Thus, a single fail-safe system can provide the pebble bed reactor with a true backup safety system.

F.3 REACTOR SYSTEM

The following drawings, Figures F-1 through F-4, show the layout for the reference reactor system. Shown in these figures are the reference duplex tube steam reformer modules.

Figure F-1 shows a plan view of the reactor containment building interior and identifies the PCRV, surrounded by the twelve non-integrated reformer-steam generator pods and the four core auxiliary cooling system loops. Figures F-1 and F-3 show the design of the reformer-generator plumbing, wherein the connections to each reformer-steam generator independently penetrate the containment building walls and are manifolded external to the containment building.

Figure F-2 (Section A-A of Figure F-1) shows pertinent details of the pebble bed reactor and the reformer-steam generator assembly. The helium flow path of the reactor primary coolant is shown schematically.

Figure F-3 (Section B-B of Figure F-1) shows the OTTO refueling concept wherein pebble fuel elements are batch loaded in the reactor service building and injected into the appropriate portion of the reactor interior via fuel conveyer and distribution mechanisms. The fuel element removal concept and the CACS are indicated.

Figure F-4 shows a plan view of the foundation for the PCRV and containment building. The fuel cart turn-table and track concept is indicated. The fast discharge system ducting arrangement and fuel reservoir are indicated.

Referring to Figure F-2, the reactor consists of a cylindrical prestressed pressure vessel containing a graphite reflector assembly. The core consists of a fixed bed of spherical graphite balls 6 cm in diameter containing the fuel. Fuel balls are added essentially continuously between one and two full-power years depending on the fuel cycle selected. The coolant flow is downwards through the fuel bed, a key element of the OTTO cycle.

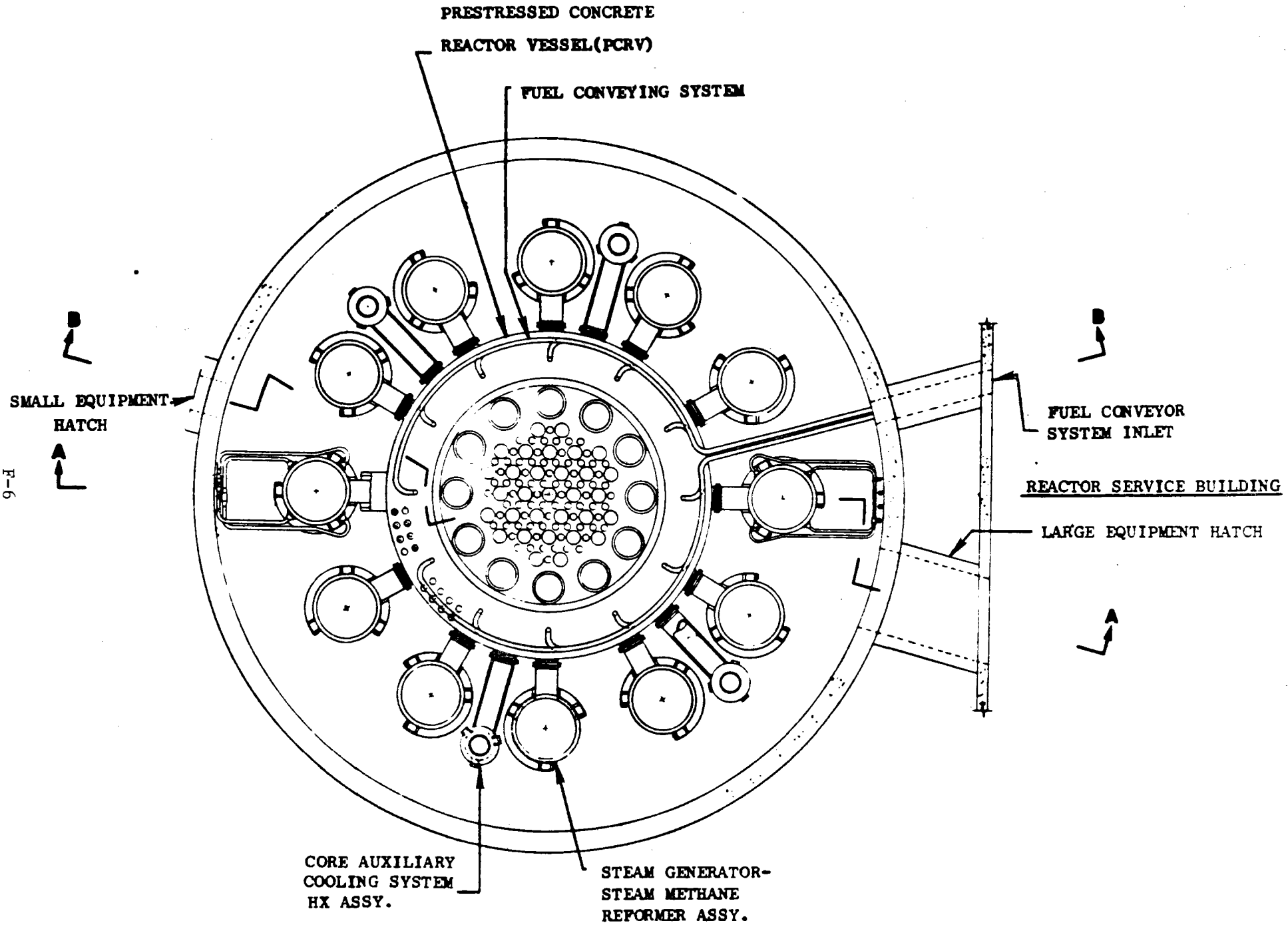

Figure F-1. Plan View of Reactor Containment Building

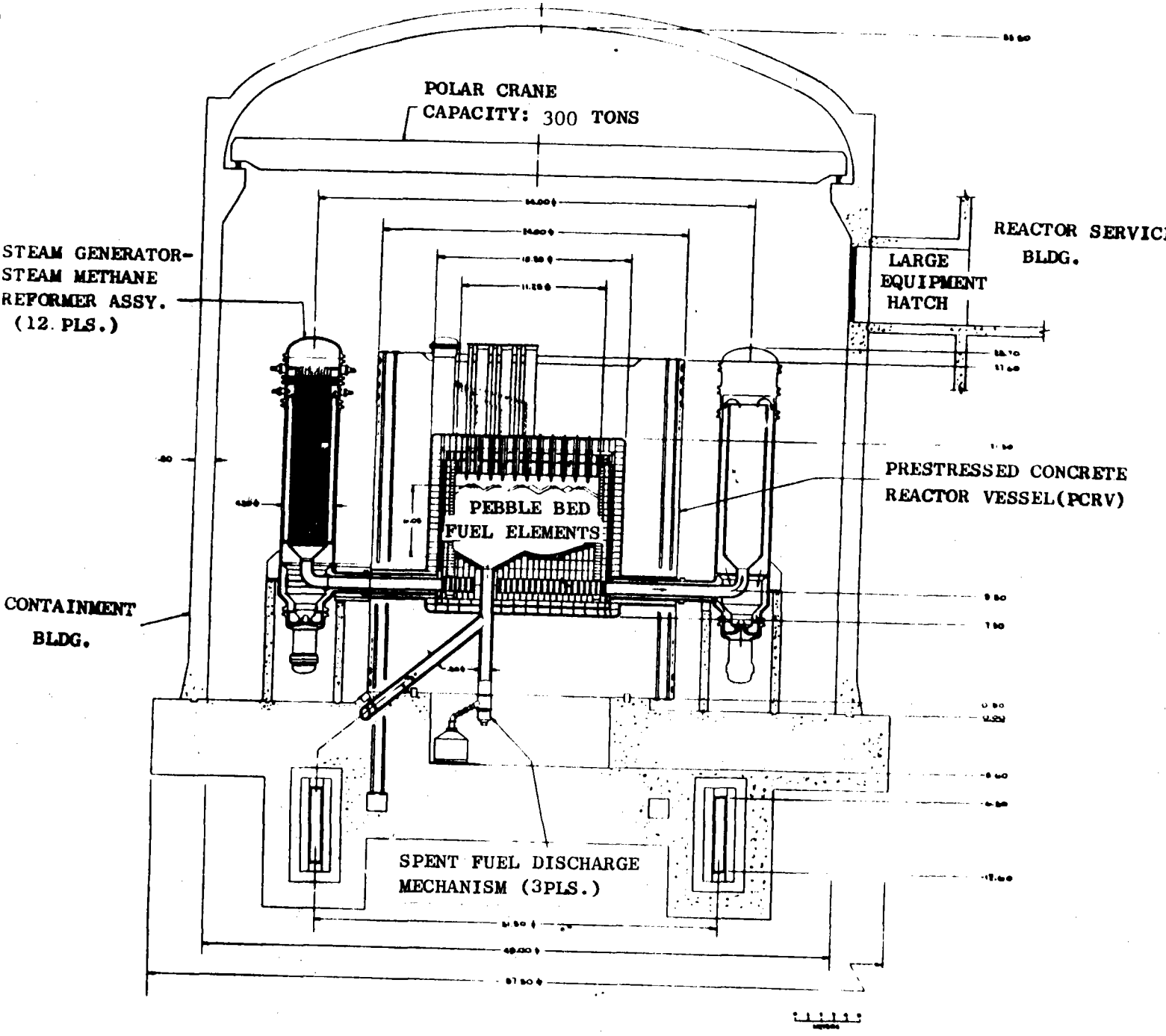

Figure F-2. Details of Pebble Bed Reactor and the Reformer-Steam Generator Assembly.

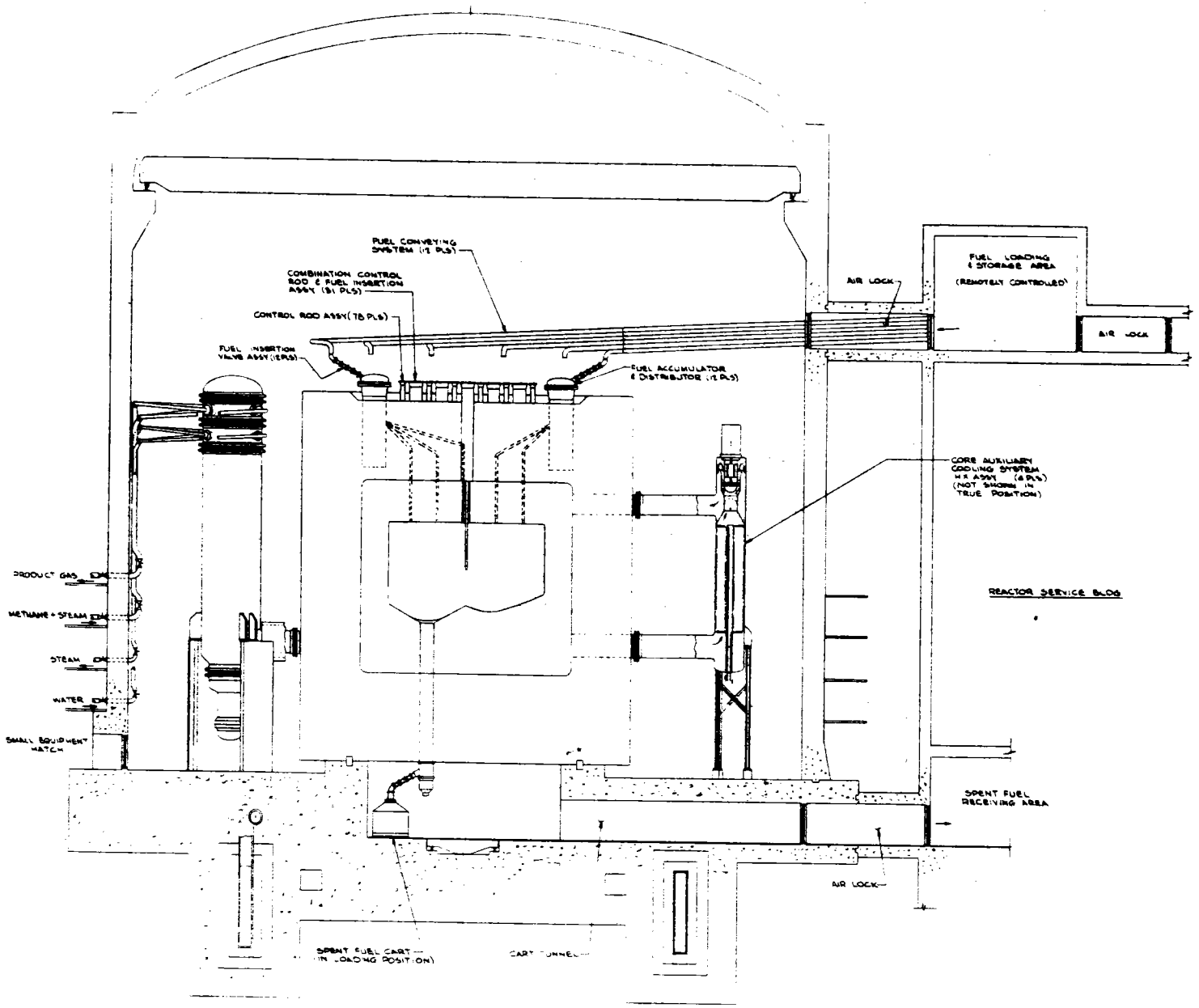

Figure F-3. Reactor Containment Building Showing Refueling Concept.

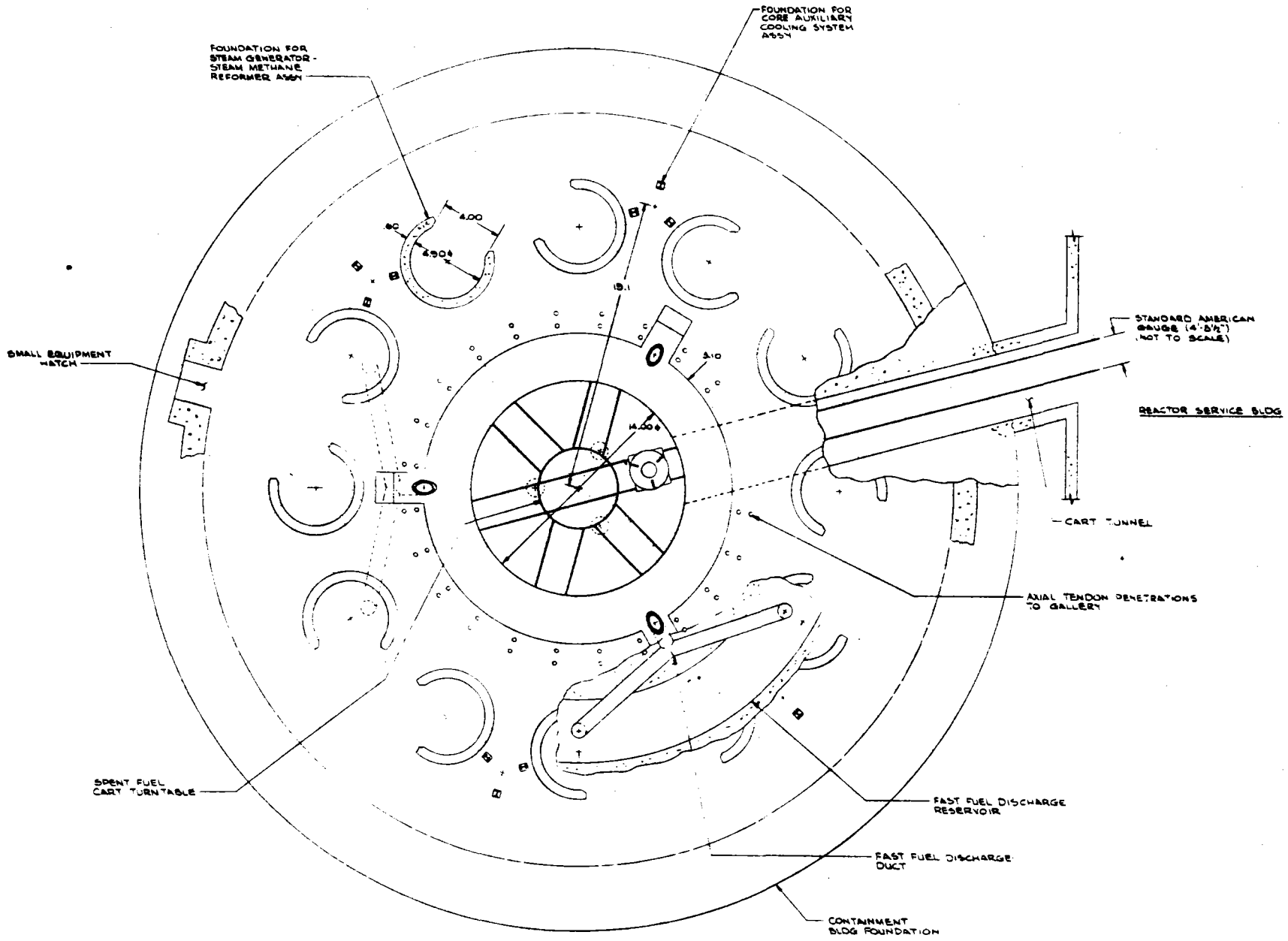

Figure F-4. Plan View of the Foundation for the PCRV and Containment Building.

In this scheme, the fissile material content of the fuel balls decreases from the top to the bottom of the core. The heat flux and power distribution tend to have the same distribution so that the highest power density occurs at the top of the core where the coolant enters at its lowest temperature. At the bottom of the core, the power density is low, where the coolant has its highest temperature. Thus, the coolant is rapidly heated in the upper portion of the core by relatively fresh fuel and with a large temperature difference while in the lower portions the temperature difference is relatively low. Thus, the difference between the maximum fuel temperature and the exit gas temperature is very small. Figure F-5 shows the temperature axial profiles in a typical OTTO cycle reactor.

The pressure vessel shown is a nonintegrated design, with the loop components in separate pods attached to the PCRV with coaxial ducts. This design appears preferable from the standpoint of cost since more factory fabrication can be used, and the cost of the field-erected PCRV should be much less than that of the alternate integrated design. However, the choice between a multicavity integrated design and the nonintegrated design shown is not crucial to the success of the PBR. Either design meets the basic requirements. The final choice will be made on the basis of cost, practicability, reliability, and safety considerations.

The PBR is designed for remote fuel handling in anticipation of the use of reprocessed U-233/thorium fuel with its attendant radioactivity. This represents an advance over the presently operating AVR and the presently under-construction THTR. Both of the above plants use fresh fuel balls which can be handled manually (initially).

As shown in Figures F-1 to F-4, four core auxiliary cooling units, each capable of providing 50 percent of the required afterheat removal, are provided. In conjunction with the triply redundant liner cooling-water circuits, these systems can handle the shutdowns and emergency heat removal requirements.

The design shown uses steam reformer/steam generator modules. Without changing the basic reactor arrangement, these modules can be replaced with steam generator modules or with the intermediate heat

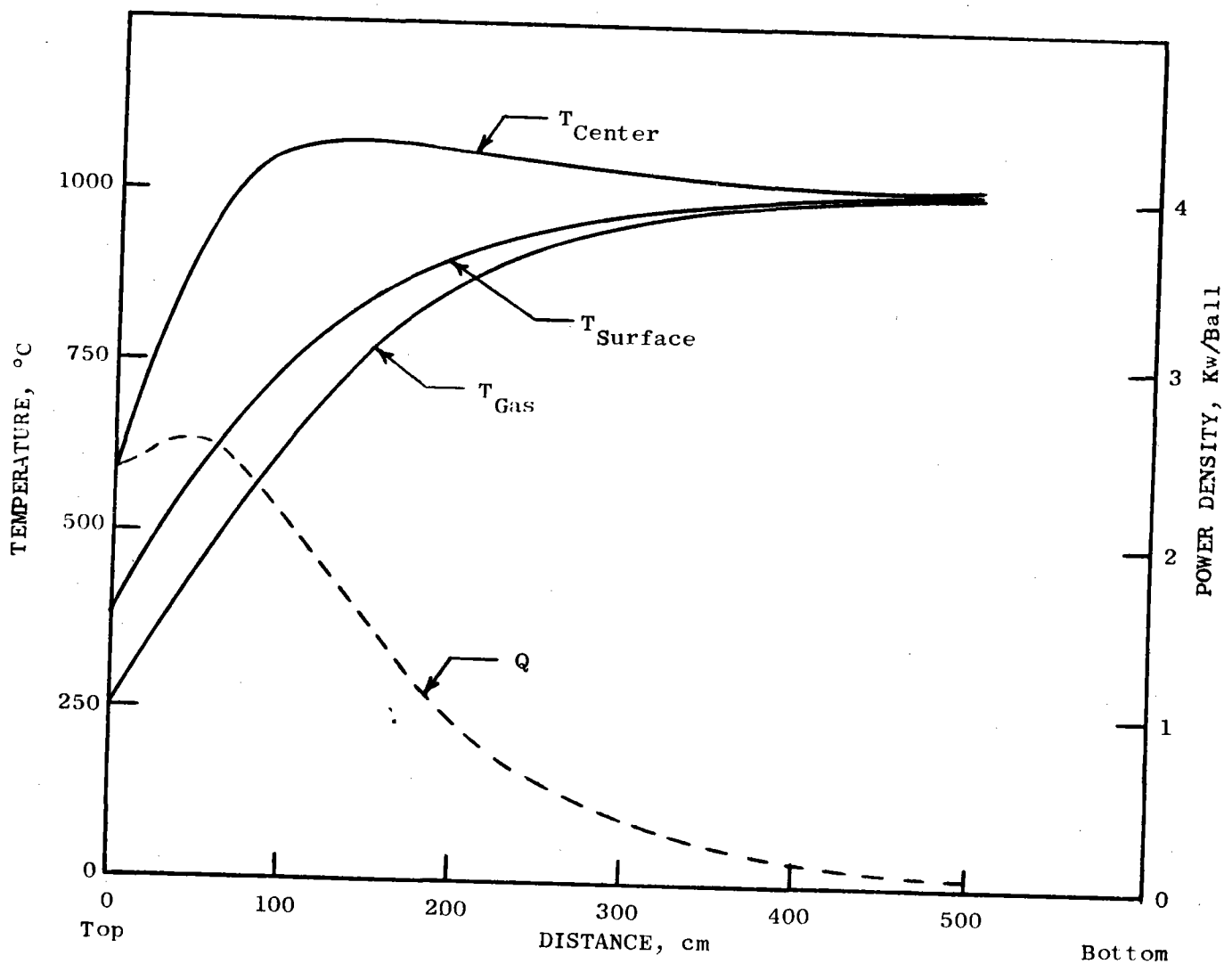

Figure F-5. Typical Axial Distribution of Power Density and Temperature.

exchanger modules. Each module is connected to the PCRV with a coaxial duct which contains both the hot discharge helium and the cool reactor inlet helium. A motor-driven circulator is located in each module. Variable guide vanes on the circulator allow flow variations down to about 20 percent of full flow and, additionally, provide for flow shutoff to enable the reactor to operate on less than the full number of modules.

The plant shown is the A-1 reference design, as discussed in Section 2 and in Appendix G. The variations in plant configuration affect such items as the PCRV, the secondary containment, and the ducting, as well as the external building housing the turbogenerators.

The following data tables and figures describe the NPH-3000 as applied to the A-1 reference duplex tube steam reforming plant.

Table F-2 is a general plant description, while Figure F-6 shows the state points, flow rates, etc. for this particular plant. Table F-3 is the plant thermal summary, again for the particular reference design. Note that in the actual optimization and selection, many of these values were changed and varied. Table F-4 describes the basic reactor core data while Table F-5 describes the fuel handling system, and Table F-6 the control rods.

The steam reformer/steam generator modules are discussed in detail in Appendix E. Table F-7 describes the primary circulator. The core auxiliary cooling system is described in Table F-8.

The weight and dimensions of the PCRV, CACS, and secondary containment building are shown in Table F-9.

F.4 NUCLEAR DESIGN AND FUEL CYCLES

The nuclear and thermal design of the PBR has been extensively discussed in other reports (F-3, F-4, F-5 and F-6). Table F-10 shows the typical performance of the U-235/thorium cycle and the U-233/thorium high conversion cycle.

Table F-2. General Plant Description

NPH A-1 Plant Output	Product Gas and Electricity
Nuclear Heat Source Power Rating	3000 MW_{th}
Fuel Element Configuration/ Refueling Cycle	Pebble Bed/OTTO*
Reactor Primary Containment Configuration	Pre-Stressed Concrete Reactor Vessel (PCRV)
Reactor Primary Coolant/ Peak Bulk Temperature	Helium/950°C
Number of Primary Coolant Loops	12
Primary Coolant Loop Components	Circulator Steam Generator (SG) Steam-Methane Reformer (SMR)
SG-SMR Assembly Description	Combined Assembly with Circulator, Duplex Tubes in SG and SMR
SG-SMR Assembly Location	Pod Mounted External to PCRV (Non-Integrated)
Number of Core Auxiliary Cooling Loops	4
Containment Building Location/ Construction Material	Above ground/prestressed concrete
Containment Building Internal Atmosphere/Pressure	Nitrogen/Slightly negative

*Once Through Then Out

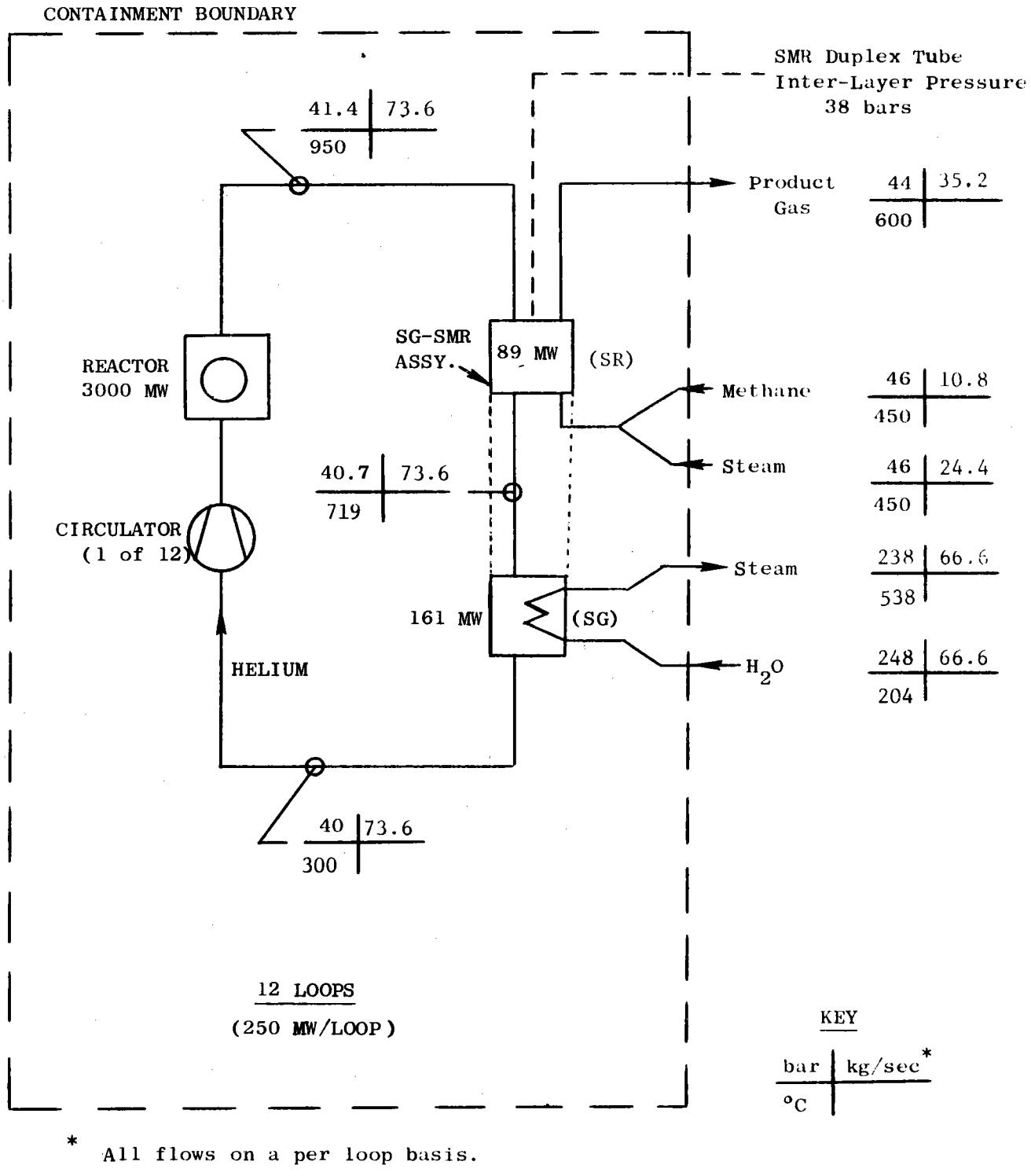

* All flows on a per loop basis.

Figure F-6. Pressure, Temperature and Flow Rates Within the Containment Building

Table F-3. Plant Thermal Summary

Thermal Reactor Power	3000 MW_t	-
Steam Generation Summary		
Exit Temperature	538°C	1000°F
Exit Pressure	238 bars	3451 psi
Total Plant Output	799.2 Kg/sec	6.34×10^6 lb/hr
Feedwater Temperature	204°C	400°F
Feedwater Pressure	∿248 bars	∿3600 psi
Duty	1932 MW_t	-
Steam-Methane Reformer Summary		
Product Gas Exit Temperature	600°C	1112°F
Product Gas Exit Pressure	44 bars	638 psi
Maximum Reactant Temperature	825°C	1517°F
Product Constituents Flow Rate (Total Plant)		
H_2	29.5 Kg/sec	
CO	72.6 Kg/sec	
CO_2	76.8 Kg/sec	
CH_4	62.1 Kg/sec	
H_2O	181.5 Kg/sec	
	422.5 Kg/sec	3.35×10^6 lb/hr
Reactant Flow Rates (Total Plant)		
Steam	292.4 Kg/sec	
Methane	130.1 Kg/sec	
	422.5 Kg/sec	3.35×10^6 lb/hr
Steam & Methane Inlet Temperature	450 °C	842°F
Steam & Methane Inlet Pressure	46 bars	667 psi
Helium Inlet/Outlet Temperature	950/ 719°C	1742/ 1326 °F
Helium Flow Rate (Total Plant)	883.2 Kg/sec	7.01×10^6 lb/hr
Duty	1068 MW_t	-

Table F-4. Reactor Core Data

Thermal Reactor Power	3000 MW
Core Power Density	5 MW/m^3
Coolant/Flow Direction	Helium/down
Coolant Inlet Temperature (Bulk)	250°C (Study Variable)
Coolant Outlet Temperature (Bulk)	950°C
Helium Pressure (Inlet)	~40 bars
Helium Mass Flow	820 Kg/sec
Core Height (mean)	6.05 M (19.85 ft)
Core Diameter	11.25 M (36.91 ft)
Number of Fuel Elements	3.25×10^6
Average Fuel Element Resident Time	1115 days
Number of Fuel Enrichment Zones	2

Table F-5

Fuel Handling System

General Data	
Diameter of Fuel Elements	6 cm
Number of Fuel Elements in Core	3.25×10^6
Number of Core Enrichment Zones	2
Average Lifetime of Fuel Elements in Core	1115 days $\sim$ 3 years
Average Flow Rate of Pebble Fuel Elements	2915 balls/day
Pressure Level in Fuel Handling System	Loading Conveyors and Isolated Removal Carts at Atmospheric Pressure. Input Fuel Accumulators, Pebble Feed Machines, Discharge Mechanisms and Removal Carts during filling all at 40 Bars Nominal.
Fuel Loading Components	
Number of Conveyor Systems from Reactor Service Building to Fuel Accumulators	12
Fuel Inlet Accumulator Location	PCRV Head
Average Pebble Input Rate/hr per Conveyor	$\sim$10 balls/hr
Number of Insertion Valves per Conveyor	4
Average Accumulator Loading Rate (Batch Loading to Accumulators Assumed @ 15 balls/batch)	1.48 hrs/batch loading (5910 loadings/year)
Pebble Feed Machine Description	Located in each Fuel Accumulator with Mechanism to Feed Individual Pebbles to Two or Three Insertion Ducts

Number of Fuel Insertion Postions into Core	31			
Enrichment Distribution Relationship	W	X	Y	Z
("W" Accumulators of "X" Enrichment	4	Hi	3	Peripherally
Level Feeding "Y" Insertion Positions)	3	Lo	3	Centrally
Located "Z")	5	Lo	2	Centrally

Fuel Removal Components

Number of Core Discharge Ducts/Diameter	3/0.8 m
Average Discharge Rate/hour per Duct	41 balls/hour
Capacity of Fuel Removal Cart	5400 balls (1 m^3 volume)
Average Time to Fill Removal Cart	5.49 days
Approximate Cart Weight (Filled)	44 Mg

Note: All fuel handling rates shown in this Table are based on average fuel life time of 1115 days. This figure is appropriate to a low enrichment core. For high conversion and for breeder fuel, the average fuel life can be as low as half of this value.

Table F-6 Control Rod Data

Number/Location	109/top of PCRV
Type	Electric Motor Driven with Rotating Spindle Advance
Rod Spacing	0.91 per m^2
Insertion Speed	Slow 2-5 cm/sec; fast $\sim$ 30 cm/sec
Absorber Material/Average Worth	B_4C/0.25$
Tip Material	High Nickel Alloy, SS Type 316L
Tip Design	Rotating Auger Bit
Rod Cooling	Primary Helium Entering through Lateral Perforations and Moving through Hollow of Absorber Section
Normal Operating Position	In Top Reflector
Design Life	6-10 Years
Primary Helium Seal	Motor and Drive Mechanism Contained in Housing, Seal-Flanged to PCRV Penetration

Table F-7. Primary Coolant Circulators (Per Loop Basis)

Number	1 per loop (12 loops)
Type	Axial; Single-Stage Impeller, Vertical, Sealed Shaft, Electric Drive
Primary Circuit Pressure Drop Distribution:	Δp, bar (psi)
Core	0.38 (5.5)
Ducting Along Primary Helium Path	0.38 (5.5)
Steam Methane Reformer, Shell Side	0.17 (2.5)
Steam Generator	0.45 (6.5)
	1.38 (20.)
Flow Rate	245 $^{Mg}/_{h}$ (0.54×10^{6} lb/hr)
Inlet/Discharge Pressures	40/41 bar (580/600 psia)
Inlet Temperature	250°C (482°F)
Outlet Temperature	252°C (486°F)
Circulator Motor Drive Power	3100 KW/circulator
Electric Motor Drive Type	Induction Motor
Circulator Speed	3600 rpm

Table F-8. Core Auxiliary Cooling System

Number of Loops	4
Duty Sizing Basis	Each CACS Heat Exchanger Assembly Sized for 50% of Reactor after Heat Duty
CACS Sink Fluid	Pressured Water (Liquid Phase Only)
Heat Exchanger Description	Helical Water Tube with Primary Helium in Cross Flow, Electric Motor Driven Circulator at Top of Heat Exchanger Assembly
Flow Schematic	Hot Helium Enters at Bottom, Flows Vertically Through CACS Heat Exchanger, Exits at Top
Ducting Arrangement	Separate Inlet and Return Ducts Connecting CACS Heat Exchanger Assembly to PCRV
Envelope	ϕ 2.13 m x 18 m Overall

Table F-9. Weights and Miscellaneous Data Related to the PCRV and Containment Building

Foundation for PCRV and Containment Building	
Overall Outside Diameter	ϕ 57.3 m (188.0 ft)
Maximum Depth Below Ground Level	16.3 m (53.5 ft)
Concrete Volume Required	25,047 m^3 (32,760 cu yds)
Approximate Weight	60,136 Mg (66,300 tons)
PCRV (Non-Integrated)	
Outside Diameter	ϕ 24 m (78.7 ft)
Overall Height	27 m (88.6 ft)
Concrete Cavity Inside Diameter	ϕ 15 m (49.2 ft)
Concrete Thickness at Head/Base	6.55/6.45 m (21.5/21.2 ft)
Concrete Volume	9740 m^3 (912,740 cu yds)
Approximate Weight (Including Reactor)	29,342 Mg (32,350 tons)
Bearing Stress on Foundation	17.2 b (250 psi)
CACS - Heat Exchanger Assembly	
Outside Diameter	2.13 ϕm (7 ft)
Overall Height	18 m (59 ft)
Containment Building	
Outside Diameter	ϕ 53 m (174 ft)
Overall Height	55 m (180 ft)
Wall Thickness	1.5 m (59 in.)
Polar Crane Capacity	272 Mg (300 tons)
Concrete Volume	15903 m^3 (920,800 cu yds)
Wall Bearing Stress	16.4 kp/cm^2 (233 psi)
Approximate Weight	38,186 Mg (42,100 tons)

Table F-10

Equilibrium Fuel Cycle Data

Parameter	Units	Thorium/Highly Enriched U-235	Thorium/U-233 (High Conversion)
Core Power Density	MW/m^3	5	5
Core Height	m	6.0	5.5
Core Diameter	m	11.28	11.78
Average Fuel Resisdence	days	1633	836
Average Gas Outlet Temp.	°C	985	985
Diameter of Fuel Ball	mm	60	60
Diameter of Fueled Zone	mm	50	54
Diameter of Fuel Kernel	µm	600	400
Coating Thickness	µm	160	130
Moderation Ratio			
Inner Core Zone	N_C/N_{HM}	250	110
Outer Core Zone	N_C/N_{HM}	230	110
Average Burnup	MWd/Mg	102,000	24,000
Conversion Ratio	-	0.625	0.958
Maximum Power per Ball	kw	2.69	1.60
Maximum Helium Temperature	°C	997	1023
Maximum Temperature at Ball Center	°C	1016	1145
Core Pressure Drop	b	0.36	0.24
Inventory - U-233	kg	813	2955
U-235	kg	702	477
Pu (239+241)	kg	3	0
Supplied - U-233	kg/d	0	3.55
U-235	kg/d	2.11	0.65
Ore Required @ 0.4% Tails	kg/d	678	66
Separative Work	SWU/d	402	39
Discharged - U-233	kg/d	0.582	3.58
U-235	kg/d	0.123	0.45
Pu(239+241)	kg/d	0.003	0.003

To achieve breeding (CR > 1.0) requires maximizing the neutrons in thorium. The capture of neutrons in thorium is maximized by increasing both the loading of thorium in the reactor and the thorium resonance integral. The resonance integral increases as the absorber is more homogenously distributed within the moderator, and the coated particle size reduced to decrease self shielding effects.

Calculations[F-7] have shown that decreasing the moderator to fuel ratio (Nc/N_{HM}) to 70 or 80 from the 110 value used in the high converter design, and decreasing the average burnup to below 20,000 MWD/T will achieve a conversion ratio greater than 1.0. Other techniques, such as purging fuel balls of volatile saturated neutrons absorbers and the addition of beryllium oxide moderator balls will increase the breeding ratio still further.

REFERENCES

F-1 "Special Issue: High Temperature Reactor for Process Heat Applications", Nuclear Engineering and Design, Volume 34 (1975), No. 1, October 1975.

F-2 Knüfer, H., "Preliminary Operating Experiences with the AVR at an Average Hot-Gas Temperature of 950°C", Page 73-84, loc. cit.

F-3 Teuchert, E. and Rütten, H. J., "Core Physics and Fuel Cycles of the Pebble Bed Reactor", pages 109-118, loc. cit.

F-4 Teuchert, E. Bohl, L., Rütten, H. J., and Haas, K. A., "The Pebble Bed High Temperature Reactor as a Source of Nuclear Process Heat", Volume 2, "Core Physics Studies", Joint GE/KFA Study, Jül-1114-RG, October 1974.

F-5 Woike, O. G., et al, "Small Nuclear Process Heat Plants (SNPH)" General Electric Co., GEEST 75-001 (ORNL-Sub-4352-1), Nov. 1975.

F-6 Tschamper, P., et al., "The VHTR for Process Heat", General Electric Co., GEAP-14018, Sept. 1974.

F-7 Teuchert, E. and Rütten, H. J., Private Communications.

APPENDIX G

SYSTEM SELECTION AND OPTIMIZATION

TABLE OF CONTENTS

LIST OF FIGURES

LIST OF TABLES

APPENDIX G

SYSTEM SELECTION AND OPTIMIZATION

G.1 INTRODUCTION

This appendix is concerned with the techniques, ground rules and assumptions used to select the reference plants described in Sections 2 and 3. Of prime importance was the investigation of at least nine different power plants for steam reforming so that an optimum choice could be made. It is extremely important to note that this study did not start from scratch. Three previous published studies, references G-1, G-2 and G-3, plus numerous unpublished studies were utilized. Furthermore, much data from the German process heat work, reference G-4, was utilized to insure a realistic result, rather than simply a "paper" optimization.

All of the detailed selection and optimization work was done on the steam reformer plant rather than the coal gasification plant. There were two reasons for this. First, the steam gasification of coal was selected early in the study as the reference design. This is a plant with intermediate heat exchangers located in the reactor containment building delivering hot helium to a coal gasifier and a steam generator outside the secondary containment. (This is, in fact, almost identical to a steam reforming plant using an IHX). Second, not enough "hard" data exists on the often-proprietary designs of the different nuclear coal gasification schemes to permit a valid optimization. (See Appendix B)

G.2 APPROACH

The first step in the General Electric approach was to review all previous steam reformer HTR plants. A matrix was established to see what common features and significant differences existed. After reference to

the work statement, Appendix J, all possible variations of intermediate heat exchanger location, type and cycle were examined. Table G-1 shows the possible variations. There are more than 36 possible combinations of these parameters, and even more when the duplex tube steam reformer option is included.

The following combinations were eliminated for basic qualitative reasons.

- Arrangements in which primary helium penetrated the secondary containment were disqualified for safety reasons.

- Arrangements in which an integrated PCRV (with heat transfer components located in pods) were combined with separate modules (containing primary coolant) were disqualified for having the disadvantages of both systems without any advantages.

- With an IHX, no gains, and some disadvantages such as space and safety problems, occur with the SG or SR inside the secondary containment. Therefore, all cases where a secondary-helium-heated PHX was used had the PHX located outside the secondary containment.

- Based on a review of the SNPH study[G-3], the use of duplex steam generator tubes appeared undesirable, since the ability to fabricate, join, and still be able to monitor the intertube helium gap was deemed very difficult. This combined with the ability to use heat exchangers outside the containment for any steam used by a customer reduces the need for the approach. Therefore the duplex tube was not considered as a replacement for the IHX for steam generation.

These considerations reduce the total possiblities drastically. Table G-2 shows all possible combinations which passed the above tests. As will be discussed later, there are some sub-options, such as having two steam generators, one for electric power only in the primary and one in the secondary loop for use in the reforming process.

A basic point for the evaluation of these plants was that, considering only those plants which meet all qualitative criteria (e.g. safety), the

TABLE G-1

CONCEPTUAL DESIGN OPTIONS

LOCATION OF IHX

- Within PCRV
- Outside PCRV but Inside Containment
- Outside Containment

LOCATION OF STEAM GENERATOR

- Within PCRV
- Outside PCRV but Inside Containment
- Outside Containment

LOCATION OF STEAM REFORMER

- Within PCRV
- Outside PCRV but Inside Containment
- Outside Containment

USE OF INTERMEDIATE LOOP

- No Intermediate Loop
- Intermediate Loop for Steam Reformers
- Intermediate Loop for Both Steam Reformer and Steam Generator

USE OF DUPLEX TUBE AS INTERMEDIATE LOOP

- For Steam Reformer Only
- For Steam Generator Only
- For Both

TABLE G-2

POSSIBLE PLANT ARRANGEMENTS

Type IHX	IHX On	Type Containment	Locations of Component*			Comments
			IHX	SG	SR	
None	-	Integrated	-	PCRV	PCRV	Basic KFA Design
None	-	Non-Int.	-	Sec.	Sec.	Alternate KFA Design
Separate	SR	Integrated	PCRV	PCRV	Outside	Reference VHTR
Separate	SR	Non-Int.	Sec.	Sec.	Outside	
Separate	SR/SG	Integrated	PCRV	Outside	Outside	
Separate	SR/SG	Non-Int.	Sec	Outside	Outside	
DSR	SR	Integrated	-	PCRV	PCRV	
DSR	SR	Non-Int.	-	Sec.	Sec	

*PCRV = Inside PCRV

Sec. = Outside PCRV but inside secondary containment

Outside = Outside secondary containment

"best" plant is the one which has the lowest energy cost. This led to the selection of the various optimization variables; Table G-3 shows the approach used.

G.3 GROUND RULES AND ASSUMPTIONS

The Chemical Heat Pipe (CHP) plant was selected as the basis for all system optimization. A complete description is included in Appendix A. For the purposes of this study, it was used to provide a common basis for all plants. Table G-4 shows some specifics of this choice. Of the many variables which might have been used for optimization, one was the fraction of reactor power transferred in the steam reformer. Figure A-3 shows the details of the CHP portion of the plant. From General Electric studies, the maximum practical steam reformer power is approximately 58.4%. At this point, the overall heat balance of the reformer plant is nearly in balance, and by use of heat exchangers, very little heat is wasted. In addition, backpressure steam turbines are used to extract electrical energy from the steam before it is used to heat the feedwater for the reformer. For this plant, an energy balance shows:

Total Reactor Power	3000 MW
Net CHP Energy	1772 MW
Gross Electric Energy	409 MW
Waste Energy	819 MW

In order to investigate the effect of variations in the power transferred to the steam reformer, the method of superposition was used. For power to the reformer of less than 58.4%, the additional thermal energy was used to generate electricity. Therefore the fraction of CHP power varied directly with the ratio of power to the reformer while the electric power also varied with the ratio of power to the reformer. Table G-5 shows the energy splits for the three values of power-to-reformer used.

Several items were fixed for all study calculations. Some of the more significant are discussed below.

The core exit helium temperature was fixed at 950°C (1742°F), which is the temperature at which the AVR has been run for over two years.

TABLE G-3

APPROACH

A. ESTABLISH CONCEPTUAL DESIGNS FOR:

- STEAM-METHANE REFORMING PLANTS USING:
  - A-1. A duplex tube steam reformer,
  - A-2. A single wall steam reformer, and
  - A-3. An intermediate heat exchanger loop (IHXL) with the steam reformer outside the secondary containment.
- STEAM GASIFICATION OF COAL PLANTS WITH AN IHXL AND WITH THE COAL GASIFIER OUTSIDE THE SECONDARY CONTAINMENT.

B. EVALUATE THESE CONCEPTUAL DESIGNS WITH RESPECT TO ECONOMIC, SAFETY, AND ENGINEERING DESIGN CONSIDERATIONS.

C. PROVIDE (BASED ON THE EVALUATIONS) PRELIMINARY DESIGN SPECIFICATIONS, AND SAFETY AND DESIGN CRITERIA FOR VHTR PROCESS HEAT SYSTEMS AND COMPONENTS, AND PROVIDE PRELIMINARY SPECIFICATIONS FOR VHTR REACTOR FUELS AND STRUCTURAL MATERIALS.

TABLE G-4

CHEMICAL HEAT PIPE ASSUMPTIONS AND GROUND RULES

- GENERAL
  - PROVIDES BASIS FOR ALL PLANTS
  - MAXIMUM PRODUCT GENERATION
  - ELECTRIC POWER AS BYPRODUCT ONLY
  - PEBBLE BED REACTOR
  - SETS OPERATING CONDITIONS
- SPECIFIC
  - 3000 MW THERMAL POWER
  - 58.3% POWER TO REFORMER OPTIMUM FROM REFORMER PLANT STANDPOINT
  - ELECTRIC POWER "BEST" USE OF HEAT LEVELS
  - RANGE OF REFORMER POWER INVESTIGATED 13% TO $\sim$ 58%

TABLE G-5

ENERGY BALANCE FOR CHP PLANTS

Power to Steam Reformer,	%	13.0	35.6	58.4
Net CHP Power to Users,	MWt	394	1080	1772
Gross Electric Power,	MWe	1023	717	409
Waste Heat (by Balance),	MWt	1583	1203	819
Net Electric Power, (less station needs)	MWe	932	591	241

From a thermodynamic and heat transfer standpoint, a higher temperature would be advantageous; the heat exchanger would be smaller, and/or higher process temperatures would be possible. However, this potential improvement would be common to all conceptual designs and therefore for optimization purposes a fixed value was used throughout the study. For many processes, such as steam gasification of coal, a higher temperature is desirable, however, and this is a goal limited primarily by heat transfer equipment, not reactor fuel capability.

A reactor pressure level of approximately 40 b (580 psia)was selected as an acceptable compromise based on previous studies. Lower pressures imply higher pumping power, a larger reactor core, less stress in vessels and ducts, while higher pressures tend in the opposite directions. As with core exit temperature, the variations of this parameter would cause a change in all systems in a nearly constant way, thus not affecting the results of the optimization.

Steam conditions were fixed at modern values, 238 b (3450 psia)and 538°C (1000°F). All steam generators were parallel, once through geometry using 25.4 mm (1.00") OD tubes.

Twelve modules were selected for both plants using SRA/SGA modules and for IHXL plants. This requires 250 MW of heat transfer capability per unit. For plants with a single-cavity PCRV (non-integrated) this is a good compromise between modules which are too large for ease of handling and too many penetrations, ducting, etc. which would be required with more. For multi-cavity PCRV's (integrated) designs, it is probable that as few modules as possible would save money in the PCRV area. This point needs additional work, requiring several designs of PCRV's, and was beyond the scope of this study.

All pressure vessels were of the prestressed concrete type. The use of prestressed steel or cast iron was not studied, although recent German work shows a very significant advantage in the prestressed cast iron vessel used with a non-integrated plant design. For integrated plants, the PCRV appears the only viable candidate.

Ducting between the modules and the PCRV was of the German coaxial design using water cooled outer containment. Hot gas ducting was of the German design as used in the HHV helium test facility, and included water cooled outer walls, fibrous insulations, and a hot gas liner of superalloy. More details are given in Appendix I.

Afterheat removal was handled by four separate core auxiliary cooling systems, each capable of removing 50% of the afterheat. This is more conservative than using the modules themselves as heat removal devices. In addition, the water-cooled liners are very nearly able to hold fuel temperatures at a safe level by themselves.

All blowers were constant speed electric motor driven radial devices, with flow control by means of variable stator vanes. Flow can be controlled down to 15% of full flow, and, with the motor shutdown, the variable vanes can effect a full flow shutoff.

G.4 PLANT DESIGN CONCEPTS

With the ground rules and assumptions described above, the following areas were selected for optimization.

- Power delivered to the reformer (as a fraction of total reactor thermal power)
- Reduction in reformer tube size (predicated on the development of advanced catalysts)
- Integrated PCRV (multi-cavity) versus non-integrated PCRV (single cavity)
- Use of a separate intermediate heat exchanger.

The reference plant, described in Section 2, consisted of the reactor plant described in Appendix F coupled with twelve 35.6% power-to-reformer, duplex tube steam reformer/steam generator modules located within the secondary containment building and coupled to a non-integrated PCRV. All variations were designed for comparison with it. Table G-6 shows the nine different design concepts which were considered.

TABLE G-6

PLANT DESIGN CONCEPTS

A-1	DUPLEX TUBE STEAM REFORMER PLANTS	
	A-1a	90 mm ID TUBES
Reference System	A-1a1	13% POWER TO REFORMER
Reference System	A-1a2	35.6% POWER TO REFORMER
Reference System	A-1a3	58.4% POWER TO REFORMER
	A-1b	50 mm ID TUBES (ADVANCED CATALYST)
	A-1b1	58.4% POWER TO REFORMER
	A-1b2	35.6% POWER TO REFORMER
	A-1c	90 mm ID TUBES WITH INTEGRATED PCRV
A-2	SINGLE WALL STEAM REFORMER PLANTS	
		35.6% POWER TO REFORMER
	A-2a	90 mm ID TUBES WITH 9 mm WALL
	A-2b	90 mm ID TUBES WITH 12 mm WALL
A-3	INTERMEDIATE HEAT EXCHANGER LOOP PLANT	
	-	35.6% POWER TO REFORMER
	-	90 mm ID TUBES, SINGLE, 9 mm WALL

The type A-1 plants explored the range of steam reformer power from 13% to 58.4%. Table G-7 shows the key variations in plant parameters, as well as some of the more important results of the study.

The use of an advanced catalyst was considered with the A-1b cases. The concept of an advanced catalyst is that of removing two limitations of the present steam reformer catalyst and tube design. First, the present catalyst life is between two and eight years, much less than the 30-40 year design life of the entire plant. The replacement of catalyst requires both costly shutdowns as well as requiring that the reformer tube be accessible enough and of such a size that the periodic catalyst removal is feasible. In addition, the present 90 mm I.D. tubes which permit catalyst removal are heat transfer limited rather than reaction rate limited. For the optimization part of this study, an "advanced" catalyst is one which by unspecified means, allows a reduction in tube diameter to a point where the reaction rate may limit heat transfer and also allows either in-place catalyst regeneration or 30 plus year catalyst life, thus permitting the use of a welded shut reformer tube. Table G-8 shows the comparison between the 90 mm reference duplex tubes and hypothetical 50 mm advanced catalyst plants. Note the significant gain in all important parameters. (See also Appendix E)

The effect of an integrated PCRV was investigated by redesigning the PCRV to hold modules within pods in the PCRV. Figure G-1 shows the fit of the twelve modules used for the A-1a2 reference plant into an integrated PCRV. The key change in parameters for this plant was an 11.1% increase in capital cost, and a 9% increase in thermal energy cost and electrical energy cost.

For comparison purposes, two plant designs were examined in which single wall reformer tubes were used. These plants, the A-2 cases, show what the economic penalties are in using either a duplex tube or IHXL plant design. They are based on German (KFA) design, but sized for the same conditions as the A-1a2 reference DSR plant. Two tube wall thicknesses were evaluated, an optimistic 9 mm wall, half of a duplex tube, and a more realistic 12 mm wall tube. For comparison, one KFA designed single wall reformer tube had an I.D. of 100 mm and a wall thickness of 15 mm. Table G-9 compares these two designs with the

TABLE G-7

A-1a PLANT DESIGN VARIATIONS

Parameter		A-1a1	A-1a2	A-1a3
Power to Reformer,	%	13	35.6	58.4
Power to CHP User,	MWt	394	1080	1772
Electric Power,	MWe	932	591	241
Height of Reactor Building,	m	51.2	52.7	54.9
Diameter of Reactor Building,	m	46.3	48.2	50.0
SRA/SGA Module				
Diameter of Shell,	m	3.00	3.83	4.82
Height of Shell,	m	18.85	20.54	22.53
Total Weight,	Mg	166.5	371.9	736.6
Number of 90 mm DSR Tubes,	-	77	270	606
Steam Generator Surface Area,	m^2	1275	1221	1333
Total Plant Investment,	$\$x10^{-6}$	695.6	723.0	813.4
Thermal Energy Cost,	¢/MBTU	326	284	305
Electrical Energy Cost,	¢/KWH	1.63	1.72	1.92

TABLE G-8

A-1b PLANT DESIGN VARIATIONS

PARAMETER		A-1a2	A-1b2	A-1a3	A-1b1
Duplex Tube I.D.	, mm	90	50	90	50
Power to Reformer	, %	35.6		58.4	
Power to CHP User	, MWt	1080		1772	
Electric Power	, MWe	591		241	
Height of Reactor Building,	m	52.7	51.8	54.9	53.0
Diameter of Reactor Building,	m	48.2	46.9	50.0	48.5
SR/SG Assembly					
Diameter of Shell	, m	3.83	3.27	4.82	3.99
Height of Shell	, m	20.54	19.42	22.53	20.85
Number of Tubes	-	270	423	606	951
Total Weight	, Mg	372	234	737	430
Steam Generator Area	, m^2	1221	1221	1337	1333
Total Plant Investment	, $\$x10^{-6}$	723.0	667.4	813.4	690.6
Thermal Energy Cost	, ¢/MBTU	284	263	305	262
Electrical Energy Cost	, ¢/KWH	1.72	1.59	1.92	165

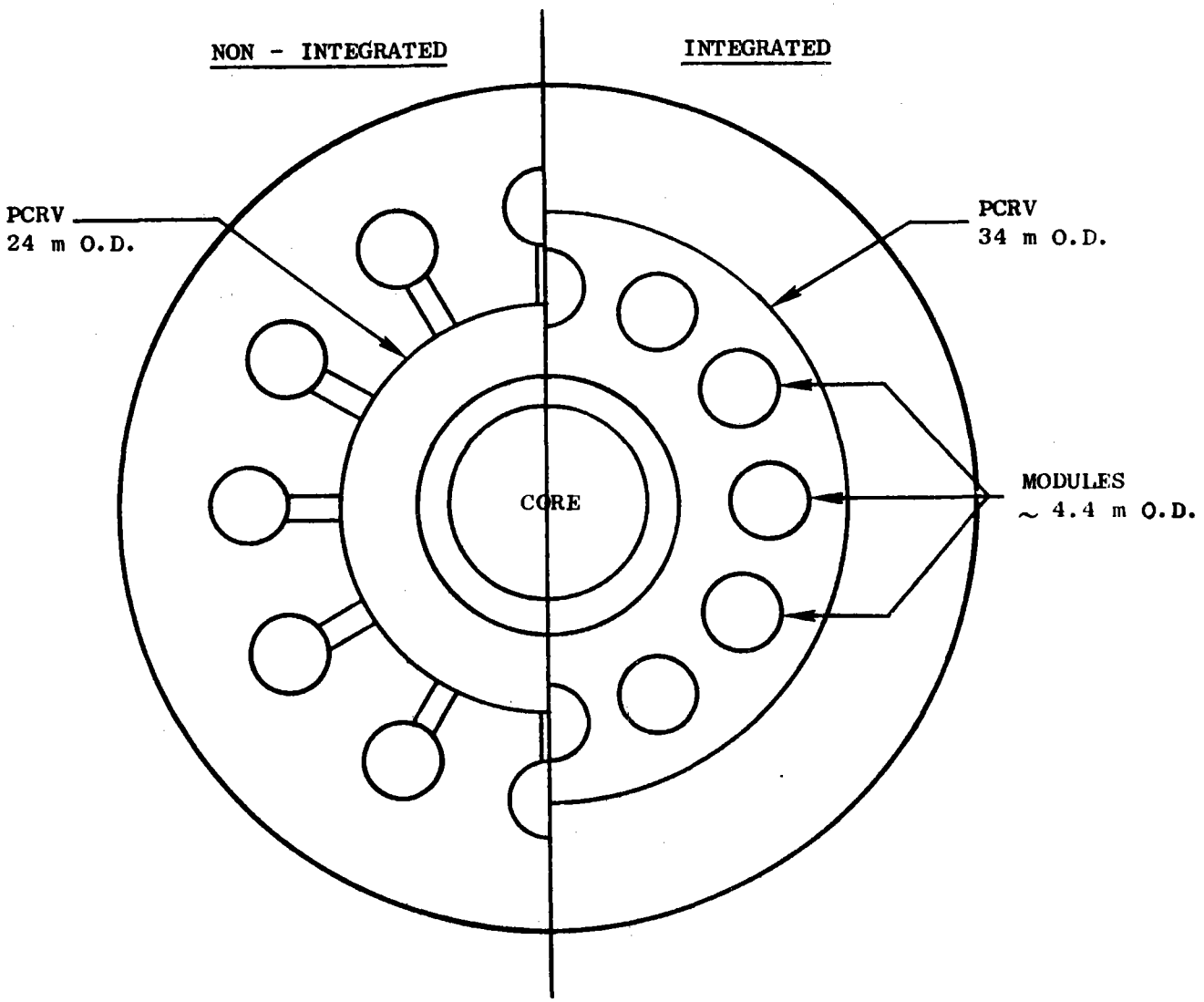

Figure G-1. Sections Through a 3000 MW_{th} Pebble Bed Reactor Showing Both Integrated & Non-integrated Design Concepts.

TABLE G-9

A-2 PLANT DESIGN VARIATIONS

PARAMETER	A-2a	A-2b	A-1a2
Tube I.D., mm	90		
Tube Wall Thickness, mm	9	12	18
Power to Reformer, %	35.6		
Power to CHP User, MWt	1080		
Electric Power, Net, MWe	591		
Height of Reactor Building, m	52.4	52.5	52.7
Diameter of Reactor Building, m	46.0	75.5	48.2
SR/SG Assembly			
Diameter of Shell, m	3.48	3.60	.83
Height of Shell, m	20.12	20.30	30.54
Number of Tubes, -	234	236	270
Steam Generator Area, m^2	1221		
Total Weight, Mg	234	272	372
Total Plant Investment, $\$x10^{-6}$	671.6	686.0	723.0
Thermal Energy Cost, ¢/MBTU	268	272	284
Electrical Energy Cost, ¢/KWH	1.62	1.65	1.72

reference DSR plant, with its 18 mm total wall thickness. Note that the maximum savings in energy cost is about 6% for the optimistic 9 mm case and only 4% for the 12 mm case.

The plant design utilizing an intermediate heat exchanger loop (the A-3 plant) has more potential degrees of freedom available than any of the other steam reforming plants. From the systems standpoint the following choices were made. Figure G-2 shows a simplified flow schematic with two potential steam generator locations indicated. The IHX and the No. 1 steam generator are both located inside the reactor building while the steam reformer and the No. 2 SG are located outside. The feed to the steam reformer consists of methane and steam. If the source of steam is the No. 1 SG, a leak in it could cause, under special conditions, contamination of the product gas. More likely, because of the high steam pressure, a leak would release water into the core, where the graphite could react in an unfavorable way. This would be true even if the steam from the No. 1 steam generator were used only for electrical power generation. Table G-10 shows the comparative advantages and disadvantages of locating part (or all) of the steam generation capacity in the primary loop. The prime advantage is that the IHX is smaller, in that it only transfers the thermal energy needed for the steam reformer, e.g. 89 MW per unit versus 250 MW for the 35.6% plant. In contrast, the following disadvantages occur with an IHX in the primary loop. First, a source of high pressure steam is now located within the primary reactor boundary. Second, since the steam generator tubing consists of a single wall, there is reduced isolation between the reactor fuel and the outside world with respect to fission products and tritium. In the case of an all-electric loop, this is probably acceptable, since another loop (the steam generator condenser cooling circuit) exists between the reactor and the energy customers. For steam reformer use, a reboiler would be necessary, as we have shown in the duplex steam reformer plants. Thirdly, as a result of transferring only the highest temperature energy by means of the IHXL, the secondary return gas is at least 600°C (1112°F) and more likely around 690°C (1274°F). This causes two serious problems. First, the secondary circulator is now a high temperature device (but not necessarily impossible) like a turbine. Second, the secondary pumping power is increased because of the higher volume of flow required.

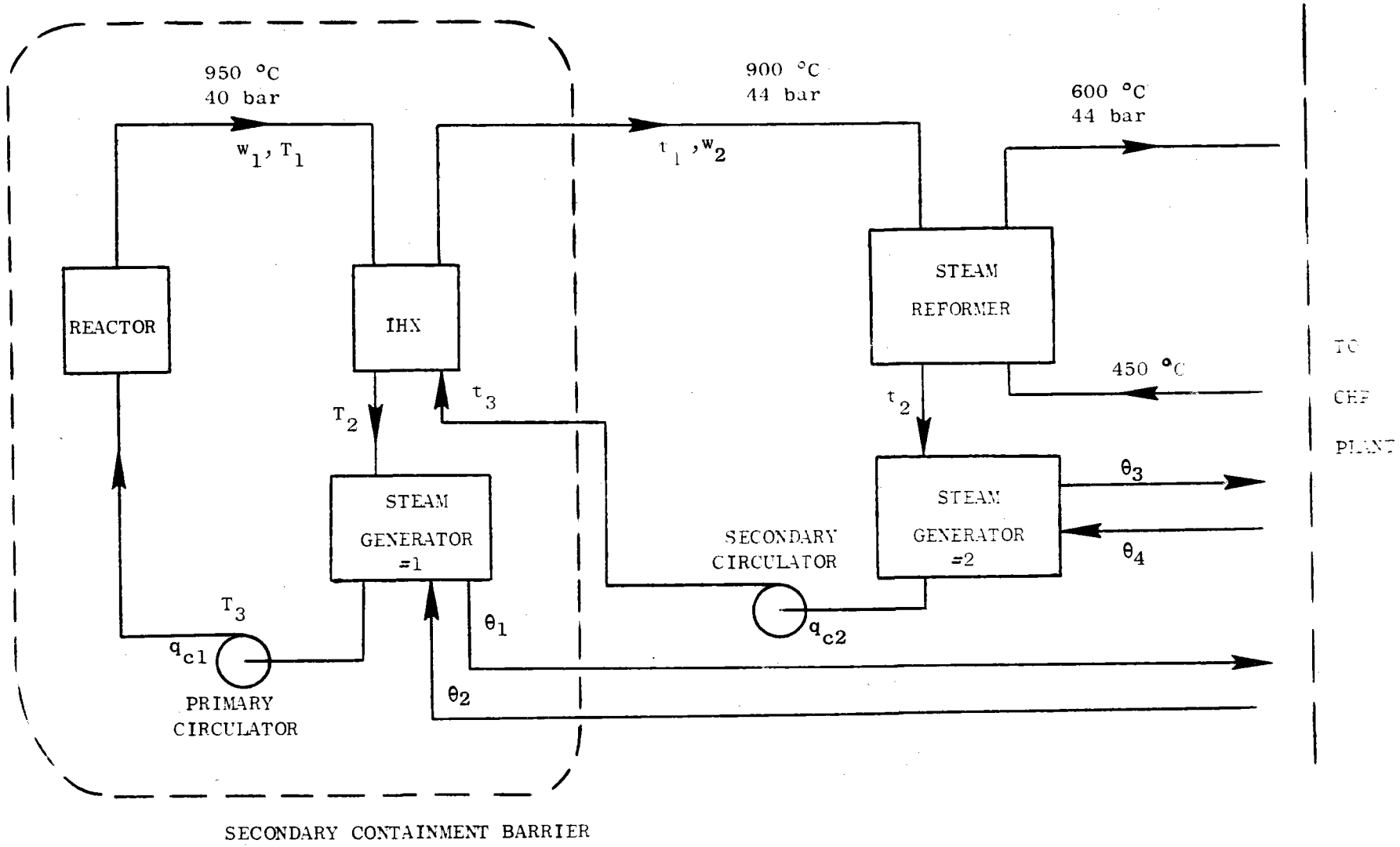

Figure G-2. Steam Reforming Plant with Intermediate Heat Transfer Loop. (Schematic)

TABLE G-10

COMPARISONS OF STEAM GENERATOR LOCATIONS IN PRIMARY LOOP

ADVANTAGES

- Reduces size of IHX

DISADVANTAGES

- Places a source of steam in primary loop
- Reduces isolation between core and customer for fission products and/or tritium
- Increases secondary circulator power
- Increases secondary circulator temperature

In summary, the use of a single steam generator in the secondary loop, with the requirement of transferring the full 250 MWt per loop, does not appear an unrealistic requirement.* As seen in Appendix C, a reasonable IHX configuration was in fact designed. The details are given there and will not be repeated here.

Another variable which was fixed for the IHX plant was the temperature difference between the core exit helium temperature and the peak intermediate loop temperature. As mentioned above, the core exit temperature was fixed at 950°C. The kinetics of the steam reformer are such that it is important to keep the SR inlet gas temperature as high as possible. There is a trade-off between maintaining a low ΔT in the IHX, thereby increasing its size drastically and having a fairly small reformer unit, and specifying a large ΔT for the IHX, thereby decreasing its size and increasing the steam reformer. The compromise reached was to use a ΔT of 50°C, giving a reformer inlet temperature of 900°C (1652°F). The steam reformer module (see Appendix E) had 33% more tubes than the corresponding non-IHXL plant, and weighed 25% more, both changes being caused by the 50°C lower inlet helium temperature.

Table G-11 shows the comparison between the A-1a2 reference plant and the A-3 IHXL plant. Note that the cost of energy is 17% higher for the IHXL plant than for the DSR reference plant. Much of this is due to the extra heat transfer equipment, e.g., the IHX and associated piping. Some of the higher energy cost is due to the extra electric power needed to run the secondary circulators.

---

*A rough calculation showed that the maximum savings in capital cost would be about 1% if <u>all</u> of the steam needed for electric power were generated in a primary loop steam generator.

TABLE G-11

A-3 PLANT DESIGN VARIATIONS

PARAMETERS		A-1a2	A-3
Type Plant		Duplex Steam Reformer	IHXL
Power to Reformer	, %	35.6	
Power to CHP User	MWt	1080	
Net Electric Power	MWe	591	547
Height of Reactor Building, m		52.7	51.2
Diameter of Reactor Building, m		48.2	50.0
Primary Heat Transfer Module			
Type		DSR/SGA	IHX
Diameter of Shell	m	3.83	4.78
Height of Shell	m	20.54	13.68
Total Weight	Mg	372	232
Total Plant Investment	$\$x10^{-6}$	723	800.8
Thermal Energy Cost	¢/MBTU	284	333
Electrical Energy Cost	¢/KWH	1.72	1.88

G.5 SYSTEM SELECTION

Table G-12 shows the evaluation criteria used to select the "best" steam-methane reforming plants. The approach used for the selection process was to divide the various criteria into "needs" and "wants". Essentially a plant had to meet all "needs" criteria, and then was rated on the "wants" criteria. In addition, for those plants which meet the mandatory criteria, the two key items which affect the selection are the cost of energy, and the required development programs. Table G-13 compares all nine plants.

The two single wall reformer plants are disqualified on the basis of not providing sufficient barriers between the customer and the reactor fission products, including tritium. All other plants meet the mandatory criteria.

Among the desired criteria, there is a trade-off between the excellent projected plant availability of the advanced catalyst plants with their long term catalyst life and the development programs required to prove out the advanced catalyst concept.

The key economic criterion is delivered energy cost. The following statements are pertinent. First, in a comparison between the IHX plant (A-3) and those plants which deliver the same amount of energy, the IHX plant is clearly more expensive. Second, the advanced catalyst plants (A-1b1 and A-1b2) are clearly superior to the reference plants at the same power ratings. Third, the integrated PCRV plant (A-1c) is more costly than its non-integrated counterpart (A-1a2). Lastly, within the power range covered by the 90 mm DSR plants, the 35.6% power-to-reformer plant (A-1a2) is slightly superior to the 58.4% plant (A-1a3).

The selected plant is thus the A-1a2 reference plant, with the second choice being the advanced catalyst plants, A-1b1 and A-1b2, when the advanced catalyst is developed.

TABLE G-12

VHTR-THX PROGRAM

EVALUATION CRITERIA

STEAM-METHANE REFORMING PLANTS

MEASUREMENT (CRITERION)	
SAFETY -	CHEMICAL EXPLOSION FISSION PRODUCT CONTAMINATION SEISMIC
CAPITAL COST Δ -	INCLUDES PIPES, DUCTS, VALVES, CLEANUP LOOPS, ETC.
ENERGY COST -	COST OF THERMAL ENERGY LESS ELECTRIC CREDIT
MAINTENANCE -	
REPAIRABILITY -	
WEIGHT -	
RELIABILITY -	
PLANT AVAILABILITY -	
HYDROGEN DIFFUSION -	H_2 TO REACTOR HELIUM T_2 TO PROCESS GAS
REQUIRED DEVELOPMENT PROGRAM-	

TABLE G-13

OVERALL PLANT EVALUATION

	PLANT DESCRIPTION								
	A-1a1	A-1a2	A-1a3	A-1b1	A-1c	A-2a	A-3	A-2b	A-1b2
Plant Description									
Type of Primary Heat Transfer	DSR	DSR	DSR	DSR	DSR	SR	IHX	SR	DSR
Power to Steam Reformer, %	13	35.6	58.4	58.4	35.6	35.6	35.6	35.6	35.6
Steam Reformer Tube I.D., mm	90	90	90	50	90	90	90	90	50
Containment Method	Non-Int.	Non-Int.	Non-Int.	Non-Int.	Integrated	Non-Int.	Non-Int.	Non-Int	Non-Int.
Notes		Reference				9mm wall		12mm wall	
Mandatory Criteria ("Needs")									
Safety									
Chemical Explosion	✓	✓	✓	✓	✓	✓	✓	✓	✓
Fission Product Contamination	✓	✓	✓	✓	✓	X	✓	X	✓
Maintenance	✓	✓	✓	✓	✓	✓	✓	✓	✓
Repairability	✓	✓	✓	✓	✓	✓	✓	✓	✓
Reliability	✓	✓	✓	✓	✓	✓	✓	✓	✓
Hydrogen Diffusion (Tritium)	✓	✓	✓	✓	✓	X	✓	X	✓
Desirable Criteria ("Wants")									
Plant Availability	Fair	Fair	Fair	Excellent	Fair	-	Good	-	Excellent
Component Weight	Excellent	Good	Poor	Good	Excellent	-	Excellent	-	Excellent
Required Development Program	Good	Good	Good	Fair	Good	-	Moderate	-	Fair
Economic Criteria									
Capital Cost, $\$x10^{-6}$	696	723	813	691	806	-	801	-	667
Delivered Thermal Energy Cost, ¢/MBTU	326	284	305	262	310	-	333	-	263
Delivered Electrical Energy Cost, ¢/KWH	1.63	1.72	1.92	1.65	1.87	-	1.88	-	1.59
Economic Rank (Based on Energy Cost)	4	2	3	1	3	-	4	-	1

REFERENCES

G-1 Tschamper, P. M., "The VHTR for Process Heat", General Electric, GEAP-14018, September 1974.

G-2 The Pebble Bed High Temperature Reactor as a Source of Nuclear Process Heat, Volume 1, 2 and 4, Conceptual Design, R. Schulten, et. al, October 1974.

G-3 Woike, O. G., "Small Nuclear Process Heat Plants (SNPH) Using Pebble Bed Reactor", General Electric Company, GEEST 75-001, November 1975.

G-4 "Special Issue: High Temperature Reactor for Process Heat Applications", Nuclear Engineering and Design, Volume 34 (1975), No. 1.

APPENDIX H

COSTING BASIS AND ASSUMPTIONS

TABLE OF CONTENTS

TABLE OF CONTENTS (Cont'd)

LIST OF FIGURES

LIST OF TABLES

APPENDIX H

COSTING BASIS AND ASSUMPTIONS

H.1 INTRODUCTION

The purpose of this appendix is to describe the methods and assumptions used to arrive at investment costs and energy costs for the eight different plants (seven steam reforming and one coal gasification) which were developed during the course of this study. Costing was performed primarily to enable each plant to be evaluated on a consistent basis, so that the absolute values obtained were of secondary importance to the cost differentials between plants.

The costs for most portions of the plant were based on prior studies, both by GE and by others. Much material was taken from unpublished data files. The prior studies included:

1) The 1974 GE and GA VHTR studies (H-1, H-2).

2) The 1975 GE SNPH study (H-3)

3) The 1973 UE&C HTGR cost study, WASH-1230, Volume V (H-4)

Costs were escalated to January 1976 using, primarily, the Handy-Whitman Index, Reference H-5. All costs are related to the ERDA (AEC) Middletown site as described in reference H-6. The format for capital cost presentation is that used by the CONCEPT code (H-7), although the CONCEPT code was not employed for the actual calculations. The cost basis was for developed components, taking into account learning curves, and specifically not accounting for development programs or escalation past January 1976.

The methodology used was to recognize that most of the cost variation between plants occurs in one sub-account, 222, Main Heat Transport Equipment, which is, of course, the primary purpose of the entire study. The rest of the plant was modeled by a simple set of equations to account for the variations caused by the different heat

transport equipment. For example, the secondary containment building was varied to account for different size heat transfer modules, and the cost of this component varied accordingly.

The cost of the heat transfer equipment was estimated in more detail. The weights of the various component parts was calculated and used as the basis for costing. In this fashion, a reasonably accurate cost for all heat transfer components was achieved.

In summary, this method should be expected to accurately show the cost trends between various design concepts, even though the absolute costs may not be as accurate.

H.2 PLANT COST MODELS

Plant capital cost and the multipliers necessary to develop a consistent investment cost were developed according to the format shown in Table H-1. The indirect costs and the spare parts and contingency allowance were all calculated as a percent of the basic direct costs. The sections following describe each direct cost classification.

H.2.1 LAND AND LAND RIGHTS (ACCOUNT NO. 20)

Land and land rights were fixed for all 3000 MWt plants at $1,000,000. This is consistent with most recent investment cost studies.

H.2.2 STRUCTURES AND IMPROVEMENTS (ACCOUNT NO. 21)

This account includes the components shown in Table H-2, consisting of almost all the building and structures not directly incorporated into another component.

The cost model was broken into three portions:

1) The reactor containment building,

2) The turbine building and turbine service building, and

3) All other components, which were fixed.

TABLE H-1

COST ACCOUNT FORMAT

ACCOUNT NUMBER	ACCOUNT TITLE	
	DIRECT COSTS	
20	Land and Land Rights	$
	PHYSICAL PLANT	
21	Structures and Site Facilities	
22	Reactor Plant Equipment	
23	Turbine Plant Equipment	
24	Electric Plant Equipment	
25	Miscellaneous Plant Equipment	
26	Special Materials	
	Subtotal	$
	Spare Parts Allowance	
	Contingency Allowance	
	Subtotal	$
	INDIRECT COSTS	
91	Construction Facilities, Equipment, and Services	
92	Engineering and Construction Management Services	
93	Other Costs	
94	Interest During Construction	
	Subtotal	$
	TOTAL PLANT CAPITAL INVESTMENT -	$

TABLE H-2

ITEMS IN ACCOUNT 21

ACCOUNT NUMBER	ACCOUNT TITLE
21	Structure and Site Facilities
211	Site Improvements and Facilities
212	Reactor Containment Building
213	Turbine Building
214	Intake and Discharge Structures
215	Reactor Service Building
216	Radioactive Waste Building (in 215)
217	Fuel Storage Building (in 215)
218	Other
218A	Control Room Building
218B	Diesel Generator Building
218C	Administration Building
218D	Turbine Service Building
218E	Helium Storage Building (in 212)
218F	Diesel Fuel Storage Building

The reactor containment building cost was based on the volume of concrete required, which in turn depends on the height, diameter, and thickness. These dimensions are derived from the space needed for the reactor, heat transfer equipment, and lift space for components (crane height). The simple formula below matched available cost data quite well.

$$\text{Cost (\$)} = 200 \times H \times D \times t$$

with all dimensions in feet. This formula is appropriate to secondary containment using reinforced concrete construction, not prestressed construction.

The turbine related building costs were fitted to a six-tenths power equation, giving:

$$\text{Cost (\$)} = 137712\ P^{0.6}$$

where P is the gross steam turbine power in MWe.

The remainder of the account 21 costs were estimated at $37,600,000. Thus the total cost for account 21 is given by:

$$C_{21}(\$) = \$37{,}600{,}000 + 200 \cdot H \cdot D \cdot t + 137712 P^{0.6}$$

where the independent variables have been described above.

H.2.3 REACTOR PLANT EQUIPMENT (ACCOUNT 22)

This account class comprises 50% of the total direct cost of the plants, typically, and hence is the key cost class from a comparison standpoint. Table H-3 shows the important elements of this account.

Account 222, Main Heat Transfer and Transport System is discussed separately in Section H.3, while the rest of this section discusses the balance of account 22.

H.2.3.1 Reactor Equipment (Account 221)

The key reactor equipment components are the PCRV and the reactor internals. Of these the PCRV is typically the most expensive component.

TABLE H-3

ITEMS IN ACCOUNT 22

ACCOUNT NUMBER	ACCOUNT TITLE
22	Reactor Plant Equipment
221	Reactor Equipment
221.1	Reactor Vessels and Accessories
221.11	PCRV Support Structure
221.12	PCRV Structure
221.13	Reactor Internals
221.16	PCRV Pressure Relief System
221.2	Reactor Control Devices
221.3	Moderator/Reflector Systems (in 221.13)
221.4	Reactor Shielding (in 221.12)
222	Main Heat Transfer and Transport Systems
223	Safeguards Cooling Systems
224	Radwaste Treatment and Disposal
225	Nuclear Fuel Handling and Storage Systems
226	Other Reactor Plant Equipment
227	Instrumentation and Control

Three elements were used to determine the PCRV cost. These are: the volume of concrete, the area of the cavities which must be lined with insulation and water cooling tubes, and the lease cost of the wire tensioning device. A relation which gave a reasonably good fit to the available data is:

1) Concrete Cost $\$510/yd^3$

2) Liner Cost $\$1100/ft^2$

3) Wire Winding Machine $\$272*A_{PC}^{0.77}$
(where A_{PC} is outer side area of PCRV in feet.)

These relationships account for the significantly different costs between single cavity PCRV's using external heat transfer modules, and multi cavity (integrated) PCRV's with many void spaces and ducts which all must be fitted with liners and insulation in the field under possibly difficult conditions.

The PCRV support cost was estimated using a simple power law:

$$C(\text{PCRV support}) = \$391 \times D^{1.513}$$

(where D is the PCRV outer diameter in feet)

This cost does not account for the fast discharge system shown in Section 2 and Appendix F. However, this item would be a constant adder to all plants considered, and would not change any conclusions reached concerning cost differences.

The PCRV pressure relief system was estimated as a constant $250,000 for all plants.

The reactor internals, consisting primarily of the graphite and coalstone structure within the main cavity of the PCRV and all attachment hardware were estimated as $1328 per square feet of primary cavity surface area. The controls for a 3000 MW_{th} PBR were estimated to cost $9,200,000. Thus the total cost of account 221 is given by:

$$C(221) = \$9,450,000 + 391D^{1.513} + 510\ V_C + 1100\ A_L + 272\ A_{PC}^{0.77} + 1328\ A_C$$

where

D = PCRV O.D., ft

V_C = Concrete Volume, yards^3

A_L = Liner area, ft^2

A_{PC} = PCRV outer surface area, ft^2

A_C = Primary (reactor) cavity area, ft^2.

H.2.3.2 Balance of Account 22

The balance of account 22, excluding account 222, consists of the following accounts.

223 Safeguards Cooling Systems
224 Radwaste Treatment and Disposal
225 Nuclear Fuel Handling and Storage
226 Other Reactor Plant Equipment
227 Instrumentation and Control

Although a wide range of cost estimates for individual accounts have been quoted in recent reports, the total of all of these should be about $60,000,000. A $\pm$ 10% variation covers almost all recent gas reactor estimates.

H.2.4 TURBINE PLANT EQUIPMENT (ACCOUNT 23)

As discussed in Section 2 and Appendix A, all process heat plants produce electric power using modern steam turbine equipment. The turbo-generator alone accounts for half of the total cost, and excellent data from other General Electric components was available for this cost. The gross electrical output was used as the parameter in the following equation.

$$C(23) = \$8,912,000 + P(MWe) \times 79,400$$

For plants with no electric power generation, the entire account is zero. The equation fits the range of approximately 300 MWe to over 1500 MWe.

H.2.5 ELECTRIC PLANT EQUIPMENT (ACCOUNT 24)

This class includes the balance of the electric plant not directly associated with the turbogenerators. In a plant producing no power, a sizeable electric plant is still required to account for the power used, such as circulators (∿40 MWe), and balance of the reforming plant. As an example, the reference plant consumes approximately 126 MWe. Thus the cost of account 24 was estimated as:

$$C(24) = \$12,949,000 + 17307*P$$

where P is the gross generated electric power in MWe.

H.2.6 MISCELLANEOUS POWER PLANT EQUIPMENT (ACCOUNT 25)

The miscellaneous power plant equipment is more nearly a function of the thermal power of the plant, which in this study is constant at 3000 MWt. Hence a constant cost was used for this estimate of $10,236,000.

H.2.7 SPARE PARTS AND CONTINGENCIES

Spare parts and contingencies were accounted for by multiplying the sum of the previous accounts 21-25 by a percentage derived from prior studies.

Spare Parts = 0.614%
Contingencies = 11.931%

H.2.8 INDIRECT COSTS

The indirect costs consist of four classes:

91 Construction Facilities, Equipment, and Services
92 Engineering and Construction Management Service
93 Other Costs
94 Interest During Construction

For the first three classes, fixed percentages, roughly equivalent to those given in WASH 1345, Figure 6, Reference H-8, were used. In the range of interest, these curves of fractional cost versus direct cost are nearly constant, thus validating the use of a single value. The following percentages were applied to the total of all direct costs plus spare parts and contingencies, but not including land cost.

Account 91, 5.7%
Account 92, 14.5%
Account 93, 4.5%

For account class 94, interest during construction, curves of percent cost spent versus percent time were generated similar to those in reference H-6 and shown in Figure H-1. By applying simple interest to this curve, the total percent cost associated with a given interest rate was calculated. Figure H-2 shows the percent increase in cost as a function of interest rate. For this study, an interest rate of 8% was chosen, giving a 30.7% total cost multiplier for account 94. This multiplier is applied to entire cost, direct, land, and indirect, to arrive at the total interest during construction.

H.3 HEAT TRANSFER COST MODELING

Cost account 222 contains the key elements in this study as listed in Table H-4. The key items which make up these elements were:

1) Helium Circulators,
2) Steam Reformer/Steam Generator Modules,
3) Intermediate Heat Exchangers, and
4) Pipes, Ducts, and Valves.

H.3.1 HELIUM CIRCULATORS

Helium circulator costs were based on prior studies. These units are described in Section 2 and Appendix E, and consist of an electric motor, a radial flow, single stage compresser, and necessary seals and support hardware. The relationship used for circulator cost was:

$$C_{CIRC}\ (\$) = \$254{,}080\ Q^{0.6}$$

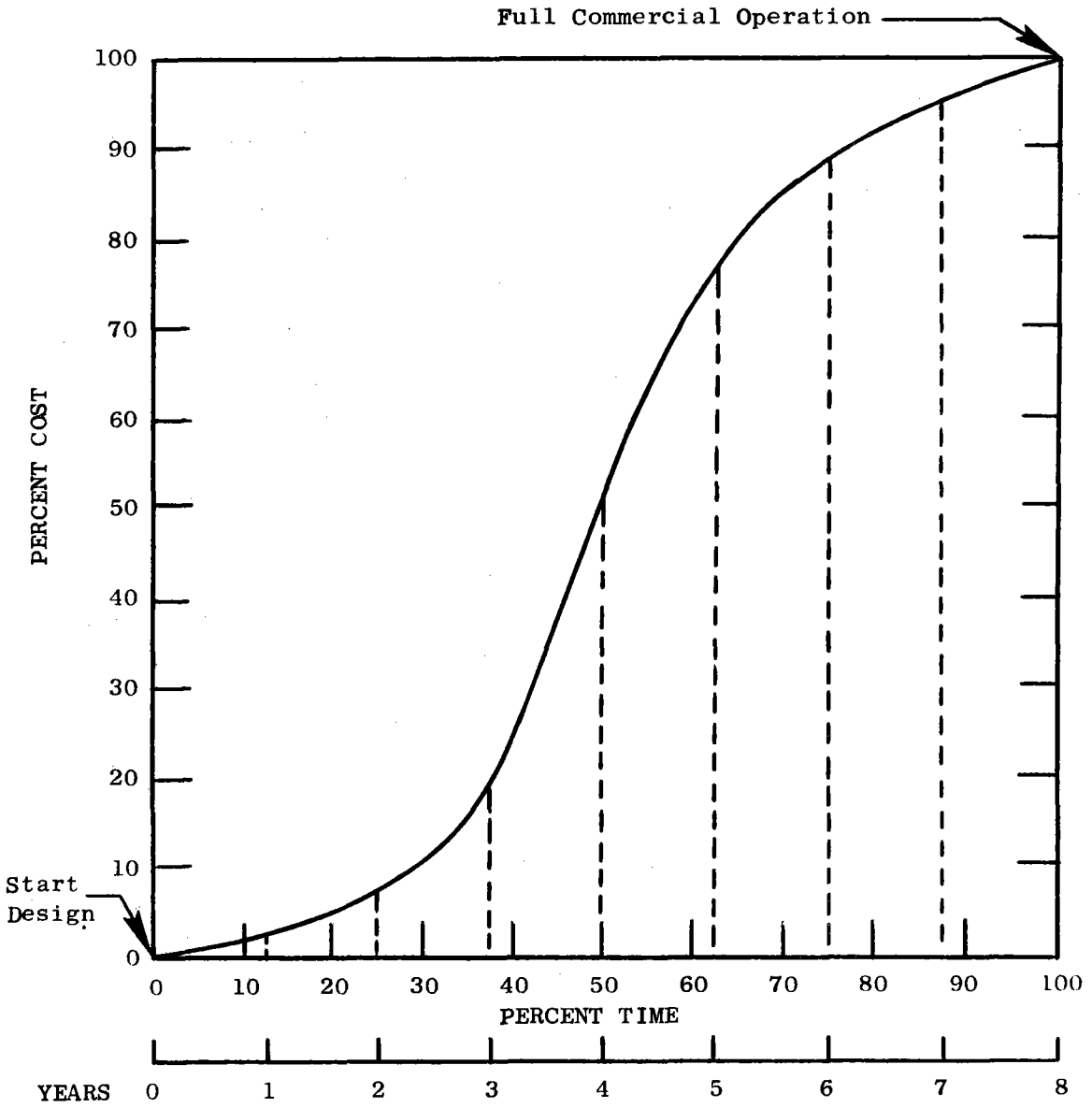

Figure H-1. Plant Capital Investment Expenditures vs. Time.

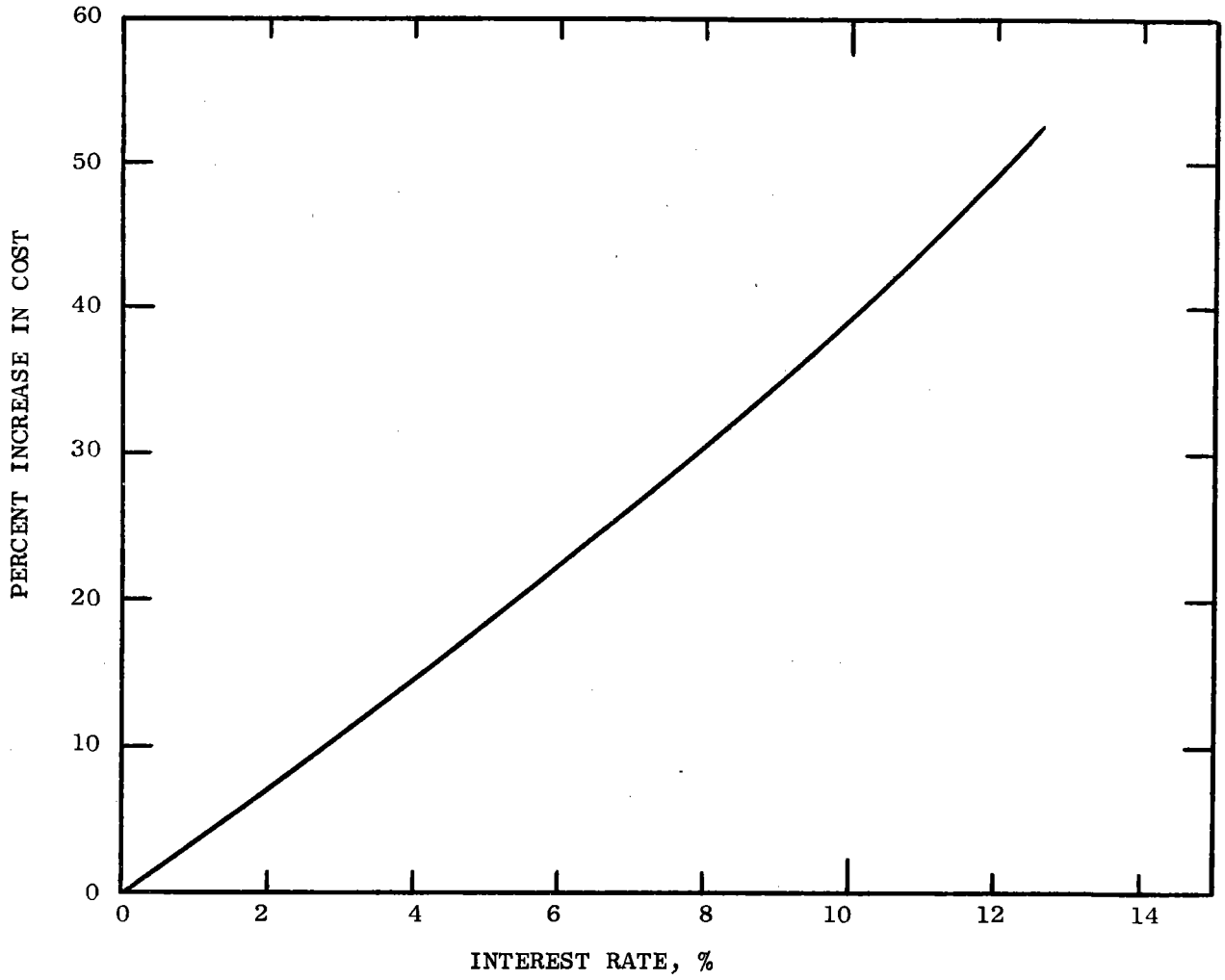

Figure H-2. Interest During Construction vs. Interest Rate.

TABLE H-4

ITEMS IN ACCOUNT 222

ACCOUNT NUMBER	ACCOUNT TITLE
222	Main Heat Transfer and Transport System
222.1	Reactor Core Coolant Systems
222.11	Main Helium Circulator System
222.12	Helium Duct Piping System - Primary
222.13	Steam Reformer/Steam Generator
222.14	Intermediate Heat Exchanger
222.15	Steam and Feedwater Lines and Valves
222.16	Hydrogen, Methane, etc. Piping & Valves
222.2	Reactor Secondary Heat Transport System
222.21	Secondary Helium Circulator System
222.22	Secondary Helium Piping System
222.23	Steam Reformer/Steam Generator
222.24	Steam and Feedwater Lines and Valves
222.25	Hydrogen, Methane, etc. Piping and Valves

where Q is the required pumping power in MW. This is approximately $75/HP at 13,600 HP. The majority of circulators in this study were between 2 and 7 MW each (∿2700 - ∿9400 HP) and costing between ∿143/HP to $87/HP.

H.3.2 STEAM REFORMER/STEAM GENERATOR MODULES

Appendix E has a quite complete description of the different steam reformer/steam generator modules used in this study. Costs were based on dividing these modules into five components and costing each separately. The five components are:

1) The Pressure Vessel,
2) The Main Tube Sheet,
3) The Steam Generator Bundle
4) The Duplex Tube Reformer Tubes, and,
5) The Internal Flow Dividers and Structure.

All costs include multipliers (overhead) to account for delivery, installation, and site materials.

H.3.2.1 Pressure Vessel Costs

Pressure vessel costs were determined from the estimated cost of LWR pressure vessels designed as primary Class I nuclear vessels. A cost of $8/lb covers all phases including fabrication, inspection, shipping and installation. This cost is applied to the entire weight of the vessel including flanges and heads. Thicknesses were based on the same nominal stresses used for LWR vessels.

H.3.2.2 Tube Sheets

A cost of $12/lb of solid tube sheet was used to account for the machinery and attachments of the steam reformers to the tube sheets. For some designs, the pitch-to-diameter ratio is so small, that the manufacture and assembly will be a difficult task, thus requiring extensive inspection and difficult welding.

H.3.2.3 Steam Generators

All steam generator tubing was 25.4 mm O.D. with a 3.18 mm wall. Based on tubing quotes for conventional boiler tubes and an estimated fabrication and inspection cost, an overall allowance of $15/lb was used.

H.3.2.4 Steam Reformer Tubes

Based on a learning curve analysis from quotes received for the DSR task of this contract, the reference 90 mm I.D. duplex tube, complete with catalyst and pigtail, was estimated to cost $9,000 per tube. The 50 mm I.D. tubes using an advanced catalyst were estimated at $3108/tube. (They weigh approximately one-third that of the 90 mm) Single wall 90 mm I.D. tubes with a 12 mm wall were costed at $5664 per tube.

H.3.2.5 Module Internals

A rough estimate of the internals was made by assuming a cylinder around the steam reformer bundle with a 25.4 mm thickness, calculating the weight and costing at $9/lb.

H.3.2.6 Summary

Table H-5 shows the weights and costs for the six modules listed in Table E-1 of Appendix E.

H.3.3 INTERMEDIATE HEAT EXCHANGERS

The same cost breakdown and component costs were used for the IHX calculations. However, the costing was performed by means of a computer program and is reported in Appendix C.

H.3.4 PIPES, DUCTS, AND VALVES

The pipes, ducts, and valves required for the various plants come under three general classes:

1) Steam Pipes, and Valves,
2) Hydrogen/Methane Pipes, and
3) Helium Ducts.

TABLE H-5

STEAM REFORMER/STEAM GENERATOR MODULE

COST AND WEIGHT DATA

Design No.	1	2	3	4	5	6
Percent Power to Reformer	13	35.6	35.6	58.4	58.4	35.6
Type	DSR	DSR	SR	DSR	DSR	SR/IHX
Diameter of Tube, I.D.,mm	90	90	90	90	50	90
Number of Reformer Tubes	77	270	234	606	951	312
Pressure Shell Height, m	18.85	20.54	19.86	22.53	20.85	20.50
Pressure Shell Diameter, m	3.00	3.83	3.48	4.82	4.00	3.81
Steam Generator Surface,m^2	1275	1221	1221	1333	1333	1260
Component Weights, Mg						
Pressure Vessel	68.2	124.0	99.5	220.4	137.3	122.3
Tube Sheet	13.1	37.9	26.6	89.9	43.9	37.0
Steam Generator	27.4	26.3	26.3	28.7	28.7	27.1
Duplex Tubes	46.8	164.2	65.2	368.4	199.7	86.9
Internals	11.0	19.5	16.7	29.2	20.9	19.4
Total	166.5	371.9	234.3	736.6	430.4	292.7
Component Costs, Thousands of Dollars						
Pressure Vessel	1203.6	2187.9	1754.3	3887.1	2421.4	2156.4
Tube Sheet	346.6	1001.9	704.9	2377.8	1160.4	979.7
Steam Generator	907.8	869.0	869.0	948.9	948.9	896.9
Duplex Tubes	693.0	2430.0	964.5	5454.0	2955.7	1286.0
Internals	218.8	387.4	332.3	580.2	414.9	384.1
Total	3369.8	6876.2	4625.0	13248.0	7901.3	5703.1

H.3.4.1 Steam Pipes and Valves

The steam pipes, feed water pipes and associated valves are entirely conventional in design, except for required "N" stamps. The steam conditions of 538°C (1000°F) at 238 b (3452 psi) and the same as those of normal fossil plants. Piping is costed from the reformer module to the secondary containment wall, through the wall using double isolation valves on each line, to a collector outside of the secondary containment.

H.3.4.2 Ducts, Pipes and Valves for Reformer Feed and Product

Costs for the product gas as well as the feed materials ducts were based on a review of the work performed on the SNPH plant (Reference H-3). As shown on the drawings in Appendix F, two smaller pipes traverse the distance from the module to the secondary containment. There they join a larger pipe and are led to the bottom of the wall. Double valves are used for isolation. An outside circulator collector is assumed for costing purposes. Since the feed material is at 450°C (842°F) and the product gas at 600°C (1112°F), reasonable conventional steam pipe technology was assumed for both duct systems. Pipe sizes range from 8-inch for the smaller pipes to 18-inches for the largest pipes. Pipe cost was based on $631/ft for 8" pipe for both temperature conditions, and other sizes were based on that cost. Valves were based on a curve of cost versus diameter with the cost ranging from $16,000 for an 8-inch valve to $65,000 for an 18-inch valve. Table H-6 shows the calculations for the three prime steam reformer plants using duplex tubes. All the other plants were derived from this basis.

H.3.4.3 Helium Ducts for Use with IHX Plant

Helium ducting is based on the German designs used for the HHV facility. These ducts, described in Appendix I, have an internal diameter of 1.0 m, compared to the approximately 0.7 m needed for the mixed flow from a single IHX module. Rough cost estimates indicate that approximately $1,000/ft would be sufficient for these ducts since the high temperature parts are located inside a low-alloy steel, water cooled pressure shell.

TABLE H-6

FEED AND PRODUCT PIPE AND VALVE COST

Plant Reformer Power, %	13	35.6	58.4
Mass Flow per Unit, kg/sec	12.8	35.1	57.6
Single Pipe Size, in.	10	15	18
Twin Pipe Size, in.	8	11	14
Total Plant Single Pipe Length, m	358	358	358
Total Plant Twin Pipe Length, m	343	343	343
Number of Large Valves	24	24	24
Number of Small Valves	24	24	24
Total Plant Costs, Thousands of Dollars			
Large (Single) Pipe	1108.3	2294.8	3183.4
Small (Twin) Pipe	712.2	1261.5	1944.8
Valves	960.0	1824.0	2568.0
Outer Collector	2017.0	3826.2	5307.0
Total Fact. Material	4797.5	9206.5	13003.2
Labor @ 0.38	1823.0	3498.5	4941.2
Site Material @ 0.02	96.0	184.1	260.1
Grand Total	6716.5	12889.1	18204.5

To reach the steam reformer modules outside the secondary containment requires a total of 688 m (2256 ft) for both hot and cold ducts. Since the "cold" duct is at 300°C (572°F), it is costed as a hot duct, although it would undoubtedly be cheaper with a smaller diameter, less insulation, and less water cooling.

Valves were estimated at $120,000 each, and 48 were needed for isolation. The cost calculation is shown below.

Helium Ducts	$2,256,000.
Valves	5,760,000
Total Factory Material	8,016,000
Site Labor at 38%	3,046,080
Site Material at 2%	160,032
Total	$11,222,112.

H.3.5 HEAT TRANSFER COMPONENT COST SUMMARY

Table H-7 summarizes the costs for all of the Account 222 components.

H.4 CAPITAL COST SUMMARY

Table H-8 summarizes the capital costs of nine different plants according to the methods previously described. Seven are the basic designs, while the last two were calculated more approximately to aid in observing the capital cost trends. Figure H-3 shows the capital cost trends for both the 90 mm duplex tube and the 50 mm duplex tube as a function of the percent power to the steam reformer. Note the significant improvement in capital cost due to the 50 mm duplex tube. Figure H-4 shows the effect of the tube wall thickness on capital costs. The duplex tube case is plotted as an 18 mm wall thickness tube to indicate the trend. The plant with an integrated PCRV (A-1c) shows an 11.5% cost increase over the A-1a2 reference design for the same output.

These costs are used in the subsequent section to calculate energy costs.

The plant using an IHXL loop (A-3) shows an 10.8% cost increase when compared with the reference designs at the same product output. However this plant does not produce as much electricity because of the secondary loop electric blowers.

TABLE H-7
VHTR IHX PROGRAM

ACCOUNT 222 TABULATION
Costs in Thousands of Dollars

Account Number	Description	A-1a1 13%/ 90mm DSR	A-1a2 35.6%/ 90mm DSR	A-1a3 58.4%/ 90mm DSR	A-1b 58.4%/ 50mm DSR	A-1c 35.6%/ INT DSR	A-2a 35.6%/ 90mm SWT(9mm)	A-3 35.6%/ 90mm IHXL	A-2b 35.6%/ 90mm SWT(12mm)	A-1b2 35.6%/ 50mm DSR
222	Main Heat Transfer & Transport Systems	73,952	117,615	195,411	131,251	99,013	90,601	158,748	98,206	89,036
222.1	Reactor Core Coolant Systems	73952	117615	195411	131251	99013	90601	59064	98206	89036
222.11	Main Helium Circulator Systems	6263	6263	6909	6909	6263	6263	5268	6263	6263
222.12	Helium Duct Piping System Primary	2880	2880	2880	2880	1500	2880	2880	2880	2880
222.13	Steam Reformer/Steam Generator	40438	82514	158976	94816	65292	55500.	0	63105	53935
222.14	Intermediate Heat Exchanger	0	0	0	0	0	0	50916	0	0
222.15	Steam & Feedwater Lines and Valves	17654	13068	8441	8441	13068	13068	0	13068	13068
222.16	Hydrogen, Methane Piping and Valves	6716	12889	18204	18204	12889	12889	0	12889	12889
222.2	Reactor Secondary Heat Transport System	0	0	0	0	0	0	99684	0	0
222.21	Secondary Helium Circulator System	0	0	0	0	0	0	7536	0	0
222.22	Secondary Helium Piping System	0	0	0	0	0	0	11222	0	0
222.23	Steam Reformer/Steam Generator	0	0	0	0	0	0	68436	0	0
222.24	Steam & Feedwater Lines and Valves	0	0	0	0	0	0	6534	0	0
222.25	Hydrogen, Methane Piping and Valves	0	0	0	0	0	0	5955	0	0

TABLE H-8

CAPITAL COST SUMMARY

Plant A-	1a1	1a2	1a3	1b1	1c	2a	3	2b	1b2
% Power to Reformer	13	35.6	58.4	58.4	35.6	35.6	35.6	35.6	35.6
Type Reformer	90 mm DSR	90 mm DSR	90 mm DSR	50 mm DSR	90 mm DSR	90 mm SR	90 mm SR	90 mm SR	50 mm DSR
Type PCRV	Non-Int	Non-Int	Non-Int	Non-Int.	Integrated	Non-Int	Non-Int	Non-Int	Non-Int
Notes		(Reference)				(9mm Wall)	(With IHXL)	(12mm Wall)	

Acct. No.	Account Title									
	Direct Costs									
20	Land and Land Rights, $	1000	1000.	1000.	1000.	1000.	1000.	1000.	1000.	1000.
	Physical Plant									
21	Structures & Site Facilities	70208	71121.	72379.	69573.	68854.	70097.	72379.	70368.	69378.
22	Reactor Plant Equipment	177240	220902.	298699.	234539.	268380.	193888.	262035.	201493.	192324.
23	Turbine Plant Equipment	90138	65842.	41387.	41387.	65842.	65842.	65842.	65842.	65842.
24	Electric Plant Equipment	30654	25358.	20028.	20028.	25358.	25358.	25358.	25358.	25358.
25	Miscellaneous Plant Equipment	10236	10236.	10236.	10236.	10236.	10236.	10236.	10236	10236.
26	Special Materials	0	0.	0.	0.	0.	0.	0.	0.	0.
	Subtotal, $	378476	393459.	442728.	375762.	438671.	365421.	435850.	373297.	363138.
	Spare Parts Allowance	2325	2417.	2719.	2308.	2694.	2245.	2677.	2293.	2231.
	Contingency Allowance	45156	46944.	52822.	44833.	52338.	43599.	52002.	44539.	43326.
	Subtotal, $	425957	442820.	498270.	422903.	493703.	411265.	490529.	420129.	408695.
	Indirect Costs									
91	Construction Facilities, Equipment, & Services	24280	25241.	28401.	24105.	28141.	23442.	27960.	23947.	23296.
92	Engineering & Construction Management Services	61764	64209.	72249.	61321.	71587.	59633.	71127.	60919.	59261.
93	Other Costs	19168	19927.	22422.	19031.	22217.	18507.	22074.	18906.	18391.
94	Interest During Construction	163376	169831.	191059.	162206.	189311.	157751.	188096.	161144.	156767.
	Subtotal, $	268587	279208.	314132.	266663.	311256.	259333.	309257.	264916.	257715.
	TOTAL PLANT INVESTMENT,$	695544	723028.	813401.	690566.	805959.	671598.	800786.	686045.	667410.

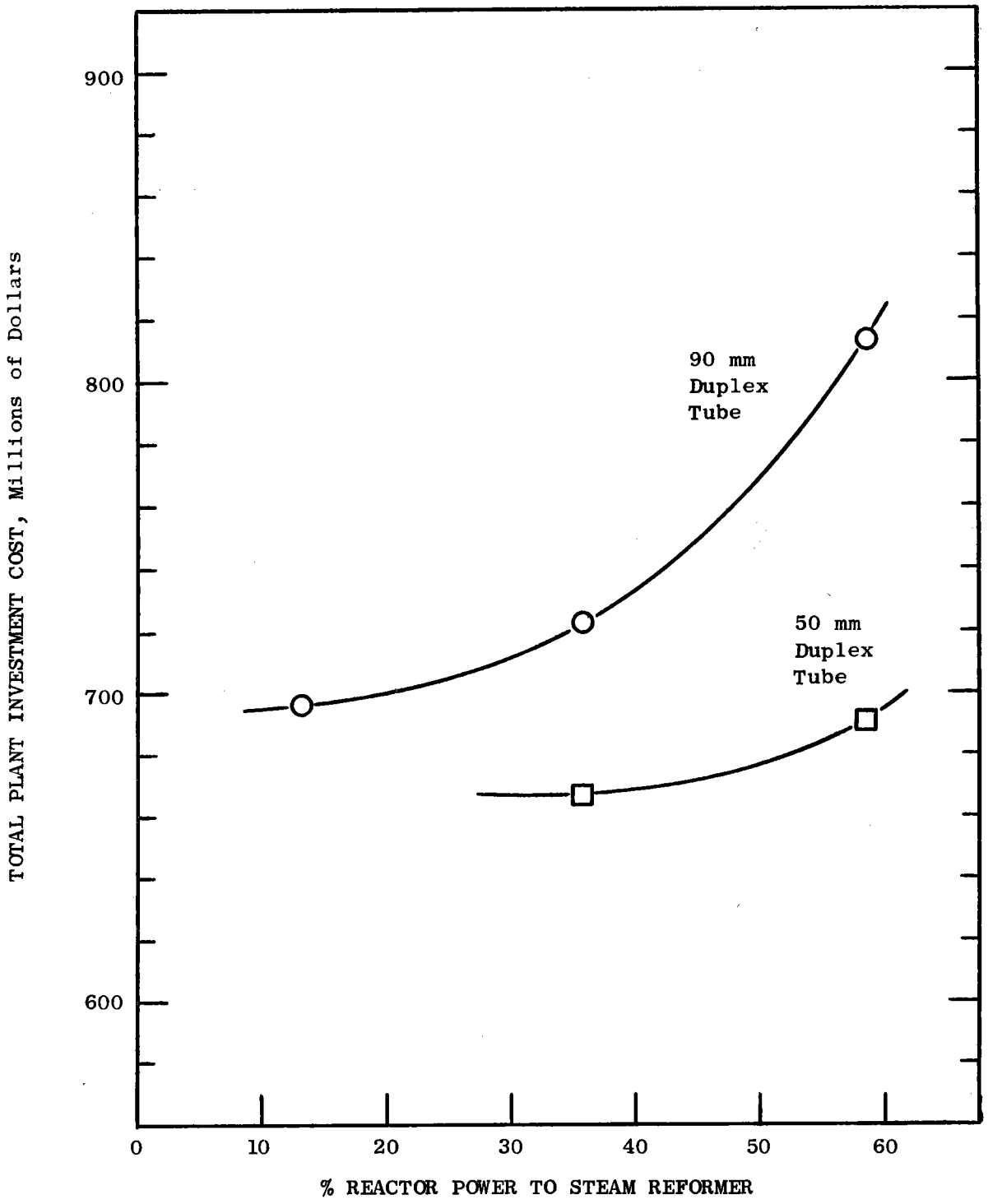

Figure H-3. Effect of Steam Reformer Power Split and Duplex Tube Size on Plant Capital Cost.

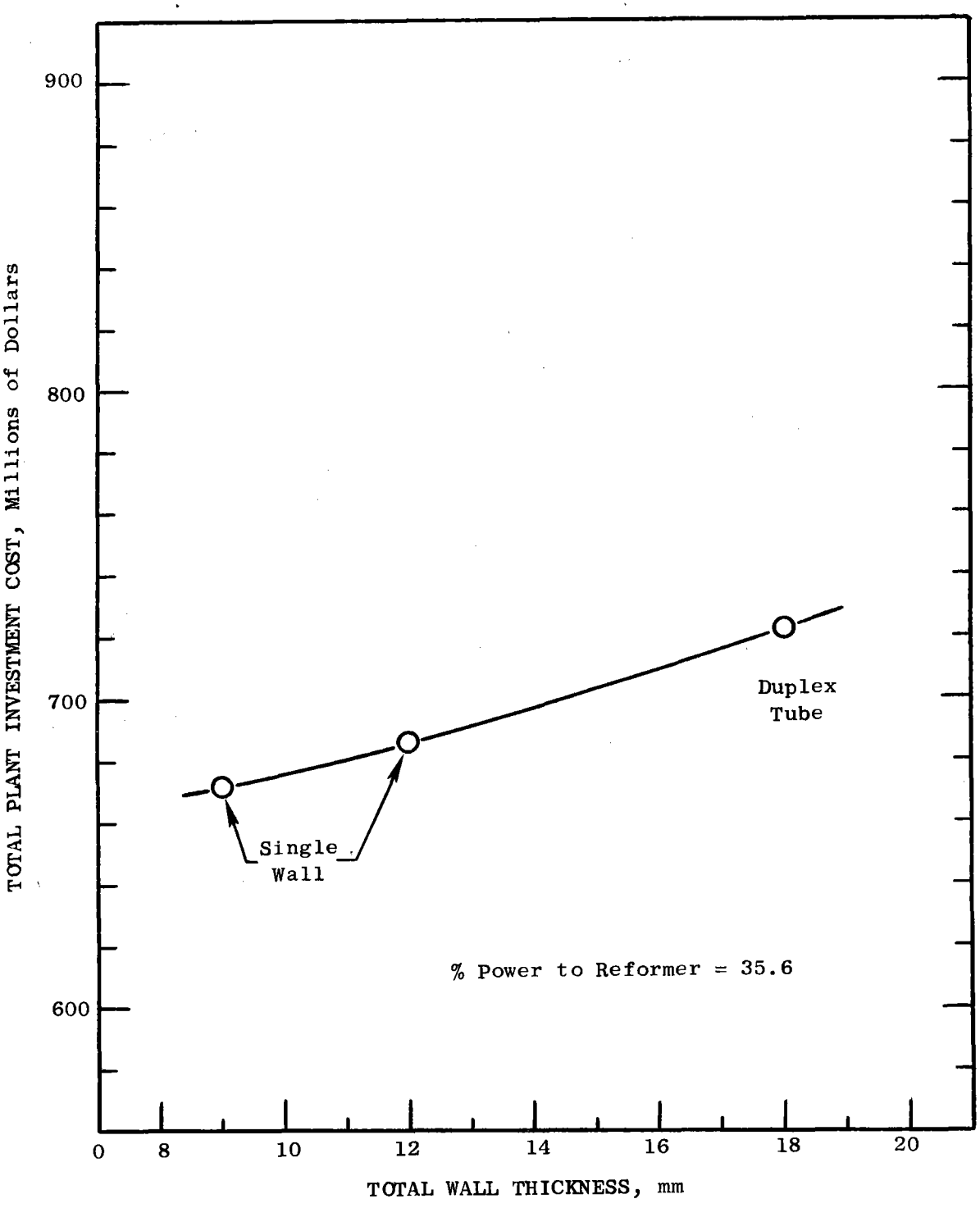

Figure H-4. Effect of Steam Reformer Wall Thickness on Capital Cost.

H.5 ENERGY COSTS

Total energy costs, consisting of plant capital costs, O&M, and fuel cycle costs are shown in Table H-9. An 18% fixed charge rate was used, corresponding to utility industry practice. O&M costs were estimated for each plant, as were the expenses of replacement catalysts, water, makeup helium, and methane. Fuel cycle costs were estimated at 30.5 ¢/MBTU.

As discussed in Appendix G, each plant consists of a reformer plant and also steam turbogenerators. The plant output thus consists of thermal energy from the reformed steam and methane, and excess electric power. The required plant power includes that required for the helium circulators, miscellaneous power plant needs, compressor power for the reformer plant, and power for pipeline pumping. This power ranges from 91 MWe to 170 MWe depending on the plant parameters.

The capital costs shown in Table H-9 include the nuclear island, but <u>not</u> the balance of the reformer plant and the off-site methanators, which would add between $\$62 \times 10^6$ to $\$280 \times 10^6$ depending on the size of the plant.

The cost of delivered thermal energy depends on the price allocated for the excess electricity.

The cost equation is:

$C_1 \times R_1 + C_2 \times R_2 = C_3 R_3$, where

C_1 = cost of electricity, \$/KWh

R_1 = amount of electricity generated (net) KWh/year

C_2 = cost of thermal energy, \$/MBTU

R_2 = amount of thermal energy, MBTU/year

C_3 = total energy cost, \$/MBTU

R_3 = total thermal core energy, MBTU/year

Figure H-5 shows the relationship for C_1 and C_2 for the 36.5% and 58.4% plants with 90 mm duplex tubes.

TABLE H-9

ENERGY COSTS, THOUSANDS OF DOLLARS

Plant Description	A-1a1	A-1a2	A-1a3	A-1b1	A-1c	A-2a	A-3	A-2b	A-1b2
Power to Steam Reformer %	13	35.6	58.4	58.4	35.6	35.6	35.6	35.6	35.6
Method of Heat Transfer	90 mm DSR	90 mm DSR	90 mm DSR	50 mm DSR	90 mm DSR	90 mm SR	90 mm IHXL	90 mm SR	50 mm DSR
Containment	Non-Int	Non-Int	Non-Int	Non-Int	Integrated	Non-Int*	Non-Int	Non-Int**	Non-Int
TOTAL PLANT INVESTMENT	695,544.	723,028.	813,401.	690,566.	805,959.	671,598.	800,786.	686,045.	667,410.
Annual Cost @ 18% FCR	125,198.	130,145.	146,412.	124,302.	145,073.	120,888.	144,141.	123,488.	120,134.
Operating & Maintenance Costs	6,600.	9,800.	13,100.	9,300.	9,800.	9,800.	11,100.	9,800.	7,500.
TOTAL PLANT & O&M COSTS	131,798.	139,945.	159,512.	133,602.	154,873.	130,688.	155,241.	133,288.	127,634.
Total in ¢/MBTU Core	160.9	170.9	194.8	163.1	189.1	159.6	189.6	162.8	155.9
Fuel Costs in ¢/MBTU Core	30.5	30.5	30.5	30.5	30.5	30.5	30.5	30.5	30.5
TOTAL ENERGY COSTS, ¢/MBTU (Core)	191.4	201.4	225.3	193.6	219.6	190.1	220.1	193.3	186.4
Delivered Thermal (CHP) Energy, MW	394	1080	1772	1772	1080	1080	1080	1080	1080
Delivered (Net) Electrical Energy, MW	932	591	241	241	591	591	547	591	591
Reactor Power Chargeable to CHP, MW	670.0	1522.5	2397.5	2397.5	1522.5	1522.5	1632.5	1522.5	1522.5
Chemical Heat Pipe "Efficiency", %	58.8	70.9	73.9	73.9	70.9	70.9	66.2	70.9	70.9
Delivered Thermal Energy Cost, ¢/MBTU	325.5	283.9	304.8	261.9	309.6	268.0	332.7	272.5	262.8
Delivered Electrical Energy Cost, ¢/KWh	1.633	1.718	1.922	1.651	1.873	1.622	1.878	1.649	1.590

*9 mm steam reformer tube wall

**12 mm steam reformer tube wall

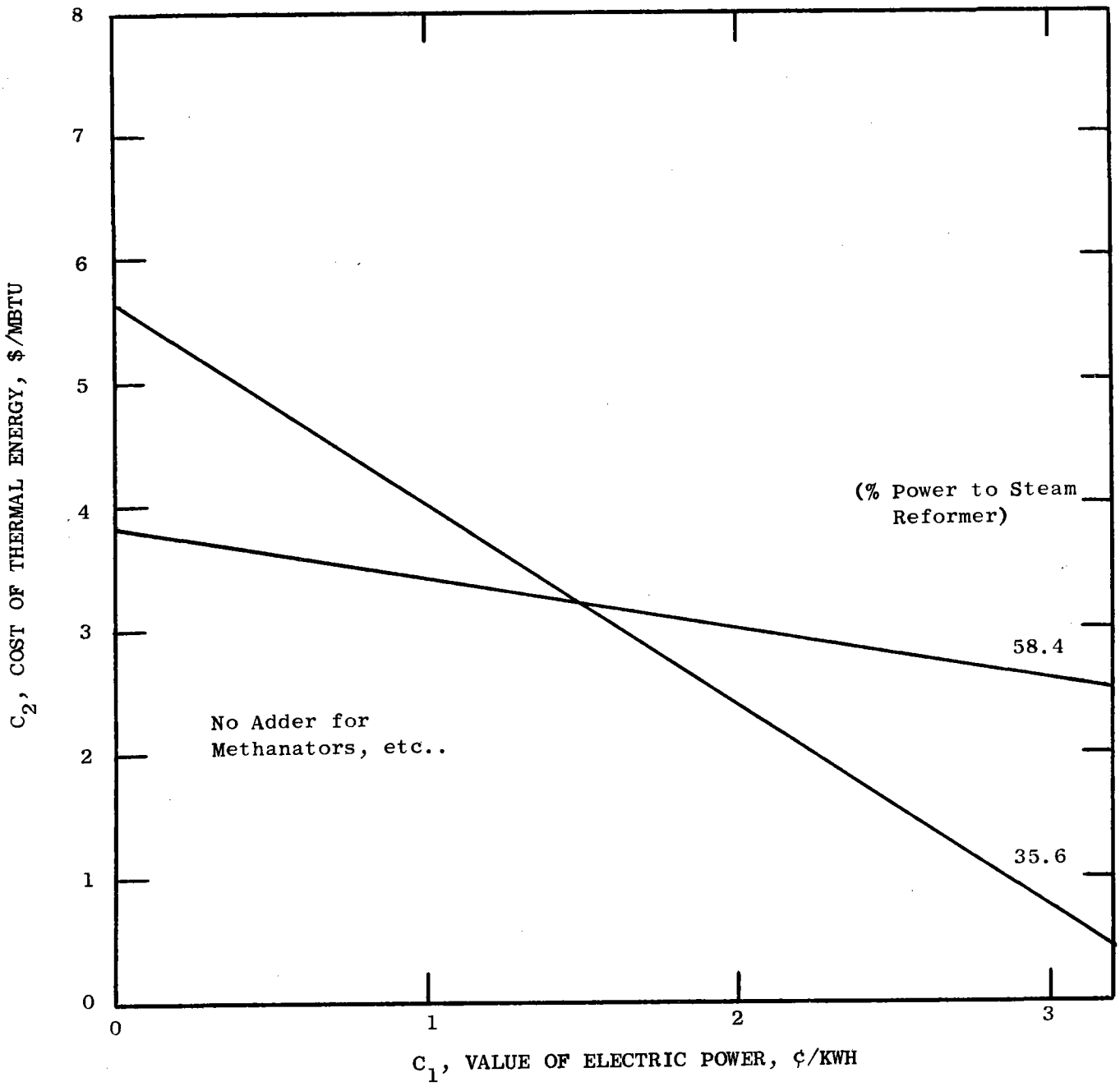

Figure H-5. Cost of Thermal Energy vs. Value of Electricity.

There are at least three logical ways to allocate the costs between thermal and electrical energy. The first involves selecting a constant value for the worth of electrical energy. This might be the way in which a user in the future would set his energy price. A second way, used in Reference H-1, converts the electrical energy to steam energy using an efficiency (of say, 40%), adds this to the delivered thermal energy to get the total delivered energy and converts this to an energy cost. This procedure tends to enhance plants generating mostly electricity. The third way calculates the fraction of the core power chargeable to the CHP system, and uses that fraction of the total core energy cost to calculate an energy cost. The balance of the cost is allocated to the electrical power.

Table H-10 shows the three sets of equations in terms of the basic parameters for each reactor plant. Figure H-6 and H-7 show the effect of the model used on the value of electricity and the value of thermal energy for the 90 mm duplex tube plants. Note that the middle curve in each figure shows a more moderate trend. In the power range of greatest interest, 30-58% steam reformer power, the conclusion one reaches is the same, i.e. that the "best" plants are in the 30-40% power range. The tabulation in Table H-9 and the balance of the discussion uses this method.

Figure H-8 shows the effect of steam reformer power on energy cost for both the 90 mm and 50 mm duplex tube plants. Note the definite superiority of the 50 mm duplex tube. It is also apparent that a 35.6% plant is the most logical choice, as it is clearly superior if 90 mm tubes must be used, and rather indifferent if 50 mm tubes can be used.

Figure H-9 shows the effect of the tube wall thickness of single wall reformer tubes on energy cost. There isn't a great deal of difference, less than 6%, between the 9 mm tube and the DSR at 18 mm total thickness.

The integrated plant, A-1c, has an energy cost 9% greater than the corresponding non-integrated reference design, while the plant with the IHX loop, A-3, has an energy cost 17% higher.

TABLE H-10

ENERGY COST/VALUE RELATIONSHIPS

METHOD	COST OF THERMAL ENERGY	COST OF ELECTRICITY
1) Constant Electrical Energy Cost	$C_c\left(\frac{Q_{CORE} - \frac{C_e}{C_c} Q_{ENET}}{Q_{CHPD}}\right)$	Fixed (C_e)
2) Constant Plant Efficiency (VHTR)	$C_c\left(\frac{Q_{CORE}}{Q_{CHPD} + \frac{Q_{ENET}}{0.4}}\right)$	$\frac{C_c}{0.4}\left(\frac{Q_{CORE}}{Q_{CHPD} + \frac{Q_{ENET}}{0.4}}\right)$
3) Constant Electrical Efficiency	$C_c\left(\frac{Q_{CORE} - \frac{Q_{ENET}}{0.4}}{Q_{CHPD}}\right)$	$\frac{C_c}{0.4}$

where:

C_c = Core energy costs

C_e = Electric energy cost (value)

Q_{CORE} = Core thermal power (3000 MW)

Q_{ENET} = Net electrical energy

Q_{CHPD} = Net thermal energy delivered

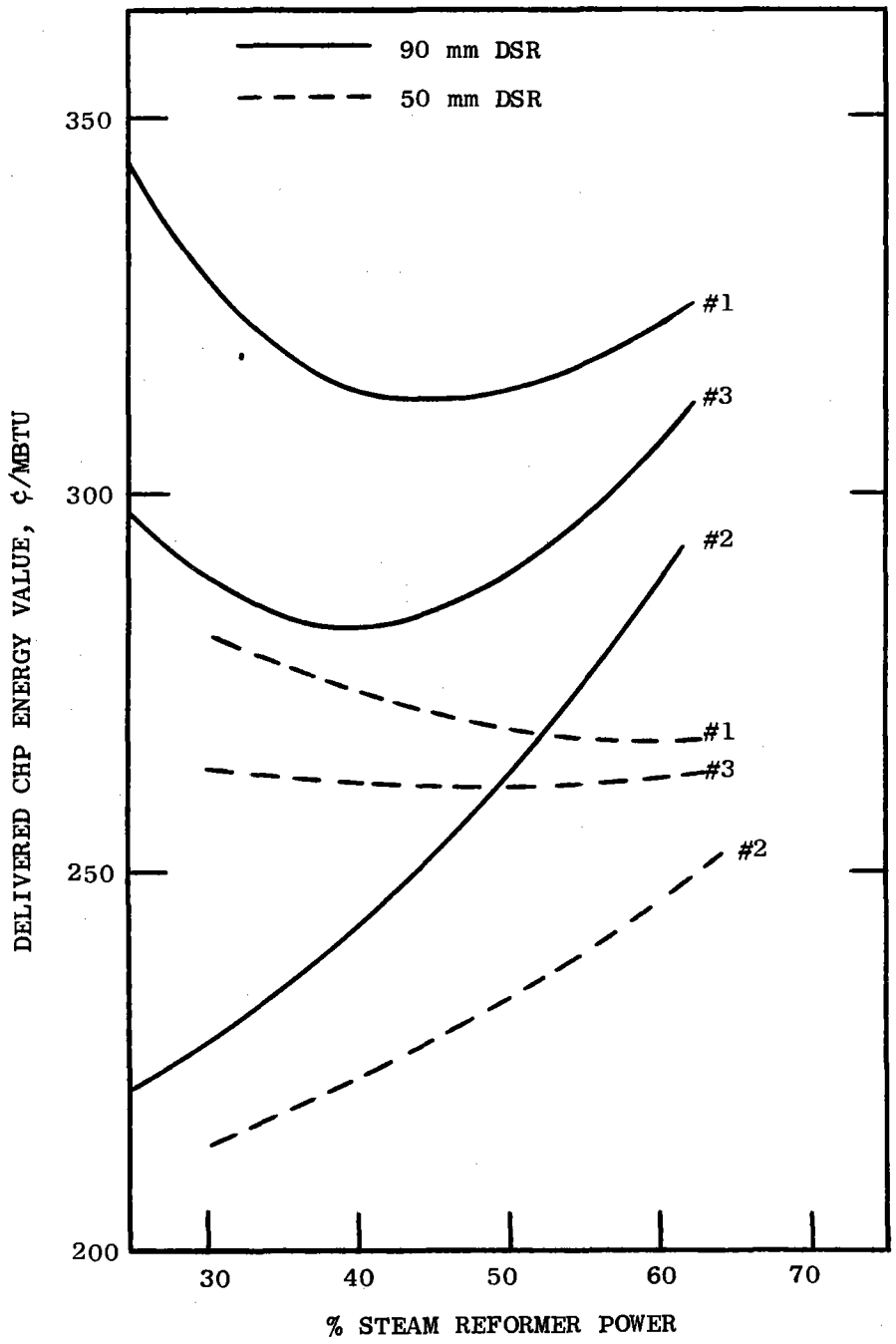

Figure H-6. Energy Value vs. Steam Reformer Power and Costing Method.

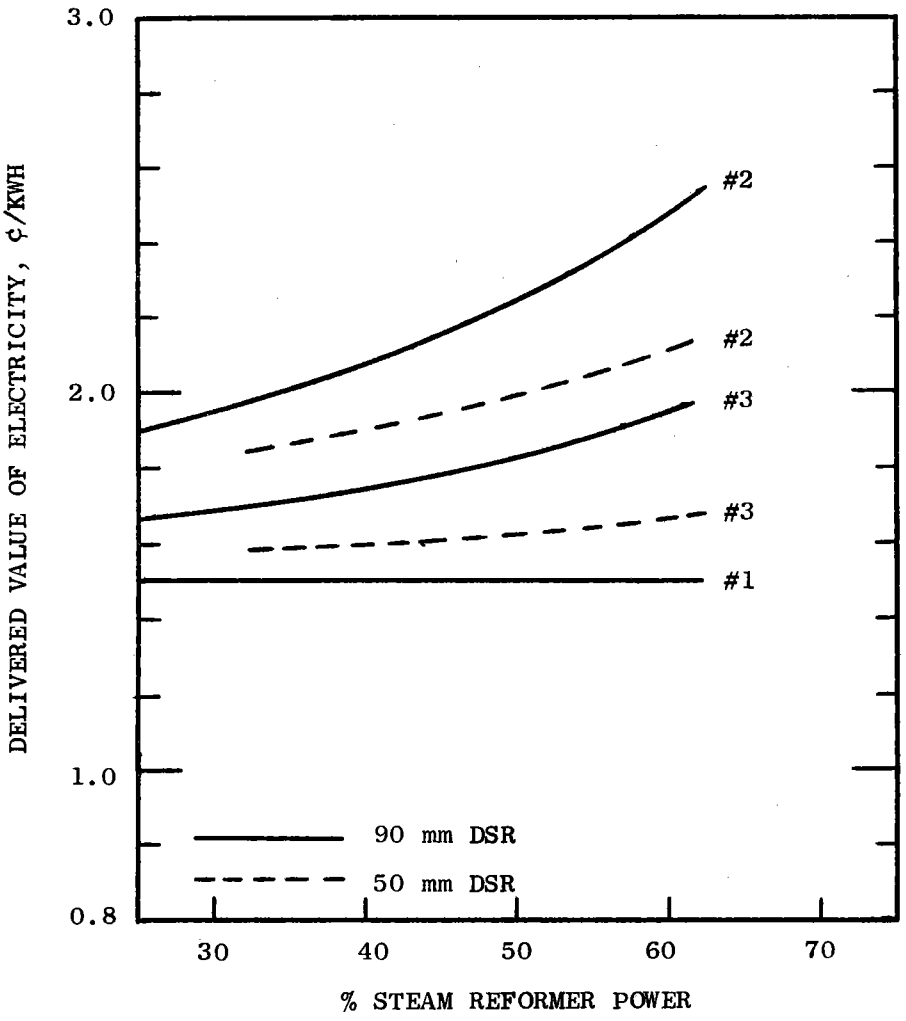

Figure H-7. Electric Power Value vs. Steam Reformer Power and Costing Model.

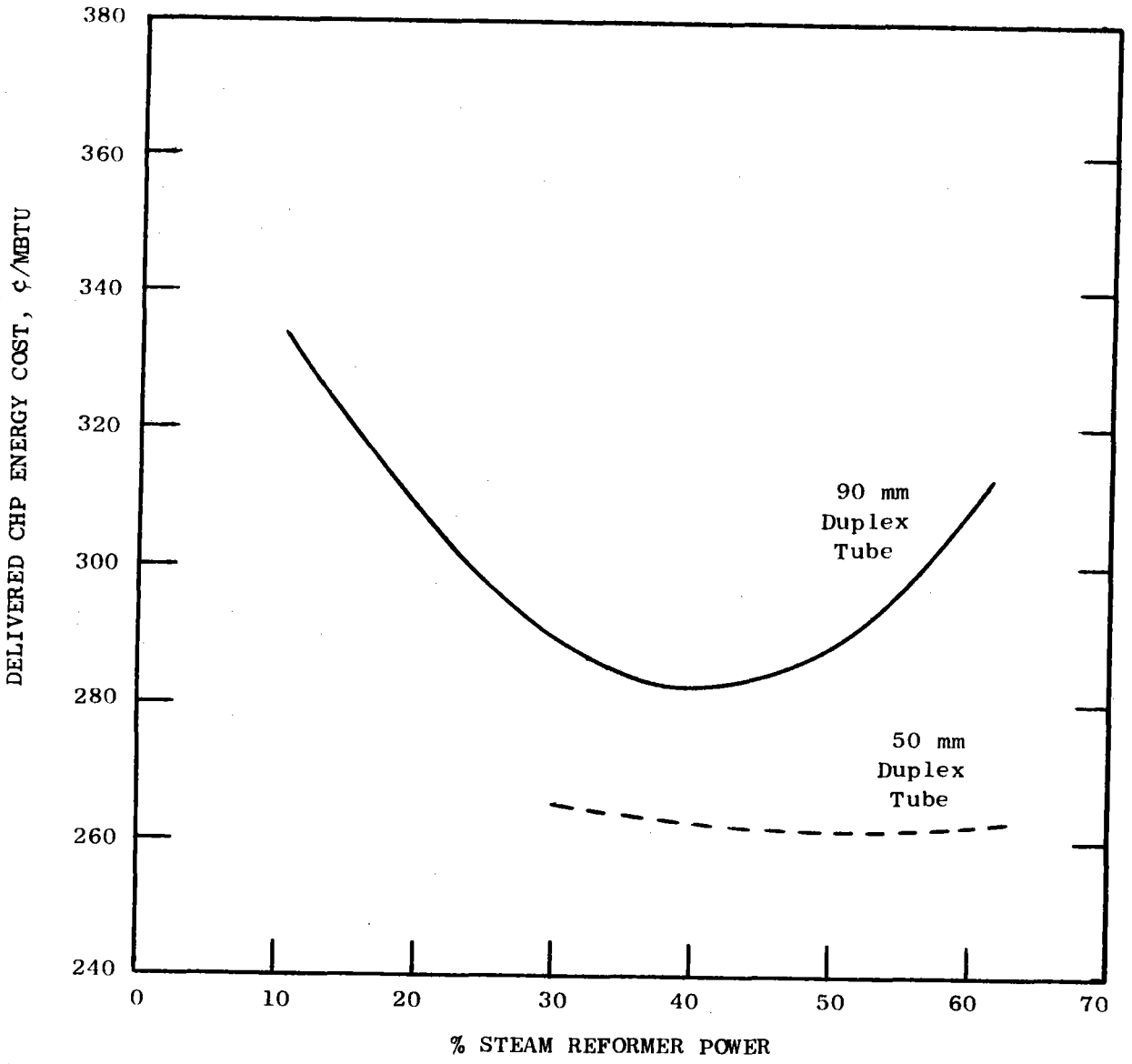

Figure H-8. Cost of Thermal Energy vs. Steam Reformer Power and Duplex Tube I.D.

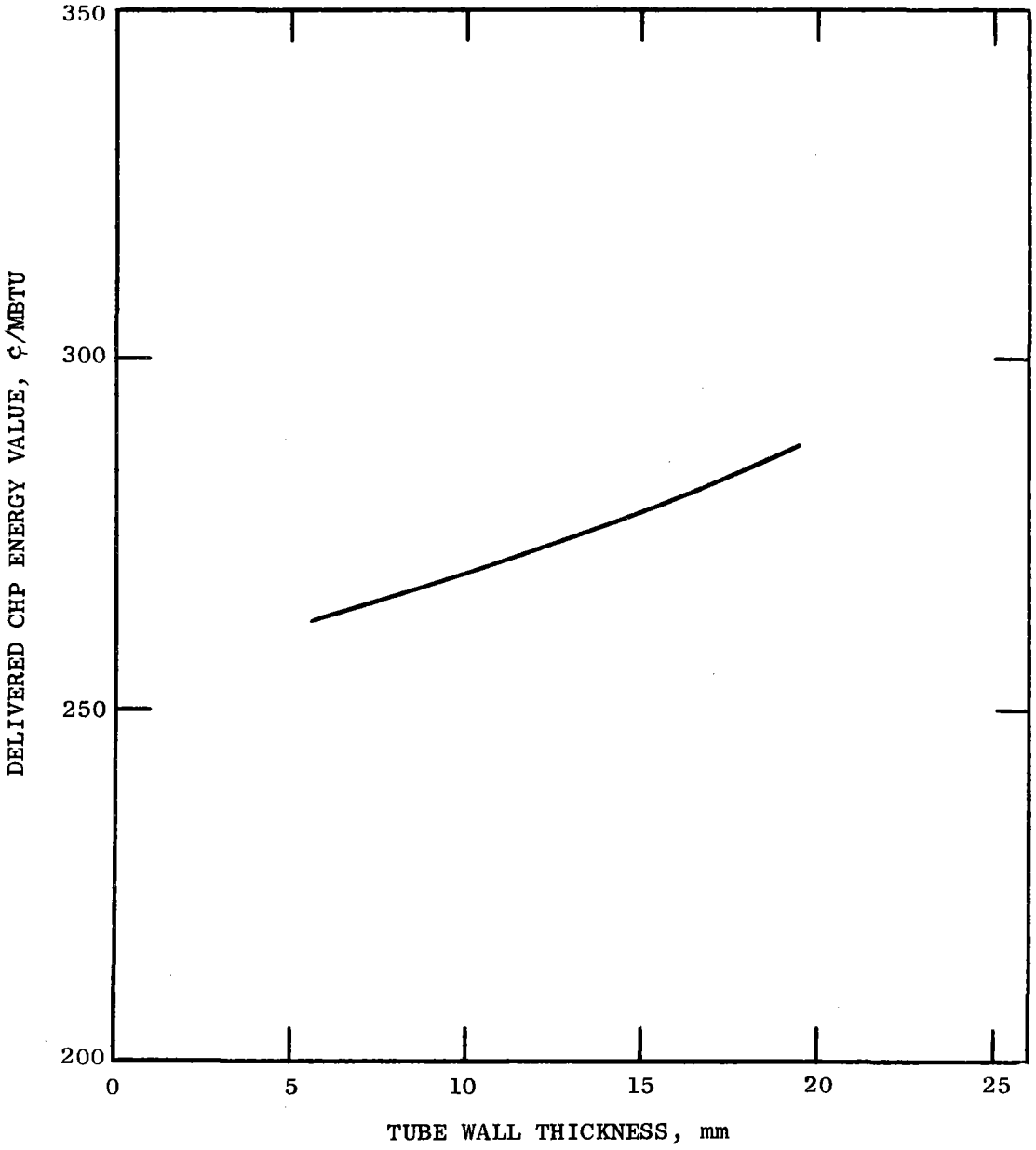

Figure H-9. Effect of Tube Wall Thickness on Energy Cost.

REFERENCES

H-1 Tschamper, P. M., "The VHTR for Process Heat", General Electric, GEAP-14018, September 1974.

H-2 "High-Temperature Nuclear Heat Source Study", General Atomic, GA-A13158, December 30, 1974.

H-3 Woike, O. G., "Small Nuclear Process Heat Plants (SNPH) Using Pebble Bed Reactor", General Electric Company, GEEST 75-001, November 1975.

H-4 "High Temperature Gas-Cooled Reactor Plant", Volume V, United Engineers and Constructors, Inc., WASH-1230, December 1973.

H-5 Handy-Whitman Index of Public Utility Construction Costs, Bulletin No. 103, Whitman, Requardt and Associates, January 1, 1976.

H-6 "Guide for Economic Evaluation of Nuclear Reactor Plant Designs" NUS Corporation, NUS-531, January 1969.

H-7 Bowers, H. I., "Concept - Computerized Conceptual Cost Estimates for Steam - Electric Power Plants", Phase II User's Manual, ORNL-4809, April 1973.

H-8 "Power Plant Capital Costs, Current Trends and Sensitivity to Economic Parameters", AEC WASH-1345, October 1974.

APPENDIX I

IHX MATERIALS CONSIDERATIONS

TABLE OF CONTENTS

LIST OF FIGURES

LIST OF TABLES

APPENDIX I

IHX MATERIALS CONSIDERATIONS

I.1 LIMITING MATERIALS REQUIREMENTS FOR THE IHX

Some major limiting requirements affecting the selection and use of materials must be integrated into a consideration of the design, development, test and successful lifetime operation of the intermediate heat exchanger (IHX). These include the following: (1) operating temperature within the various components, (2) the mix of stress-time-temperature relationships for critical, life limiting components, (3) environmental effects on materials, (4) tritium and hydrogen diffusion characteristics of heat exchanger surfaces, (5) cold wall insulation concepts, (6) sliding wear and galling, and (7) the potential for future growth to higher operating temperatures.

I.1.1 OPERATING TEMPERATURES

The IHX design required for the steam gasification of coal requires metal operating temperatures in the 800-950°C range (1500-1750°F), as indicated below, with growth versions extending the temperature capability to the 900-1150°C range (1650-2100°F).

	Temperature °C	
	Initial Designs	Growth Versions
Primary Helium Temperature	950	1050-1150
Secondary Helium Temperature	900	1000-1100
Peak Process Temperature	771	783-800

It is apparent that the use of nickel base superalloys can be considered for initial designs, but that growth versions will require the use of unique fabricable heat exchanger materials (such as oxide dispersion strengthened alloys (ODS) with useful long term mechanical properties at

temperatures above those normally considered for conventional iron and nickel base alloys. Although alloys are not now ASME-code qualified above 815°C (1500°F), ASME criteria for design allowable stresses can be applied to typical alloy data for purposes of conceptual designs; it is intended that alloys selected and qualified for the various materials requirements might be ASME code qualified during the course of the necessary development program and prior to final commercial design. At the higher operating temperatures of the gas cooled reactor components, such as the IHX, the microstructural instabilities of various potential alloys and the effects of these instabilities on strength and ductility requires that ASME code qualification be based upon comprehensive test programs of long test duration.

I.1.2 LIFE REQUIREMENTS

The IHX has a design life goal of 30 year useful life (over 260,000 hours) in a helium atmosphere at a pressure level of about 600 psia; nevertheless, long life stresses are very low since the pressure differential across the high temperature components is very small (∿30 psi). The stresses within the outer pressure vessel shell can be readily tolerated since the vessel itself is insulated and water cooled. In addition to the low steady state stresses, the hot components may be subjected to a very maximum of 1000 significant thermal excursions produced by start up and shut down, and to short term high internal pressure stresses occasioned by a postulated abrupt failure of the secondary containment system.

In the present conceptual design*the tubing wall thickness was sized, using ASME type design criteria, by the assumption of a 10 hour fault. In this fault mode, failure of the secondary containment was assumed and, after the loss of pressure on the secondary side it was assumed that primary pressure was maintained at full pressure and temperature for a ten hour period. Stress levels were assumed based upon ASME code type stress allowables which might be expected of an alloy such as Inconel 617; the fault analysis criteria limited the stress to the lesser of the ten hour properties for 1% creep, rupture or initiation of third stage creep. The 0.5 inch diameter tubes feature a 0.050 inch wall thickness which includes a 0.022 inch corrosion allowance.

*See Appendix C

In analyzing design requirements of component development and commercial components, more rigorous design criteria must be used based upon established design allowables and upon a linear damage approach involving a summation of the fractional life used by various alternative life degradation processes (creep, fatigue, mixed mission stresses, etc.). The current conceptual design illustrates the need for code approved design allowable stresses.

I.1.3 IMPURE HELIUM ENVIRONMENT EFFECTS

Most of the widely used high temperature alloys such as those listed in Table I-1 were developed primarily for use in oxidizing environments such as air, where thin adherent oxide films are formed on the surface and tend to retard further oxidation. The oxidizing potential of HTR helium coolants, which results from its O_2 and H_2O impurities, is too low to oxidize major alloy components such as Fe and Ni. Instead, Cr and the more reactive trace elements, such as Al and Ti, are selectively oxidized. This is understandable considering the free energy curves of Figure I-1, compared to the oxidation potentials of HTR helium. According to an explanation offered by Mazandarany and Rittenhouse[I-1], oxidation proceeds initially with Cr at the surface, where it is in relatively high concentration ($\sim$21% for Incoloy 800), to form a scale and a Cr-depleted layer beneath the scale. The resultant oxygen potential at the interface of the scale/Cr-depleted region drops to a value below that required for further oxidation of Cr in the depleted layer until sufficient Cr diffuses into this region. During this period, the oxygen that diffuses into the depleted region is of sufficiently high potential to oxidize Ti and Al. Depending upon relative concentrations and diffusivities, Ti and/or Al tends to move to the Cr_2O_3-metal interface to form a complex oxide. The formation and growth of this oxide further lowers the oxygen potential and concentrations of Ti and Al to a level where only Al_2O_3 (and sometimes TiO_2 depending upon relative concentration and mobility) can form below the oxide-metal interface. Because of the very low driving forces involved (low oxygen potential and low Al content in this region) Al_2O_3 tends to nucleate at preferred high energy sites such as existing grain boundaries and nucleating sub-boundaries near the surface. Internal oxidation along grain boundaries tends to degrade the properties of austenitic and high-nickel alloys.

TABLE I-1

TYPICAL CHEMICAL COMPOSITIONS OF SEVERAL CANDIDATE IHX TUBE ALLOYS

ALLOY	C	Cr	Ni	Fe	Co	Mo	W	Cb	Al	Ti	Other
AISI 316	0.08	17.0	12.0	Bal.		2.5					Si 1.0 Max Mn 2.0 Max
INCONEL 601	0.05	23.0	Bal.	14.0					1.35	0.35	Cu 1.0 Max
INCONEL 617	0.07	22.0	Bal.		12.5	9.0			1.0	0.35	
INCONEL 625	0.05	22.0	Bal.	5 Max	1.0 Max	9.0		3.75	0.4 Max	0.4 Max	Si 0.3 Mn 0.15
INCOLOY 800H	0.07	21.0	32.5	Bal.					0.38	0.38	Si 0.5 Mn 0.75
HASTELLOY S	0.02	16.0	Bal.	1.0		14.5			0.2		B 0.02 La 0.02
HASTELLOY X	0.1	22.0	Bal.	19.0	1.5	9.0	0.6		0.2		
TD NiCr		20	78								2 ThO_2
MA 754		20	Bal.						0.3	0.6	0.6 Y_2O_3

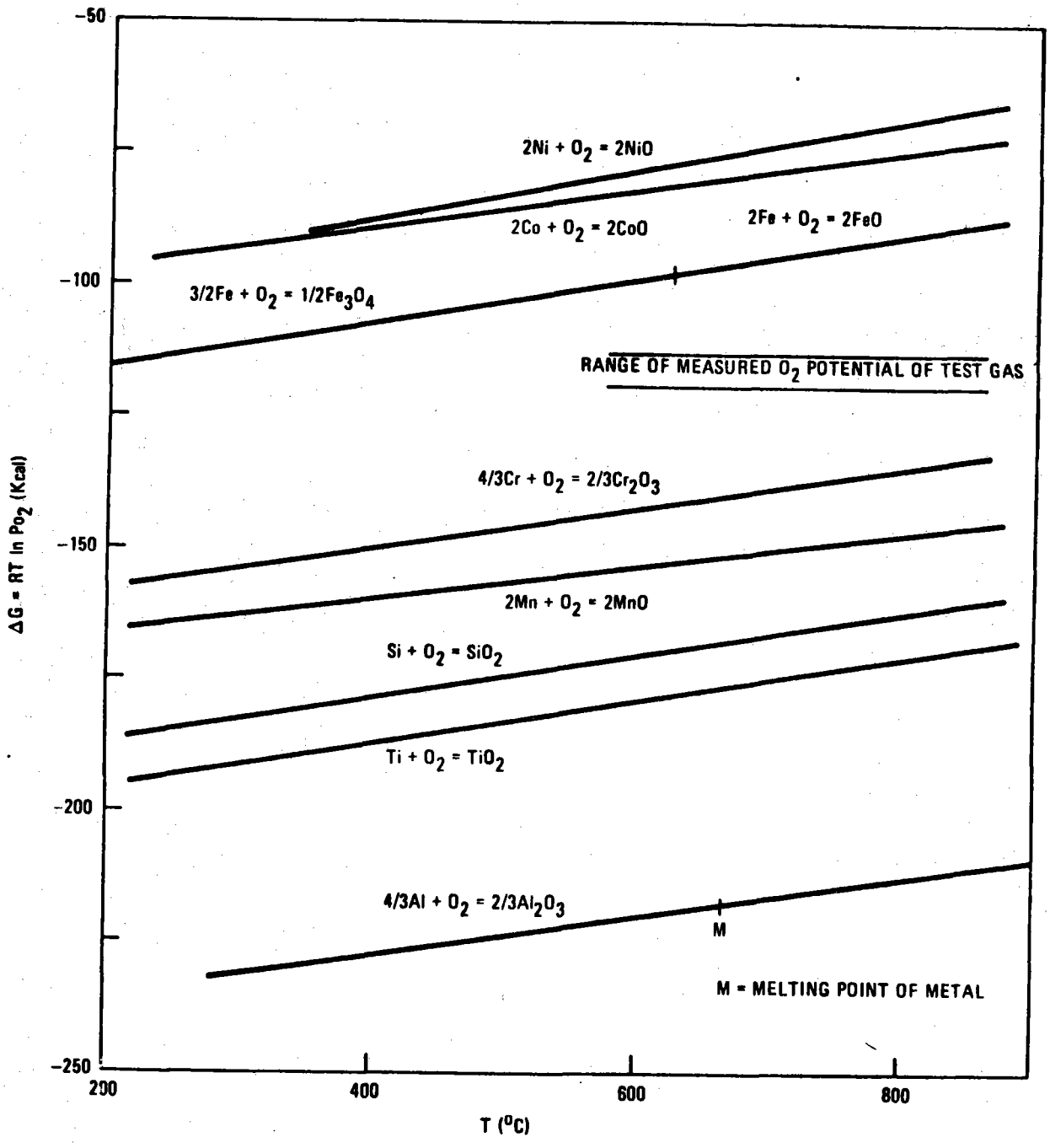

Figure I-1. Standard Free Energy of Formation of Metal Oxides. (Ref. I-1).

Even in those instances where sufficient oxygen is present to form an oxide film, vaporization of the oxide may occur at temperatures above 800°C (1470°F)[I-2]. The vaporization rate is dependent upon the type of oxide film formed as shown in Figure I-2, and is also dependent on helium flow rate[I-3].

HTR helium coolants also may be reducing and carburizing with respect to individual elements within the alloys, depending on temperature, impurity gas levels, and gas partial pressure ratios. This is illustrated by Figure I-3 which shows that either oxidation or carburization, both, or neither can occur depending on the conditions of temperature and hydrogen/water partial pressure ratio.

Carburization can be either detrimental or beneficial, depending upon the concentration, morphology, and location of the carbides. Plate-like carbide particles in a continuous film in grain boundaries are very detrimental, whereas well distributed, fine carbide particles within the matrix can increase strength. Although the exact mechanism of carburization has not been established, it is known that the degree and rate of carburization generally increase rapidly at temperatures above 1500°F. Carburization seems to be promoted by high nickel contents and by internal oxidation[I-5]. The expected corrosion behavior of several commercial alloys in HTR helium, based on current thinking, is given in Table I-2.

Investigations of the effect of helium on the properties of materials have been undertaken in several foreign countries as well as in this country. Although some early test results indicated that creep and rupture strength were adversely affected by the impure helium environment, more recent testing has indicated that creep and rupture strengths in impure helium are comparable to those in air[I-6]. Creep testing in HTR helium has been accomplished on only a few alloys suitable for use at 950°C (1750°F). Certainly, much additional data is needed to adequately determine the effect of the impure helium environment on the mechanical properties of the specific alloys selected for use, and to generate sufficient data to support design calculations.

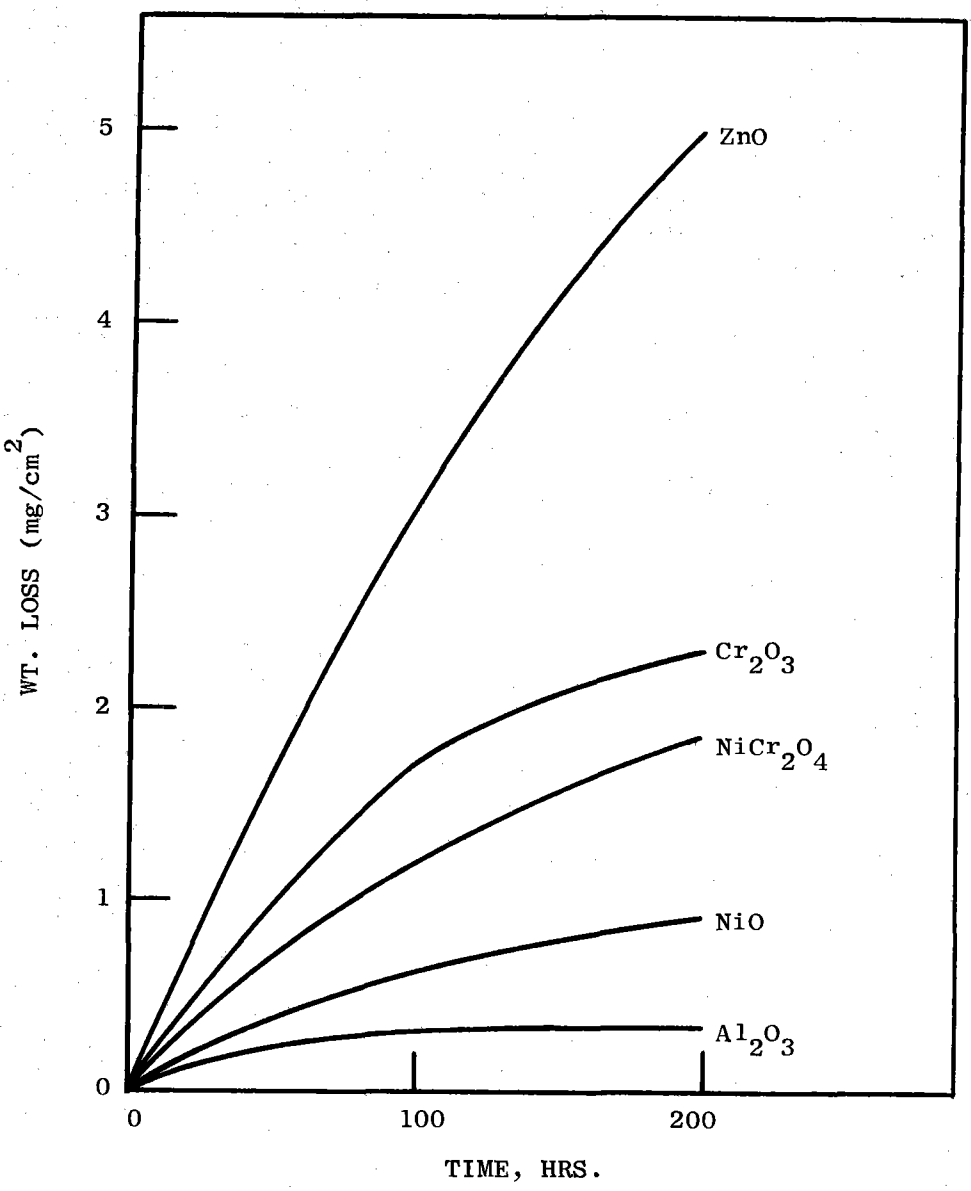

Figure I-2. Relative Vaporization Rate of Oxides in Air at 1090°C (2000°F) (Ref. I-4).

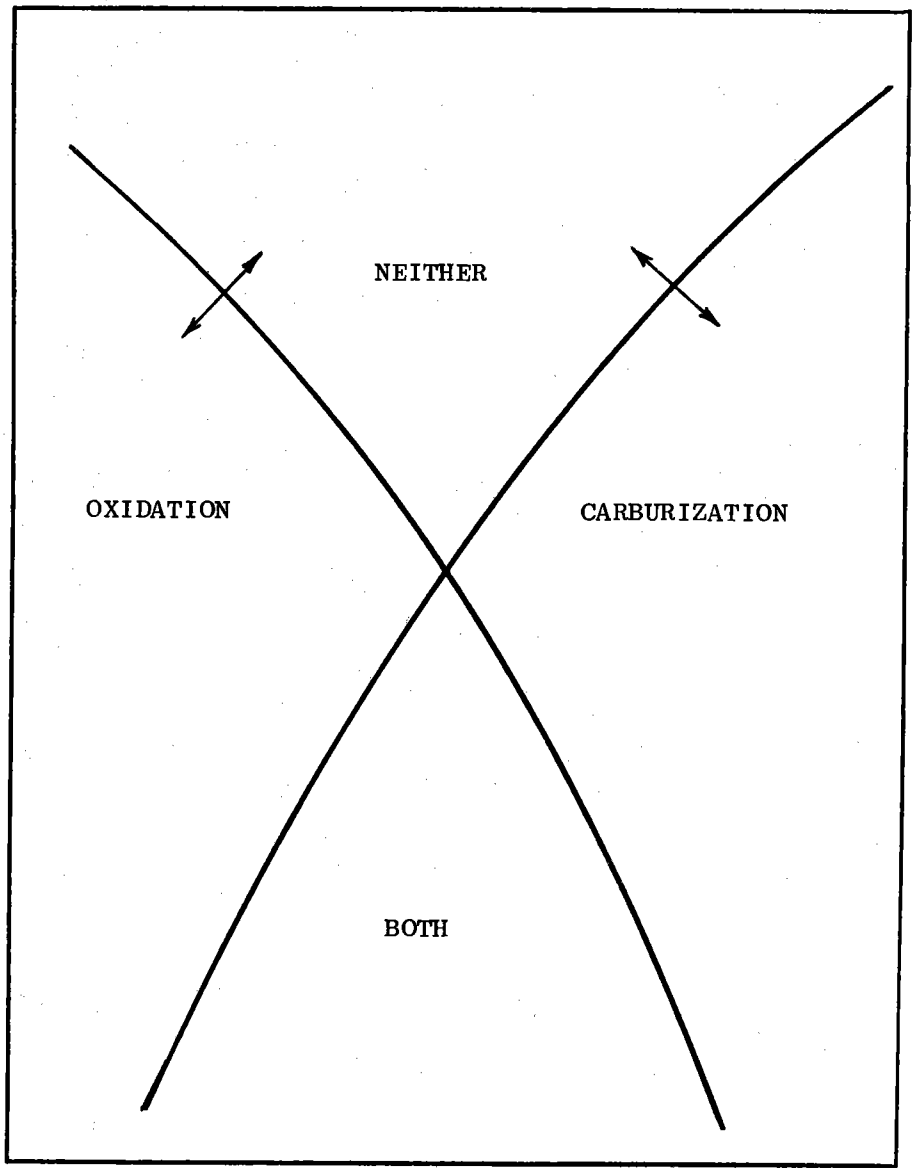

Figure I-3. Oxidation and Carburization Reactions in HTR Helium as a Function of Temperature and P_{H_2}/P_{H_2O} Ratio.

TABLE I-2

EXPECTED CORROSION BEHAVIOR OF COMMERCIAL ALLOYS IN HTR HELIUM

ALLOY	COMMENT
Incoloy 800H	Oxidation of Cr, Forming Thin Non-protective Surface Film; Internal Oxidation of Al and Ti; Some Sub-surface Carburization.
Incoloy 802	Very Similar to Incoloy 800H.
Incoloy 807	Cb in Alloy Should Promote Stable Oxide Film; Would Expect No Internal Oxidation (As This Alloy Contains No Al or Ti) or Carburization.
Inconel 601	Surface Oxidation of Cr and Internal Oxidation of Al.
Inconel 617	Surface Oxidation of Cr and Probably Less Internal Oxidation Than Inconel 601 Because of Lower Al Content.
Inconel 625	Presence of Cb Should Promote Stable Oxide Film; Expect Little Carburization.
Hastelloy C	Contains No Al or Ti; Would Expect No or Little Internal Oxidation; Contains Mo and W.
Hastelloy S	Expect Little or No Internal Oxidation of Al; La Effect Unknown.
Hastelloy X	Same as Hast. C.

I.1.4 HYDROGEN AND TRITIUM PERMEATION*

Tritium, the heavy isotope of hydrogen (^3H) is formed in all nuclear reactor systems through the fission process and through neutron interactions with various materials. To minimize the transfer of tritium, which is a radiological hazard, from the primary coolant loop to the secondary loop, consideration must be given to the permeability characteristic of candidate alloys during the selection process.

Permeation rates are slightly lower for tritium than for hydrogen through nickel and Incoloy 800 according to the data of Figure I-4. Although several recent papers[I-7 -I-12] have addressed the subject of tritium permeation, only a few alloys have been involved. Hydrogen permeabilities may be used to compare materials with respect to tritium permeability on a relative basis for screening purposes. The relative permeabilities of several metals and alloys to hydrogen are shown in Figure I-5. Also shown in the figure are two curves for Incoloy 800 which demonstrate the results of experiments on diffusion at high temperatures of pure hydrogen and a steam-hydrogen mixture. Hydrogen permeation was reduced by one to two orders of magnitude in the presence of steam, indicating that a diffusion barrier is formed by oxides of chromium and iron. Strehlow and Savage[I-8] also showed that an oxide film can produce a large reduction in hydrogen permeation rate, but that the effectiveness of such films was dependent on the presence or absence of defects in the film and also on hydrogen pressure.

One method of taking advantage of this reduction in hydrogen permeation rates by oxide films is to oxidize the surface of the tubes prior to assembly of the IHX and to "dope" or to intentionally add oxygen impurity to the helium in the secondary loop to assist in maintaining the oxide film and to "heal" any defects in it.

Some of the hydrogen on the process side of the process heat exchanger will permeate through the walls of that heat exchanger and into the secondary coolant loop from which it then will permeate through the walls of the IHX and into the primary loop. Minimizing transfer of hydrogen into the primary loop helps protect the graphite fuel elements and reflectors from corrosion by the reaction: $C + 2H_2 \rightarrow CH_4$. It is clear, therefore, that development effort aimed toward measuring and minimizing hydrogen and tritium

*See also Appendix D.4

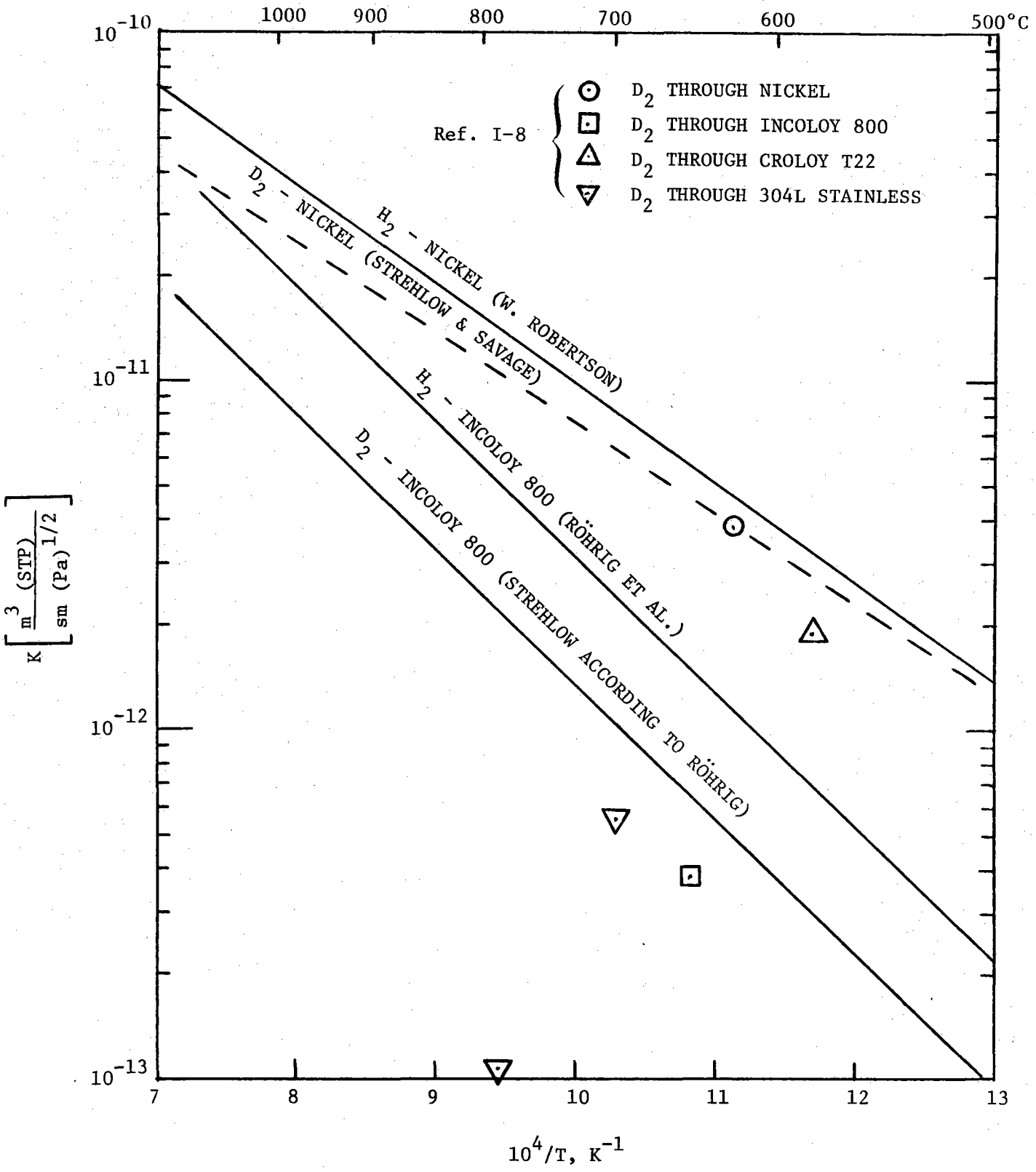

Figure I-4. Hydrogen Permeation Data

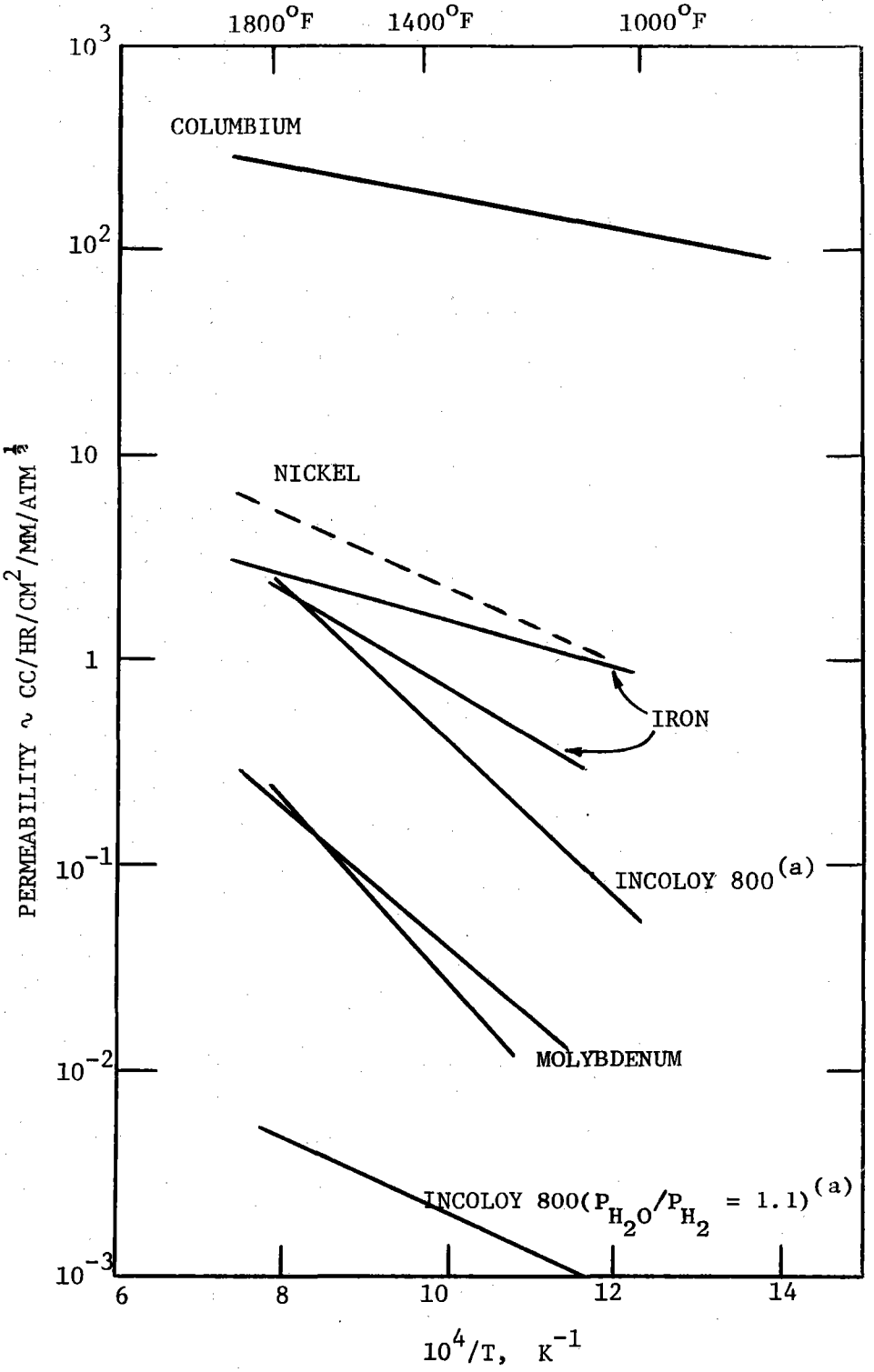

Figure I-5. Comparative Permeabilities of Hydrogen Through Various Metals (Ref. I-13).

(a) Incoloy 800 data converted to these permeability units assuming a square root of pressure relationship (Ref. I-14).

permeation through alloys suited to HTR service is needed. In addition, the effectiveness of oxide films in reducing permeation rates requires additional study.

I.1.5 HIGH TEMPERATURE COLD WALL INSULATION

Thermal insulation is required for the IHX pressure vessel and for high temperature pipes serving the IHX at temperatures up to 900-950°C (1652-1742°F) with growth possibilities to 1050°C (1922°F). These insulation systems can be based upon an extrapolation of techniques either used in earlier gas cooled reactors or planned for various hot gas closed cycle heat transfer systems. The types of materials and design of such insulation systems and the principal factors governing them are discussed below.

L. A. Feathers of the General Electric Company, Breeder Reactor Operation has summarized [I-15] the status of thermal insulation system designs for Pre-stressed Concrete Reactor Vessels (PCRV) and piping system, through 1973. Three basic types of thermal insulation have been used. These include (1) reflective metal (sheet or mesh) radiation control systems, (2) light weight porous ceramic insulating bodies, such as Glass-Rock (fused quartz) foam, and (3) ceramic fiber blankets, such as Kaowool Fiberfrax or Dyna Quartz. Typical materials are listed in Table I-3. The Peach Bottom I, AVR and THTR reactors were designed with reflective metal insulation as were many of the English gas cooled reactors with startup dates through 1971. The Fort St. Vrain reactor and various English gas cooled reactors with startup dates after 1972 featured designs with fibrous ceramic thermal insulation. Currently BBC/KFA has designed and manufactured water cooled hot gas ducts one meter in diameter using fibrous insulation; these insulated pipes will be used in the HHV non-nuclear gas turbine test facility: Figure I-6 indicates the type of construction involved. The Fort St. Vrain reactor uses four inch-thick-Kaowool felt batts at 8 $\#/ft^3$, compressed in place to 12 $\#/ft^3$.

Many references cited by Feathers and the extensive efforts of the English and others in the gas cooled reactor field indicates a strong

TABLE I-3

TYPICAL INSULATION MATERIALS

Designation	Vendor	Composition	Description	Max. Temp.	Bulk Density
Bulk Fireous Materials Kaowool	Babcock & Wilcox Co. Augusta, Georgia	$45Al_2O_3$-$52SiO_2$ $1.3Fe_2O_3$-$1.7TiO_2$	Fiber Mat 2.8 Micron Avg Dia	--	96 & 160 kg /m^3 (6 & 10 lb/ft^3)
Fiberfrax Felt	Carborundum Co. Niagara Falls, N.Y.	$50.9Al_2O$-$46.8SiO_2$- $1.2B_2O_3$-$0.8Na_2O$	Fibermat 2-40 Micron Dia.	1530 K (2300°F)	96 & 160 kg /m^3 (6 & 10 lb/ft^3)
Fiberfrax Block	Carborundum Co. Niagara Falls, N.Y.	$50.9Al_2O_3$-$49.4SiO_2$ $1.2B_2O_3$-$0.8Na_2O$ Inorganic Binder	Pressed Fiber Block	1530 K (2300°F)	256-320 kg /m^3 (16-20 lb/ft^3)
Cerafelt/Thermoflex	Johns Manville Manville, N.J.	$50.3Al_2O_3$-$49.4SiO_2$ $0.14Fe_2O_3$-$0.02TrO_2$ 2.3 Organic Binder	Fibermat 3 Micron Avg Dia	1530 K (2300°F)	48-384 kg /m^3 (3-24 lb/ft^3)
Fiberchrome	Johns Manville Manville, N.J.	Similar to cerafelt but with small amt of Cr_2O_3 added	Fibermat 3 Micron Avg Dia	1530 K (2300°F)	64-160 kg /m^3 (4-10 lb/ft^3)
Micro-Quartz	Johns Manville Manville, N.J.	Porous Quartz Fiber	Fibermat 3 Micron Drawn "E" Glass Fiber, Leached & Felted into Mat	Unspecified	48-96 kg /m^3 (3-6 lb/ft^3)
WRP - XZQ	Refractory Products Co. Evanston, Illinois	$34Al_2O_3$-$64SiO_2$- 1.1 Inorganic	Fibermat	1530 K (2300°F)	272-304 kg /m^3 (17-19 lb/ft^3)
Dyna-Quartz	Johns Manville Manville, N.J.	Porous Quartz Fiber	Sintered Micro Quartz	Unspecified	72-160 kg /m^3 (4.5-10 lb/ft^3)
S-Glass Fiber Mat	Owens Corning Fiberglass Granville, O.	$25Al_2O_3$-$64SiO_2$ - 10 Mgo	Fibermat Cloth ∿9.5 Micron Dia (375 x 10^{-6} in.) Continuous Filament	1088 K (1500°F) Static 810 K (1000°F) Dyn.	80 kg /m^3 (5 lb/ft^3)

TABLE I-3 (Cont'd)

TYPICAL INSULATION MATERIALS

Designation	Vendor	Composition	Description	Max. Temp.	Bulk Density
Porous Ceramics Glass Rock Foam	Glass Rock Products, Inc Atlanta, Georgia	Sintered Fused Quartz	65-80% Porosity 0.0156 Avg Pore Size	1200 -1370 K (1700°-2000°F) Continuous	480-800 kg /m^3 (30-50 lb/ft^3)
Foamed Al_2O_3	Various	Al_2O_3	Porosity to 95%	1923 K >(3000°F)	200-1000 kg /m^3 (12.5-62 lb/ft^3)
Foamed ZrO_2	Various	ZrO_2	Porosity to 95%	2478 K >(4000°F)	280-1400 kg /m^3 17.5-87 lb/ft^3)

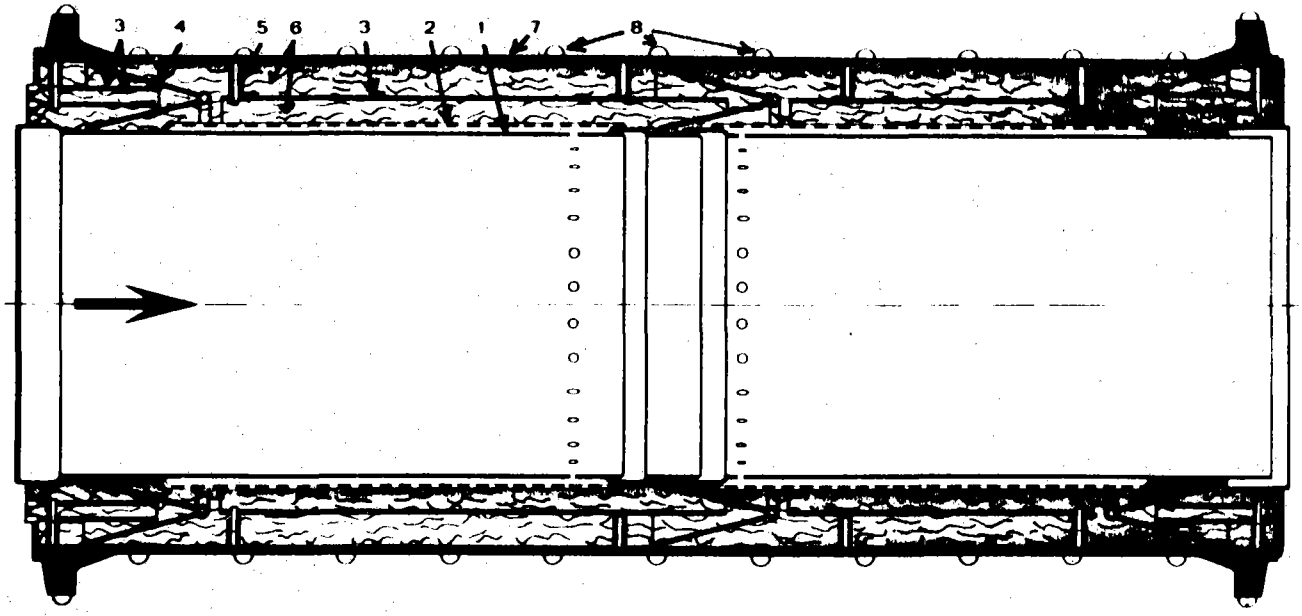

1 - Inner Liner
2 - Perforated Sheet Metal
3 - Intermediate Sheet Metal
4 - Support Member
5 - Spacer Bolt
6 - Insulation
7 - Pressure Containment
8 - Water Cooling

Figure I-6. Cross-section of a Hot Gas Duct.

background is at hand in hot gas insulation systems. The technical data and experience in reflective metal, porous ceramics, and fibrous insulation systems are available on which to base the growth of such insulation systems to meet higher temperature requirements. This background includes an appreciation of the principal factors governing design and materials selection.

I.1.6 SLIDING WEAR RESISTANCE

At various locations within the IHX differential expansion will occur as the result of operating temperature differences between components, use of dissimilar expansion alloys, temperature transients, etc. Relative movements, which can cause sliding wear between mating parts, can be minimized by design; use of material with higher temperature characteristics and lower thermal expansion in the hotter side of hairpin heat exchanger tubes, making the hot length of the hairpin tube shorter than the cold length, and installation of flexible bellows are some means which can be employed to minimize the relative movement of mating wear surfaces and/or the introduction of differential expansion stresses. Nevertheless, some relative sliding motion is still likely for which control of wear will be necessary to prevent component degradation and possible failure. The application of surface protection and wear resistant coatings on these mating wear surfaces will be necessary.

The principal locations where wear is likely to occur include (1) the OD surfaces of the heat exchanger tubes in contact with the primary helium flow baffles, (2) the outer diameter surfaces of these flow baffles in contact with primary helium flow containment in the hairpin heat exchanger modules, (3) the 5-inch diameter sliding seal joint in the primary helium flow between the center manifold and the individual hairpin heat exchanger modules, and (4) the large diameter sliding seal joints in the primary helium at both the inlet and outlet ducts of the IHX. Operating temperatures at these locations will vary depending upon the location of the sliding wear surfaces from a maximum temperature near 950°C (1750°F) to a mini-

mum of about 350°C (670°F). The presence of the helium atmosphere may grossly affect rubbing and wear conditions through the inability of surface oxide films to re-establish themselves. In some cases design effort may permit the location of the wear surface on a colder, thermally insulated surface.

Hot wear applications in aircraft gas turbines, in the space craft program,and in other high temperature applications will provide the background of technology needed for initiation of development efforts on the specific wear problems in the IHX. Table I-4 indicates the types of plasma arc sprayed coatings which have been considered and/or used in aircraft engine fretting and wear conditions over a wide temperature range; they include, principally, metal bonded carbides, molybdenum,and copper-nickel-indium alloys. Use temperatures are limited by the wear characteristics and by the oxidation behavior of the materials in an oxidizing atmosphere. For the gas cooled reactor IHX application the inert helium atmosphere may have effects which either extend the application temperature of potential wear coatings such as tungsten carbide and molybdenum or which inhibit the wear resistance of mating couples through the instability of surface oxide films.

Additional coatings and surface treatments involving molybdenum disulphide, graphite,and materials with similar lamellar structures such as the sulphides and selenides of rhenium, tantalum, columbium,and molybdenum are also worthy of consideration.

Based upon prior wear testing experiences in hot combustor gas and space applications, it is expected that a detailed review of the literature would provide a well defined background on which to base further wear testing and evaluation efforts.

TABLE I-4

TYPICAL PLASMA ARC SPRAYED FRETTING AND WEAR COATINGS FOR AIRCRAFT ENGINES

MATERIAL AND TYPE	SPECIFICATION		COATING THICKNESS			USEFUL TEMP. RANGE °F	DEPOSITION METHOD	SURFACE PREP.	REMARKS
	RAW MATERIAL	FINISH COATING	USEFUL RANGE MIN.	USEFUL RANGE MAX.	PROCESS CAPABILITY				
Tungsten Carbide WC	B50TF27	F50TF15	.003	.012	±.0015	900	P/A	60-90 RMS	Best P/A WC Coating, Self-bonding.
Tungsten Carbide	-	F50T19D	.003	.010	±.002	900	D		Extremely hard, dense coating.
Chromium Carbide Cr_3C_2	B50TF28	F50TF14	.004	.010	±.002	1200-1600	P/A	60-90 RMS	Material picks up where titanium carbide leaves off.
Molybdenum 99.0 + % Mo	B50TF41	F50TF19	.003	0.12	±.002	600	P/A	60-90 RMS	Exhibits excellent lubricity and anti-fretting wear.
Copper Nickel CuNi	B50TF42	-	.003	0.12	±.002	1000	P/A	105-130	Seal faces and some anti-fretting applications.
Copper Nickel Indium CuNiIn	B50TF72	F50TF13	.003	.010	±.002	1000	P/A	105-130	Excellent anti-fretting protection.
Titanium Carbide TiC	B50TF112	F50TF21	.005	.010	±.002	900-1200	P/A	105-130	Material fits between temperature ranges of WC (900) and Cr_3C_2 (1200). Bond coat not recommended.

I.2 MATERIAL TEST PROGRAMS

I.2.1 SEPARATELY FUNDED PROGRAMS

Development of the IHX will be supported by several separately funded programs appropriate to many components of the high temperature gas cooled reactor; in addition, it will be supported by materials programs directly related to the specific needs of the IHX design. The former includes the broad materials evaluation and development program[I-16] covering (1) the long term environmental effects of helium on the creep, stress-rupture, fatigue and tensile properties of selected alloys, (2) the evaluation of the thermal stability of alloy matrix, surface films and subsurface chemical composition, (3) the characterization and quantitative extent of corrosion and, (4) the development of new or modified alloys with improved characteristics for use in helium cooled reactor environments. A similar basic program would involve fundamental studies of the diffusion of tritium and hydrogen through selected coolant containment alloys in both anticipated helium cooled reactor gases and in helium doped with oxidants. Studies in the latter atmosphere will be performed for the purpose of developing stabilized surface oxides which might be demonstrated to be more resistant to diffusion by tritium or hydrogen. It is presumed that both of these mechanical property and diffusion study programs will continue in effect as needed to provide information regarding the basic environmental behavior of selected gas cooled reactor component materials.

I.2.2 IHX DIRECTLY RELATED PROGRAMS

In addition to such basic programs as those above, material development and evaluation effort will be necessary to meet the specific engineering design requirements of such components as the IHX. Particularly pertinent are the following types of necessary effort.

I.2.2.1 Design Data

The development will be required of ASME code qualified design data on the final selected heat exchanger alloy or alloys in those environmental areas and for those temperature regimes where the alloys are not currently code qualified. Note that design calculations were based on strength properties of a material such as Inconel 617 or its cobalt-free counterpart, Inconel 618 for the hotter portion of the heat exchanger; austenitic stainless steels would be suitable for the lower temperatures. The design data must include all mechanical property data relevant to ASME code qualification including short term tensile properties, high and low cycle fatigue, creep strength,and the structural stability effects on both ductility and impact properties after long term operation under stress.

I.2.2.2 Fabrication Development

Effort will be required to confirm the manufacturability of the various components, to certify the weld joining processes, to determine weld joint mechanical properties of specific joint configurations such as tube to header joints and joints between dissimilar alloys,and to certify other special processes such as the application of wear coatings on different components.

I.2.2.3 Cold Wall Insulation Development

Additional effort will be required to further develop insulation systems and prove their reliability. A detailed and current assessment should be made of the actual operating performance characteristics, maintenance experience,and life of various types of insulating materials in actual reactors. Evaluation of more promising insulation systems, design features, and insulating materials should be made at the higher proposed temperatures (950°C and higher). The work should be guided by design effort intended to optimize the insulation system at these higher temperatures; it would require determination or confirmation of the resiliency characteristics of fibrous materials at elevated temperatures, the consideration of composite materials insulation systems, and the measurement of thermal conductivity, decompression rates and fatigue resistance characteristics of modeled insulation systems in test component sizes.

I.2.2.4 Wear Coating Development

A basic testing program for the selection and evaluation of wear coating materials will be required. Plasma arc spraying and other forms of coating application, will be used to apply wear coatings on one or both mating alloy surfaces in simple materials rub test experiments. These tests will be run in helium environments at the temperatures and rubbing conditions anticipated in the IHX design. Various combinations of materials will be evaluated in rubbing contact including metal bonded tungsten, titanium and chromium carbides, refractory metal sulfides and selenides, and refractory metal elements such as molybdenum. Selection of mating rub surfaces will be made upon the basis of fundamental considerations of rubbing wear and prior rubbing material compatibility experience; consideration will be given to the existence of the protective helium atmosphere and its effect upon avoidance of adverse oxidation of wear surfaces such as molybdenum and the refractory metal carbides and upon the instability of rub surface oxide films on the bare metal of uncoated IHX component surfaces. These wear tests will provide the basis for the reliable selection of materials and processes for protecting wear surfaces in the final design components and for the later conduct of simulated component rub tests involving modular forms of final design configurations.

I.3 BENCH TEST PROGRAMS

Several component design confirmation testing programs will be required using modular components or simulations of final design configurations.

Cold-flow mockups of "U" tube bundle section will be required for initial evaluation of flow distribution and pressure drop in the primary and secondary fluid flow areas.

Simulations of various design configurations for rub test evaluation of wear surface coatings will be required. These will be performed under representative design configuration and under the environment and sliding conditions of temperature, contact pressure, displacement, frequency, and number of cycles expected in final design components. Such testing will utilize the most promising technology developed in the materials rub tests; it will confirm the satisfactory nature of the selected design and the materials and

processes for expected resistance to wear, seizing and excessive gas leakage at each of the critical sliding contact areas in the IHX design.

The preparation of closely simulated tube-to-header joints, the fabrication of process demonstration components, and the preparation of dissimilar alloy welds in full size components will be necessary both for the final certification of the fabrication processes and also for non-destructive and destructive tests necessary to certify the design capability.

I.4 COMPONENT TEST PROGRAMS

Single module heat exchanger "U" tube bundles provide a relatively economic basis for evaluating the design limits, performance characteristics and endurance capability of the IHX. The construction of a total of 3 modules is suggested. One module would be operated in air or combustion gases over the design temperature range at a test facility in the USA. This module test would provide data concerning such performance characteristics as hot gas flow, pressure drop in both circuits, preliminary heat transfer data, tube bundle thermal distortions under transient conditions, tube vibration characteristics, and high cycle fatigue problem analysis at design and off-design conditions. In addition to various tests involving exploration of design capabilities, this component could serve as a test vehicle to evaluate the adequacy of the design in the event of a simulated abrupt rupture failure in the secondary loop. The design calculations establishing the acceptability of retaining full pressure in the primary loop for a ten hour fault period could be verified, the capability of the system to withstand a significant number of low cycle fatigue cycles could be verified, and the mode of failure of the module under the large pressure differential occasioned by a fault period much longer than ten hours could be determined.

Two additional "U" tube bundles are suggested, one for test at the Los Alamos Scientific Laboratories and one for test at KFA in the Federal Republic of Germany. Both tube bundles would be tested under helium atmospheres at temperatures and heat flux rates required by the design. Design performance could be verified and off-design characteristics could be determined. Tests could be run to determine the effect of tube plugging; effects of variations in leakage at various seal areas could be noted; and the long term performance reliability and structural endurance characteristics of the component

could be verified. In addition special techniques could be developed for determining the presence of primary to secondary circuit leakage and for borescopic examination of the tubes on each side of the hairpin tube bundle by entry through the secondary flow passages above the tube headers.

It is expected that the test program involving the above three modular "U" tube heat exchanger bundles would provide a wealth of performance data, corrective design information, operating experience and reliability information which would reduce, to a minimum, any further problems in the design and construction of a full size multi-module IHX.

I.5 GROWTH VERSIONS OF THE IHX

Growth versions of the IHX can achieve higher operating temperatures through the selection and use of materials with higher temperature capability. A review of the broad spectrum of materials which might be considered and a brief statement of their advantages and disadvantages is in order. These materials include, but are not limited to, the following typical alloy and ceramics.

- Weldable iron, nickel and cobalt base tubing alloys
  - Incoloy 800
  - Hastelloy X
  - HA 188
  - Inconel 617
- Weldable cast cobalt base alloys
  - X40
- Turbine blade materials
  (not applicable as tubing, but cited for reference to strength characteristics)
- Refractory alloys
  - Molybdenum
  - Molybdenum TZM
- Oxide dispersion strengthened alloys
  - TD Nichrome
  - MA 754

- Ceramics
  - Si_3N_4
  - Si C

The relative strengths of the above materials are shown as a function of temperature in Figure I-7.

The current reliable heat exchanger tubing materials technology is represented by the weldable iron, nickel and cobalt base alloys of which nickel base alloy INCO 617, and cobalt base alloy, HA-188, are two materials with the highest temperature capability. Weldable cast alloys such as cobalt base X-40 might add additional high temperature capability in the application and use of weldable alloys; effort would be required in the processing of quantities of long lengths of X-40 pipe; however, the possibility of induced radioactivity from cobalt particles in the reactor area must be considered.

The next higher temperature materials capability exists among the non weldable turbine materials of which INCO 738 is a typical example; these alloys would not be suitable for heat exchanger tubes or headers because of lack of weldability and limited ductility; they are shown only to indicate the presence of a group of higher temperature materials.

The refractory alloys exemplified by molybdenum and the very high strength molybdenum alloy TZM, offer increased temperature capability. The high strength refractory alloys, such as molybdenum, generally have poor weldability; alloying with rhenium and the choice of other refractory elements, such as columbium and tantalum,as alloy base systems, provide much improved weldability; nevertheless, the cost of these, their susceptibility to embrittlement, their gross oxidation and their need for protective coating systems (which have not demonstrated long life reliability), makes the choice of refractory alloys highly unlikely.

The oxide dispersion strengthened alloys, such as TD Nichrome and MA 754, do provide a substantial temperature improvement in use of ductile, oxidation and corrosion resistant materials; they merit attention.

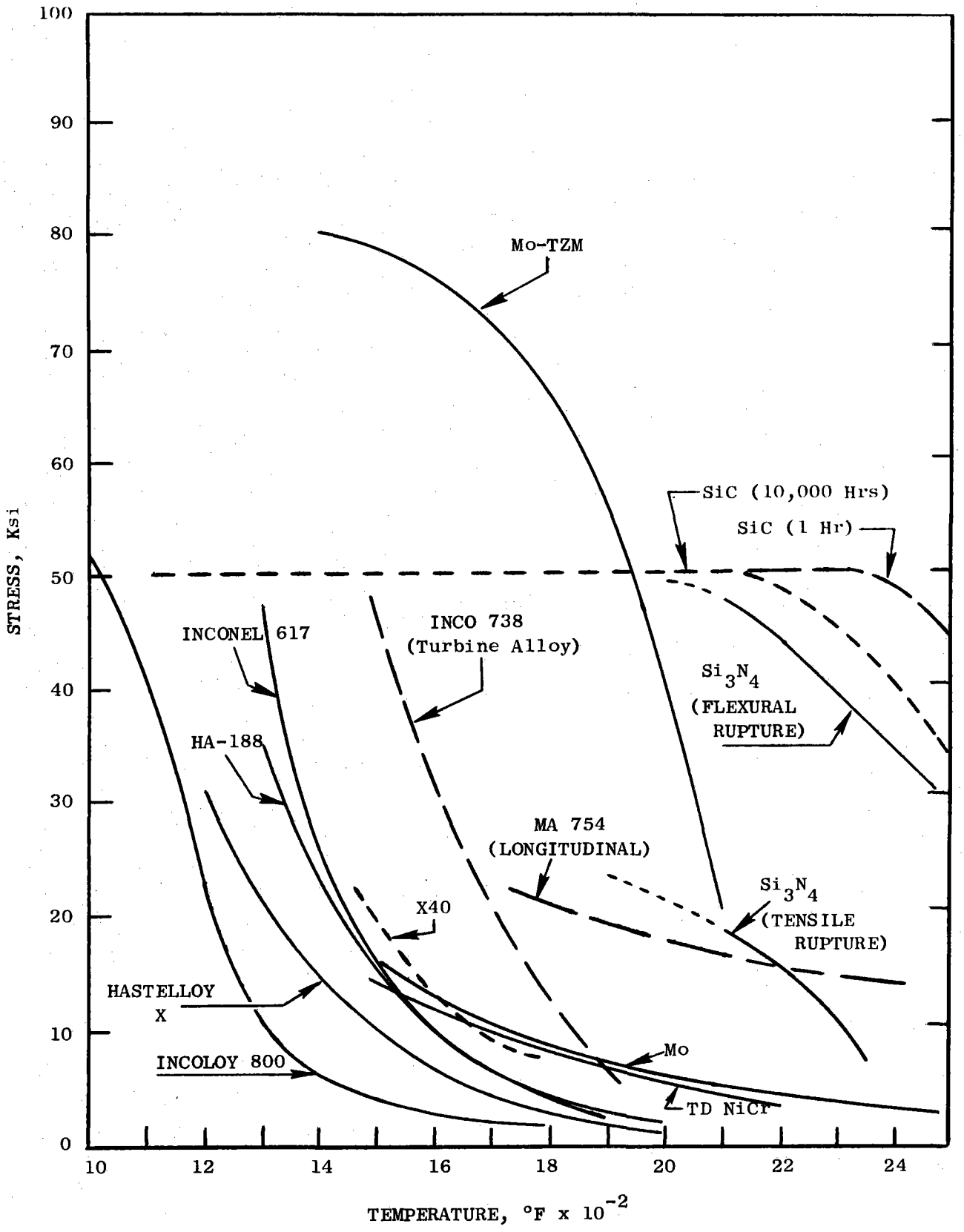

Figure I-7. Strengths of Typical Potential Heat Exchanger Materials (1000 Hr. Rupture Strengths are Shown Except Where Indicated).

At the highest temperatures ceramic materials, alone, provide the strength necessary for heat exchanger surfaces. Some work is being done now to explore the possibilities of using these high temperature, but very brittle materials, in heat exchangers. Much development effort and unique, advanced design criteria for use of brittle materials are necessary before these materials can be strongly considered.

The most likely candidate materials for use in the higher temperature IHX are the oxide dispersion strengthened alloys. The formability of the high strength ODS alloys is relatively poor and, when welded, the ODS structure, which provides their basic strengthening mechanism, is lost. Thus, the use of ODS alloys in aircraft turbine engines, as nozzle vanes employing limited air cooling at extremely high temperatures, has been in extruded bar form rather than in formed and welded sheet metal structures. Parts are joined by brazing instead of welding; brazing alloys and processing techniques are well established both in the brazing process, itself, and in the satisfactory behavior of brazed joints operating at very high temperatures.

For use in the growth version of the IHX, the ODS alloys would probably be employed as extruded tubes. An immediately achievable development goal would be the production of extruded tubes in ten foot lengths. Brazed joints with relatively large lap shear areas would be used to minimize stresses in the brazed joint. The design would provide essentially a mechanical joint with the braze acting as a leak tight sealant and providing shear resistance against joint disassembly. Joining with dissimilar alloys, such as Inconel 617, using brazed joints, should not cause any great difficulties.

While the ODS alloys are limited in available sizes and in their fabricability and while their cost is currently somewhat excessive ($25-40/lb), there appears to be no reason why such alloys could not be used in growth versions of the IHX in those limited areas where uncooled hot gas tubing, header plates or heat exchanger tube surfaces were required.

REFERENCES

I-1. F. N. Mazandarany and P. L. Rittenhouse, "Effects of Service Environments on the Behavior of HTGR Steam Generator Structural Materials", General Atomic Report GA-A13553, July 15, 1975.

I-2. C. T. Sims and W. C. Hagel, Editors, The Superalloys, John Wiley and Sons, New York, 1972.

I-3. L. A. Charlot, R. A. Thiede, and R. W. Westerman, "Corrosion of Superalloys and Refractory Metals in High Temperature Flowing Helium", BMWL-SA-1137, March, 1976.

I-4. K. Hauffae and K. Pschera, Z. Anorg, Chem., 262, Nos. 1-5, 147, 1950.

I-5. P. L. Rittenhouse, "Initial Assessment of the Status of HTGR Metallic Structural Materials and Technology", ORNL-TM-4760, Dec. 1974.

I-6. L. W. Graham, et al., "Environmental Conditions in HTRS and the Selection and Development of Primary Circuit Materials", International Symposium on GCR with Emphasis on Advanced Systems, Jülich, RFG, October, 1975.

I-7. Robertson, W. M., "Hydrogen Permeation, Diffusion and Solution in Nickel", Zeitschrift Für Metalkunde, Vol. 64, No. 6, June, 1973.

I-8 Strehlow, R. A., and H. C. Savage, "The Permeation of Hydrogen Isotopes Through Structural Metals at Low Pressures and Through Metals with Oxide Film Barriers", Nuclear Technology, Vol. 22, April, 1974.

I-9 Röhrig, H. D., J. Blumensaat, and J. Schaefer, "Experimental Facilities for the Investigation and Hydrogen and Tritium Permeation Problems Involved with Steam Methane Reforming by Nuclear Process Heat" British Nuclear Energy Society - International Conference, 26-28, Nov., 1974.

I-10 Bell, J. T., Strehlow, R. A., Redman, J. D., and Smith, F. J., "Tritium Permeation Through Steam Generator Materials", International Conference on Radiation Effects and Tritium Technology for Fusion Reactors, Gatlinburg, Tenn., October 1-3, 1975.

I-11 Bell, J. T., Strehlow, R. A., Redman, J. D., Savage, H. C., and Smith, F. J., "Tritium Permeation through Materials for Steam Generator Systems", Proc. 23rd Conf. Remote Systems Technology, 1975.

I-12 Röhrig, H.D., Hecker, R., Blumensaat, J., and Schaeffer, J., "Studies on the Permeation of Hydrogen and Tritium in Nuclear Process Heat Installations", Nuclear Engineering and Design, Vol. 34, No. 1, October 1975.

I-13 Steigerwald, E.A., "The Permeation of Hydrogen Through Construction Materials", TAPCO Report ER-4776, June 1962.

I-14 Schuster, H., and Jakobeit, W., "High Temperature Alloys for the Power Conversion Loops of Advanced HTR's IAEA-SM-200/36.

I-15 Feathers, L.A., "A Study of the High Temperature Reactor (HTR) Insulation System, AE-73-5, October 31, 1973.

I-16 Anon, Advanced Gas Cooled Nuclear Reactor Materials Evaluation and Development Program, General Electric Co. Proposal CFES P-75-12 (ERDA RFQ, Dated October 9, 1975), December 8, 1975.

APPENDIX J

SCOPE OF WORK FOR FY-1976 VHTR

ENGINEERING DESIGN STUDIES

APPENDIX J

SCOPE OF WORK FOR FY-1976 VHTR ENGINEERING DESIGN STUDIES

I. This study is a follow-on effort to earlier VHTR design studies which have been conducted by GA, GE, and W. This follow-on effort is designed to have two primary objectives:

1. To evaluate VHTR process heat systems with respect to various criteria, plant layout and design options for the systems and components used to transport heat from the reactor core to a process stream with respect to economic, safety, and engineering design considerations.

2. To provide preliminary design specifications, and safety and design criteria for VHTR process heat systems and components, and to provide preliminary specifications for VHTR reactor fuels and structural materials. This information is needed to define development objectives for the VHTR reactor fuels and materials development programs.

II. In conducting these studies, the following assumptions should be used:

1. The process applications of primary interest are assumed to be steam-hydrocarbon reforming (carried out at maximum process temperatures in the range of 1,400 to 1,600°F.), thermochemical water-splitting (carried out at maximum process temperatures of 1,600 to 1,800°F.); and steam-coal gasification (carried out at temperatures ranging from 1,600 to 1,800°F. and above).

2. Capital costs should be estimated in 1976 dollars with no escalation. Capital costs of affected areas should be presented in the NUS-531 type format used for earlier VHTR studies.

3. Hydrogen and tritium should be assumed to diffuse through metallic components in measurable amounts during normal operation, and attention should be given to this consideration in evaluating safety, materials of construction, and various plant layout options.

4. It should be assumed that the VHTR process heat plant will be totally dedicated to one of the processes above. If the core inlet temperatures are unreasonably high for some processes, the temperature may be moderated by adding steam generators and assuming the generation of electrical power.

III. The study shall include, but not be limited to the following:

1. Development of conceptual designs applicable to either steam-hydrocarbon reforming or thermochemical water-splitting for the following plant layout options;

   a. No intermediate loop, i.e., process heat exchangers and steam generators in primary circuit.

   b. With intermediate loop for process heat exchanger, steam generator in primary circuit.

   c. With intermediate loop for both process heat exchanger and steam generator.

   In developing these designs, consideration should be given to the options for locating heat exchangers and steam generators within the reactor primary vessel structure (as with PCRV, PCSV, or PCIV concepts), within the reactor secondary containment vessel, and outside the reactor secondary containment. The optimum layout configurations should be determined insofar as possible, and the rationale for choosing these configurations should be presented.

2. As for the previous studies, estimates of capital costs for the reference nuclear systems will be presented in sufficient detail to permit independent assessment and normalization of costs. Costs will be estimated for a 3000 MWt plant capacity with appropriate scaling factors to be provided for plant sizes down to approximately 300 MWt or to another appropriate size after evaluating the scaling factor limitation.

3. Conceptual design information for VHTR components and systems should then be translated to preliminary system design and safety criteria, and specifications and development requirements for reactor fuels and structural materials. More specifically, the temperature requirements for VHTR fuels should be established based upon the reference fuel configuration most favored by the contractor, and any associated fuel development requirements should be described in detail. With respect to materials, specifications should be developed with respect to component and system requirements for operating temperatures, strength, creep-fatigue, environmental control, lifetime, and fabricability, corrosion resistance, permeability, etc. The information developed under this task is particularly crucial with respect to providing development goals for the ongoing VHTR fuel development efforts and the high temperature materials program now being initiated.

4. Development of a conceptual design applicable to steam-coal gasification process. Conceptual design information for the VHTR components and systems should be translated to preliminary component and system design and specifications and development requirements for reactor fuels and materials. VHTR fuel temperature and materials requirements should be developed as described in "3" above. This information will provide development goals for fuel development and high temperature materials programs now being initiated.

5. For further details of the various contractor approaches to VHTR design see technical reports GA-13158, GEAP-14018, and WANL-2445-1.

APPENDIX K

ACRONYMS

APPENDIX K

ACRONYMS

AVR	Arbeitgemeinschaft Versuchsreaktor, Germany (Gas Cooled Pebble Bed Reactor, 50 MWt)
CACS	Core Auxiliary Cooling System
CHP	Chemical Heat Pipe
DBA	Design Basis Accidents
DSR	Duplex Steam Reformer
ERDA	Energy Research and Development Administration
EVA	Einrohr Vergasungsanlage, Pilot Plant, Jülich (Steam Reformer Test Facility)
FBR	Fast Breeder Reactor
FDS	Fast Discharge System
FEA	Federal Energy Administration
FPC	Federal Power Commission
FRC	Federal Radiation Council
FRG	Federal Republic of Germany
GA(GAC)	General Atomics Corporation
GCR	Gas Cooled Reactor
GE	General Electric
GE-KAPL	General Electric - Knolls Atomic Power Laboratory
HHV	Hochtemperatur-Helium-Versuchsanlage
HTGR	High Temperature Gas-Cooled Reactor
HTR	High Temperature Reactor
ICRP	International Commission on Radiological Protection
IHX(L)	Intermediate Heat Exchanger (Loop)
KFA	Kernforschungsanlage, Jülich, Germany
LASL	Los Alamos Scientific Laboratory
LMFBR	Liquid Metal Fast Breeder Reactor
LOCA	Loss-of-Cooling Accident
LWPBR	Light Water Pre Breeder Reactor
LWBR	Light Water Breeder Reactor
LWR	Light Water Reactor
MPC	Maximum Permissible Concentration
NRC	Nuclear Regulatory Commission
O&M	Operating and Maintenance
OTTO	Once Through Then Out Fuel Cycle
PBR	Pebble Bed Reactor
PCRV	Prestressed Concrete Reactor Vessel
PWR	Pressurized Water Reactor
SG(A)	Steam Generator (Assembly)
SNG	Substitute Natural Gas
SNPH	Small Nuclear Process Heat Plants
SR(A)	Steam Reformer (Assembly)
THTR	Thorium High Temperature Reactor, Germany, 200 MWe
USA	United States of America
VHTR	Very High Temperature Reactor
W	Westinghouse

APPENDIX L

METRIC CONVERSIONS

APPENDIX L

METRIC CONVERSIONS

Quantity	Metric	English Engineering
Area	1 m^2	10.765 ft^2
Density	1 gm/cm^3	62.428 lb/ft^3
Energy	1 kcal	3.968 Btu
Enthalpy	1 cal/gm	1.8 Btu/lb m
Flow	1 Mg/hr = 1000 kg/hr	2205 lb/hr 0.6125 lb/sec
	1 kg/sec	2.205 lb/sec
Heat Flux	1 w/m^2	0.317211 $Btu/hr-ft^2$
Heat Transfer Coefficient	1 $w/m^2-°C$	0.17619 $Btu/hr-ft^2-°F$
Length	1 m	3.281 ft
Mass	1 kg	2.205 lbs
	1 Mg (1 metric tonne)	2205 lbs
Pressure	1 b	0.9869 atm 14.504 psi
Specific Heat	1 cal/gm-°C	1 Btu/lmb-°F
Stress	1 kp/cm^2	14.223 psi
Temperature	°C	°F = 1.8 (°C)+32
Volume	1 m^3	35.3198 ft^3
Work	1 kw	3414 Btu/hr